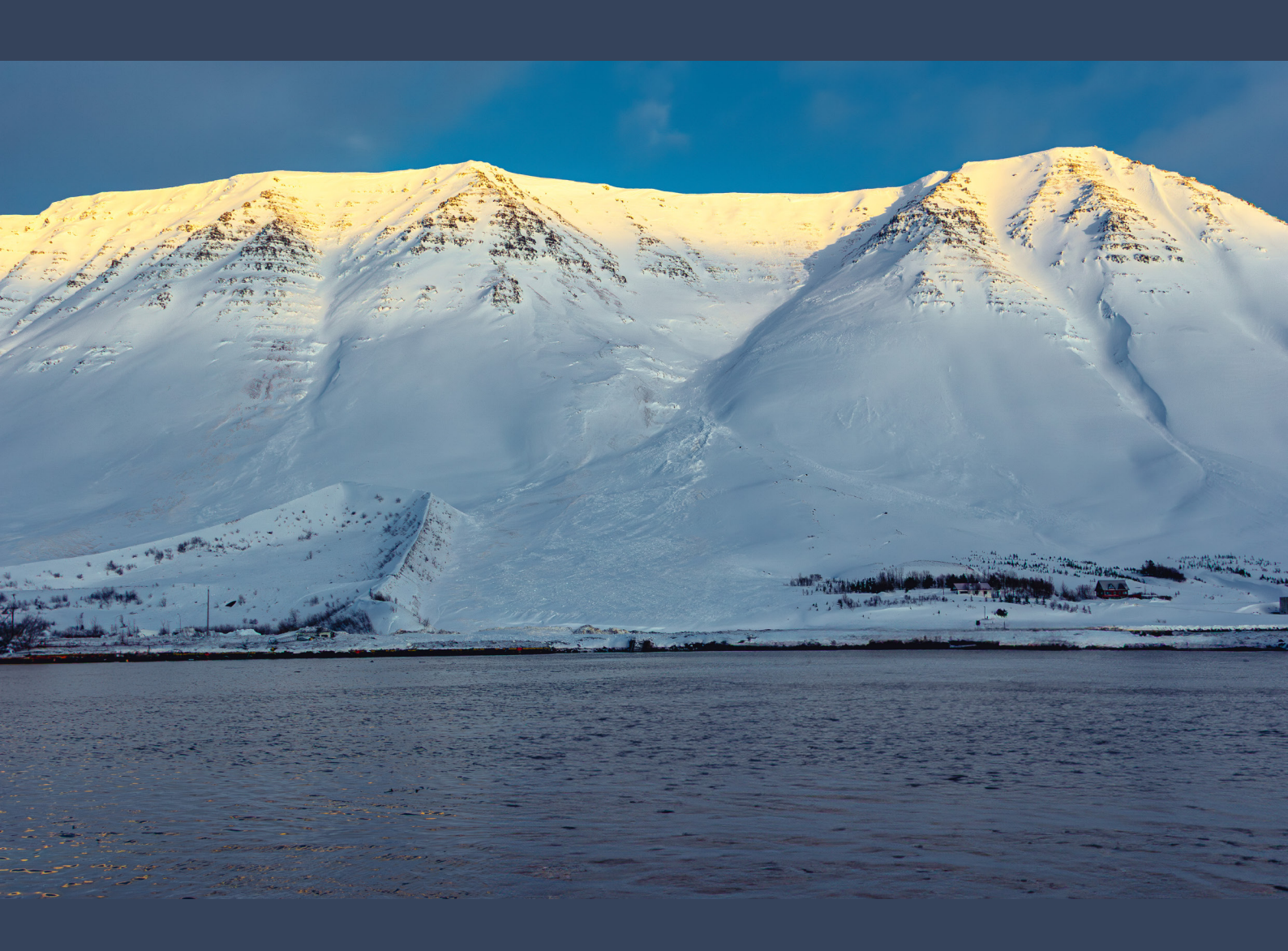


International Symposium on Mitigation Measures against Snow Avalanches and other Rapid Gravity Mass Flows



Ísafjörður, Iceland September 30 – October 3, 2025



International Symposium on Mitigation Measures against Snow Avalanches and other Rapid Gravity Mass Flows

Ísafjörður, Iceland September 30 - October 3, 2025

Organizing Committee

Árni Jónsson, chairman, Association of Chartered Engineers in Iceland (VFÍ)
Bergþóra Kristinsdóttir, Icelandic Road and Coastal Authorities (IRCA)
Ester Anna Ármannsdóttir, The National Planning Agency
Geir Sigurðsson, Icelandic Road and Coastal Authorities (IRCA)
Örn Baldursson, The Government Property Agency (FSRE)

Scientific & Editorial Committee

Árni Jónsson, Association of Chartered Engineers in Iceland (VFÍ)
Fjóla Guðrún Sigtryggsdóttir, Norwegian University of Science and Technology (NTNU)
Peter Gauer, Norwegian Geotechnical Institute (NGI)
Sólveig Þorvaldsdóttir, University of Iceland (UI)
Stefan Margreth, WSL Institute for Snow and Avalanche Research (SLF)
Þorbjörg Hólmgeirsdóttir, COWI

Note! All work and viewpoints expressed in these proceedings are solely the responsibility of the authors. Only minor editing has been done to submitted documents.

Recommended citation

Jónsson, Á., Sigtryggsdóttir, F. G., Hólmgeirsdóttir, Þ., Gauer, P., Margreth, S., and Þorvaldsdóttir, S. (eds) 2025, International Symposium on Mitigation Measures against Snow Avalanches and other Rapid Gravity Mass Flows, Ísafjörður, Iceland September 30 - October 3, 2025.

The proceedings are available online via QR code:



Previous SNOW conferences

SNOW2008 https://vedur.is/gogn/snjoflod/varnarvirki/EgilsstadirProceedingsEAbstractsRS.pdf SNOW2019 https://www.vfi.is/media/utgafa/SNOW2019 conference proceedings web.pdf

Photo front- & back cover: Flateyri January 17, 2020, Arni Jonsson

Sponsors

Gold



Silver





Bronze







Other Financial Support



Government of IcelandMinistry of the Environment,
Energy and Climate





Supporters









Organizers





















Foreword

In 2025, Iceland will mark the 30th anniversary of the devastating avalanches that struck the communities of Súðavík and Flateyri, resulting in tragic loss of life, widespread community disruption, and severe infrastructure damage. The Association of Chartered Engineers in Iceland (VFÍ) believes it is important to honor these events and their lasting impact by holding the next SNOW conference in the Westfjords in 2025.

For many decades, and even centuries, various locations around the world have implemented mitigation measures to counter snow avalanches and other rapid mass movements in steep terrain. Advancements in knowledge and equipment have enabled the construction of significantly larger and more complex structures than before. These measures are primarily intended to protect human lives and infrastructure, like roads and communication networks, but they also influence people in various other ways. Large structures typically have a notable impact on the environment, either in the avalanche starting zones or in the run-out zones. Often, run-out zone structures must be erected near densely populated areas; they can be imposing and may even alter the local climate and snow accumulation near them.

Relocating communities involves making difficult choices, as individuals must leave their established homes for new locations. A key question arises: why demolish an existing developed area instead of protecting it? The value of vulnerable buildings often comes into question. How do mitigation measures impact people's daily lives? Do residents trust these measures and feel secure living nearby? How do these mitigation measures influence the value of protected buildings and the area's future development?

Does a poor avalanche reputation affect the community and its future growth? In recent years, travel has surged, making the demand for safe transportation a global priority. Avalanches pose a significant threat to roads and railways in mountainous regions, resulting in numerous fatalities each year. Traffic disruptions and rerouting also lead to substantial financial losses annually.

The symposium covers four distinct themes: *Risk Management, Society and Environment, Planning, Design, Construction, and Management of Protective Measures, and Observations and Simulations of Avalanches.* The aim is to present the current state of knowledge, provide insights into future developments, and broaden the perspectives of participants from each group. The symposium encourages the exchange of experiences and ideas, fostering collaboration to enhance life in regions at risk of avalanches.

The organizing committee welcomes you all to Ísafjörður in September 2025.



Árni Jónsson, chairman of the organizing committee

Index

Foreword		4
Programme		8
Abstracts (w	ith presenting author underlined if not the first author)	13
Keynotes		14
K1	Designing for Safety and Liveability: Collaborative Approaches to Avalanche Defences in Iceland Þórhildur Þórhallsdóttir	14
K2	Managing natural hazards risk: Perspectives from far-flung. Andrea Taurisano	15
К3	Avalanche and landslide protection measures in Iceland – 30 years of design innovations protecting tw	elve
	villages across Iceland.	16
	Kristín Martha Hákonardóttir, Tómas Jóhannesson, Gísli Steinn Pétursson and Hafsteinn Pálsson	
K4	From granular mechanics to 3D modeling: Advancing avalanche hazard assessment and mitigation	25
	Michael L. Kyburz, Lars Blatny and Johan Gaume	
Oral Session	ns	
01.1	History of snow avalanches and settlements in hazard areas in Iceland Harpa Grímsdóttir	31
01.2	Seven years of research on snow avalanches in Nunavik, northern Quebec, Canada: hazard and vulner	abilities
	Armelle Decaulne, Vincent Filion, Beatriz Funatsu, Sasha Griffin and Najat Bhiry	38
O2.1	Development of a guidelines for site-specific avalanche warning – needs, method, and content	44
	Karin Bergbjørn and Priska H. Hiller	
O2.2	Towards an operational avalanche forecasting tool using RAMMS::Extended	49
	<u>Cam Campbell</u> and Eirik Sharp	
O2.3	Systems-Thinking Analysis of the Seyðisfjörður Landslide Programme: Understanding Feedback	55
	Control Mechanisms.	
	Sólveig Thorvaldsdóttir and Benedikt Halldórsson	
O2.4	Temporary risk reduction methods in protected areas	61
	Óliver Hilmarsson, Harpa Grímsdóttir and Tómas Jóhannesson	
03.1	Guidelines and digital toolboxes for mitigation measure planning and assessment from an Austrian	66
	Perspective The Control of the Contr	
	Felix Oesterle, Matthias Granig, Paula Spannring, Anna Wirbel, Jan-Thomas Fischer and Christian Tol	C
O3.2	Numerical analysis of reinforced soil barriers subjected to avalanche dynamic loads	71
02.2	Oltion Korini and Anthony Austin	
O3.3	Monitoring Umbrella Nets – A Full-Scale Test Site in Tirol	77
02.4	Engelbert Gleirscher, Anselm Köhler, Matthias Granig and Michael Brauner	0.2
O3.4	HELIOPLANT® – PV structure in avalanche protection	83
02.5	Alexander Ploner, Thomas Sönser and Florian Jamschek	0.0
O3.5	Preventive Avalanche Control on Arnøya – Securing Critical Infrastructure	88
	Thomas Berger, Olafur Stitelmann, Cedric Larcher, Siiri Wickstrom, Kalle Kronholm, Maxence Carrel,	,
041	Sindre Linstad, Andreas Per Ola Persson,	0.4
O4.1	Are avalanche pressure requirements still necessary for the design of modern ropeways?	94
044	Philippe Berthet-Rambaud, Lucas Le Bouquin, Michel Gillard	
O4.2	Mitigating the natural hazard risk in Longyearbyen, Svalbard	100
	Árni Jónsson, Stian Bue Kanstad, Jan-André Jansen	100

04.3	Swiss experience with direct avalanche protection measures on buildings Stefan Margreth	108
O4.4	Planning & structural limitations of RACS – making structures survive in avalanche release areas	114
	Martin Venås, Walter Steinkogler, Andreas Egger, Stian Langeland	
O5.1	Keeping the power on: Quantitative avalanche risk assessment and operational decision making for a	
	transmission in British Columbia, Canada	121
	Alan Jones and Christ Argue	
O5.2	Comparing benefit-cost-analyses of snow avalanche mitigation measures obtained by two hazard and	
	risk analysis approaches	122
	Michael Bründl, Jan Kleinn, and Linda Zaugg	
O5.3	Integral snow avalanche risk management for national roads in Norway	131
	<u>Markus Eckerstorfer</u> , Njål Farestveit, Jeanette, Gundersen, Tore Humstad, Knut Inge Orset, Emil Solbakker Jens Tveit	1,
O5.4	The Pollfjellet powder snow avalanche: Building model scenarios for a mass dependent model and	
03.4	mitigation Case study	137
	Hallvard Skaare Nordbrøden, Siiri Wickström and Kalle Kronholm	137
O5.5	Risk management from natural hazards for the new European Road E10, Halogalandsveien	143
03.3	Christian Jaedicke, Vidar Kveldsvik, Anders Kleiven, Sunniva Skuset, Holt Hancock, Elise Morken, Peter	143
	Gauer, Piotr Kupiszewski, Kjersti Gisnås, and Graham Gilbert	
O5.6	Land use and planning of settlements in hazard zones and under defense structures	150
03.0	Magni Hreinn Jónsson and Tómas Jóhannesson	130
O6.1	Three-dimensional simulations of snow-avalanche flow for assessing the effectiveness of protections	
00.1	measures in the run-out zone	152
	<u>Tómas Jóhannesson</u> , Alexander H. Jarosch and Magni Hreinn Jónsson	132
O6.2	Turbulence-Based Modeling of Powder-Snow Avalanches and Air-Blast Pressures Using RAMMS::Extended	153
00.2	Perry Bartelt, Lukas Stoffel, Stefan Margreth, Yu Zhuang and Marc Christen	133
O6.3	Large scale avalanche hazard indication modelling adapted for Iceland	159
00.5	Yves Bühler, Sigríður Sif Gylfadóttir, Pia Ruttner, Marc Christen, Andreas Stoffel and Stefan Margreth	13)
O6.4	Bridging the Gap: Scenario-Based Avalanche Modeling vs. Back-Calculation of Events	166
00.4	Lukas Stoffel, Stefan Margreth and Perry Bartelt	100
O7.1	Towards a Physics-Based Quantification of Run-Up and Impact Pressure Using Numerical and	
07.1	Physical Experiments	172
	Michael J. Kohler, Johan Gaume, Julius Kruse, Christophe Ancey, and Betty Sovilla	1/2
O7.2	Use of OpenFOAM and $\mu(I)$ rheology in design of protective structures for avalanches for Flateyri	178
07.2	Reynir Leví Guðmundsson, Snorri Gíslason, Hafþór Pétursson and Kristín Martha Hákonardóttir	170
O7.3	Numerical simulation of slushflow and assessment of proposed protective measures in Patreksfjörður,	
07.0	Iceland	186
	Ragnar Lárusson, Reynir Leví Guðmundsson, Gísli Steinn Pétursson, Snorri Gíslason, Kristín Martha	100
	Hákonardóttir	
O8.1	Artificial intelligence supported extra long-range Doppler radar: avalanche activity measurement and	
0011	RACS blasting verification in Evolène	203
	Maxence Carrel, Ólafur Y. Stitelmann, Martin Hahner, François Fellay, Pascal Mayoraz	_00
O8.2	Detailed, high temporal resolution snow surface monitoring for avalanche hazard management: A case	
	study from a controlled avalanche release	208
	<u>Pia Ruttner</u> , Julia Glaus, Annelies Voordendag, Andreas Wieser and Yves Bühler	_00
08.3	Low-Cost Lidar Monitoring to Inform Planning and Implementation of Avalanche Mitigation	214
	Thomas Goelles Stefan Wallner and Markus Eckerstorfer	

	O9.1	Impact of Snow Depth Initialization on Avalanche Modeling: Comparing Station Data with High-Resolution	on
		Measurements	220
		Julia Glaus, Pia Ruttner, Johan Gaume and Yves Bühler	
	O9.2	Comparing simulated pressure profiles with measurements from a power line assembly at the Ryggfonn	
		test site.	226
		Peter Gauer, Piotr Kupiszewski, and Callum Tregaskis	
	09.3	Next-Generation Modular Avalanche Radar with Multi-Hazard Capabilities	235
		Susanne Wahlen, Lorenz Meier and Severin Staehly	
	O9.4	Development of snowsensors in Ísafjörður	236
		Harpa Grímsdóttir and Örn Ingólfsson	
	O10.1	Experiences in designing mitigation measures against slush flows	239
		Elise Morken, Sunniva Skuset and Peter Gauer	
	O10.2	Slush Flows – A review of a poorly explored phenomenon and its protection measures	244
		Nadine Feiger and Corinna Wendeler	
	O10.3	Advancing Snowdrift Forecasting with Physically-Based Snow Models and High-Resolution	
		Weather Data	252
		Sveinn Gauti Einarsson	
	O10.4	Can wind simulation help optimize function of snow avalanche mitigation measures?	256
		Árni Jónsson and Peter Gauer	
Poster	Session	ns	
	P1.1	Avalanche control systems and traditional mitigation structures.	264
		Ines Waltl and Jón Páll Eyjólfsson	
	P1.2	Avalanche Monitoring in Flateyri using Doppler Radar	269
		<u>Lars Krangnes</u> and Ragnhild Lie	
	P1.3	Samuelsberg catching dam partial failure and rebuild – A case study.	270
		Árni Jónsson and Anders Bjordal	
	P1.4	Adapting and using active rigid modules in a passive way against avalanches	277
		Rémy Martin, Nadia Hassine and Philippe Berthet Rambaud	
	P1.5	Detection of liquid water accumulations during snow block sliding experiments	283
		James Glover, Fabian Wolfsperger, Silvio Ziegler	
	P1.6	Roof avalanche mitigation through photovoltaic panel heating to induce controlled snow removal	284
		James Glover, Michael Sattler, Dylan Longridged, Philip Crivelli, Jann Ambühl	
	P2.1	Engineering Approaches to Avalanche Mitigation in Japan: Current Status, Challenges, and Future	
		Perspectives.	285
		Yusuke Harada	
	P2.2	Snow net instrumentation at Snoqualmie Pass, Washington, USA.	291
		Chris Wilbur and John Stimberis	
	P2.3	New experiments and measurments to improve operational practices for preventive avalanche triggering.	297
		Philippe Berthet-Rambaud, Jean-François Bellin, Eric Viallet, Amandine Molinier, Sonam Bourlon de Rou	vre,
		Fanny Bourjaillat and Stéphane Bornet	
	P2.4	Monitoring site Ranalt – Flexible barrier designed for catching avalanches exposed to an unexpected	
		debris flow event.	303
		Gernot Stelzer, Engelbert Gleirscher, Daniel Illmer, Georg Nagl, Marcel Fulde	
	P2.5	Snow fences on Eyrarfjall above Flateyri: A pilot study on avalanche risk reduction.	304
		Gísli Steinn Pétursson, Þorbjörg Anna Sigurbjörnsdóttir, Kristín Martha Hákonardóttir, Tómas Jóhannesson	n,
		Örn Ingólfsson, Skúli Þórðarson, Áki Thoroddsen	
	P2.6	Development of a calculation method for flexible rockfall barriers under static and dynamic snow loads	314
		Dennis Gasteiger, Peter Utz, Gabriel Marc, Alexander Michalski and Maximilian Kramer	



Programme

Monday September 29

18:30 – 20:00 The welcome reception will be held at The Westfjords Heritage Museum. Invitation by Ísafjarðarbær

The Westfjords Heritage Museum is located in Neðstakaupstaður in Ísafjörður, and its exhibitions are in the Turnhúsið, which was built in 1784-1785. The museum's main is about fishing and its development in the Westfjords, as well as what the growing fishing industry meant for the people living there. In Neðstakaupstaður stands the oldest cluster of houses in the country, consisting of four houses that all belonged to Danish mer chants in the area.

Light refreshments will be served at the museum.

Tuesday September 30

n •		
П	m	e

08:00 Registration 08:30 Opening

09:00 Keynote 1 – Environment and Society

Designing for Safety and Liveability: Collaborative Approaches to Avalanche Defences in Iceland.

ÞÓRHILDUR ÞÓRHALLSDÓTTIR, LANDMÓTUN

09:30 - 10:00 Oral Sessions 1

09:30 O1.1 History of snow avalanches and settlements in hazard areas in Iceland.

HARPA GRÍMSDÓTTIR, ICELANDIC METEOROLOGICAL OFFICE

09:45 O1.2 Seven years of research on snow-avalanche in Nunavik, northern Quebec, Canada:

hazards and vulnerabilities.

ARMELLE DECAULNE, CNRS LETG

10:00 QA 10:15 Break

10:30 Keynote 2 – Risk management

Managing natural hazards risk: Perspectives from far-flung.

ANDREA TAURISANO, NVE

11:00 - 12:00 Oral Sessions 2

11:00 **O2.1** Development of a guidance for site-specific avalanche warning – needs, method, and content.

ANNA KARIN BERGBJØRN / PRISKA HELENE HILLER, NVE

11:15	O2.2	Towards an operational avalanche forecasting tool using RAMMS::Extended.
		CAM P. CAMPBELL, ALPINE SOLUTIONS
11:30	O2.3	Systems-Thinking Analysis of the Seyðisfjörður Landslide Programme: Understanding Feedback Control Mechanisms.
		SÓLVEIG THORVALDSDÓTTIR, UNIVERSITY OF ICELAND
11:45	O2.4	Temporary risk reduction methods in protected areas.
		ÓLIVER HILMARSSON, ICELANDIC METEOROLOGICAL OFFICE
12:00	QA	
12:15	Lunch	
13:15	Keyn	ote 3 – Planning, design, construction
		Avalanche and landslide protection measures in Iceland: 30 years of design innovations protecting ten
		Icelandic communities.
		KRISTÍN MARTHA HÁKONARDÓTTIR, THE MINISTRY OF THE ENVIRONMENT, ENERGY AND CLIMATE
13:45 - 15:00	Oral	Sessions 3
13:45	O3.1	Guidelines and digital toolboxes for mitigation measure planning and assessment from an Austrian Perspective.
		FELIX OESTERLE, AUSTRIAN RESEARCH CENTRE FOR FORESTS
14:00	O3.2	Numerical analysis of reinforced soil barriers subjected to avalanche dynamic loads.
		OLTION KORINI, GEOQUEST
14:15	03.3	Monitoring Umbrella Nets – A Full-Scale Test Site in Tirol.
		ENGELBERT GLEIRSCHER, BFW
14:30	03.4	HELIOPLANT® – PV structure in avalanche protection.
		THOMAS SÖNSER / ALEXANDER PLONER, I.N.N.
14:45	03.5	Preventive Avalanche Control on Arnøya – Securing Critical Infrastructure.
		THOMAS BERGER / SIIRI WICKSTRÖM/ SINDRE LINSTAD, MND FRANCE
15:00	QA	
15:15 - 15:45		x + Postersession 1
	P1.1	Avalanche control systems and traditional mitigation structures.
	20.0	INES WALTL, INAUEN SCHÄTTI AG
	P1.2	Avalanche Monitoring in Flateyri using Doppler Radar
	D1 2	LARS KRANGNES, CAUTUS GEO AS
	P1.3	Samuelsberg catching dam partial failure and rebuild – A case study
	D1 4	ÁRNI JÓNSSON, ORION CONSULTING SLF
	P1.4	Adapting and using active rigid modules in a passive way against avalanches
	D1 5	PHILIPPE BERTHET-RAMBAUD, ENGINEERISK
	P1.5	Detection of liquid water accumulations during snow block sliding experiments
	P1.6	JAMES GLOVER, UNIVERSITY OF APPLIED SCIENCES GRISONS Pacf cyclopela mitigation through photographic monel heating to induce controlled grown removal
	1 1.0	Roof avalanche mitigation through photovoltaic panel heating to induce controlled snow removal
15:45	WS1	JAMES GLOVER, UNIVERSITY OF APPLIED SCIENCES GRISONS The avalanche incidents 1995 documented through the camera
13.43	W 51	-
16:15	WS2	RAGNAR AXELSSON, RAX Officers on duty during the avalanche incidents 1995.
10.13	11 132	RÖGNVALDUR ÓLAFSSON/HLYNUR SNORRASON, THE NATIONAL POLICE COMMISSIONERS OFFICE
16:45	WS3	A Historical Perspective: Events Leading Up to, During, and Following the 1995 Avalanches.
1∪.⊤J	1100	ÁRNI JÓNSSON, ORION CONSULTING SLF
17:15	End of	Tuesday program
1,	2114 01	

Programme (Continue)

Wednesday October 1

09:00 - 17:30 - Field excursion / symposium tour

At 9:00 the buses will depart from the conference hall, heading first to Súðavík for a brief stop at the memorial site. From there, the tour continues to Flateyri, where we will observe the existing mitigation measures and ongoing construction projects.

A lunch break is planned at Café Gunna.

Afterward, we will travel to Bolungarvík to visit Iceland's highest catching dam. The final three stops of the day will be in Ísafjörður, where we will examine catching and deflecting dams. The tour is scheduled to conclude no later than 18:00.

Thursday October 2

Time			
08:00	Venue opens		
8:30 - 9:30	Oral	Sessions 4	
08:30	O4.1	Are avalanche pressure requirements still necessary for the design of modern ropeways?	
		PHILIPPE BERTHET-RAMBAUD, ENGINEERISK	
08:45	O4.2	Mitigating the natural hazard risk in Longyearbyen, Svalbard	
		ÁRNI JÓNSSON, ORION CONSULTING SLF	
09:00	O4.3	Swiss experience with direct avalanche protection measures on buildings	
		STEFAN MARGRETH, WSL INSTITUTE FOR SNOW AND AVALANCHE RESEARCH SLF	
09:15	O4.4	Planning & structural limitations of RACS – making structures survive in avalanche release areas	
		MARTIN VENÅS, WYSSEN NORWAY	
09:30	QA		
09:45	Break		
10:00 - 11:30	0 Oral Sessions 5		
10:00	O5.1	Keeping the power on: Quantitative avalanche risk assessment and operational decision making for a	
		transmission in British Columbia, Canada	
		ALAN JONES, DYNAMIC AVALANCHE CONSULTING LTD	
10:15	O5.2	Comparing benefit-cost-analyses of snow avalanche mitigation measures obtained by two hazard and	
		risk analysis approaches	
		MICHAEL BRÜNDL, WSL INSTITUTE FOR SNOW AND AVALANCHE RESEARCH SLF	
10:30	05.3	Integral snow avalanche risk management for national roads in Norway	
		MARKUS ECKERSTORFER, NORWEGIAN PUBLIC ROADS ADMINISTRATION	
10:45	O5.4	The Pollfjellet powder snow avalanche: Building model scenarios for a mass dependent model and	
		mitigation Case study	
		HALLVARD SKAARE NORDBRØDEN, SKRED AS	
11:00	05.5	Risk management from natural hazards for the new European Road E10, Halogalandsveien	
		CHRISTIAN JAEDICKE, NORWEGIAN GEOTECHNICAL INSTITUTE	
11:15	O5.6	Land use and planning of settlements in hazard zones and under defense structures	
		MAGNI HREINN JÓNSSON, ICELANDIC MET OFFICE	

11:30	QA	
11:45	Lunch	
12:45	Keynote 4 – Mitigation measures; simulations, experiments, experiences	
		From granular mechanics to 3D modeling: Advancing avalanche hazard assessment and mitigation
		MICHAEL LUKAS KYBURZ, CHAIR OF ALPINE MASS MOVEMENTS, ETH ZÜRICH
13:15 - 14:15		
13:15	O6.1	Three-dimensional simulations of snow-avalanche flow for assessing the effectiveness of protections
		measures in the run-out zone
12.20	061	TÓMAS JÓHANNESSON, ICELANDIC METEOROLOGICAL OFFICE
13:30	O6.2	Turbulence-Based Modeling of Powder-Snow Avalanches and Air-Blast Pressures Using
		RAMMS::Extended
13:45	06.3	PERRY ANDERS BARTELT, RAMMS AG Large scale avalanche hazard indication modelling adapted for Iceland
13.43	00.5	YVES BÜHLER, WSL INSTITUTE FOR SNOW AND AVALANCHE RESEARCH SLF
14:00	O6.4	Bridging the Gap: Scenario-Based Avalanche Modeling vs. Back-Calculation of Events
11.00	00.1	LUKAS STOFFEL, WSL INSTITUTE FOR SNOW AND AVALANCHE RESEARCH SLF
14:15	QA	ECKIS STOTTEE, WISE INSTITUTE FOR SHOW IN INVIDENCE IE RESERVED SEE
14:30	Break	
14:45	Sponso	r session
15:00 - 15:45	Oral S	Sessions 7
15:00	O7.1	Towards a Physics-Based Quantification of Run-Up and Impact Pressure Using Numerical and
		Physical Experiments
		MICHAEL JOSEF KOHLER, WSL INSTITUTE FOR SNOW AND AVALANCHE RESEARCH SLF
15:15	O7.2	Use of OpenFOAM and $\mu(I)$ rheology in design of protective structures for avalanches for Flateyri.
		REYNIR LEVÍ GUÐMUNDSSON, VERKÍS
15:30	O7.3	Numerical simulation of slushflow and assessment of proposed protective measures in Patreksfjörður,
		Iceland.
15.45	0.4	RAGNAR LÁRUSSON, VERKÍS
15:45 16:00	QA Brook	x + Postersession 2
10.00	P2.1	Engineering Approaches to Avalanche Mitigation in Japan: Current Status, Challenges, and Future
	1 2.1	Perspectives.
		YUSUKE HARADA, CIVIL ENGINEERING RESEARCH INSTITUTE FOR COLD REGION
	P2.2	Snow net instrumentation at Snoqualmie Pass, Washington, USA.
		CHRIS WILBUR, WILBUR ENGINEERING, INC.
	P2.3	New experiments and measurments to improve operational practices for preventive avalanche
		triggering.
		PHILIPPE BERTHET-RAMBAUD, ENGINEERISK
	P2.4	Monitoring site Ranalt - Flexible barrier designed for catching avalanches exposed to an unexpected
		debris flow event.
		GERNOT STELZER, TRUMER SCHUTZBAUTEN GMBH
	P2.5	Snow fences on Eyrarfjall above Flateyri: A pilot study on avalanche risk reduction.
	De :	GÍSLI STEINN PÉTURSSON, VERKÍS
	P2.6	Development of a calculation method for flexible rockfall barriers under static and dynamic snow loads.
16.00	n • •	DENNIS GASTEIGER, GEOBRUGG AG
16:30		Thursday program
19:00	Dinner at Hótel Ísafjörður	

Friday October 3

Time			
08:00	Venue opens		
08:30 - 09:30	Oral Sessions 8		
08:30	O8.1	Artificial intelligence supported extra long-range Doppler radar: avalanche activity measurement and	
		RACS blasting verification in Evolène	
		MAXENCE CARREL, GEOPREVENT	
08:45	O8.2	Detailed, high temporal resolution snow surface monitoring for avalanche hazard management: A case	
		study from a controlled avalanche release	
		PIA RUTTNER, WSL INSTITUTE FOR SNOW AND AVALANCHE RESEARCH SLF	
09:00	O8.3	Low-Cost Lidar Monitoring to Inform Planning and Implementation of Avalanche Mitigation	
		THOMAS GOELLES, UNIVERSITY OF GRAZ	
09:15	QA		
09:30	Break		
09:45 - 11:00	Oral S	Sessions 9	
09:45	09.1	Impact of Snow Depth Initialization on Avalanche Modeling: Comparing Station Data with	
		High-Resolution Measurements	
		JULIA GLAUS, WSL INSTITUTE FOR SNOW AND AVALANCHE RESEARCH SLF	
10:00	O9.2	Comparing simulated pressure profiles with measurements from a power line assembly at the Ryggfonn	
		test site.	
		PETER GAUER, NORWEGIAN GEOTECHNICAL INSTITUTE	
10:15	09.3	Next-Generation Modular Avalanche Radar with Multi-Hazard Capabilities	
		SUSANNE WAHLEN, GRAVIMON LTD.	
10:30	O9.4	Development of snowsensors in Ísafjörður	
		ÖRN INGÓLFSSON / HARPA GRÍMSDÓTTIR, ICELANDIC METEOROLOGICAL OFFICE	
10:45	QA		
11:00	Break	Break	
11:15 - 12:30		Oral Sessions 10	
11:15	O10.1	Experiences in designing mitigation measures against slush flows	
		ELISE MORKEN, NORWEGIAN GEOTECHNICAL INSTITUTE	
11:30	O10.2	Slush Flows – A review of a poorly explored phenomenon and its protection measures	
		NADINE FEIGER, MOUNTAIN HAZARD ENGINEERING GMBH	
11:45	010.3	Advancing Snowdrift Forecasting with Physically-Based Snow Models and High-Resolution	
		Weather Data	
		SVEINN GAUTI EINARSSON, VEÐURVAKTIN	
12:00	O10.4	Can wind simulation help optimize function of snow avalanche mitigation measures?	
		ÁRNI JÓNSSON, ORION CONSULTING SLF	
12:15	QA		
12:30	Conference Closing		

Saturday October 4

Seljalandsdalur to Hnífsdalur Valley Hike

09:00 - 14:00 - Mountain hiking tour - Optional

Join us on a scenic hike from the Seljalandsdalur ski area in Ísafjörður to the village of Hnífsdalur, taking in the stunning land-scapes of the Westfjords. The route takes you through the Seljalandsdalur and Hnífsdalur valleys, offering views of surrounding mountains, mountain lakes, and clear streams.

The area is also marked by history—particularly the tragic avalanche that fell in Seljalandsdalur in 1994. As we make our way through the valley, we'll reflect on this event, which shaped both the landscape and the community. Your guides will provide context and ensure a safe and enjoyable experience.

Included:

- Professional guide
- Transport to and from Ísafjörður
- Light lunch
- Optional: Hiking poles

Itinerary:

09:00 – 09:30: Meet at the harbor in Ísafjörður and head for a brief 5-minute drive to the Seljalandsdalur ski area. After a quick safety briefing, we start the hike, following gentle slopes as we approach the base of the Þjófatindar peaks.

09:30 - 10:30: After an hour of hiking, we reach the base of the mountains. From here, we begin a steady ascent towards the pass between the peaks. This portion provides scenic views of the surrounding area, giving you a sense of the raw power of the glaciers that shaped this region.

10:30 - 11:00: After reaching the pass, we'll stop for a break and enjoy the sweeping views of the mountains and fjords in the distance. This is the perfect spot for a photo or just to take in the scenery.

11:00 – 11:45: Continuing our hike, we begin the descent into the valley on the opposite side of the pass, heading towards the village of Hnífsdalur. There is a short, steeper section of the trail, but your guides will be with you to assist as needed.

11:45 – 12:00: Arriving in Hnífsdalur, we'll take some time to enjoy the peaceful atmosphere of this small village by the fjord. The hike ends with a short ride back to Ísafjörður, where we'll arrive around 13:30.

Important Notes:

The descent includes a short steep section, but it is manageable with guidance from our experienced team. Remember to wear sturdy hiking boots, bring clothing suitable for changing weather conditions, and stay hydrated. Duration: 4,5 hours approximately.

This hike provides an excellent opportunity to appreciate the beauty of the Westfjords while learning about the region's history, perfect for those attending the avalanche research conference.

Designing for Safety and Liveability: Collaborative Approaches to Avalanche Defences in Iceland

Þórhildur Þórhallsdóttir¹

¹ Landmótun Iceland

ABSTRACT

Following the catastrophic avalanches that struck the Westfjords of Iceland in 1995, the country undertook a comprehensive reorganization of its avalanche defence systems. Landscape architects have been involved from the outset, and their role has expanded considerably over time. Initially focused on mitigating environmental disturbance, it soon became evident that their input was essential to fully integrate defence structures into the built and natural environment.

Many of these defences have evolved into multifunctional spaces, providing not only protection but also recreational opportunities for local residents. Early integration of landscape design into technical planning has proven crucial in ensuring the long-term success and public acceptance of these structures.

In practice, constructing effective defences has often required substantial landscape modifications—reshaping hillsides, removing forests and berry fields, and, in some cases, extending works into private gardens, roads, and paths. To manage these impacts, close collaboration with municipalities is essential. This includes early engagement with municipal officials, technical staff, and residents through formal presentations and informal consultations. Design proposals are communicated clearly, and community feedback is actively considered.

Though construction phases often involve unexpected adjustments, the core objectives remain consistent: to safeguard communities while improving local environments, supporting outdoor activity, and enhancing public health. Many defence sites now feature various rest areas and educational signage, reinforcing their role as valued public spaces.

This presentation outlines lessons learned from Iceland's interdisciplinary approach, emphasizing the importance of early collaboration between engineers, landscape architects, and municipalities in designing effective and socially integrated avalanche defences.

P. Þórhallsdóttir K1 - Page 14

Managing natural hazards risk: Perspectives from far-flung

Andrea Taurisano*

The Norwegian Water Resources and Energy Directorate (NVE), Middelthuns gate 29, 0368 Oslo, NORWAY

*Corresponding author, e-mail: anta (at) nve.no

ABSTRACT

Risk management encompasses policies, strategies, measures, and methods that aim to reduce risk to a tolerable level. Managing the risk from natural hazards, in particular, is a daunting task that involves legislators, local administrations and communities, scientists, practitioners and product developers. How do we find our place in it and contribute to effective risk management? And what should we focus on? The keynote shares perspectives gained during a recent revision of the Norwegian technical regulations for new buildings, as well as 15 years of hazard mapping in Norway and work with disaster risk reduction in Afghanistan. However, the experiences and perspectives the keynote lecture offers are likely to have an even more international relevance.

A. Taurisano K2 - Page 15

Avalanche and landslide protection measures in Iceland – 30 years of design innovations protecting twelve villages across Iceland

Kristín Martha Hákonardóttir,^{1*} Tómas Jóhannesson,² Gísli Steinn Pétursson³ and Hafsteinn Pálsson¹

¹ The Ministry of the Environment, Energy and Climate, Reykjavík, ICELAND
² The Icelandic Meteorological Office, IS-105 Reykjavík, ICELAND
³ Verkís, Ofanleiti 2, IS-103, Reykjavík, ICELAND
*Corresponding author, e-mail: kristin.hakonardottir (at) urn.is

ABSTRACT

The Icelandic Avalanche and Landslide Fund was established in 1996 following catastrophic avalanches in Flateyri and Súðavík in 1995. The fund is operated by the Ministry of the Environment, Energy and Climate under the 1997 Act on Protection Against Avalanches and Landslides (No. 49). Its primary role is to finance mitigation measures, risk assessments, and hazard monitoring. Since 1996, defence structures have been built in ten municipalities across Iceland, with approximately 70% of planned projects completed. These include 27 catching dams, 23 deflecting dams, 83 braking mounds, four splitters and 13.5 km of supporting structures.

To date, 58 avalanches have interacted with these defence structures (Jóhannesson et al., 2019). Notably, the deflecting dams above Flateyri, constructed in 1997, have been struck by multiple avalanches, including four large avalanches, two with developed fluidized heads (in 2020). The Boli-dams above Siglufjörður, built in 1998–1999, have deflected small to medium-sized avalanches. In 2023, large fluidized to dense snow avalanches interacted with supporting structures, steep mounds and dams in Neskaupstaður (Jóhannesson et al., 2024), built in two phases (1999–2002 and 2012–2015).

These events, combined with advances in numerical modelling and small-scale experiments, have improved understanding of avalanche—dam interaction. They underscore the need for reexamining the design of existing defence layouts at nine locations in Iceland to assess the need to improve their effectiveness. The presentation will focus on these design innovations.

1. INTRODUCTION

The Icelandic Avalanche and Landslide Fund was established in 1996 following catastrophic avalanches in Flateyri and Súðavík in 1995. The fund is operated by the Ministry of the Environment, Energy and Climate under the 1997 Act on Protection Against Avalanches and Landslides (No. 49). Its primary role is to finance mitigation measures, risk assessments, and hazard monitoring. Since 1996, defence structures have been built in ten communities across Iceland. Approximately 70% of planned projects are completed. These include 27 catching dams, 23 deflecting dams, 83 braking mounds, four splitters and 13.5 km of supporting structures. These have cost approximately 43 billion ISK or 350 million USD, at the price level of 2024. The projects are located in avalanche prone areas of Iceland, mainly in the Westfjords, the Troll peninsula in the North and in the East fjords of Iceland, see Figure 1. The following villages and farms have been protected fully or partially, grouped by municipalities, clockwise starting at the Snæfellsnes peninsula in West Iceland:

Snæfellsbær: In Ólafsvík, guiding walls for slushflows along the Bæjarlækur channel have been constructed and supporting structures installed in the starting zone at Tvísteinahlíð, protecting a nursing home.

Vesturbyggð: In Patreksfjörður, a catching dam has been built above the hospital and school, and deflecting- and catching dams above the harbor at Urðir, Hólar, and Mýrar, near the lower part of Litladalsá river, and supporting structures in the starting zone of Stekkagil gully. The testing of snow fences is ongoing at the Brellur mountain plateau. In Bíldudalur, protection dams have been built below Búðargil, and in Tálknafjörður, houses have been purchased below Geitárhorn.

Ísafjarðarbær: In Flateyri, two deflecting dams have been built below the Innra-Bæjargil and Skollahvilft starting zones. In Ísafjörður, a deflecting dam and braking mounds were constructed below Seljalandshlíð, catching dams were built below Kubbi and Gleiðarhjalli, and supporting structures constructed in the starting zones of avalanches in Kubbi mountain. An avalanche splitter was constructed above the Funi waste incinerator in Engidalur. In Hnífsdalur, the settlement below Búðarhyrna has been purchased.

Bolungarvík: Protection dams and braking mounds have been built below Traðarhyrna.

Súðavík: The settlement below Súðavíkurhlíð was relocated.

Fjallabyggð: In Siglufjörður, supporting structures have been constructed in the starting zones of Hafnarhyrna and Gróuskarðshnjúkur, and catching dams below Hafnarhyrna and deflecting dams below Strengsgil, and Jörundarskál. In Ólafsfjörður, a deflecting dam has been built above the Hornbrekka nursing home.

Eyjafjarðarsveit: A splitter for debris flows was constructed above the farm Grænahlíð.

Múlaþing: In Seyðisfjörður, protection dams have been built at the Bjólfsbrún plateau and a deflecting dam was constructed above the farm Tóarsel in Norðurdalur.

Fjarðabyggð: In Eskifjörður, guiding dams for slushflows have been built along Lambeyrará, Ljósá, Hlíðarendaá, and Bleiksá rivers. In Fáskrúðsfjörður, protection dams have been built above the settlement by Nýjabæjarlækur. In Neskaupstaður, protection measures have been built below Drangagil, Tröllagil, Miðstrandarskarð, Urðarbotnar, and Sniðgil, combining braking mounds, catching dams and deflecting dams. Supporting structures have been installed in the starting zones of Tröllagil and Drangagil.

Reykjavík: A deflecting dam for landslides was constructed above the farm Vellir in Kollafjörður, Kjalarnes.

Avalanche protection measures are under construction in the following communities:

Snæfellsbær: Improvements to the Bæjargil channel and guiding walls.

Vesturbyggð: In Patreksfjörður, the final finishing work on the Stekkagil preliminary slush flow defences and the avalanche protective dams above the harbor. In Bildudalur, construction of catching dams and braking mounds is scheduled to begin in 2025.

Ísafjarðarbær: In Flateyri, improvements to the already constructed deflecting dams is under construction and steep braking mounds upstream of the dams are under construction and testing of snow fences is ongoing at the Eyrarfjall mountain plateau (Figure 6).

Múlaþing: In Seyðisfjörður, a deflecting dam, a catching dams and five steep mounds have been constructed and the final deflecting dam is under construction below mountain Bjólfur (Figure 6). Preliminary dams against landslides have been constructed in the Botnar area.

Fjarðabyggð: In Neskaupstaður, braking mounds and a catching dam are being built below Nesgil and Bakkagil (Figure 7). Upgrades to the supporting structures (nets) in the Drangagil release area started in 2025.

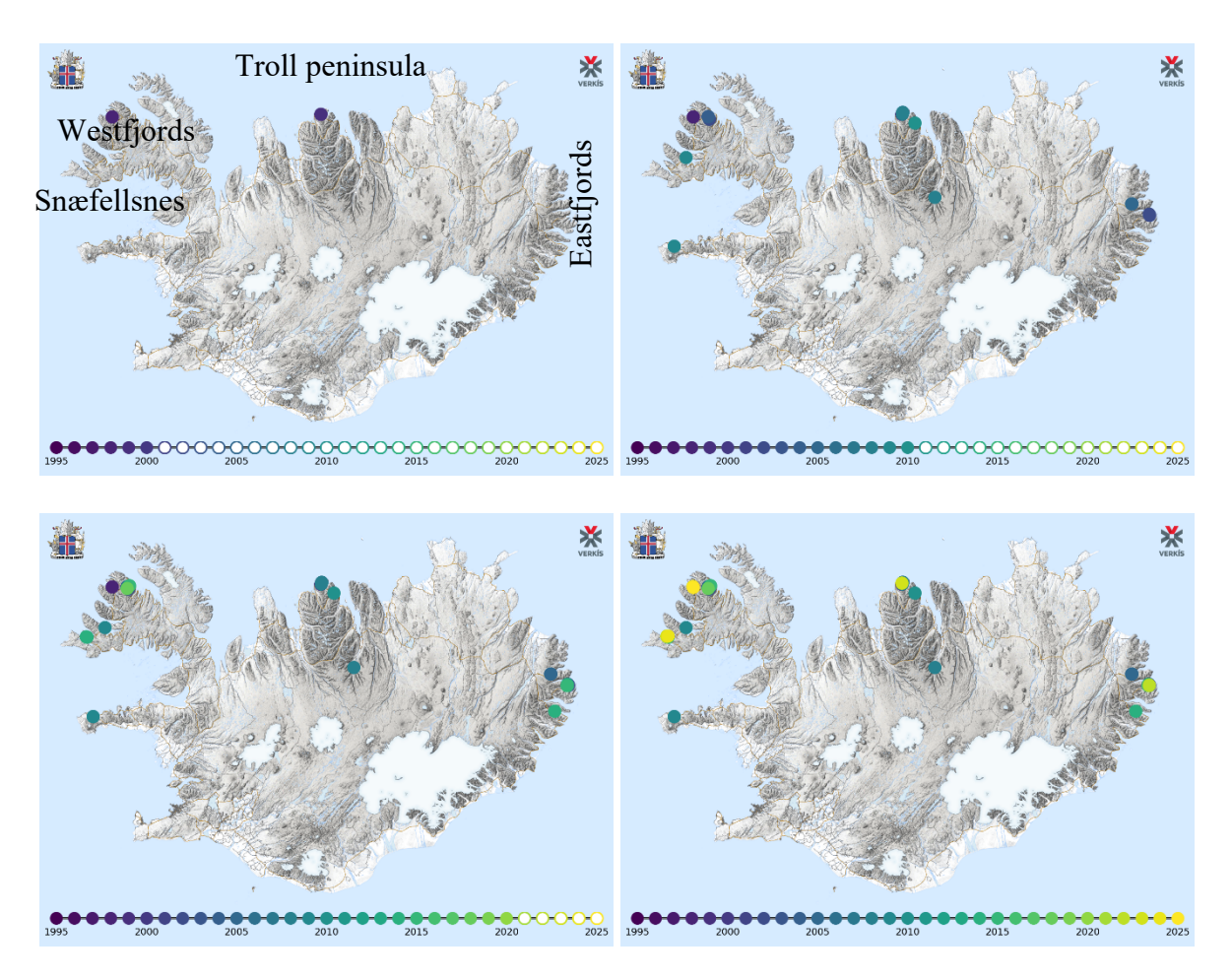


Figure 1 Maps of Iceland showing locations were protection measures have been built since 1995. The maps are arranged chronologically: 2000 (upper left), 2012 (upper right), 2020 (lower left) and 2025 (lower right). The relatively small dams above farmhouses in Norðurdalur and Kollafjörður are not shown.

The investment in avalanche defence measures has not been at a constant rate. During a ten years period from 1996 to 2008 approximately 500 to 1000 million ISK were spent yearly on the investment (in current prices for each year). During 2009 to 2020 approximately 1200 million ISK were used, but since 2020, the amount was increased and is currently approximately 4500 million ISK per year (36 million USD). The increase came as a response to avalanches overflowing the deflecting dams at Flateyri in January 2020 (Hilmarsson et al., 2020) a large landslide in Seyðisfjörður in December 2020 and avalanches in Neskaupstaður in March 2023. At present, the goal is to finish the construction of protection measures for villages in Iceland within the coming ten years. The additional cost of the planned future projects is estimated approximately 30 billion ISK or 243 million USD and further 10 billion ISK to enhance the

efficiency of already built structures, such as at Flateyri, West Iceland. The reason for the relatively high cost of the remaining constructions is partly that problematic areas remain to be protected. They call for complicated and expensive solutions, e.g. the landslide defence measures at Seyðisfjörður and guiding dams in Eskifjörður.

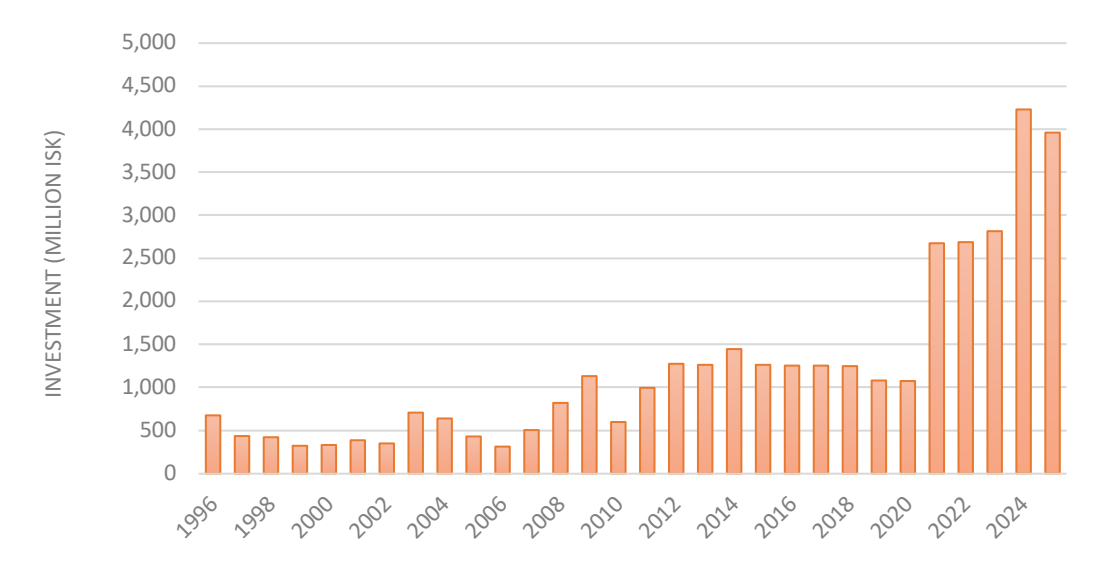


Figure 2 Annual investments by the Icelandic Avalanche and Landslide fund for construction of avalanche and landslide protection measures since 1996, in current prices for each year.

2. THE DESIGN OF PROTECTION MEASURES IN ICELAND

The Icelandic Avalanche and Landslide Fund has funded research on the interaction of avalanches and dams which has led to new design guidelines of protection dams (Jóhannesson et al., 2009; Rudolf-Miklau et al., 2015) based on the formation of shocks in the interaction between rapid granular flows and dams (Hákonardóttir and Hogg, 2005) and ballistic trajectories launched over relatively small braking mounds (Hákonardóttir et al., 2003a), see Figure 3. Further small-scale experiments on loading on mast-like obstacles from supercritical granular flow were carried out in 2007 (Hauksson et al., 2007).

Small scale laboratory experiments on the efficiency of slushflow barriers and the possibility of stopping slushflows were conducted as a part of the design of slushflow barriers above the village of Patreksfjörður in West Iceland (Hákonardóttir and Andrésdóttir, 2019; Hákonardóttir et al., 2024a). In the experiments, a violent initial splash was identified in the interaction of supercritical water flows with steep dams, and the experiments showed the effectiveness of utilizing relatively low mounds upstream of a catching dam to stop such flows, see Figure 4. This behavior was recreated with full scale 2D simulations as shown in Figure 5 (Hákonardóttir et al., 2024a).



Figure 3 Left and middle: Small scale laboratory experiments showing photographs of oblique shocks in a granular flow at Froude number 5, looking downstream onto the deflector, and in water flow at Froude number 4.5, looking upstream into the flow along the deflector (Hákonardóttir and Hogg, 2003). Right: A photograph of snow experiments at Weissfluhjoch in Davos. An avalanche launched over two 0.6 m high mounds. The snow is deflected both over and around the mounds and an interaction between jets launched from adjacent mounds takes place (Hákonardóttir et al., 2003c).



Figure 4 Stills from slushflow experiments at a dimensional scale of 1/10. Supercritical water flow at a Froude number of approximately 5 hits a 1 m high catching dam. The pictures show the different flow stages of the interaction. Left: The initial violent splash. Middle: The semi-steady fountaining, approximately 1.25 s after initial impact. Right: Hydraulic jump, approximately 2 s after initial impact (Hákonardóttir and Andrésdóttir, 2019; Hákonardóttir et al., 2024a).

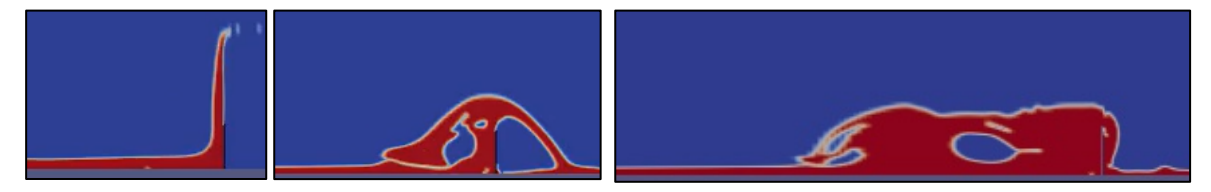


Figure 5 Stills from 2D and 2 phase simulations of water (red) and air (blue) in Open FOAM. The simulations reproduce the experiments shown in Figure 5 where flow of water interacts with a 1 m high catching dam (Hákonardóttir et al., 2024a).

These experimental results highlight the importance of using barriers with steep upstream faces for the effective dissipation of energy in the initial impact between the structures and the current (dry avalanche, wet avalanche, slushflow). Such effective dissipation of energy leads to an abrupt transition in flow state to a hydraulic jump at the face of high dams. Steep structures are, however, more expensive than structures constructed of soil with gentler sloping sides, see Figure 6 and Figure 7.



Figure 6 Left: The construction of two steep, 10 m high braking mounds upstream of the Flateyri, Innra-Bæjargil deflecting dam. Right: The recently finished, 9 m high braking mounds and the 18 m high deflecting dam below Kálfabotnar in Seyðis-fjörður. Photos: Kristín Martha Hákonardóttir, July and August 2025.



Figure 7 Protection measures above Neskaupstaður, East Iceland. From left to right: Construction site below Nesgil and Bakkagil. Ten 10 m high mounds below Nesgil have been constructed and foundation work laid for a 800 m long and 23 m high catching dam. To the right are 13 mounds below Drangagil, located upstream of the 17 m high catching dam. These protection measures were built in 1999 and interacted

with fluidized to wet avalanches in the avalanche cycle in 2023 (Jóhannesson et al., 2024). To the right is the eastern end of a catching dam and braking mounds below Urðarbotnar.

Full-scale tests of the efficiency of snow fences in the windy climate in Iceland are ongoing at two locations: The Brellur mountain plateau above Patreksfjörður; and at Eyrarfjall plateau above Flateyri, with promising results for Flateyri (Pétursson et al., 2025; see Figure 8).



Figure 8 Testing of two rows of 5 m high and 150 m long snow fences started in winter 2022. Photo: Veðurstofa Íslands, January 15th 2023.

The Icelandic Avalanche and Landslide Fund has also funded the development of numerical models to capture these phenomena numerically (Xinjun et al., 2007; Jarosch et al., 2022) and aid with the design of more complicated structures, such as at Flateyri northwestern Iceland, see Figure 9. The models have also been used to evaluate the design of existing dams in Iceland against the dense core of avalanches. The results underscore the need to re-examine the design of existing defence layouts at nine locations in Iceland to assess the need to improve their effectiveness.

The interaction of fluidized avalanches with dams and mounds in Iceland in 2020 and in 2023 has furthermore highlighted the importance of designing steep barriers (Hákonardóttir et al., 2024b; Jóhannesson et al., 2024). It is also worth noting that 1) the earthfill structures withstood the loading from these events without major damage, and 2) even suttle directional change in the deflecting angle of deflecting dams leads to increased run-up on the dams and potential overtopping, e.g. at the end of both dams at Flateyri.

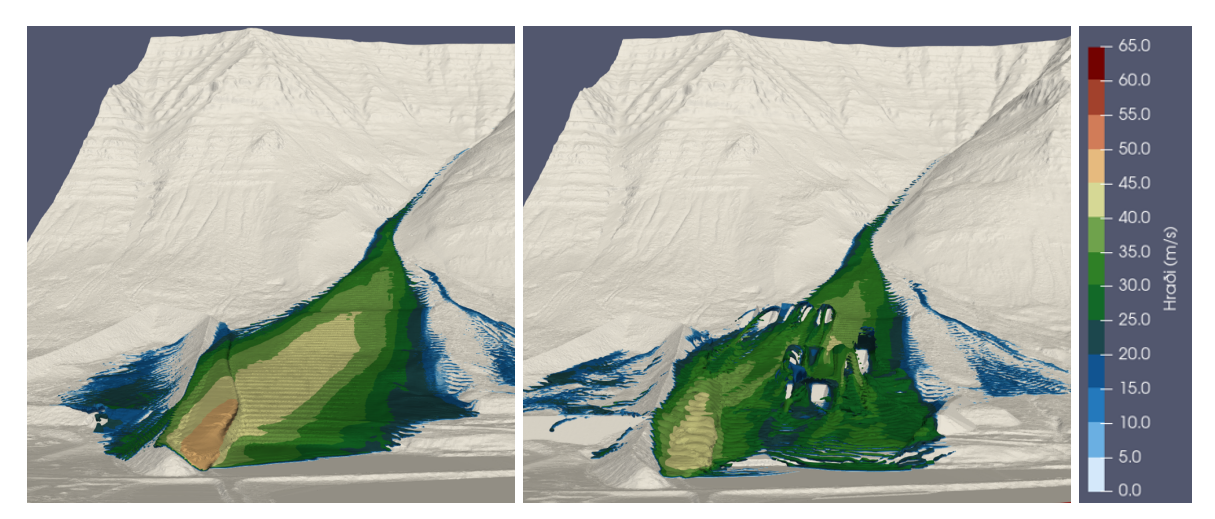


Figure 9 Stills from a 3D avalanche simulation in OpenFOAM. A design avalanche with an estimated frequency of 1000 years and a volume of 675 thousand m³ is released from the Skollahvilft gully, above Flateyri and hits the (left) existing 14 to 19 m high deflecting dam and (right) the proposed braking mounds upstream of the dam and higher and steeper catching dam. An oblique hydraulic jump is formed at the deflecting dam during the interaction and the direction of the flow becomes parallel to the dam. The picture on the right shows that the flow launches ballistically over the mounds and the mounds break the flow and the speed of the hydraulic jump at the deflecting dam is reduced (Guðmundsson et al., 2025).

REFERENCES

Guðmundsson, R. L., Gíslason, S., Pétursson, H. and Hákonardóttir, K. M., 2025. Use of OpenFOAM and μ(*I*)-rheology in the design of protective structures for avalanches for Flateyri NW Iceland. In: Jónsson, Á., Sigtryggsdóttir, F. G., Hólmgeirsdóttir, Þ., Gauer, P., Margreth, S., Þorvaldsdóttir, S. (eds.), International Symposium on Mitigative Measures against Snow Avalanches and Other Rapid Gravity Mass Flows Ísafjörður, Iceland, Sept. 29 to Oct. 3, 2025. The Association of Chartered Engineers in Iceland, Reykjavík.

Hauksson, S., M. Pagliardi, M. Barbolini, T. Jóhannesson 2007. Laboratory measurements of impact forces of supercritical granular flow against mast-like obstacles. Cold Regions Science and Technology, 49, 54–63, doi: 10.1016/j.coldregions.2007.01.007.

Hákonardóttir, K. M., Hogg, A. J., Batey, J. og Woods, A.W., 2003a. Flying Avalanches. Geophys. Res. Lett., 30, 23, 2191, doi:10.1029/2003GL018172.

Hákonardóttir, K. M., Hogg, A. J., Jóhannesson, T. og Tómasson, G. G., 2003b. A laboratory study of the retarding effect of braking mounds on snow avalanches. Journal of Glaciology, 49, 165, 191–200.

Hákonardóttir, K. M., Hogg, A. J., Jóhannesson, T., Kern, M. and Tiefenbacher, F, 2003c. Large-scale avalanches braking mound and catching dam experiments with snow: A study of the airborne jet. Surveys in Geophysics, 24, 5–6, 543–554.

Hákonardóttir, K.M., Hogg, A.J., 2005. Oblique shocks in rapid granular flows. Physics of Fluids, 17, 071101, doi: 10.1063/1.1950688.

Hákonardóttir, K. M., Andrésdóttir, K. H., 2019. The design of slushflow barriers: Laboratory experiments. In: Jóhannesson, T., Gauer, P., Hákonardóttir, K. M., Margreth, S., Pálsson, H., Sigtryggsdóttir, F. G., (eds.), International Symposium on Mitigative Measures

- against Snow Avalanches and Other Rapid Gravity Mass Flows Siglufjörður, Iceland, April 3–5, 2019, 83–94, The Association of Chartered Engineers in Iceland, Reykjavík.
- Hákonardóttir, K. M., Pétursson, H. Ö., Guðmundsson, R. L., Thoroddsen, Á., Jóhannesson, T.,
 2024a. Stopping slushflows: Small-scale laboratory experiments and full-scale numerical simulations. In: Gisnås, K. G., Gauer, P., Dahle, H., Eckerstorfer, M., Mannberg, A.,
 Müller, K. (eds.), Proceedings of the International Snow Science Workshop ISSW 2024,
 Tromsø, Norway, 23–27 Sept. 2024, 737–744, Montana State University.
- Hákonardóttir, K. M., Lárusson, R., Kristjánsson, Á., and Pétursson, G., 2024b. Loading on structures from fluidized avalanche fronts overflowing deflecting dams at Flateyri, Iceland, January 2020. In: Gisnås, K. G., Gauer, P., Dahle, H., Eckerstorfer, M., Mannberg, A., Müller, K. (eds.), Proceedings of the International Snow Science Workshop ISSW 2024, Tromsø, Norway, 23–27 Sept. 2024, 932–939, Montana State University.
- Hilmarsson, Ó., Jóhannesson, T. & Grímsdóttir, H., 2020. Snjóflóðin úr Skollahvilft og Innra-Bæjargili 14. janúar 2020. The Icelandic Meteorological Office (VÍ) report nr. 2020-010. December 2020.
- Jarosch, A. H., Jóhannesson, T., Hákonardóttir, K. M., Pétursson, H. Ö., 2022. Full three-dimensional simulations of snow-avalanche flow with two-phase, incompressible, granular μ(I) rheology using OpenFOAM / interFoam, EGU General Assembly 2022, Vienna, Austria, 23–27 May 2022, EGU22-7984, doi: 10.5194/egusphere-egu22-7984.
- Jóhannesson, T., Gauer, P., Issler, D, Lied, K., (eds.), 2009. The design of avalanche protection dams. Recent practical and theoretical developments. Brussels, Directorate-General for Research, Environment Directorate, European Commission, Publication EUR 23339, 195 pp., doi: 10.2777/12871.
- Jóhannesson, T., Hansson, G., Ingólfsson, Ö., Brynjólfsson, S., Jónsson, M. H., Hilmarsson, Ó., Grímsdóttir, H., 2019. Snow avalanches hitting deflecting and catching dams in Iceland 1997–2018, In: Jóhannesson, T., Gauer, P., Hákonardóttir, K. M., Margreth, S., Pálsson, H., Sigtryggsdóttir, F. G., (eds.), International Symposium on Mitigative Measures against Snow Avalanches and Other Rapid Gravity Mass Flows Siglufjörður, Iceland, April 3–5, 2019, 132–139, The Association of Chartered Engineers in Iceland, Reykjavík.
- Jóhannesson, T., Grímsdóttir, H., Hákonardóttir, K. M., Brynjólfsson, S., Hilmarsson, Ó., Jarosch, A. H., 2024. Lessons from several avalanches impacting avalanche protective structures in Iceland in January 2020 and March 2023. In: Gisnås, K. G., Gauer, P., Dahle, H., Eckerstorfer, M., Mannberg, A., Müller, K. (eds.), Proceedings of the International Snow Science Workshop ISSW 2024, Tromsø, Norway, 23–27 Sept. 2024, 820–827, Montana State University.
- Pétursson, S. P., Sigurbjörnsdóttir, Þ. A. and Hákonardóttir, K. M., 2025. Snow fences on Eyrarfjall above Flateyri A pilot study. In: Jónsson, Á., Sigtryggsdóttir, F. G., Hólmgeirsdóttir, Þ., Gauer, P., Margreth, S., Þorvaldsdóttir, S. (eds.), International Symposium on Mitigative Measures against Snow Avalanches and Other Rapid Gravity Mass Flows Ísafjörður, Iceland, Sept. 29 to Oct. 3, 2025. The Association of Chartered Engineers in Iceland, Reykjavík.
- Rudolf-Miklau, F., Sauermoser, S., Mears, A. I., 2015, (eds.): Technical Avalanche Protection Handbook, John Wiley & Sons, Berlin.
- Xinjun Cui, J. M. Nico T. Gray, Tómas Jóhannesson. 2007. Deflecting dams and the formation of oblique shocks in snow avalanches at Flateyri, Iceland. J. Geophys. Res., 112(F04012). doi: 10.1029/2006JF000712.

From granular mechanics to 3D modeling: Advancing avalanche hazard assessment and mitigation

Michael L. Kyburz, 1,2,3* Lars Blatny 1,2,3 and Johan Gaume 1,2,3

¹ Chair of Alpine Mass Movements, ETH Zürich, Zürich, Switzerland

² WSL Institute for Snow and Avalanche Research SLF, Davos, Switzerland

³ Climate Change, Extremes and Natural Hazards in Alpine Regions Research Center CERC, Davos, Switzerland

*Corresponding author, e-mail: michael.kyburz (at) slf.ch

ABSTRACT

Accurately assessing and mitigating avalanche hazards remains a central challenge in mountainous and snow-prone regions, where complex terrain and material behavior limit the predictive power of traditional numerical models. Fully three-dimensional (3D) numerical modelling has long been prohibitive due to the computational cost involved. Here, we present an advanced numerical framework that integrates granular mechanics with cutting-edge threedimensional modeling to improve our understanding and simulation of snow, rock, and debris avalanches. At the core of this approach is the SLAB3D solver, a computationally efficient 3D implementation of the Material Point Method (MPM) coupled with physics-based rheologies, in particular the $\mu(I)$ - rheology. In contrast to the widely used Voellmy model, the $\mu(I)$ rheology accounts for pressure-dependent friction and velocity saturation effects—critical factors for simulating dynamic flow behavior and interactions with natural and engineered structures. SLAB3D enables high-resolution simulations over complex topography, capturing key processes such as run-up, overflow, and structural loading, while considering obstacles like forests and avalanche dams. We showcase practical applications of this modeling approach through detailed case studies, including the 2019 "Salezer" avalanche in Switzerland and an avalanche dam performance analysis in Siglufjörður, Iceland. These examples illustrate how the integration of granular flow physics with efficient 3D computation can support more reliable hazard assessment and provide actionable insights for engineers and decision-makers involved in risk management and infrastructure planning.

1. INTRODUCTION

Recent times are marked with a growing population, causing dwellings to expand into locations of increased risk of natural hazards and an increase in frequentation of mountainous regions for recreational purposes. Simultaneously, a warming climate leads to an increase in the frequency and severity of catastrophic gravitational mass movements. Consequently, more people and infrastructure are subjected to an increased exposure to natural hazards.

To date, geophysical mass flows, including snow avalanches, are commonly simulated using depth-averaged numerical methods and empirical rheological models, which are calibrated by matching simulations to observations from events in the past (e.g., Christen et al., 2010; Mergili et al., 2012; Rauter et al., 2018; Vila, 1984; Zugliani and Rosatti, 2021). This implies that the predictive capacity of these models is strongly limited, especially in the light of a changing

climate, where unprecedented and severe events are expected to occur with increased frequency (e.g., Castebrunet et al., 2014; Lazar and Williams, 2008; Naaim et al., 2016).

In research, a recent implementation of the Material Point Method has proven its ability to simulate the dynamics of a range of hazardous geophysical mass movements. Compared to the current methods used in practice, fully three-dimensional MPM simulations allow to explicitly simulate avalanche-structure interaction, and can thus contribute to the development of more cost-efficient design of protective structures or simulate impact forces on structures with complex geometries. More physics-based and precise analyses of natural hazards can also help to improve decision making e.g. for road closures, reducing the disruptions, and therefore also minimizing the negative impact of these measures on the economy.

In this contribution, we present two different case studies using MPM at either end of the range between research and practice: The 2019 Salez (Davos, Switzerland) avalanche event, and a potential 1,000-year return period avalanche interacting with a deflection dam in Siglufjörður, Iceland.

2. METHODS

The Material Point Method (MPM) is a combined Eulerian and Lagrangian numerical technique solving the momentum balance equation and naturally respecting mass conservation. This method is notably effective for capturing free surface flows of materials with substantial deformations, impacts, and fractures, which are challenging for mesh-based methods, on complex topography in depth-resolved and real-scale simulations. In recent times, MPM has drawn significant interest in the fields of snow and avalanche research (e.g. Cicoira et al., 2024, Gaume et al., 2024). In our modeling framework, we apply a finite strain elasto-plasticity approach featuring snow models that stems from critical state soil mechanics and granular mechanics (Gaume et al., 2018; Blatny et al., 2024, Blatny and Gaume, 2025).

To efficiently analyze the simulation results, we recently developed a routine for post-processing the complex 3D model outputs to derive key dynamic properties of the mass movement, such as run-out, maximum velocity, slope-parallel and slope-normal velocity components, vertical flow height, flow thickness, and deposition heights (Kyburz et al., 2024; Vicari et al., 2025). This tool also offers a GIS interface, enabling users to visualize simulation outcomes like the run-out in the context with topography maps and nearby infrastructure for hazard assessment purposes.

3. RESULTS AND DISCUSSION

3.1 2019 Salez Avalanche Davos

This case study (Kyburz et al., 2025) investigates both the potential and challenges of simulating large-scale snow avalanches using 3D MPM and model. Thereby, we focus on the model's ability to capture complex flow dynamic processes, and evaluate the model's performance by comparing simulation results with data from the well-recorded Salezer snow avalanche that occurred in Davos, Switzerland, in January 2019. A particular novelty of this simulation is that, not only we simulate the avalanche in 3D and real scale, but also simulate the snow cover on the day of the event distributed on the whole terrain to explicitly capture erosion and deposition processes.

The simulation results match well with real-world observations, particularly in terms of the avalanche's approach velocity captured in an eyewitness video and the flow outline documented in a drone survey. Additionally, the model effectively qualitatively replicates the main erosion and deposition patterns of the actual event.

The detailed 3D simulation results allows us to examine intermittent flow structures at the flow front in the gully, identifying numerous snow particle clusters that separate from the dense basal layer and remain airborne for short periods, despite the model not simulating turbulent air-snow interactions (Figure 1 b, c). We hypothesize that these structures arise from rapid topographic changes in the gully where the avalanche flows at high kinetic energy (Figure 1 d).

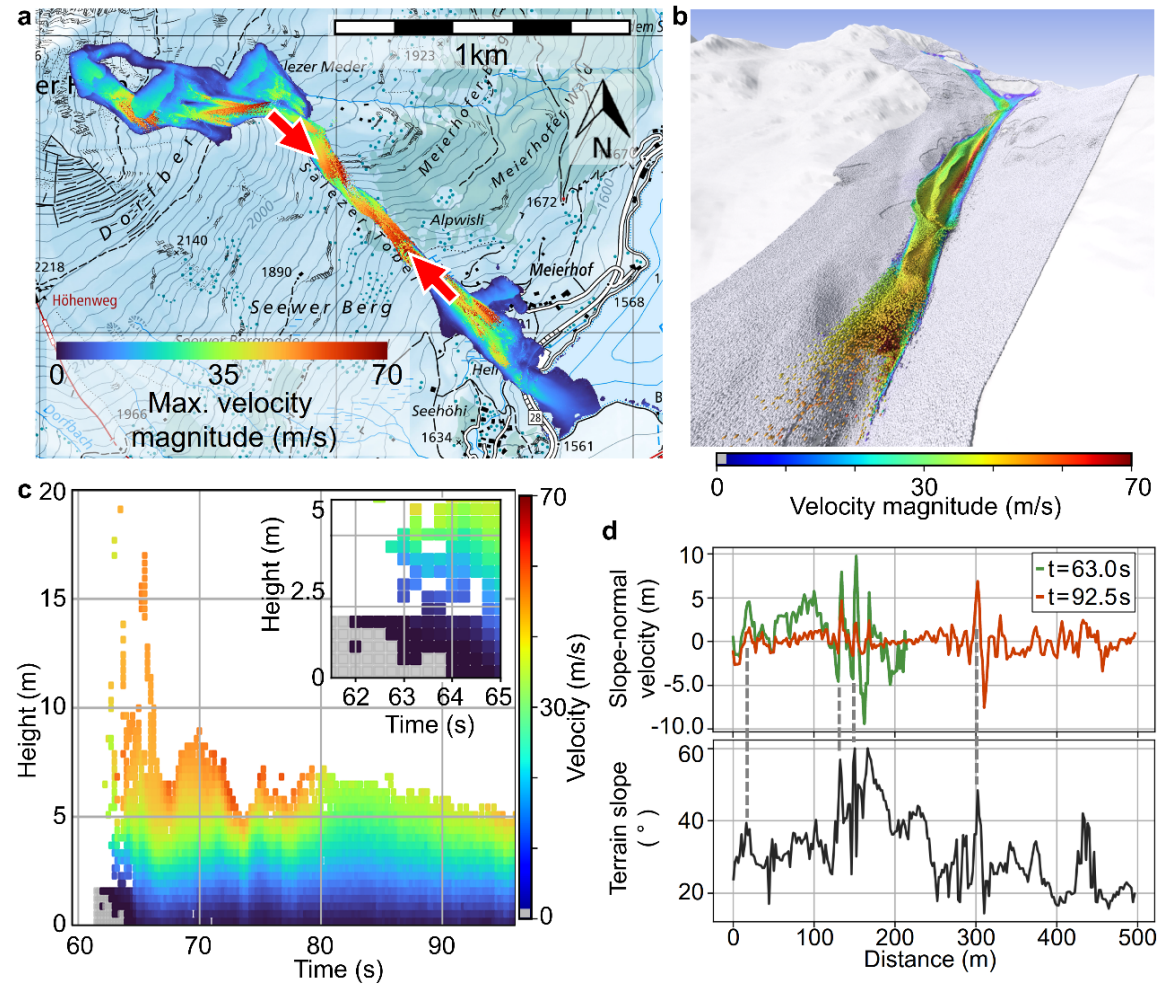


Figure 1: a) Distribution of the maximum avalanche velocity magnitude over all time frames, b) Rendering of the avalanche front in the gully, c) Temporal evolution of flow velocity as a function of the flow height near the location of the upper red arrow in panel a). The inset shows a close-up of the same data at the flow front, d) Slope-normal velocity and the terrain slope in a 500 m long transect between the two red arrow tips in panel a) in the gully. The gray-dashed lines highlight the correlation of exemplary peak values in both plots. Figure adapted from Kyburz et al. (2025). Map source: Swiss Federal Office of Topography

Considering the detailed insight and numerous dynamic processes naturally emerging from the 3D simulations, we believe MPM simulations hold great potential for conducting detailed analyses, particularly in identifying critical impact pressure peaks due to transient flow features. Furthermore, the model could serve as a valuable tool in research aimed at examining dynamic flow attributes that are challenging to measure in the field.

3.2 Avalanche dam in Siglufjörður

In this case study, we focus on a more practical application of 3D MPM simulations and assess the protective capacity of an avalanche deviation dam in Siglufjörður, Iceland. More specifically, we back-calculate a design avalanche for the Strengsgil avalanche path. Subsequently, we use the same calibrated parameters and initial conditions with a DEM that includes the deflecting dam and additional non-erodible snow deposits upstream of the dam to assess the potential hazard of an avalanche overflowing the dam and affecting the town. One fully 3D simulation of the whole avalanche path with a spatial resolution of 1m lasted 2.4 hours.

MPM predicts peak particle velocities of 50m/s and depth-averaged velocities around 45m/s (Figure 2 a), which aligns well with the design estimate of 45m/s. The maximum vertical flow heights of approximately 20m are located in the upper part of the flow path (Figure 2 b).

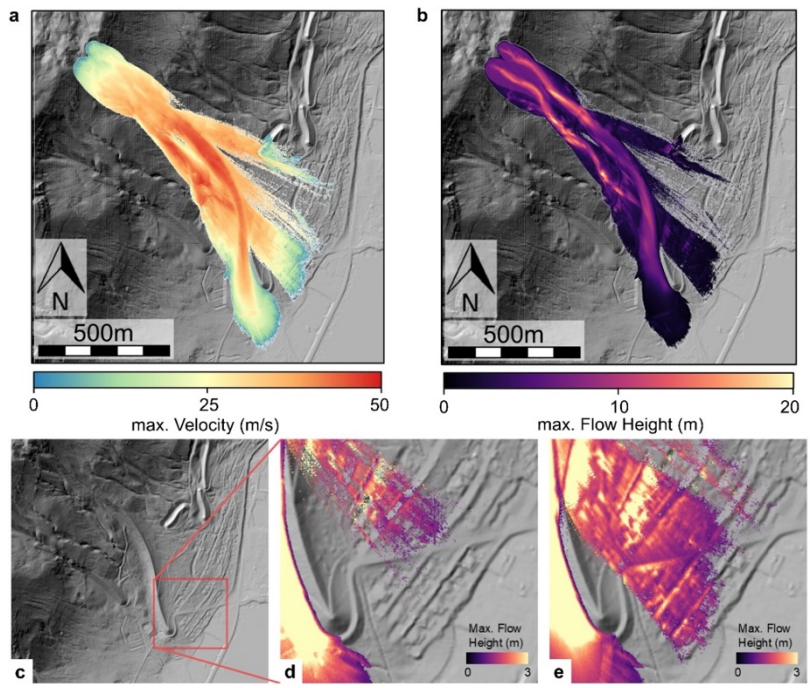


Figure 2: For the simulation case with the dam and snow deposit a) shows the maximum particle velocity and b) the maximum vertical flow height. c) Zoomed region of the inhabited area showing the maximum vertical flow height in d) the dam case and e) the dam and snow deposit case.

Our 3D simulations reveal that the dam would experience only a minor overflow under the design scenario, with overflow volumes amounting to 0.4 % of the avalanche volume without snow deposits and 17.8 % when snow deposit is included. Importantly, the deposits of the overflow are very thin in both cases and likely highly fluidized (Figure 2 d, e). Excluding

regions where flow height exceeds 3 m due to steps in the topography (Figure 2 c–e), the simulated flow and deposit thickness remains below 1 m for the dam-only scenario and reaches about 1.5 m when previous snow deposits are present. These observations need careful consideration for two reasons. Firstly, the flow thicknesses below common hazard-mapping thresholds (typically 0.2-0.4 m) are often considered negligible. Secondly, our measurements carry an uncertainty tied to the simulation grid spacing, here ± 0.5 m.

By resolving impacts and interactions in full three dimensions, our simulations inherently capture momentum losses that depth-averaged models cannot, underscoring the advantages of 3D approaches for complex flow phenomena. Overall, these results demonstrate the necessity of advanced 3D modeling to accurately represent intricate overflow behavior and pressure-dependent rheological effects, thereby providing a more reliable basis for assessing mitigation structure reliability and guiding the development of safer dam designs.

4. CONCLUSIONS

In the two exemplary case studies presented here, as well as in numerous other cases involving rock or rock-ice avalanches, MPM shows great potential for both research and practical applications. Our computationally highly efficient 3D MPM simulations can e.g. help to design avalanche dams that fully prevent overflow in complex topography or simulate the interaction of avalanches with infrastructure with complex geometries, thereby ensuring robust safety margins for practice.

In research, we currently develop more realistic constitutive models, for example to capture rate dependency and pore pressure effects, which will be available for practice in the future. For engineering applications, we continue to make the pre-processing and post-processing more intuitive and easier to use, also allowing for integration with widely used engineering tools. The GIS post-processing interface used to present the data in this contribution already enables effective result interpretation and hazard assessment.

ACKNOWLEDGEMENT

We acknowledge the whole Alpine Mass Movements team for contributing to the development of our MPM simulation framework. We thank Stefan Margreth for the insightful discussions.

REFERENCES

Blatny, L., Gray, J. M. N. T., and Gaume, J., 2024. A critical state μ(I)-rheology model for cohesive granular flows. *Journal of Fluid Mechanics*, 997, A67. 10.1017/jfm.2024.643

Blatny, L. and Gaume, J., 2025. Matter (v1): An open-source MPM solver for granular matter, EGUsphere, 10.5194/egusphere-2025-1157

Castebrunet H, Eckert N, Giraud G, Durand Y and Morin S, 2014. Projected changes of snow conditions and avalanche activity in a warming climate: the French Alps over the 2020-2050 and 2070-2100 periods. The Cryosphere, 8(5), 1673–1697, 10.5194/tc-8-1673-2014

- Christen M, Kowalski J and Bartelt P, 2010. RAMMS: Numerical simulation of dense snow avalanches in three-dimensional terrain. Cold Regions Science and Technology, 63(1-2), 1-14
- Cicoira A, Blatny L, Li X, Trottet B and Gaume J, 2022. Towards a predictive multi-phase model for alpine mass movements and process cascades. Engineering Geology, 310, 106866, ISSN 0013-7952, 10.1016/j.enggeo.2022.106866
- Gaume, J., Gast, T., Teran, J., van Herwijnen, A., Jiang, C., 2018. Dynamic anticrack propagation in snow. Nat. Commun. 9 (1) 10.1038/s41467-018-05181-w.
- Gaume, J., Kenner, R., Bühler, Y., Stoffel, A., , Kyburz, M. L., Cicoira, A. and Blatny, L., 2024. Blind prediction of the Brienz rock avalanche runout using a 3D Material Point Method. In Interpraevent 2024 Conference Proceedings, pages 302–306.
- Kyburz, M. L., Vicari, H., Troilo, F. and Gaume, J., 2024. Advancements in GIS-based visualization and analysis of 3D depth-resolved MPM simulations of alpine mass movements. In Interpraevent 2024 Conference Proceedings, pages 258–262
- Kyburz, M. L., Sovilla, B., Bühler, Y. and Gaume, J, 2025. Potential and challenges of depthresolved three-dimensional MPM simulations: a case study of the 2019 'Salezer' snow avalanche in Davos. Annals of Glaciology, 65, e19.
- Lazar B and Williams M, 2008. Climate change in western ski areas: Potential changes in the timing of wet avalanches and snow quality for the aspen ski area in the years 2030 and 2100.
 Cold Regions Science and Technology, 51(2), 219–228, ISSN 0165-232X, 10.1016/j.coldregions.2007.03.015, International Snow Science Workshop 2006
- Mergili M, Schratz K, Ostermann A and Fellin W, 2012. Physically-based modelling of granular flows with open source GIS. Natural Hazards and Earth System Sciences, 12(1), 187-200
- Naaim M, Eckert N, Giraud G, Faug T, Chambon G, Naaim-Bouvet F and Richard D, 2016. Impact du réchauffement climatique sur l'activité avalancheuse et multiplication des avalanches humides dans les alpes françaises. La Houille Blanche, (6), 12–20, 10.1051/lhb/2016055
- Rauter M, Kofler A, Huber A and Fellin W, 2018. fasavage-hutterfoam 1.0: depth-integrated simulation of dense snow avalanches on natural terrain with OpenFoam. Geoscientific Model Development, 11(7), 2923–2939
- Vicari, H., Kyburz, M. L. and Gaume, J., 2025. Brief communication: Depth-averaging of 3D depth-resolved MPM simulation results of geophysical flows for GIS visualization. EGUsphere, 2025, 1–12
- Vila JP, 1984. Modélisation mathématique et simulation d'écoulements à surface libre. La Houille Blanche, 6/7, 485–489, 10.1051/lhb/1984034
- Zugliani D and Rosatti G, 2021. Trent2d: An accurate numerical approach to the simulation of two-dimensional dense snow avalanches in global coordinate systems. Cold Regions Science and Technology, 190, 103343, 10.1016/j.coldregions.2021.103343

History of snow avalanches and settlements in hazard areas in Iceland

Harpa Grímsdóttir*

Icelandic meteorological Office, IS-105 Reykjavík, Iceland *Corresponding author, e-mail: harpa (at) vedur.is

ABSTRACT

Snow avalanches are the type of natural hazard that has claimed the highest number of human lives in Iceland, when storms at sea and on land are not considered. Many areas in Iceland, especially in the Westfjords, Northern Iceland and the Eastfjords, are characterized by steep mountains, and narrow valleys and fjords. Vegetation is sparse and potential avalanche starting zones are above the treeline. Strong winds and frequent precipitation are typical for the winter weather in Iceland due to the passage of low-pressure systems. The Icelandic people have had to deal with avalanche danger since the country was first settled in the ninth century CE, even though other risks, such as famine, disease and other weather-related accidents, were probably more important causes of premature death in the society in earlier centuries.

The formation of towns and villages started in Iceland in the second half of the 19th century. Prior to that, people would get caught in avalanches when travelling over mountains and individual farms would occasionally be hit. Soon after urbanization started at the end of the 19th century and the beginning of the 20th century, the first avalanche accidents occurred in towns and villages with many casualties. In 1995, two avalanche catastrophes, with a total of 34 fatalities, became a turning point for avalanche hazard assessment and construction of avalanche protection measures in Iceland.

1. INTRODUCTION

Natural hazards have affected society in Iceland since settlement in 874. Volcanic eruptions have caused damage to fields and livestock due to pollution, ash and lava flow, jökulhlaups have destroyed fields and settlements and earthquakes have damaged buildings. Fierce winds, heavy precipitation and icing have claimed many human lives both on land and sea.

However, it is snow avalanches, followed by landslides, that have claimed the greatest number of human lives when looking at direct consequences of natural hazards when storms on land and sea are not considered. Many areas in Iceland are characterized by steep mountains, and narrow valleys and fjords. Vegetation is sparse and protective forest is usually not found in potential avalanche starting zones. This combination of geography and weather is favorable for avalanche formation and long run-outs.

2. AVALANCHE RECORDING IN ICELAND

Annal writers in Iceland have documented important events through the centuries, and church books contain information about the lives and deaths of people. Information on historical avalanches can be found in different registers and, since the 19th century, in newspapers. In 1957, the two-volume book *Skriðuföll og snjóflóð* (English: Landslides and avalanches) by

H. Grímsdóttir O1.1 - Page 31

Ólafur Jónsson (1957, second edition in three volumes in 1992) was first published. The book is the result of tremendous work of Jónsson who gathered records of landslides and avalanches in Iceland. An updated version of the book was published in 1992. All avalanches and landslides described in this book are now registered in the database of the Icelandic Meteorological Office (IMO) which hosts and manages a database on snow avalanches, landslides and slushflows in Iceland. In addition to records from these books, a systematic search has been carried out in an online database that hosts most of the magazines and newspapers that have been published in Iceland. As part of hazard mapping efforts, a search for historical avalanches is done by conducting interviews with local people. Additionally, for the last 25–30 years, snow observers have systematically recorded avalanches in the areas where they work, and these get entered directly into IMO's database. Furthermore, the public is encouraged to give IMO information on avalanches they see. The avalanche database of IMO is, thus, probably one of the most comprehensive national avalanche databases in the world. It is, however, known that most avalanches outside settled areas go unobserved, and even in areas that are monitored by snow observers, many avalanches are not recorded because they fall during blizzards that erase all indications of the avalanches before visibility returns.

It is likely that the majority of avalanches and landslides that have killed people or destroyed homes are in the national database, but it can still be assumed that several catastrophic incidents went unreported or unrecorded and are, therefore, missing. However, avalanches causing little or no damage were not systematically recorded until the past few decades. This makes it difficult to accurately describe long-term trends regarding avalanche activity in Iceland, but the rich historical documentation still provides incredible insight for the current avalanche work at the IMO.

3. SNOW AVALANCHES IN A RURAL ICELAND 874-1880

Up until 1880, avalanches would occasionally destroy single farms, and injuries or death were often the result for people staying inside the houses. Farmhouses in Iceland were small buildings made of turf and stones that needed constant maintenance (Þjóðólfur, 1863). The location of many *landnámsbæir* (English: settlement farms, i.e., farms that have existed since the period 875–1100) is quite good with respect to avalanche danger. It is possible that the exact locations of the farmhouses changed a little over the decades and centuries in response to the local conditions. For example, if avalanches, landslides or flash floods threatened or damaged buildings, then they might have been moved away from the hazard the next time they were renovated or rebuilt, thus, ending up in the best spot in the area over time.

Avalanche accidents in uninhabited areas were common, as people needed to visit steep mountain slopes for various reasons and would occasionally be caught in avalanches.

Life was tough in Iceland, and it is unlikely that avalanches were considered a major problem in people's day-to-day lives, even though avalanche accidents were quite frequent. Famine, diseases, bad weather and other hardships were a greater threat to most people. The child mortality rate was high, and the annual risk of death for people was, in general, much higher than it is today. The acceptable level of risk in society due to avalanches was almost certainly higher than it is today. However, people had to learn to live with nature and read the weather, and that was probably also the case with avalanche danger.

4. FORMATION OF TOWNS AND SETTLEMENTS AND EARLY URBAN AVALANCHE ACCIDENTS 1880–1919

Urbanization in Iceland started around 1880 when the first towns and villages began to form. Increased fishing was the main reason, and the towns often developed close to the sea where harbor conditions were favorable (Hall, A., et al., 2002). This development happened quite rapidly, and many houses were built in areas without previous settlement history. In many cases, the settlements expanded into avalanche areas, and soon, the first avalanche accidents occurred in densely populated areas. During this period, some harsh winters resulted in widespread avalanche cycles that caused many accidents in rural areas and uninhabited areas as well. Below, the most serious accidents in towns and villages are described shortly along with other fatal accidents happening nearby. Of course, there were more avalanche accidents than the ones described, but this selection helps to paint a picture of the avalanche conditions faced by the Icelandic people in settled areas during this time.

4.1 Seyðisfjörður 1885

The largest avalanche catastrophe in the history of Iceland happened in Seyðisfjörður on February 18, 1885. A village was starting to form at the bottom of the fjord and the avalanche destroyed 15 houses and carried some of them into the sea. A total of 24 people were killed and many were injured. February 1885 was harsh and snowy in the north and east, and snow and avalanches caused damage in various places. Later, in February in the same year, an avalanche hit two farmhouses in Norðfjörður, south of Seyðisfjörður. Three people died but some were rescued from the avalanche debris up to 7 hours after the avalanche hit (Jónsson et al., 1992).

4.2 Hnífsdalur 1910

In Hnífsdalur, a dense settlement formed under the mountain Búðarhyrna, where houses had been built near the sea for fishermen and their families. On February 18, 1910, exactly 25 years after the avalanche catastrophe in Seyðisfjörður, an avalanche from Búðargil gully killed 20 people. The winter was harsh, and in the beginning of March, a fierce blizzard caused an avalanche that killed four people in the farm Breiðaból in Skálavík, a remote valley not far from Hnífsdalur. The blizzard continued, and it was only two days later that two young men managed to get through the snow to the next town and ask for help. A rescue mission was formed, and surprisingly, a woman and four children were found alive after lying for about 40 hours in the ruins of their house, buried in the snow (Jónsson et al., 1992).

4.3 Siglufjörður 1919

In Siglufjörður, the biggest herring factory in Iceland had been built by Norwegian brothers on the opposite side of the fjord from the current main town of Siglufjörður. The factory started operating in the year 1911, and a cluster of houses formed around it. A big avalanche fell on April 12, 1919, from the bowl Skollaskál destroying the factory and many houses. People in the town of Siglufjörður noticed that boats and piers had been heavily damaged during the night, and ship crews that spent the night in their boats in the harbor, talked about a flood wave happening around 4 am. Some people remembered stories about a similar event in 1839 when a large avalanche from Skollaskál triggered a flood wave causing damage to boats, but at that time, there was no settlement in the area. A decision was made to send 12–15 men to check the situation on the other side of the fjord, and their suspicions were confirmed; a large avalanche had swept away the herring factory, along with the houses where the people lived. Seven people

H. Grímsdóttir O1.1 - Page 33

were rescued, but nine people died in the avalanche. During the herring seasons, 80–100 people worked at the factory, but when the avalanche fell it was empty (Jónsson et al., 1992).

Four days later, a sailor phoned Siglufjörður and expressed worries about the farm Engidalur, which was close to Siglufjörður. The sailor said he could not land his boat in the area, so a boat was sent from Siglufjörður to investigate. It was discovered that an avalanche had hit the farm, and all seven people living there had died. This likely occurred the same night as the avalanche destroyed the herring factory. Two other fatal accidents took place in Héðinsfjörður around this same time. In total, 18 people died in avalanches in the northernmost part of Tröllaskagi (English: the Troll's peninsula) in this avalanche cycle (Jónsson et al., 1992).

5. THE AVALANCHE HISTORY 1920–1973

After the the year 1919, serious avalanche accidents did not occur in urban areas until December 1974. During this period, there were only two avalanches that struck buildings and resulted in more than two fatalities. One of these avalanches fell in 1925 and hit a house on the farm Sviðningur in the North. While a farmer living in another house in Sviðningur was able to rescue three people from the avalanche debris, three other people in the house lost their lives. The other accident was a residence on the farm Goðdalir in the eastern part of the Westfjords in December 1948. An avalanche hit and destroyed the house, and all seven people in the building were buried. It took a while for the tragedy to be discovered, as there was no one else living in the vicinity, and the phone connection to the farm had been lost. The severed phone connection did not raise suspicion, as communications were often hampered in bad weather. Four days after the avalanche, a teenage boy was sent to Goðdalir to deliver mail, and he called for help from a neighbouring farm when he discovered what had happened at Goðdalir. Three members of the household were still alive but two of them died shortly after being rescued. The farmer survived the accident, but his leg was amputated due to frostbite (Jónsson et al., 1992).

Although there were few large avalanche events in settlements during this period, there were still 30 fatal avalanche accidents in rural areas, on roads and in the wilderness (IMO's avalanche database, 2025). The reason that fewer large avalanche accidents happened during this period is not entirely clear. Perhaps it was mostly the result of chance. There is evidence, however, that winters may not have been as harsh in the decades following 1920 as in the decades before and after, as this period is sometimes referred to as a warm spell (Jónsson, 2007).

6. EVOLVEMENT OF FISHING TOWNS AND AN AVALANCHE ACCIDENT IN NESKAUPSTAÐUR IN 1974

Fishing towns and villages in Iceland expanded rapidly in the 20th century due to technological development in the fishing industry. The introduction of motorboats, followed by trawlers and the construction of fish factories, created many new jobs and fuelled rapid growth (Hall et al., 2002) In many "avalanche towns", the initial development of the village was close to the sea and the harbour, and then expansion that stretched towards the mountains.

This style of development was especially common in the period around 1960–1980 (Grímsdóttir, 1997, 1998a,c, 1999). Large residential areas were built closer to the mountains than before, as the fishing industry continued to expand. There is little sign of avalanche and landslide consideration in the planning of settlements during this period, with the notable exception of areas where large catastrophes with many fatalities had occurred. Perhaps, too many decades had passed since the last large avalanche accidents in urban areas. In some cases,

there were historical records of avalanches reaching down to areas that were being densely settled at this time, but their destructive force might have been underestimated because they didn't cause fatalities.

On December 20th, 1974, two avalanches killed 12 people in an industrial area and in a residence in Neskaupstaður (IMO's avalanche database, 2025). At that time, no hazard maps existed, and no monitoring system was in place anywhere in Iceland and the avalanches came as a total surprise. The rescue work was complicated, since there was a lot of debris from the industrial area mixed with the snow from the avalanche. Fuel oil from a large storage tank and a whole stock of car tires were among things the rescuers had to deal with in the avalanche debris (Grímsdóttir, 1998b). The avalanches also reached the sea, which is not uncommon in Iceland, carrying some of the victims and debris with them.

In the aftermath of these avalanches, an avalanche committee was formed by the municipality of Neskaupstaður in 1975, and a working group was established by the national government of Iceland. These groups drafted proposals on hazard mapping that would take avalanches into consideration when planning settlements. Suggestions were made about avalanche monitoring and research, and specialists from other countries were brought in for consultation (Grímsdóttir, 1998b). Most of these suggestions were not implemented at that time.

In 1984, an avalanche destroyed an industrial building in Ólafsvík, injuring two people. Another avalanche was released above the hospital of the town, stopping just a few meters from the building (IMO's avalanche database, 2025). These incidents seem to have been a wake-up call. In 1985, a report by an avalanche specialist at NGI in Norway (Erik Hestnes) concluded that the avalanche risk at the most exposed dense settlements in Iceland was perhaps 10 times higher than in Norway and that surprisingly large construction activity was taking place in avalanche hazard areas without any apparent consideration of the potential consequences (Hestnes, 1985). Then, in 1985, the first laws on avalanche prepardness were enacted in Iceland. The laws stated that municipalities with known avalanche history should hire snow observers, and a basis for avalanche hazard mapping was created.

7. THE AVALANCHE CATASTROPHES IN SÚÐAVÍK AND FLATEYRI IN 1995 AND AVALANCHE WORK IN THE AFTERMATH

On January 16th, 1995, an avalanche fell on the village of Súðavík in the Westfjords damaging or destroying 16 residential houses and some other buildings. The avalanche killed 14 people and injured another 12. It happened during a severe blizzard that lasted until the next day, which made it challenging to bring in rescue teams. During the night of October 26th the same year, an avalanche in the neighboring village of Flateyri hit 30 buildings, destroying 16 of them. Most of the buildings were residential houses, and the avalanche killed 20 people and injured five others (IMO's avalanche database, 2025). October is a highly unusual month for such large avalanches in Iceland. The avalanche was the result of a few days of blizzard conditions. Soon after the avalanche struck, the weather shifted to higher temperatures and rapid snowmelt, which made the catastrophe appear quite absurd. The winter that followed in the area was quite mild with rather little snow according to locals.

In 1995, the avalanche laws from 1985 were in effect, and avalanche hazard maps existed for both villages. Snow observers had been hired in the area, and evacuations had been ordered prior to the avalanches. Most of the victims, however, were in houses that were outside of the

H. Grímsdóttir O1.1 - Page 35

hazard zones according to hazard maps at that time. These two avalanches had reached farther than most people could imagine. Two conclusions could be drawn from these events:

- 1. Many towns and villages in Iceland had probably expanded into avalanche areas where the risk was completely unacceptable for the residents.
- 2. Avalanche hazard maps would need to be revised, and new methods for hazard assessment would have to be developed.

In the years after 1995, the avalanche laws and regulations were revised and a new hazard mapping method was developed. Hazard maps have been made for towns and villages where the hazard is considerable, and the hazard zones are much larger than according to the former zoning. The criterion is annual probability of death for an individual staying in an unreinforced house. This reflects the political decision that the risk to people should be the most important factor when calculating possible consequences of this highly deadly natural phenomenon. The monitoring system was also strengthened and centralized within the IMO.

For the most hazardous zones in residential areas (C-zones or red zones on hazard maps), the municipality is required to reduce the risk permanently with relocation of houses or construction of defense structures. Monitoring and evacuations is not considered acceptable as the only solution for these areas. Therefore, the installation of defense structures for these areas in many towns and villages was started following the catastrophes in 1995.

Since 1995, only one avalanche fatality has occurred in a settlement in Iceland, In 2004, a farmer was killed in his farmhouse Bakki in Ólafsfjörður when he visited his farm to feed his livestock during a period of evacuation. There have been some close calls, especially at Flateyri in 2020 when a part of an avalanche overran a deflecting dam, and in Neskaupstaður in 2023, when an avalanche reached down to an unprotected area of the town where houses had not been evacuated. The avalanches caused extensive damages but luckily nobody was seriously injured.

Evacuations have been quite frequent since 1995, and on a few occasions, they may have prevented damages or injuries. Many avalanches have reached down to avalanche dams or have been released from gullies partly covered with supporting structures that have reduced the size of the avalanches. It is likely that those defense structures have saved many houses from damage by avalanches and probably some lives.

8. CONCLUSIONS

Many houses as well as industrial areas in towns and villages in Iceland are located in avalanche hazard zones. The severity of the situation became apparent after two avalanche catastrophes in 1995. Before avalanche laws were enacted, avalanche hazard did not have notable effect on the planning of settlements, with two exceptions: 1) Where avalanches were very frequent, with return period lower than 5–10 years, settlements were not developed, and 2) areas where large accidents with many fatalities had occurred were mostly uninhabited. However, there are examples from various places around the country of dense settlements being built up in areas that had been overrun by historical avalanches. Taking avalanche hazard into account when planning and developing settlements is the best way to avoid accidents. For that, the history shows us that laws and regulations are necessary.

LIST OF REFERENCES

- Grímsdóttir, H., 1997. Byggingarár húsa á Seyðisfirði. Reykjavík. VÍ-G97016-ÚR12. Icelandic Meteorological Office.
- Grímsdóttir, H., 1998a. Byggingarár húsa í Neskaupstað. Reykjavík. VÍ-G98011-ÚR09. Icelandic Meteorological Office.
- Grímsdóttir, H., 1998b. Viðhorf og viðbrögð við ofanflóðahættu í Neskaupstað. Reykjavík. BSc thesis. University of Iceland.
- Grímsdóttir, H., 1998c. Byggingarár húsa á Siglufirði. Reykjavík. VÍ-G98049-ÚR36. Icelandic Meteorological Office.
- Grímsdóttir, H., 1999. Byggingarár húsa á Ísafirði, Reykjavík. VÍ-G99014-ÚR08. Icelandic Meteorological office
- Hall, A., Jónsson, Á., Agnarsson, S., 2002. Byggðir og Búseta. Þéttbýlismyndun á Íslandi. Reykjavík. Hagfræðistofnun Háskóla Íslands.
- Hestnes, E., 1985. Skredfare i arealbruksammenheng. Studietur I Island 30.07–05.08.84. Oslo. NGI report.
- IMO's avalanche database, 2025. The avalanche database hosted and maintained by the Icelandic Meteorological Office.
- Jónsson, Ó., 1957. *Skriðuföll og snjóflóð* (Landslides and avalanches). Akureyri, Bókaútgáfan Norðri.
- Jónsson, Ó., Rist, S., Sigvaldason, J., 1992. *Skriðuföll og snjóflóð* (Landslides and avalanches). Reykjavík, Bókaútgáfan Skjaldborg.
- Jónsson, T., 2007. Hitafar á Íslandi eftir 1800. Icelandic Meteorological Office website. https://www.vedur.is/loftslag/loftslag/fra1800/hitafar/
- Þjóðólfur, 1863. Húsakynni og húsabyggingar á Íslandi. Þjóðólfur (newspaper), January 24th 1863, p. 50.

H. Grímsdóttir O1.1 - Page 37

Seven years of research on snow avalanches in Nunavik, northern Quebec, Canada: hazard and vulnerabilities

Armelle Decaulne^{1*}, Vincent Filion², Beatriz Funatsu¹, Sasha Griffin^{3,1}, and Najat Bhiry²

¹ CNRS LETG-Nantes, Chemin de la Censive du Tertre, F-44300 Nantes, FRANCE
 ² Université Laval, Geography Department & Centre d'études nordiques, 2405 rue de la Terrasse, Québec, G1V 0A6, CANADA

³ Nantes Université, Chemin de la Censive du Tertre, F-44300 Nantes, FRANCE *Corresponding author, e-mail: armelle.decaulne (at) cnrs.fr

ABSTRACT

In Nunavik (northern Quebec, above 55°N), over the past two centuries, Inuit territorial organization has experienced a profound spatial reconfiguration. From the dispersion of Inuit nomadic camps, the way of life gradually changed with the establishment of trading and commercial posts; since 1950s structured settlement of Inuit communities is done in 14 villages. With rapid population growth, villages are still expanding. Until recently, snow avalanches in Nunavik had seldom been documented. However, ongoing research highlights that short steep slopes are prone to snow avalanches, both in village surroundings and in remote areas. To improve our understanding of snow avalanches, a network of automatic cameras monitors snow avalanches since winter 2017-2018. Slopes were selected based on geomorphologic investigations. Over the last seven winters, more than 600 snow-avalanche deposits have been identified and their paths delineated. Runout distances vary according to two distinct regimes: winter (from November to April) and spring (May-June). Weather data were analyzed to identify the range of triggering factors. There is both inter- and intra-winter variability in snow cover conditions (duration, thickness). Topographic analyses of avalanche slopes identify potential source areas for snow avalanches as well as runout distances, where infrastructures are found in some instances.

1. INTRODUCTION

As in similar mountain areas worldwide, Nunavik experiences snow avalanches. Yet, scholarly and institutional attention to this hazard is recent, as the interplay between snow-avalanche processes and human settlements has emerged over the past decades as a pressing concern in this Inuit territory. On the New Eve's night 1999, the most dreadful known snow avalanche in Quebec stroke Kangiqsualujjuaq. Until 2019, this event has been one of the very few documented in the literature in Nunavik (e.g., Schaerer et al., 1999; Stethem et al., 2003; Germain and Martin, 2011; Germain, 2016). Details were mainly extracted from the post-event report by Lied and Domaas (2000), which compiled different standards of archives based on inhabitants remembering. Following the snow-avalanche event affecting the Nunavik northeasternmost village, few other snow avalanches, of lesser magnitude, were revealed, witnessed in the 1980s and in 1993. However, detailed information is lacking, with uncertainties regarding dates and runout distances. The further urban-planning of the community has been impacted (Decaulne et al., 2021), as the village needed to develop away from the avalanche slope that was already known, in a context constrained by the valley topography and thawing permafrost. Therefore, the few existing studies attest that snow

avalanches are an active process on the short but steep slopes of rolling Nunavik landscape (Fig. 1) in a context of demographic growth demanding terrain for further dwellings.

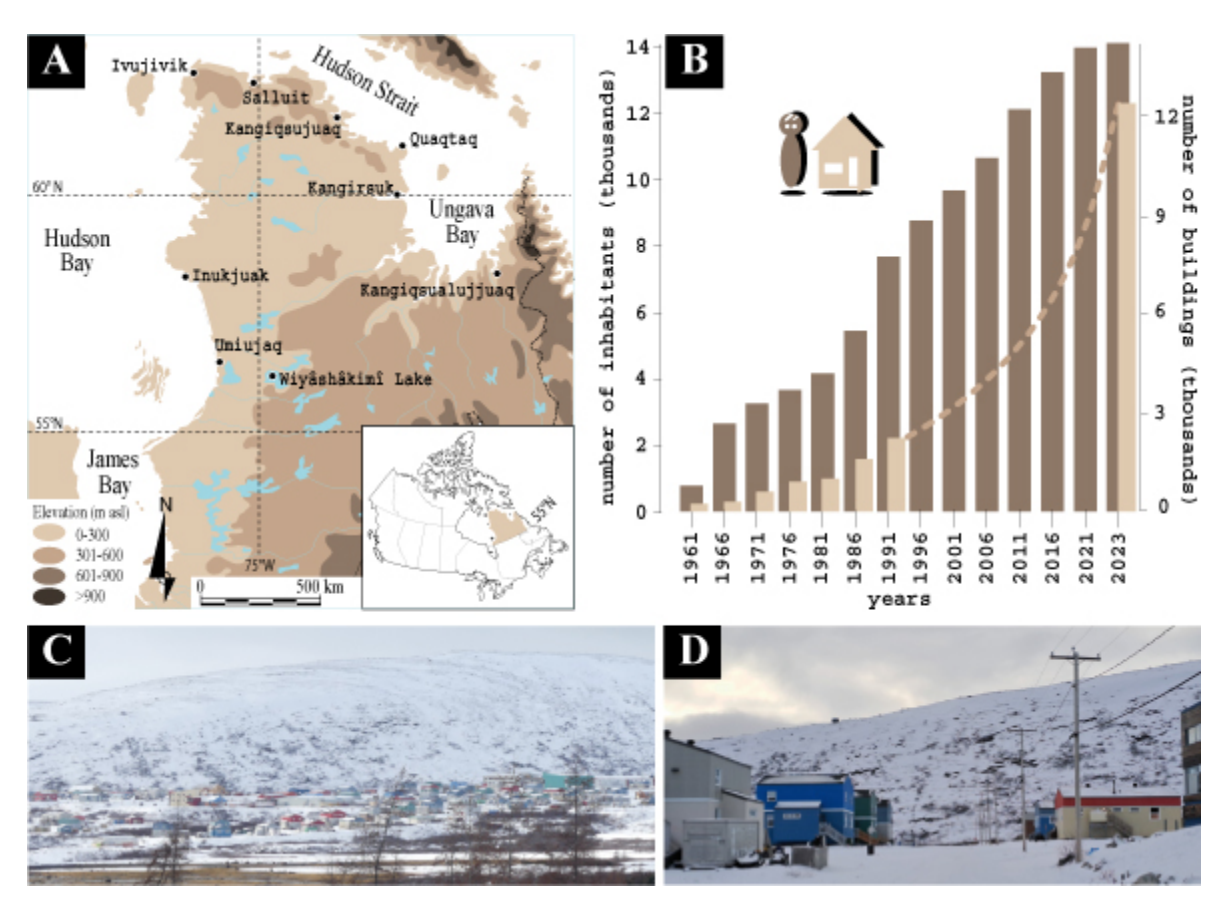


Figure 1 Location of Nunavik Northern Villages, surrounding areas and a remote site within Tursujuq national park, affected by snow avalanches (A), associated to population and building growth since 1960s (B - data from Statistics Canada), underlining the need for snow-avalanche research in the area. C & D show views of the slope above the Northern Village of Kangiqsualujjuaq, hit in 1999 by a dreadful slab snow avalanche (photos: A. Decaulne).

The aims of the ongoing research are (i) to document snow-avalanche activity in a territory where little is known on the process; (ii) to determine the meteorological triggering factors for snow avalanches in Nunavik; (iii) to define the slope profiles, and prone source-areas for snow avalanches. The objective of this contribution is to highlight the diversity of snow-avalanche regimes, deposits and runout distances that were encountered at several locations in Nunavik over the last seven winters. We focus on inhabited areas and transportation corridors where snow avalanches could represent a threat.

2. METHODS

To document snow-avalanche activity in Nunavik, a set of complementary methods is used. A geomorphological approach was first carried out on talus slopes at several locations, to attest evidence of past and recent snow-avalanche deposits through morphometric measurements of slopes and clasts on talus (Decaulne et al. 2018, 2025; Veilleux et al., 2020). Then a network

of automatic cameras (from ReconyxTM) has been deployed on targeted slopes, to inventory snow-avalanche occurrences (Veilleux et al., 2021; Grenier et al., 2023). In 2025, 19 automatic cameras record hourly images (from 9:00 am to 17:00 pm) in four villages and their close surroundings, as well as in remote areas (Wiyâshâkimî Lake), providing a reliable calendar of snow-avalanche events. Weather data from nearby ground stations (from Centre d'études nordiques-CEN climate monitoring network) enable to access the snow-avalanche triggering factors. From the collected images, snow-avalanche contours and runout distances are extracted. To overpass the narrow frame of the camera images at the scale of all mountain slopes surrounding communities, LiDAR data were used to extract topographic profiles along the main slopes within community borders, highlighting the potential zones for snow accumulations, *i.e.*, potential source areas for snow avalanches, and associated runout distances. As snowpack conditions and its development throughout winter are still unknown in Nunavik territory, topographic model to determine snow-avalanche terrains remains the only reliable one (Filion, 2025; Filion et al., 2025).

3. RESULTS AND DISCUSSION

3.1 Exploiting the camera images: snow-avalanche calendars, outline and runout, weathers

Camera images enable to acquire essential data on snow-avalanche occurrences over several winters (Fig. 2). Dates are known for all avalanche deposits, and hours are precise for daytime events; they are differentiated from the nocturne avalanches, which occur from 5:00 pm to 9:00 am. On the most active path in the valley near Umiujaq, for instance, 52% avalanches overpass the β =10° inflection point, *i.e.*, the distal part of the slope; 38% reach the mid-slope, and 10% do not pass the rockwall. At this site, 61% avalanches occurred during daytime, and 39% during nighttimes. Additionally, 55% of avalanches transport dry snow (from November to May), while 45% transport wet snow (in May and June).

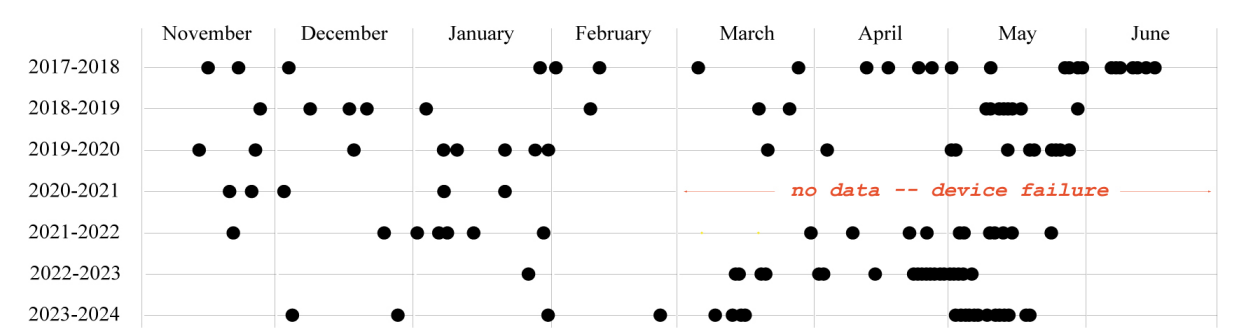


Figure 2 Days with observed snow-avalanche deposits (one or several) from 2017 to 2024 on one of the most active areas, close to Umiujaq, from a single automatic camera. The largest extent deposits occur from February to early May (modified from Veilleux et al., 2021; Grenier et al., 2023).

Accurate knowledge of the avalanche timing enables to examine the main triggering factors. Two regimes are distinct, according to the hourly air temperature recorded at the nearest weather stations, located only a few hundred meters away from some of the investigated slopes (Grenier et al., 2023): winter regime has air temperatures constantly negative; spring regime has positive and negative air temperature variations during the day. During winter regime, results show that a 10 cm of snow accumulating over three days is conducive to

snow-avalanche release. During spring regime, the combination of a minimum daily air temperature of 2°C with forty-six cumulative melting degree-days are the most prone conditions for snow-avalanche release.

3.2 Slope profiles of snow-avalanche prone paths in Northern Villages

Based on 315 longitudinal slope profiles in the communities of Umiujaq, Salluit, Kangirsujuaq and Kangiqsualujjuaq, some recurrent topographic characteristics are identified (Fig. 3). Slopes are mainly concave (57%), with or without distal debris talus; then 11% slopes present a rocky face in the shape of a hockey stick; 11% have convex profile, developing on slopes covered with glacial till; only 5% of slopes profiles are stepped, corresponding to alternating sedimentary layers of different resistance, such as limestone and sandstone. Profiles that fit none of these shapes are estimated to 8%.

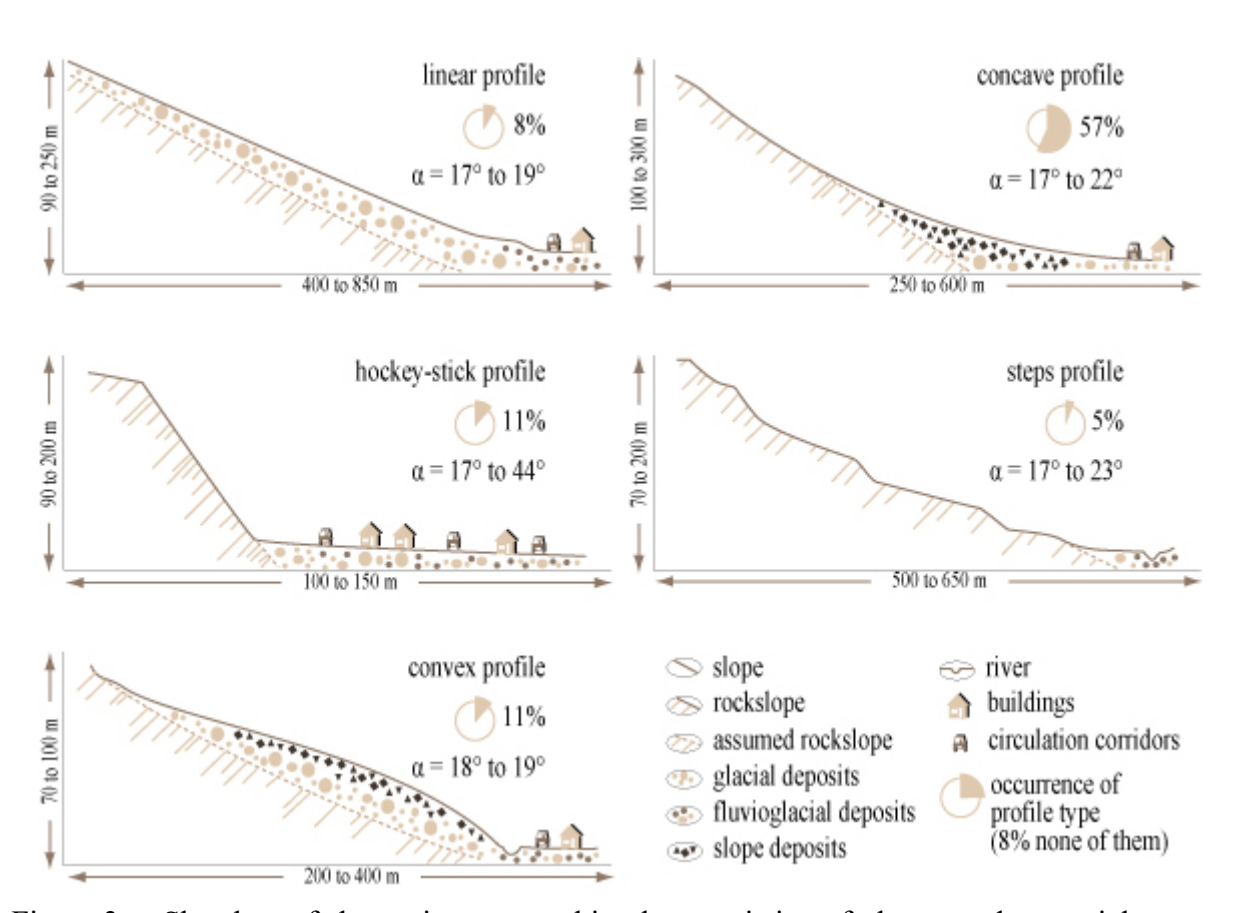


Figure 3 Sketches of the main topographic characteristics of slopes and potential snow-avalanches runout distances in four Nunavik Northern Villages, based on 315 slope profiles.

Alpha angles are rather low, comprised between 17° and 23°. Most of the Northern Villages have parts of their infrastructures, either transportation corridors or buildings (dwellings, municipal facilities, sheds), within the deposit zone of potential snow-avalanche paths (Filion, 2025; Filion et al., 2025), as shown in Fig. 4 for Kangiqsualujjuaq. In fact, over the last seven winters, some of the events captured by the cameras reached human infrastructures, for instance the road at one site near Umiujaq.

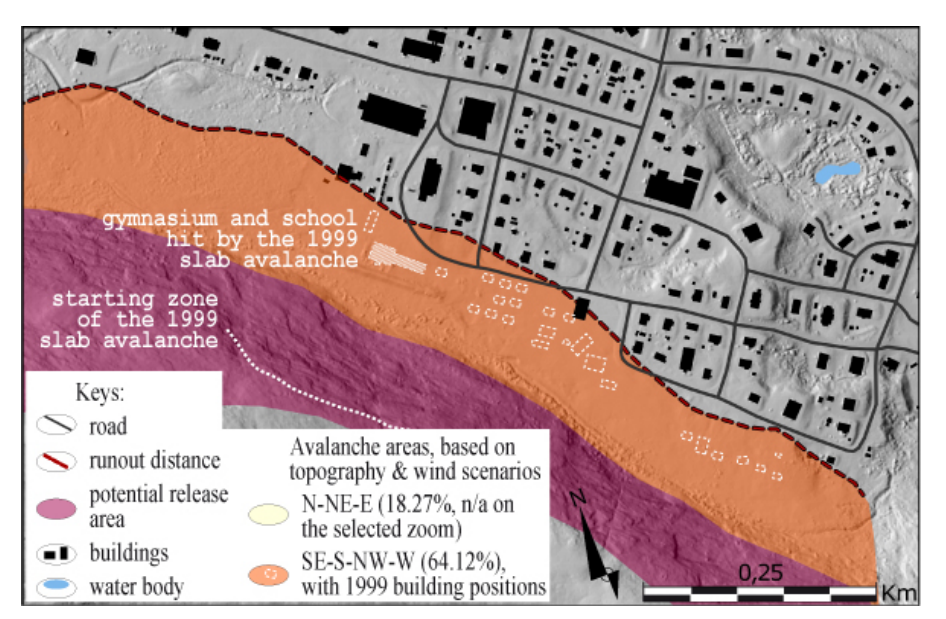


Figure 4 Snow-avalanche maximum runout distance according to the topographic and wind analyses carried out on part of Kangiqsualujjuaq (modified from Filion et al., in press). In 1999, prior to the avalanche, several houses and buildings were located within the potential runout zone; some encountered damage in 1980s and 1993. All buildings were relocated after the 1999 event, and few are newly built.

4. CONCLUSION

Snow avalanches in Nunavik occur on a range of slope profiles and are triggered under a large variety of weather conditions. Over the last seven winters, we documented inter- and intra- annual variability regarding snow thickness, wind regimes, temperatures. The automatic cameras are a useful tool to document snow-avalanche events. The snow-avalanche collection is an essential basis to decipher the fundamentals of snow-avalanche research, *i.e.*, timing, outlines, runout distances, triggering factors. In a context of few information regarding snowpack characteristics over winter, or with the lack of specific snow-avalanche landforms, tracking the topographic conditions prone to snow avalanching helps to focus on specific slopes. The research is ongoing, and results are shared with the stakeholders in Northern communities to support informed decision-making regarding land-planning in a context of climate change. This represents a challenge in the fast-evolving subarctic and arctic environments.

ACKNOWLEDGEMENT

This research is supported by OHMi Nunavik (Labex DRIIHM program "Investissements d'avenir" referenced ANR-11-LABX-0010), Institut Polaire Français Paul-Emile Victor (IPEV project #1148 DeSiGN) and CNRS laboratory Littoral, Environnement, Télédétection, Géomatique UMR 6554, as well as Natural Sciences and Engineering Research Council of Canada (NSERC). We thank former MSc students Raphaël Loiseau, Chiara Saporiti, Claire Morillon, Thomas Dias and Jeanne Jaillard for their work on part of the data compiled in this document, while on training at LETG lab. We thank also Denis Sarrazin and Carl Barrett for their valuable collaboration in retrieving part of the data when the research team was unable to reach the field, during the COVID pandemic in 2020 and Quebec forest fires in 2023.

REFERENCES

- Decaulne, A., Bhiry, N., Lebrun, J., Veilleux, SS., Sarrazin, D., 2018. Geomoprhological evidence of Holocene slope dynamicson the Canadian shield a study from Lac à l'Eau-Claire, western Nunavik. Ecoscience, 25(4), 343-357.
- Decaulne, A., Bhiry, N., Faucher-Roy, J., Pelletier Boily, C., 2021. The development of Kangiqsualujjuaq and the threat of snow avalanches in a permafrost degradation context, Nunavik, Canada. Espace Populations Sociétés, 1, 10497.
- Decaulne, A., Bhiry, N., Delwaide, A., 2025. Geomorphic properties of a complex subarctic slope and dynamic implications: granulometric characteristics and tree-ring patterns (Raspberry slope, Wiyâshâkimî Lake, Nunavik, Canada). Géomorphologie: relief, processus, environnement, 31(1), 13w4n.
- Filion, V., 2025. Identification et caractérisation des terrains avalancheux à proximité des villages du Nunavik (Québec, Canada). MSc thesis, Université Laval, 142 p.
- Filion, V., Decaulne, A., Bhiry, N., in press. Avalanche terrain analysis in Nunavik, Quebec: a multi-criteria approach combining topographic and meteorological data. CATENA.
- Germain, D., 2016. Snow avalanche hazard assessment and risk management in northern Quebec, Canada. Natural Hazards, 80, 1303-1321.
- Germain, D., Martin, J.-P., 2011. The vulnerability of northern cities to weather-related hazards: case studies from the Province of Quebec, Eastern Canada. In Daniels, J.A. (ed.), Advances in Environmental Research. ISBN: 978-1634832786, Nova Science Publishers, pp. 143-160.
- Grenier, J., Bhiry, N., Decaulne, A. (2023). Meteorological conditions and snow-avalanche occurrence over three snow seasons (2017–2020) in Tasiapik Valley, Umiujaq, Nunavik. Arctic, Antarctic, and Alpine Research, 55(1), 2194492.
- Lied, K., Domaas, U., 2000. Avalanche hazard assessment in Nunavik and on Côte-Nord, Québec, Canada. Ministère de la Sécurité publique du Québec.
- Schaerer, P., Jamieson, B., Stethem, C., 1999. Avalanche hazard mitigation for Kangiqsualujjuaq, Québec. Technical report, Ministère de la sécurité publique, Gouvernement du Québec.
- Stethem, C., Jamieson, B., Schaerer, P., Liverman, D., Germain, D., Walker, S., 2003. Snow avalanche hazard in Canada a review. Natural Hazards, 28, 487-515.
- Veilleux, S., Bhiry, N., Decaulne, A., 2020. Talus slope characterization in Tasiapik Valley (subarctic Québec): Evidence of past and present slope processes. Geomorphology, 349(15), 106911.
- Veilleux, S., Decaulne, A., Bhiry, N., 2021. Snow cornice and snow avalanche monitoring using automatic time lapse cameras in Tasiapik Valley, Nunavik (Québec) during the winter of 2017–2018. Arctic Science, 7(4), 798-812.

Development of a guidelines for site-specific avalanche warning – needs, method, and content

Karin Bergbjørn^{1*} and Priska H. Hiller¹

¹ NVE Norwegian Water Resources and Energy Department, Middelthunsgate 29, NO-0368 Oslo, NORWAY *Corresponding author, e-mail: kabe (at) nve.no

ABSTRACT

Site-specific avalanche warning comprises avalanche hazard evaluation for one or a few specific avalanche tracks and recommendation for appropriate awareness levels regarding chosen objects at risk. It differs clearly from regional avalanche warning services, which cover larger areas, are mostly directed towards travelling in avalanche prone terrain and give more general recommendations (NVE, 2025).

The need for site-specific avalanche warnings for buildings, infrastructure and temporary facilities in avalanche-prone areas has increased in Norway. Hence, the demand from municipalities, the Norwegian Public Roads Administration, and private actors has increased. Consequently, there is a need for guidelines both for customers and providers of site-specific avalanche warning services. The aim of the guidelines is to secure minimum requirements for quality, better coordination, and more efficient use of resources.

The guide is based on experience from several warning projects in Norway and the recommendations for site-specific avalanche warning by European Avalanche Warning Services (EAWS, 2023). Both consultants and customers from the public administration contributed to the work led by the Norwegian Water Resources and Energy Directorate (NVE).

The guidelines distinguish between preparation and operation of a site-specific avalanche warning service and also include the risk owner's responsibility for preparedness and risk acceptance.

The contribution will provide insight into the background of the guidelines, central principles, structure, and content.

1. INTRODUCTION

Site-specific avalanche warning has only occurred systematically in Norway for buildings since 1997 (Waaler, 2015), with an increase in objects since 2015. It is only recently that it has become a more common service to reduce the risk from avalanches to objects. Site-specific avalanche warning is more commonly used for roads or temporary objects such as job sites prone to avalanche risk. However, there are as of 2025 ongoing warning services concerning residential houses in Longyearbyen, Honningsvåg, Mosjøen and a consortium of communities

in Northern Norway, in addition to infrastructure, such as power lines, substations, and aquaculture farms.

An increase in locations with site-specific warning, and consultants providing warning services, has spurred the need for consensual guidelines for providers as well as customers. In particular, municipalities may need support when calling for tenders as they may lack expertise about snow avalanche risk mitigation. Even the preliminary risk assessment for defining the objects at risk, is quite demanding if you are unfamiliar with avalanches, potentially resulting in disproportionately high costs or unacceptable risk acceptance. This need for guidelines has also been expressed by the industry itself, needing a benchmark for quality, safety, and performance.

NVE has initiated and led the work on the guidelines, in close collaboration with Norwegian Public Roads Administration, including municipality administration, and consultants. The guidelines are based on the recommendations by EAWS published in 2023, with slight modifications.

The project has had five online workshops, since the start in autumn 2024, with dedicated tasks assigned to each subject. The written draft for the guidelines has been constantly open for adding content and comments by everyone involved. In late spring 2025, everyone attended a physical workshop spanning two days to go through the written guidelines. In addition, three topics were specifically analysed and separately reported within subprojects addressing:

- Snow observations related to site-specific warning,
- instrumentation for site-specific warning, and
- using unmanned aerial vehicles (UAVs) for analysing snow distribution

The guidelines have undergone a final review process and legal check. The publication is scheduled for autumn 2025.

2. CONTENT AND STRUCTURE OF THE GUIDELINES

The guidelines will be published digitally on https://veiledere.nve.no/veileder-stedspesifikk-snoskredvarsling/ in Norwegian. It contains an introduction, description of the risk owners' responsibilities and tasks, and a recommendation of the competence level for providers. The guidelines distinguish between preparation and operation of a site-specific avalanche warning service.

During preparation an avalanche warning plan is elaborated. It describes how the avalanche hazard will be evaluated in the warning service using measurements, snow observations, weather data and predefined scenarios, resulting in a recommended awareness level. The risk owner needs a corresponding emergency response plan which transfers the awareness level into predefined actions.

In the following, we describe those responsibilities and tasks.

2.1 Risk owner

Before starting the work with the avalanche warning plan, the risk owner must identify and describe the objects at risk sufficiently (Statens vegvesen, 2021). Usually, the risk is assessed including vulnerability, exposure and potential consequences such as loss of life, economic losses, or loss or interruption of infrastructure.

The results of the assessment form the base to evaluating different mitigation strategies, where avoiding risk or permanent mitigation should be the preferred solutions. However, in some cases site-specific warning in combination with an emergency response plan turns out to be the most suitable if there is sufficient time available to react to the warning, and the residual risk is acceptable. The risk acceptance depends on objects at risk, the risk owner, and which laws apply. Consequently, this defines the scope of the service.

The risk owner also must prepare an emergency response plan before the warning service starts. This plan must outline the acceptable level of risk for each site and/or object and clearly define roles and responsibilities. The plan facilitates good communication between different stakeholders such as police, mayors, or public roads. The risk owner is also responsible for deciding which specific mitigation actions to implement at each awareness level defined in the avalanche warning plan.

The emergency response plan must also describe the management, operation, maintenance, and implementation of measures. Furthermore, the plan should include routines for maintaining measures such as signage, barriers, and instrumentation.

Finally, the risk owner must have a plan for communicating with locals and is strongly encouraged to hold public meetings with anyone affected in connection with the site-specific warning.

2.2 Preparation of a warning service

The level of detail the site-specific warning service depends on the vulnerability and exposure of the object, and complexity of the avalanche site. This is defined in the avalanche warning plan which is inspired by the one described in Technical Aspects of Snow Avalanche Risk (Canadian Avalanche Association, 2016).

Elaborating the avalanche warning plan includes a thorough site investigation, mapping both the release and run-out areas of potential avalanches. The required level of detail varies depending on the type of object or infrastructure at risk. Historical avalanche events, digital terrain models, weather data, fieldwork, and the availability or absence of monitoring equipment must all be described.

It is important to specify all factors that can increase avalanche danger, such as critical weather and snow conditions. Monitoring these factors usually include instrumentation and observations in the field. The plan should specify which instrumentation is essential and how uncertainties can be reduced. Snow observations should be specified by type, purpose, and potential locations. Particular attention should be paid to the topography and terrain, as these factors influence the potential for snow avalanche release and the extent of the run-out area. Defining all the avalanches that could impact the object is essential. All documentation, including modelling inputs, results, and GIS data, must always be stored and remain available for the risk owner.

The avalanche warning plan also includes mitigation zones and predefined awareness levels, with mitigation actions, see Figure 1. Combining the risk matrix for each site, the awareness levels and actions allow seamless transitions from the awareness level in the avalanche warning plan to the mitigation levels or actions defined in the emergency response plan.

		,	Actions	
	Level	Awareness	Road closure	Road maintenance
	Green	Normal		No actions, avalanches are reported
Awareness level	Yellow	Increased	Traffic shouldn't stop at site	Daily site-spesific warning, no manual operations at site
	Orange	Some restrictions	May happen in short notice, opening is evaluated	Some restrictions ons work operations, convoy driving should be risk evaluted
	Red	Extensive restrictions	Road closure, opening is evaluated	Avoid working operations at site

Figure 1 Awareness levels and associated mitigation actions Source.

The awareness levels replace the impact probability from definitions in EAWS (2023). This adaptation is based on feedback from ongoing services. The impact probability is indirectly still present when combining probabilities for avalanches and sizes. However, mitigation actions might be necessary even if the avalanche might not impact the object directly. For example an avalanche impact can cause flood waves endangering objects, or if the avalanche stops higher in the avalanche path, not reaching the actual object, it still may cause reduced visibility which can be dangerous on a high-speed road.

2.3 Operation of the warning service

The avalanche warning plan serves as a guiding document throughout the operational warning service, supporting consultants in their decision-making processes. They communicate the awareness level to the risk owner as specified in the avalanche warning plan, and display the uncertainty in all communication (Øyen, Albrechtsen, Hancock, & Indreiten, 2022). The avalanche warning plan should be evaluated periodically, typically after each warning season, and after events activating the emergency response plan. If needed, the avalanche warning plan should be revised and updated. Changes must be communicated to all stakeholders, especially to the risk owner, who maintains overall responsibility.

The guidelines further elaborate on the various methods used for site-specific warning in Norway, discussing their respective strengths and weaknesses. There are specific requirements regarding the format for communicating awareness levels to the risk owner. For example, the awareness levels and corresponding mitigation actions should be clearly stated in the beginning of the warning, similar to the recommendations from EAWS.

Our guidelines recommend four awareness levels, aligning more closely with regional warning services in Norway, as highlighted in several research projects (Albrechtsen & Øien, 2022). This harmonization improves public understanding, particularly since regional and site-specific avalanche warnings may differ.

3. CONCLUSIONS

The guidelines presented for site-specific avalanche warning aim for a common understanding of the service, roles and responsibilities as well as to ensure quality. They will also support risk owners who have limited experience in snow avalanche risk mitigation.

The broad collaboration with other public services and private providers of avalanche warning services provided many important inputs and was appreciated during the writing of the guidelines. This process also allowed us to incorporate experience from ongoing site-specific warning projects, follow recent findings in research, and make minor adjustments to the EAWS recommendations. The guidelines hence distinguish between the avalanche warning plan and the emergency response plan. The avalanche warning plan results in a recommended awareness level which is picked up by the emergency response plan connecting the awareness level to an appropriate action for mitigating the risk.

There are some final tasks remaining before the guidelines can be published digitally, and we are curious how the guidelines will be used in practice.

ACKNOWLEDGEMENT

We appreciate the input from risk owners such as Norwegian Public Road Administration, Tromsø and Nordkapp municipalities, Troms County municipality and consultants Georisiko AS, NGI, Skred AS and Wyssen Avalanche. Varsom also contributed with warning service experience. Thank you for the contribution and great collaboration.

REFERENCES

Albrechtsen, & Øien. (2022). Lokalt snøskredvarsel for Longyearbyen. Evaluering av nåværende system. Arctrisk.

Canadian Avalanche Association. (2016). *TASARM-Technical aspects of snow avalanche risk management*. Revelstoke, BC: Canadian Avalanch Association.

EAWS. (2023). Site-specific avalanche warning, definitions and recommendations. EAWS.

NVE. (2025, 07 04). *Snøskredvarslingen*. Retrieved from Varsom: https://www.varsom.no/snoskred/snoskredvarsling/om-snoskredvarslingen/

Statens vegvesen. (2021). Håndbok V721 Risikoanalyse veg. Statens vegvesen.

Waaler, H. S. (2015). Nordnorsk skredovervåkning. Bergen: Universitet i Bergen.

Øyen, K., Albrechtsen, E., Hancock, H., & Indreiten, M. (2022). *Evaluation of a Local Avalanche Forecasting System in Svalbard*. European Safety and Reliability Conference.

Towards an operational avalanche forecasting tool using RAMMS::Extended

Cam Campbell* and Eirik Sharp

Alpine Solutions Avalanche Services *Corresponding author, e-mail: ccampbell@alpinesolutions.com

ABSTRACT

Integrating near-real-time LiDAR measurements of start-zone snow depth data with RAMMS:Extended avalanche simulations to estimate runout and assess the potential of avalanches to reach specific elements at risk, is an emerging opportunity for avalanche forecasting. However, while the use of dynamic simulations such as RAMMS is promising, they require further research into the appropriate model parametrization to accurately simulate non-extreme events before they can be broadly implemented as a predictive tool.

We present initial sensitivity assessment results using RAMMS::Extended for simulating late-season, low-volume avalanches in Path 51 (Highway 99, British Columbia, Canada) to support an operational forecast tool. Across 224 simulations, erodible snow depth dominated runout distance; colder initial snow temperatures increased reach, while air temperature (5–10 °C) had a negligible effect.

1. INTRODUCTION

Determining the end of avalanche season is often a difficult decision that avalanche forecasters face. These decisions typically hinge on estimations of potential avalanche runout extent given the amount and stratigraphy of snow in the starting zones (i.e., potential release volume), the condition of the track (e.g., smooth or rough), and the avalanche flow regime (e.g., dry or wet).

Dynamic numerical avalanche simulations, such as RAMMS (Rapid Mass Movement Simulation; Christen et al., 2010) are commonly used in planning stage risk assessments to model extreme magnitudes for long return-period avalanches (Canadian Avalanche Association, 2016). However, these models have seen limited use as a predictive tool for operational risk assessments. This limitation stems from model sensitivity to input variations, which have historically been calibrated against extreme avalanche events (Buser & Frutiger, 1980); the use of snow-free topography as a sliding surface (Bühler et al., 2011); and challenges in accurately initializing simulations because release volume, entrainment, and snow temperature all affect runout extent (Vera Valero et al., 2015).

For this study, we use RAMMS::Extended (Bartlet & Christen, 2025) to perform a sensitivity analysis of measurable flow regime parameters (e.g., snow temperature, air temperature, erodible snow depth, and water content) to explain variations in runout extent for a given release volume in an avalanche path with smooth track conditions.

C. Campbell, E. Sharp O2.2 - Page 49

1.1 Study Site

Path 51 is the most active path on Highway 99 in the Coast Mountains of British Columbia, Canada, with an average of three avalanches reaching the highway annually. It's broad alpine starting zone (1700–2300 m elevation) feeds into a highly channelized (20-50 m wide) 1000 m long track that descends to Duffy Lake at 1000 m. The highway intersects the path at the top of the runout zone. (Figure 1).

The path is monitored and controlled by full-time Ministry of Transportation and Transit (MoTT) avalanche forecasters with the aid of a GazEx system installed in 1992. "Fickle Finger" (Figure 2) is an aptly named release area in the lower starting zone that typically does not release with avalanches flowing from above and has a history of producing post-control natural avalanches that reach the highway. It is a relatively small release area ($< 5000 \text{ m}^2$) compared to the $\sim 100,000 \text{ m}^2$ starting zone area.



Figure 1 Explosive-triggered avalanche in Path 51, May 14, 2012 with debris accumulation visible along Highway 99 (Source: MoTT).

Figure 2 Path 51 starting zone after extensive control, showing the Fickle Finger release area (dashed red outline) that did not release.

1.2 Previous Research

Several studies (e.g., Dillon & Hammonds, 2021; Glaus et al., 2024; Stoffel et al., 2018; Vera Valero et al., 2016, 2018) have demonstrated that RAMMS::Extended, when initialized with measured or modelled snowpack and weather data, can capture runout distances under varying flow regimes. While these approaches are promising, they require further research into the appropriate model parametrization to accurately simulate non-extreme events before they can be broadly implemented as a predictive tool.

Campbell et al. (2024) found a weak correlation between release volume and runout distance for Path 51, with relatively low release volumes of less than 5000 m³ often reaching the highway. They examined dynamic friction parameters to explain variations in the relationship between release volume and runout distance for low-volume end-of-season avalanches and found that friction coefficients (μ) ranging from 0.100 to 0.430, corresponding to different track

conditions, can explain these variations. However, discussions with MoTT avalanche forecasters indicated that avalanche flow regime also plays a critical role in whether low-volume late-season avalanches reach the road. These avalanches have a dense, wet snow, pluglike flow, with little volume increase in the track, similar to those analyzed by Vera Valero et al. (2016).

Building on this work, this study examines how erosion depth, snow temperature, air temperature, and water content affect simulated runout in Path 51, to evaluate their potential as forecasting parameters.

2. METHODS

We ran 224 RAMMS::Extended simulations for Path 51 to test the sensitivity of runout distance to measurable flow parameters. Simulations were initialized with release conditions based on observed Fickle Finger avalanches and use a snow-covered 2 m DEM acquired in mid-April. Erosion depth, snow temperature, snow temperature gradient, water-content gradient with elevation, and air temperature were varied in stepwise fashion across realistic ranges (Table 1) for a fixed release volume of 7660 m³. These parameters were selected for their influence on wet-snow avalanche flow and feasibility for real-time measurement. All other model inputs followed Bartlet & Christen (2025), late-season observations from Path 51, and prior studies (e.g., Vera Valero et al., 2016, 2018). Runout distance was calculated relative to the highway, with negative values indicating simulations that stopped above the road.

Table 1 RAMMS::Extended parameters and associated range of values used in the sensitivity analysis.

Parameter	Value(s) Used
Release Volume (m³)	7660
Water content (%)	0
Erosion depth - d0* (m)	0 to 1
Snow temperature (°C)	0 to -4
Snow temperature gradient - ΔT (°C/100m)	0 to 0.4
Water content gradient with elevation - ΔW (%/100m)	0.04 to 0.52
Air temperature (°C)	5 or 10

3. RESULTS AND DISCUSSION

Erosion depth emerged as the most dominant parameter affecting runout distance. Simulations initiated with shallower erosion (< 0.4 m) consistently stopped well above the highway with any realistic water content gradient (Figure 3).

C. Campbell, E. Sharp O2.2 - Page 51

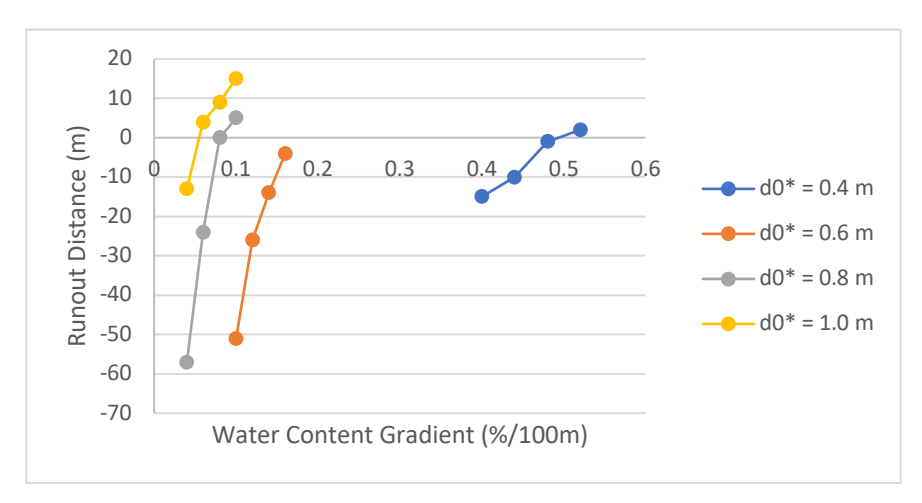


Figure 3 Runout distance relative to the road versus water content gradient for different erosion depths (d0*) for an air temperature of 10 °C, a snow temperature of -4 °C, and a snow temperature gradient of 0.4 °C/100 m.

Initial snow temperature also had a significant effect on runout distance. Colder initial snow temperature (-4 °C) produced the longest runouts. Initial snow temperature of -2 °C produced the shortest runouts, whereas an initial snow temperature of 0 °C resulted in intermediate runout distance (Figure 4). Furthermore, runout distance decreased with increasing snow temperature gradient for simulations initiated with a snow temperature of -4 °C, while runout distance increased with increasing snow temperature gradient for simulations initiated with a snow temperature of -2 °C (note that no snow temperature gradient was used for simulations initialized with a snow temperature of 0 °C, because snow cannot be warmer than 0 °C).

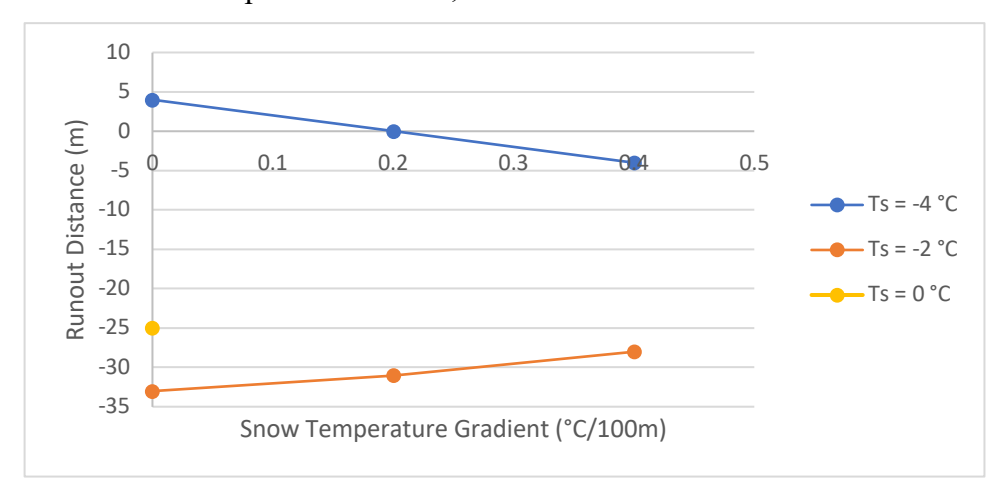


Figure 4 Runout distance relative to the road versus snow temperature gradient with elevation for different initial snow temperatures (Ts) for an erosion depth of 0.6 m, an air temperature of 10 °C, and a water content gradient of 0.16 %/100 m.

The effect of initial snow temperature on runout distance also increased with decreasing erosion depth (Figure 5). Furthermore, runout distance remained relatively constant for an erosion depth of 1.0 m, regardless of initial snow temperature. However, with an erosion depth of 0.6 m, runout distance decreased significantly with an increase in initial snow temperature from -4 °C to -2 °C, only to increase slightly as the initial snow temperature warmed from -2 °C to 0 °C.

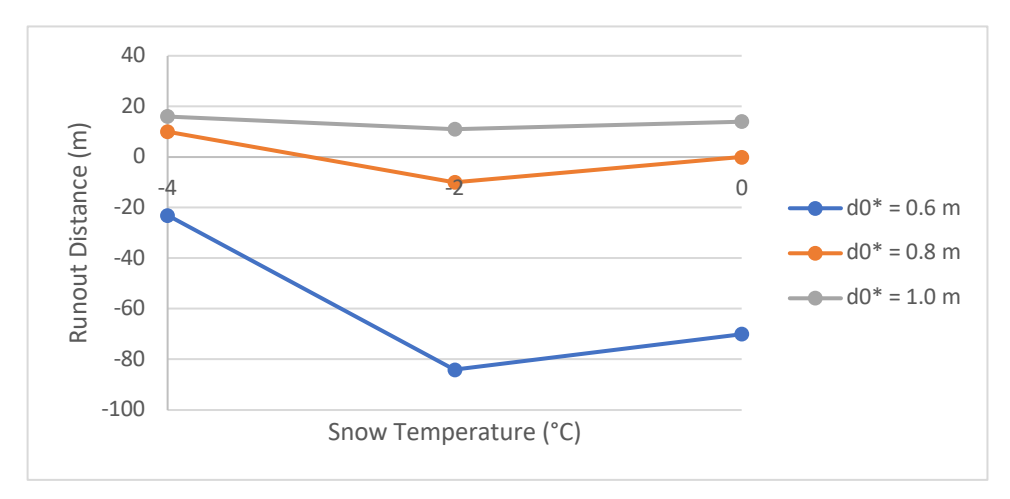


Figure 5 Runout distance relative to the road versus initial snow temperature for different erosion depths (d0*) for an air temperature of 10 °C, a water content gradient of 0.1%/100 m, and a snow temperature gradient of 0 °C/100 m.

Air temperature (within the range analysed) had little effect on runout distance under any combination of other parameters.

4. CONCLUSIONS

This study explored measurable parameters that affect runout distance in RAMMS::Extended simulations for low-volume, late-season avalanches in an avalanche path with a highly channelized track. Erosion depth, snow temperature, and water-content gradient with elevation were the most influential factors, with snow temperature gradient playing a secondary role; air temperature had little effect.

Because they can be observed in real time, these parameters could be incorporated into operational forecasts. This study is a first step toward building such a tool with RAMMS::Extended. Future efforts will examine the sensitivity of runout extent to initial water content and release volume supported by drone surveys and SNOWPACK modelling (Lehning et al., 1999) to define realistic parameter ranges. Ultimately, the goal is to develop a tool that estimates the potential for late-season avalanches to reach the highway based on lidar measurements of release volume and measured or modelled flow regime parameters.

ACKNOWLEDGEMENT

We would like to acknowledge the MoTT avalanche personnel for providing data and discussions used for this analysis.

REFERENCES

Bartlet, P., and Christen, M. 2025. Snow Avalanche Dynamics with RAMMS::Extended. RAMMS AG. June 1, 2025.

Bühler, Y., Christen, M., Kowalski, J., and Bartelt, P. 2011. Sensitivity of snow avalanche simulations to digital elevation model quality and resolution, Ann. Glaciol., 52, 72–80.

Buser, O. and Frutiger, H. 1980. Observed Maximum Runout Distance of Snow Avalanches and the Determination of the Friction Coefficients μ and ξ , J. Glaciol., 26, 121–130.

C. Campbell, E. Sharp O2.2 - Page 53

- Campbell, C., Sharp, E., and Tessier, A. 2024. Investigating Dynamic Model Friction Parameters for Low-Volume End-Of-Season Avalanches. in: Proceedings, International Snow Science Workshop, Tromso, Norway.
- Canadian Avalanche Association. 2016. Technical Aspects of Snow Avalanche Risk Management Resources and Guidelines for Avalanche Practitioners in Canada (C. Campbell, S. Conger, B. Gould, P. Haegeli, B. Jamieson, & G. Statham Eds.). Revelstoke, Canada.: Canadian Avalanche Association.
- Christen, M., J. Kowalski and P. Bartelt. 2010. RAMMS: Numerical Simulation of Dense Snow Avalanches in Three-Dimensional Terrain. Cold Regions Science and Technology, 63(1-2), 14.
- Dillon, J. and Hammonds, K. 2021. Brief Communication: Initializing RAMMS with High-Resolution LiDAR Data for Avalanche Simulations, Cryosphere Discuss., 2021, 1–1.
- Glaus, J., Jones, K. W., Bartelt, P., Christen, M., Stoffel, L., Gaume, J., and Bühler, Y. 2024 Simulation of cold powder avalanches considering daily snowpack and weather situations to enhance road safety, EGUsphere, 2024, 1–31.
- Lehning, M., Bartlet, P., Brown, B., Russi, T., Stockli, U., and Zimmerli, M. 1999. SNOWPACK model calculations for avalanche warning based upon a network of weather and snow stations. Cold Regions Science and Technology, 30, 145-157.
- Stoffel, L., Bartelt, P., Margreth, S., and Schweizer, J. 2018. Can scenario-based avalanche dynamics calculations help in the decision making process for road closures? In: Proceedings, International Snow Science Workshop, Innsbruck, Austria.
- Vera Valero, C., Wilkstroem Jones, K., Bühler, Y., and Bartelt, P. 2015. Release temperature, snow-cover entrainment and the thermal flow regime of snow avalanches. J. Glaciol., 61, 173–184.
- Vera Valero, C., Wever, N., Bühler, Y., Stoffel, L., Margreth, S., and Bartelt, P. 2016. Modelling wet snow avalanche runout to assess road safety at a high-altitude mine in the central Andes, Nat. Hazards Earth Syst. Sci., 16, 2303–2323.
- Vera Valero, C., Wever, N., Christen, M., and Bartelt, P. 2018. Modelling the influence of snow cover temperature and water content on wet-snow avalanche runout. Nat. Hazards Earth Syst. Sci., 18, 869-887.

Systems-Thinking Analysis of the Iceland Avalanche and Landslide Programme:

Understanding Feedback Control Mechanisms (Seyðisfjörður Case Study)

Sólveig Thorvaldsdóttir^{1,*} and Benedikt Halldórsson^{1,2}

¹Earthquake Engineering Research Centre, University of Iceland, Selfoss, ICELAND

²Icelandic Meteorological Office, Reykjavik, Iceland.

*Corresponding author, e-mail: solvth@hi.is

ABSTRACT

The study aim was to gain an understanding of how risk policy shapes risk management. The objective was to find leverage for improving risk management by evaluating policy aspects of the Icelandic avalanche and landslide mitigation programme, initiated in 1995. The progress towards reducing the risk of disaster in Seyðisfjörður village was used as a case study. According to the original plans, mitigation barriers in Seyðisfjörður were to be completed by 2010. Due to various delays, they are not yet complete. In 2020, in a span of one week, 24 landslides fell above or onto the village, calling for evacuations, recovery efforts, and emergency barriers. A systems-thinking approach was used to study the programme system structure and its behaviour, how they relate to policy, and characterize unintended consequences. Analytical steps were to (i) identify key activities, decisions and delays, (ii) compare the outcome of the actual programme with the intended programme, (iii) draw a causal loop diagram of the programme feedback structure and behaviour, and (iv) identify leverage points for corrective action to monitor and avoid unintended consequences. The study revealed that the relationship between policy targets and risk management was simple, it is defined by a risk gap, but that policy strategy and planning have been significantly affected by multiple decisions leading to programme deficiency. Feedback control on unintended consequences are important elements to monitor and maintain efficiency of DRR programmes.

1. INTRODUCTION

Government Disaster Risk Reduction (DRR) programmes are established to increase citizen safety. The avalanche and landslide risk mitigation programme in Iceland was revised in 1995 after two urban avalanches in the Westfjörds killed 34 people. A new institutional DRR structure was established by law in 1997. The programme was driven by the policy that the risk of dying in your home in a village should be no greater than dying in a car crash in the capitol. A plan was set in motion signed by the minister of environment to update risk assessments, design mitigation measures, and build them in 8 villages by 2010. Specific tax revenues were installed on homeowners to ensure national programme funding. The programme did not meet the 2010 goal for the 8 municipalities. Almost half of the projects planned in 1996 were completed by the end of 2008. After two urban avalanches in 2020, the government increased the 2021 national budget, and a new completion date for all projects was set to 2030.

Hazards in Seyðisfjörður, a village in the Eastfjörds in the programme, are both landslides and avalanches. Risk assessments began in 2000, had to be repeated a few times due to new

evidence, but were completed by 2002. By 2016 the initial mitigation design was completed. In 2020, 24 landslides fell above or onto Seyðisfjörður, causing significant damages. The entire village was evacuated for a few days. This led to a revised risk assessment and new barrier design. Construction in Seyðisfjörður is estimated to start in 2028 and be completed in 2032.

This paper presents a systems-thinking approach to analyse the DRR programme and its application in Seyðisfjörður. Systems thinking is an efficient approach for finding solutions to complex disaster management problems (Gillespie, 2004). Systems thinking defines a system as (i) its elements, (ii) their interconnectedness, and (iii) the function (what the system actually does) of the system as a whole (Meadows, 2008). The basic operating unit of a system is a feedback loop (Meadows, 2008). A study of systems seeks to identify feedback structures and understand system behaviour. The term *systems archetype* signifies generic system structures that are commonly found in organizations (Kim and Lannon, 1987).

2. METHODS AND TECHNIQUES

The analysis of the Icelandic DRR programme involved the following steps:

- 1) Elements Building a timeline of key activities and decisions made in the programme and for the Seyðisfjörður project in order to identify key system elements. The activities of the National Flow Flood Fund (NFFF) are from the fund's reports (Ofanflóðasjóður, 1996-2021) based on the programme law (Act, 1997). All hazard reports and maps from the Icelandic Meteorological Office (IMO) are available on their website. Illmer et al., (2016), a multi-agency report, shed light on mitigation efforts.
- 2) **Function** Determining deviation of actual from intended system. Delays were characterized based on policy aspects. The policy-related definitions used: *Policy* The disaster risk reduction goals; *Strategy* The system structure established to reach objectives in order of priority; *Plans* The timeline of activities and associated resources; and *Tactics* The act of putting the plan in motion, (BESTrategicPlanning, 2024). *Policy integration* is the act of merging multiple overlapping conflicting policies of multiple sectors (Persson, 2004).
- 3) **Interconnectedness** Drawing a Causal Loop Diagram (CLD) that shows the programme feedback structure (i.e., the interconnectedness of the elements). System Dynamics methodology was applied. System dynamics is a mental and computer modelling technique used for the analysis of policy and strategy (Sterman, 2000; Deegan, 2016) and used for testing policy control by modelling feedback control mechanisms in systems.
- 4) Consequences Building a timeline of key relief and recovery activities performed by municipality staff due to 2020 landslides. The timeline included perspectives of the current mayor, office manager, social services, engineering and urban planning, employment and culture representative, a former mayor of Seyðisfjörður and resident. Use the timeline to understand what to use for leverage for avoiding unintended consequences.





Figure 1. Municipality staff constructing a timeline (Photos: Sólveig Thorvaldsdóttir).

3. RESULTS

3.1 Elements and function

The year and key activity for the programme and Seyðisfjörður project based on the NFFF and IMO reports are presented in Table 1. Each activity has been assigned a system element type.

Table 1. Timeline: Mainly Seyðisfjörður. Mainly landslides, but includes avalanches.

Year	Activity	Element type
1995	Fatalities in urban avalanches.	Event
1996	Initial assessment report.	Hazard/Risk
2000	Project work starts. New info on moving landmass, requiring new assessments.	Hazard/Risk
2001 Feb	JHZC* establish for Seyðisfjörður. JHZC authorizes a detailed assessment.	Strategic
2001 Sep	Hazardous events (rains, fissure expansion) in September and October	Event
2001-2002	Detailed assessments carried out. New traces of prehistoric large landslides.	Hazard/Risk
2002	Landslides and evacuations.	Event
2002	Detailed assessment approved by JHZC, NFFF, and signed by minister in July.	Strategic
2002	Tender for mitigation design.	Mitigation
2003	Additional hazard assessments.	Hazard/Risk
2003-2004	Various minor mitigation efforts.	Mitigation
2011	Draft risk assessment for existing and new areas presented to local authorities.	Strategic
2015	JHZC authorises preliminary survey of landslide hazard and mitigation design.	Mitigation
2018-2020	Environmental assessment	Strategic
2019	Risk assessment results presented to public for comments.	Strategic
2020 Mar	Revised and expanded risk assessment sign by minister.	Strategic
2020	Avalanches in two villages (not in Seyðisfjörður)	Events
2020 Dec	24 landslides in 5 days. Evacuations.	Event
2020 Jan	Mitigation barriers, critical.	Mitigation
2021 Jan	Mitigation barriers, emergency.	Mitigation
2021	Increased programme funding due to the two avalanches (not in Seyðsifjörður)	Strategic
2021	Tender completed. Design of barriers begins.	Hazard/Risk
2021	Revised risk assessment	Hazard/Risk
2022	Mitigation design finalized. Design approved by JHZC, residents, council,	Mitigation
	NFF, minister. Design incorporated into Seyðisfjörður master plan.	
2023	Detailed report on state of hazard, risk and estimated mitigation cost for Iceland.	Hazard/Risk
2028-2032	Future activities: Construction estimated to take place in Seyðisfjörður	Mitigation

^{*} Joint Hazard Zoning Committee

The DRR programme did not meet its 10-year completion goal for Seyðisfjörður, therefore, the actual system did not function as intended. Table 2 divides key delays in the Seyðisfjörður project based on policy aspects. Key changes were either related to strategy or planning. No changes have been made to the original policy risk target during the project, and no notable changes have been made at the tactical level.

Table 2. Delays in the Seyðisfjörður project

Delays based on policy aspects Strategic: changes in funding to programme or projects Control of flood tax revenue was moved from the NFFF to the national treasury. Reduction in government spending in 2004-2006 due to overheating in the economy due. Expansion, e.g., new municipalities, exposure types (e.g., farms), hazards (e.g., volcanic eruptions). Plans: delays in completion dates Changed priority due to new projects. New hazard information, requiring updated risk assessments. Environmental assessments. Archaeological assessments.

The main deviation of the actual DRR programme function from the intended programme are delays in the completion date. Systems that do not reach their goal due to internal pressures are termed "drifting goal" system archetypes (Kim and Lannon, 1987), (Figure 2). Taking corrective action will eventually close the gap between actual and planned completion time. However, multiple decisions over time place pressure on the system to postpone completion time, thus drift away from its original goal. The drifting-goal behaviour is a "boiling frog" syndrome, as delays can go undetected for a long time before a problem surfaces and corrected.

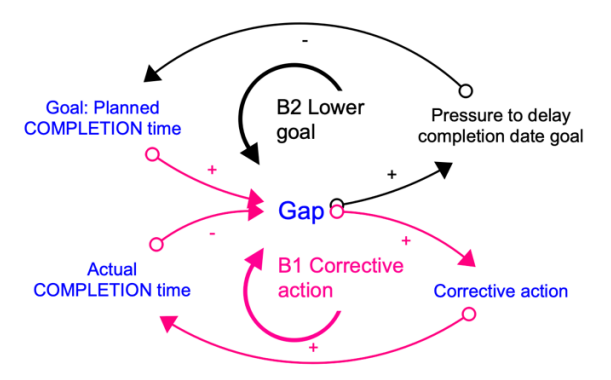


Figure 2 CLD for Drifting-goal archetype (Boiling frog syndrome). B: balancing loop, +/-: changes in same/opposite direction.

Drifting-goal archetype states that the problem can be easily solved with corrective action, but various pressures take away people's attention away from what people are trying to achieve and make it easier and quicker, and therefore tempting, to close the gap by lowering the planning goal (like delaying the completion date). Another reason for drift is time from the inspiring event (fatal avalanches); the longer since the inspiring, the less likely action is going to be taken.

3.2 Interconnectedness and consequences

A CLD of connectedness of the elements in the programme, in a project, and the risk policy shows locations of delays that can generate goal drift (Figure 3), and reads as follows:

B1 Programme inspiration: Avalanches and landslides cause fatalities (and damages). The more fatalities, the higher the perceived risk, greater the political will, the larger the national programme budget, the more risk assessments, the more mitigation, the fewer fatalities. R1 Budget: The larger the national budget, the larger the project budgets, the smaller the national budget. B2 Village risk: The bigger the village budget, the more risk projects, the more mitigation projects, the less the perceived risk, the less the political will for risk reduction in a village, the lower the budget. B3 Risk feedback control: Initially, there is a gap between actual risk and policy risk target. The larger the gap, the more mitigation, the lower the actual risk, the smaller the gap. The gap eventually closes, which ends the project.

The risk policy tethered to B3 corresponds to the goal in Figure 2. The Risk gap in B3 corresponds to Gap in Figure 2. Mitigation in B3 corresponds to Corrective action in Figure 2. The strategic delays (double lines) in Figure 3 correspond to Pressure to delay completion date goal in Figure 2 due to policies: Reduce funding to national budget; Policy integration; and Programme expansion.

The CLD shows two additional unintended consequences of the delays: a) The more time since the last events, the more time to forget, the lower perceived risk, and b) the less mitigation, the longer the buildings are exposed to risk, the higher the actual risk.

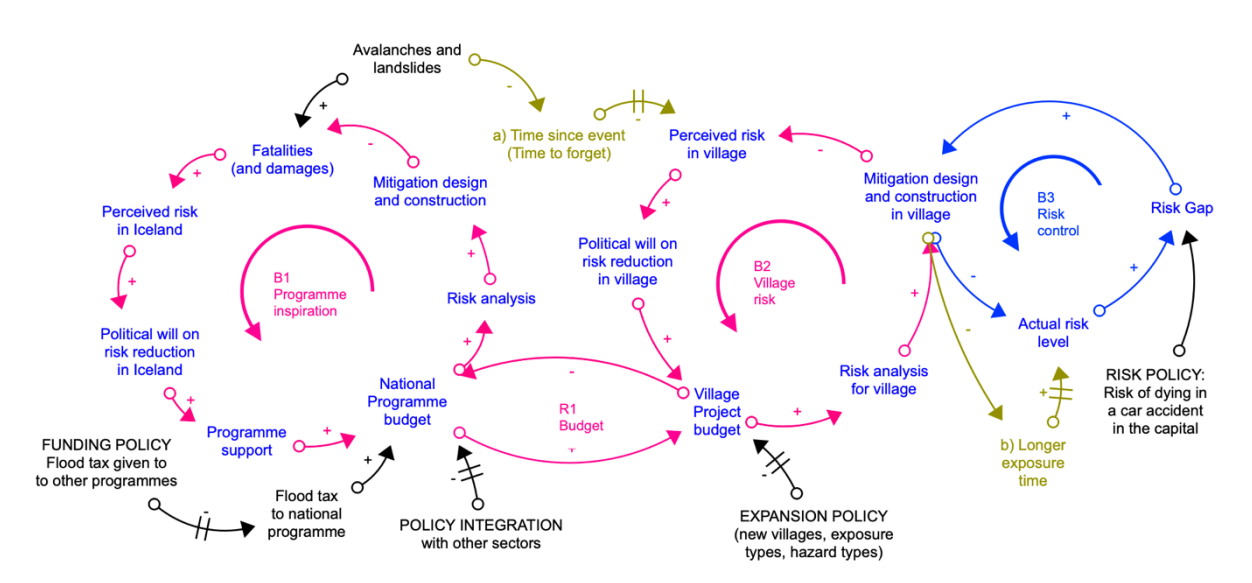


Figure 3. CLD for the DRR programme. B: balancing loop, R: reinforcing loop, +/-: changes in same/opposite direction. Double lines: delays.

The municipality staff members listed the following activity groups due to the 2020 landslides: Emergency activities, recovery project management, housing projects (emergency shelter, temporary housing, building new apartments), communication with residents on emergency and recovery issues, national collaboration on recovery, and land use planning changes due to new perceived risk. These activities had been suddenly added to their normal workload in 2020.

The unintended consequences of programme delays for the municipality staff can be divided into recovery efforts and staff pressure. Recovery management is a balancing act between speed and quality of recovery (Johnson and Olshansky, 2017). A hasty recovery leads to insufficient planning time resulting in poor decisions and processes. Slow recovery will extend suffering and the effected are more likely to take matter into their own hands rather than follow official directives. Recovery demands will increase staff work pressure. Poorly management recovery efforts will aggravate the problem. Setting policy targets on recovery management and staff wellbeing enables managers to apply counter pressures in the system to advocate keeping original projects goal as goal drift may lead challenges in closing recovery and pressure gaps.

Figure 4 shows the relationship between risk control, recovery management control, and of staff-wellbeing control. *B3 Risk control* is the same risk control as in B3 of Figure 3. If mitigation is delayed, the likelihood of a disaster increases. *B4 Recovery management* tethers recovery actions to a pre-defined target. The better the recovery management, the lower the staff work-pressure. *B5 Staff wellbeing* tethers staff pressure to a sustainable work pressure.



Figure 4. Integrated policy targets for risk, recovery management and staff wellbeing.

4. CONCLUSIONS

A risk-policy target shapes risk management by setting boundaries for mitigation efforts, which are implemented according to policy strategy and plans. However, DRR programme efficiency can be threatened by policy integration with conflicting sectors (e.g., economic, environmental, cultural), and other factors that pressure risk managers to lower project goals, such as completion dates. Efficiency decay may be gradual, and may go undetected, leading to the intended but also unintended consequences. Knowledge of programme system behaviour, including location and reason for delays, gives risk managers leverage in dealing with undesirable programme pressures. Additionally, by setting policy targets on unwanted consequences enables risk managers to monitor increasing risk of unintended consequences as project goals drift.

The approach presented here applies to any disaster risk reduction programme. Further work includes model simulation of a DRR system behaviour to identify which delays lead to critical goal-drifts and to quantify possible corrective actions.

ACKNOWLEDGEMENT

This work was done within the project MEDiate, Multi-hazard and Risk-informed System for Enhanced Local and Regional Disaster Risk Management, funded by the European Union. The contributions of Mulathing municipality staff, Austurbrú, Esther Hlíðar Jensson at the IMO, and Jón Haukur Steingrímsson at Efla Consultancy are gratefully acknowledged.

REFERENCES

- BESTrategicPlanning (n.d.). https://bestrategicplanning.com/difference-between-policy-and-strategy. Retrieved 2023.
- Deegan, M. A. (2006). Defining the policy space for disaster management: A system dynamics approach to US flood policy analysis. *Policy*, *1009*(1), 1-29.).
- Gillespie, D. F., Robards, K. J., & Cho, S. (2004). Designing safe systems: Using system dynamics to understand complexity. *Natural Hazards Review*, *5*(2), 82-88.
- Icelandic Meteorological Office (n.d.) Hættumat fyrir Seyðisfjörð (1995-2022, 1996, 2002, 20021, 2010, 2010a, 2019, 2012)
 - https://www.vedur.is/ofanflod/haettumat/seydisfjordur/
- Illmer, D., Jón Kristinn Helgason, J.K., Jóhannesson, T., Gíslason, E., Hauksson, S (2016) Overview of landslide hazard and possible mitigation measures in the settlement southeast of Fjarðará River in Seyðisfjörður. https://www.vedur.is/media/vedurstofan-utgafa-2016/VI 2016 006 rs.pdf
- Johnson, L. A., and Olshansky, R. B. (2017). *After great disasters: An in-depth analysis of how six countries managed community recovery*. Cambridge: Lincoln Institute of Land Policy.
- Kim, D. H., and Lannon, C. (1997). *Applying systems archetypes*. Waltham: Pegasus Communications.Meadows, D. H. (2008). *Thinking in systems: A primer*. chelsea green publishing.
- Act (1997). Lög um varnir gegn snjóflóðum og skriðuföllum. https://www.althingi.is/lagas/nuna/1997049.html
- Ofanflóðasjóður (1996-2021). Reports from Nation Flow Flood Fund.
 - https://www.stjornarradid.is/verkefni/almannaoryggi/vedur-og-natturuva/ofanflod/
- Persson, Å. (2004) Environmental policy integration: an introduction. *PINTS—Policy Integration for Sustainability Background Paper. Stockholm Environment Institute.*).
- Sterman, J. (2000). Business dynamics (p. 982). Irwin/McGraw-Hill

Temporary risk reduction methods for protected areas

Óliver Hilmarsson,* Harpa Grímsdóttir and Tómas Jóhannesson

Icelandic Meteorological Office, IS-105 Reykjavik, Iceland *Corresponding author, e-mail: oliver (at) vedur.is

ABSTRACT

Following the avalanche catastrophes in Súðavík and Flateyri, NW-Iceland, in 1995, where a total of 34 people lost their lives, new methods and criteria for avalanche hazard mapping were developed. Since then, new hazard maps have been made for all towns and villages where there is significant avalanche hazard. The municipalities are required to take action for the most hazardous areas and lower the risk with permanent measures, either with relocation of settlements or construction of defense structures. The aim is to eliminate the so-called C-zones (red zones) which are the most dangerous hazard zones. Milder hazard zones (so-called A- and B-zones) are usually defined beneath defense structures to reflect the rest risk due to uncertainty about the effectiveness of the structures and the fact that avalanches larger than the design avalanches are possible. The effectiveness of defense structures on the fluidized front of high-speed, dry-snow avalanches is especially uncertain, and in January 2020 a teenage girl was buried in her bedroom when the fluidized part of an avalanche partially overrode a deflecting dam above the village of Flateyri.

Evacuation and action plans are, therefore, made for the parts of settlements next to defense structures. Sometimes it is considered enough to advise people to stay away from rooms with doors or windows facing the mountain. In other cases, evacuations may be ordered under extreme conditions or when the defenses structures are not fully functional, e.g. when supporting structures become buried by snow or when avalanche deposits reduce the effective height of braking mounds or dams.

1. HAZARD MAPS AND UTILIZATION OF HAZARD ZONES

Following the avalanche catastrophes in Súðavík and Flateyri, NW-Iceland, in 1995, where a total of 34 people lost their lives, new methods and criteria for avalanche hazard mapping were developed in Iceland. Hazard assessment is the basis for measures to reduce the danger posed by avalanches and since 1995, new hazard maps have been made for all towns and villages where there is significant avalanche hazard. Alongside the preparation of the hazard assessment, a plan for the construction of protective structures was initiated. The municipalities are required to take action for the most hazardous areas and lower the risk with permanent measures, either with relocation of settlements or construction of defense structures. The aim is to eliminate the so-called C-zones (red zones) which are the most dangerous hazard zones. Milder hazard zones (so-called A- and B-zones) are usually defined beneath defense structures to reflect the rest risk due to uncertainty about the effectiveness of the structures and the fact that avalanches larger than the design avalanches are possible.

At the time of this paper, 24 deflecting dams, 27 catching dams and five splitters for the protection of settlements, with heights in the range 10–22 m, have been built. One or two rows of steep braking mounds, typically 10-m high, are located above five of the catching dams and to

the side of one deflecting dam. Snow supporting structures have, furthermore, been constructed for six avalanche paths.

Among the challenges that municipalities and planning authorities face is how to utilize the protected areas below the defenses. According to the law and regulations on avalanches in Iceland, defense structures should only be built to increase the safety of people in areas already populated and utilization and town development in defined hazard zones must follow strict criteria where the goal is to limit the avalanche risk to humans.

- In hazard zones A, new residential and commercial buildings, as well as cottages intended for overnight stays in skiing areas, can be erected. Schools, daycare centers, hospitals, community centers, multifamily dwellings with more than four apartments and other comparable buildings may be erected provided they are reinforced to withstand a defined impact pressure..
- In hazard zones B, new single- and multifamily dwellings with up to four apartments may be built, and additions made to schools, day-care centres, hospitals, community centres, multifamily dwellings with more than four apartments and other comparable buildings, provided the buildings and/or additions are reinforced to withstand a defined impact pressure. Commercial buildings may be erected, as well as cottages in skiing areas, which are not intended for overnight stays, without reinforcement requirements. No new schools, daycare centres, hospitals, community centres, multifamily units with more than four apartments, or other comparable buildings may be erected.
- In hazard zones C, only new structures, which people are not expected to occupy on a regular basis as a residence or place of employment, may be built, such as pumping or transmission stations, power lines and other comparable structures, and provided that they will not create increased risk to other settlement if the structure is subjected to the impact of a snow- or landslide. Residential and commercial buildings may, however, be modified but only in such manner that the total risk in the area concerned does not increase, e.g. due to increase in the number of apartments or number of employees.

Even though the law and regulations are fairly clear on how land in avalanche-prone areas should be used, this can still be challenging, as usable land is often limited.

2. UNCERTAINTY IN THE EFFECTIVENESS OF PROTECTIVE MEASURES

Since the implementation of the Act on Protection against Snow Avalanches and Landslides in 1997, scientific knowledge about the nature of avalanches and the effects of protective structures has increased significantly. New and powerful three-dimensional avalanche models enable scientists to simulate avalanches above populated areas, both with and without protective structures, and to observe how effective they are in diverting the dense core of avalanches away from the respective settlements.

2.1 New knowledge and experience

Extensive insights have been gained from over fifty snow avalanches that have interacted with defense structures in Iceland (Jóhannesson et al., 2019). Particularly valuable data on the performance of different types of defense structures came from two major dry-snow avalanche cycles: one at Flateyri in northwest Iceland in January 2020, and another at Neskaupstaður in east Iceland in March 2023 (Jóhannesson et al., 2024). They confirm earlier findings of experimental studies on the interaction of the dense core of avalanches with obstacles. Additionally, valuable insight was obtained into the not-as-well-understood interaction of fluid-

ized avalanches and protection measures. The observations from Flateyri indicate that the dense core of the avalanches was successfully deflected away from the settlement by the dams whereas a fluidized front travelled faster and was able to overflow the dams (Hilmarsson et al., 2020; Hákonardóttir et al., 2024). The observations at Neskaupstaður show that a fluidized front travelled on the order of a hundred meters farther than the dense core. The supporting structures in Neskaupstaður most likely reduced the size of avalanches from three main starting areas substantially and the avalanches were subsequently stopped above the settlement by steep braking mounds and catching dams in the run-out areas.

2.2 Uncertainty

Despite improved understanding about avalanches and the effectiveness of defense structures, there will always remain some uncertainty about rest risk to humans in areas below these structures – for instance, regarding the potential maximum size of avalanches in a given path, the effectiveness of structures when partially or fully buried by previous avalanches or snow, and, finally, their ability to stop dry-snow avalanches with a powerful fluidized front. Observations from both Flateyri and Neskaupstaður highlight the importance of the fluidized layer as a hazard element that needs to be considered in hazard zoning and in the design of avalanche protection measures. Lack of understanding of the fluidized regime of snow avalanches underscores the need for improved snow-avalanche models that can represent this flow regime realistically in the design of protection measures in the run-out zone.

2.3 Revision of hazard assessment

An existing, confirmed hazard assessment may need to be updated. This could be due to new insights, such as those gained during the dry-snow avalanche cycles at Flateyri and Neskaupstaður, the implementation of protective measures in previously unprotected areas, or other changed conditions. The Icelandic Meteorological Office is responsible for revising the hazard assessment.

3. EVACUATION PLANS FOR TOWNS

According to the Act on Protection Against Avalanches and Landslides, the Icelandic Meteorological Office is responsible for issuing warnings about impending avalanche hazards. Buildings in areas specified in a warning from the Meteorological Office must then be evacuated. In consultation with local authorities, the Meteorological Office has created special evacuation maps of the country's urban areas where avalanche hazards are considered significant, and evacuation plans for these locations are based on these maps. An evacuation plan for a town consists, first, of a sector-based evacuation map; second, a report from the Icelandic Meteorological Office on which buildings/sector should be evacuated and when; and last but not least, the plan of the local police authorities on how the evacuation will be carried out when such a notification is received from the Meteorological Office.

In places where protective measures are already in place, it is sometimes considered enough to advise people to stay away from rooms with doors or windows facing the mountain. In other cases, evacuations are ordered under extreme conditions or when the defenses structures are not fully functional, e.g. when supporting structures become buried by snow or when avalanche deposits reduce the effective height of braking mounds or dams (see Figure 1).



Figure 1. Screenshot from a web viewer showing the evacuation zones and their names in Neskaupstaður. For areas next to defense dams, two types of avalanche warnings are planned. The first advises caution – avoiding being outdoors for extended periods or in rooms with windows facing the slope when large, dry-snow avalanches that could be accompanied by a fluidized layer are considered possible. The second involves evacuation of buildings if it is considered a possibility that extreme avalanches could partially overtop the defense wall.

3.1 Decision making and uncertainty

As mentioned above, the Icelandic Meteorological Office (IMO) is responsible for issuing warnings and evacuation orders in collaboration with the local police authorities. These warnings are made by an avalanche team that assesses the local avalanche hazards, based on current weather observations and forecasts, as well as information about snowpack stability and recent avalanche activity. Snow observers play a key role by providing valuable insights into snow conditions and offering on-the-ground descriptions of the weather, which can be difficult to gauge from dispersed weather stations. The final decision on whether, what, and when to evacuate buildings is always made by the group from the avalanche team. Various factors influence whether the group makes good decisions, for example uncertainty in weather forecasts, hidden or unknown weak layers in older snow, group dynamics and experience, and how effectively team members communicate and log valuable information. Active avalanche monitoring and evacuations are always subject to uncertainties, and on few occasions, disaster has been narrowly avoided, such as in Flateyri in 2020 and Neskaupstaður in 2023.

The construction of new defense structures and the improvement of older ones with known weaknesses is the most important step in enhancing the safety of residents living in avalanche-prone areas. The challenge for society, once this development is completed, will be to recognize when extreme conditions arise and to ensure that people remain aware of the residual risk that can occur below the protection measures.

LIST OF REFERENCES

- Hákonardóttir, K. M., Lárusson, R., Kristjánsson, Á., and Pétursson, G., 2024. Loading on structures from fluidized avalanche fronts overflowing deflecting dams at Flateyri, Iceland, January 2020. In: Gisnås, K. G., Gauer, P., Dahle, H., Eckerstorfer, M., Mannberg, A., Müller, K. (eds.), Proceedings of the International Snow Science Workshop ISSW 2024, Tromsø, Norway, 23–27 Sept. 2024, Montana State University.
- Hilmarsson, Ó., Jóhannesson, T., and Grímsdóttir, H., 2020. Snjóflóðin úr Skollahvilft og Innra-Bæjargili 14. janúar 2020 [The snow avalanches from Skollahvilft and Innra-Bæjargili on 14 January 2020; In Icelandic], Report 2020-010, Icelandic Meteorological Office, Reykjavík.
- Jóhannesson, T., Hansson, G., Ingólfsson, Ö., Brynjólfsson, S., Jónsson, M. H., Hilmarsson, Ó., Grímsdóttir, H., 2019. Snow avalanches hitting deflecting and catching dams in Iceland 1997–2018, In Jóhannesson, T., Gauer, P., Hákonardóttir, K. M., Margreth, S., Pálsson, H., Sigtryggsdóttir, F. G., (eds.), International Symposium on Mitigative Measures against Snow Avalanches and Other Rapid Gravity Mass Flows Siglufjörður, Iceland, April 3–5, 2019, 132–139, The Association of Chartered Engineers in Iceland, Reykjavík.
- Jóhannesson, T., Grímsdóttir, H., Hákonardóttir, K. M., Brynjólfsson, S., Hilmarsson, Ó., Jarosch, A. H., 2024. Lessons from several avalanches impacting avalanche protective structures in Iceland in January 2020 and March 2023. In: Gisnås, K. G., Gauer, P., Dahle, H., Eckerstorfer, M., Mannberg, A., Müller, K. (eds.), Proceedings of the International Snow Science Workshop ISSW 2024, Tromsø, Norway, 23–27 Sept. 2024, Montana State University.

Guidelines and digital toolboxes for mitigation measure planning and assessment from an Austrian perspective

Felix OESTERLE ^{1*}, Matthias GRANIG ², Paula SPANNRING ¹, Anna WIRBEL ¹, Jan-Thomas FISCHER ¹ and Christian TOLLINGER²

¹ Austrian Research Centre for Forests, Innsbruck, AUSTRIA
² Austrian Torrent and Avalanche Service, Innsbruck, AUSTRIA
*Corresponding author, e-mail: felix.oesterle (at) bfw.gv.at

ABSTRACT

Consistent and effective avalanche hazard and risk mitigation depend on technical guidelines, reliable tools, and best practice approaches. New, official norms, digital toolboxes, and supplementary recommendations for the planning and evaluation of avalanche mitigation measures are used to illustrate Austria's approach. These include everything from how to assess and plan mitigation measures (like dams, steel snow bridges, and so on) to how to use common simulation tools. Further, we provide an explanation of the significance of this unified approach for decision makers, planning entities, and the general public. To support this approach, we introduce the digital toolbox AvaFrame and its tools, demonstrating the potential to assist practitioners in the development of mitigation strategies. As an example, we look at how our thickness integrated avalanche simulation tool AvaFrame::com1DFA could be used for evaluating the effectiveness of release mitigation with steel snow bridges. Lastly, we discuss the applicability of simulation tools operated for protection forest assessment and management on a local and regional scale, specifically the AvaFrame::com4FlowPy module.

1. INTRODUCTION

Avalanches are among the rapid mass movements that can cover large distances and develop enormous destructive potential. Protective measures are therefore critically essential to prevent damage. As they mostly occur at exposed locations and often at high altitudes, they must meet strict criteria regarding strength, robustness, and safety factors. To support planning and assessments, a unified approach is propagated in Austria, and common tools and guidelines are provided.

2. MOTIVATION/EXPLANATION FOR UNIFIED APPROACH

Our unified approach to hazard mapping, including the planning and assessment of protection measures, offers significant advantages for decision-makers, planners, and the public. It establishes clear, standardized parameters grounded in existing scientific and industry norms. The main points of the Austrian approach are:

- Norms and guidelines are provided, giving clear advice on the applicability of tools.
- Norms and guidelines give strategies and formulas for dimensioning and planning of mitigation measures.

Felix Oesterle and others

O3.1 - Page 66

- Methodologies for determining input information (for example release height in the case of avalanches) are given.
- Necessary data are provided, or the method to obtain them is described.
- Digital simulation tools are provided with a standard set of model/input parameters.

We see the following benefits: it ensures consistency and reproducibility through transparent logs of inputs, adjustments, and methodologies. It promotes fairness and equity as all stakeholders (public, private, and research) are evaluated against the same standards. And it minimizes unsubstantiated changes as results are easily comparable across projects/institutions with discussions concentrating on core issues.

Of course, drawbacks and limitations exist: general configurations cannot cover every possible circumstance (prioritizes reliability for the majority). It requires significant effort/resources: model assumptions need constant (re)evaluation and setting to accepted values. And it mandates accessibility: all stakeholders require access to tools (or simplified versions), documentation, and training.

The following sections discuss tools that are used in the Austrian approach, starting with the Austrian Standard Norm B4801—Technical Avalanche Protection.

3. AUSTRIAN STANDARD: NORM B4801

The Norm B4801 came into force on October 1, 2024, with the goal of establishing uniform terminology for the planning, structural design, construction, and maintenance of protective structures within permanent technical avalanche protection. Although the norm is not legally binding because it is not a law, it is the de facto standard to which all stakeholders should adhere. To date, B4801 is the first standard in the European Union to comprehensively cover technical avalanche protection from the starting zone to the runout zone (forestry-biological measures and technical building protection are not included). However, parts of it are based on preexisting work and research. For example, the Swiss guideline "Lawinenverbau im Anbruchgebiet" by Margreth (2007) served as the authoritative basis for the chapter about avalanche starting zone protection structures.

At the beginning of the standard, general terms and fundamentals are defined. Subsequently, the different requirements and measures are described in detail. Focus was placed on the most common state-of-the-art measures.

Further topics covered are:

- Specific procedures for structure height dimensioning and foundation design.
- Snowdrift protection structures as well as glide snow protection measures.
- Temporary technical avalanche protection. This regulates requirements in the planning and approval phase for stationary avalanche triggering systems anchored in place via foundations.
- Dimensioning concepts for avalanche deflection and catching structures .
- Avalanche galleries.
- Inspection and maintenance strategy to keep structures functional and protective for as long as possible.
- Maintenance management

4. ADDITIONAL GUIDELINES

In addition to the norm, Tollinger et al. (2024) provide an operational guide (German: Praxisleitfaden Lawinen). This guide outlines the avalanche modeling workflow used in the operational service of the Torrent and Avalanche Control (WLV). It (a) aims to provide an overview of avalanche calculations and to serve as a decision-making aid. (b) Acts as a quality assurance tool for handling avalanche simulations within the department and for external collaborations. (c) Makes the procedures and protocols used within the WLV transparent and accessible. It is constantly being reevaluated and updated regarding emerging topics or adjusted to new tools and data. The guide describes the avalanche modeling procedure within the WLV, which is typically carried out on a catchment-area basis with the following topics covered in the guideline:

- Preparatory work including (a) Data Collection, (b) Data Analysis and Evaluation, and (c) Preparation for Modeling
- Model/Tool Application with (a) Avalanche Simulation, (b) Result Interpretation/Documentation
- Data Utilization with (a) Further Application and (b) Documentation
- Additional section in which standardized snow statistics data are provided

5. DIGITAL TOOLBOX AVAFRAME

The AvaFrame digital toolbox (Oesterle, 2025) has tools to handle tasks within the unified approach. In 2020, development began on this project as a joint effort between the Austrian Avalanche and Torrent Service (Wildbach- und Lawinenverbauung; WLV) and the Austrian Research Centre for Forests (Bundesforschungszentrum für Wald; BFW). Since early 2023, the first version of AvaFrame has been available for practical use. AvaFrame provides planners with a toolbox of avalanche models that preserves 20 years of avalanche simulation knowledge while continuously incorporating the latest developments. Thanks to its various modules, ranging from general pre- and postprocessing, modeling and simulation modules to visualization and analysis tools, it enables (end) users to complete many tasks. For all modules, a standard setup is provided. Tools used in operations at the WLV are accessible via a GUI for end users, in which the adjustability of inputs is pared down to a minimal set. However, power users or scientific user can adjust all available parameters. As one example, case studies furthering process knowledge need full flexibility. The toolbox's open source framework status (licensed under the European Union Public License (EUPL)) is a crucial factor making it available to the general public.

5.1 Practical application: scenarios with dense flow model AvaFrame::com1DFA

AvaFrame::Com1DFA is a module for dense flow (snow) avalanche computations (DFA). Calculations are based on the thickness integrated governing equations and solved numerically using a particle-grid method that relies on the smoothed particle hydrodynamics (SPH) method (Tonnel, 2023). Approximations of processes such as entrainment and additional resistance (for example through forests) can be included. One of the ways this module is used in Austria in relation to mitigation measures is the definition of scenarios. This allows for comparisons of simulated setups, for example one with a forest and one without a forest, or scenarios in which different release heights are used. At the time of writing, the recommendation for a simple approach to the generation of scenarios regarding the assessment of snow steel bridges is still

Felix Oesterle and others

O3.1 - Page 68

being developed. The approach currently favored is using half of the original design event release heights within areas with snow bridges. In any case, AvaFrame provides visualization and analysis tools in which these different scenarios can be compared in a quantified manner. It thereby offers more comprehensive and concrete information than just a simple visualization of fields in GIS – software. This gives the user additional information and various visualizations for a more informed decision-making process.

5.2 Practical application: protective forest via AvaFrame::com4FlowPy

Lastly, we discuss the AvaFrame::com4FlowPy module operated for assessment and management of protective forests on a local and regional scale. Com4FlowPy is an empirically motivated simulation tool for gravitational mass flows (GMF), such as snow avalanches. The model simulates runout distance and intensity based on the runout-angle concept (Heim, 1932) and a raster-based routing routine for modeling lateral process spreading. Simulations can be used to identify process areas (paths and runout zones) and corresponding intensities of the respective GMFs (e.g. Huber et al., 2024).

Com4FlowPy was used to generate a map of protective forest for all of Austria (Fig. 1; available online). It is based on simulations of rockfall, snow avalanches, and near-surface landslides combined with data on forests and endangered objects, including settlements, roads, and other important infrastructure. It serves as a tool for forest assessment and management decisions.

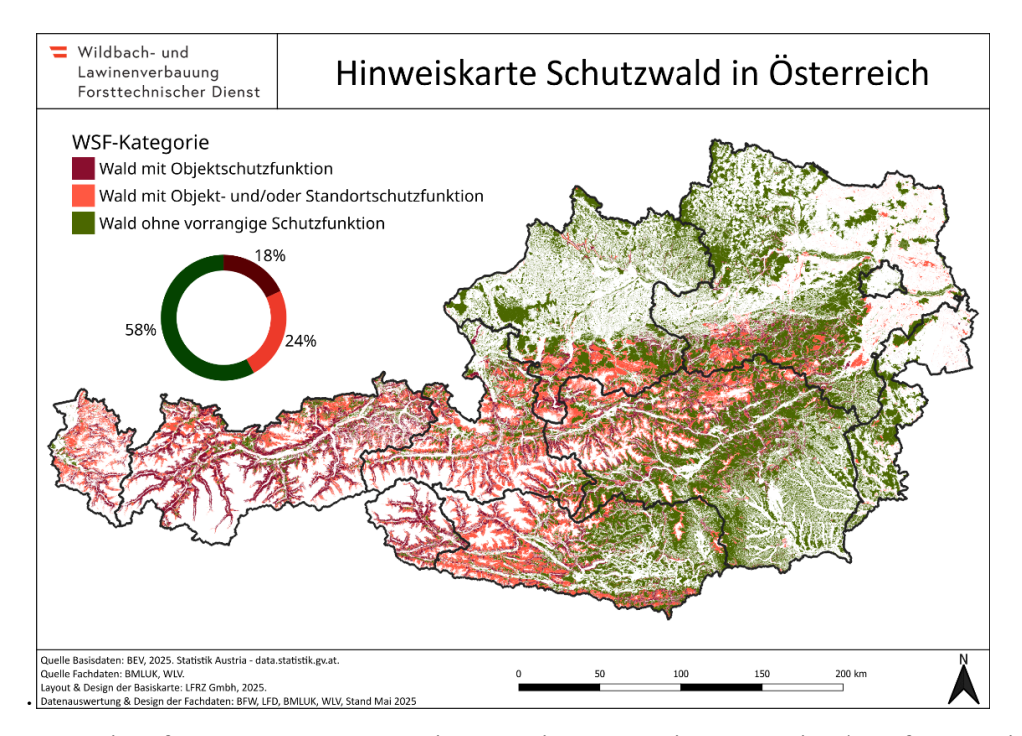


Fig 1: Protective forest coverage map in Austria. Forest is categorized as forest with object-protective function (dark red), forest with object-protective or site-protective function (light red) and forest without primary protective function (green). Available at https://www.protective-forest.at/maps.html.

6. CONCLUSIONS

We propagate the use of a unified approach for hazard mapping, planning, and assessments of mitigation measures. Cornerstones of such an approach include a clear communication of accepted norms and guidelines, available simulation tools with standard parameter sets, and well defined approaches to various stages of such a process. While prioritizing reliability for most scenarios through validated inputs and minimizing subjective adjustments, it allows justified deviations in edge cases based on expert assessment. The approach's success relies on comprehensive documentation, traceability, accessible resources, and continuous effort to keep it up to date. As part of the approach, Norm B4801 establishes the first comprehensive EUwide standard for technical avalanche protection, providing unified terminology and detailed information on requirements for planning, design, construction, and maintenance regarding all parts of an avalanche track. While not legally binding, it serves as the essential de facto standard, consolidating decades of experience and introducing unified strategies and procedures for avalanche protection. In addition to the norm, practical guides give further advice on workflows for avalanche modeling. Another component, the open-source AvaFrame toolbox, standardizes avalanche simulations through preconfigured modules while offering tiered accessibility—from simplified GUI workflows for practitioners to full parameter control for experts. It allows for exploration of different avalanche scenarios, quantified assessment of potential differences including informative visualizations, and estimation of the effect of mitigation measures such as protective forests.

REFERENCES

- Heim, A., 1932. Bergstuerze und Menschenleben, in: Beiblatt zur Vierteljaehresschrift der Naturforschenden Gesellschaft in Zuerich, Fretz & Wasmuth, Zuerich, CH.
- Huber, A., Saxer, L., Spannring, P., Hesselbach, C., Neuhauser, M., D'Amboise, C., Teich, M., 2024: Regional-Scale Avalanche Modeling with com4FlowPy Potential and Limitations for Considering Avalanche-Forest Interaction Along the Avalanche Track. In: Proceedings of the International Snow Science Workshop, Tromsø, 23-28 September, pp. 587-594.
- Margreth, S., 2007. Lawinenverbau im Anbruchgebiet. Technische Richtlinie als Vollzugshilfe. Umwelt-Vollzug Nr. 0704. Bundesamt für Umwelt, Bern, WSL Eidgenössisches Institut für Schnee- und Lawinenforschung (SLF), Davos.
- Oesterle, F., Wirbel, A., Fischer, J., Huber, A., Spannring, P., 2025. avaframe/AvaFrame: 1.12 (1.12). Zenodo. DOI: 10.5281/zenodo.4721446
- ÖNORM B 4801 Technischer Lawinenschutz Einwirkungen, Bemessung und Instandhaltung, 2024. Austrian Standards International, Wien.
- Tollinger, C., Granig M., Jenner A., Oesterle F., Siegele P., Hochreiter, H., 2024. Praxisleitfaden – für Lawinensimulationen in der WLV (v1.4). Bundesministerium für Landwirtschaft, Regionen und Tourismus, Wien.
- Tonnel, M., Wirbel, A., Oesterle, F., Fischer, J.-T., 2023. AvaFrame com1DFA (v1.3): a thickness-integrated computational avalanche module -- theory, numerics, and testing. Geoscientific Model Development, 16, 7013–7035. DOI: 10.5194/gmd-16-7013-2023

Felix Oesterle and others

O3.1 - Page 70

Numerical analysis of reinforced soil barriers subjected to avalanche dynamic loads

Oltion Korini^{1*} and Anthony Austin²

¹ Geoquest, 280 avenue Napoléon Bonaparte, 92500, Rueil-Malmaison, France
² Geoquest UK Solutions Ltd, Innovation House, Euston Way, Telford TF3 4LT, United Kingdom
*Corresponding author, e-mail: oltion.korini@geoquest-group.com

ABSTRACT

Avalanches may have devastating effects on human lives and infrastructure in mountainous areas. Reinforced soil barriers have been efficiently used to mitigate this risk, while having minimal influence on the landscape. The rapid loading nature of avalanches requires a dynamic analysis for a realistic design. This article presents a numerical analysis approach of reinforced soil barriers using Flac2D software. The avalanche load is applied as a pressure that is variable in time as per local design standards. Large deformations and inertial effects are considered by the software. The upstream facing of the structures consists of a welded steel mesh that is held in place by reinforcing strips that are embedded in the soil backfill. The mobilization of the reinforcements is monitored during the dynamic load application as well as the facing deformation. Two case studies are chosen to show the performance of reinforced soil barriers subjected to dynamic avalanche loads. It is observed that the load amplitude and duration have an important effect on the final deformed shape of the structure.

Keywords: reinforced soil barrier, dynamic load, avalanche protection, numerical modelling

1. INTRODUCTION

1.1 Background

Reinforced soil embankments are among the most efficient solutions for resisting avalanche loads due to their robustness and shock absorbing capacity. Traditionally, the design of such avalanche protection structures has relied on simplified approaches that consider the avalanche impact load as a static force (Barbolini et al., 2009; Margreth, 2007). This simplification treats the impact as a permanently applied pressure, which, while providing a conservative estimate in some cases, does not accurately represent the transient and dynamic nature of avalanche events. A real avalanche impact is a rapid phenomenon, with significant forces being applied and dissipated within a matter of seconds.

Numerical analysis has experienced a significant growth in the latest decades. Several software applications like Flac (ITASCA, 2024) and Plaxis (Bentley, 2024) are now available for performing dynamic analyses on reinforced soil barriers subjected to avalanche loads. Studies show that the response of the barrier subjected to a dynamic variable pressure is different compared to the case when the load is an equivalent pseudostatic one (Cuomo et al., 2020). Moreover, the dynamic pressure and duration of an avalanche load can vary depending on the terrain topography. This means that for each design case, a site-specific load needs to be determined.

O. Korini, A. Austin

1.2 Geoquest company technology

In the last years, Geoquest company (formerly Terre Armée) has designed several avalanche protection barriers located in the Nordic countries. The technology used consists of a facing with C-shaped welded steel mesh and connectors that transfer the loads to the steel strips embedded in the compacted soil. The backfill material is usually crushed stone processed from a local quarry, while at the facing are used larger stones with 100-200 mm diameter (Figure 1). All the metallic elements are galvanized and designed to resist during the lifetime of the structure.

Different configurations can be designed with the above-mentioned technology. The typical barrier has 1H/4V reinforced front slope and 2H/1V unreinforced back slope. However, a reduced width structure with back-to-back reinforcement is also possible. In some cases, splitter mounds are constructed uphill for reducing the avalanche energy before it reaches the main barrier. The splitter mounds have three reinforced facings due to their limited length.





Figure 1 Technology used in avalanche barriers of Geoquest

This article presents a numerical analysis approach for reinforced soil embankments used as avalanche barriers. The finite difference software Flac is used for this purpose and case studies are shown for illustration.

2. METHODOLOGY

Flac2D software uses a Lagrangian formulation meaning the computational grid deforms together with the material it represents. This allows the software to handle large deformations as it may happen in dynamic analyses. The Flac2D solver uses an explicit time integration that propagates forces and motion through the model elements. Although this operation is fast and does not require the creation of large stiffness matrices, the explicit solver needs a relatively low timestep to converge, which leads to a longer analysis time. In its dynamic formulation inertia components are added to the equilibrium equations.

The avalanche load is typically represented by a pressure diagram applied at the upstream facing of the barrier (Figure 2). The initial pressure (P_1) is usually several times higher than the following dynamic pressure (P_2) . The application time T_1 is generally quite short (< 0.1 s), while T_2 can be several seconds.

O. Korini, A. Austin

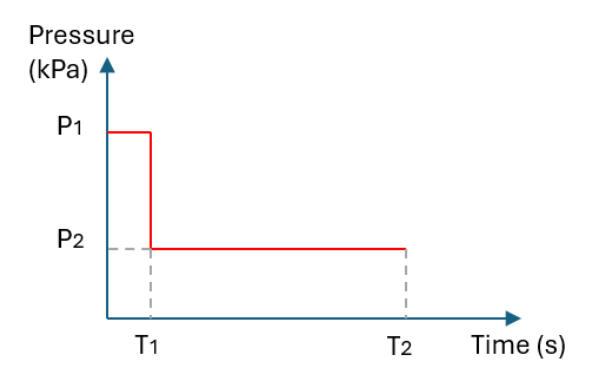


Figure 2 Typical avalanche load vs time used in the analyses

The analysis in Flac2D is performed in steps. Firstly, the structure is constructed and calculated layer by layer by installing each time the backfill soil, facing panel and reinforcement. In this way, the internal stresses and the mobilized tension in the reinforcement are more realistic. Then the peak load of the avalanche (P_1) is applied in the specified area of the barrier facing, while on the horizontal (or less steep surfaces) it is applied the vertical load of 2 m snow. The model is run up to time T_1 and then the peak load is replaced with the dynamic pressure (P_2) . At the last stage the model is run up to time T_2 keeping constant the pressure applied on the facing as per Figure 2.

3. ANALYSIS RESULTS

Two case studies are chosen to illustrate the numerical analysis of avalanche barriers using Flac software. The loads are different in each case as they depend on the terrain configuration and local design standards. They are summarized in Table 1 below.

TC 11 1	D	1 1 0.1	1	, 1'
Table 1	Llynamic	loade of the	chosen	case studies.
I abic i	Dynamic	ivaus of the	CHOSCH	case studies.

	Seyðisfjörður S2	Flateyri S21
	(14.5 m)	(13.8 m)
Pressure P ₁ (kPa)	370	416
Time $T_1(s)$	0.1	0.1
Position P ₁ (m)	0 - 2	2 - 3.5
Pressure P ₂ (kPa)	23	19
Time $T_2(s)$	20	20
Position P ₂ (m)	Full height	2 - 13.5

Both projects are located in Iceland and have similar loads. The Seyðisfjörður (section S2) has one reinforced facing, while the Flateyri (section S21) is a back-to-back case. The effect of dynamic loads on the barriers is monitored both on the soil and reinforcements.

3.1 Avalanche load propagation

The peak avalanche pressure (P_1) initiates a shock wave on the facing of the embankment, which is then spread and attenuated in the soil volume. The application time of the peak load is short (0.1 s) and its effect on the barrier is dissipated in less than a second. On the other hand, the dynamic pressure (P_2) acts for a longer time (20 s), but its amplitude is much lower and therefore not visible in the chosen output scale (Table 2).

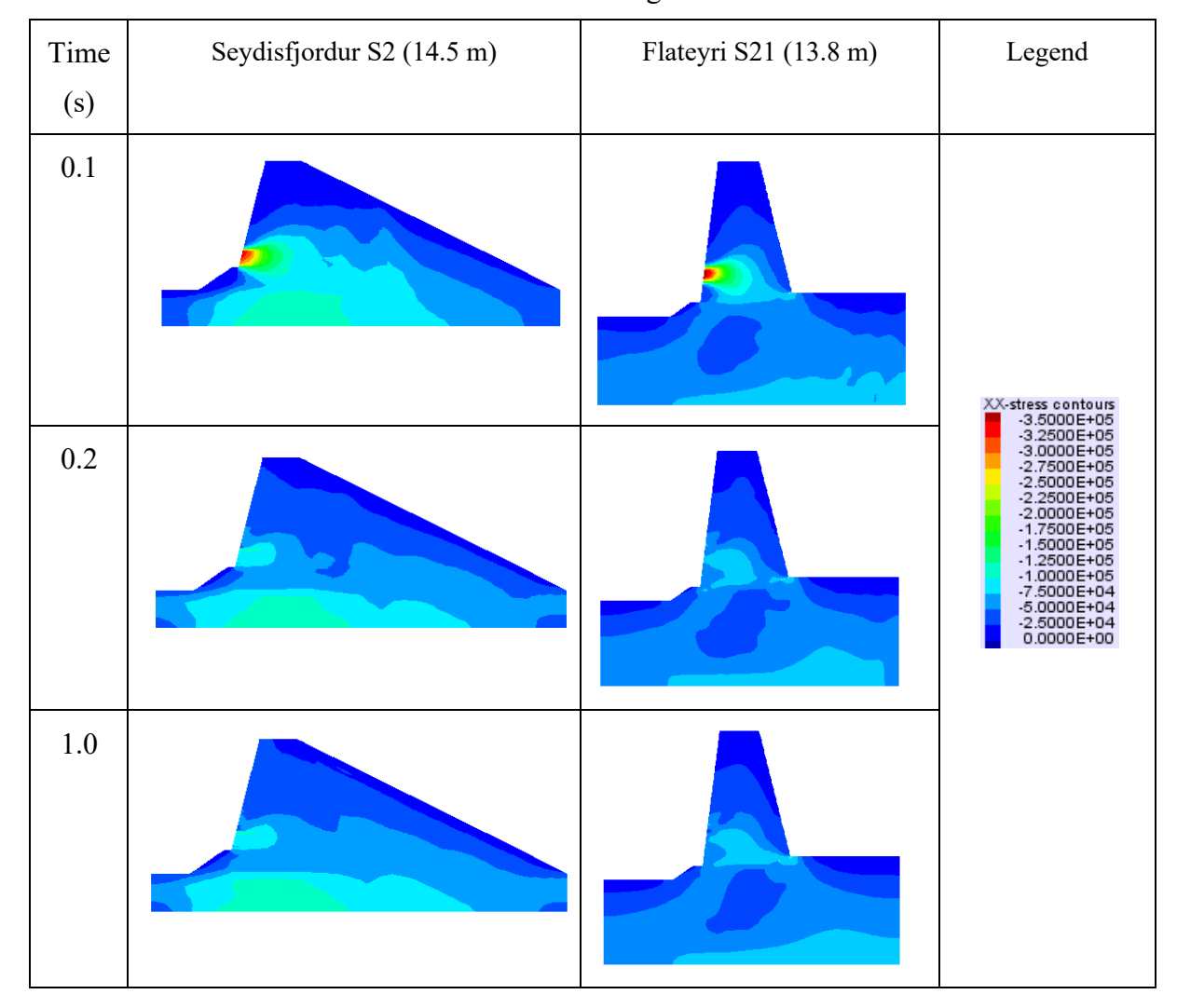


Table 2 Horizontal stresses on the barriers during avalanche load.

3.2 Displacements of the facing

Despite its amplitude, the peak load does not usually cause considerable deformation because the application time is quite short (0.1 s). On the other hand, the dynamic pressure (P_2) acts for a much longer time, so it is more able to cause permanent deformation on the structure. Most of the displacement caused by the peak load seems reversible and temporary. In addition, the peak load seems to affect only its application area (Figure 3).

The dynamic pressure starts to act after the peak load, and it applies on a greater area. The structure response due to this load depends on its robustness. For example, Seyðisfjörður section is stiffer compared to Flateyri and as such is less affected from the dynamic pressure. In fact, between the chosen sections the effect of the avalanche loads is inversed. The stiffer structure has a higher initial peak displacement and lower residual one, while the other has the opposite due to its flexibility. However, in both cases the amplitude of the displacements is in the range of few centimetres.

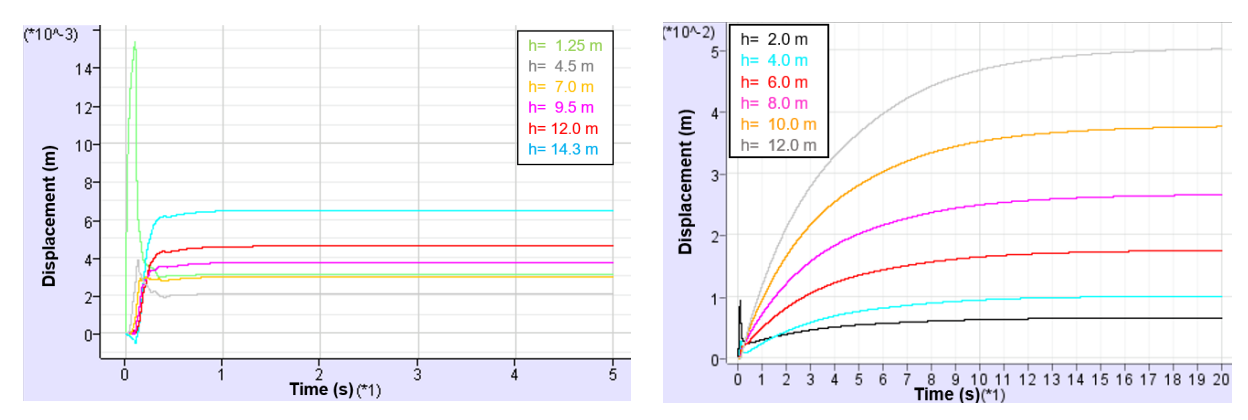


Figure 3 Front facing displacements at different levels for Seyðisfjörður (left) and Flateyri (right)

3.3 Tension on reinforcement

The avalanche load is applied at the facing and then it is transmitted to the reinforcements. The most critical position is close to the facing, because further inside the barrier the load is dissipated in the soil. The reinforcement is sensitive to the peak load, which is governing the reinforcement design. Usually, the initial design is done using static loads and then it is checked in dynamic analysis. There are cases where the strip density is increased in the zone of peak load application after the dynamic modelling.

As shown in Figure 4, the maximal tension on the strips occurs during the peak load (0.1 s). The removal of the peak load causes a reverse loading due to soil inertia in the opposite direction.

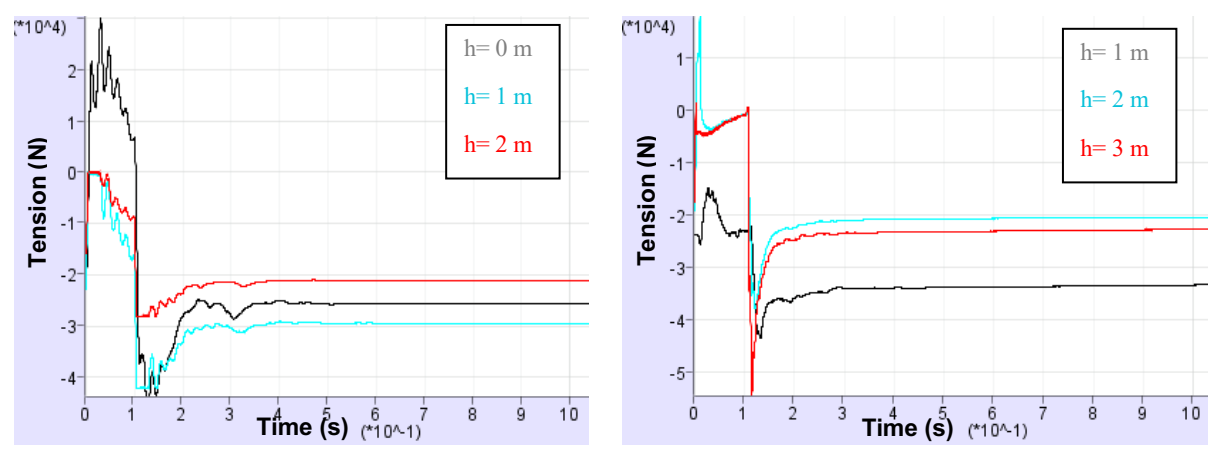


Figure 4 Reinforcement tension at different levels for Seyðisfjörður (left) and Flateyri (right) during the initial peak load

4. CONCLUSIONS

This article presents the technology of reinforced soil barriers that Geoquest company uses as avalanche protection. The barriers are designed to withstand static and dynamic loads using advanced numerical tools such as Flac2D software. Examples of avalanche barriers with just the front facing reinforced and back-to-back reinforcements are shown above. Based on the numerical analyses it results that the barrier's behaviour under dynamic loading is strongly related to their section width.

The numerical analyses using Flac2D software allows for an in-depth understanding of reinforced soil structures subjected to dynamic loads. The application of dynamic load as a pressure that varies with time, is a more realistic approach compared to pseudostatic analysis. Through modelling it is shown that the initial peak load has not an important effect on the deformation of the structure because its application time is quite short. On the other hand, the peak load is directly affecting the reinforcements tension, and it governs their design.

The Geoquest company is endorsing the use of sophisticated numerical approaches for dynamic loads such as avalanches. This allows for a more optimized and accurate design thus allowing material quantities to be minimised.

REFERENCES

- Barbolini, M., Domaas, U., Faug, T., Gauer, P., Hakonardottir, K.M., Harbitz, C.B., Issler, D., Johannesson, T., Lied, K., Naaim, M., 2009. The design of avalanche protection dams Recent practical and theoretical developments. Brussels, Directorate-General for Research, Environment Directorate, European Commission, Publication EUR 23339, 195 pp., doi: 10.2777/12871.
- Bentley, 2024. Plaxis2D. [Software]. https://www.bentley.com/software/plaxis-2d/
- Cuomo, S., Moretti, S., Frigo, L., Aversa, S., 2020. Deformation mechanisms of deformable geosynthetics-reinforced barriers (DGRB) impacted by debris avalanches. Bull. Eng. Geol. Environ. 79, 659–672.
- ITASCA, 2024. Flac2D. [Software]. https://itascasoftware.com/products/flac2d/
- Margreth, S., 2007. Defense structures in avalanche starting zones: Technical guideline as an aid to enforcement. Environment in Practice no. 0704. Bern, Federal Office for the Environment FOEN; Davos, WSL Swiss Federal Institute for Snow and Avalanche Research SLF, 134 pp.

Monitoring Umbrella Nets – A Full-Scale Testsite in Tirol, Austria

Engelbert Gleirscher^{1*}, Anselm Köhler¹, Matthias Granig², Michael Brauner³

¹ Federal Research Centre for Forests (BFW), Institute for Natural Hazards, Department of Snow and Avalanches, Hofburg – Rennweg 1, A-6020 Innsbruck, Austria

² Avalanche and Torrent Control, Wilhelm-Greil-Straße 9, A-6020 Innsbruck, Austria

³ ÖBB Infrastructure AG, Lassallestraße 5, A-1020 Vienna, Austria

*Corresponding author: engelbert.gleirscher@bfw.gv.at

ABSTRACT

Umbrella-shaped net structures are a possible solution for mitigating snow creep and stabilizing smaller gullies and slopes in alpine terrain. Unlike conventional anvalanche release protection systems, these flexible installations rely on a single uphill anchorage, offering advantages in adaptability and ease of installation. Despite their increasing deployment, empirical data on actual loading and structural performance remain limited. To address this, a full-scale testsite was established in the Axamer Lizum region (Austria), equipped with four umbrella net systems and a comprehensive force monitoring setup.

During the 2023–2024 winter season, tensile and compressive forces were recorded at 15-minute intervals using load shackles and base plate sensors. Snow height data were reconstructed from a nearby weather station and calibrated using manual measurements at the testsite. Guideline-based force estimates were calculated from snow height and density to be compared with the measured values. While maximal calculated forces generally exceeded measurements, the difference was largest in edge fields. A notable temporal offset between peak snow depth and peak force suggests significant influence of snow creep and settlement after snowfall and during warmer periods. These findings highlight the importance of ongoing refinements of design assumptions, site-specific snowpack assessment, and continued monitoring for improving the reliability and safety of umbrella net systems.

1. INTRODUCTION

Umbrella-shaped net structures (umbrella nets) are an innovative protective measure for mitigating snow creep and stabilizing smaller gullies and slopes in alpine terrain. Unlike conventional release protection systems, described for example in Rudolf-Miklau and Sauermoser (2015), umbrella nets are anchored by a central attachment point and two floormounted support piles. This offers high flexibility with simple and therefore cost-effective installation requirements. However, their application as snow retention systems is still at an early stage, with limited operational experience and scarce empirical data on actual load magnitudes and failure modes. Some previously installed umbrella nets have exhibited damage requiring repairs, attributed to overloading from snow accumulation. This raises important questions about their structural performance, long-term durability and maintenance needs. A critical drawback of umbrella net systems is their reliance on a single anchorage point: failure of this anchorage would result in total system failure, unlike conventional structures with multiple supporting elements.

E. Gleirscher et al. O3.3 - Page 77

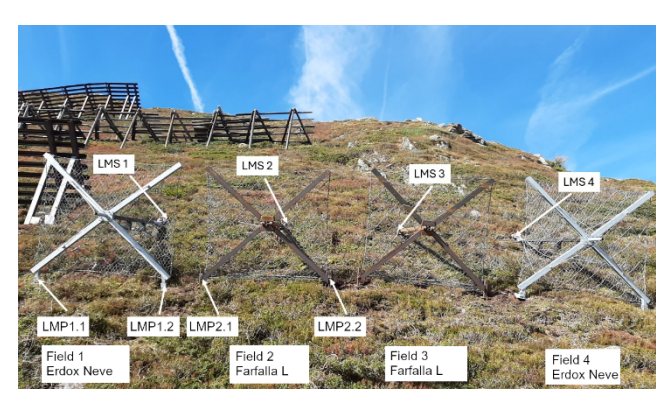




Figure 1 left: Overview of the testsite with some of the installed force gauges, note the existing protection structures on the left side. right: Picture at time of maximal snow height showing the uneven snow distribution across the testsite.

Previous research on snow retention structures in release zones includes measurements on both rigid and flexible systems. Studies such as Margreth (1995), Nicot et al. (2002), Platzer et al. (2004), Rainer et al. (2008), and Gleirscher et al. (2018) examined flexible net structures, while Hiller and Bader (1990) and Borner et al. (2024) focused on rigid installations. These measurements are essential for calibrating and improving guideline-based design approaches such as ÖNORM B 4801 or Margreth (2007). The primary objective of this study was to instrument and monitor a dedicated testsite of umbrella nets in the Axamer Lizum area during several winter seasons. By systematically recording the forces acting on the structures and documenting snowpack development, the project aimed to provide empirical evidence for design criteria and to identify potential improvements for monitoring techniques and the guideline estimations.

2. METHODS

2.1 Testsite and Structures

The testsite was set up near the Pleisen summit in the Axamer Lizum ski area at an elevation of approximately 2080 m, see Figure 1. Four umbrella nets were deployed, including two FARFALLA L models and two ERDOX Neve systems provided by the manufacturers Mair Wilfried GmbH and Betonform GmbH. Each net was anchored to a micropile foundation with both tensile and compressive anchors. The unique configuration allows the nets to function under a combination of snow creep forces and settlement pressure. The effective net height of both systems is 3 m. The net width measures 3.25 m for the FARFALLA system and 3.6 m for the ERDOX system. The ERDOX nets were specifically installed at the lateral positions of the testsite, as these units were delivered in a reinforced configuration suitable for edge placement. The spacing between adjacent net structures is approximately 0.5 m. On the orographic right-hand side, the installation is bounded by an existing protection structure at a distance of 2.4 m. In contrast, the orographic left-hand edge opens toward an unconfined snow field, see Figure 1.

2.2 Instrumentation

The testsite was equipped with a sensor setup to monitor snowpack development and structural response. The core force measurements focused on four load shackles (LMS, SHK B 55T, Althen GmbH) measuring tensile forces at the upper anchor points of each net, and four load pins (LMP, LAUMAS Elettronica S.r.l.) installed at the base plates of the two orographically right-side nets to record vertical compressive forces.

Additional instrumentation includes strain gauges on selected ropes and environmental sensors (e.g., air temperature, humidity, and wind). In this publication, we focus exclusively on the load measuring shackles (LMS) and load measuring pins (LMP) datasets, which provided the most direct insights into structural loading. The other sensors served to complement the understanding of environmental conditions and are used for ongoing verifications.

2.3 Data Acquisition and Analysis

All sensor signals are recorded using a Campbell CR1000X data logger at a 15-minute interval. Time-lapse images are captured at the same interval using a Canon EOS 2000D digital camera, providing visual context for sensor data. Measurements were conducted during the winters of 2023–2024 and 2024–2025. However, the analysis here focuses on the 2023–2024 season with still below average, but higher snow heights than the later one. Consequently, the resulting forces in the structure were larger and therefore of higher interest.

3. RESULTS AND DISCUSSION

3.1 Snowpack parameters

During the 2023–2024 winter season, no automated snow depth sensor was installed directly at the testsite. Therefore, snow height was reconstructed based on data from a nearby weather station (Speicherteich, Kühtai, 2103m). Several manual measurements at the testsite were used to calibrate this external dataset, and assign a different snow height for the testsite. Scaling factors were derived for days with available manual data and interpolated to generate an adjusted snow height time series. This series was used as the basis for the force calculations. Snow density values were obtained from manual snow profiles recorded at selected dates. These values, ranging between $280 \, \text{kg/m}^3$ and over $500 \, \text{kg/m}^3$, were interpolated to generate a continuous density evolution over the season. Both snow height and snow density were varied by $\pm 10\%$ in the force calculations in accordance with the Austrian guideline ÖNORM B 4801 to account for potential measurement uncertainties and spatial variability.

3.2 LMS - measurements

The LMS recorded tensile forces at the upper anchor points of each net system. During the 2023–2024 winter season, the sensors provided reliable and high-resolution data on structural loading across the different net fields, see Figure 2. The highest tensile force was observed in LMS 4, reaching approximately 120 kN, while center nets exhibited values between 50–70 kN (LMS 2/3). In contrast, LMS 1 reaches maximal values mostly below 50 kN. These lower values are attributed to reduced snow accumulation and the influence of the adjacent existing structural protection on the orographic right-hand side, which likely constrained snow loading in this zone. These differences reflect both the snow accumulation pattern as shown in Figure 1 and the influence of boundary conditions of each field. Particularly notable was the delayed onset of peak tensile force compared to maximum snow depth, suggesting the increasing relevance of new snow settling and snow cover creep in late winter. Until February, snow accumulation had little effect on the measured forces. From February onward, however, forces increased more markedly. This pattern is consistent with higher temperatures during late winter, making snow creep a plausible contributing factor. A notable temporal lag of around one week between peak snow height and peak force further supports this interpretation.

E. Gleirscher et al. O3.3 - Page 79

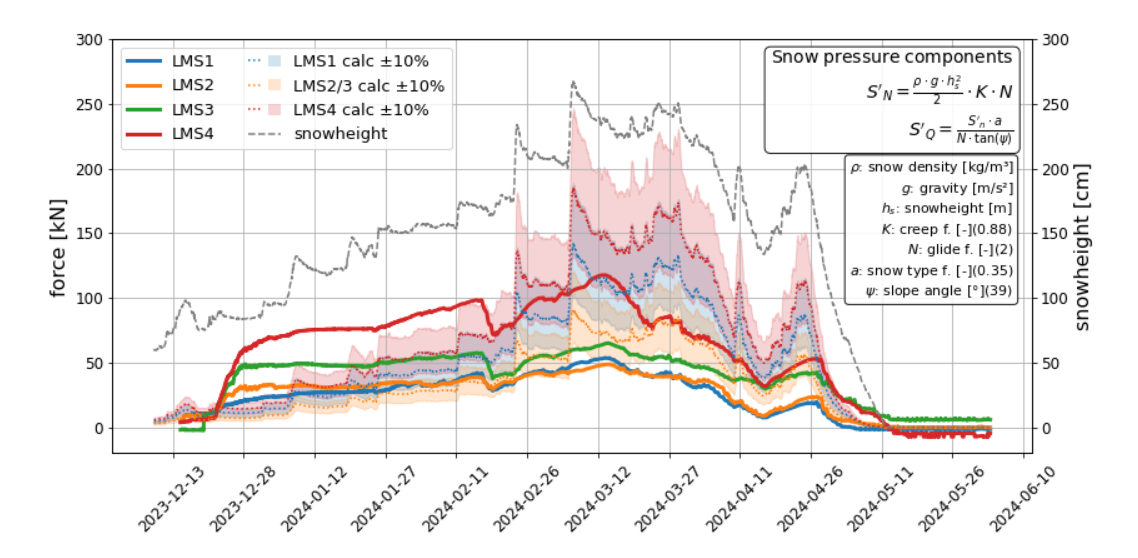


Figure 2 Measured and calculated tensile forces in the shackels of the umbrella systems over the winter period 2023-2024.

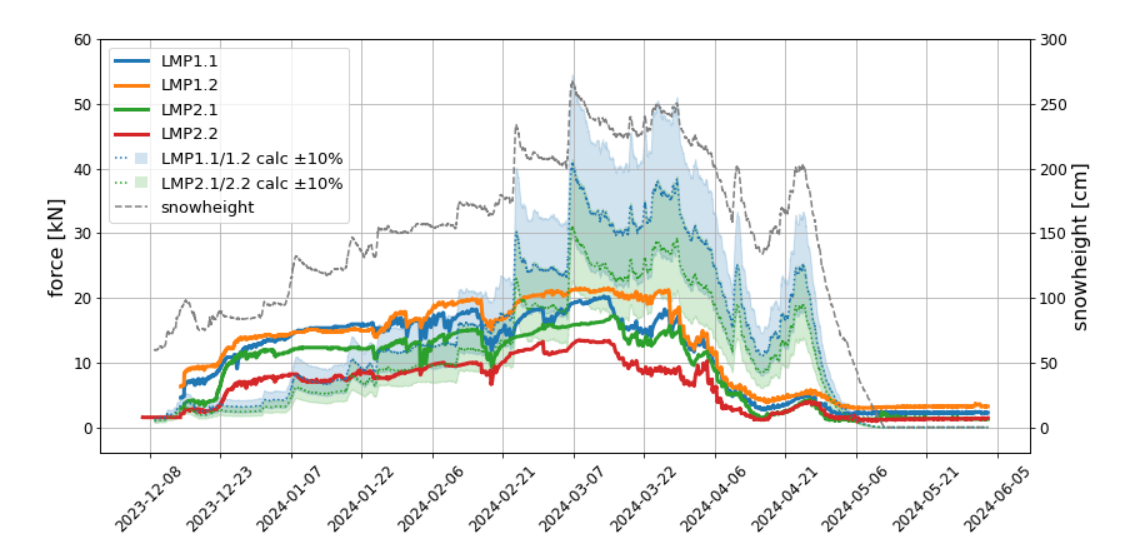


Figure 3 Measured and calculated normal forces in the load pins of the umbrella systems over the winter period 2023-2024.

3.3 LMP – measurements

The LMP were installed at the base plates of the two nets located on the orographic right-hand side. These sensors measure the normal force transmitted through the support foundations to the ground surface, resulting from both the dead load and the snow load. The highest normal forces were observed in the edge field sensors (LMP 1.1 and LMP 1.2), which is attributed to boundary effects and reduced lateral support for the edge field. Maximum measured values across all sensors ranged between -13 kN and -22 kN. Given the baseplate dimensions of 30 × 30 cm for the ERDOX Neve system and 24 × 24 cm for the FARFALLA L system, the resulting surface pressures were calculated between 150 kN/m² and 380 kN/m², respectively. These values reflect the localized ground loads transmitted by the foundation under varying snow conditions and structural geometry, as shown in Figure 3.

3.4 Comparison Measured Forces - Guidelines

The measured LMS forces were compared with snow-load-based force estimations derived according to the Austrian guideline ÖNORM B 4801, which incorporates the calculation scheme proposed by Margreth (2007). Based on the formulas for snow pressure, and considering the geometric configuration of the structures including edge effects, the resulting forces in the respective sensors were derived, see Figure 2 and 3. For this purpose, snow height and snow density were varied ± 10 % from the assumed value to account for uncertainties, resulting in a force range depicted as shaded bands. The comparison shows that calculated forces reach up to ~200 kN in the most exposed edge fields, whereas the maximum measured force was approximately 120 kN. More specifically, measured peak values were ~50 kN in Field 1, 50-70 kN in Fields 2 and 3, and ~120 kN in Field 4. Corresponding calculated maximum values were ~140 kN for Field 1, ~90 kN for Fields 2 and 3, and ~180 kN for Field 4. Thus, the calculated peak forces exceeded the measured values in all cases, with the largest discrepancy observed in the edge field (Field 4). Notably, the peak force did not coincide with the maximum snow height but occurred later in the season, likely due to snow creep effects, which intensify under higher temperatures. The edge field LMS (LMS 4) showed significantly higher values than the central sensors, due to increased snow accumulation and reduced lateral restraint at the free boundary.

Forces normal to the slope from LMP measurements were available from the orographic right-side nets. Here, the calculation was based on geometrical relationships between the force in the shackles and the force in the pins, assuming symmetric load transfer onto the two base plates. The comparison shows that the maximum measured compressive forces were approximately half of the calculated ones — consistently observed for both Field 1 (LMP 1.1 and 1.2) and Field 2 (LMP 2.1 and 2.2). This indicates that either the assumptions regarding load transfer might overestimate the ground reaction or that not all calculated load components fully reach the foundation due to redistribution within the structure. Conversely, at lower snow heights during early winter, both LMS and LMP calculations underestimated the measured forces. This can partly be attributed to the omission of dead load and to discrepancies between assumed and actual snow height at the testsite.

3.5 Discussion of Variability and Structural Implications

During the early winter until February, measured forces increased steadily without distinct peaks, despite noticeable snow accumulation events. This suggests that low temperatures may have suppressed snow creep, resulting in gradual loading only. From February onward, forces rose more sharply and coincident with new snow events, likely due to higher temperatures and increased creep effects. As no continuous snow height measurements were available directly at the testsite during the 2023–2024 season, snow depths were derived from a nearby station and calibrated with occasional on-site measurements. This introduces uncertainty in the calculated forces. To reduce this limitation, we are currently developing a method to extract snow height data from time-lapse images. This approach aims to provide more accurate, site-specific snow height inputs for each net structure for load estimations.

4. CONCLUSIONS

The measurement campaign, which is designed to cover several measurement periods to capture different relevant load situations, has already delivered preliminary but interesting results in its first season. The monitoring of umbrella net structures under real snow load conditions revealed

E. Gleirscher et al. O3.3 - Page 81

systematic deviations between measured and calculated forces. While the guideline-based estimations (ÖNORM B 4801) lie on the conservative side, they tend to overestimate the actual structural loads—especially in edge fields. This indicates that current design assumptions may not fully reflect the real load transfer mechanisms, particularly under time-dependent effects such as snow settlement and creep. The observed delay between maximum snow depth and peak structural loads further highlights the influence of snowpack behavior on load development. These findings underscore the value of continuous in-situ monitoring for capturing complex loading processes.

To reduce uncertainties in future calculations, we are developing methods to extract snow height directly from image data. The insights gained from this project provide a robust basis for improving practical design approaches and may inform future adjustments to normative frameworks governing flexible protective structures in alpine terrain.

ACKNOWLEDGEMENT

The authors acknowledge the valuable support of Mair Wilfried GmbH and Betonform GmbH for providing the structures, Axamer Lizum GmbH for granting access to the testsite. Special thanks go to all project partners and technical staff involved in the installation and maintenance of the testsite.

REFERENCES

- Borner J., Rusterholz P., Margreth S., Bartelt P. (2024) Measuring snow pressure forces on supporting structures using low-cost strain gauges. In K. Gisnås, P. Gauer, H. Dahle, M. Eckerstorfer, A. Mannberg, & K. Müller (Eds.), Proceedings of the international Snow Science Workshop 2024. Oslo: Norwegian Geotechnical Institute. 1127-1132.
- Gleirscher, E., Kofler, A., Gigele, T., Graf, A., Granig, M., & Fischer, J.-T. (2018). Monitoring forces in steel wire rope nets: Evaluation of short and long term influences. Proceedings of the International Snow Science Workshop (ISSW), Innsbruck, Austria, pp. 139–142.
- Hiller, M. and Bader, H.: Schneedruck auf Stützwerke, Tech. rep., WSL Institute for Snow and Avalanche Research SLF, Interner Bericht Nr. 660, 1990
- Margreth, S. (1995). Snow pressure measurements on snow net systems. In: Proceedings of the ANENA Symposium, Chamonix, May 30–June 3, pp. 241–248.
- Margreth, S. (2007). Lawinenverbau im Anbruchgebiet. Technische Richtlinie als Vollzugshilfe. Umwelt-Vollzug: Vol. 0704. Bern; Davos: Bundesamt für Umwelt (BAFU); WSL Eidgenössisches Institut für Schnee- und Lawinenforschung SLF.
- Nicot, F., Gay, M., and Tacnet, J. (2002). Interaction between a snow mantel and a flexible structure: a new method to design avalanche nets. Cold Regions Science and Technology, 34(2):67–84
- Platzer, K., Mears, A., Margreth, S. (2004). Guidelines for the design and construction of flexible avalanche protection systems made of wire rope nets. In: ISSW 2004 Proceedings, Jackson Hole, Wyoming, pp. 545–553.
- Rainer, E., Rammer, L., and Wiatr, T. (2008). Snow loads on defensive snow net systems. In International Symposium on Mitigative Measures against Snow Avalanches Egilsstadhir, Iceland
- Rudolf-Miklau, F., Sauermoser, S., Mears, A. (2015). The Technical Avalanche Protection Handbook. Wien: Federal Ministry for Agriculture, Forestry, Environment and Water Management (BMLFUW).

HELIOPLANT® – PV structure in avalanche protection

Alexander Ploner^{1*}, Thomas Sönser² and Florian Jamschek³

1.2 i.n.n. ingenieurgesellschaft für naturraum-management mbH & CoKG, Maria-Theresien-Straße 42a, 6020 Innsbruck, AUSTRIA

3 ehoch2 energy engineering e.U., Flösserweg 17, 6423 Mötz, AUSTRIA

*Corresponding author, e-mail: alexander.ploner (at) inn.co.at

ABSTRACT

The vertical tree-like structure of HELIOPLANT® and the selected spacing ensure that the vertex effect interrupts the redistribution of stress in the snowpack so that avalanches are no longer possible. A HELIOPLANT® field in an avalanche start area behaves like a secured highaltitude afforestation. The great advantage of this structure is that the cross shape of the wind field creates such turbulence even at low wind speeds that the system itself remains free of snow and a scour ring of transported snow forms at around 2 m from the outer edge of the module. Considering high wind speeds and an allowance for the transported snow, this results in a design load of approx. 3 kN/m² (ÖNORM B 4801). The support structure consists of four frames, which are mounted on a post. Each element has a total of 15 bifacial PV modules, which are aligned vertically. The cross-shaped structure ensures almost continuous solar radiation. The distances between the individual elements are set between 8-14 m depending on the exposure. Four IBO R38-500 nails or GEWI 40 are used to integrate the upright into the substrate. The snow reflection also ensures improved yields. One HELIOPLANT® has a nominal output of approx. 8.3 kWp. Depending on the altitude, yields of up to 1.500 kWh/kW can be achieved. The chosen design of HELIOPLANT® allows the system to be adapted to the existing relief on the one hand by leaving out geologically and ecologically sensitive areas on the other. Projects are currently being prepared in Austria and Switzerland.

1. INTRODUCTION

HELIOPLANT® represents a new form of cross-shaped support structure for bifacial PV modules. The system design was derived from the field of mitigation structures (Margreth, 2015).

The major advantage of this structure is that the cross shape generates turbulence in the wind field, even at low speeds (from approximately 3 m/s), which keeps the system largely free of snow. A scour ring also forms at a distance of up to 2 metres from the outer edge of the module. The eroded snow is transported and deposited outside the area affected by the turbulence. The turbulence breaks up the snow crystals and causes them to accumulate with a higher density. Due to the system effect between the HELIOPLANT® structures, any snow load that can no longer be deposited is transported away from the construction site.

A. Ploner and others
O3.4 - Page 83

2. METHODS

2.1 HELIOPLANT® Layout

A HELIOPLANT® element consists of a mast with four vertical wings arranged in a cross formation. Each of these four wings typically contains four bifacial, vertically aligned photovoltaic modules. In steep areas with a slope of more than 22°, the lowermost module on the mountain side is omitted, meaning that each element has up to 15 bifacial modules. This design is also intended for use in avalanche starting areas. The distance between the individual elements is set between 8 and 14 meters, depending on exposure and slope inclination (see Figure 1).

The cross-shaped structure generates turbulence in the wind field, even at low speeds (from approximately 3 m/s), which keeps the system largely free of snow. Depending on the slope gradient, an up to 1 m ground distance ensures that a thin layer of snow still forms on the ground in the scour area. This is important for reflection and, consequently, energy generation.

The snow redistribution process takes place in different forms of movement depending on the wind speed. Approximately 90% of the mass displacement occurs in the form of particle creep and saltation up to a height of approximately 2 m above the ground level. Above this, transport occurs as an aerosol up to a height of several tens of metres. The specific weight of the transported air/snow mixture is highly dependent on altitude, reaching a maximum of 10 kg/m³ near the ground (Dimensioning basis: Institute for Geotechnics / Ice and Snow Mechanics, University of Innsbruck in: i.n.n. 2009).

The HELIOPLANT® element is designed for wind speeds corresponding to a 100-year event and adding a surcharge for transported snow. The design load is approximately 3 kN/m², which corresponds to the design load for snowdrift structures in Austria as specified in ÖNORM B 4801 (Gabl, Lackinger, 2024).

No concrete foundation is required to anchor the construction to the ground. The foundation is laid using a walking excavator via a steel plate on the pole, which is connected to the ground with four IBO R38-500 bolts or GEWI 40 bolts. Furthermore, a 1 m long casing pipe is inserted beneath the steel plate for reinforcement. Minor ground unevenness is not problematic and does not require levelling. The micro piles are dimensioned according to the existing ground conditions (i.e. drilling logs), with an approximate length of 4-6 metres.

Depending on the surface conditions, the cables are laid in cable protection pipes either at a shallow depth in the ground or fixed to the rock.

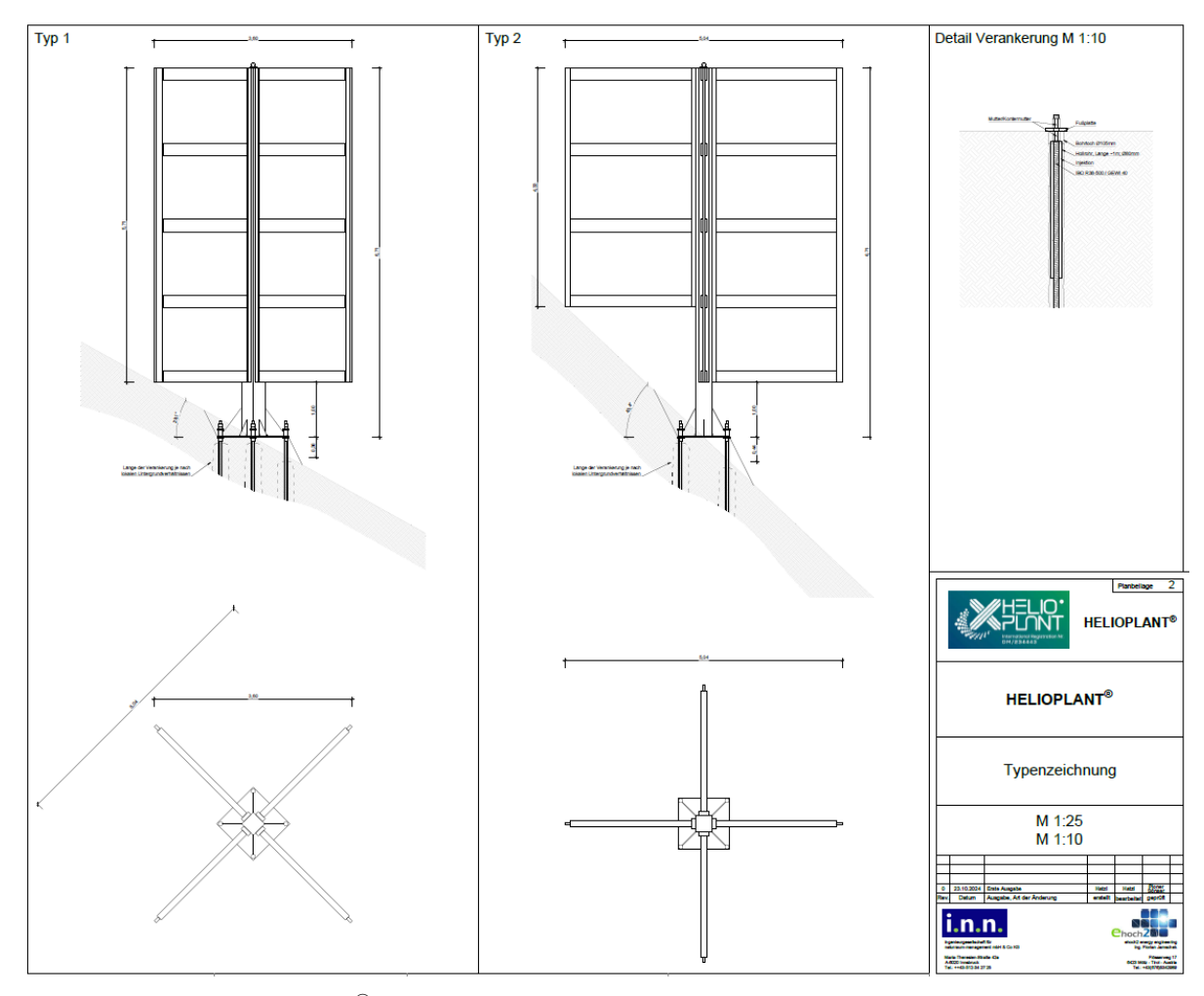


Figure 1 HELIOPLANT® schema for different slope inclination

2.2 Wind deflector plates to enhance the scour effect

In particularly exposed locations – pronounced lee areas – the HELIOPLANT® wings are equipped with wind deflectors in the area of the ground clearance (approx. half the wing width) to reinforce the vortex effect at large scour depths. The deflectors are generally 3 mm thick steel sheets that are screwed into place in a trapezoidal shape underneath the lowest PV modules. For terrain inclines more than 25°, the wind deflector on the uphill wing is triangular. The wind deflectors are fixed to the mast and the respective wing in such a way that the ground clearance is significantly reduced.

2.3 General electrical concept

The PV modules of a HELIOPLANT® element are aligned in different directions. The modules of the north and south wings are aligned towards the west and east respectively. The modules of the west and east wings are aligned towards the south.

The cross-shaped structure ensures almost continuous sunlight exposure. However, depending on the time of day and the position of the sun, it is not possible to prevent partial shading of the PV-modules. This shading primarily occurs from wing to wing, with one wing shading the adjacent wing, and moves outwards from the mast. This results in asymmetrical shading. The

A. Ploner and others O3.4 - Page 85

outer parts of the modules are shaded less frequently than the inner. In addition, the modules' frames cause shading in the cells.

Despite the fact that the cross-shaped structure results in a reduction of the specific yield due to internal shading. This problem was solved by cleverly interconnecting the optimized modules.

One HELIOPLANT® has a nominal output of approx. 8,3 kWp. Depending on the altitude, yields of up to 1.500 kWh/kW can be achieved.

2.4 Avanlanche protection with HELIOPLANT® elements

The major advantage of the element structure is that, as already explained, the cross shape creates turbulence in the wind field even at low wind speeds so that the system itself mostly remains free of snow and a scour ring of drifted snow forms at a distance of about 2 m from the outer edge of the wings (see Figure 2).

In avalanche starting areas HELIOPLANT® elements with up to 15 bifacial PV modules are used. The vertical tree-like structure of HELIOPLANT® and the selected spacing (8-14 m) ensure that the scouring effect interrupts the redistribution of tension in the snow cover, preventing avalanche starts. A HELIOPLANT® field in an avalanche starting area behaves like a protective mountain forest. For this reason, the HELIOPLANT® rows are arranged in a staggered pattern, unlike a layout on gently sloping terrain, so that there are no continuous lanes.

The eroded snow is transported and deposited outside the area affected by the turbulence. The turbulence breaks up the snow crystals and causes them to accumulate with a higher density. The snow load that can no longer be deposited due to the interlocking effect between the HELIOPLANT® elements is transported out of the avalanche starting area.

3. RESULTS AND DISCUSSION

A 6.3 MWp HELIOPLANT® system is currently being built in Sölden, Tirol, with parts of the site also securing small avalanche starting zones above the access road to the Tiefenbach glacier.

The wind turbulence creates swirls that ensure the system remains largely free of snow. This interrupts the stress redistribution in the snow layer, similar to a protective mountain forest, significantly reducing the probability of triggering an avalanche. In addition, the problem of reduced yield is solved by HELIOPLANT®-specific electrical wiring, which also leads to a balanced yield curve without a midday peak.

Natural environment aspects

The chosen design of HELIOPLANT® allows the system to be adapted to the existing terrain and, by avoiding geologically and ecologically sensitive areas, to be better integrated into the landscape without causing negative effects because of snow drifting, unlike linear systems.

Viewed from a distance, the entire system resembles a protective mountain forest, which is further emphasised by the dark colour scheme.



Figure 2 View of the vortex effect shown from above (test field Sölden, Austria) – similar to a protective mountain forest

4. CONCLUSIONS

The approach outlined above makes it possible to combine avalanche protection with energy generation in mountain regions. This dual benefit results in high cost-effectiveness in the implementation of avalanche protection measures.

REFERENCES

Gabl, K., Lackinger B., 2024. Meteorologisch-nivologisches Gutachten zur Windeinwirkung. Projekt: Helioplant Photovoltaikanlagen. Innsbruck, St. Anton am Arlberg.

i.n.n., 2009. Ausführungsplanung PV-Anlage Wildkogel, Salzburg: Dimensioning Basis Institute for Geotechnics / Ice and Snow Mechanics, University of Innsbruck.

Margreth S., 2015. Basics for the design of snow drift measures, Grundregeln für das Erstellen von Verwehungsverbauungen. Davos, Eidgenössisches Institut für Schnee- und Lawinenforschung

A. Ploner and others

O3.4 - Page 87

Preventive Avalanche Control on Arnøya – Securing Critical Infrastructure

Thomas Berger^{5*} Siiri Wickstrom¹ Kalle Kronholm¹ Maxence Carrel² Olafur Stitelmann² * Sindre Linstad³ Andreas Per Ola Persson⁴ Cedric Larcher^{5*}

SKRED AS, avd Tromsø Sjølundsvegen 1, 9015 Tromsø, NORWAY
 GEOPREVENT, Räffelstrasse 28, 8045 Zürich, SWITZERLAND
 MHM, Entreprenør & Service AS, Kåsegrend 63, NO-3870 Fyresdal, NORWAY
 ⁴Troms fylkeskommune,, Tromsø, NORWAY
 ⁵MND SAFETY, 74 voie Magellan, 73800 Ste Helene du Lac, FRANCE
 *Corresponding author, e-mail: thomas.berger@mnd.com

ABSTRACT

In 2024, a major avalanche mitigation project was implemented on Arnøya, a remote island in Troms County, Northern Norway. The main objective was to protect vital road infrastructure from snow avalanches, ensuring year-round access for the local population and supporting the operations of Arnøy Laks, a key local industry. A total of 24 remotely operated avalanche control towers (ObellX+), supplied by MND France, were installed across two high-risk zones: Singla and Oterelvene. The civil works and installation were completed during the summer of 2024, and the system is planned to be operated for five years, with options to extend the service until 2044. In addition to RACS, the Arnøya project includes two real-time Doppler radars, with both a PTZ and an infrared camera completed by two weather stations that overall detect and map the avalanche activity. The project was a collaborative effort involving Skred AS (technical consultancy), Troms County Council (project owner), MHM Entreprenør & Service (local contractor and project coordinator), and MND France & Geoprevent (technology providers). During its first operational season, the system has functioned optimally, significantly improving avalanche safety and reduction of road closure. Troms County Council, the regional authority responsible for the roads, has expressed strong satisfaction with the results. The successful implementation has proven to work well in the challenging conditions of Arnøya with a snowy Arctic coastal climate, with possible polar lows, and limited light conditions during the snow season.

1. INTRODUCTION

Arnøya (Northern Sami: Árdni) is an island located in Skjervøy Municipality, Northeast of Tromso in the artic region of Norway. The island is characterized by its mountainous terrain, with several peaks rising above 900 meters above sea level. The highest point is Arnøyhøgda,1,170 m.a.s.l. Arnoya has a maritime climate with humid and mild air masses and precipitation reaching the island from the northerly and westerly sector with a drier inland climate south and east of the island. Creating a dynamic and challenging-to-predict snow climate with frequent intense storms followed by occasional dry and cold continental airmasses. Arnøya experiences dark season from late November to late January, making it hard to observe mountain sides visually.

T. Berger and others O3.5 - Page 88



Figure 1: Arnoya island location

County road fv. 7940 running from the Lauksunskaret Ferry around the southern coast of the island is exposed to snow avalanches from paths above Oterelvene (and south facing avalanche paths from Singeltind in the southeastern corner of the island. Both these zones accumulate snow in the release areas with the prevailing wind direction of winter precipitation yelding in rapid loading in the release areas. Singla present approximately 10 main avalanche paths, some of which have several independent release areas. Oterelvene, presents three large release areas that can be divided into many small paths, approximately 10–20 in total. Hence, the reliability of this coastal road in southern Arnoya Island, is largely driven by avalanche risk during the winter. A report released by the Norwegian Road Authorities (Statens Vegvesen, 2019) states that in the 10 years preceding the report the stretch of road was on average closed 10 days in a winter with 2-4 avalanches reaching the road. These road closures affect both local businesses, including salmon farms, and the access to the mainland of the inhabitants of the local community.

To increase the reliability and to shorten the road closure time ,Tromsø county tendered an integrated avalanche mitigation project in 2024. The design and implementation of this mitigation solution was a collaborative effort between the Troms County and other local authorities and a panel of companies from the natural hazard sector, namely SKRED AS, MHM AS, MND, and GEOPREVENT. The solution, implemented in November 2024 consists of 24 RACS' (Remote Avalanche Control Systems) to release avalanches, two radars to detect and warn about avalanche activity, and two weather stations to provide knowledge about the local meteorological conditions.

2. METHODS

2.1 The Mitigation Concept

The mitigation concept is active removal of snow from the avalanche paths in a controlled way using RACS systems. The timing of active avalanche control is decided by an on-duty avalanche forecasting team at Tromsø County assessing the snowpack and incoming weather. The forecasting team having access to data detected by the radars and both the infrared camera (dark season) and the PTZ camera are valuable sources of information. The radar and camera combination also detect, and record avalanche released by RACS's. This is especially valuable in the dark season and during poor weather. Given the complex topography this concept also

includes weather stations at the height of the release areas to give the forecaster real-time information about the temperature and wind conditions in these zones. The RACS's are operated by a local contractor who also performs daily snow depth measurements.

2.2 Remote Avalanche Control Systems

The Obellx+ Remote Avalanche Control System (RACS) is an autonomous, gas-based solution. Each unit comprises modular gas generators mounted on a 4-meter-high tower, anchored to the ground and deployed via helicopter, eliminating the need for on-site personnel and reducing logistical risks. With an operational autonomy of at least 12 shots per module, the system ensures sustained functionality throughout the winter season. Obellx+ is remotely operated through cellular network using a dedicated web platform or from the extremities of the road by a contractor on a radio mode. The software modular architecture allows for both individual and synchronized multi-tower activations, enabling operators to combine energy outputs for enhanced avalanche release efficiency and time efficiency. This system offers significant advantages over traditional methods, including improved safety, operational flexibility, and minimal environmental impact, (Bourgeaillat et al, 2010).

2.3 Radars

In addition to RACS the Arnøya project includes two real-time Doppler AVYX radars that detect and map avalanche activity (Fig 2) as experienced by (Persson, A et al, 2016). These systems, one looking at Singla and one looking at Oterelvene, are connected to an SMS-based alarm system that informs users of avalanche activity and if an avalanche released in a Region-of-Interest (ROI) affected the road. The radars can detect both natural and triggered avalanches 24/7 in any weather conditions. On the same mast as the radar, a PTZ camera and an infrared camera are also providing information about the snow cover conditions and provides a possibility to record and validate avalanche activity in the slopes. These cameras are also used by forecasters to study snow distribution and current conditions.

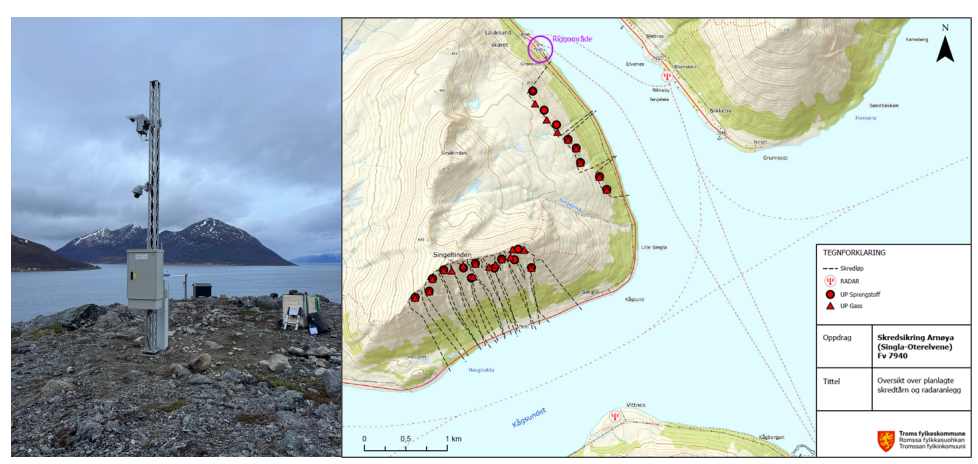


Figure 2 Radar looking at Singla Figure 3 Map of the two zones with RACS positions and avalanche paths. East facing paths are Oterelvene and South facing paths are Singla.

2.4 Automatic Weather Stations (AWS)

Two automatic weather stations measuring wind and temperature were installed to provide realtime data of the meteorological conditions in the release areas. The first station is located on

T. Berger and others O3.5 - Page 90

Singeltind at approximately 700 m.a.s.l. and the second one above the Oterelvene release areas above at approximately 300 m.a.s.l. The weather stations have a solar panel and battery to provide data throughout the dark season. The wind sensors are mechanical anemometers (propeller and vane) and mounted on 3-meter masts. The temperature sensor is mounted at 2-meter. Data is collected every 15 minutes and sent to live data portal every 30-minutes where it is available for the forecasters and other users.

3. LESSONS LEARNED - RESULTS AND DISCUSSION

3.1 Implementation of the RACS system

To manage the tight timeline of the project and the extent of the work in Arnøya's challenging terrain the workforce from MHM operated on a 14-days-on / 14-days-off rotation. During their shifts, personnel were accommodated in the mountain-based site rig (Fig 4), which was equipped with eight sleeping quarters, a kitchen, two restrooms, two showers, and a common living area. Supplies and provisions were delivered by helicopter once a week. To optimize drilling operations, six air compressors were transported to various locations across the mountainous terrain, allowing multiple drilling points to be executed simultaneously. In total, 24 tower foundations were drilled, shuttered, cast, and installed within a four-week period. This set-up allowed for efficient installation in the short Northern-Norwegian summer!



Figure 4 Mountain base site on Singla

3.2 Radars

The two AVYX radars were installed in early November 2024 in both Singla and Oterelvene. The installation was conducted in challenging weather with strong wind. Nevertheless, all components of the radar system, including the PTZ camera, could be mounted on the radar masts. The radar itself is equipped with a wind blower to clear snow from the radar head. Once the installation was completed on both sites, Geoprevent's team remotely fine-tuned the systems' calibration and set up the automated alarm notifications. The radars have been successfully monitoring avalanches most of t the 2024-2025 winter season, with the exception of the Singla in early season. The malfunction was possibly caused by lightning in a intense cold front, but this was not confirmed. The radar ROI and the RACS operations for best capture of the avalanches have been finetuned throughout the season. The location of the radar looking at Singla is very windy and the vibrations in the mast affected the zoom on the camera in stormy periods and it was decided to stabilize the mast in the summer of 2025.

3.3 Weather Stations and Meteorological Data

The weather stations were installed by Skred AS in July 2024 at Singla and Oterelvene. These stations provided valuable data throughout the season. Icing on the propeller of the anemometer was a larger than anticipated problem demonstrating the harsh conditions at Singeltind. We investigated the possibility of having a heated anemometer but with a battery driven station in a climate with a dark season (no solar charge) this wasn't feasible. The silver lining was that the station managed to shake itself free from icing without assistance. Further, the location proved to be a highly turbulent location, not giving data representative of the release area especially in situations with high wind speeds. To receive the highest possible operational benefit from this station we have suggested raising the mast or alternatively move the station further from the wake of the ridge. These lessons show that placement of a point measurement is key to high-quality data and that the use of robust instrumentation pays off in these harsh environments.

3.4 Discussion of the first season

3.4.1 Lessons learned after the first winter

The first season has shown that for an effective mitigation of the avalanche risk timing is everything! The control must be done at the right time after the snowfall event requiring a continuous dialogue with contractors in charge of the avalanche control and the avalanche forecasters monitoring the situation. The PTZ cameras have proven to be a highly valuable tool to study snow accumulation as there are no precipitation measurements, and it allows zoom into the release areas.

Underestimated snow volumes. This first season has revealed an underestimation of the snow accumulation in some sectors. Especially, wind loading has been challenging in Singla sector, and the release areas fill in quickly. Hence, snow depths appear to be high relative to the tower height, something that wasn't accounted for. This led to an additional snow load on the structure which resulted on damages on 3 units. In addition, some towers snowed over at season's end. This needs to be considered in future improvement of the system and has resulted in repositioning of some towers in summer 2025. The years to come will also gain more experience for snow conditions, and evaluate the need for more adjustments, to optimize the system further.

Another lesson learned is the value of public consultation with the local community that proved to be an effective way to communicate and build trust in this mitigation concept, as many locals would have originally preferred the avalanche risk being mitigated with a tunnel.

The project has a clear goal to mitigate the avalanche risk on county road 9740. The first winter shows that implementation of advanced avalanche monitoring and mitigation systems on Arnøya gave significant operational advantages for the local community. Notably, the infrastructure ensured that avalanche debris does not accumulate on open roads, thereby maintaining uninterrupted access and reducing the risk of traffic disruptions. As a result, prolonged road closures were effectively eliminated. Instead, the system facilitates targeted avalanche control actions, which require only short-term closures of 30 to 60 minutes per intervention. Over the observed period, a total of 15 such controlled actions were conducted, demonstrating the efficiency of the system in managing avalanche hazards without causing substantial inconvenience to residents or commuters.

T. Berger and others O3.5 - Page 92

Furthermore, the need for post-avalanche debris clearing on roadways is minimized, with only a single clearing operation required throughout the season. This reduction in maintenance efforts translates to both cost savings and enhanced safety for road users. Additionally, the integration of a Vehicle Traffic System (VTS) provides advance notifications of potential avalanche risks, with alerts issued at least six hours prior to anticipated events. This proactive approach allowed residents, emergency services, and transportation authorities to prepare adequately, further mitigating the impact of avalanches on daily life and infrastructure.

Finally, this system shows that such an avalanche mitigation measure is a feasible alternative for permanent measures also in remote Arctic areas, such as Arnøya. However, these systems will need continuous management and a period of finetuning, the team getting familiar and gaining experience of the site for best possible operations. Contrary to gray measures such as tunnels, this mitigation measure anchors local knowledge of the snow climate and avalanche dynamics in the local community, the forecasting team and the project owner.

4. CONCLUSIONS

The project is considered a success and to have reached its goal for this first year of implementation, despite the not so unexpected challenges in the early phase. These operational improvements on road management underline the effectiveness of modern avalanche monitoring technologies in enhancing both safety and logistical efficiency in snow-prone regions.

5. ACKNOWLEDGEMENT

We would like to thank the Troms County team who trust the gas technology in such severe environment. A special Thanks to Andreas for his continued support from the initial implantation studies and nice walks over the ridges of Singla. County engineers for input and support from the project owners team.

6. REFERENCES

- Bourjaillat Fanny, Dr Berthet-Rambaud Philippe, 2010 Avalanche control: inventory and analysis of preventive triggering methods in the world. ISSW 2010, 831-832
- Meier, L., Jacquemart, M., Blattmann, B., Arnold, B., 2016. Real-time avalanche detection with long-range, wide-angle radars for road safety in Zermatt, Switzerland. In: Proceedings ISSW, Breckenridge, Colorado, 304-308.
- Persson, A., Venås, M., Humstad, T., Meier, L., 2018. Real-time radar avalanche detection of a large detection zone for road safety in Norway. In: Proceedings ISSW, Innsbruck, Austria, 597-600.
- Stähly, S., Yount, J., Gorsage, B., Greene, E., Wahlen, S., 2023. Optimizing road management with Doppler radar for automatic avalanche detection at I-70. In: Proceedings ISSW, Bend, Oregon, 1565-1568.
- Statens Vegvesen, 2019. Viktige fylkesveger for næringstrafikk i Troms Framkommelighet, sikkerhet og strekningsvise tiltak Report Region nord Vegavdeling Troms

Are avalanche pressure requirements still necessary for the design of modern ropeways?

Philippe Berthet-Rambaud^{1*}, Lucas Le Bouquin¹, Michel Gillard²

¹ ENGINEERISK, 690, route de la Motte Servolex, 73160 Saint-Sulpice FRANCE

² DCSA, 43 Bd des Alpes, 38240 Meylan FRANCE.

*Corresponding author, e-mail: pbr (at) engk.fr

ABSTRACT

Carrying out an avalanche risk assessment is a regulated requirement, particularly in Europe for any new ski lift. Various standards exist, considering different avalanche scenarios, as well as snow-gliding, integrating the associated combinations according to different return periods. The main result expected by the designer and manufacturer is the height and pressure profile detailed data, allowing them to dimension and design pylons and foundations. In parallel, these same structures are subjected to various other loads, intrinsic to operation (risk of derailment, for example) but also external (wind, earthquake, etc.). With the continuous increase in power, comfort, capacity, and speed of recent ropeways, other load cases are being integrated and weighted, which can become largely predominant. In particular, the wind becomes particularly impacting when the vehicles are large (gondola for example) and especially when the pylons are very high (25m or more) and spans long (several hundreds of meters): the corresponding shear or mechanical momentums sometimes represent the load of "monster" avalanches which would be totally unrealistic, and which directly cover a majority of real avalanches. However, and beyond the purely mechanical aspect, directions of application cannot be neglected which can be very different from those of the other loads and specific effects. Other aspects must also be taken into account, particularly regarding stations and for the safety of people (including possible evacuation to the ground) which continue to justify avalanche analyses.

1. INTRODUCTION

By definition, ski lifts need to reach uphill mountains points to offer good ski and doing that, are regularly crossing avalanche trajectories, from starting to runout zones and steep slopes prone to snow gliding. Ideally, pylons shall be located in a way to minimize corresponding loadings, but ropeways also include their own constraints so that at least some pylons can be directly threatened.

At the same time, ropeways technologies continuously improve in parallel to changes in skiers' behaviours: fixed-grip double chairlifts are close to disappear, replaced by detachable 6-seater chairlift sometimes with bubbles. To ensure connections between zones or promote various uses (also in summer), gondolas are also developing: modern lifts mean now capacities of several thousand passengers per hour thanks to bigger vehicles, higher speed and (much) more powerful systems able to manage bigger cable ropes, less supports and longer spans. It is common that the replacement of an old chairlift can lead to a number of pylons divided by 2 for the new modern line.

In the meantime, regulations have also evolved with more safety and more reliability, which means totally different pylons structures. This paper aims to illustrates the consequences in terms of avalanche prescriptions.

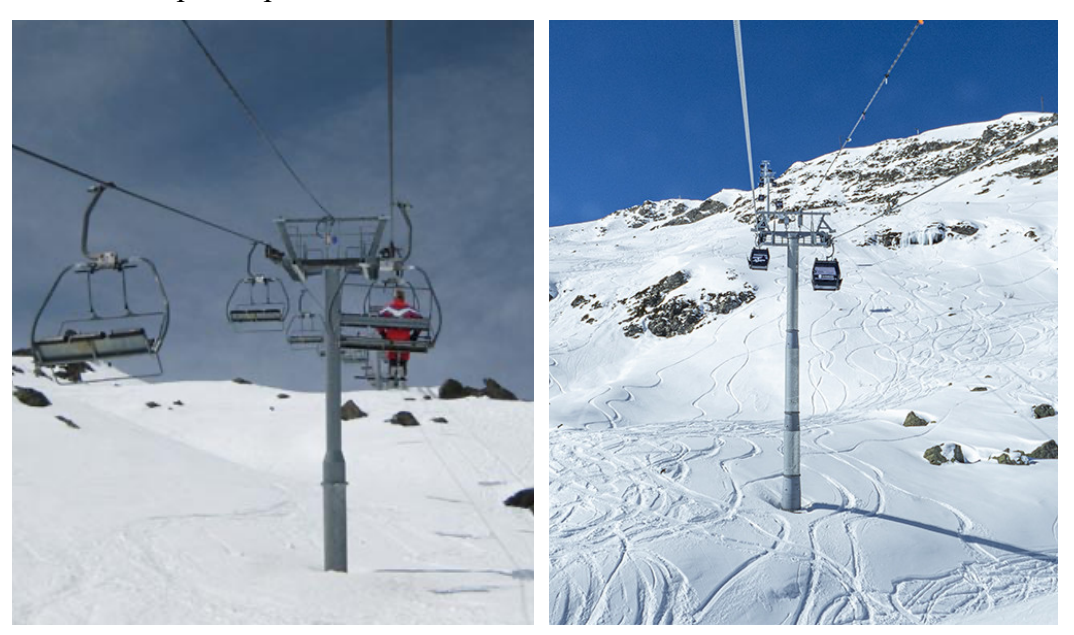


Figure 1 Left: typical design and size of a fixed-grip chairlift built in the 1980s (Creux Noirs at Courchevel). Right: modern gondola (La Masse at Les Ménuires)

2. REGULATIONS

When planning a new ropeway project, the designer must follow a regulated procedure, especially to ensure that the structure will resist the different load cases it would possibly face. In France, the European standards EN 12930:2015 and EN13107:2015 are applied and coordinated in the national guide RM2. These documents specifically refer to the ropeway systems. More generally, regarding concrete and steel structures, Eurocodes 2, 3 and 4 must be also followed. In spite of some differences (Siegele P. and Walter G., 2019), equivalent standards exist in different countries which cooperate within the International Organization for Transportation by Rope (OITAF) since 1959. Avalanche topics are within the scope of the Study Commission No. VII: Environment.

However, CEN (2015a, b) give very few requirements about snow and avalanches action except that a 50-years return period event shall be taken into account. In comparison, Margreth et al (2016) provides a more detailed and comprehensive framework to address the question of snow avalanche and snow gliding loadings. It is also partly used in France to structure corresponding analyses.

Main other load cases defined in the specific documents are wind, snow, icing, earthquakes and cable derailments. Regarding wind, the most restrictive load is the pressure the ropeway should withstand while non-operating: 1.2 kPa (STRMTG 2023) which corresponds to about a 50 m/s speed. This pressure applies on the surface of the system, and so, depends on the presence of a storage building for vehicles to remove them during non-operating period. Icing impact is taken into account by considering a larger cable diameter (up to a 40% increase of the windward surface) but reducing the wind pressure by 35%. Concerning earthquakes, Eurocode 8-2 give a

reference ground acceleration depending on the geographic zone (from 0.4 to 3 m.s⁻² in Fance). A complete method is then given to find the induced shear force, although specialists agree to say that it is almost never dimensioning the final project.

3. PRACTICAL EXAMPLE

One interesting example is pylon #4 of La Flégère recent (2019) gondola at Chamonix. This ropeway has replaced different successive cable cars since 1956 to access the homonymous ski area: if the cable car technology allowed to jump easily over the transit and runout zones of the 'Lanchers' major avalanche path (and the golf course of Chamonix) thanks to no limitation of the height above ground, it faced also limited passengers capacity and strong wind sensitivity.

The choice for a gondola has solved these last points but needs also more pylons to better follow the terrain and not overpass the standards value of 60m above ground (STRMTG 2023. In fact, even less for landscape and aviation local constraints). That means that at least one pylon had to be located at best in the avalanche-prone zone, well known from the history, confirmed during February 1999 famous avalanche period and more recently in January-February 2018 (2 major avalanches), just before the building of this new gondola.

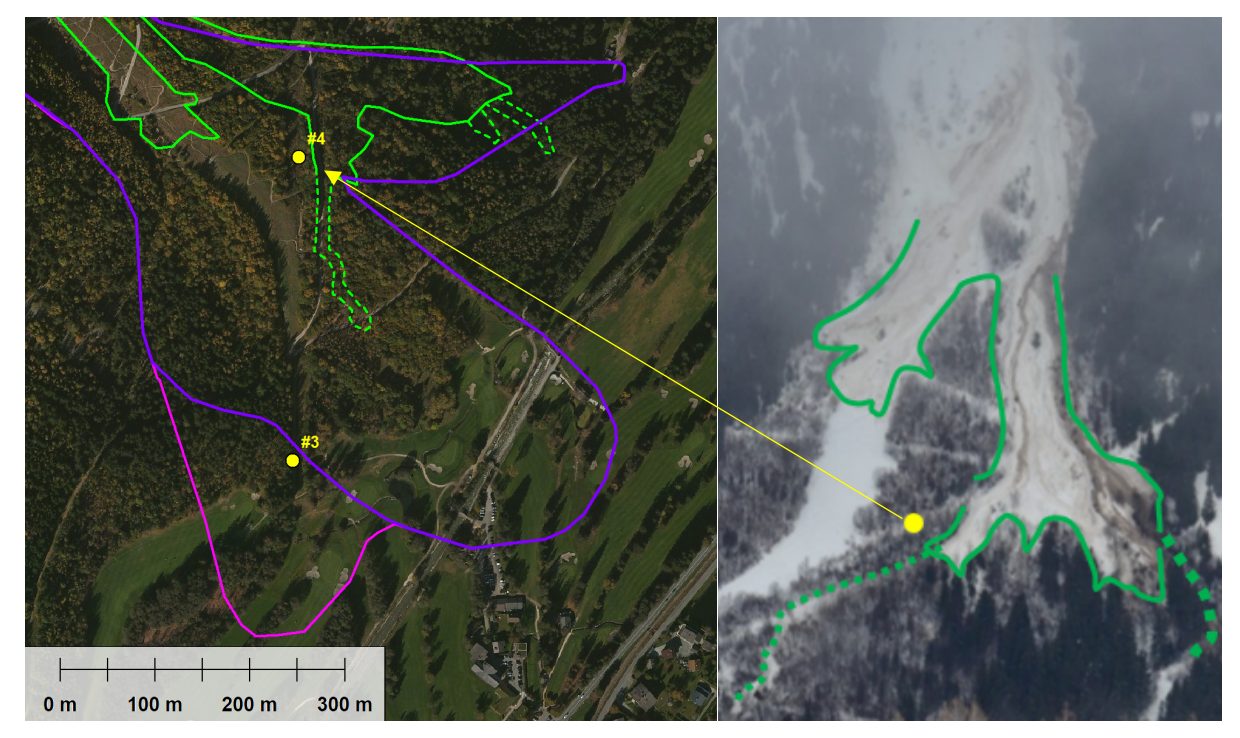


Figure 2 Left: evolution of the CLPA avalanche map limits (Bourova et al 2016) before (purple) and after (pink) February 1999 famous avalanche period by comparison to February 2018 avalanche (green). Right: picture of February 2018 avalanche and location of pylon #4.

In this situation, the general analysis of the exposure of this gondola (Engineerisk 2019) provided rather important pressure values, up to 40 kPa on 2m high (30-years return period scenario) and 120 kPa on 3m high (100-years return period scenario) for the design of pylon #4. It was also expected that avalanches could transport some trees or rocks in a location where small debris flows are also possible. Consequently, the design of this pylon seemed to have an obvious problem regarding the different flows which could impact it (hopefully, the main

trajectory of a possible powder cloud avalanche is going straight between pylons #3 and 4# with limited overloads on them).

But, finally, looking at the size of this impressive tower #4 (30.50m high, cylindric section between 2.14m and 0.70m), these avalanche loadings were largely competed by regulatory wind consequences: among the 51 loads combinations which were examined for its design, momentums are clearly maximized by wind, even without any vehicles attached to the ropeline and especially along the transverse direction. The value due to the centennial avalanche is about 3 times smaller!

Regarding shear force on the foundation, the comparison is more nuanced as the maximum value due to the wind is between the 2 avalanches scenarios: if the 100-years return period avalanche is not taken into account (which is sometimes the case depending on the context, as the result of a negotiation between local authorities and the gondola owner endorsing a larger responsibility), that means that the design of both the pylon and its foundation can be not influenced prejudicially by avalanches in spite of a strong avalanche situation.

In the current case, the main protection against flows consisted in adding a crushable wood layer at the basis of the exposed face of the pylon (Figure 3) to avoid that a possible hard part inside a flow (avalanche, debris) can cause apparent marks and superficial damages which do not compromise the integrity and resistance of the structure but can raise long questions and discussions, often first leading to the closure of the gondola according to the precaution principle. Here, only the fuse layer should be damaged and can be easily replaced.

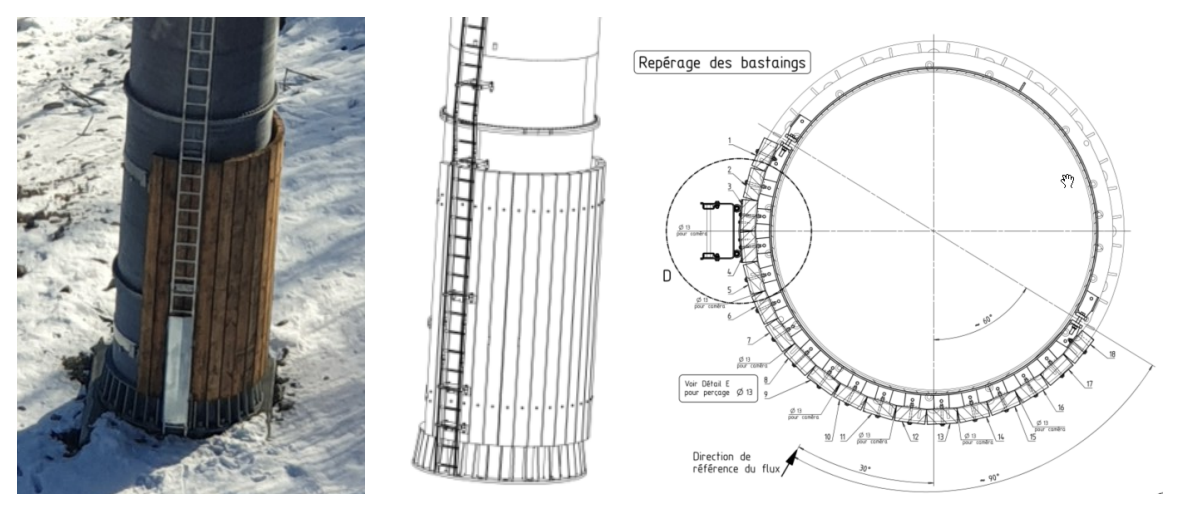


Figure 3 Additional layer of wood at the basis of pylon #4 of Flégère gondola at Chamonix-Mt-Blanc to protect it against secondary impacts – Technical schemes and details (source: Doppelmayr).

4. PSEUDO-STATISTICAL ANALYSIS AND SCHEMATIC MODEL

Based on the data of 6 recent ski lifts in avalanche situations, accounting for 91 usual cylindric pylons (steel lattice structures are surely more sensitive, Margreth 2007), a pseudo-statistical analysis has been performed based on the contribution of every external load in each direction. The aim of this analysis was to approach how (often) avalanche requirements were prejudicial or not, compared to other 'natural' loads. For each pylon, the two main load types, shear force and momentum, are considered along 3 directions (\vec{x} = ropeline axis, \vec{y} =transversal axis, \vec{z}),

being possibly positive or negative. So, each load case (and/or actions combination result – there can be several hundred per pylon) corresponds to six different values: F_X , F_Y , F_Z , M_X , M_Y , M_Z .

A load value is considered as a prejudicial or "sizing" value if its load type gives the maximum positive value (or the minimum negative value) in a considered direction. For example, let's consider a pylon for which, along the \vec{x} axis, the wind shear force is 600 kN, the avalanche shear force -800 kN and the snow gliding shear force is -400 kN. The sizing load case regarding F_{X} + is the wind (maximum shear force positive value) whereas the sizing load case regarding F_{X} - is the avalanche (minimum shear force negative value).

Finally, there are up to 12 sizing values for each pylon and foundation. For instance, for La Masse gondola (Figure 1) with 24 pylons in total and only 13 subjected to snow avalanche prescriptions, that means 156 sizing values (actually 150 as 6 individual directions had no negative values). Among them, "only" 4 were due to snow gliding and 23 to the 100-years return period avalanche scenario and wind is largely predominant, especially regarding transverse situations.

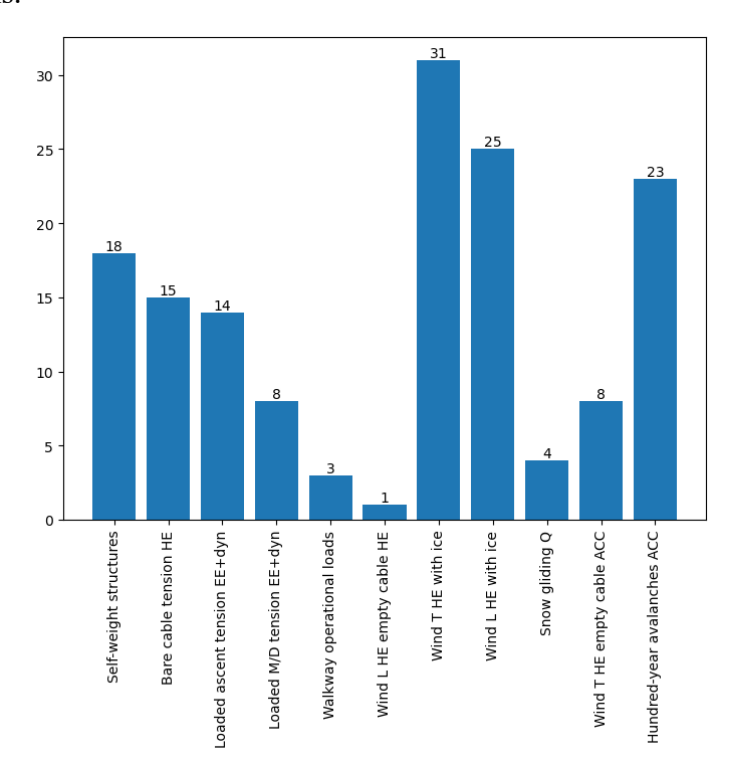


Figure 4 Number of sizing values due to each load cases for the 13 pylons of La Masse gondola.

To complete this analysis, a simple analytical model is being developed to evaluate the shear forces and momentums induced by wind, avalanche and snow gliding, based on a limited number of geometric parameters to describe the considered pylon (height, section) including its head components (using equivalent surfaces from an internal database of recent project and ropeways model). Mainly along the transverse direction, it confirms that with an increasing

geometry, usual avalanche requirements are anyway overpassed by wind loads, firstly through the momentum but then through also the shear force.

5. CONCLUSION

For the design of ropeway pylons, avalanche prescriptions compete with other external loads: with wider and higher towers, modern ski lifts are particularly subjected to the transverse fixed wind pressure of 1.2 kPa which can easily become predominant. Geometric thresholds could be simply defined to determine, with safety margins, in which situations, avalanche requirements become even useless.

However, the first goal is not to remove work to avalanche specialists but to better apply their resources and focus on most important points of an avalanche design assessment: Sometimes, trying to refine some (biggest) values is less important than confirming the exact range of more usual ones which finally enter directly in the foundations design. For instance, the comparison with other loads is more balanced along the line axis and in case of a sufficiently thick powder cloud, its aerial pressure can become the main criteria able to lay down a pylon (Caviezel et al 2021).

And finally, avalanche considerations must also apply to the rest of the infrastructure (stations that may be threatened as buildings) and to the safety of skiers in the vicinity.

REFERENCES

- Bourova, E., Maldonado, E., Leroy, J.-B., Alouani, R., Eckert, N., Bonnefoy-Demongeot, M., and Deschatres, M. 2016. A new web-based system to improve the monitoring of snow avalanche hazard in France, Nat. Hazards Earth Syst. Sci., 16, 1205–1216, https://doi.org/10.5194/nhess-16-1205-2016.
- Caviezel A., Mergreth S., Ivanova K., Sovilla B., Bartelt P., 2021. Powder snow impact of tall vibrating structures, COMPDYN 20218th ECCOMAS Thematic Conference on Computational Methods in Structural Dynamics and Earthquake Engineering, M. Papadrakakis, M. Fragiadakis (eds.)
- CEN 2015. (European Committee for Standardization), EN 12930:2015, Safety requirements for cableway installations designed to carry persons Calculations
- CEN 2015. (European Committee for Standardization), EN 13107:2015 Safety requirements for cableway installations designed to carry persons Civil engineering works
- Engineerisk, 2019. Diagnostic des risques nivologiques, TC Flégère, Chamonix Mt Blanc. Report version 2bis
- Margreth, S., 2007. Snow pressure on cableway masts: Analysis of damages and design approach. Cold Regions Science and Technology 47, 4–15.
- Margreth S., Stoffel L., Schaer M. 2016: Prise en compte du danger d'avalanches et de la pression de la neige pour les installations à câbles. Guide pratique. WSL Ber.46:44p
- Siegele P., Walter G. 2019. Hazard managing in Austrian ski areas, International Symposium on Mitigative Measures against Snow Avalanches and Other Rapid Gravity Mass Flows Siglufjörður, Iceland, April 3–5, 2019
- STRMTG, 2023. RM2 Guide technique relatif à la conception générale et à la modification substantielle des téléphériques, version 3, 2023

Mitigating the natural hazard risk in Longyearbyen, Svalbard

Árni Jónsson^{1,2*}, Stian Bue Kanstad², Jan-André Jansen²

 ORION Consulting slf, Foldarsmára 6, IS-201 Kópavogur, ICELAND
 The Norwegian Water Resources and Energy Directorate (NVE), Middelthuns gate 29, NO-0301 Oslo, NORWAY

*Corresponding author, e-mail: arni (at) orion.is

ABSTRACT

Between 2018 and 2024, a series of mitigation measures were implemented in Longyearbyen to address the risks posed by avalanches and slush-flows. These measures were prompted by deadly avalanches in 2015 and 2017. In December 2015, an avalanche from the Lia hillside struck eleven houses, resulting in two fatalities and highlighting the need for mitigation measures. In February 2017, an avalanche from Mt. Sukkertoppen caused significant structural damage to two buildings.

A row of snowdrift fences was installed to accumulate snow away from the release area, and a channel was constructed to divert meltwater away from the residential area. Later, rows of rigid supporting structures were built in Lia and Mt. Sukkertoppen, along with 5.5 m high and 400 m long catching dam was built to prevent avalanches from reaching the residential area.

To address the risk of slush-flows in Vannledning valley (Vld), 14 debris-flow barriers were installed throughout the valley, along with modifications to existing deflecting dams. The purpose of this paper is to summarize the actions taken and their potential impact on future settlement in Longyearbyen.

1. INTRODUCTION

The Svalbard archipelago, with its administrative hub in Longyearbyen (LYR), is situated at latitude 78° north, within the permafrost region, see Fig. 1. Since approximately 1970, Svalbard has been experiencing significant climate change, making it one of the areas in the world with the highest temperature increases, particularly during the winter months (Isaksen et al., 2017). Precipitation is generally sparse, averaging 196 mm from 1971-2000 at Svalbard airport (Isaksen et al., 2017). Since 1912, it has increased by approximately 2 mm pr. 10 years. Recent studies (Isaksen and others, 2017) suggest further increases. The median projection of RCP8.5 (IPCC, 2013) indicates an approximate 40 % increase in annual precipitation by the end of the century.

Most of the settlement in LYR is located on a narrow stretch between the mountain side and the Longyear river (see Fig. 1). This narrow stretch can be affected by natural processes such as snow avalanches, debris flows, rockfall, and slush-flows. Slush-flows from Vannledning valley have threatened the residential area of Haugen for a long time. In 1953 3 people perished and 30 people were injured, when a slush-flow hit the residential area at Haugen. In 1989 a slush-flow hit one house at Haugen and destroyed water and heat pipelines (Hestnes et al., 2016).

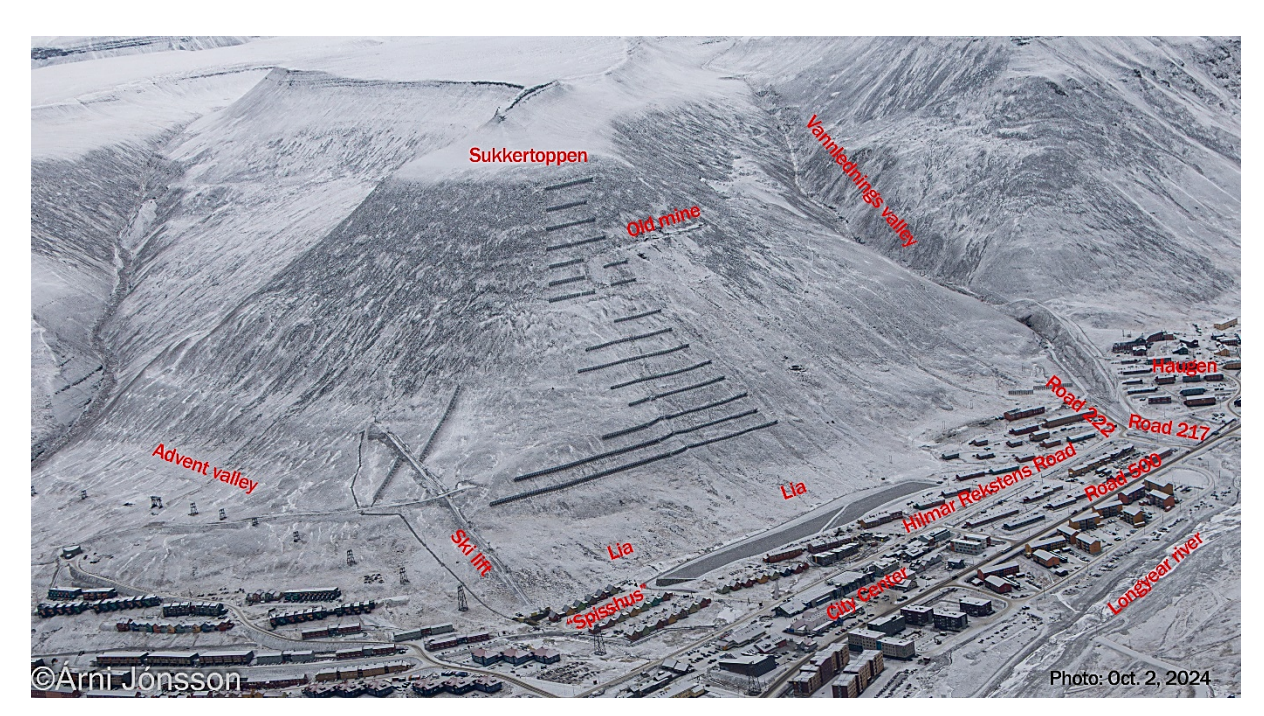


Fig. 1 An aerial view of Longyearbyen and the mitigation measures.

The natural hazard processes have been studied for at least 40 years. Large part of the study has been done by The Norwegian Geotechnical Institute (NGI) (Hestnes et al., 2016). Mitigation measures aimed to protect the residential area have been proposed, primarily by NGI (Norges Geotekniske Institutt NGI, 2015, 1996, 1991). An informing review of NGIs work in Longyearbyen can be found in (Hestnes et al., 2016).

2. INCIDENTS IN 2012, 2015 AND 2017

2.1 January 2012

During the last week of January 2012, an unusually warm period occurred with heavy rain and high temperatures. Numerous slush-flows were released from mountainsides in the vicinity of LYR, and one was released from Vld, approximately 200 m above the alluvial fan apex (Norges Geotekniske Institutt NGI, 2012). The slush-flow from Vld caused only minor damage, mainly to a pedestrian bridge that connects the Haugen area with the town center. Following this incident the local authorities asked NGI to propose mitigation measures for the Haugen- and the residential area at road 222 and 217. NGI proposed two deflecting dams along the stream on the alluvial fan to guide the slush-flow past residential sites (Norges Geotekniske Institutt NGI, 2015). The report discusses also net alternatives in Vld, more about them later.

2.2 **December 2015**

A fatal avalanche struck the residential area below Lia (mountain site) in LYR on December 19th, 2015. Tragically, two persons lost their lives: a two-year-old child and a 45-year-old man. An intense low-pressure system formed by the merging of two separate systems in the Norwegian Sea on December 17th, gaining strength as it moved towards the Svalbard islands (Jonsson and Jaedicke, 2017). The wind was blowing from southeast and transporting large quantities of snow out Advent valley into the release area above "Spisshus" buildings at road

230. The bad weather ended early on Dec. 19th, about three hours before the avalanche. The width of the avalanche was approximately 200 m, and the average fracture height was close to 2 m. The avalanche hit eleven houses and displaced them from 5 m to over 80 m (Jonsson and Jaedicke, 2017). Further details can be found in (Issler et al., 2016; Jaedicke et al., 2016; Jonsson and Jaedicke, 2017; Norges Vassdrags- og Energi Direktorat NVE, 2017; Spesialenheten for Politisaker, 2017).

2.3 February 2017

The first part of February 2017 experienced warm weather and rain. However, from February 12th onwards, the temperature dropped, and precipitation occurred as slush or snow. The lowest temperature recorded was -21°C. Prior to the avalanche on February 21st, there was light snowfall and increased wind (Jonsson and Jaedicke, 2017). The first avalanche release occurred at Sukkertoppen, and the second release happened at approximately the same location as the avalanche in December 2015. There were no fatalities, but the avalanche impacted several buildings, but only one building, which was closest to the mountain side, with three apartments, was destroyed.

3. MITIGATION MEASURES



Fig. 2 Red areas in the figure show areas with constructions to mitigate the avalanche danger from Sukkertoppen and slush-flow danger from Vannledningsdalen. Photo taken on April 1, 2025.

3.1 Timeline

The timeline of incidents and key mitigation milestones is presented in Fig. 3.

3.2 Deflecting dams along Vannledning stream at Haugen

Following a slush-flow incident in late January 2012, the local authorities in LYR tasked NGI with planning mitigation measures to protect the residential area on Haugen and along roads 222 and 217. The plan included constructing two deflecting dams, one on each side of the stream on the alluvial fan from the apex of the fan to road 500, which is the main road connecting the residential areas on both sides of Vld stream. The project was not implemented. The project is described in (Jónsson and Gauer, 2014; Norges Geotekniske Institutt NGI, 2015).

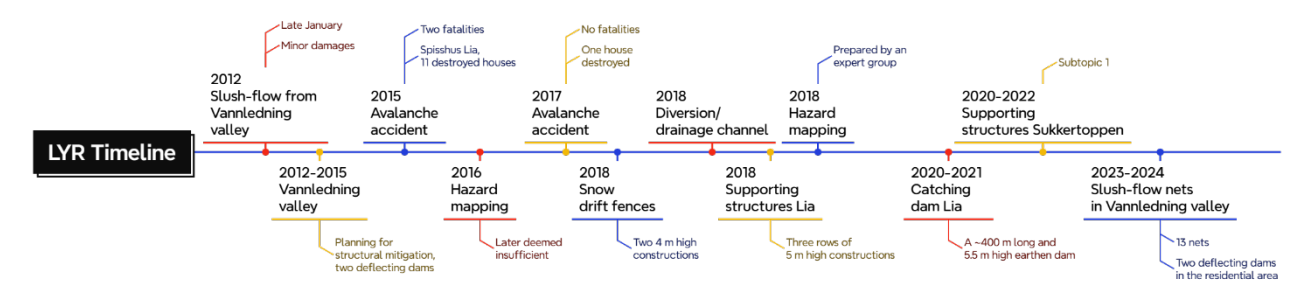


Fig. 3 shows the timeline for various milestones in Longyearbyen.

3.3 2015 and 2017 mitigation work

The avalanches in Dec. 2015 and Feb. 2017 were a wakeup call for the authorities. In 2016 a consultant was engaged to map the natural hazard for Longyearbyen and several other locations in Svalbard (Multiconsult AS, 2016). As a part of a plan for mitigating the avalanche danger NVE tendered the detailed design of snow drift fence and supporting structures in 2017; NGI was awarded the contract. During the design phase the local authorities (abr. LL) requested a diversion channel above road 232 to compensate for increased meltwater from the snow drift fences.

3.4 Snowdrift fences, a diversion channel and supporting structures Lia

One of the primary causes of avalanche release in Lia mountain side in 2015 was the rapid snow accumulation in the release area above road 228 and 230 (the "Spisshus", e: Pointed Gable houses). The wind blew from southeast along and out the Advent valley to the Lia release site. An estimation of snow height in the release area indicated an average 2 m snow height and at least 5 m snow height with the likelihood of even more in some locations.

A diversion channel, about 450 meters long, was constructed above the residential area at road 232 to redirect meltwater from snow drift fences away from the housing zone at Gruvedalen. The open channel has a depth of around 2 meters from the embankment top, and excavation for the impermeable membrane is roughly 3 meters deep. The membrane is intended to remain frozen within the permafrost.

A snow drift fence was planned to limit snow buildup in the release zone. During design, LL informed NGI of a future ski lift crossing, so the fence was divided into two sections to accommodate it. To address ground creep, the fence was constructed using individual 5 m long segments with gaps between them to account for ground movement. Total length is approximately 220 m. During the first summer, it was observed that the creep ranged from 3 to 5 cm. Today, the snowdrifts on the lee side are used for preparing ski slopes.

Three rows of steel bridges, each 5 meters in height, were constructed in the release zone in Lia, with a total length of approximately 470 m. The original plan was to install snow or rock fall nets, but contractors suggested steel bridges during the tender. After reviewing proposals, rigid steel bridges with anchored support were chosen as a more favorable solution than nets with floating baseplates. Due to permafrost and active layer summertime the length of the anchors is extra-long. The steep slope combined with permafrost and active layer causes significant ground movement that impacts the foundations especially the foundation of support. Further information about this work can be found in (Norges Geotekniske Institutt NGI, 2017).

Because the mountain side beneath the supporting structures poses an avalanche risk, plans were made to build a catching dam at the base of Lia. When mitigation work shifted to studying a catching dam below Mt. Sukkertoppen, it was decided to merge both into a single, longer catching dam.

3.5 Supporting structures in Sukkertoppen

After the incident in February 2017, various mitigation measures were evaluated for the Sukkertoppen mountain side. The final plan involved partially covering the mountain side with supporting structures, and the residential buildings nearest to the mountain below the uncovered section, were scheduled for removal.

The construction of the steel bridges encountered challenges similar to those experienced with the Lia site, and in addition the proximity of cultural heritage sites (old coal mines) and the presence of coal layers, that raised concerns regarding the foundations. In total there were constructed 15 rows of supporting structures ranging from 3,5 m to 5,0 m in height. Total length of supporting structures is approximately 1500 m.

3.6 Catching dam Lia

Since the supporting structures do not reach the mountain's base, a 400 m long, 5.5 m high catching dam was planned where the uppermost row of houses stood before. Unlike an extra row of steel bridges, the catching dam can also stop debris flows, shallow landslides and divert surface water.

The facing material on impact side is a reinforced dry-block rock wall, and the supporting fill is gravel from the Longyear riverbed. An earth material with low coal content (usually a material close to coal layers, in Norway called "Skeidestein") is embedded in the fill area of the dam construction as transport of this toxic material to special landfill site on the mainland was deemed too expensive and not environmentally friendly. The material is above groundwater level and is surrounded by watertight membrane to hinder leakage from it. When in contact with water it forms a sulfur acid.

The presence of permafrost and the active layer influenced the dam's design. During the planning and construction phases, efforts were made to improve stability and minimize settlement by excavating into the permafrost beneath the active layer. Multiple thermistors were installed within the dam to monitor its temperature. The permafrost is projected to take several years to extend into the fill material. Located just above central Longyearbyen, the catching dam was designed with aesthetics in mind to serve as an appealing landmark where locals and tourists can enjoy viewing the construction and the town from its top.

3.7 Slush-flow nets in Vannledningsdalen

For many years, slush-flows have posed a significant threat to residential areas at Haugen, as well as to roads 222 and 217. Traditionally, such events have been associated with snowmelt during late May or early June. However, climate change has led to an increase in midwinter rainfall, resulting in more frequent occurrences during the dark winter months. While local authorities typically excavate trenches in the valley snowpack each spring to facilitate water drainage, this practice is not safe during the winter's prolonged darkness.



Fig. 4 This photo shows the valley's largest net, which stands 7 m tall on a 1 m foundation. The photo is taken on Oct. 2, 2024.

The client (NVE and LL) ultimately chose the net solution, which comprises 14 modified debris flow nets along a 1200 m valley. The nets range from 3 to 7 m in height, each with about 1 m high foundations and approximately 1 m clearance for the stream. To our knowledge, debrisflow barriers have not previously been used on this scale to mitigate slush flows.

4. DISCUSSION

This article outlines various mitigation measures implemented in Longyearbyen since 2018. These measures share common factors, including permafrost conditions, the presence of an active layer, creeping soil, coal layers and the quality of existing materials. Cultural heritage imposed certain limitations and regulations regarding travel and employment outside the town are strict. Ground conditions have been studied mainly through test drilling, georadar and ERT surveys.

The client has recognized that there is limited information available regarding the expected lifespan of these structures in arctic environments; consequently, relatively high safety factors have been incorporated into both the substructure and superstructure design. Climate change, particularly in the Arctic region, is a significant concern. Accordingly, a study was undertaken to project climatic conditions approximately 50 years from now and for the year 2100.

The design lifetime was specified as 40-50 years; however, several of these structures are expected to last beyond that period especially the superstructures. Test anchors have been installed in Vannledning valley for evaluation in 40 years.

Following reports can be found to be interesting for these projects. A short description of mentioned measures can be found in (Jonsson, 2024). Future climate is discussed in (Kronholm et al., 2019). Detailed design is outlined in (Norges Geotekniske Institutt NGI, 2018a), (Norges Geotekniske Institutt NGI, 2018b), (HNIT Verkfræðistofa, 2021), (HNIT Verkfræðistofa, 2025a), (HNIT Verkfræðistofa, 2025b), (HNIT Verkfræðistofa, 2025c), (Skred AS, 2022), (Geobrugg AG, 2024).

ACKNOWLEDGEMENT

Some of the authors' original text in this article is rewritten with the help of Microsoft Copilot.

5. REFERENCES

- Geobrugg AG, 2024. Design report slush flow barriers Vannledningsdalen Longyearbyen, Svalbard. Romanshorn.
- Hestnes, E., Bakkehøi, S., Jaedicke, C., 2016. Longyearbyen, Svalbard Vulnerability and Risk Management of an Arctic Settlement under Changing Climate A Challenge to Authorities and Experts, in: International Snow Science Workshop 2016. ISSW, Breckenridge, pp. 1–8.
- HNIT Verkfræðistofa, 2025a. Vannledningsdalen Longyearbyen. Detailed Design Of Slush-Flow Nets. OPM Report. HNIT Verkfræðistofa, Reykjavík.
- HNIT Verkfræðistofa, 2025b. Sukkertoppen Lonbgyearbyen. Detaljprosjektering av støtteforbygninger. HNIT Verkfræðistofa, Reykjavík.
- HNIT Verkfræðistofa, 2025c. Sukkertoppen Longyearbyen. Detaljprosjektering av fangvoll sentrumsområdet. HNIT Verkfræðistofa, Reykjavík.
- HNIT Verkfræðistofa, 2021. Longyearbyen. Detaljprosjektering av støtteforbygninger, RIB (No. Rapport 18247-SK01-00). HNIT verkfræðistofa hf, Reykjavík.
- IPCC, 2013. Climate Change 2013: The Physical Science Basis. Contribution of Working Group I to the Fifth Assessment Report of the Intergovernmental Panel on Climate Change. Cambridge University Press, Cambridge, United Kingdom and New York, NY, USA, Cambridge and New York.
- Isaksen, K., Førland, E.J., Dobler, A., Benestad, R., Haugen, J.E., Mezghani, A., 2017. Klimascenarioer for Longyearbyen-området, Svalbard. Delrapport 1, Statsbygg oppdrag: «Bygging og forvaltning på Svalbard i et langsiktig klimaperspektiv», in: Isaksen, Ketil Førland, Eirik J Dobler, Andreas Benestad, Rasmus Haugen, Jan Erik Mezghani, A. (Ed.), . Statsbygg, Oslo, p. 55.
- Issler, D., Jónsson, Á., Gauer, P., Domaas, U., 2016. Vulnerability Of Houses And Persons Under Avalanche Impact The Avalanche At Longyearbyen On 2015-12-19, in: ISSW 2016 International Snow Science Workshop, Proceedings. Breckenridge.
- Jaedicke, C., Hestnes, E., Bakkehøi, S., Mørk, T., Brattlien, K., 2016. Forecasting The Fatal Longyearbyen Avalanche. Possibilities And Challenges, in: International Snow Science Workshop 2016. International Snow Science Workshop, Breckenridge.
- Jonsson, A., 2024. Longyearbyen mitigation measures. Norges vassdrags og energi direktorat NVE, Narvik.
- Jónsson, Á., Gauer, P., 2014. Optimizing Mitigation Measures against Slush Flows by Means of Numerical Modelling A Case Study Longyearbyen, Svalbard -, in: Fujita, M., Araki, Y., Daimaru, H., Gomi, T., Kaibori, M., Miyata, S., Nakatani, K., Takebayashi, H., Tsutsumi, D., Uchida, T., Yamada, T., Huebl, J., Mikos, M., Rudolf-Miklau, F., Portner, N.B. (Eds.), Extended Abstracts of the Interpraevent2014 in the Pacific Rim. November 25-28, 2014 in Nara Japan. Nara, p. 6.

- Jonsson, A., Jaedicke, C., 2017. Avalanches in Longyearbyen Svalbard 2015 and 2017. Zeitschrift für Wildbach-, Lawinen-, Erosions- und Steinschlagschutz/Journal for Torrent, Avalanche, Landslide and Rock Fall.
- Kronholm, K., Jonsson, A., Pedersen, M.B., Husdal, E., Sollie, I.L., Isaksen, K., 2019. Mulige effekter av klimaendringer på valgte sikringstiltak (No. 18241- 09–2). HNIT verkfræðistofa hf, Skred AS, Rambøll Norge AS, Met No.
- Multiconsult AS, 2016. Skredfarekartlegging i utvalgte områder på Svalbard (No. .713416-RIGberg-RAP-001). Multiconsult AS, Tromsø.
- Norges Geotekniske Institutt NGI, 2018a. Detaljprosjektering av sikringstiltak-Lia mellom veg 230 og 228 Prosjekteringsrapport for snøsamleskjerm og avskjærende grøft/voll (No. 20170299- 01- R). Oslo.
- Norges Geotekniske Institutt NGI, 2018b. Detaljprosjektering av sikringstiltak Lia mellom veg 230 og 228. Prosjekteringsrapport for støtteforbygninger (No. 20170299- 05- R). Norges Geotekniske Institutt NGI, Oslo.
- Norges Geotekniske Institutt NGI, 2017. Detaljprosjektering av sikringstiltak Lia mellom veg 230 og 228. Longyearbyen: Alternativ fremgangsmåte for prosjektering og utlysning av sikringstiltak. (No. 20170299- 01- TN). Oslo.
- Norges Geotekniske Institutt NGI, 2015. Vannledningsdalen, Longyearbyen. Forprosjektering av sikringstiltak for bebyggelse og infrastruktur nedenfor Vannledningsdalen (No. 20120650-01-R), 20120650-01-R. Norges Geotekniske Institutt, Oslo.
- Norges Geotekniske Institutt NGI, 2012. Longyearbyen, Svalbard, akuttbistand for snø- og sørpeskred. Vurdering av akutt skredfare 31.01-02.02 2012 (No. NGI rapport 20120153-00-1-TN). Oslo.
- Norges Geotekniske Institutt NGI, 1996. Det gamle sykehuset, Longyearbyen. Skredfarevurdering. Oslo.
- Norges Geotekniske Institutt NGI, 1991. Longyearbyen. Vurdering av tiltak mot snøskred, sørpeskred og drivsnø i Longyearbyen (No. 904025–1). Norges Geotekniske Institutt, Oslo.
- Norges Vassdrags- og Energi Direktorat NVE, 2017. Gjennomgang og evaluering av skredhendelsen i Longyearbyen 21.02.2017 (No. NVE Rapport nr 31-2017). Oslo.
- Skred AS, 2022. Vannledningsdalen debris flow barriers handling of floods and sediment transport (No. 18241-27–1). Skred AS, Ål.
- Spesialenheten for Politisaker, 2017. Vurdering av straffansvar etter snøskred i vei 228 og 230 i Longyearbyen 19. Desember 2015. Hamar.

Swiss experience with direct avalanche protection measures on buildings

Stefan Margreth^{1*}

¹ WSL Institute for Snow and Avalanche Research SLF, Flüelastr. 11, CH-7260 Davos Dorf, SWITZERLAND *Corresponding author, e-mail: margreth (at) slf.ch

ABSTRACT

Around 10,400 residential buildings in Switzerland are situated in areas prone to avalanches. Many of these buildings have direct protection measures, which are among the oldest methods of avalanche protection. Since the 16th century, splitting wedges and avalanche ramp roofs have been used. Today, endangered buildings are mostly protected by the implementation of reinforced concrete walls and lateral wing walls. In Switzerland, construction in blue hazard zones, i.e. areas where 300-year avalanches reach pressures of less than 30 kN/m², is only permitted if direct protection measures are implemented. It is essential to consider avalanches from the start of the design process of a building in hazard-prone areas. Details such as the position of the roof connection or the flow direction of an avalanche are often crucial to ensure the successful functioning of direct protection measures. The Swiss standard SIA 261/1 (2020) is decisive for designing new buildings at risk from gravitational natural hazards. This standard specifies a 300-year event as the protection goal for typical residential and commercial buildings.

1. INTRODUCTION

As an alpine and densely populated country, Switzerland is particularly exposed to natural hazards. One in six residential buildings in Switzerland is exposed to natural hazards (Schellenberg and Horehájová, 2025). Around 10,400 residential buildings are at risk from avalanches. That is 0.8% of the approximately 1.8 million residential buildings. Many of these buildings have direct protection measures. In blue hazard zones (Margreth, 2014), which are areas at moderate risk of 300-year avalanches with a pressure of less than 30 kN/m², the construction of new buildings is generally permitted. However, the buildings require special structural reinforcement. The goal is to ensure that people, animals, and significant property are not endangered. Direct protection measures are among the oldest types of avalanche protection. As early as 1603, the church in Davos Frauenkirch was protected by a splitting wedge that saved the church from damage during several major avalanches (Figure 1a). At around the same time, ramp roofs were built to divert avalanches over the roof (Figure 2b). Earth embankments, wood, and stones were used as building materials. From around 1800, underground cellars were built where residents could take refuge in the event of an avalanche. After the avalanche winter of 1951, a growing number of buildings were reinforced directly, for example, by making the exterior walls stronger. Today, direct protection measures are an important part of integrated natural hazard management. In most cantons, it is mandatory to insure buildings against natural hazards.

S. Margreth O4.3 - Page 108



Figure 1: (a) The church in Davos Frauenkirch was protected in 1609 with a splitting wedge that extends beyond the roof. (b) Since its destruction in 1968, the Länta SAC hut has been protected by an avalanche ramp roof, but the chimney and the outdoor area are still at risk of avalanches (Photos S. Margreth a, SLF b).

2. DAMAGE TO BUILDINGS CAUSED BY AVALANCHES

Unreinforced buildings are susceptible to damage when hit by avalanches (Figure 2). A wooden building is destroyed by avalanche pressure of around 12 to 24 kN/m², and a masonry building by avalanche pressure of around 25 to 45 kN/m². One of the reasons why buildings are relatively vulnerable to avalanches is that their structural system is mostly designed to withstand vertical loads such as snow loads on roofs or live loads. However, they are only designed to a limited extent to withstand horizontal loads. Horizontal loads caused by wind or earthquakes are usually smaller than avalanche loads. For a typical single-family home in the blue hazard zone, the resulting horizontal wind load is 30 to 50 kN, the resulting horizontal earthquake load is about 40 to 140 kN, and the resulting load of a dense flow avalanche with a flow height of 2 m is about 200 to 600 kN. If these horizontal loads cannot be transferred safely to the foundation by the structural system, the building may collapse. To prevent this, reinforced concrete walls and ceiling slabs are usually required. Powder snow avalanches pose an additional problem by causing uplifting forces on the roof, side walls, and rear wall. If the roof is ripped off, the building is likely to be severely damaged. Openings such as doors and windows are often weak points in the building envelope. If they fail, people inside the building are at risk, although the building itself is somewhat unlikely to collapse. Individual components carried by an avalanche, such as stones or tree trunks, can cause high single impact loads.

In Switzerland, around 1,700 buildings, mostly outside residential areas, were affected by avalanches in the extreme winter of 1999, resulting in damage amounting to CHF 100 million. 15% of the damage affected residential buildings. It is interesting to take a closer look at the total damage. Only 20 buildings had damage of more than CHF 0.2 million. For 80% of the buildings, the damage amounted to less than CHF 0.06 million. Minor damage can often be prevented by relatively simple measures such as reinforced shutters. On long-term average, around 80 buildings are damaged by avalanches in Switzerland every year. This is more than 20 times less than in the extreme winter of 1999. Only in exceptional winters, when avalanches extend beyond their usual run-out zone, is a larger number of buildings damaged.

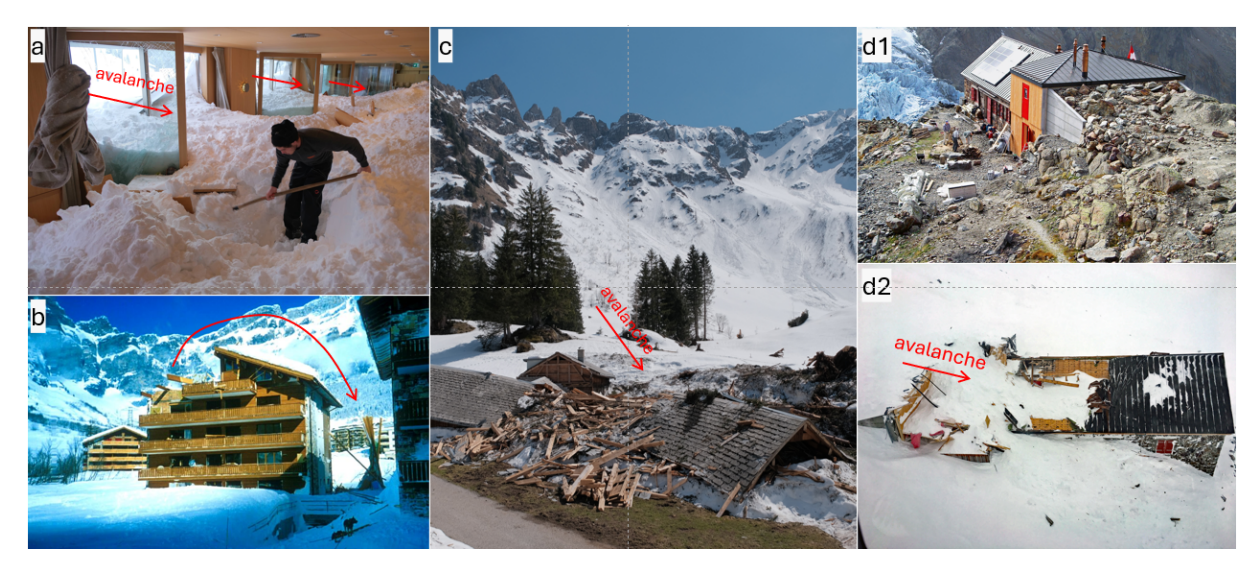


Figure 2: (a) On Jan. 10, 2019, the Hotel Schwägalp was hit by an avalanche. Several windows were broken by an avalanche pressure of 3 to 4 kN/m² and the restaurant was filled with snow. (b) On Feb. 25, 1999, a powder snow avalanche hit a residential building in Leukerbad. The roof was uplifted. (c) On 11 January 2019, the Alp Schottenloch was destroyed by an avalanche carrying several tree trunks, which increased its destructive force. (d2) On Jan. 28, 2021, the SAC Trift hut was damaged by an avalanche. The hut was protected by a ramp roof (d1). The damage was caused by underestimating the impact pressure and by the ramp roof being higher than the concrete wall. (Photos S. Margreth a and c, SLF b, SAC d).

3. OVERVIEW OF DIRECT PROTECTION MEASURES

3.1 Structural reinforcement

The risk to people and property can be significantly reduced through the reinforcement of the building envelope and structural system, the integration of the building into the terrain, and the optimisation of its design and orientation. Structural reinforcement is the most common direct protection measure applied in Switzerland. The main impact wall is typically made of 25-35 cm thick reinforced concrete (Figures 3a and 4b). To reduce the impact area on the wall, a storyhigh embankment can be added on the avalanche side. It is best if the building axis is aligned in the direction of the avalanche flow. To protect the side facades, the impact wall can be built with lateral wing walls (Figure 3a). It is unfavourable if the building geometry has recessed corners, as force concentrations can occur there. Entrances and windows should be avoided in the main impact area. On the other hand, entrances and windows must be protected. Windows can be protected with appropriately dimensioned bulletproof glass or shutters. The design of the roof must be carefully planned, especially if the roof is affected by avalanches. The roof coverage should not extend beyond the reinforced concrete wall. If there is a risk of powder snow avalanches, roof overhangs should be minimized.

3.2 Splitting wedge

Splitting wedges serve to protect buildings and towers. The snow masses are split and diverted past the structure to be protected. The wedge is placed directly on the object or immediately in front of it (Figure 1a). There may be an increased risk in the direction of the deflected avalanche.

S. Margreth O4.3 - Page 110

The maximum opening angle of the wedge should not exceed 60°. The wedge must be high enough so that the avalanche does not flow over it and hit the roof. The wedge should be wider as the building so that the side walls are also protected (Figure 3b). If the wedge is placed directly on the object, no further protective measures need to be taken on the building. Otherwise, pressure and friction forces on the side walls must be taken into account in the structural design.



Figure 3: (a) Residential buildings with a retaining wall and wing walls on the mountain side. The lower building has windows with reinforced shutters. It is unfavorable that the roof protrudes beyond the wall. (b) The residential building is protected by a massive wedge. The wedge protrudes above the roof and protects the side entrance. (c) Ramp roof, which was integrated into the terrain without deflecting the avalanche. It is important that the roof is designed to withstand horizontal friction forces (Photos S. Margreth).

3.3 Avalanche ramp roof

A ramp roof connects without a gap to the terrain or a fill on the mountainside (Figures 1b and 3c). The avalanche flows over the roof of the building. Particular attention must be paid to the design of the roof edges. Special solutions are also required for chimneys, for example in the form of a removable structure. Furthermore, a step or sharp deflection between the terrain and the roof must be avoided. The roof must be designed to withstand horizontal friction forces and the roof beams must be anchored. It is important that there are no bends in the roof surface, as this can cause increased deflection forces. The design of a ramp roof is like that of a snow shed. In addition to the weight of the natural snow cover, the weight of the flowing avalanche, friction forces, deflection forces and the weight of the deposited avalanche snow must be considered. The backwall of the building must be designed for lateral earth pressure. It should be noted that the entire area around the building is at risk of avalanches and that there are no safe accesses.

4. DESIGN OF DIRECT PROTECTION MEASURES

The Swiss standard SIA 261/1 (SIA, 2020) is decisive for the design of new buildings at risk from gravitational natural hazards. This standard specifies a 300-year event as the protection goal for normal residential and commercial buildings. 300-year events are considered to be accidental actions. The determined avalanche parameters are characteristic values. A load coefficient γ_F of 1.0 is used to verify the structural safety. The snow load on the roof is taken into account as a variable accompanying action with a reduction coefficient ψ_0 of 0.8. When determining the avalanche pressure q_{fn} , the importance of the structure is considered with a coefficient γ_f depending on the structure class (SC). For example, the importance coefficient γ_f is 1.0 for residential buildings (SC I), 1.2 for school buildings (SC II), and 1.5 for hospitals (SC III). The avalanche pressure q_{fn} exerted by dry dense flow avalanches on large objects (width >

5 m) is calculated as a function of velocity v_f , density ρ_f and deflection angle α . The recommended value for the bulk density of dry snow avalanches ρ_f is 300 kg/m^3 . The deflection angle α is varied by +/- 20° to take account of any alterations in the flow path of the avalanche (Figure 4a). In the case of an angled impact, an additional frictional stress q_{fr} arises, which depends on the roughness of the surface. The coefficient of friction μ_{fr} for a smooth surface such as concrete is 0.3. Increased pressures occur in wet avalanches and on narrow objects.

$$q_{fn} = \gamma_f \cdot \rho_f \cdot \left(v_f \cdot \sin \alpha \right)^2 \quad [kN/m^2] \quad (1) \qquad q_{fr} = \mu_{fr} \cdot q_{fn} \quad [kN/m^2] \quad (2)$$

Load distribution (Figure 4a) is considered using a three-layer model that considers the natural snow cover h_n (no force transfer), the flow height h_f (uniform avalanche pressure), and the runup height h_{stau} (linear reduction to 0). The energy conversion constant Δ is 1.5 for loose, dry avalanches and 2 to 3 for dense, wet avalanches. If necessary, the impact of individual components is considered. The static equivalent force A_k of an impacting tree trunk acts simultaneously with the avalanche pressure q_{fn} . Formula (4) is based on the impact of a 10 m long tree trunk with a diameter of 0.25 m on a 0.25 m thick and 2.5 m wide concrete slab.

$$h_{stau} = \frac{(v_f \cdot \sin \alpha)^2}{(2 \cdot g \cdot \Delta)} \quad [m] \quad (3) \qquad A_k = \frac{q_{fn}}{0.3} \quad [kN] \quad (4)$$

In addition, powder snow avalanches can occur, which act simultaneously with the dense part. The suspension layer is treated in the same way as wind, whereby the dynamic pressure of the wind is replaced by that of the powder snow avalanche. Suction forces act on the roof, side walls, and rear wall of a building.

5. PLANNING DIRECT PROTECTION MEASURES

When planning a structure in an avalanche area, it is advisable to involve an avalanche expert at an early stage (SIA, 2019). The first step is to assess the avalanche risk at the building's location. The type of avalanche (dense flow or powder snow avalanche) and its characteristics (e.g. velocity, impact pressure, flow height, flow direction, deposit height), as identified through avalanche simulations for a specific scenario, are decisive factors in selecting the most suitable direct protection measure. Experience shows that dry dense flow avalanches are usually decisive, rather than wet snow avalanches. This could change in the future as a result of climate change. In simple cases, standardized avalanche characteristics are used depending on the location of the object in the blue hazard zone (GVG, 1994). The avalanche pressure of a dry dense flow avalanche varies often between 10 and 20 kN/m² and the flow height is between 4 and 5 m. The structure should be integrated into the terrain as well as possible. For example, an avalanche ramp roof is easier to build on a slope or at a terrain step than on flat terrain. In a terrain depression, the action of powder snow avalanches is reduced, but the flow height of dense flow avalanches is increased. Whenever possible, the building should be aligned with the avalanche axis, with the narrower side facing the avalanche. Depending on the situation, natural obstacles such as big boulders or terrain ridges can be considered. If there are several buildings nearby, any increase in risk must be prevented. This can make the use of splitting wedges impossible. It is important to consider how the interior and exterior areas of a building will be used. Access points and openings on the avalanche side should be avoided. Underground entrances, e.g., through a parking garage or an access protected by the building, simplify any evacuations. Permanent protective measures are preferable to removable ones (e.g. protecting a window with reinforced glass instead of shutters).

S. Margreth O4.3 - Page 112

Most cantons in Switzerland have cantonal building insurance companies, which play a key role in the planning process of direct protection measures. When granting building permits, they define the avalanche actions to be considered at the site, review the planned mitigation measures, and approve the mitigation measures once they have been implemented. If the implementation does not comply with the project plan, the avalanche risk may be excluded from the insurance coverage.

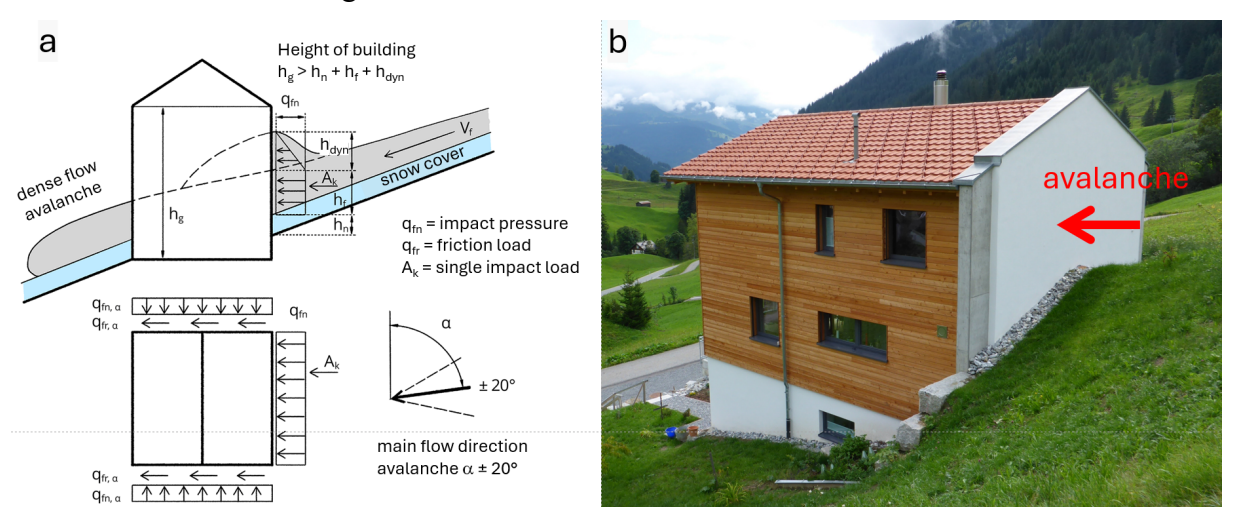


Figure 4: (a) Action of a dense flow avalanche on a building following standard SIA 261/1. (b) Residential building on a slope protected by a concrete wall on the mountain side. The concrete wall is filled with earth material up to the first floor. The wall protrudes above the roof and is wider than the building (Photo S. Margreth).

6. CONCLUSIONS – LIMITS OF DIRECT PROTECTION MEASURES

Direct protection measures are a key method when building in hazard areas. Such measures are suitable for blue hazard zones with moderate risk and avalanche pressures of less than $30 \, \text{kN/m^2}$. For higher pressures, area protection measures such as avalanche dams or supporting structures are often more cost-effective. New buildings are much easier to reinforce against avalanches than existing buildings. It is very important to involve avalanche experts at an early stage of planning to optimize the building concept regarding avalanche actions. The aim should be to plan robust measures whose effectiveness is guaranteed under various conditions. Access to the building must be always given the necessary attention. Openings on the avalanche side should be avoided or protected accordingly. In addition to correctly determining the avalanche actions, small planning details are often decisive whether a direct protection measure will work well.

REFERENCES

GVG, 1994. Vorschriften für bauliche Massnahmen an Bauten in der blauen Lawinenzone. Gebäudeversicherung Graubünden, Chur. (https://gvg.gr.ch/)

Margreth, S., 2014. Hazard mapping in Switzerland. Avalanche Review, 33(2), 31-32.

Schellenberg, J. and Horehájová, A. 2025. Achtung Gefahr. Immobilien aktuell. Nr. 1/25. Zürcher Kantonalbank. p. 19-25.

SIA, 2020. Actions on structures - Supplementary Specifications. Swiss code SIA 261/1. Swiss Society of Engineers and Architects SIA, Zürich.

SIA, 2019. Entwerfen & Planen mit Naturgefahren im Hochbau. Dokumentation D0260. Swiss Society of Engineers and Architects SIA, Zürich.

Planning & structural limitations of RACS - Making structures survive in avalanche release areas

Martin Venås^{1*}, Walter Steinkogler², Andreas Egger², Stian Langeland¹

Wyssen Norway AS, Campus Fosshaugane Trolladalen 30, NO-6856, Sogndal, NORWAY
 Wyssen Avalanche Control AG, Feld 1, CH-3713 Reichenbach, SWITZERLAND
 *Corresponding author, e-mail: venas (at) wyssen.com

ABSTRACT

To protect objects at risk from snow avalanches, remote avalanche control systems (RACS) have been successfully applied operationally for several decades. Wyssen Avalanche Control has been a supplier of RACS solutions since the year 2000. Pre-engineered scenarios have been developed for dry snow avalanche scenarios with flow velocities and snow height up to 25 m/s and 1.5 m respectively. In many instances these scenarios can streamline the planning process. However, cases that fall outside of the pre-engineered solutions might still be realized in cooperation with the supplier to find safe and effective placements. To illustrate this, we present cases from Switzerland, USA and Canada that show a wide spectrum of challenges and requirements, leading to vastly different tower placements. Ultimately, determining tower placement requires balancing maximal release area coverage for each system against favourable geotechnical conditions and other real world factors such as access and communications, while staying inside the structural design limitations of the systems and ensuring operational requirements are fulfilled.

1. INTRODUCTION

Since 2000, Wyssen Avalanche Control (WAC) has supplied avalanche towers for Remote Avalanche Control Systems (RACS). RACS enables triggering artificial avalanches from a safe distance. Over the past decades RACS have proven to be a safe and cost-effective method for protecting roads, railways, ski resorts and mines around the world. As of May 2025, Wyssen has 917 operational avalanche towers worldwide. The tower construction has undergone optimization through several iterations, and over the years, we have gained extensive experience through close dialogue with our customers and their consultants, as well as through in-house design, construction, and operation.

A thorough planning phase for the placement of towers is important and depends on a variety of factors. In this extended abstract we will focus on safety of the object at risk and safety of the towers themselves, where the following three factors are most important:

- Optimal explosive effect to release avalanches from release areas of interest
- Minimizing the exposure of the tower to natural or artificially triggered avalanches
- Geotechnical ground conditions (based on input from geotechnical engineer)

Other considerations such as risk of rockfall, safe access, helicopter longline operation and communication coverage are not included in this article.

2. PLANNING METHOD / PROJECT METHODOLOGY

2.1 Early planning phase

The release area to be controlled by RACS is mainly defined by the objects at risk and their avalanche paths. Typically, the goal is to affect the release area by direct effect from the explosive detonation. Lower release areas in the avalanche path can also be indirectly affected by the released avalanches. It is important to clearly define the effective range of the system early in the planning phase, as this will impact the number of RACS and their suggested placement. Key factors influencing the effect include distance from the blast, snowpack structure at the time of detonation, and terrain shadow effects. WAC recommends a 120-to-130-meter line-of-sight radius for a standard 4 to 5 kg charge, based on measurements and operational experience (Gubler, 1976; Meier, 2023; Meier, 2024 and Seitz; 2021). Visibility analyses of the affected area can be conducted using GIS tools to identify terrain shadowing.

Operational requirements may justify smaller spacing between towers than the recommended range, for example, to reduce the need for reloading during the season. In areas with high accessibility demands, such as busy roads or above settlements, overlapping coverage from multiple towers ensures redundancy. Nonetheless, we recommend striving for the minimum number of towers required for effective control, as the method has proven reliable within the recommended range and offers substantial benefits in terms of cost, maintenance, and environmental impact. It is important that the operations team is informed of any financial or other constraints during the planning phase, such that operations can be tailored accordingly (Campbell et.al., 2016). An example of this is given in chapter 3.

2.2 Tower structural limitations

Wyssen Avalanche Towers are engineered to withstand snow and avalanche forces under a wide range of conditions. To define their load limits, independent consultants (A. Burkard AG, Paul Glassey SA) modeled various scenarios using both Swiss (Stoffel et al., 2006; Margreth, 2007) and international calculation methods (Jóhannesson et al., 2009), followed by structural analyses using standardized safety factors according to Swiss standards (SIA)/Eurocode.

Scenarios included dynamic impacts from dry slab avalanches (10–30 m/s), static snow pressures and wind load. For critical cases, additional load by avalanche powder clouds was considered. Dry slab scenarios assumed a snow height of 1.5 m (vertical) with a flow height of 1.2 m at a density of 300 kg/m³. Results of structural analysis show that towers can withstand dry avalanches with velocities up to 25 m/s with the given parameters, also in south-facing slopes with high snow creep and glide. Forces on the tower due to wet avalanches have potential to reach the maximum force scenario at lower velocities, partly due to the higher density of snow and higher run-up height.

2.3 Recommendations for placement selection

To support safe placement of avalanche towers, a simplified method has been developed to assess avalanche hazard at potential tower sites by estimating avalanche velocity as a function

of slope angle and distance from the fracture line. We generally suggest that towers can be placed provided certain conditions are met:

- 1. Less than 200 m line-of-sight distance to expected fracture line, or where the avalanche velocity is < 25 m/s.
- 2. Where the release area and the avalanche path above the tower are not channeled to avoid accumulation of flowing snow mass.
- 3. Avoidance of gully shaped terrain features and utilize ridge features to avoid increased flow heights, to minimize rock fall potential and optimize the affected area by the explosive detonation.
- 4. Wet snow avalanches can be avoided by placing towers outside of the main flow path.

If any of these conditions are not satisfied, we suggest a more detailed expert assessment.

2.4 Foundation and anchor design

In the next step detailed measurements and a terrain assessment are conducted during a field visit. These values are then used to determine appropriate anchor dimensions and anchoring lengths for the local ground conditions of each tower and foundation type (Figure 1). Locations with good (or as good as possible) geotechnical conditions should be favored, allowing construction of a regular foundation without special adaptions or design changes (e.g. special anchors). Poor ground conditions may limit the areas where foundations can be placed and must be surveyed by a geotechnical engineer. Based on the pre-engineered design this leads to a maximum allowed force of 332 kN per vertical anchor and 543 kN on the shear relief anchor.





Figure 1 Wyssen concrete (left) and concrete-less foundation (right) with 4 vertical and 1 shear relief anchor.

3. APPLICATION IN PRACTICE

Wyssen Avalanche towers have been placed in a variety of mountainous terrain. As a system provider, we strive for customers and consultants to position the towers following the procedure and criteria presented in section 2. A complete overview of all possible concept parameters is outside of the scope of this article, but here we present a few examples of different operational settings and typically faced boundary conditions.

3.1 Spacing between RACS

Operational requirements can demand both tighter or sparser spacing of towers. A large spacing (= beyond the assumed effective range) between RACS can be used if the main goal is to disturb the snow cover and mitigate the hazard of large avalanches with wide fracture lines, whereas smaller (natural) avalanches are acceptable to the operation as they do not endanger the infrastructure in the runout. At Breitzug close to the town of Davos (Switzerland), RACS have been installed in 2017 for the protection of the road and railway. Four towers were placed on natural ridge features with spacing of up to 320 m. Since the installation of the RACS, no natural or controlled avalanche reached a size that would endanger the underlying infrastructure.

An example in the opposing end of the scale is the ski resort of Alta (USA), where towers were placed relatively close together to directly affect individual release areas to mitigate hazard of (natural or human triggered) small avalanches which could reach ski slopes (Figure 2 left). In the alpine town and ski resort of Samnaun (Switzerland), 87 RACS are used to protect the access road, the settlement and ski slopes (Figure 2 right). Most avalanche paths are very steep and can directly affect the objects at risk, especially for the settlement. Some towers are placed closely together and often overlap in effective range for system redundancy. With more than 20 years of operational experience with RACS this client continuously refined its operational concept and even relocated some towers after a few winters to optimize positions and effectiveness.

3.2 Limited locations due to geotechnical limitations or overhead hazard

In some cases, suitable tower installation locations are very limited due to overhead avalanche hazard or rock fall potential. Also, geotechnical limitations can dictate where tower foundations can be constructed (in a cost-efficient manner).

At the Brucejack mine (Canada) access road, RACS was installed in 2019 to mitigate avalanches from upper release areas and with an additionally row of RACS on the lower parts just above the main access road (Figure 3 left). The lower row of towers has seen minor damages, e.g. to the uphill ladders placed on the tower, by the avalanches released from the top.

For the road between Sils and Maloja (Switzerland), suitable locations for installation of RACS has been limited by rockfall hazard. Exposure of the towers was minimized by selecting placements on natural rock features and ridges. Also, the concrete-less design (Figure 1 right) was chosen for construction efficiency, e.g. no formwork or concrete needed, and to minimize exposure time of workers during construction.

Towers are generally placed on natural ridges for maximum explosives effect to the side (based on spherical wave propagation from the detonated explosive charge). These placements also minimize the expected forces acting on the tower by natural or controlled avalanches. This also

applies to reducing the risk of rockfall to the tower and furthermore reduces the visual impact of a tower protruding above ridge line. E.g. due to the very steep terrain in Samnaun (Switzerland), the expected velocities would have been too high if towers were not placed on ridge features (Figure 2 right).

Special adaptations of the towers are possible but usually require a significant amount of additional engineering and (material and construction) costs. Often a lot of knowledge and operational experience exists with the RACS suppliers, and it is recommended to consult and involve them early in the planning phase.



Figure 2 Left: Alta ski resort (USA) – towers are placed close together to directly affect individual release areas to mitigate hazard of (natural or human triggered) small avalanches which could reach ski slopes. Right: Samnaun (Switzerland) – 87 RACS are used to protect the access road, the settlement and ski slopes.



Figure 3 Left: Brucejack mine (Canada) access road, RACS (yellow dots) installed to mitigate avalanches from upper release areas and with an additionally row of RACS on the lower parts above the main access road. Right: Sils-Maloja (Switzerland) –Limited locations due to geotechnical conditions. Risk of rockfall was minimized by selecting natural ridges.

4. DISCUSSION

When planning any sort of structure in mountainous terrain, the existing design and construction standards, which are typically aimed at e.g. residential buildings or road construction, are often inadequate. Thus, deviations from these standards (e.g. SIA standard) have been compiled and

engineered for a variety of structures resulting in cost-efficient and suitable designs – e.g. Swiss guidelines for construction of defense structures in avalanche starting zones (Margreth, 2007).

This also applies to Wyssen Tower, where the construction is a balance between the maximum forces where the structure must withstand (which affects the thickness and weight of steel) and the constructability and suitability for transport via helicopter (especially at higher altitudes). After 25 years of applying the Wyssen RACS towers design to nearly 1000 towers, experience shows that the design is robust and cost-efficient. In most cases it is not possible to find the "ideal" location for an avalanche tower. In reality, it is much more a compromise between affected area, effective use of explosive power and the number of RACS while still staying within the design parameters.

As wet avalanches often cannot be completely excluded, we found our guidelines to be imprecise and difficult to apply. In discussions with clients and consultants in such cases, we have suggested that, if towers are actively operated to ensure continuous disturbance of weak layers, the potential size of wet avalanches will generally be very limited. We are not aware of any cases where wet snow avalanches have caused critical damage to the main structure or foundation. Further research and measurements on the impact pressures applied to objects caused by wet snow avalanches could improve the planning of RACS.

5. CONCLUSION

Remote Avalanche Control Systems (RACS) are a cost-efficient and long-term solution for an operation if placed well. For the installation of Wyssen towers we conclude with the main points:

- The operational requirements and the effective range of the RACS set the boundaries the project-specific design.
- To achieve the most cost-efficient solution, it is recommended to stay within the suppliers design limitations, while simultaneously optimizing RACS placements to maximize release area covered.
- Pre-engineered scenarios allow for simplified planning. If scenario limits are exceeded and for complex projects, it is advised to consult the supplier.
- A field visit is necessary to finalize each position. During this visit, geotechnical conditions, constructability and local terrain should be assessed.
- Final tower placement is a trade-off between a variety of factors that should be considered during the planning phase.

REFERENCES

Campbell, C., Conger, S., Gould, B., Haegeli, P., Jamieson, B., Statham, G., 2016. Technical Aspects of Snow Avalanche Risk Management. Resources and Guidelines for Avalanche Practitioners in Canada. Canadian Avalanche Association, Revelstoke, BC, ISBN: 978-1-926497-00-6, pp. 6-8.

Gubler, H., Wyssen, S., & Kogelnig, A., 2012. Guidelines for Artificial Release of Avalanches. Wyssen Avalanche Control AG: Reichenbach, Switzerland.

- Gubler, H., 1976. Kunstliche Ausloesung von Lawinen durch Sprengungen, Mitteilungen des Eidgenossischen Institutes fuer Schnee- und Lawinenforschung, Davos, Switzerland...
- Jóhannesson, T., Gauer, P., Issler, D, Lied, K., (eds.), 2009. The design of avalanche protection dams. Recent practical and theoretical developments. Brussels, Directorate-General for Research, European Commission.
- Margreth, S., 2007. Defense structures in avalanche starting zones. Technical guideline as an aid to enforcement. Environment in Practice no. 0704. Federal Office for the Environment, Bern; WSL Swiss Federal Institute for Snow and Avalanche Research SLF, Davos, Switzerland. 134 pp.
- Meier, B., 2023. A model approach to describe the Effects of Explosives on a Snowpack, Proceedings: International Snow Science Workshop 2023, Bend, Oregon, USA.
- Meier, B., 2024. On Triggering Avalanches. What Happens Between Explosion and Release. Proceedings: International Snow Science Workshop 2024, Tromsø, Norway.
- Seitz, B., 2021. Measuring Explosive Airblast of Remote Avalanche Control Systems, Montana State University. Montana, USA.
- Stoffel, L., Schär, M., Margreth, S., & Müller, R., 2006. Berücksichtigung der Lawinen-und Schneedruckgefährdung bei touristischen Transportanlagen. Bern: Bundesamt Verkehr.

Keeping the power on: Quantitative avalanche risk assessment and operational decision making for a transmission in British Columbia, Canada

Alan Jones^{1*} and Christ Argue ¹

¹ Dynamic Avaalanche Consulting Ltd. Revelstoke Canada,

ABSTRACT

The power supply between Terrace and Prince Rupert, British Columbia, Canada is provided by BC Hydro's 287 kV transmission line. This is the primary power supply to over 12000 residents in Prince Rupert, which is also an important Pacific port that moves \$60 billion of cargo annually. Since construction in the 1960's, avalanches have damaged one structure four times, which was relocated and replaced in 2019 by two 62 m reinforced, steel poles to increase conductor clearance. Another fifty-five structures or conductor spans are exposed to avalanche hazard along the 126 km route.

In 2023 and 2024, week-long generator maintenance outages were scheduled for the backup power system. The reliability of the transmission line was critical during this time to avoid extended power disruption due to avalanches. A quantitative risk assessment was completed to express baseline risk as the annual probability of service disruption. Results were communicated using a semi-quantitative risk matrix incorporating probability and consequence.

To determine if the risk was tolerable and generator maintenance should proceed, baseline risk was adjusted based on current and forecast avalanche conditions. This assessment considered the snowpack structure, snow distribution in the avalanche track and runout zones, and the forecast weather. This assessment was compared to the baseline avalanche risk assessment to inform a decision to proceed with generator maintenance.

This paper summarizes historical avalanche damage to the line, implemented mitigation measures, and presents a methodology to link long-term avalanche risk to short-term, operational decisions.

A. Jones and C. Argue O5.1 - Page 121

Comparing Benefit-Cost Analyses of Snow Avalanche Mitigation Using Two Hazard and Risk Assessment Approaches

Michael Bründl^{1,2*}, Jan Kleinn^{1,2}, and Linda Zaugg^{1,2}

WSL Institute for Snow and Avalanche Research SLF,
 Climate Change, Extremes and Natural Hazards in Alpine Regions Research Centre CERC, both Flüelastrasse 11, 7260 Davos Dorf, SWITZERLAND
 *Corresponding author, e-mail: bruendl@slf.ch

ABSTRACT

In Switzerland, protective measures against gravitational natural hazards, such as snow avalanches, are planned according to economic, ecological and social criteria. Since 2008, the economic assessment of planned mitigation measures is carried out with the software EconoMe.

The methodological basis for EconoMe is the risk concept for natural hazards which was formally introduced in 2009 as part of the Swiss national strategy for natural hazards. It is based on hazard intensity maps with three to four predefined release return periods. This approach has its limits, which is why the concept of probabilistic risk assessment is currently being further developed for the assessment of gravity-driven natural hazards in Switzerland.

We compare the results of a benefit-cost analysis using the EconoMe method with the results obtained using a probabilistic hazard and risk analysis. The results show that the benefit-cost ratio obtained by both approaches is in a comparable range in this case study. The probabilistic assessment leads to a lower benefit-cost ratio in this case study given equal assumptions on the effectiveness of measures but it provides a wealth of additional possibilities for hazard and risk assessment.

1. INTRODUCTION

Since 2008, Swiss authorities base decisions on mitigation measures against gravity-driven natural hazards, such as snow avalanches, on quantitative risk assessment. Hereby the expected reduction of annual damages is compared to the annual cost of the planned mitigation measures (Bründl and Zaugg, 2019). Additionally, the individual risk of death for a person in the affected area is considered. If it exceeds the value of 1 x 10⁻⁵ per year, mitigation measures for reducing the risk at reasonable expense should be examined (Bründl and Margreth, 2021, PLANAT, 2015). To evaluate the effectiveness and efficiency of mitigation projects, the software EconoMe was introduced in 2008 (EconoMe, 2025), so that federal subsidies for mitigation projects are based on a uniform approach.

In the current practice, this type of risk assessment is based on hazard intensity maps, which typically depict the maximum intensity at 30, 100, and 300 years of release return periods. If possible, an intensity map of 500 - 1,000 years of return period should be included. These intensity maps are primarily developed for hazard mapping relevant in land-use planning. According to Swiss regulations, hazard maps indicate where construction of new buildings and building extensions are not allowed (red zone), where restrictions apply (blue zone) and where low (yellow zone), residual (yellow-white hatched zone) or no hazards (white zone) are

expected (FOEN, 2016). For snow avalanches, the information shown in an intensity map is based on the snow accumulation over a three-day period (Δ HS3D) at a specific meteorological station for selected return periods. These return periods are derived using extreme value statistics applied to the snowfall data. Intensity maps depict the maximum expected physical impact at objects at risk across all possible and conceivable process pathways. The intensity I is typically divided into three classes (I < 3kPa, 3kPa < I < 30 kPa; $I \ge 30$ kPa). The exceedance probability of Δ HS3D and therefore of an avalanche release is assigned to the exceedance probability of the intensity maps and hence to the exceedance probability of the damage occurring. Using such intensity maps for risk assessments results in an overestimation of damage at the return periods. To counteract this overestimation, a factor – the spatial probability of occurrence, ranging from 0 to 1 – is applied to the damage values. This factor reflects that, depending on the return period of release, only part of the process area is usually affected during a single avalanche event. This also reduces the expected annual damage (Bründl et al., 2009).

Probabilistic hazard and risk modelling is based on a large number of simulated hazard events and their associated event probabilities. The outcome of such a probabilistic modelling allows to derive continuous intensity-frequency curves at any given location. Therefore, maps can be generated, which represent the intensity through probabilistic modelling at the location for the given return period. Combined with object values and vulnerabilities, it allows to derive continuous loss-frequency curves for single objects or groups of objects.

Probabilistic hazard and risk assessment has been common practice for decades for earthquakes (e.g. Silva et al., 2015, Gerstenberger et al., 2020) with the approach being based on Cornell (1968). Since then, the approach has been adapted to tropical cyclones (Bloemendaal et al., 2020, Emanuel et al., 2006, Hall and Jewson, 2007, Hall et al., 2021, Lee et al. 2020) and to more localized hazards such as hail (Schröer et al. 2022). Recently, this approach has been introduced to hazard analysis of snow avalanches (Kleinn et al., 2024a; Glaus et al., 2024) and rockfall (Kleinn et al., 2024b).

Here, we compare benefit-cost analyses using the EconoMe approach and results from a probabilistic hazard and risk assessment for a case study with the identical assumptions for exposed values, vulnerabilities, and mitigation measures. Both approaches are based on the same set of simulations, which has not been formally validated in the field.

2. METHODS

2.1 Case Study Site and Exposed Values

To illustrate our approach, we chose the area "Ausserschwand" in Adelboden, canton of Berne. The investigated release area and the runout area is located at an altitude between 1,330 and 1,800 m a.s.l. In the investigated area, 25 buildings are located in the red and 15 in the blue hazard zone (Figure 1). We determined the type and usage of buildings and derived their monetary values and their vulnerabilities according to the standard values in EconoMe (EconoMe, 2025). The standard vulnerabilities in EconoMe are only defined for three ranges of intensity: I < 3kPa, 3kPa < I < 30 kPa; $I \ge 30$ kPa. For each housing unit we assume 2.24 persons are present for 18 hours per day, which are standard values in EconoMe.

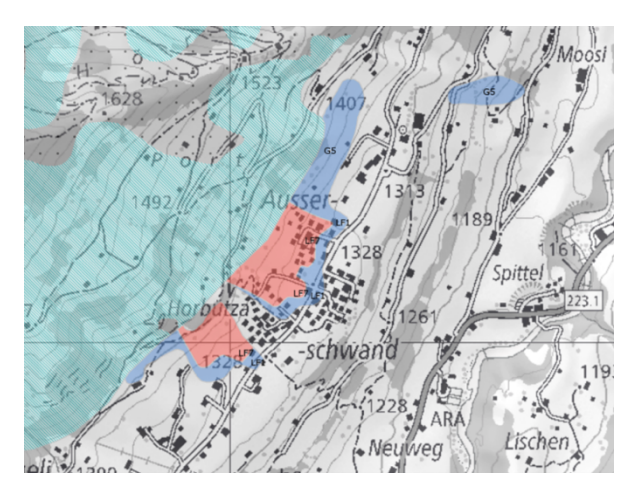


Figure 1 Current official avalanche hazard map of the area "Ausserschwand" near Adelboden (left). 40 buildings are located either in the red or the blue hazard zone.

2.2 Hazard Modelling

For the probabilistic hazard analysis, we simulated the avalanches for 13 release depths (Δ HS3D) from 70 cm to 310 cm in steps of 20 cm using the operational version of RAMMS and standard values for friction parameters μ and ξ . According to the extreme value statistics of the weather station Jaunpass, we determined the return periods of Δ HS3D as shown in

Table 1 for selected values of Δ HS3D. In our pilot study, the return periods of the release depths did not match the standard return periods of 30, 100 and 300 years. Therefore, we chose release depths with return periods of 22, 74, and 217 years to be representative of the standard return period values. We derived the maximum pressure from all simulations based on these release depths for the EconoMe approach.

Table 1 Selected release depths and their return periods as used for hazard and risk modelling.

ΔHS3D [cm]	Return period [years]
110	6
130	22
150	74
170	217
190	570
210	1364

For the probabilistic approach, we ran a total of about 14,000 simulations across all release depths in the entire region. 356 of these simulated avalanches affect the buildings of this pilot study.

2.3 Estimation of Expected Annual Damage

For the standard EconoMe approach, we combine the spatial distribution of avalanche hazard, expressed as impact pressure [kPa], for each of the three return periods to determine the expected damage. This calculation accounts for building vulnerabilities and the assumed number of occupants. The calculated damage is reduced by the spatial probability of occurrence for each return period (standard values of EconoMe; EconoMe, 2025). The expected annual damage is then calculated from the three data points using a step function.

In the probabilistic approach, we consider the simulated pressure at each building for each simulated avalanche. In combination with building vulnerabilities, values and number of occupants, we derive a damage for each simulated avalanche. The damage of each simulated avalanche and its probability are combined to a continuous loss-frequency curve. The expected annual damage is the integral of the loss-frequency curve.

The results of both approaches can be depicted in loss-frequency curves (Kleinn et al., 2022).

2.4 Mitigation Measures

The area of Ausserschwand is prone to avalanches releasing from a 30 - 40° steep south-east facing slope at an altitude of 1,800 m a.s.l. As a fictitious mitigation measure, we planned two areas with 1,005 m wooden support structures (effective height D_k =2.5 m) and two areas with 769 wooden tripods, both combined with afforestation (Figure 2). The total cost of investment for these measures is estimated at 1,770,000 CHF. We assumed maintenance costs of 0.2 % and a lifespan of 30 years for the support structures and the tripods. For afforestation, we assumed 1 % maintenance costs and a lifespan of 100 years. This results in annual costs for all measures of 71,200 CHF per year (EconoMe, 2025). As a simplified assumption of the measures' effectiveness, we assume no avalanche release for release depths of up to 150 cm within the mitigation measure polygons for both approaches. In the EconoMe approach, this leads to a reduced damage for 22 years and 74 years of return period. Damages at 217 years of return period (release depth of 170 cm) were considered to remain unchanged. For the probabilistic approach, the avalanche events originating within the mitigation measure polygons with release depths of up to 150 cm were removed from the avalanche event set for analyses of hazard and risk with measures.

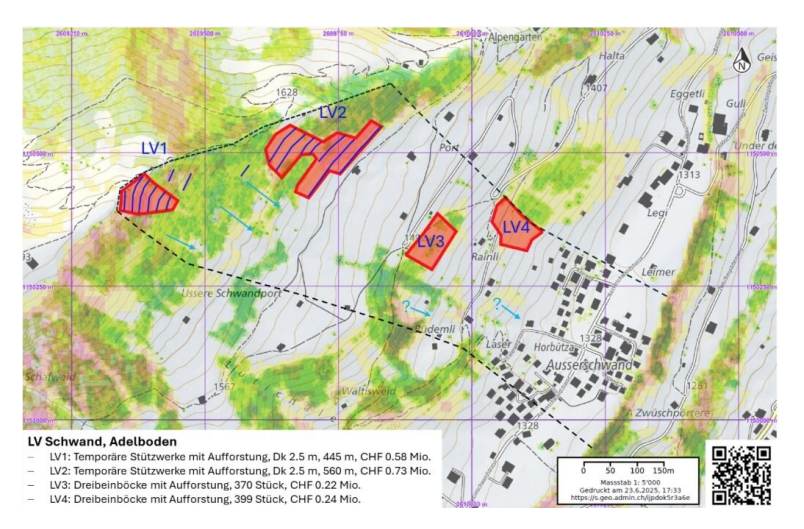


Figure 2 Overview of the fictitious mitigation measures to reduce avalanche hazard in the area "Ausserschwand" in Adelboden, canton of Berne. LV1 and LV2 consist of wooden supporting structures. LV3 and LV4 consist of wooden tripods. All four areas include afforestation.

3. RESULTS AND DISCUSSION

3.1 Hazard Modelling

In total, we ran 14,000 simulations for the region around Adelboden, of which 356 affect the slope of our case study around Ausserschwand. RAMMS provided information on avalanche velocity, flow height and avalanche pressure for each grid cell. These simulations can be used to calculate the maximum impact of all releases of a given release depth and return period according to the current Swiss hazard mapping procedures (top row of Figure 3). In combination with the event probabilities of the simulated avalanches, intensity frequency curves can be calculated for each grid cell and the intensity at any given return period can be derived. We extracted intensities for the return periods of avalanche release depth used for the current hazard mapping approach (bottom row of Figure 3).

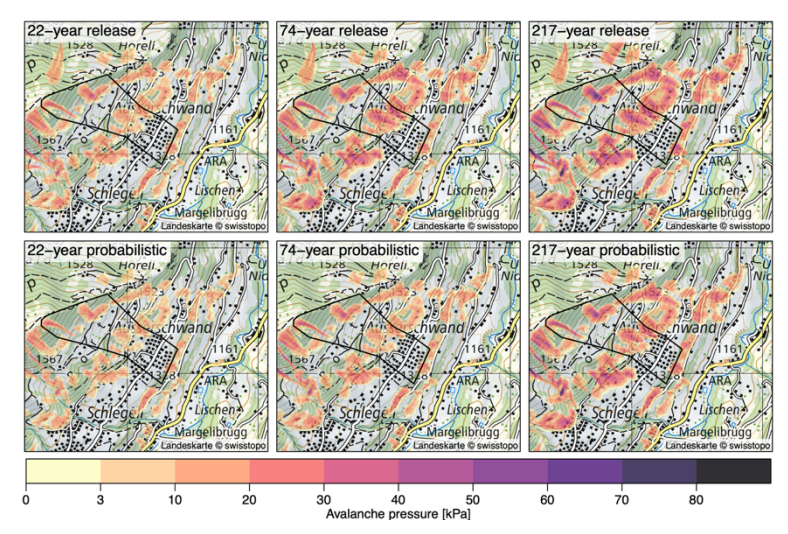


Figure 3 Avalanche hazard as modelled with RAMMS. The top three figures show the maximum pressure [kPa] in each grid cell from all simulations of release depth of the return periods of 22, 74, and 217 years, respectively. The lower three figures show the effective pressure [kPa] in each grid cell derived from all avalanche simulations and their corresponding probabilities. The expected annual damage is estimated for the buildings including persons within the polygon.

3.2 Loss-Frequency Curves

Loss-frequency curves are required for characterizing risk (Kleinn et al., 2022). The expected annual damage, which is commonly used for benefit-cost analyses, is one of the characteristics of risk. When loss-frequency curves are depicted using a linear loss scale and linear exceedance probabilities or non-exceedance probabilities as axis, the surface underneath the loss-frequency curve corresponds to the annual expected damage.

The loss-frequency curve of the EconoMe approach consists of a step-function to connect the damage values of the three return periods of avalanche release (Figure 4). The loss-frequency curves of the probabilistic approach were constructed using all event damages and the corresponding event probabilities. This results in continuous loss-frequency curves for the probabilistic approach.

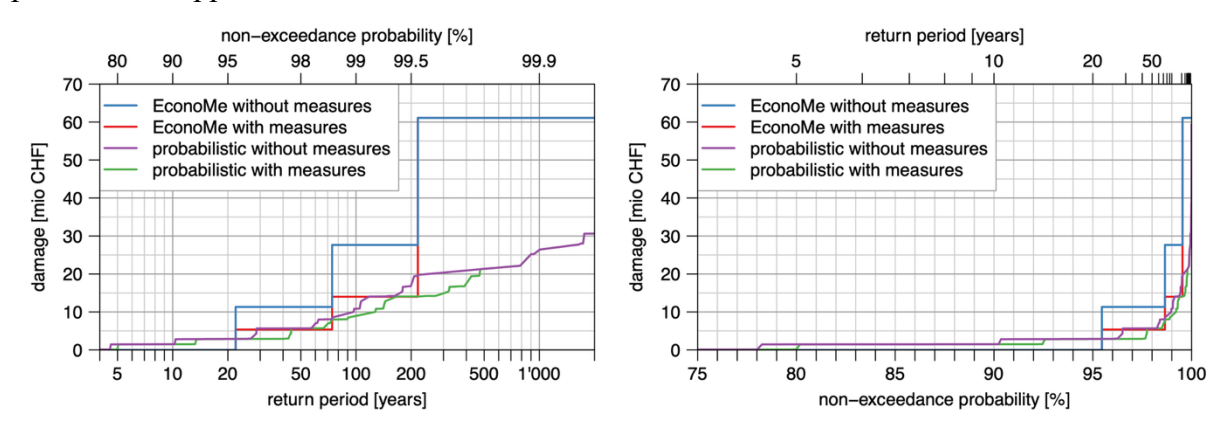


Figure 4 Loss frequency curves without (initial value) and with consideration of the fictitious mitigation measures. The two panels show the same loss-frequency curves with different probability scales. In the panel to the right, the surface underneath the curves correspond to the annual expected damage. The figure on the right thus allows a visual comparison of risk characteristics, due to the area-preserving representation of annual losses. This not only allows different risks to be compared but also enables the contribution to the annual loss of rare and frequent events to be identified.

3.3 Expected Annual Damage

The expected annual damages as derived from the loss-frequency curves are shown in Table 2 for both the EconoMe and the probabilistic approach.

Table 2 The expected annual damage (EAD) for the initial state before mitigation and the mitigated state (remaining EAD) as well as the resulting reduction in EAD are shown for both risk assessment approaches.

Approach	Initial EAD [CHF/a]	Remaining EAD [CHF/a]	Reduction [CHF/a]
EconoMe	888,089	576,676	311,412
probabilistic	733,533	605,606	127,928

3.4 Benefit-Cost Ratio

The results from both risk assessment approaches provide the information to estimate the economic efficiency of the planned mitigation measures. The EconoMe approach estimates a reduction in expected annual damages of 311,412 CHF/year, annual costs of 71,200 CHF/year for the measures, resulting in a benefit-cost ratio of 4.4. Using the probabilistic approach, the benefit-cost ratio is 1.8.

4. CONCLUSIONS

This comparison of a risk-based benefit-cost analyses for avalanche mitigation measures, using two different hazard and risk assessment approaches in a case study, shows that the results are within a comparable range. The probabilistic approach yields a lower benefit-cost ratio, which is attributed to its more differentiated hazard and risk representation. The results should be interpreted with caution, considering the specific hazard and exposed values of this case study. In other cases, the difference between the two approaches may be different.

Probabilistic modelling provides a range of advantages compared to the EconoMe approach. Since damages are calculated for all simulated events, mitigation measures can be designed in a much more targeted manner by reducing the most damaging release areas. Furthermore, the probabilistic approach allows to take multiple damaging events per year into account in the risk assessment and hence also in the benefit-cost-analyses. The continuous intensity-frequency and loss-frequency curves provide more information on possible jumps in intensity or damages compared to EconoMe. Probabilistic hazard and risk assessment also takes the spatial correlation into account, i.e. the possibility of multiple objects being hit in a single event. Changes induced by climate change or changes in the building stock, can be taken into account in a more realistic manner in the probabilistic approach.

ACKNOWLEDGEMENT

We thank the Foundation for Prevention of the Public Insurance Companies for Real Estate and the Department Natural Hazards (DNH) of the Office for Forest and Natural Hazards of the Canton of Berne for the financial support and fruitful discussions. We thank Nils Hählen (DNH) for recommending the case study area and Stefan Margreth, SLF for assisting us in planning the fictitious mitigation measures. We further thank the Canton of Grisons for the support of the research centre CERC, which is the financial basis of this research.

REFERENCES

- Bloemendaal, N., Haigh, I.D., de Moel, H. et al., 2020. Generation of a global synthetic tropical cyclone hazard dataset using STORM. Sci Data 7, 40, https://doi.org/10.1038/s41597-020-0381-2.
- Bründl, M., & Margreth, S., 2021. Integrative risk management: the example of snow avalanches. In *W. Haeberli & C. Whiteman (Eds.), Snow and ice-related hazards, risks, and disasters* (pp. 259-296). https://doi.org/10.1016/B978-0-12-817129-5.00002-0.
- Bründl, M., & Zaugg, L., 2019. Risk management of gravitational driven processes in Switzerland. In *International Symposium on Mitigative Measures against Snow Avalanches and Other Rapid Gravity Mass Flows* (pp. 31-38). Association of Chartered Engineers in Iceland.
- Bründl, M., Romang, H. E., Bischof, N., & Rheinberger, C. M., 2009. The risk concept and its application in natural hazard risk management in Switzerland. *Natural Hazards and Earth System Sciences*, 9(3), 801-813. https://doi.org/10.5194/nhess-9-801-2009.
- Cornell, C.A., 1968. Engineering seismic risk analysis, Bulletin of the Seismological Society of America 58 (5): 1583–1606, https://doi.org/10.1785/BSSA0580051583.
- EconoMe, 2025. EconoMe 5.3. Wirkung und Wirtschaftlichkeit von Schutzmassnahmen gegen Naturgefahren. Dokumentation. https://econome.ch/eco_work/eco_wiki_main.php, last access 25 July 2025.
- FOEN, 2016. Protection against Mass Movement Hazards. Guideline for the integrated hazard management of landslides, rockfall and hillslope debris flows. Federal Office for the Environment, Bern. The environment in practice no. 1608: 97 p.
- Gerstenberger, M. C., Marzocchi, W., Allen, T., Pagani, M., Adams, J., Danciu, L., et al., 2020. Probabilistic seismic hazard analysis at regional and national scales: State of the art and future challenges, Reviews of Geophysics, 58, e2019RG000653, https://doi.org/10.1029/2019RG000653.
- Hall, T.M., and S. Jewson, 2007. Statistical modeling of North Atlantic tropical cyclone tracks, Tellus A, 59A, 486-498, https://doi.org/10.1111/j.1600-0870.2007.00240.x.
- Hall, T.M., J.P. Kossin, T. Thompson, and J. McMahon, 2021. US tropical cyclone activity in the 2030s based on projected changes in tropical sea-surface temperature, J. Climate, 34, no. 4, 1321-1335, http://dx.doi.org/10.1175/JCLI-D-20-0342.1.
- Lee, C.-Y., Camargo, S. J., Sobel, A. H., and, Tippett, M. K., 2020. Statistical-dynamical downscaling projections of tropical cyclone activity in a warming climate: Two diverging genesis scenarios. J. Climate, 33, 4815–4834, https://doi.org/10.1175/JCLI-D-19-0452.1.
- Kleinn, J., Aller, D., Oplatka, M. (2022). Characteristics of Risk. In: Collins, J.M., Done, J.M. (eds) Hurricane Risk in a Changing Climate. Hurricane Risk, vol 2. Springer, Cham. https://doi.org/10.1007/978-3-031-08568-0_2
- Kleinn J., Christen M., Bartelt P., 2024. Probabilistic event-based rockfall modelling for deriving continuous intensity-frequency curves in the impact area. In J. Schneider (Ed.), Interpraevent 2024. Conference proceedings. Klagenfurt: Interpraevent. 648-652.
- Kleinn J., Bühler Y., Glaus J., Aller D., Berger C., Rinderer M., ... Singeisen C., 2024. A probability-based modelling approach beyond a few selected return periods for comprehensive and robust hazard and risk assessment. In K. Gisnås, P. Gauer, H. Dahle, M. Eckerstorfer, A. Mannberg & K. Müller (Eds.), Proceedings of the international Snow Science Workshop 2024. Oslo: Norwegian Geotechnical Institute. 841-847.
- PLANAT, 2015. Sicherheitsniveau für Naturgefahren Materialien. Nationale Plattform für Naturgefahren PLANAT, Bern. 68 S.

- Schröer, K., Trefalt, S., Hering, A., Germann, U., Schwierz, C., 2022. Hagelklima Schweiz: Daten, Ergebnisse und Dokumentation Fachbericht MeteoSchweiz, 283, 1-82, http://dx.doi.org/10.18751/PMCH/TR/283.Hagelklima-Schweiz/1.0.
- Silva, V., Amo-Oduro, D., Calderon, A., et al., 2015. Development of a global seismic risk model, Earthquake Spectra, 36 (1_suppl): 372-394. https://doi.org/10.1177/8755293019899953.

Integral snow avalanche risk management for national roads in Norway

Markus Eckerstorfer*, Njål Farestveit, Jeanette Gundersen, Tore Humstad, Knut Inge Orset, Emil Solbakken, Jens Tveit

Norwegian Public Roads Administration (NPRA), NORWAY *Corresponding author, e-mail: markus.eckerstorfer@yegvesen.no

ABSTRACT

The Norwegian Public Roads Administration manages 10,000 km of national roads, with 354 sections exposed to snow avalanches and slush flows. We apply a holistic risk management approach, selecting mitigation methods based on hazard type, residual and perceived risk, and cost-effectiveness. Our mission is to ensure a transport system that is safe, accessible, and environmentally sustainable. We highlight how technology—such as detection, monitoring, and active control systems—helps reduce uncertainty, improve situational awareness, and enhance safety for road users. Avalanche mitigation is integrated into a broader natural hazard risk management system. A 24/7 national preparedness framework issues daily regional alerts and supports emergency response. For roads with active avalanche control, site-specific forecasts provide daily risk levels to road operators. To support effective risk communication, we use RESPONS—a custom-built mapping and forecasting tool. Our forecasting and emergency response efforts are closely coordinated nationally through the Varsom platform. Collaboration with private consultants and international partners strengthens our comprehensive approach to avalanche risk management.

1. INTRODUCTION

The Norwegian Public Roads Administration (NPRA) manages approximately 10,000 km of national roads, including 354 sections exposed to snow avalanches and slush flows (Farestveit et al., 2024). Around 2,500 natural hazard events are registered annually, with 63% being rockfalls or rockslides—often from artificial cuts—16% snow avalanches and slush flows, and 13% landslides. The remainder includes debris flows and other disruptive events such as collapsing ice.

To address these risks, NPRA applies a holistic management approach that combines physical and organizational mitigation with technological innovation and a 24/7 preparedness system. This strategy is grounded in a broad understanding of risk—including physical, residual, and perceived risk—alongside cost-benefit considerations, ensuring that measures are tailored to each road section in a changing climate.

This paper presents an overview of NPRA's integrated snow avalanche risk management system, highlighting its components, implementation, and coordination.

M. Eckerstorfer et.al. O5.3 - Page 131

2. HISTORICAL SHIFT TOWARDS TECHNOLOGY-DRIVEN AVALANCHE MANAGEMENT

Historically, the Norwegian Public Roads Administration (NPRA) relied on physical protection structures—such as tunnels, deflection dams, and breaking mounds—to mitigate avalanche risk (Humstad, 2024). Since the 1980s, however, the agency has increasingly embraced technological solutions, a shift led by the NPRA's Snow Committee.

Early detection systems like analog geophones required manual verification, often causing prolonged road closures. These evolved into digital platforms with remote access, enabling real-time monitoring and faster, more informed decisions. Today, NPRA employs advanced technologies including Doppler radar, infrasonic sensors, ground-based radar interferometry, and distributed acoustic sensing (Persson et al., 2018; Humstad et al., 2016, 2018; Turquet et al., 2024). Integrated into user-friendly dashboards, these systems allow operators to monitor avalanche activity, verify events via cameras, and distinguish real events from false alarms through automated post-processing—reducing uncertainty and improving operational efficiency.

Currently deployed at over 20 locations (Figure 1), these systems are also used for rockfalls and debris flows. Supplied by fewer than ten consultancies under more than 50 contracts, this evolution marks NPRA's strategic shift from reactive to proactive hazard management. However, the success of both active mitigation and modern detection depends on continuous follow-up and integration within a robust preparedness system.



Figure 1: Left panel: Map of Norway showing road locations with physical mitigation measures (red) and active mitigation measures (green). Three locations with active mitigation measures are highlighted. Right panels: Map and picture of Rv15 Knutstugugrove where a doppler radar monitors the avalanche path and informs a traffic light and road barrier.

3. NATURAL HAZARD PREPARDENESS AND OPERATIONAL COORDINATION

Although traffic volumes are relatively low, expectations for road accessibility and connectivity remain high (Orset & Frekhaug, 2024). To manage natural hazard risks across the national road network, NPRA operates a coordinated 24/7 preparedness system, in collaboration with the

Norwegian Water Resources and Energy Directorate (NVE), private consultancies, and international partners. This system covers a wide range of hazards, including snow avalanches, debris flows, slush flows, and flooding.

The preparedness system serves two main functions:

- 1. Issuing daily diligence levels to alert road owners to potential disruptions.
- 2. Providing expert support during acute events.

Diligence levels are issued daily for the entire country, divided into sub-regions (Figure 2). Hazards are categorized into four levels, from normal operations to significant restrictions. These levels are based on regional hazard forecasts (e.g., avalanches, floods) and NPRA's own weather analysis, tailored to the road network. Each level is accompanied by a short, written forecast published in the decision-support tool RESPONS (Figure 2).

During acute events, expert assistance is available via an on-duty forecaster. Local experts may be dispatched for field investigations, though remote support using photos is often sufficient. Since 2020, the system has handled over 1,100 inquiries (Orset & Frekhaug, 2024).

4. TECHNOLOGICAL EVOLUTION AND ACTIVE AVALANCHE CONTROL

In 2024, the NPRA launched a national initiative to reduce avalanche risk through technological innovation, responding to a request from the Ministry of Transportation (Farestveit et al., 2024). The goal was to implement Remote Avalanche Control Systems (RACS) at 25 high-risk road sections and to test additional technologies for avalanche monitoring and detection. Among these, the use of unmanned aerial systems (UAS) for artificial avalanche control has shown promising results (Tveit & Bøckman, 2024).

By summer 2025, RACS were operational on Rv7 Hardangervidda and E134 Haukelifjell, with installations underway on Rv15 Strynefjellet and Rv13 Vikafjellet. Feasibility assessments have also been conducted for several other avalanche-prone locations. To support this effort, NPRA established a framework agreement with two RACS providers.

Effective active control depends on detailed knowledge of snowpack stability, allowing for the frequent triggering of small, controlled avalanches to prevent larger, natural ones. This has required the development of site-specific avalanche forecasting systems, tailored to support operational decision-making at each RACS site.

M. Eckerstorfer et.al. O5.3 - Page 133

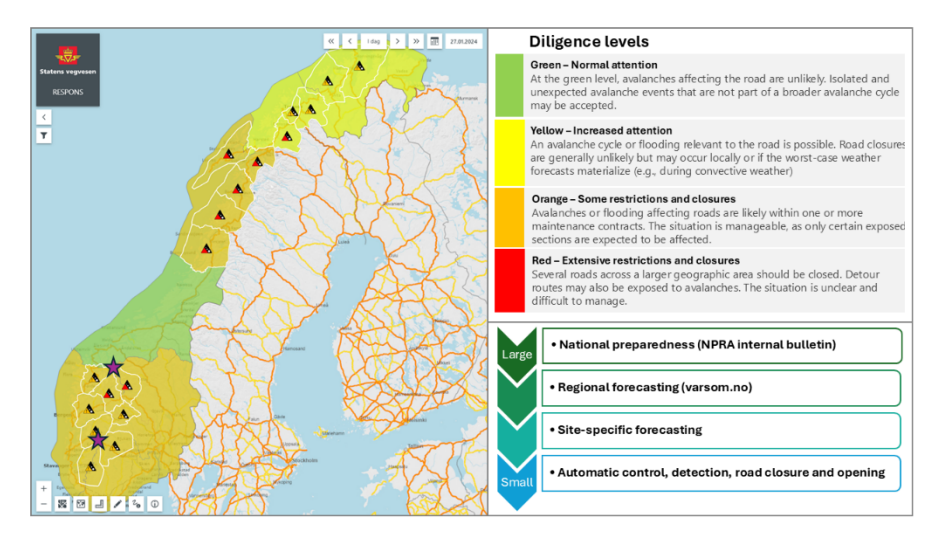


Figure 2: Left panel: Screenshot from RESPONS showing Norway with national diligence levels imposed, from 27.1.2024. Regional avalanche forecasting regions and danger level are also shown. Right panel: Definition of the diligence levels as well as a flow chart of the different forecasting systems, from national to avalanche pathscale.

5. SITE-SPECIFIC AVALANCHE FORECASTING

As part of the 24/7 national preparedness framework, NPRA currently operates two site-specific avalanche forecasting projects at Rv13 Strynefjellet and E134 Haukelifjell. A third project was conducted at Rv80 near Bodø during the 2023–24 winter season to forecast slush flow hazards (Andreassen et al., 2024). With RACS being implemented at additional locations, more forecasting projects will be established in the coming years.

Daily forecasts are issued throughout the winter season and are based on snowpack stability assessments, runout probabilities, and the potential consequences of avalanches reaching the road. These forecasts follow a four-level diligence scale (green to red), each linked to specific operational responses such as work restrictions, road closures, or active control measures.

Technological tools play a key role in reducing uncertainty and improving forecast accuracy. These include SNOWPACK simulations for snowpack evolution, drone-based snow surface modeling for terrain and snow distribution, and ultrasonic snow depth sensors for real-time calibration. Especially our use of drone-based sensors for data collection has in recent years increased (McCormack, et al, 2024).

6. INTEGRAL SNOW AVALANCHE RISK MANAGEMENT FOR NATIONAL ROADS IN NORWAY

NPRA has transitioned from relying solely on physical avalanche protection to a proactive, technology-driven approach embedded in a national 24/7 preparedness system. We now combine passive measures like snow sheds and deflection dams with active interventions such as RACS, supported by site-specific forecasting and advanced detection technologies. These innovations enhance situational awareness and reduce uncertainty (Figure 3).

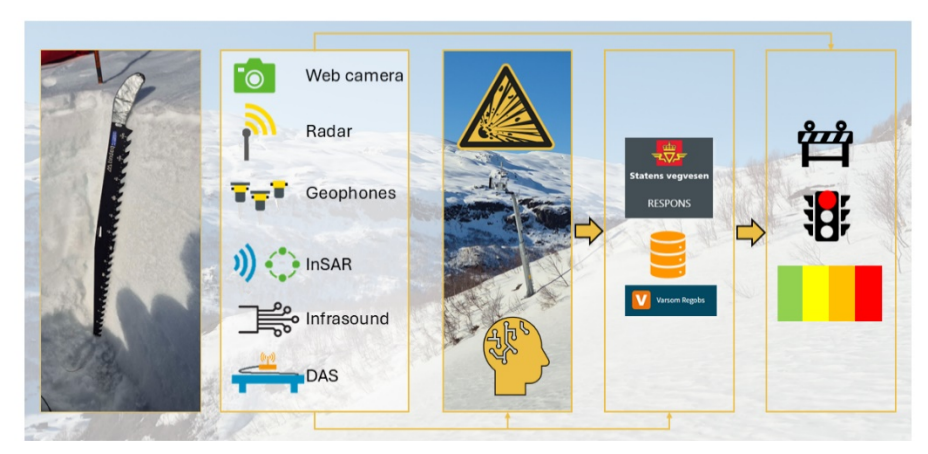


Figure 3: Components of our proactive approach to avalanche mitigation, combining field observations, technology for detection, monitoring and active control and site-specific forecasting. Data and forecasts are made available via different web platforms.

This proactive model also enriches the professional experience of our forecasters and hazard specialists. With increased responsibility comes a need for continuous learning, scientific engagement, and fieldwork. Staying updated with research and maintaining local knowledge makes the work both meaningful, dynamic and interesting.

Cost-benefit analyses (CBAs), as emphasized in the National Transport Plan (NTP, 2022-2033, National Transport Plan 2022–2033 - regjeringen.no), guide the prioritization of mitigation efforts. They ensure that investments deliver maximum societal value by balancing safety improvements, reduced road closures, and operational efficiency against implementation costs—especially important in remote areas with low traffic but high connectivity demands.

Importantly, the NTP also recognizes the growing impact of climate change on natural hazards. As a result, climate adaptation has become a key priority, with a focus on the life cycle of mitigation measures and integrating climate risk into planning and operations.

Despite the many benefits of Norway's proactive avalanche risk management approach, it also presents notable operational challenges and technical limitations. Continuous forecasting and preparedness demand significant human resources, with experts having to balance remote forecasting with on-site fieldwork. Besides the time intensity of this work, deep knowledge and ongoing professional development is needed. Forecasting is an intuitive, experienced-based work where uncertainty is inherent. The reliance on advanced technologies demands ongoing maintenance, calibration and error finding. High false alarm rates add uncertainty and can increase the experienced risk for road users. While proactive measures aim to reduce residual risk, they cannot eliminate it entirely – such as a tunnel can. Unexpected weather events, technology failure, communication breakdowns or misinterpretation of data can compromise safety.

7. CONCLUSION AND FUTURE DIRECTIONS

Norway's integrated approach demonstrates how innovation, preparedness, and economic rationale can converge to create a resilient and efficient transport system. The NPRA's integral approach to snow avalanche risk management exemplifies best practices in hazard mitigation.

M. Eckerstorfer et.al. O5.3 - Page 135

By combining traditional engineering solutions with cutting-edge technology and inter-agency coordination, within a 24/7 national preparedness system, Norway ensures the safety and accessibility of its national road network. Continued investment in research, technology, and collaboration will be key to addressing future challenges. Future developments will focus on enhancing forecast accuracy, expanding the use of AI in decision support, and strengthening cross-border collaboration.

REFERENCES

- Andreassen, D.T.R, et al. 2024. Site-specific slush flow warning on highway Rv80, Northern Norway. Proceedings of the International Snow Science Workshop, Tromsø, Norway. 750-753.
- Farestveit, N., et al, 2024. Technology for handling of natural hazards in the Norwegian Public Roads Administration. Proceedings of the International Snow Science Workshop, Tromsø, Norway. 912–914.
- Humstad, T., 2024. Forty years with avalanche detection systems in Norway. Proceedings of the International Snow Science Workshop, Tromsø, Norway. 990-996.
- Humstad T., Søderblom, Ø., Ulivieri, G., Langeland S., Dahle., H. 2016. Infrasound Detection of Avalanches in Grasdalen and Indreeidsdalen, Norway. Proceedings of the International Snow Science Workshop, Breckenridge, CO. 621-627.
- Humstad, T., Dahle H., Orset K. I., Venås M., Skrede I. 2018. The Stavbrekka glide avalanche in Norway evaluations after three years of monitoring. Proceedings of the International Snow Science Workshop, Innsbruck, Austria. 457-461.
- McCormack, E., et al, 2024. Operational integration of uncrewed aerial vehicles into roadway agencies' snow avalanche risk assessment process. Proceedings of the International Snow Science Workshop, Tromsø, Norway. 1100 1006.
- Orset, K.I., Frekhaug, M.H. 2024. Natural hazard preparedness in the Norwegian Public Roads Administration. Proceedings of the International Snow Science Workshop, Tromsø, Norway. 252-256.
- Persson A., Venås M., Humstad T., Meier L. 2018. Real-time Radar Avalanche Detection of a large Detection Zone for Road Safety in Norway. Proceedings of the International Snow Science Workshop, Innsbruck, Austria. 597-600.
- Tveit, J., Bøckman, J. 2024. Avalanche control with unmanned aerial systems on Norwegian roads. Proceedings of the International Snow Science Workshop, Tromsø, Norway. 1336-1340.
- Turquet, A., Wuestefeld, A. Svendsen, G. K., Nyhammer, F. K., Nilsen, E., Persson, A., P-O, Refsum, V. 2024. Automated avalanche monitoring, detection and classification systems powered by distributed acoustic sensing. Proceedings of the International Snow Science Workshop, Tromsø Norway. 1005-1012.

The Pollfjellet powder snow avalanche: building model scenarios for a mass dependent model and mitigation case study

Hallvard Skaare Nordbrøden, 1* Siiri Wickström 1 and Kalle Kronholm 1

1 Skred AS, Torget 3, 3570 Ål, NORWAY *Corresponding author, e-mail: hallvard (at) skred.as

ABSTRACT

On the eastern edge of the Lyngen alps in Arctic Northern Norway lies Furuflaten. Parts of the village is threatened by the powder part from large snow avalanches from several release areas. As part of a mitigation study, a climate analysis adopted for building an avalanche scenario in the mass-dependent avalanche model RAMMS::Extended was made. We show how this was adopted from the method proposed by Stoffel et al. (2024) by utilizing a gridded meteorological dataset called SeNorge2018. We address the uncertainty related to input parameters from interpolated climatological data and show how we built our avalanche scenario. Finally, we show our proposal for how the Pollfjellet avalanches can be mitigated.

1. INTRODUCTION

On the eastern edged of the Lyngen alps in Arctic Northern Norway lies Furuflaten. Parts of the village is threatened by the powder part from large snow avalanches from several release areas. Hazard zone maps defined 40 buildings with unacceptable risk. Consequently, a feasibility study for mitigation measures has been made.

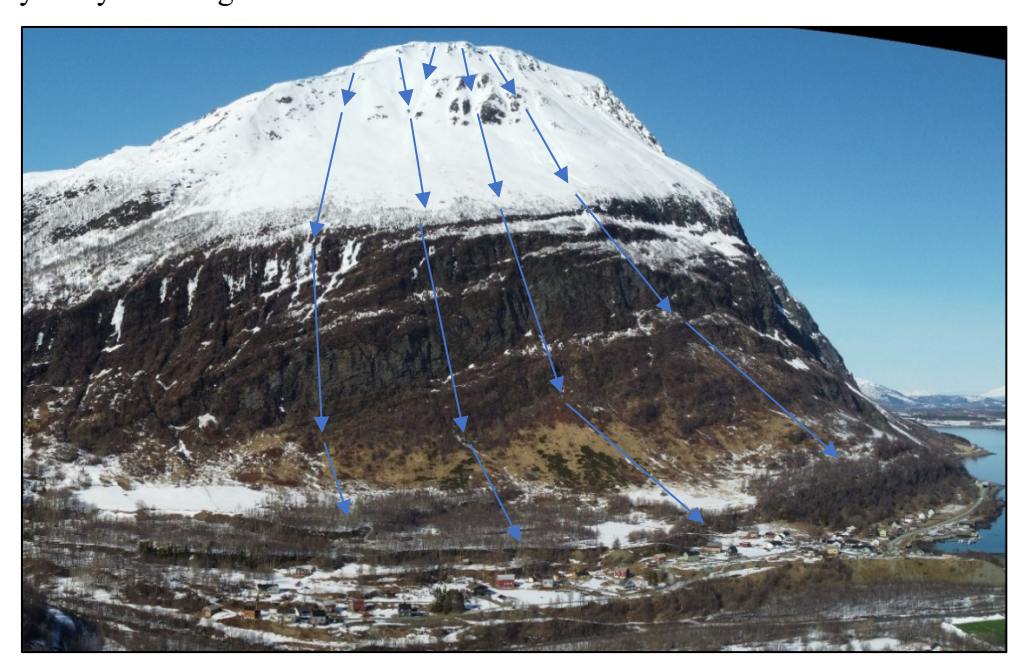


Figure 1 The mountain Pollfjellet (1213 m. a.s.l.) and Furuflaten village at its base. Blue arrows show flow paths of avalanches from different release areas.

A key part of this study was to develop a realistic avalanche scenario for modelling the powder cloud. Mass-dependent powder cloud models are becoming widely available, offering greater accuracy in reproducing observed events through many adjustable parameters. However, this makes scenario-based modelling more difficult and can lead to variability between practitioners since the scientific community has not yet to set enough focus on how to build realistic scenarios with this kind of models. Stoffel et al. (2024) proposed a method based on long-term snow depth data, an altitude-driven climate, and long experience with modelling in Switzerland. In contrast, Norway lacks extensive snow depth records and has a more complex snow climate influenced by altitude, latitude, and maritime effects. We demonstrate how Stoffel's method was adapted for the Pollfjellet avalanches as input to RAMMS::Extended (Bartelt & Christen, 2025) by using available data sources in Norway.

2. SETTING

The Pollfjellet avalanche paths face S–SE with a drop height of 700–1000 m. The western release area is a large bowl (~90,000 m²), while the eastern areas comprise steep, narrow gullies prone to cross-loading, situated above an open flank. The convex mountain form in the eastern paths spread the avalanches into multiple flow paths (Figure 1). Avalanches drop over a cliff around 300–500 m a.s.l., becoming airborne and generating powder clouds with long runouts (Figure 2). Historic records document destroyed buildings (now relocated) and roofs being torn off by the powder cloud.

Major avalanches in at Pollfjellet typically occur with intense snow fall from NW from polar lows loading on top of a depth hoar which is very common. The eastern release areas also release as wet avalanches due to rapid warming and cross loading from SW.

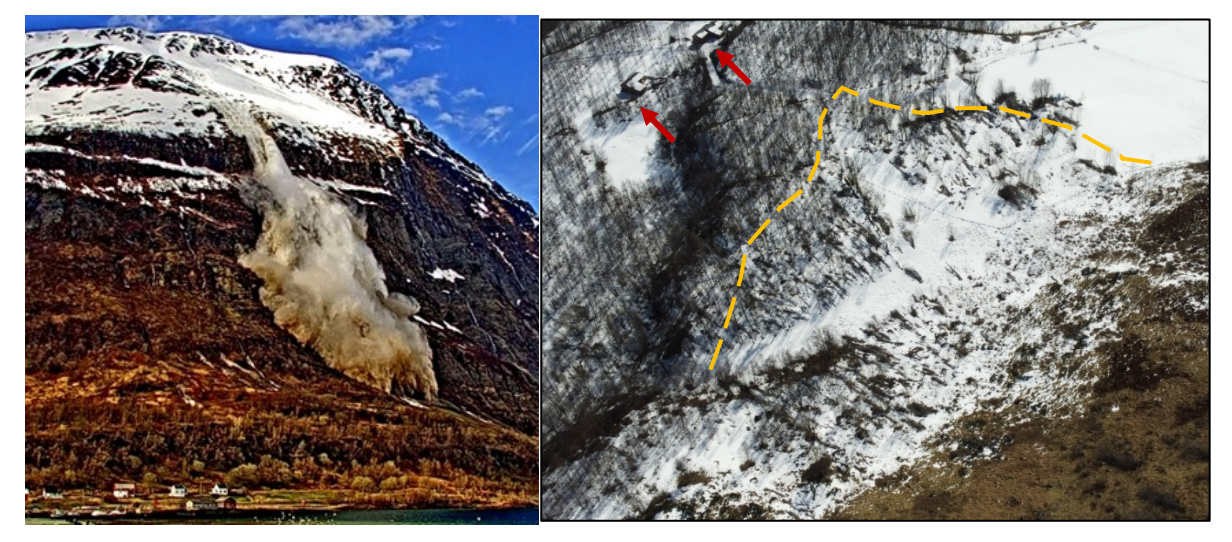


Figure 2 Left: A wet avalanche plunges over the cliff in the avalanche path Geitlirenna right next to the village. Right: Drone photo where yellow dashed line indicates forest which is completely damaged by the powder cloud. Broken trees with age estimated 50-80 years were observed in this area. Red arrows indicate two of the exposed houses.

3. METHODS

3.1 The gridded data set SeNorge2018

As basis for calculating extreme values for fracture heights in Norway, the SeNorge2018 1 × 1 km gridded dataset is used. This dataset of daily temperature and precipitation across Norway is generated by interpolation, combing station data with a high-resolution, model-based reference climate (Lussana et al., 2019). In regions with few observations like Pollfjellet, the model climate component dominates, limiting the accuracy of precipitation estimates.

Snowfall in SeNorge is inferred from precipitation and temperature with precipitation classified as snow when the daily mean $T < 0.5\,^{\circ}\text{C}$. Undercatch due to wind is corrected, and snow height is calculated using a temperature-dependent snow density (Saloranta 2012) on level ground. The three-day snow accumulation is a running total, while total snow depth includes a simple densification model. Snow depth above treeline is corrected to account for wind compaction (higher density), therefore the model at times gives higher snow depth in forested areas than at the mountain top. Most weather stations measuring precipitation are placed at valley bottoms, making the interpolation at high elevation very model climate dependent. Steep mountainous topography within the $1x1\,\text{km}$ cells give a smoothing that unlikely resolves complex topographic effects precisely.

There is inherent uncertainty in the dataset stemming from interpolation, station density and modelled snow related parameters. The interfaces between purely observation-based interpolation and the model climate are also a source of inconsistency and uncertainty. These are magnified in mountainous regions with low data density generally especially at high elevations, making the data set difficult to validate for avalanche related use.

For extreme value analyses (EVA) we use SeNorge2018 (1957–2025), treating the three-day snow height with a specific return period as a proxy for fracture height. Both Gumbel and GEV distributions are applied with a block maxima approach of yearly maximum values. Fit-distribution is based on Kolmigorov-Smirnov test and visually on how the empirical CDF fit. The uncertainty is a combination of embedded uncertainties in SeNorge combined with the long return intervals 100, 1000 and 5000 years (representing the hazard zones in Norway) assessed on 68 years of data.

3.2 Scenario building from SeNorge

In Norway, scenario building is based on the same principles as in Switzerland and Austria where fracture depth d0 is correlated to the three-day new snow and three-day snow height increase respectively, with a snow drift contribution. While common mass-independent dense flow models only require a fracture depth as input from climatological data, the extended version of RAMMS is mass-dependent and requires several climatological input parameters with their own inherent uncertainty.

An adapted method for defining fracture height and consistency is therefore necessary to build realistic avalanche scenarios. To avoid the uncertainties for snow parameters in SeNorge, we

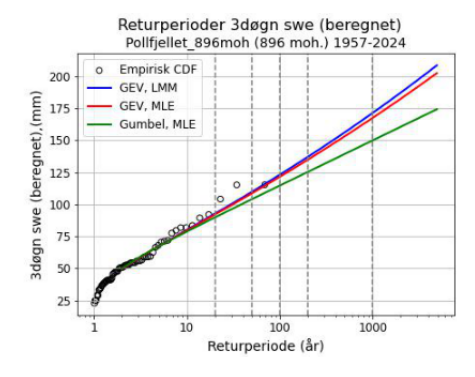
apply an approach using Snow Water Equivalent (SWE) on the approach Stoffel et al. (2024) suggested with slight adjustments:

- Snow cover temperature at release area elevation
 - Since temperature regime is much more complex than in Switzerland, we use regional climate, latitude and elevation as basis, as well as experience from reproducing documented events.
 - Generally, we use $T = -6^{\circ}C$ as a standard value. For release areas at low elevation and at lower latitudes -5°C is often applicable. For dry, cold continental climates, release areas at relative high elevation and special cases at higher latitudes we apply -7°C.
- Fracture depth d0 and basic value d0*
 - o Carefully consider how well the EVA based on SWE data corresponds to observed of given return periods avalanches and experience with modelling.
 - \circ Snowdrift is added as a percentage of SWE, typically in the range 0-50%. This scales the snow drift relative to the snow available for transport and have shown good results for typical Norwegian mountainous topography where fetches can be large.
 - We use the densities suggested by Stoffel et al. (2024) for the chosen snow cover temperature to calculate d0 and d0*.
 - Slope correction solely for slope angle and not the f(w) formula of Salm (1990) in accordance with what seems to be common practice in Norway.

Forest

In Norway, forest input can be estimated from a satellite-based map showing DBH, crown coverage and tree type. The data should always be validated by field investigations.

Figure 3 show extreme value analysis of SWE and calculated d0 and d0* for the feasibility study.



72h SWE [mm]	% of SWE due to snowdrift	d0 [cm]	d0* [cm]
170 mm	50 %	103 cm	86 cm

Figure 3 - Left: Extreme value analysis of SWE at Pollfjellet from a grid cell with elevation 896 m by three different methods (colored lines). Data values used in the analysis are shown by circles. Right: Calculated d0 and d0* for Pollfjellet from suggested method for return period 1/1000. Snow density ρ =175 kg/m³ and mean slope angle 40°.

4. RESULTS

Example of modelling results is shown in Figure 4. The chosen model setup is the result of carefully choosing a grid cell from SeNorge. For calibration, few events were well-documented, so the observed forest damage (Figure 2), estimated tree age and calculated fracture height for a representative return period was used for calibration purposes and verification. This especially helped define the snow drift contribution and give confidence to the precipitation values used for scenario-building.

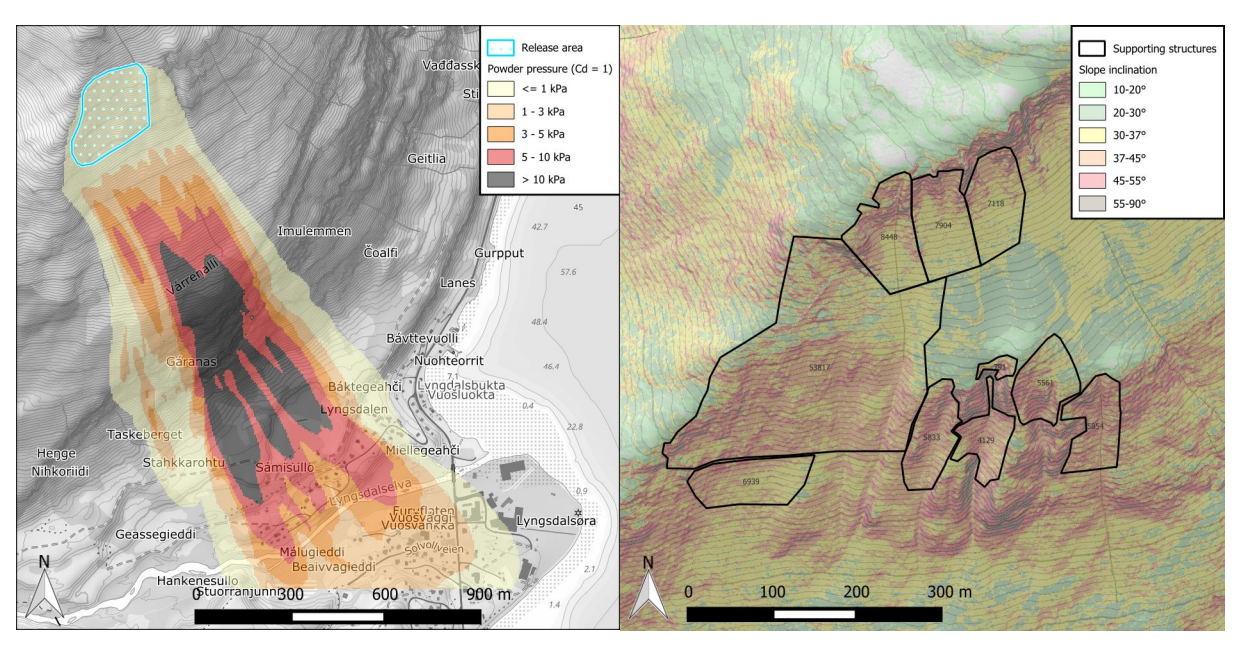


Figure 4 Left: Example of model result from the western and largest release area with the avalanche scenario. Right: Preliminary suggestion on layout for planning of supporting structures. Numbers are m² in plan view.

Since the avalanches plunge and are airborne when they reach the valley floor, mitigation is only reasonable to do with protection measures in the release areas, such as supporting structures, or reinforced buildings. Since buildings are mainly wooden buildings reinforcement of existing buildings was considered not feasible. Based on iteration of the avalanche scenario with different release areas an estimation of supporting structures was done (Figure 4 & Table 1). During the iteration, avalanche size used in RAMMS was carefully considered from the eastern release areas because both forest and documented events show less damage from avalanches in these paths. This is likely because the convex form of the mountain channelizes the avalanches in several smaller flows, making them less mobile and destructive in the runout than avalanches from the western release area. Therefore, a relatively little part of the possible release areas in this part was suggested to be mitigated.

Table 1 Estimated amount of supporting structures based on iteration with the avalanche scenario for different release areas.

Average slope [º]	Total area in plan view [m ²]	Dk 4 [m]	Dk 5 [m]
39,8	106 394	2 132	2 593

5. CONCLUSION

The village Furuflaten is threatened by avalanches from Pollfjellet. As part of a mitigation study, we adapted a method for building avalanche scenario from Stoffel et al. (2024) to utilize a gridded data set in a region with few observations. In this work, the embedded uncertainties were handled and treated carefully with insight to the data sets limitations and uncertainties. This is crucial for the avalanche engineer to account for when building scenarios for the ever more sophisticated mass-dependent avalanche models which emerge from the scientific community these days. From our point of view, it is crucial that the scientific community continue to work with how scenario-based approaches can best be done when the avalanche engineer applies these models in practice.

REFERENCES

- Bartelt, P., Christen, M., 2025: Snow Avalanche Dynamics with RAMMS::Extended. RAMMS AG report, 2025.
- Lussana, C., Tveito, O. E., Dobler, A., and Tunheim, K., 2019 : seNorge_2018, daily precipitation, and temperature datasets over Norway, Earth Syst. Sci. Data, 11, 1531–1551, https://doi.org/10.5194/essd-11-1531-2019.
- Salm, B., Burkard, A., Gubler, H. U., 1990. Berechnung von Fliesslawinen. Eine Anleitung fuer Praktiker mit Bleispielen. Davos, Eidgenössisches Institut für Schnee- und Lawinenforschung, Mitteilungen Nr. 47.
- Saloranta, T. M.,2012: Simulating snow maps for Norway: description and statistical evaluation of the SeNorge snow model, The Cryosphere, 6, 1323–1337, https://doi.org/10.5194/tc-6-1323-2012, 2012.
- Stoffel, L., Bartelt, P., Margreth, S., 2024. SCENARIO BASED AVALANCHE SIMULATIONS INCLUDING SNOW ENTRAINMENT, SNOW TEMPERATURE AND DENSITY. In: Proceedings of the International Snow Science Workshop, Tromsø, Norway, 2024.

Risk management from natural hazards for the new European Road E10, Halogalandsveien

Christian Jaedicke^{1,2*}, Vidar Kveldsvik¹, Anders Kleiven¹, Sunniva Skuset¹, Holt Hancock^{1,3}, Elise Morken¹, Peter Gauer¹, Piotr Kupiszewski¹, Kjersti Gisnås¹, and Graham Gilbert^{1,4}

Norwegian Geotechnical Institute, P.O. Box 3930 Ullevål Stadion, NO-0806 Oslo, NORWAY
 University of Oslo, Department of Geosciences, Blindern, NO-0371 Oslo, NORWAY
 UiT, The Arctic University of Norway, Department of Geosciences, Tromsø, NORWAY
 The University Centre in Svalbard, P.O. Box 156 N-9171 Longyearbyen, NORWAY
 *Corresponding author, e-mail: Christian.jaedicke@ngi.no

ABSTRACT

The 82 km section of the European Road E10 from Tjelsund Bridge to the Sigerfjord tunnel is currently under reconstruction. Seven tunnels with a total combined length of 27 km will be drilled to make the road shorter and to avoid exposure to avalanche terrain. Outside of the tunnels, other road sections will require protection from structural mitigation measures to limit the risk from rockfalls, avalanches and slushflows. A variety of mitigation measures will ultimately protect the exposed stretches of road against slope hazards. For rockfalls, local rock anchors and nettings will secure smaller outcrops, while catching nets will provide protection from larger release areas. Bridges with sufficient clearance will elevate the road over known slushflow channels and will be supplemented by catching basins, which retain the slush before it enters the road. Several types of dams such as retention and guiding dams are used to mitigate avalanches. Where the new roadway parallels the shoreline of Gullesfjord, dams with sufficient dimensions to protect the road proved to be too expensive to realistically complete. Therefore, a combination of smaller dams and remote avalanche control systems is suggested for the area. During construction of the roadway and the protection structures, workers and construction sites are exposed to avalanche hazard. A site-specific avalanche warning service was established to manage the avalanche hazard. In daily forecasts, the avalanche impact probability is assessed individually for each exposed work site. Predefined working routines corresponding to the forecast impact probability were implemented. This allowed the daily work plan to be adapted to the avalanche risk and ensured safe execution of the construction work during winter.

1. INTRODUCTION

Constructing roads in Norway frequently meets challenges with all kinds of natural hazards (NVE, 2016). Therefore, the Norwegian Public Roads Administration (NPRA) has developed detailed handbooks for the design and construction of public roads (Statens Vegvesen, 2021). In these guidelines, risk acceptance criteria are given for natural hazards, such as rapid mass movements based on the average daily traffic (ADT). For each class of ADT, a nominal annual probability for a rapid mass movement to reach one kilometre of a road is defined (These criteria are valid for roads where the traffic flows normally. However, location locations such as rest areas, parking lots, or stretches of the road where traffic backs up in the event of a road closure or are subject to the stricter regulations of the building act (Direktoratet for byggkvalitet, 2017). For all new road construction as well as the renovation of existing roads, these criteria are required to be used for a) identification of critical points along the road, b) quantification of the anticipated annual probability for a rapid mass movement to reach the road and c) assessment and design of required mitigation to satisfy the given criteria.

Table 1).

Jaedicke, Kveldsvik, et al. O5.5 - Page 143

These criteria are valid for roads where the traffic flows normally. However, location locations such as rest areas, parking lots, or stretches of the road where traffic backs up in the event of a road closure or are subject to the stricter regulations of the building act (Direktoratet for byggkvalitet, 2017). For all new road construction as well as the renovation of existing roads, these criteria are required to be used for a) identification of critical points along the road, b) quantification of the anticipated annual probability for a rapid mass movement to reach the road and c) assessment and design of required mitigation to satisfy the given criteria.

Table 1 Risk acceptance criteria for rapid mass movements on public roads in Norway (Statens Vegvesen, 2021, table 1.12)

Dimensioning ADT	Nominal annual event probability per km
< 500	1/20
500 – 3999	1/50
4000 – 5999	1/100
6000-11999	1/300
≥ 12000	1/1000

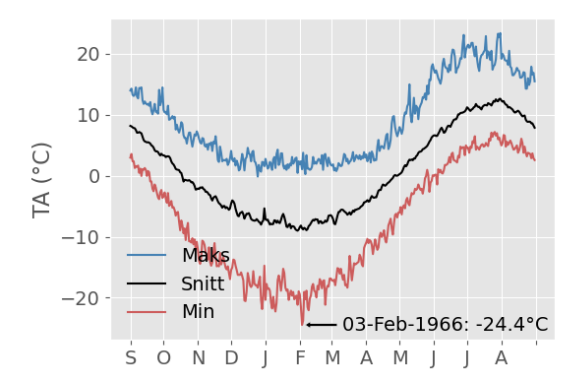
In addition to the requirements for the completed road, one must consider the natural hazards during the construction of the road and the mitigation measures. The workers' safety in areas exposed to natural hazards is regulated in the Norwegian Work Environment Act (Ministry of Labour and Social Inclusion, 2005) and in the corresponding regulations on work safety (Ministry of Labour and Social Inclusion, 2011).

The required safety for the workers and the final road can be achieved by a wide range of mitigation measures often described as temporary/permanent and passive/active. The total avoidance of avalanche terrain by thorough mapping and land use would be a permanent + passive mitigation, while the use of avalanche warning in the construction phase would be a temporary + passive mitigation. Several handbooks (McClung and Schaerer, 2022; Rudolf-Miklau et al., 2015) give guidelines for mitigation against avalanches, and similar guidelines are available for mitigation against rockfalls (Volkwein et al., 2011) and landslides (Highland and Bobrowsky, 2008).

Together, these regulations form the framework of the risk management along the E10 road. The objective of this paper is to describe the natural hazards along the road and the wide range of risk mitigation strategies used to reduce the apparent risk from natural hazards to an acceptable level, both for the construction phase and the operational phase of the road.

2. SITE DESCRIPTION

The new road is approximately 82 km long and passes through three municipalities (Kvæfjord, Lødingen and Tjeldsund) in the counties Nordland and Troms (Figure 2). 35 km of the road consist of new or upgrades of the existing line, 20 km are completely new open road, and 27 km will be in tunnels. The tunnels are specifically located to reduce the length of the road and to pass the most exposed areas safely. The road leads from the Tjelsund bridge out to the Ofoten and Lofoten Islands and is the only land access to these areas. The new road aims to reduce the length of the road by 30 km, travel time by 40 minutes and increase regularity by reducing the influence of severe winter weather in the traffic.



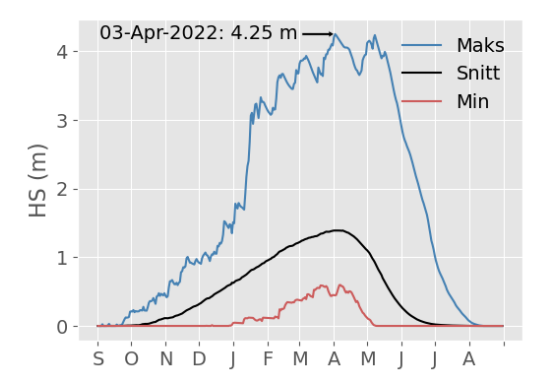
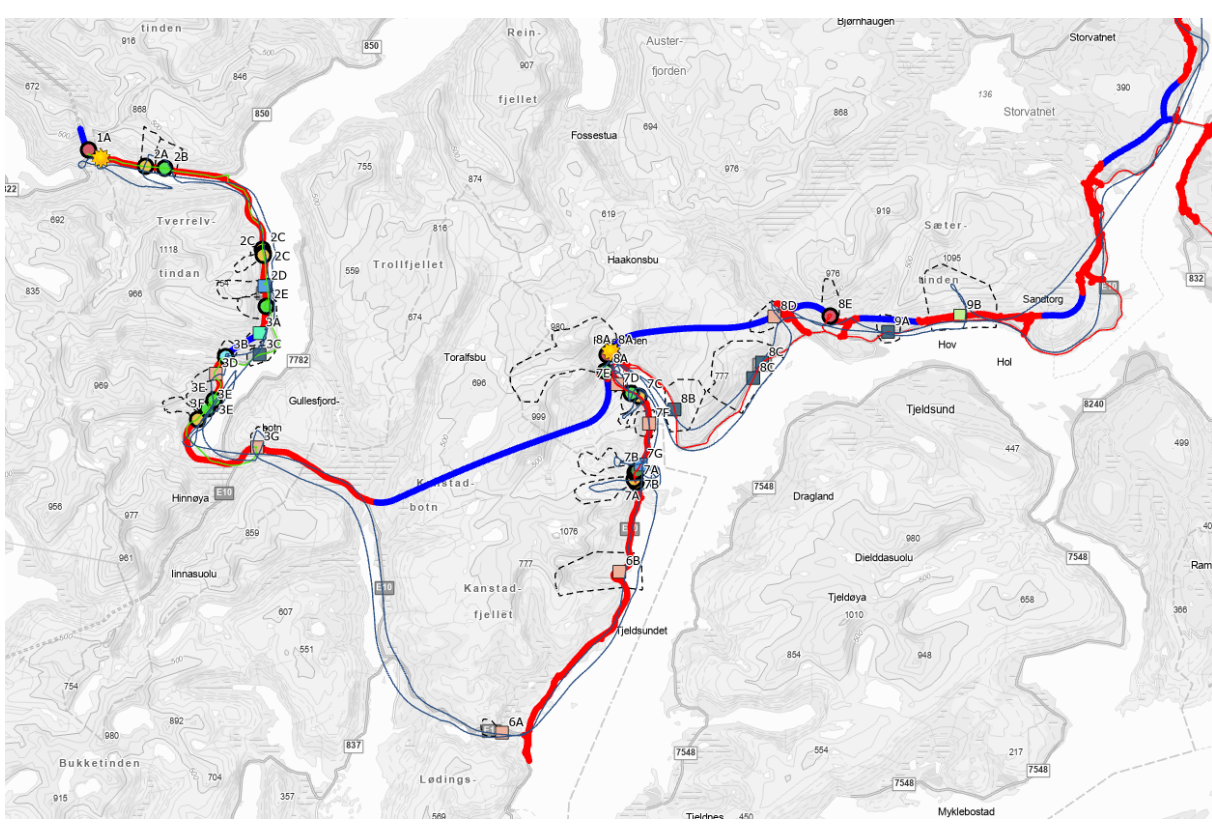


Figure 1 Min, max and mean temp. (left) and snow height (right) at a selected point along the road.

The terrain around the road rises from sea level up to 1000 m a.s.l. and is dominated by geomorphology from the last glaciation with u-shaped valleys and moraine deposits. The bedrock is stable granite, well suited for tunneling.

The climate in the area is dominated by the close proximity to the ocean. Temperatures in winter vary widely from several plus degrees and rain to intense cold periods with minus ten degrees Celsius or less. Rain on snow is a common phenomenon. This leads to a highly stratified snowpack and a large variation in snow properties (Figure 2). Bare ground at sea level can often be accompanied by eminent avalanche danger in the higher ranges of the mountains. The annual mean precipitation in the area ranges between 1600 mm and 2500 mm across distances of only 20 km.

Annual mean temperature at sea level is more regionally homogenous with 4.3 °C and a range of -10 °C to +20 °C. (Lussana et al., 2018; Saloranta, 2016). Polar low-pressure systems (Noer et al., 2011) can lead to high local variations in snow and rain precipitation such that the different sections of the road can experience totally different weather conditions at the same time.



Jaedicke, Kveldsvik, et al. O5.5 - Page 145

Figure 2 Map of the roads to be built in the E10 project. Blue lines are tunnels, red lines are open road stretches. The coloured dots show the location of the planed mitigation measures.

3. MATERIALS AND METHODS

The first hazard assessment for the planned road was done by the NPRA and documented in four reports (Statens Vegvesen, 2017a, 2017a, 2017b, 2016) which pointed out sections that could be exposed to natural hazards and which also included some preliminary suggestions for mitigation measures. These points were reassessed by the Norwegian Geotechnical Institute on contract from SKANSKA prior to the final bid for the project to get updated information on the required resources and investments that are needed for the mitigation. The assessment by NGI was based on a high resolution (1 m) DEM from the area ("Høydedata", 2024), areal pictures, historical events and on site field work by helicopter and on the ground. The numerical models RAMMS (Christen et al., 2010) and SAMOS AT (Sampl and Zwinger, 2004) were used for simulation of dimensioning avalanches, rockfalls, debris and slushflows.

In the second phase of the project, after SKANSKA was awarded the final project, the suggested mitigation measures were designed in the digital design tools Grasshopper and Rhino (Robert McNeel & Associates, 2024). Parts of the process were automated in Rhino models to address repetitive tasks more efficiently. The final detailed design was then done by structural engineers in AutoCAD.

For the workers safety, a daily avalanche warning service was established that follows the weather and snow situation through the whole winter (EAWS, The European Avalanche Warning Services, 2022). The warning service issues an impact probability for each working site at three levels, low, middle and high. Site-specific action plans are enforced according to the forecasted impact probabilities and workers in exposed areas are equipped with avalanche safety gear and are schooled in its proper use.

4. RESULTS

4.1 Assessment of natural hazards

In total 20 points of concern were mentioned in the original reports from the NPRA. NGI's assessment showed 24 points where mitigation was considered necessary. The points most commonly considered slushflows as the dominant hazard type (13 points), followed by debris flows (11) and snow avalanches (11). Rockfalls were considered a hazard at 6 points. Slushflows and debris flows were often assessed to be possible in the same location. While slushflows, debris flows, and also rockfall were limited to well defined locations, mostly minor creeks or other water flows, snow avalanches showed a wider area of influence asking for mitigation along longer stretches of the road.

4.2 Design of mitigation

The expected ADT of the new road is between 500 and 3999 leading to an accepted nominal annual probability of 1/50 for an event to reach the road within 1000 m of road (These criteria are valid for roads where the traffic flows normally. However, location locations such as rest areas, parking lots, or stretches of the road where traffic backs up in the event of a road closure or are subject to the stricter regulations of the building act (Direktoratet for byggkvalitet, 2017). For all new road construction as well as the renovation of existing roads, these criteria are required to be used for a) identification of critical points along the road, b) quantification of the

anticipated annual probability for a rapid mass movement to reach the road and c) assessment and design of required mitigation to satisfy the given criteria.

Table 1). The NPRA handbook (Statens Vegvesen, 2021) also states that probabilities should be aggregated when several points of concern are identified within 1000 m. This leads to much higher acceptance criteria in e.g. a case where four points of concern are identified within 1000 m of road. This would lead to an accepted probability of 1/(50x4) for each point.

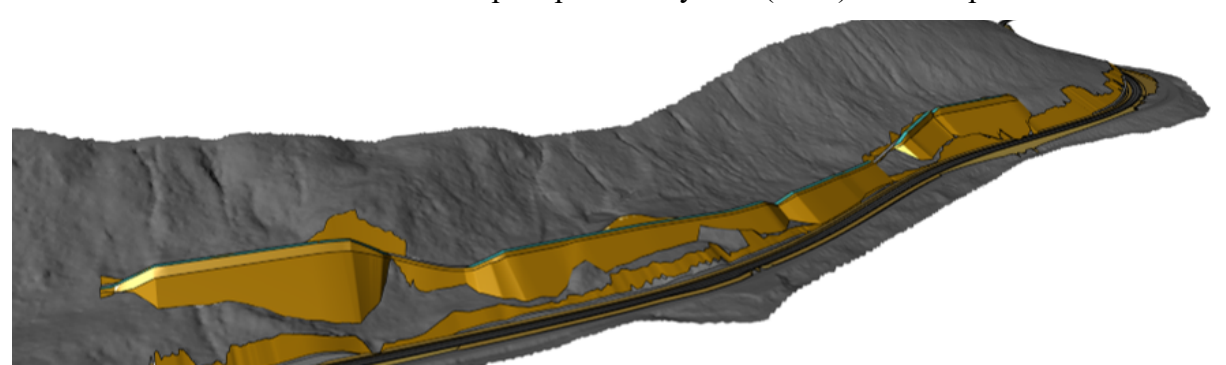


Figure 3 Three-dimensional view of the avalanche protection dams at Karitinden/Gullesfjord. Mitigation against a dimensioning 1/200 event at four points is naturally far more expensive than mitigating only against single 1/50 events. After a thorough discussion with the entrepreneur SKANSKA and the NPRA, the general design event was set to be 1/50 for each point independently.

Results from numerical modelling of the design events were then used to address possible mitigation measures. In many cases a single solution was efficient, but at Langvatn, the calculations showed that the required avalanche dams would be too high and costly to be realized. Instead, a combination of remote avalanche control and dams was chosen. Debris- and slushflows were mitigated with wide and reinforced bridges as well as with catching basins. Rockfalls are secured with nets, rock anchors and cleaning of the rock faces.

4.3 Avalanche warning



Figure 3 Webcamera image showing the avalanche paths over the road on Karitind/Gullesfjorf.

The avalanche warning issues daily forecasts valid for the next 24 hours and has been operational over the past two winters. The forecasts provide hazard assessments for up to eight different locations such that work could continue even if 1/8 locations were assessed to high impact probability. Several periods with high impact probability have been identified and operations were shut down in the respective areas. Most affected by avalanche and slushflow danger is the section Brattelva to Karitind, where multiple avalanches and slushflows have reached down to the construction site. Due to the avalanche warning and associated action plans, neither persons nor machinery were involved in any incidents.

Jaedicke, Kveldsvik, et al. O5.5 - Page 147

5. DISCUSSION

Mitigation against natural hazards along the new E10 road required an open mind and a broad overview over possible mitigation strategies and tools. The formal requirements from the NPRA handbook proved to be too expensive to achieve and a simpler approach with the same probability for each point of concern was chosen. The individual assessment of design events and internally-adjusted design of each mitigation measure supported cost effective and innovative solutions for each point. The use of digital design tools improved the workflow and effectiveness of the design process. With the help of daily avalanche warning, work in exposed areas could be continued during winter to keep up the progress of construction during the whole year.

6. CONCLUSIONS

The topography and local climate create a challenging environment for the new European Road 10. Rockfalls, slushflows, and avalanches are abundant in the area and affect the terrain where the new road is located. A multi hazard approach, close cooperation between entrepreneur, natural hazard consultants and continuous contact due to the avalanche warning quarantined both safe mitigation for the road as well as high workers safety in the construction period. The developed tools and procedures are today used successfully in several other projects and will be further developed for general use in other road construction projects.

ACKNOWLEDGEMENT

The authors want to thank our partners in SKANSKA and Hæhre and their trustful cooperation and valuable observations throughout the project. We also thank the NPRA for providing the foundation for this work and helping to knowledgeably steer this project to completion.

REFERENCES

- Christen, M., Kowalski, J., Bartelt, P., 2010. RAMMS: Numerical simulation of dense snow avalanches in three-dimensional terrain. Cold Regions Science and Technology 63, 1–14. https://doi.org/10.1016/j.coldregions.2010.04.005
- Direktoratet for byggkvalitet, 2017. Byggteknisk forskrift (TEK17) med veiledning.
- EAWS, The European Avalanche Warning Services, 2022. Site-specific avalanche warning, Definitions and Recommendations.
- Highland, L., Bobrowsky, P., 2008. The Landslide Handbook, Circular. United States Geological Survey, Verginia, USA.
- Høydedata [WWW Document], 2024. URL https://hoydedata.no/LaserInnsyn2/ (accessed 7.30.24).
- Lussana, C., Saloranta, T., Skaugen, T., Magnusson, J., Tveito, O.E., 2018. seNorge2 daily precipitation, an observational gridded dataset over Norway from 1957 to the present day. Earth system Sciences data 10, 235–249.
- McClung, D., Schaerer, P., 2022. The avalanche handbook, 4th ed. Mountaineers Books, Seattle, WA.
- Ministry of Labour and Social Inclusion, 2011. Regulations concerning the performance of work, use of work equipment and related technical requirements, FOR-2011-12-06-1357.

- Ministry of Labour and Social Inclusion, 2005. Act relating to the working environment, working hours and employment protection, etc. (Working Environment Act), LOV.
- Noer, G., Saetra, Ø., Lien, T., Gusdal, Y., 2011. A climatological study of polar lows in the Nordic Seas. Quarterly Journal of the Royal Meteorological Society 137, 1762–1772. https://doi.org/10.1002/qi.846
- NVE, 2016. NIFS sluttrapport (No. 43–2016). Norges vassdrags- og energidirektorat, Oslo, Norway.
- Robert McNeel & Associates, 2024. Rhino.
- Rudolf-Miklau, F., Sauermoser, S., Mears, A.I., 2015. The Technical Avalanche Protection Handbook, The Technical Avalanche Protection Handbook. https://doi.org/10.1002/9783433603840
- Saloranta, T.M., 2016. Operational snow mapping with simplified data assimilation using the seNorge snow model. Journal of Hydrology 538, 314–325. https://doi.org/10.1016/j.jhydrol.2016.03.061
- Sampl, P., Zwinger, T., 2004. Avalanche simulation with SAMOS. Annals of Glaciology 38, 393–398. https://doi.org/10.3189/172756404781814780
- Statens Vegvesen, 2021. N200 Vegbygging. Statens Vegvesen Håndbok N200.
- Statens Vegvesen, 2017a. Rv. 85/E10 HÅLOGALANDSVEGEN, parsell 3. Skredfare og skredsikring, rapport til reguleringsplan (Skredfaglig rapport No. 50831- SKRED- 002), Region Nord. National Public Road Administration, Bodø, Norway.
- Statens Vegvesen, 2017b. E10 HÅLOGALANDSVEGEN, parsell 8- 9: Fiskefjord KongsvikHårvika. Skredfare og skredsikring, rapport til reguleringsplan (Skredfaglig rapport No. 50831- SKRED- 003), Region Nord. National Public Road Administration, Bodø, Norway.
- Statens Vegvesen, 2016. RV.85 HÅLOGALANDSVEGEN, parsell 2 i Kvæfjord kommune. Skredfare og sikring, skredfaglig rapport til reguleringsplan (Skredfaglig rapport No. 50831- SKRED- 001), Region Nord. National Public Road Administration, Bodø, Norway.
- Volkwein, A., Schellenberg, K., Labiouse, V., Agliardi, F., Berger, F., Bourrier, F., Dorren, L., Gerber, W., Jaboyedoff, M., 2011. Rockfall characterisation and structural protection a review. Natural Hazards And Earth System Sciences 11, 2617–2651. https://doi.org/10.5194/nhess-11-2617-2011

Jaedicke, Kveldsvik, et al. O5.5 - Page 149

Land use and planning of settlements in hazard zones and under defense structures

Magni Hreinn Jónsson* and Tómas Jóhannesson

Icelandic Meteorological Office, IS-105 Reykjavik, ICELAND *Corresponding author, e-mail: magni (at) vedur.is

ABSTRACT

Following the catastrophic avalanches in Súðavík and Flateyri in 1995, new laws and regulations were enacted concerning avalanche and landslide monitoring, hazard mapping, and land use in hazard zones. Strict rules govern land use in undeveloped areas, where new houses are only permitted if the risk is considered acceptable. In existing settlements, exemptions are made to allow for continued development with some restrictions. New residential buildings are allowed in A-zones and in B-zones if the buildings are reinforced. Construction of new hospitals, schools, apartment blocks, and similar buildings are permitted in A-zones if they are reinforced, but not in B-zones. In existing settlements, the same rules apply for the use of A-zones below defense structures. In recent years, increased population growth in several municipalities threatened by snow avalanches around Iceland has led to a renewed interest in building new homes below avalanche defense structures. As the official reviewer of land-use plans, the Icelandic Meteorological Office (IMO) has advocated for a cautious approach to developing such areas. These recommendations are made due to uncertainty about the effectiveness of defense structures — especially with regard to the fluidized front of high-speed drysnow avalanches, which most protection measures were not originally designed for.

INTRODUCTION

Following the catastrophic avalanches in Súðavík and Flateyri in 1995, new laws and regulations were enacted concerning avalanche and landslide monitoring, hazard mapping, and land use in hazard zones.

It was decided that hazard zones should be based on individual risk, and an acceptable level of avalanche risk was defined. Three types of hazard zones were defined:

A-zone: where the annual risk is 0.3–1.0 out of 10 000,

B-zone: where the annual risk is 1.0–3.0 out of 10 000,

C-zone: where the annual risk is greater than 3.0 out of 10 000.

This risk refers to an individual spending all of their time in one unreinforced house. The acceptable risk was chosen to be 0.2 out of 10,000 when exposure of individials to the hazard is taken into account. When considering the time people typically spend at home and at work, the acceptable risk level corresponding to 100% exposure is defined as 0.3 per 10,000 or lower for residential buildings, and 1.0 per 10,000 or lower for commercial buildings (excluding schools and hospitals).

HAZARD ZONING AND LAND USE

Strict rules govern land use in undeveloped areas, where new construction is only permitted if the risk is considered acceptable. In existing settlements, exemptions allow for continued development under certain restrictions. New residential buildings are allowed in A-zones, and in B-zones if the buildings are reinforced. New hospitals, schools, apartment blocks, and similar structures are permitted in A-zones but only if they are reinforced.

In existing settlements, the same rules apply to A-zones located below defense structures. However, in undeveloped areas, the protective effect of defense structures is not considered in land-use planning. Local governments, which oversee land-use planning, are required to adhere to these rules in both regional and local plans and when issuing building permits. In towns and villages, local authorities must take permanent action to either defend or buy out residential buildings located in C-zones, whereas safety plans based on evacuations and other non-permanent measures are allowed in rural areas.

Hazard assessments are mandatory for urban areas where avalanches, landslides, or slush flows are a concern. Assessments have been completed for 25 towns and villages across the country. In 16 of these, permanent actions are needed for houses in C-zones. Protection measures have been constructed for tens of avalanche paths in twelve towns and villages at a total cost of ~250 million €, in addition to a few projects in rural areas, the relocation of the residential buildings of the village of Súðavík after the avalanche accident in 1995 and buyout of houses in other places. In total, 24 deflecting dams, 27 catching dams, and five wedges for splitting avalanches have been constructed in run-out areas and >12 km of supporting structures have been installed in avalanche starting areas. In ten settlements, planned defenses are still in the planning phase or under construction, and some defenses are in place.

In rural areas, hazard assessments are less formal. Avalanche or landslide hazard is described for individual homes to support government decision-making regarding warnings and emergency actions, such as evacuations. However, the government is not obligated to take permanent defensive measures for rural properties. Outside of areas with formal hazard assessments, local assessments are required before issuing building permits. More than 200 such local assessments have been conducted.

In recent years, increased population growth in several municipalities around Iceland has led to a renewed interest in building new homes below avalanche defense structures. As the official reviewer of land-use plans, the Icelandic Meteorological Office (IMO) has advocated for a cautious approach to developing such areas. The IMO recommends that in hazard zones below defence structures: (1) New residential buildings should not be built closer to the mountain than existing ones. (2) New residential buildings should not make up a large proportion of buildings in the area. New buildings in the uppermost one or two rows of settlements should be reinforced. These recommendations are made due to uncertainty about the effectiveness of defense structures — especially with regard to the fluidized front of high-speed dry-snow avalanches, which most protection measures were not originally designed for.

Protecting against avalanches and landslides requires costly measures. It is therefore essential that new construction and development in protected areas and elsewhere do not significantly increase overall risk by expanding the number of people living and working in hazard zones. In the long term, local governments should focus development and new construction in areas outside of hazard zones or in zones with lower risk where that is possible. When opportunities arise, efforts should be made to reduce human presence and activity in the most hazardous zones.

Three-dimensional simulations of snow-avalanche flow for assessing the effectiveness of protections measures in the run-out zone

Tómas Jóhannesson, 1* Alexander H. Jarosch, 2 and Magni Hreinn Jónsson 1

¹ Icelandic Meteorological Office Reykjavík Iceland ² Theta Frame Solutionns Austria

ABSTRACT

The design of protections measures in the run-out zone is traditionally based on simplifying assumptions about snow avalanche dynamics, some of which have been validated with laboratory experiments with granular flow and interpretation of field observations of snow avalanches. We present an efficient computational fluid dynamics (i.e. OpenFOAM) implementation of an incompressible granular-flow rheology based on recent advances in the theory of $\mu(I)$ rheology that we call "Open- $\mu(I)$ ". Our approach represents an important improvement with respect to existing, depth-averaged models as it is able to simulate the full three-dimensional flow at impact with obstacles such as catching and deflecting dams and braking mounds. For example, our simulations faithfully represent the formation and timedependent development of hydraulic jumps in the shallow granular snow-avalanche flow. Splashing is simulated at impact with obstacles as well as granular wedges behind the upstream face of dams or mounds alongside many other flow features expected in such complex granular flows. Variations of the flow direction with depth within the moving material are simulated and, thus, shearing overflow of the upper part of avalanches at impact with a deflecting dam that deflects the main avalanche flow. We present several simulations of avalanches against protective dams and natural terrain obstacles in Iceland. The model does not represent the fluidized regime of some dry-snow avalanches and can, therefore, not be used to assess the rest risk due to the possible overflow of rapid fluidized heads of dry-snow avalanches as have recently been observed near settlements in Iceland.

Turbulence-Based Modeling of Powder-Snow Avalanches and Air-Blast Pressures Using RAMMS::Extended

Perry Bartelt^{1*}, Lukas Stoffel², Stefan Margreth², Yu Zhuang³ and Marc Christen¹

¹ RAMMS AG, Davos Wiesen, SWITZERLAND
² WSL Institute for Snow and Avalanche Research SLF, Davos, SWITZERLAND
³ College of Civil Engineering, Hunan University, Changsha, CHINA
*Corresponding author, e-mail: perry@ramms.ch

ABSTRACT

RAMMS::Extended is a physics-based model for simulating powder-snow avalanches, in which the turbulent suspension cloud is treated as an inertial flow of fine ice particles suspended in air. Once lofted by the dense avalanche core, the cloud evolves as a decoupled turbulent flow, governed by conservation laws for mass, momentum, and turbulent kinetic energy. A central tenet of the model is that all dissipative processes in the flow act first by feeding energy into turbulence, which then decays through the classical energy cascade. This turbulence governs not only entrainment and drag but also the generation of air-blast pressures, which arise from both mean flow and fluctuating components. The pressure field is computed by accounting for the anisotropic structure of turbulence, acknowledging that only a fraction of turbulent kinetic energy projects in the direction of motion. Model predictions align closely with observed forest and infrastructure damage in real avalanche paths, suggesting that this turbulence-first dissipation hypothesis offers a valid and physically coherent framework for simulating powder-snow avalanches.

1. INTRODUCTION

Developing and calibrating models for powder-snow avalanches—particularly the prediction of air-blast pressures—is a significant challenge due to the scarcity of direct field measurements. Air-blast pressure sensors are rarely deployed in active avalanche paths, and when they are, they often fail to capture the full spatial and temporal evolution of the powder cloud. As a result, model validation relies heavily on back-analysis of real events. In this context, forest damage offers a valuable proxy: trees act as natural pressure sensors, providing spatial constraints on air-blast intensity and extent.

Physically, the powder cloud (Π) behaves as a turbulent, inertial suspension current composed of fine ice particles entrained in air, see Figure 1 (Bozhinskiy and Losev, 1998). It originates from the momentum imparted by the dense avalanche core (Φ) —a granular, shear-driven flow of snow clods—and evolves as a detached, airborne flow. RAMMS::Extended is formulated to capture the full spatial development of this cloud, solving conservation equations for co-volume height (mass), physical height (volume), mean velocity, and turbulent kinetic energy,

P. Bartelt and others O6.2 - Page 153

Figure 1 RAMMS::Extended separates the avalanche into a core (Φ) and an overlying powder cloud (Π) . Air trapped and accelerated by the core defines the initial velocity of the powder cloud. The mean cloud velocity \vec{u}_{Π} , as well as the turbulent kinetic energy R_{Π} associated with the velocity fluctuations \vec{u}'_{Π} are calculated.

The co-volume height \hat{h}_{Π} represents the total suspended mass in the cloud, normalized by a reference density $\hat{\rho}_{\Pi}$, which reflects the initial "seeding" density of the suspension originating from the avalanche core.

The cloud incorporates air from two sources: $\dot{M}_{\Phi \to \Pi}$: ice-dust and embedded air transferred from the core, and $\dot{M}_{\Lambda \to \Pi}$: ambient air entrained as the cloud expands. This entrained air drives cloud growth, affecting density, velocity, and height. Notably, the model does **not** include any mechanisms for cloud settling or mass loss to the ground.

The cloud velocity \vec{u}_{Π} is governed primarily by momentum injection from the core, expressed as $\dot{M}_{\Phi \to \Pi} \vec{u}_{\Phi}$. In this process, the core acts as a momentum engine—especially when dispersed—ejecting ice-dust and air at high velocity. This mixture rapidly entrains additional air $(\dot{M}_{\Lambda \to \Pi})$, leading to upward and outward cloud expansion.

Although gravity \vec{G} contributes to motion, its effect is moderated by the buoyancy of the cloud: the density difference $\frac{(\hat{\rho}_{\Pi} - \rho_{\Lambda})}{\hat{\rho}_{\Pi}}$ is small, and thus the gravitational force is secondary to the dominant core momentum. Once airborne, the cloud decouples from terrain interactions and propagates as a self-sustaining flow. Without further input from the core, it gradually slows due to drag forces S_{Π} , which dissipate energy over time.

The **turbulent energy equation** captures the generation and dissipation of turbulence, which governs both cloud drag and air-blast pressure. Turbulence is generated by:

A key assumption is that all energy input is initially converted into large-scale turbulence, with **no immediate thermal losses**. This turbulence then cascades to smaller eddies and ultimately dissipates as heat, represented by the term $\beta_{\Pi}\hat{h}_{\Pi}R_{\Pi}$ is the turbulence decay coefficient. This framework is consistent with the classical energy cascade model of turbulence.

2. TURBULENCE GENERATION AND PRESSURE CALCULATION

At each computational time step, the total rate of turbulence generation in the powder cloud, denoted \dot{P}_{II} , is computed as:

$$\dot{P}_{\Pi} = \dot{M}_{\Phi \to \Pi} R_{\Phi} + \dot{W}_{\Pi} + \frac{1}{2} \rho_{\Lambda} \dot{M}_{\Lambda \to \Pi} ||\vec{u}_{\Pi}||^{2}$$

Each term represents a distinct physical mechanism contributing to turbulence:

- $\dot{M}_{\Phi \to \Pi} R_{\Phi}$: random kinetic energy transferred from the avalanche core,
- \dot{W}_{Π} : shear-induced turbulence within the cloud,
- $\frac{1}{2}\rho_{\Lambda}\dot{M}_{\Lambda\to\Pi}\|\vec{u}_{\Pi}\|^2$: turbulence generated by air entrainment at the cloud's upper boundary.

To describe the vertical distribution of turbulence, we define the parameters:

$$\theta_0 = \left(\dot{M}_{\Phi \to \Pi} R_{\Phi} + \dot{W}_{\Pi}\right) / \dot{P}_{\Pi}, \ \theta_h = \frac{1}{2} \dot{M}_{\Lambda \to \Pi} u_{\Pi}^2 / \dot{P}_{\Pi}$$

Here, θ_0 and θ_h represent the relative turbulence contributions at the base and top of the powder cloud, respectively. The turbulent energy profile $R_{\Pi}(z)$ follows a parabolic distribution in height constrained by:

$$R_{\Pi}(z=0) = \frac{\theta_0}{3} R_{\Pi} , R_{\Pi}(z=h_{\Pi}) = \frac{\theta_h}{3} R_{\Pi}$$

This formulation captures the dual turbulence regimes in the cloud: near the base, turbulence is driven by shear and energy transfer from the core, while at the top, air entrainment dominates. This vertical structure causes the region of maximum turbulence—and therefore pressure—to shift upward, elevating the effective nose of the avalanche (see Figure 2).

The total air-blast pressure in RAMMS::Extended is computed as the square of the sum of laminar (mean flow) and turbulent contributions. Let $V_{\Pi} = \|\vec{u}_{\Pi}\|$ and $V_{\Pi}^{T} = \|\vec{u}_{\Pi}'\|$

$$(p_{\Pi})_{max} = \frac{1}{2} \rho_{\Pi} [V_{\Pi} + V_{\Pi}^T]^2$$

Here, V_{Π}^{T} is the turbulent velocity is calculated from the local turbulent energy as:

P. Bartelt and others O6.2 - Page 155

$$V_{\Pi}^{T}(z) = \sqrt{\frac{2R_{\Pi}(z)}{3\rho_{\Pi}(z)}}$$

This formulation assumes that only one-third of the turbulent kinetic energy is effectively aligned with the direction of the mean flow—a simplification that accounts for the multidirectional nature of turbulence within the powder cloud. Because turbulent fluctuations are not fully oriented with the flow, only a portion of their energy contributes directly to dynamic pressure. This adjusted contribution is visualized as the grey region in the pressure plots (Figure 2). The minimum air-blast pressure, shown as the red line, can be computed as:

$$(p_{\Pi})_{min} = \frac{1}{2} \rho_{\Pi} [(V_{\Pi}^2) + (V_{\Pi}^T)^2] \text{ or } (p_{\Pi})_{min} = \frac{1}{2} \rho_{\Pi} [V_{\Pi} - V_{\Pi}^T]^2$$

The first expression captures the individual contributions of the mean and turbulent velocity components without considering their directional alignment or any compounding effects. The second formulation assumes the turbulent fluctuations act against the mean flow field.

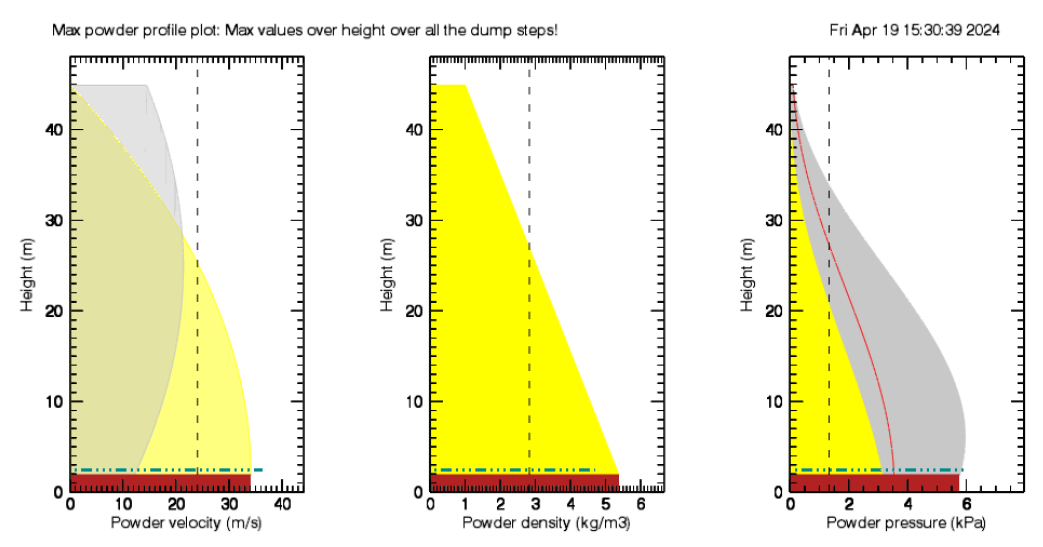


Figure 2 Velocity (left), density (middle) and air-blast pressure (right) profile in the powder cloud. The yellow and grey regions in the pressure plots depict the laminar and turbulent components, respectively.

In RAMMS::Extended the air entrainment rate $(\dot{M}_{\Lambda \to \Pi}, \text{ in m/s})$ depends on turbulent energy (R_{Π}) and the density difference between the powder cloud and surrounding air $(\rho_{\Pi} - \rho_{\Lambda})$. This relationship is expressed as:

$$\dot{M}_{\Lambda \to \Pi} = \left(1.16 \, \psi + 0.013 \sqrt{R_{\Pi} \hat{h}_{\Pi}}\right) (\rho_{\Pi} - \rho_{\Lambda})$$

In RAMMS::Extended, the powder cloud drag S_{II} is modeled as a combination of laminar and turbulent contributions, reflecting the dual nature of resistance encountered by the suspension cloud:

$$S_\Pi = \mu_L \|\vec{u}_\Pi\| + \mu_T R_\Pi \hat{h}_\Pi$$

where μ_L represents the laminar viscous drag, and μ_T denotes the turbulent viscosity. The transition between these two regimes is governed by the state of turbulence within the cloud.

3. CASE STUDY: MONBIEL KLOSTERS AVALANCHE, JANUARY 15, 2019

On January 15, 2019, a significant powder-snow avalanche descended the Inner Chinn track near Monbiel, Klosters, in Canton Grisons, Switzerland. This windy torrent, with steep sides lined by spruce trees, channeled the avalanche from a release zone at 2500 m elevation down to 1250 m, where it reached the Landquart River, depositing forested snow and tree debris. The avalanche reached a peak velocity of approximately 50 m/s (Figure 3) while confined by the torrent's deep sides, exiting at 40 m/s before stopping on the opposite riverbank. The powder cloud, constrained by the torrent walls, destroyed many 50-year-old spruce stands with stem diameters of 30–50 cm (see Figure 3). Although the cloud traveled up a gentle counterslope, overrunning the village of Monbiel, no damage occurred in the late runout stages. Within the torrent, however, the air-blast caused extensive damage, with estimated fracture heights of 1.2–1.5 m, suggesting a 100-year event. Powder pressures exceeded 3kPa at the river Landquart.

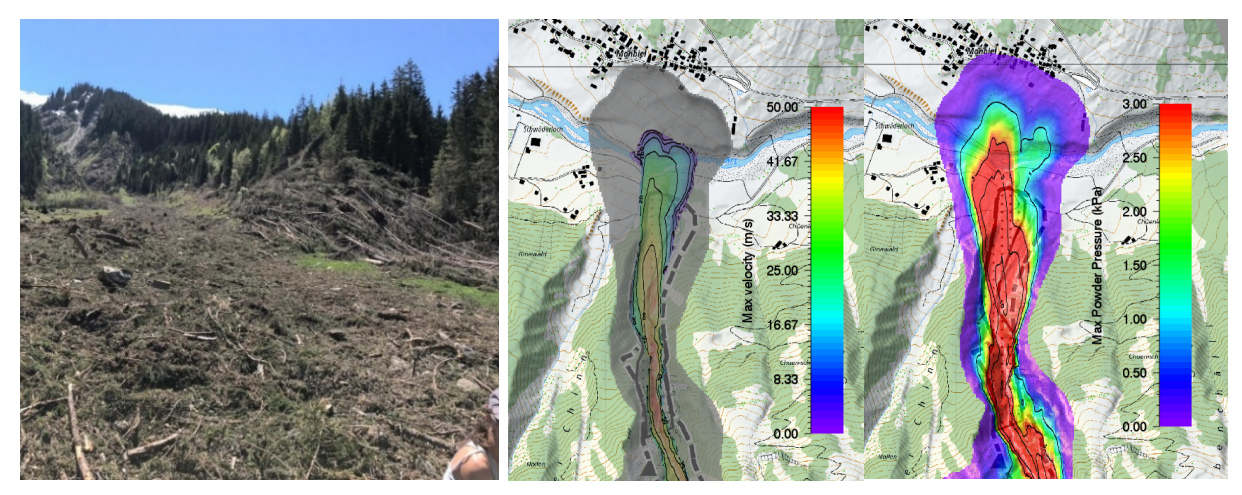


Figure 3 Forest destruction caused by the 2019 Inner Chinn avalanche (left). The avalanche core reached the river Landquart (middle) and the powder cloud travelled to the village of Monbiel Klosters with heights of 50m (right).

We simulated the avalanche using **RAMMS::Extended**, specifying a fracture height of 1.2 m, an initial release volume of 77,600 m³, and friction category 100L. Following a cold winter storm, we applied a 3-day snow settlement option with a low snow density of 175 kg/m³. The avalanche entrained 320,000 m³ of snow, mostly on upper slopes before entering the Inner Chinn torrent. Simulated powder cloud heights reached 50 m, consistent with observations. The model accurately captured forest destruction patterns, as detailed in Zhuang et al. (2023), where the turbulent component of the air-blast pressures enabled modeling of stem breakage with failure bending stresses exceeding 100 MPa—impossible without turbulence (see Figure 4).

The model requires specification of snow properties, and due to the cold winter storm, we defined a mean snow temperature of -6°C in the release zone, with snow height gradients of 5 cm/100 m to reflect the thinning snowcover as the avalanche descended, and a temperature gradient of 0.2°C/100 m fall height. These parameters aligned the simulated air-blast damage with empirical tree failure thresholds under pressures of 5–15 kPa, as reported by Fuchs and Bründl (2005). We did not consider curvature effects (centripetal accelerations), consistent with the idea that the winter snowcover smooths out sharp curvature in mountain torrents. This

P. Bartelt and others O6.2 - Page 157

allowed RAMMS::Extended to capture the complex behavior of the powder cloud, especially in such terrain.

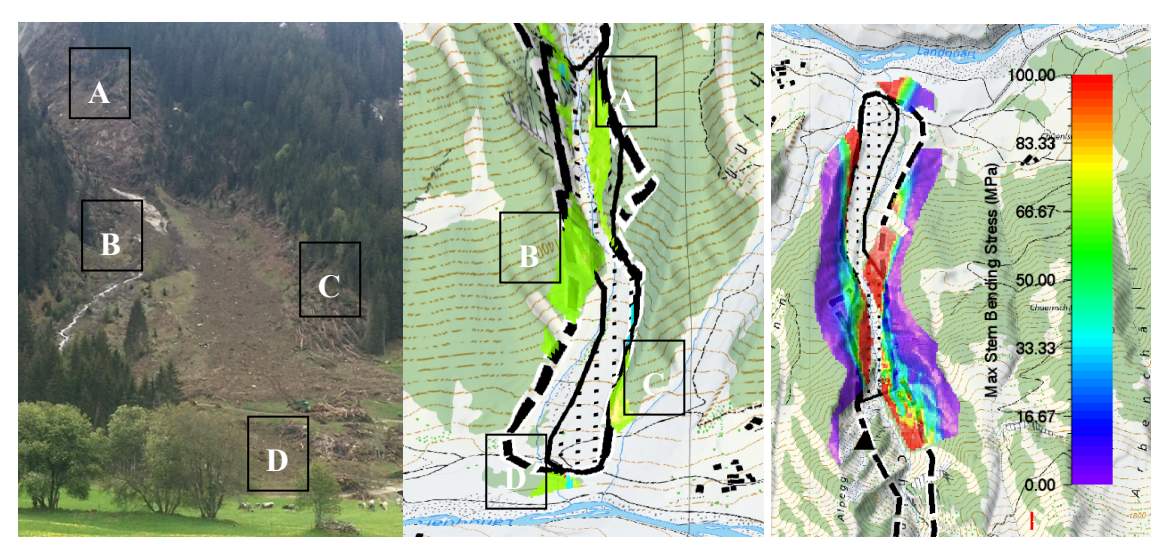


Figure 4 Forest destruction caused by the 2019 Inner Chinn avalanche, observation (left) and calculated (middle). Calculated bending stresses (>100MPa) in the tree stems.

4. CONCLUSIONS

RAMMS::Extended provides a turbulence-resolving framework for modeling powder-snow avalanches in which all dissipative processes are assumed to first generate turbulent kinetic energy, which then decays through classical inertial and viscous mechanisms. This assumption allows for a physically consistent representation of momentum diffusion, entrainment, and pressure generation within the powder cloud. The model resolves the spatial structure of turbulence and its role in producing air-blast pressures arising from both mean flow and velocity fluctuations. Application to the 2019 Monbiel Klosters avalanche confirms the validity of this approach: observed forest damage and stem failure are reproduced only when turbulence is explicitly modeled. By capturing both laminar and turbulent drag contributions, RAMMS::Extended enables smooth transitions across flow regimes and provides a predictive tool grounded in the physics of energy transfer and turbulent transport.

REFERENCES

Fuchs, S., Bründl, M. (2005). Damage Potential and Losses Resulting from Snow Avalanches in Settlements of the Canton of Grisons, Switzerland. *Natural Hazards*, 34, 53–69.

Bozhinskiy, A. N., & Losev, K. S. (1998). *The fundamentals of avalanche science. Mitteilungen des Eidg. Institutes für Schnee- und Lawinenforschung: Vol. 55.* Davos: Eidg. Institut für Schnee- und Lawinenforschung.

Zhuang, Y., Piazza, N., Xing, A., Christen, M., Bebi, P., Bottero, A., Bartelt, P. (2023). Tree blow-down by snow avalanche air-blasts: dynamic magnification effects and turbulence. *Geophysical Research Letters*, 50(21), e2023GL105334.

Large scale avalanche hazard indication modelling (LSHIM) adapted for Iceland

Yves Bühler^{1,2*}, Sigríður Sif Gylfadóttir³, Pia Ruttner^{1,2,4}, Marc Christen⁵, Andreas Stoffel^{1,2} and Stefan Margreth¹

¹ ¹WSL Institute for Snow and Avalanche Research SLF, Flüelastrasse 11, 7260 Davos Dorf, SWITZERLAND
 ² Climate Change, Extremes and Natural Hazards in Alpine Regions Research Center CERC, SWITZERLAND
 ³ Icelandic Meteorological Office

⁴ Institute of Geodesy and Photogrammetry, ETH Zurich 8092 Zurich, SWITZERLAND ⁵ RAMMS AG, Riedweg 35, 7494 Davos Wiesen, SWITZERLAND *Corresponding author, e-mail: buehler (at) slf.ch

Abstract

Large-scale simulations of avalanche hazards, such as those conducted over entire countries, enable continuous spatial estimation of hazards even in regions not covered by official hazard maps. In Switzerland, this encompasses approximately 90% of the mountainous areas. Hazard indication maps are crucial for planning new infrastructure and transportation routes as well as risk management, especially in areas lacking legally binding hazard maps.

In recent years, we have developed an automated approach called Large Scale Hazard Indication Modelling (LSHIM) to generate hazard indication maps based on digital elevation models and information on the snow climatology. This method allows for the calculation of various scenarios with return periods ranging from frequent to extreme. Our approach integrates the automated delineation of potential release areas, estimation of release depths, and numerical simulation of avalanche dynamics using the well-established RAMMS::Avalanche model, which is employed for hazard mapping in Switzerland and other countries. This procedure can be applied globally, provided high-resolution digital elevation models and snow climate data are available. It facilitates reproducible hazard indication mapping in regions without existing hazard maps, making it invaluable also for studies estimating potential impact of climate change on avalanche hazard. In this contribution, we present our strategy for adapting the LSHIM methodology to the very different terrain and meteorological conditions in Iceland.

1. INTRODUCTION

Avalanche hazard maps are vital tools for managing risks in alpine regions, helping to identify areas where construction should be avoided due to high avalanche danger. In Switzerland and other mountain regions, these maps are created by experts using a combination of historical avalanche records, terrain and forest analysis, field surveys, and numerical simulations. They have proven effective in reducing damage and saving lives (Margreth and Romang, 2010; Slf, 2000). However, their production is expensive and time-consuming, and coverage is limited—often restricted to areas with existing infrastructure. For instance, only about 10% of the alpine terrain in the canton of Grisons is currently covered with hazard maps.

To address this limitation, we developed an automated method to generate large-scale avalanche hazard indication maps using digital elevation models, information on snow climatology and protection forest (Bühler et al., 2022). These maps provide a spatially continuous overview of areas potentially endangered by avalanche events for the scenarios

Y. Bühler and others O6.3 - Page 159

applied in Switzerland with 10, 30, 100 and 300 years return periods. While the automatically generated maps do not include detailed interpretation and expert judgments gained through field visits, they are reproducible and offer valuable insights for early planning and risk awareness as well as a review of existing hazard maps using a uniform method.

Various approaches have been tested, including statistical models, GIS-based mapping, and simplified avalanche simulations. However, most approaches lack reliable avalanche dynamic models of avalanche runouts considering local terrain features —an essential component for assessing hazards in populated alpine valleys. Some methods also rely on coarse data or single-scenario simulations, limiting their practical use. Next to the LSHIM methodology (Bühler et al., 2022) applied in this paper, the most widely applied methodologies are NAKSIN in Norway (Issler et al., 2023) and ATES (Statham and Campbell, 2025) in North-America. However, the ATES model is, like the CAT product (Harvey et al., 2024; Harvey et al., 2018), aimed at backcountry activities planning and not for extreme scenarios and hazard mitigation for traffic lines and buildings.

Our approach builds on a validated algorithm for identifying potential release areas (Bühler et al., 2018), enabling the use of the RAMMS avalanche dynamics user model (Christen et al., 2010) for large-scale hazard indication mapping. RAMMS::Avalanche is widely used and trusted by avalanche experts worldwide for its robustness and ability to simulate multiple hazard scenarios based on standard return periods used in Switzerland.

In close collaboration with experts from the Icelandic Meteorological Office we now develop and test a strategy to adapt this well-established methodology to the very different topographic and climatological conditions in Iceland.

2. MAIN ADAPTION NEEDS

In various discussions we identified the following main adaption needs to transfer the methodology to Icelandic conditions. This process is still ongoing, and we are currently working on the testing and optimisation of these topics. Here we present first results.

2.1 Potential Release Areas PRA

A first critical step in the methodology is the delineation of the potential release areas PRA based on terrain parameters. The approach was developed over several years integrating a lot of expert know how and feedback from avalanche professionals (Bühler et al., 2013; Veitinger et al., 2016; Bühler et al., 2018). However, all this development and testing was performed in the Swiss Alps.

The topography and elevations in Iceland are very different to the Swiss Alps, typically with flat-top mountain shapes close to the ocean. Therefore, we develop and test adaptations of the delineation algorithm for better representing of large terrain bowls, and the very rough cliffs and gullies often present in Iceland. Even though the mapped PRA outlines cannot be reproduced exactly, the adapted version of the algorithm provides a better representation of the bowls, the ridges and gullies than the original version.

2.2 Fracture depth d0

In combination with the PRA the avalanche fracture depth d0 defines the release volume and with that the friction value classes used by RAMMS::Avalanche to calculate the runout distances. Therefore, it is a critical parameter for the large-scale hazard modelling.

The climatic conditions in Iceland are more extreme than in the Swiss Alps, in particular considering wind speeds and the amounts of windblown snow. In Switzerland we applied three days snow depth increase Δ HS(3) values derived and extrapolated from the dense network of manual long term snow depth measurements (Bühler et al., 2022).

Snow depth measurements in Iceland are mainly located at weather stations near the coastline and give rather limited information on conditions near the top of mountains, where wind-blown snow is an important factor for snow accumulation in potential release areas. Therefore, an alternative approach for defining Δ HS(3) was adopted using weather data from the Copernicus Arctic Regional ReAnalysis (CARRA) project (CITE), where the HARMONIE-AROME model (Bengtson et al., 2017) was run on historical data from 1990 to the present. Data from selected CARRA grid points are used as input in the Norwegian seNorge degree-day snow model (Saloranta, 2012; 2016) to generate a time series of snow depths. The grid has a resolution of 2.5 km. For each grid point, a time series of Δ HS(3) is then generated and using extreme value analysis, the value for a given return period is estimated.

In Iceland, the combination of the flat-top mountains with very frequent winds with high speeds leads to a higher importance of windblown snow for the avalanche fracture depth. In Switzerland we started to quantify the amounts of windblown snow in an avalanche release area applying high temporal resolution measurements with low-cost laser scanners (Ruttner et al., 2025). In Iceland first attempts with drone based photogrammetric measurements are performed. Based on these findings, we will adapt the d0 calculations for the simulations in Iceland. While these measurements are not available, we plan use a simple way to represent wind-drifted snow. In earlier approaches simulation important avalanche tracks with SAMOS (Sampl and Zwinger, 2004) the slopes have been classified into different classes of gullies and bowls with varying snow accumulation potential. This involves increasing the precipitation by a factor that grows with third power of wind speed if the wind direction is within +/- 45° of the release area aspect. Preliminary tests and comparison with measurements indicate that this method captures the significant difference in snow accumulation between release areas that align with the main wind direction during snowfall and those that do not.

2.3 Model Friction Parameters

The friction parameters μ and ξ that control the simulation of the avalanche flow in RAMMS::Avalanche have an elevation component calibrated based on avalanches in Switzerland (Christen et al., 2010). The basic idea behind this is that the snow at higher elevations (> 1500 m a.s.l.) is dryer than at lower elevations (< 1000 m a.s.l.) in Switzerland. These limits have to be adapted in Iceland as the avalanches often reach the ocean. We propose to set the limits at 200 and 500 m a.s.l. but we need further data on snowpack density and avalanche characteristics to identify the ideal thresholds.

Y. Bühler and others O6.3 - Page 161

3. RESULTS AND DISCUSSION

We used the region around Neskaupstaður in eastern Iceland as test case to adapt the algorithm to delineate the potential release areas (PRA) because manually delineated release zones of frequently observed avalanches are available. Figure 1 presents the resulting PRAs of the original approach (Bühler et al., 2018) and a first adapted version to better incorporate the rough terrain (gullies and ridges) and the large bowls present in this region.

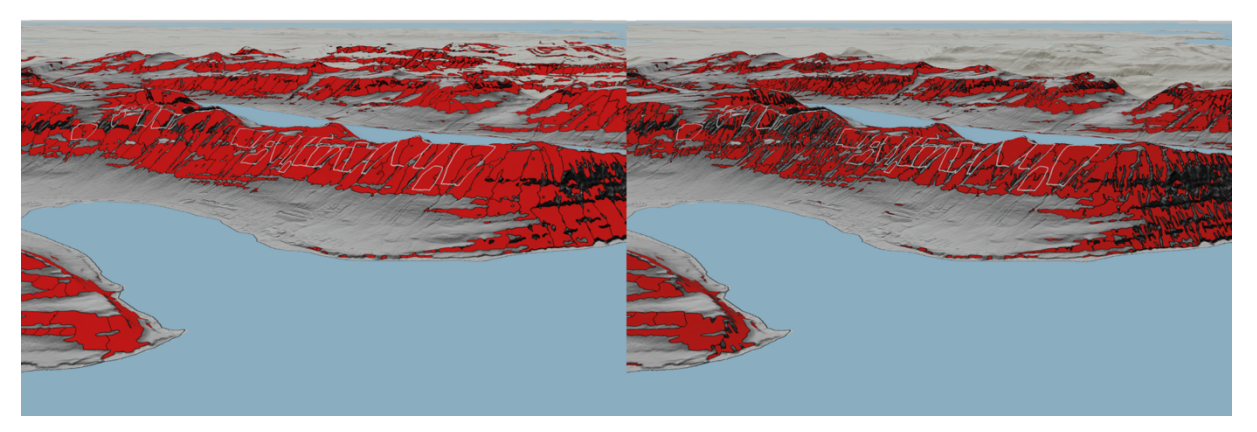


Figure 1 Result of the original PRA algorithm (left) and an adapted version (right), which is better representing bowls and the effect of terrain ridges and gullies in the region of Neskaupstaður. The white lines are the reference avalanche outlines mapped by the local avalanche experts.

The PRA generated with the adapted approach are then used to set up a simulation run for extreme avalanches in this region (Figure 2). A detailed analysis of these first results will help to further optimize the parameter setting. In particular, a better definition of the fracture depth d0 and the implementation of larger amounts of windblown snow for the extreme scenario (300 year return period in Switzerland) are expected to have a strong effect on the calculated runout distances and impact pressures. Further tests will be performed in the region around Ísafjörður (north-western Iceland) and Siglufjörður/Ólafsfjörður (north Iceland).

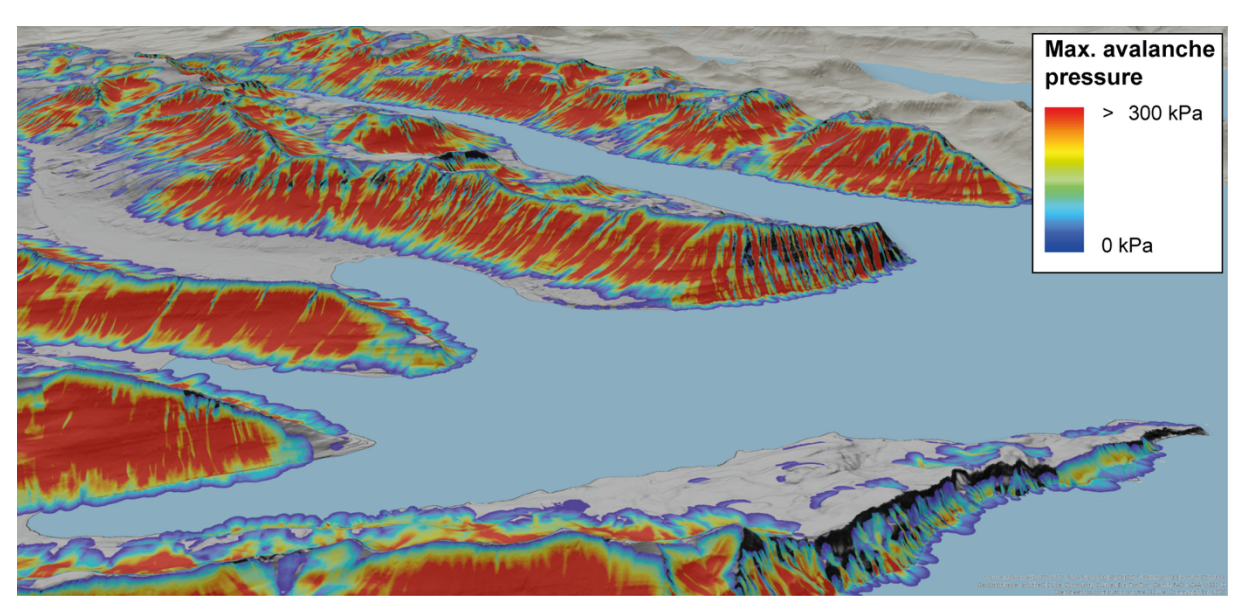


Figure 2 Result of a preliminary simulation run for extreme avalanches in the Neskaupstaður region.

4. CONCLUSIONS

Applying the Large Scale Hazard Modelling (LSHIM) approach, which was developed in Switzerland for avalanches in the Swiss Alps, in Iceland where the topography and meteorology is very different is challenging. Even though the approach has already been applied in various regions around the world (e.g. New Zealand, Afghanistan, Uzbekistan, Canada, Chile etc.) the specific challenges in Iceland are unprecedented.

The delineation of the potential release areas (PRAs) and the definition of meaningful fracture depth values (d0) need a lot of testing and refinement. We need to characterize the snow conditions defining the specific hazard scenarios from frequent to extreme. However, one simplification in the model compared to other mountain regions, is the omission of protective functions of forests.

In the future we plan to compare the simulations using the RAMMS::Avalanche model (Christen et al., 2010) with the more detailed RAMMS::Extended model, which is able to also calculate impact pressures of the powder cloud (Glaus et al., 2025). We also plan a comparison with existing hazard/risk maps, the results of the already performed SAMOS simulations and the NAKSIN approach (Issler et al., 2023), which is currently already implemented for some regions in Iceland.

ACKNOWLEDGEMENT

We thank Tómas Jóhannesson and Harpa Grímsdóttir for initiating the project and Daniel Govoni and Magni Hreinn Jónsson for valuable project inputs and discussions.

Y. Bühler and others O6.3 - Page 163

REFERENCES

- Bengtsson, L., et al. The HARMONIE–AROME model configuration in the ALADIN–HIRLAM NWP system. Mon. Weather Rev. 145, 1919–1935. https://doi.org/10.1175/MWR-D-16-0417.1. 2017
- Bühler, Y., Kumar, S., Veitinger, J., Christen, M., and Stoffel, A.: Automated identification of potential snow avalanche release areas based on digital elevation models, Natural Hazards and Earth System Sciences, 13, 1321-1335, 10.5194/nhess-13-1321-2013, 2013.
- Bühler, Y., von Rickenbach, D., Stoffel, A., Margreth, S., Stoffel, L., and Christen, M.: Automated snow avalanche release area delineation validation of existing algorithms and proposition of a new object-based approach for large-scale hazard indication mapping, Natural Hazards and Earth System Sciences, 18, 3235-3251, 10.5194/nhess-18-3235-2018, 2018.
- Bühler, Y., Bebi, P., Christen, M., Margreth, S., Stoffel, L., Stoffel, A., Marty, C., Schmucki, G., Caviezel, A., Kühne, R., Wohlwend, S., and Bartelt, P.: Automated avalanche hazard indication mapping on a statewide scale, Nat. Hazards Earth Syst. Sci., 22, 1825-1843, 10.5194/nhess-22-1825-2022, 2022.
- Christen, M., Kowalski, J., and Bartelt, P.: RAMMS: Numerical simulation of dense snow avalanches in three-dimensional terrain, Cold Regions Science and Technology, 63, 1 14, 10.1016/j.coldregions.2010.04.005, 2010.
- Glaus, J., Wikstrom Jones, K., Bartelt, P., Christen, M., Stoffel, L., Gaume, J., and Bühler, Y.: Simulation of cold-powder snow avalanches considering daily snowpack and weather situations, Natural Hazards and Earth System Sciences, 25, 2399-2419, 10.5194/nhess-25-2399-2025, 2025.
- Harvey, S., Christen, M., Bühler, Y., Hänni, C., Boos, N., and Bernegger, B.: Refined Swiss avalanche terrain mapping CATv2/ ATHv2, International Snow Science Workshop (ISSW 2024), September 23-27, 20242024.
- Harvey, S., Schmudlach, G., Bühler, Y., Dürr, L., Stoffel, A., and Christen, C.: Avalanche terrain maps for backcountry skiing in Switzerland, International Snow Science Workshop ISSW, Innsbruck, Austria2018.
- Issler, D., Gisnås, K. G., Gauer, P., Glimsdal, S., Domaas, U., and Sverdrup-Thygeson, K.: Naksin a New Approach to Snow Avalanche Hazard Indication Mapping in Norway., SSRN, 10.2139/ssrn.4530311, 2023.
- Margreth, S. and Romang, H.: Effectiveness of mitigation measures against natural hazards, Cold Regions Science and Technology, 64, 199-207, 2010.
- Ruttner, P., Voordendag, A., Hartmann, T., Glaus, J., Wieser, A., and Bühler, Y.: Monitoring snow depth variations in an avalanche release area using low-cost lidar and optical sensors, Nat. Hazards Earth Syst. Sci., 25, 1315-1330, 10.5194/nhess-25-1315-2025, 2025.

- Sampl, P. and Zwinger, T.: Avalanche simulation with SAMOS, Annals of Glaciology, 38, 393-398, 2004.
- SLF, Ammann, W., and Bründl, M. (Eds.): Der Lawinenwinter 1999 Ereignisanalyse, Eidgenössisches Institut für Schnee- und Lawinenforschung, Davos, 588 pp.2000.
- Statham, G. and Campbell, C.: The Avalanche Terrain Exposure Scale (ATES) v.2, Natural Hazards and Earth System Sciences, 25, 1113-1137, 10.5194/nhess-25-1113-2025, 2025.
- Veitinger, J., Purves, R. S., and Sovilla, B.: Potential slab avalanche release area identification from estimated winter terrain: a multi-scale, fuzzy logic approach, Natural Hazards and Earth System Sciences, 16, 2211-2225, 10.5194/nhess-16-2211-2016, 2016.

Y. Bühler and others O6.3 - Page 165

Bridging the Gap: Scenario-Based Avalanche Modeling vs. Back-Calculation of Events

Lukas Stoffel^{1*}, Stefan Margreth¹ and Perry Bartelt²

¹ WSL Institute for Snow and Avalanche Research SLF, Flüelastrasse 11, 7260 Davos Dorf, Switzerland

² RAMMS AG, 7494 Wiesen, Switzerland

*Corresponding author, e-mail: stoffell (at) slf.ch

ABSTRACT

Avalanche engineers are often required to assess hazards before any event occurs, using scenario-based approaches and calibrated avalanche dynamic models. Parameters such as release area, fracture depth, snowpack characteristics, and friction values are defined according to standardized procedures linked to specified return periods. Model outputs are validated with reference to avalanche history, terrain features, and vegetation patterns.

Back-calculations, by contrast, are performed after an event has occurred and benefit from known outcomes. Field data such as avalanche extent, release volume, and snow temperatures can be used to refine inputs. However, even in well-documented events, certain key parameters like entrained snow, snow density along the avalanche path, and friction values remain uncertain and must be determined through additional data and considerations.

This presentation draws on a case study from Switzerland to illustrate differences between scenario-based modeling and back-calculation. We present a structured procedure for defining model parameters, aimed at improving clarity and reproducibility. Additionally, we demonstrate how the RAMMS::Extended model - incorporating entrainment processes and temperature-dependent rheology - enhances the understanding of avalanche dynamics. These advances support a more nuanced, physically informed approach to avalanche simulation, ultimately improving hazard zoning and risk mitigation strategies.

1. INTRODUCTION

Avalanche hazard assessment plays a critical role in protecting infrastructure and communities in mountainous regions. A key challenge for engineers is to predict the runout distances and impact pressures of avalanches associated with specific return periods - a requirement for hazard mapping and mitigation planning. Two primary modeling strategies are applied for such purposes. The **scenario-based approach** simulates hypothetical avalanche events by defining model inputs such as release area, snowpack properties, and friction values - based on statistical and procedural standards linked to return periods. This method, which is based on general assumptions, can be applied with or without knowledge of historical events. By contrast, **back-calculation** is applied after an avalanche has occurred and leverages observed data such as release volume, snow temperature, and deposition extent. However, even with field data, key inputs like entrainment and friction still involve uncertainty.

This paper presents a structured 8-step procedure for scenario-based avalanche simulations and compares it to back-calculation using a documented case from Switzerland. The aim is to

L. Stoffel and others
O6.4 - Page 166

highlight differences in methodology, parameter sensitivity, and simulation outcomes - ultimately contributing to robuster hazard assessments.

2. OVERVIEW OF THE SCENARIO-BASED 8-STEP APPROACH

Scenario-based avalanche simulations estimate potential avalanche behavior for defined return periods by systematically assigning input parameters based on terrain, snowpack conditions, and standardized procedures. The approach described here applies to both dense flow and powder snow avalanches, with Steps 1-4 relevant for dense flows when applying RAMMS::Avalanche and Steps 1-8 used for powder snow avalanches when applying RAMMS::Extended (v3.0.2). The 8-step procedure is overviewed in Figure 1.

2.1 Avalanche return period

The return period has a significant influence e.g. on the avalanche runout. In Switzerland, 10-, 30-, 100-, 300- and >300-year avalanche return periods are taken into account for hazard assessment. The RAMMS friction parameters (section 2.4) are defined for these return periods.

2.2 Release area

The selection of the release areas for avalanche calculations is based on the terrain characteristics (slopes between 28 and 55° , ridges, cliffs, planarity, roughness, aspect), possible snow distribution, the return period (T = 300 y.: generally larger release area than for T = 30 y.) and also on considerations that in avalanche simulations the entire release mass is set in motion simultaneously and therefore the entire potential release area should usually not be taken into account for simulations. Means, the selected release area is part of the potential avalanche release area.

2.3 Fracture depth do

The slope-perpendicular fracture depth d_0 is calculated for dry avalanches according to the SLF procedure as follows (Salm et al., 1990; Stoffel et al., 2024):

- 1) Three-day snow height increase Δ HS3 for a specific return period: extreme value statistical analysis of data from a representative study plot preferably with long-term data.
- 2) Altitude correction of Δ HS3: difference in altitude between measurement field and release area. For the Swiss Alps typically an increase of 5 cm / 100 m is used
- 3) Correction to 28° slope: Conversion of $\Delta HS3$ measured on a flat study plot (value of 1) and 2)) to a 28° inclined slope which is the base value for the calculation of the fracture depth d_0 and the depth of erodible snow d_0^* (see section 2.5); with the factor $\cos 28^{\circ}$.
- 4) Snow drift addition due to wind influence: depending on the return period and the terrain situation we propose 0 to 50 cm, which is added to d_0 *.
- 5) Fracture depth d_0 taking into account the mean slope angle of the release area: d_0 * is corrected with the slope angle factor $f(\Psi)$ which is for example for $35^{\circ} = 0.71$. The reason for this assumption is that less snow can accumulate on a steep slope until the start of avalanches than on a less steep slope.

2.4 Friction Category

The friction parameters μ and ξ are defined based on the release volume and the assigned return period. Release volumes are categorized as follows: large (L) > 60'000 m³, medium (M) 25'000-60'000 m³, small (S) 5000-25'000 m³, and tiny (T) < 5000 m³.

If the avalanche splits into two or more distinct tracks over a significant portion of its path, it may be appropriate to assign a lower volume category for friction. This adjustment assumes that each track could be modeled as a separate avalanche with a smaller effective release volume.

2.5 Erodible snow in the Track

In RAMMS::Extended, the base value d_0^* is the input parameter for the erodible snow depth along the avalanche track and is referenced to the release area elevation. In the Swiss Alps, d_0^* is typically derived from the standard procedure used to calculate fracture depth d_0 (see Section 2.3, point 3). This base value excludes drift snow; if significant drift accumulation is present, d_0^* should be adjusted accordingly. The assumption that all new snow is eroded simplifies real conditions where beside parts of new snow, also parts of the old snow can be eroded.

To account for decreasing snow depth downslope, we recommend applying a gradient of Δd_0^* = 5 cm per 100 m.

2.6 Snow Temperature

Snow profile measurements during snowfall periods at 2100-2700 m a.s.l. showed mean temperatures of -3.5°C to -9°C (topmost meter), excluding the uppermost 20 cm to avoid surface effects (Stoffel et al., 2024). Snow temperatures generally decrease with elevation, supporting the use of the values proposed in Section 2.7 for scenario-based modeling.

A vertical gradient of $\Delta Ts = 0.28^{\circ}C/100$ m was reported in (Stoffel et al., 2024); we recommend using 0.2°, 0.3°, or 0.4°C/100 m, depending on conditions.

For air temperature (measured 2 m above the ground), we suggest applying the same values as for snow temperature.

2.7 Snow Density

Few snow density measurements from high-altitude snow profiles during prolonged snowfall events are available (Stoffel et al., 2024). However, average values between 150 and 200 kg/m³ appear realistic for new snow that has accumulated over two or more days, accounting for some settlement. Slightly higher densities are assumed for warmer snow temperatures. For the Swiss Alps we propose:

- Release area 1700-2100 m a.s.l.: snow temperature -5°C, density 190 (175-200) kg/m³
- Release area 2100-2600 m a.s.l.: snow temperature -6 $^{\circ}$ C, density 175 (160-190) kg/m³
- Release area 2600-3000 m a.s.l.: snow temperature -7°C, density 160 (150-175) kg/m³

2.8 Other parameters, e.g. Generate, Curvature

Model-specific inputs like "Generate" and "Curvature" are adjusted based on terrain. A value of 7 is commonly used for "Generate", and "Curvature Off" is reserved for long, gentle gullies.

L. Stoffel and others
O6.4 - Page 168

	1) Return period T	2) Release area	3) Fracture depth d0	4) Friction T/S/M/L	5) d0* Base value+∆d0*	6) Snow temp. + ΔTs	7) Snow density	8) Other
Scenario- based	10 30 100 300	f(T) f(terrain: sub-areas)	f(T) Based on extrem value stat.	f(T) f(release volume)	f(T) f(d0)	f(altitude release area / climate)	f(snow temp. / climate)	Generate Curvature
Details		From RAMMS:: Avalanche simulations		No. of tracks	At altitude release area		3-day settlement	Curvature off: long gentle gully

Figure 1 Overview of the Scenario-Based 8-step Approach. Input parameters are based on measurements or statistical data. Return period T influences size of release area, fracture depth, friction values, and erodible snow (d₀*). Defining the release area is crucial. The size and location of the release area has a big influence on the result. Green: defined / derived. Yellow: small uncertainty. Red: high uncertainty.

3. OVERVIEW ON THE BACK-CALCULATION OF OBSERVED AVALANCHES

As shown in Fig. 2 some of the input parameters of documented avalanches can be measured or are observed. Parameters like fracture depth or size of release area are difficult to assess when weather is poor. The biggest challenge might be the selection of the friction parameters which is explained in our case study in section 4. The available data often makes it possible to assign a return period to the back-calculated avalanche.

	1) Return period T	2) Release area	3) Fracture depth d0	4) Friction (T/S/M/L)	5) d0* Base value+Δd0*	6) Snow temp. + ΔTs	7) Snow density	8) Other
Back- Calculation	Com- parison with aval. history	e.g. observed, by drone	e.g. observed, by drone	f(cond.)	e.g. observed, measured	f(condi- tions)	f(cond- itions)	Generate Curvature
Details	e.g. runout		! Mean value of release area	f(rel.vol. + no. of tracks?)	Control: Erodible snow in runout	SnowPack simulations	SnowPack simulations	

Figure 2 Overview on the back-calculation of avalanches (RAMMS::Extended). Green: defined / derived. Yellow: small uncertainty. Red: high uncertainty.

4. CASE STUDY: WILDI AVALANCHE IN THE DISCHMA VALLEY NEAR DAVOS

Avalanche records from 1960 to 2025 indicate a return period of 10 years for events reaching the local road just northeast of the small river. One such event was the 15 January 2019 avalanche, triggered by heli bombing (Fig. 3).

4.1 10-year avalanche calculated with the Scenario-based Approach

The 10-year avalanche simulated with RAMMS::Avalanche crosses the open field near the river but falls short of the observed runout by about 40 m (Fig. 4, left). The fracture depth d_0 is 0.8 m, based on extreme value statistics (Δ HS3, Davos Dorf, T=10y.). The release volume is 30'100 m³, and the assigned friction category is 10-year Medium.

The 10-year core simulated with RAMMS::Extended reaches the road (Fig. 4, middle; Table 1), consistent with historical records (same release area used as for RAMMS::Avalanche).



Figure 3 Avalanches of 15 January 2019: no. 1: Wildi Avalanche (Glaus et al., 2024).

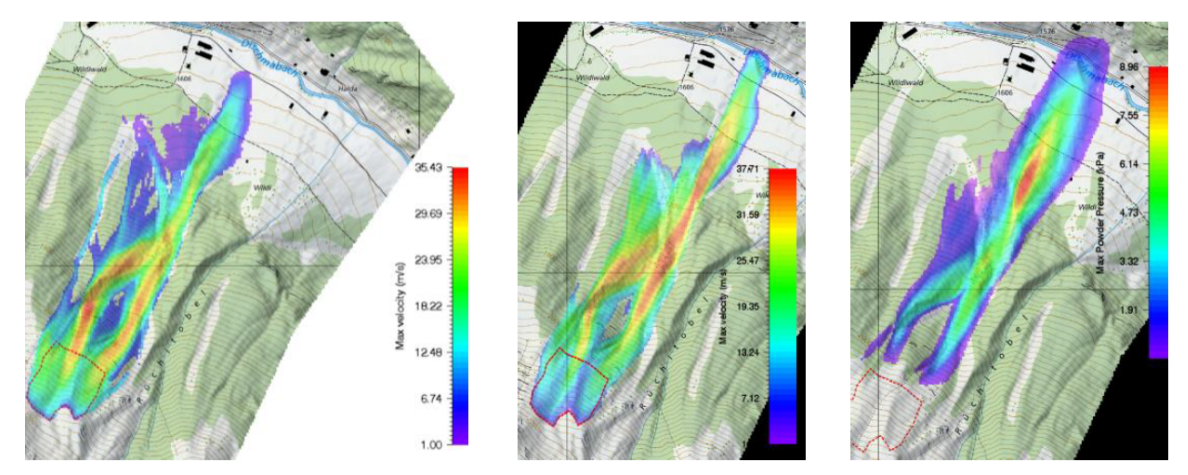


Figure 4 10-year dense flow avalanche (RAMMS::Avalanche left); core and powder cloud (RAMMS::Extended middle and right)).

4.2 Back-calculation of the Wildi avalanche of 15 January 2019

It is notable that the January 2019 avalanche, despite its small release volume of only 4200 m³, reached the road. This suggests extreme flow conditions, which were also needed in the model to reproduce the long runout (Table 1, Fig. 5). For such "tiny avalanches," we recommend testing different friction categories from 10y. to 300y. tiny - as used here. Selecting appropriate

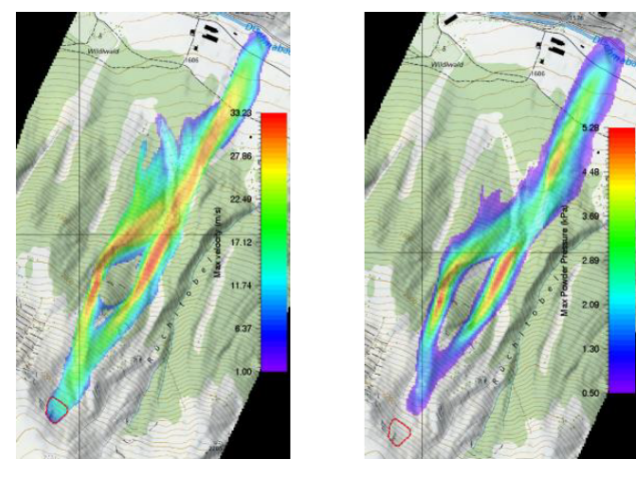


Figure 5 Back-calculation with RAMMS::Extended of the 2019 Wildi avalanche using the observed small release area and selected low friction (core left, powder cloud right).

L. Stoffel and others O6.4 - Page 170

friction values remains one of the key challenges in avalanche back-calculations (see Section 3). The input parameters in regard of the weather and snow conditions refer to (Glaus et al., 2024).

Table 1 RAMMS::Extended: Scenario-based input parameters and back calculation.

Input parameter	Values of Scenario-	Back calculation: avalanche of 15 Jan. 2019		
	based Approach (Section 4.1)	Value	Source	
Fracture depth d ₀	0.8 m	0.95 m	Drone	
Release volume	30'100 m ³	4200 m ³	Drone	
Erosion depth d_0^* Δd_0^*	0.95 m 0.05 m / 100 m	1.00 m 0.01 m / 100 m	Measured (in the run out) Measured	
Snow temp. (rel. area) Δ Snow Temperature	-6° 0.3° / 100 m	-7° 0.4° / 100 m	Snowpack data from Weiss- fluhjoch (WFJ) and Davos Dorf	
Snow density	175 kg/m ³	195 kg/m ³	Snowpack data from WFJ	
Friction	10y. Medium	300y. Tiny	Expert decision	

5. CONCLUSIONS

We analyzed the two modeling approaches, scenario-based simulations and back-calculations of observed events. The scenario-based method follows a structured 8-step procedure and is widely used for hazard mapping due to its reproducibility and linkage to standardized return periods. However, it involves simplifications such as uniform snow entrainment and predefined friction values. The back-calculation of the 2019 Wildi avalanche showed how field data can refine inputs but also highlighted the challenge of selecting friction values, which strongly affect runout. In this case, a small avalanche required unusually low friction to match observations, indicating complex flow not captured by standard settings. Back-calculations of observed avalanches can help calibrate models and better understand outlier events and allow a better understanding of the characteristics of an avalanche track. Parameter transfer between the two approaches should be done with caution due to explained differences.

REFERENCES

- Salm, B., Burkard, A., Gubler, H. U., 1990. Berechnung von Fliesslawinen. Eine Anleitung für Praktiker mit Beispielen. Davos, Eidgenössisches Institut für Schnee- und Lawinenforschung, Mitteilungen Nr. 47.
- Stoffel, L., Bartelt, P., and Margreth, S.: Scenario-based avalanche simulations including snow entrainment, snow temperature and density. In: Proceedings of the International Snow Science Workshop, Tromsö, September 23–29, 2024.
- Glaus, J., Wikstrom Jones, K., Kleinn, J., Stoffel, L., Ruttner-Jansen, P., Gaume, J., Bühler, Y.: Probability-based avalanche run-out mapping for road safety. In: Proceedings of the International Snow Science Workshop, Tromsö, September 23–29, 2024.

Towards a Physics-Based Quantification of Run-Up Height and Impact Pressure Using Numerical and Physical Experiments

Michael J. Kohler^{1,2,*}, Johan Gaume^{1,3}, Julius Kruse^{1,3}, Christophe Ancey², and Betty Sovilla¹

WSL Institute for Snow and Avalanche Research SLF, Davos, SWITZERLAND
 École Polytechnique Fédérale de Lausanne (EPFL), Lausanne, SWITZERLAND
 Eidgenössische Technische Hochschule Zürich (ETH Zurich), Zürich, SWITZERLAND
 *Corresponding author, e-mail: michael.kohler (at) slf.ch

ABSTRACT

Assessing how pylon-like structures respond to snow avalanche impact is a critical, yet challenging, part of risk mitigation. Central to this challenge is the quantification of run-up height and impact pressure distribution, both of which directly influence structural design.

Current engineering practice mostly relies on simple theoretical models incorporating empirical parameters, whose selection requires extensive experience. Although these models have proven to be effective in most cases, they may lead to inappropriate designs in some specific scenarios due to the simplifying assumptions postulated in their derivation. A more physics-based description of avalanche impact has the potential to improve our understanding and support more targeted and economical structural mitigation design. It is in this context that computer-based numerical approaches such as the material point method (MPM) have gained increasing interest. Elasto-plastic MPM frameworks can accurately reproduce the mechanical response of snow, offering a powerful approach to snow avalanche simulations. In our research, we use MPM to investigate the three-dimensional impact of avalanches on pylon-like structures. In addition to the numerical work, we have developed a small-scale experimental setup to calibrate and validate the model for controlled impact scenarios. This dual approach enhances confidence in the simulations and facilitates process understanding.

In this contribution, we present selected findings from our recent work, with a focus on the integration of numerical and physical modeling. Preliminary results highlight the potential of 3D simulations not only to inform future mitigation design but also to revisit and assess long-standing theoretical concepts in snow mechanics, such as the view of Haefeli (1939) on impact pressure.

1. INTRODUCTION

Pylon-like structures, such as ski lift pylons or transmission towers, are essential components of alpine infrastructure. Owing to their exposed and often remote locations, they are frequently subject to snow avalanche impact. These slender structures are usually completely surrounded by the flowing avalanche, resulting in complex, three-dimensional impact dynamics. For the design of such structures, engineers commonly rely on semi-empirical design formulae to estimate key quantities such as avalanche impact pressure and run-up height (e.g. Margreth et al. (2015), European Commission (2009)). These methods include simple analytical approaches (e.g. Voellmy (1955)), supplemented by experience from field observations, experiments or

engineering consulting (e.g. Salm (1990)). Although these tools have been shown to be effective in many practical applications, they rely on simplified rheological models. This means that their predictions can be inaccurate, which can be problematic in some cases.

Recent advances in numerical modeling, particularly in three-dimensional particle-based methods, offer a more physics-based representation of avalanche processes and could support more targeted, efficient structural design. For example, recent studies using the Discrete Element Method (DEM), have revealed important rheological mechanisms that govern impact pressures of avalanche-like flows (Kyburz et al. 2020; 2022a; 2022b). Nevertheless, DEM simulations remain computationally intensive and are thus restricted to idealized or small-scale scenarios.

To complement these developments, we adopt a continuum-based approach using the material point method (MPM), which allows for a balance between physical detail and computational efficiency. MPM is well-suited to simulate cohesive granular materials such as avalanching snow and has been increasingly used both in avalanche dynamics (Gaume et al. 2018; Li et al. 2021; Kyburz et al. 2024) and granular impact studies (Mast et al. 2014; Kohler et al. 2024). In this contribution, we present a dual approach that combines our 3D MPM model and a newly developed small-scale experimental setup for process understanding and validation. We present recent findings and outline how this approach could improve our understanding of the impact of avalanches and inform future design practices.

2. METHODS

2.1 Physical Modeling

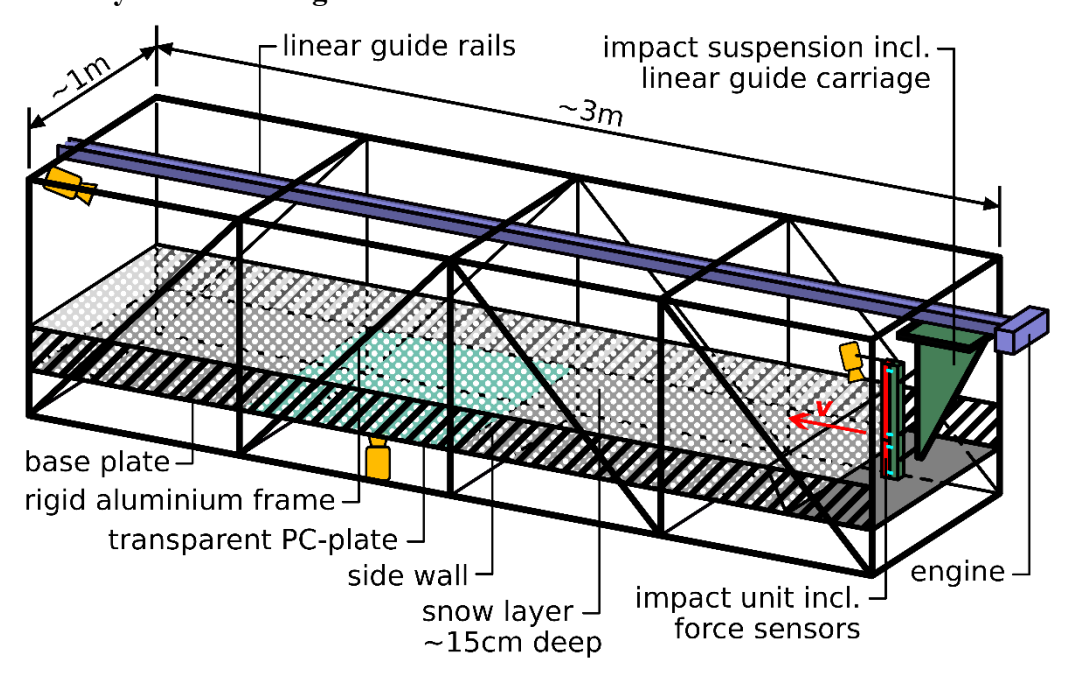


Figure 1 Schematic of the experimental setup

The experimental setup is located outdoors in a shaded area near Davos, Switzerland, at an altitude of 1600 m. It consists of a rigid aluminum frame measuring over 3 m in length and 1 m in width. The frame supports a laterally confined platform and a linear guide, powered by an

electric motor. Attached to the carriage of the linear guide is a 4.4 cm wide, rectangular obstacle, referred to as the impact unit. For each experiment, we sieve a 15 cm thick layer of snow onto the platform and drive the impact unit through the stationary snow at a fixed speed. This procedure is equivalent to considering that we are working in the moving Cartesian coordinate system attached to the avalanche rather than a fixed coordinate system.

For each experiment, we record the impact pressure distribution on the impact unit across two beams, each of which is supported by 2 uniaxial load cells. In addition, three video cameras record the scene synchronously. Two of them are stationary, one provides an overview of the entire setup, while the other captures images from beneath the snow layer through a transparent polycarbonate (PC) plate. A third camera is mounted on the impact unit and moves with it, capturing a top-down view of the interface between the snow and the obstacle. Figure 1 shows a schematic of the experimental setup with its most relevant components. A photo of the experimental setup is also shown in Figure 2a, which displays a video frame of a running experiment.

2.2 Numerical Modeling

MPM is a continuum-based particle method that captures many aspects of snow avalanche dynamics by accommodating large deformations, collisions, and fractures. Owing to its continuum formulation, MPM is more computationally efficient than discrete methods such as the DEM and enables the incorporation of sophisticated material models. In this work, we use the elasto-plastic Modified-Cam-Clay model, originally developed by Roscoe and Burland (1968) and extended to finite-strain and cohesive behavior by Gaume et al. (2018) for the simulation of snow slabs.

The numerical setup closely follows the geometry and boundary conditions of the physical experiment (see Figure 2b). The mechanical snow properties are estimated from density, grain type, grain size and snow temperature measurements as well as from video footage of the corresponding experiment.

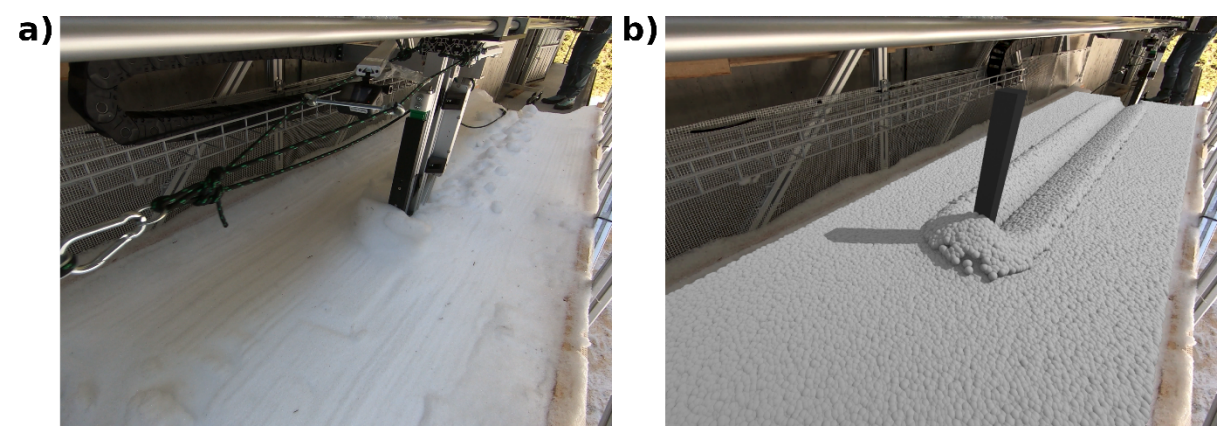


Figure 2 a) Video frame of a running experiment. b) Frame of the corresponding simulation

3. RESULTS AND DISCUSSION

To demonstrate the capabilities of our dual approach, we focus on a single experiment and simulate it using our MPM model. The selected test involves depth-hoar-like snow with a bulk density of approximately $480 \, \mathrm{kg/m^3}$ and an impact velocity of $0.75 \, \mathrm{m/s}$, corresponding to a

Froude number of around 0.6. The ambient air temperature was approximately -1.6 °C, and the snow temperature was -2.3 °C.

For the simulation, we estimated a cohesionless internal friction angle of about 25°, and assumed a moderate cohesion level, resulting in an effective internal friction angle of roughly 32°. Given the already high initial density, excessive compaction was prevented by enabling rapid material hardening, with the preconsolidation pressure set to 2 kPa. We used a Young's modulus of 1000 kPa and a Poisson's ratio of 0.25 and set the simulation resolution to 8.8 mm, which equals 1/5 of the obstacle width.

In this contribution, we focus on the impact force within the initial height of the snow layer. A

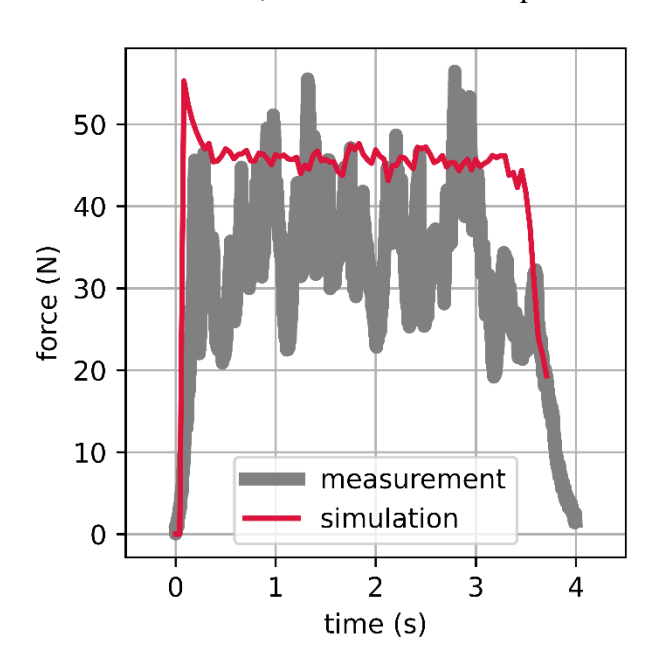


Figure 3 Comparison of the impact force time history within the initial snow height between the experiment and the simulation

comparison of the force-time histories from the experiment and the simulation is shown in Figure 3. The simulated curve lies between the measured average and the peak impact pressures. Notably, the simulation yields a smooth force curve, whereas the experimental data exhibit several pressure peaks of short duration. These peaks may be attributed to stick-slip behavior, commonly phenomenon observed experimentally in granular materials (Albert et al. 2001) but also in full-scale snow avalanche impact measurements (Sovilla et al. 2008).

At this preliminary stage, we are satisfied with this match. Reproducing the observed stick-slip behavior is possible with our model, but would require more rigorous parameter calibration, e.g. tuning the material parameters to produce a stiffer and more brittle behavior, which is subject for future work.

Apart from progressing toward a quantitatively predictive tool for quantities relevant to engineering, such as impact pressure, our model also allows us to better understand the physics of impact. For instance, as it is based on continuum mechanics, it provides the stress tensor at any Material Point. In Figure 4a, we visualize the principal stress directions as pressure and tension trajectories for a representative simulation frame. This visualization reveals a striking qualitative agreement with the conceptual model proposed by Haefeli (1939), for the load transfer onto support structures in creeping snow, formulated at a time when spatial stress fields could not yet be computed readily. This correspondence highlights the potential of modern numerical methods to revisit and validate long-standing theoretical concepts in snow mechanics.

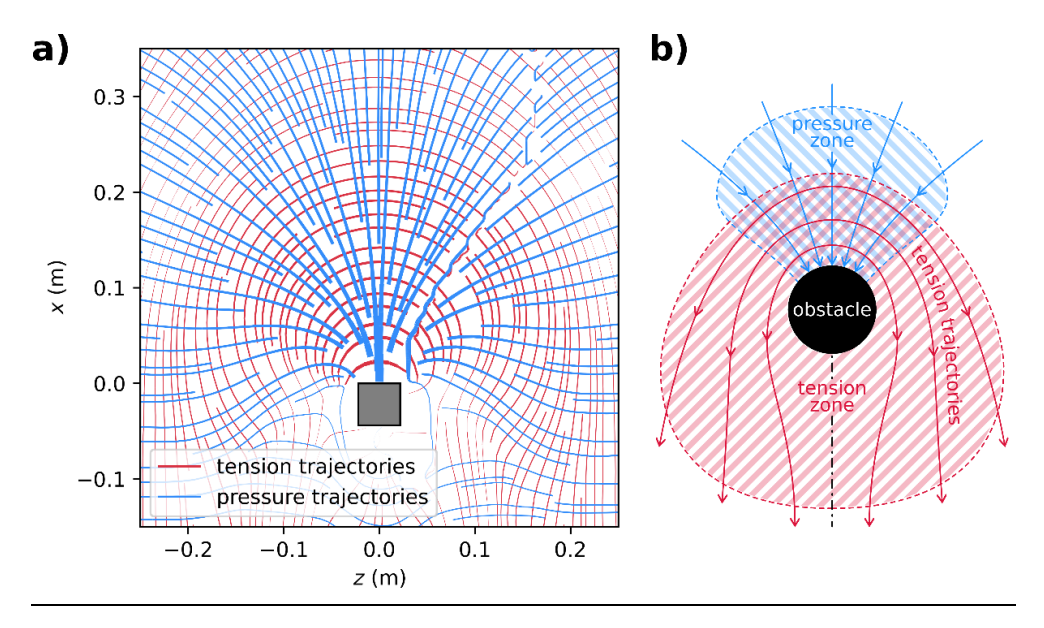


Figure 4 a) Pressure and tension trajectories of the simulation compared to b) Haefeli's (1939) conception of a support structure's mode of action in creeping snow

4. CONCLUSIONS

In this contribution, we have presented a combined numerical-experimental modeling approach and a selection of applications to avalanche impact. Our goal is to enhance traditional empirical methods by improving our understanding of the physical processes involved and enabling the systematic validation of numerical models. With accurate mechanical material characterization, the model captures the key mechanisms of impact pressure build-up. While the present study focused on the impact force within the initial flow height, future work will address additional variables such as run-up height. The fully spatially resolved numerical model provides detailed insights into the main impact processes and can thus contribute to the refinement of current engineering design practices. In the long term, this dual approach has the potential to establish 3D numerical modeling as a predictive and reliable method for avalanche engineering applications.

ACKNOWLEDGEMENT

This work was supported via the Swiss National Science Foundation project "The pulsing nature of powder snow avalanches" under Grant No. 200021 207323.

REFERENCES

Albert, I., P. Tegzes, R. Albert, et al. 2001. "Stick-Slip Fluctuations in Granular Drag." *Physical Review E* 64 (3): 031307. https://doi.org/10.1103/PhysRevE.64.031307.

European Commission, Directorate-General for Research and Innovation, D. Issler, P. Gauer, and T. Jóhannesson. 2009. *The Design of Avalanche Protection Dams - Recent Practical and Theoretical Developments*. Publications Office. https://data.europa.eu/doi/10.2777/12871.

Gaume, J., T. Gast, J. Teran, A. van Herwijnen, and C. Jiang. 2018. "Dynamic Anticrack Propagation in Snow." *Nature Communications* 9 (1): 3047. https://doi.org/10.1038/s41467-018-05181-w.

- Haefeli, Robert. 1939. "Schneemechanik mit Hinweisen auf die Erdbaumechanik." Doctoral Thesis, ETH Zurich. https://doi.org/10.3929/ethz-a-000096665.
- Kohler, Michael J., Johan Gaume, and Betty Sovilla. 2024. "Are Our Avalanche Impact Pressure Equations Fit for a Warming Climate? Insights from 3D Avalanche Modeling." *Proceedings of the International Snow Science Workshop* 2024, 299–305.
- Kyburz, M. L., B. Sovilla, Y. Bühler, and J. Gaume. 2024. "Potential and Challenges of Depth-Resolved Three-Dimensional MPM Simulations: A Case Study of the 2019 'Salezer' Snow Avalanche in Davos." *Annals of Glaciology*, April 4, 1–14. https://doi.org/10.1017/aog.2024.14.
- Kyburz, M. L., B Sovilla, J. Gaume, and C. Ancey. 2020. "Decoupling the Role of Inertia, Friction, and Cohesion in Dense Granular Avalanche Pressure Build-up on Obstacles." *Journal of Geophysical Research: Earth Surface* 125 (2): e2019JF005192. https://doi.org/10.1029/2019JF005192.
- Kyburz, M. L., B. Sovilla, J. Gaume, and C. Ancey. 2022a. "The Concept of the Mobilized Domain: How It Can Explain and Predict the Forces Exerted by a Cohesive Granular Avalanche on an Obstacle." *Granular Matter* 24 (2): 45. https://doi.org/10.1007/s10035-021-01196-1.
- Kyburz, M. L., B. Sovilla, J. Gaume, and C. Ancey. 2022b. "Physics-Based Estimates of Drag Coefficients for the Impact Pressure Calculation of Dense Snow Avalanches." *Engineering Structures* 254 (March): 113478. https://doi.org/10.1016/j.engstruct.2021.113478.
- Li, Xingyue, Betty Sovilla, Chenfanfu Jiang, and Johan Gaume. 2021. "Three-Dimensional and Real-Scale Modeling of Flow Regimes in Dense Snow Avalanches." *Landslides* 18 (July). https://doi.org/10.1007/s10346-021-01692-8.
- Margreth, Stefan, Lukas Stoffel, and Mark Schaer. 2015. "Berücksichtigung der Lawinen- und Schneedruckgefährdung bei Seilbahnen. Ein Leitfaden für die Praxis." WSL Berichte, no. 28. https://www.dora.lib4ri.ch/wsl/islandora/object/wsl%3A9091/.
- Mast, Carter M., Pedro Arduino, Gregory R. Miller, and Peter Mackenzie-Helnwein. 2014. "Avalanche and Landslide Simulation Using the Material Point Method: Flow Dynamics and Force Interaction with Structures." *Computational Geosciences* 18 (5): 817–30. https://doi.org/10.1007/s10596-014-9428-9.
- Roscoe, Kenneth Harry, and John Boscawen Burland. 1968. "On the Generalised Stress-Strain Behaviour of 'Wet' Clay." *Engineering Plasticity*, 535–609.
- Salm, B., A. Burkard, and H. U. Gubler. 1990. *Berechnung von Fliesslawinen. Eine Anleitung fuer Praktiker mit Beispielen*. https://www.dora.lib4ri.ch/wsl/islandora/object/wsl%3A26106/.
- Sovilla, Betty, Mark Schaer, and Lambert Rammer. 2008. "Measurements and Analysis of Full-Scale Avalanche Impact Pressure at the Vallée de La Sionne Test Site." *Cold Regions Science and Technology*, International Snow Science Workshop (ISSW) 2006, vol. 51 (2): 122–37. https://doi.org/10.1016/j.coldregions.2007.05.006.
- Voellmy, A. 1955. "Über die Zerstörungskraft von Lawinen; Stau- und Druckwirkungen." *Schweizerische Bauzeitung* 73 (17). https://doi.org/10.5169/SEALS-61903.

Use of OpenFOAM and $\mu(I)$ -rheology in the design of protective structures for avalanches for Flateyri NW Iceland.

Reynir Leví Guðmundsson^{1*}, Snorri Gíslason¹, Hafþór Pétursson² and Kristín Martha Hákonardóttir³

¹ Verkís, Ofanleiti 2, IS-103 Reykjavík, ICELAND
 ² Landsvirkjun, Katrínartún 2, IS-105 Reykjavík, ICELAND
 ³ Ministry of the Environment, Energy and Climate, Borgartún 26, IS-101 Reykjavík, ICELAND
 *Corresponding author, e-mail: rlg (at) verkis.is

ABSTRACT

This study presents the application of a newly implemented $\mu(I)$ -rheology module in OpenFOAM/interFoam for simulating the three-dimensional interaction between the dense core of snow avalanches and protective dams. The module was developed and integrated into the OpenFOAM framework by Thetaframe Solutions in collaboration with the Icelandic Meteorological Office. It was in part made to support the redesign of avalanche defence structures above the village Flateyri, in the Westfjords of Iceland, after the fluidized heads of two avalanches overran the existing dams in 2020.

The $\mu(I)$ -rheology model, which captures the complex behaviour of granular flows, has been validated using historical data from large natural Icelandic avalanches in different types of terrain and avalanches interacting with defence structures. The model realistically reproduces the three-dimensional interaction of avalanches with steep obstacles, forming granular jumps at dams and capturing ballistic trajectories over smaller features such as mounds.

Simulations were carried out to evaluate the effectiveness of various design improvements above Flateyri. These included steeper dams, the placement of braking mounds upslope of existing structures, and the addition of a deflecting dam above the harbour. The final design features three rows of steep, 10 and 11 m high braking mounds located upslope of the current deflecting dams, a reconstructed catching dam with increased height and a steep upstream face, and a new 5–7 m high, steep deflecting dam above the harbour.

The model was used to optimize the layout of the braking mounds—including aspect ratio, spacing between rows, and distance to the deflecting dam—and to calculate time-dependent loading on the structures.

1. INTRODUCTION

Avalanches are frequent from the starting zones above the village Flateyri, in NW Iceland and there are records of numerous avalanche occurrences, most notable the catastrophic avalanche of 1995 that claimed 20 lives. The defence structures above the village entail two, 14–19 m high earth fill deflecting dams and one 10 m high earth fill catching dam. The main starting zones above the village are Innra-Bæjargil and Skollahvilft. Several avalanches have hit these protective structures since their construction. In January 2020, two large avalanches from both starting zones hit the protective structures (Hilmarsson et al., 2020). Both avalanches had developed fluidized heads, that hit the deflecting dams. In both instances, the fluidized heads

overran the dams, though the dams directed the denser core (approximately 90% of the avalanche mass) successfully away from the town, see Figure 1. The overflow caused some damage of houses and vehicles downstream from the dams, and a young child was buried but saved from her bedroom. A large part of the avalanche from Skollahvilft entered the harbour causing severe damage to boats and the surrounding harbour structures.

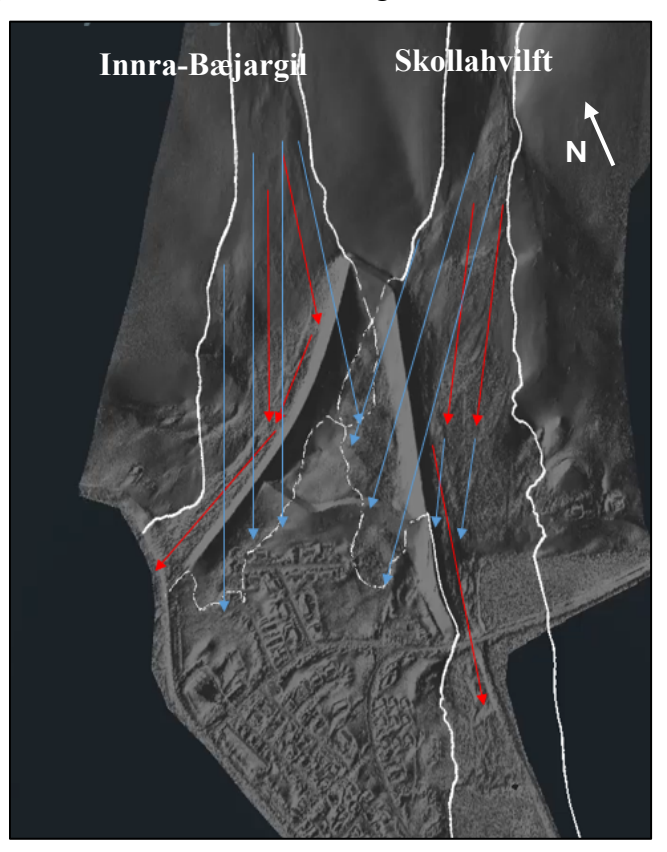


Figure 1 Outlines of the two avalanches from January 2020. Blue lines indicate the path and direction of the fluidized layer and red lines the path and direction of the denser core.

The initial design of the dams was made by the companies VST (Verkfræðistofa Sigurðar Thoroddsen) and NGI in Norway. Following the events, VST (now Verkís ltd.) was tasked with reviewing the design and functionality of the protection structures, submitting proposal for improvement, and exploring possibilities to protect the harbour area.

2. IMPROVING THE PROTECTION STRUCTURES

A newly implemented $\mu(I)$ -rheology module in OpenFOAM/interFoam (Jarosch, 2021) was applied in the design process for improving the protection structures. The purpose of the $\mu(I)$ -rheology (Baker and Gray, 2017) module is to capture the complexity of the flow of the dense core of snow avalanches (Jarosch et al., 2022).

Using this module, it is possible to simulate interaction between the dense core of snow avalanches and protective structures in three dimensions. This is a certain advance from using depth-integrated two-dimensional models.

There are mainly two physical parameters in the $\mu(I)$ -rheology module, dynamic friction coefficient (μ_d) and static friction coefficient (μ_s), that can be adjusted. To validate the choice of parameters known avalanches, that included the two avalanches in 2020, were simulated (Jarosch et al., 2022).

2.1 Improvement process

In this work, avalanche simulations at Flateyri were conducted for the two different release areas, Innra-Bæjargil and Skollhvilft, which are independent of each other. The same physical properties were used for both situations. Design avalanches for different release areas were established based on current hazard zoning (Hættumatsnefnd Ísafjarðarbæjar, 2004) and correspond to a frequency of 1 in 1000 years. This was verified by simulation on the terrain without current protection structures.

Initially, the efficiency of the current protection dams was analysed and based on those results various improvements were tested. These included a number of different structures and layouts, e.g. steeper dams, the placement of braking mounds upslope of existing structures, different geometry of flow channels along existing deflecting dams, and the addition of a deflecting dam above the harbour.

3. NUMERICAL SIMULATION

3.1 Solver and numerical scheme

The simulations were made with InterFoam, a three-dimensional OpenFOAM solver that simulates two incompressible, isothermal, immiscible fluids using the Volume of Fluid method (VOF). The two phases that are simulated are the snow or dense core and the air surrounding the avalanche. For the snow phase the $\mu(I)$ -rheology module was used with the corresponding parameters.

Friction parameters: $\mu_d = 0.11$ and $\mu_s = 0.75$. Density $\rho_{snow} = 300 \text{ kg/m}^3$.

Due to density differences between the two phases the air has negligible influence on the snow phase. It was assumed that the air phase was laminar. To secure simulation stability a first order upwind scheme was used.

3.2 Simulation geometry, boundary conditions and computational grid

A model of the current terrain was acquired through an aerial LiDAR scan. The area below 400 m a.s.l. was LiDAR scanned by Svarmi in autumn 2020 and the area above was based on a courser scan by TopSCAN in 2009. The simulated terrain with current protection structures for the two gulleys are shown in Figure 2. For the relevant suggestions for protection structures, different protective constructions or modifications were added to the terrain.

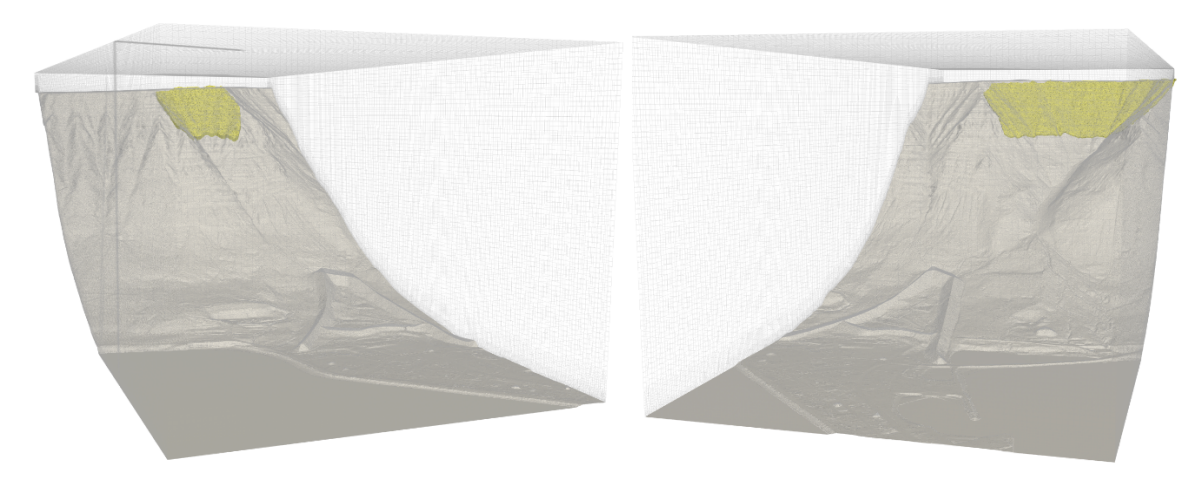


Figure 2 The computational domains of Innra-Bæjargil (left) and Skollahvilft (right). Current terrains with the corresponding release areas. Size of both domains is 2190 x 890 x 700 m (L x W x H).

The mesh of the computational domain with the protective structures consists of around 8 million cells for the simplest case, that is when there are limited protection structures, to almost 10 million cells. The cells are primarily hexahedral. It should be noted that the computational domains are in both cases relatively large.

Since many different layouts were simulated, a simple meshing strategy was implemented. A more strategic refinement could have produced smaller domains with fewer cells and somewhat shorter computational time. For this work, the adopted work flow was more effective.

Initially a relatively large (10 x 10 x 10 m) cells throughout the domain were used with a refinement strategy close to the ground and around protective structures. Three refinement levels were used, where the smallest cell was around 1.25 x 1.25 x 1.25 m in size. The length and width of the refinement areas, as well as the height, depends on expected flow trajectories and splashing. This is important around braking mounds as well close to both deflecting and catching dams. Table 1 shows relevant information about grid size strategy and refinement zones, Figure 3 shows an example of the refinement zone around a row of braking mounds.

Table 1 Grid refinement

Terrain and dams	
1.25 x 1.25 x 1.25 m grid size	From ground to 5 m height*
2.5 x 2.5 x 2.5 m grid size	From 5 m to 20 m height*
5 x 5 x 5 m grid size	From 20 m to 50 m height*
Braking mounds	
1.25 x 1.25 x 1.25 m grid size	L: 135xB: Width of dam row + 24xH:60 m**
2.5 x 2.5 x 2.5 m grid size	L: 155xB: Width of dam row + 44xH:80 m**
5 x 5 x 5 m grid size	L: 175xB: Width of dam row + 64xH:100 m**

^{*}Sizes cover the whole terrain. **L: length, B: width, H: height from ground.

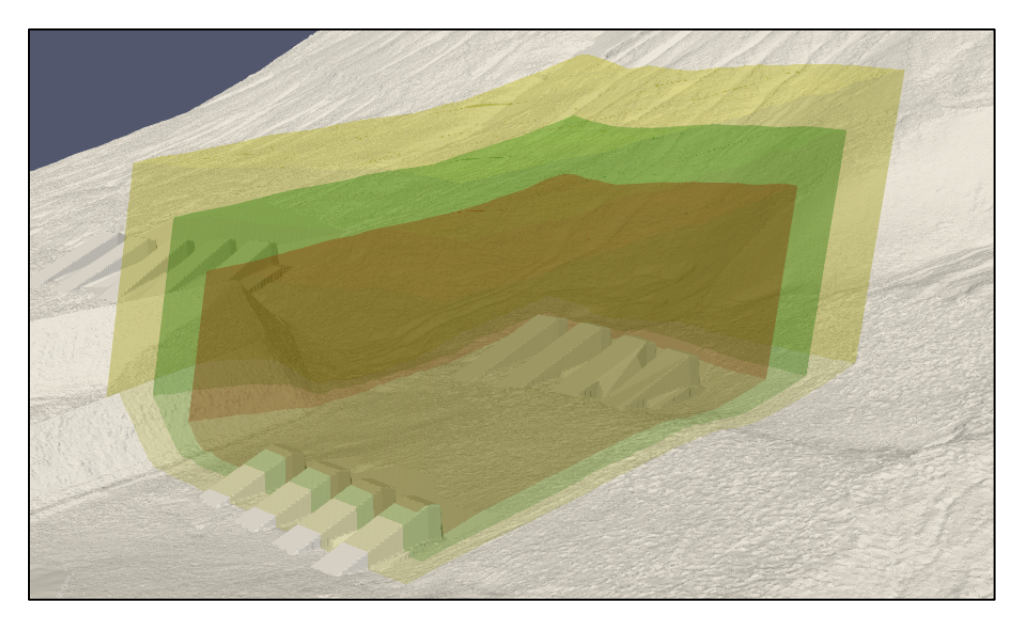
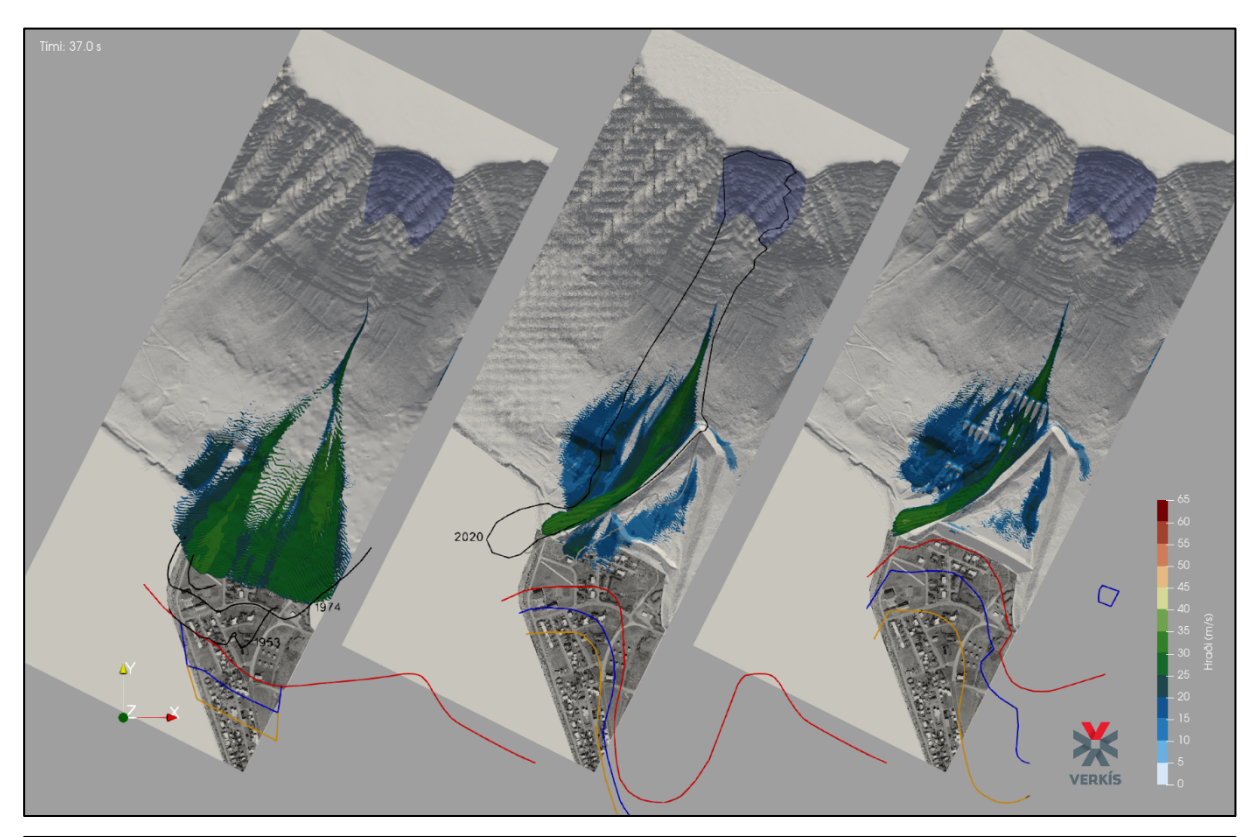


Figure 3 An example of mesh refinement zones around the uppermost row of braking mounds below Skollahvilft gully.

4. RESULTS

In total, 10 different layouts were tested for Innra-Bæjargil and >23 different layouts for Skollahvilft. The situation below Skollahvilft is more complex due to the harbour and Sólbakki, a residential house east of Flateyri. The proposed modifications in the protective structures shows a significantly improved protection, both for the residential area as well for the harbour, and the additional mounds play a key role in protecting the harbour (see Figure 4 and Figure 5 for Innra-Bæjargil and Skollahvilft respectively).

In addition to all the different layouts that were simulated, various other scenarios were investigated, e.g. one with uppermost row of mounds being completely buried by avalanche deposits. Both to validate the results and to analyse the effectiveness of different protective structures. Additionally, the mounds are assumed to dissipate energy in fluidized avalanches as well. Fluidized avalanches where, however, not modelled in the study. Figure 6 shows an example of the interaction of the dense core with braking mounds.



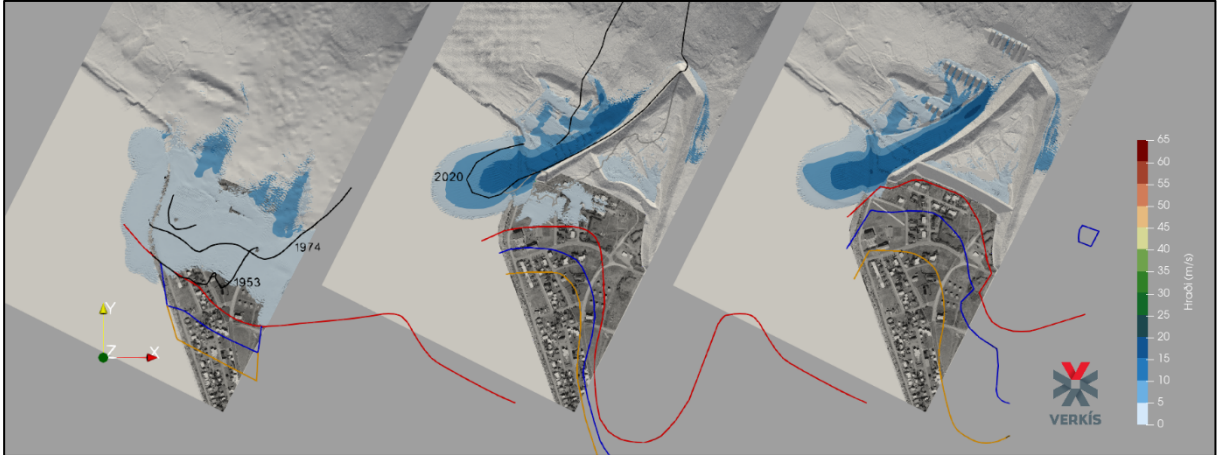
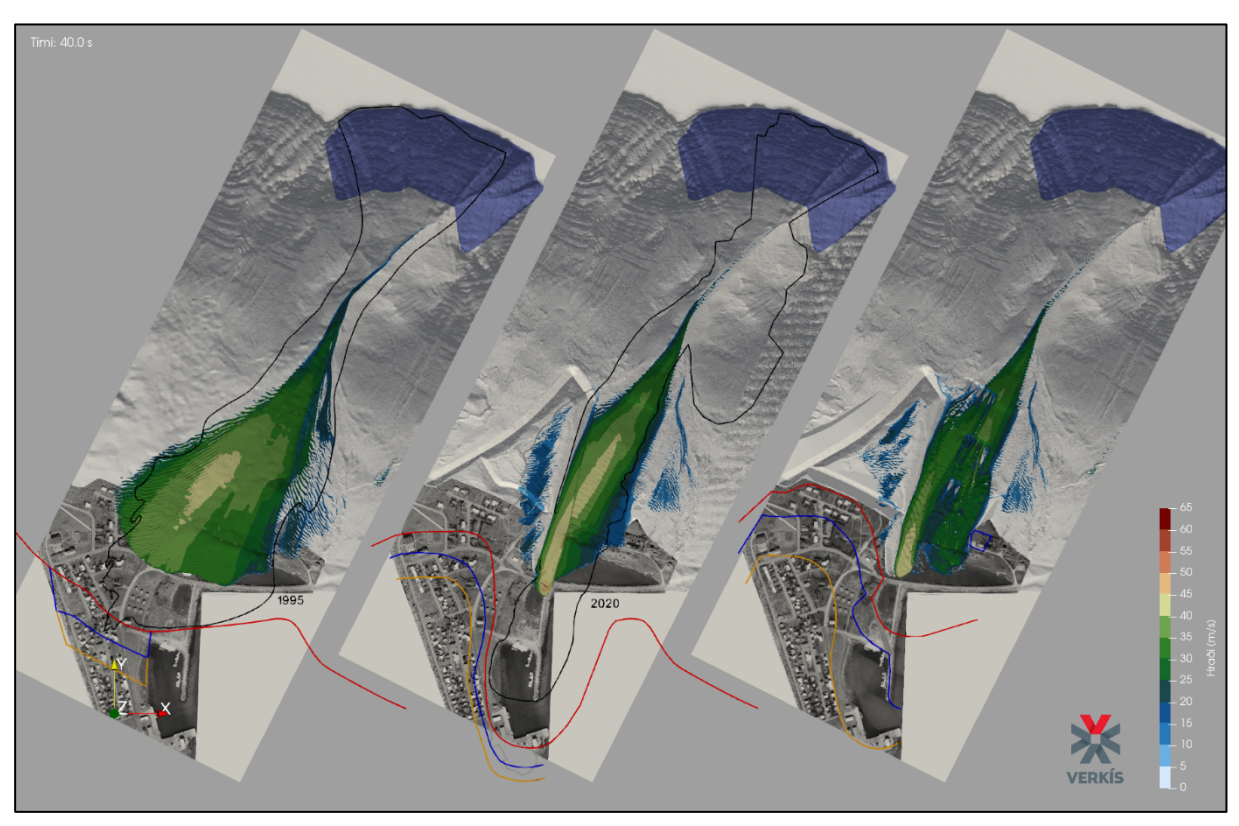


Figure 4 OpenFOAM results of the dense core of the design avalanche from Innra-Bæjargil. Volume: 460 k m³. To the left is terrain in 1997, in the middle the protective structures in 2020 and to the right the proposed improved protective structures. Colors represent the velocity at the surface at 37 s and 57 s. Hazard lines from 2004 are on the left, revised hazard lines, with respect to structures from 2020 are shown in the middle, and on the right are proposed revised hazard lines. Black lines show outlines of the largest known avalanches with or without protective structures.



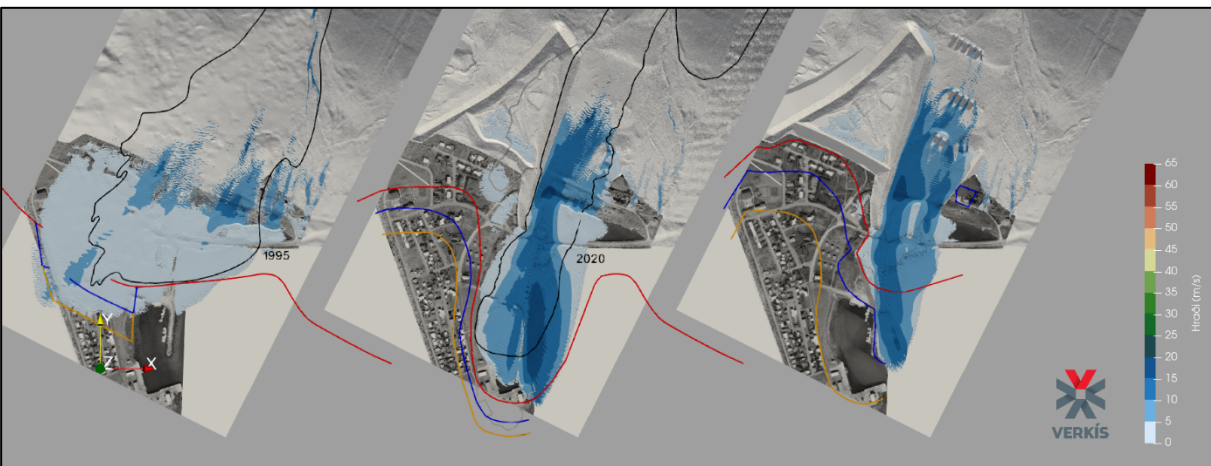


Figure 5 OpenFOAM results of the dense core of the design avalanche from Skollahvilft. Volume: 675 k m³. To the left is terrain in 1997, in the middle the protective structures in 2020 and to the right the proposed improved protective structures. Colors represent the velocity at the surface at 40 s and 60 s. Hazard lines from 2004 are on the left, revised hazard lines, with respect to structures from 2020 are shown in the middle, and on the right are proposed revised hazard lines. Black lines show outlines of the largest known avalanches with or without protective structures.

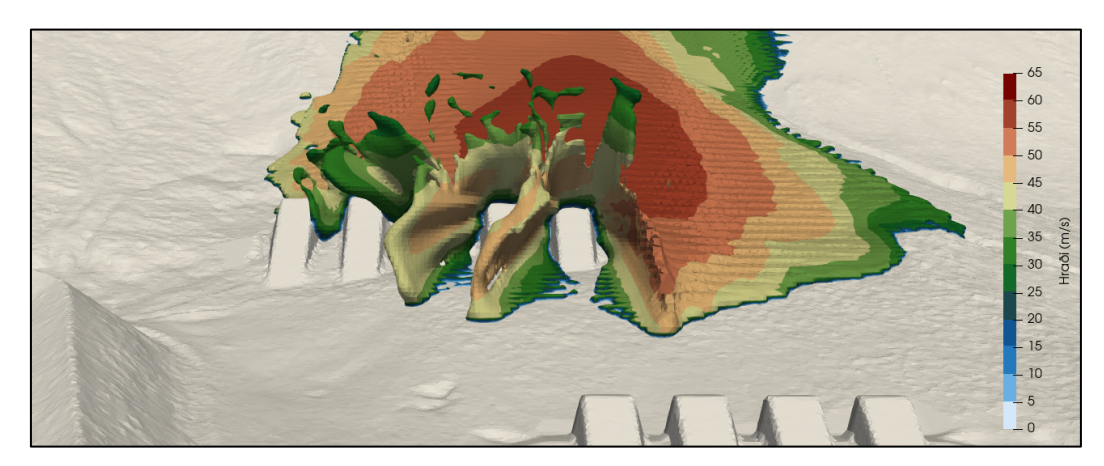


Figure 6 OpenFOAM results of dense core of the design avalanche from Skollahvilft at 26 s. Showing splashing as the avalanche collides with the uppermost row of braking mounds. Colors represent the velocity at the surface.

5. DISCUSSION AND CONCLUSION

When analysing three-dimensional interaction of avalanches with steep obstacles it is important to use three-dimensional solver such as OpenFOAM. With OpenFOAM it is possible to capture more complex flow structures than can be simulated with depth-integrated solvers. It should be noted that only the flow of the dense core is captured in these simulations, currently other parts, i.e. the fluidized regime and suspension cloud are not simulated.

The simulations gave a detailed perception of the flow of large avalanches from the starting zones and seem to capture the highly three-dimensional interaction with barriers convincingly. Splashing and ballistic jets resulting from the collision of the avalanches with braking mounds were simulated, as well as the formation of hydraulic jumps along deflecting dams. Though not shown here, it is possible to estimate time-dependent loading on relevant obstacles by the simulations. A disadvantage is the computational time, which is significantly longer than for depth-averaged models.

REFERENCES

Barker, T. & Gray, J.M.T. 2017. Partial regularisation of the incompressible $\mu(I)$ -rheology for granular flow. Journal of Fluid Mechanics, 828, 5–32.

Hilmarsson, Ó., Jóhannesson, T. & Grímsdóttir, H. 2020. *Snjóflóðin úr Skollahvilft og Innra-Bæjargili 14. janúar 2020*. The Icelandic Meteorological Office (VÍ) report nr. 2020-010. December 2020.

Hættumatsnefnd Ísafjarðarbæjar. 2004. *Mat á hættu vegna ofanflóða á Flateyri*. Report with maps of hazard zones. September 2004.

Jarosch, A. H. 2021. alexjarosch/OpenFOAM-muI: v1.0. OpenFOAM mu(I) rheology (v1.0.1). Zenodo. https://doi.org/10.5281/zenodo.4964189.

Jarosch, A. H., Jóhannesson, T., Hákonardóttir, K. M., and Pétursson, H. Ö. 2022. Full three-dimensional simulations of snow-avalanche flow with two-phase, incompressible, granular μ(I) rheology using OpenFOAM / interFoam, EGU General Assembly 2022, Vienna, Austria, 23–27 May 2022, EGU22-7984, https://doi.org/10.5194/egusphere-egu22-7984.

Numerical simulation of slushflow and assessment of proposed protective measures in Patreksfjörður, Iceland

Ragnar Lárusson^{1*}, Reynir Leví Guðmundsson¹, Gísli Steinn Pétursson¹, Snorri Gíslason¹, Kristín Martha Hákonardóttir²

¹ Verkís, Ofanleiti 2, IS-103, Reykjavik, ICELAND ² Ministry of the Environment, Energy and Climate, Borgartún 26, IS-105, Reykjavik, ICELAND *Corresponding author, e-mail: rl (at) verkis.is

ABSTRACT

Numerical simulations were conducted to assess the effectiveness of proposed protective measures against slushflows released from the Stekkagil gully above the village of Patreksfjörður in Northwestern Iceland. A devastating slushflow from the gully claimed three lives and damaged sixteen buildings in January 1983. Series of small-scale laboratory experiments and numerical simulations of flow interactions with various mound and dam configurations have been conducted and documented over the past several years leading up to the current design. This study presents an assessment of the final design which consists of two rows of steep 4-6 m high braking mounds upstream of a steep 12 m high catching dam. The assessment is achieved through three-dimensional numerical simulation of a 30,000 m³ slushflow coming from the gully. The flow was also simulated over the current terrain without protective structures and its distribution compared to the flow marks of the 1983 flow. The simulations predict satisfactory performance of the mounds and dam with no overflow. They furthermore provide estimates of the hydrodynamic pressure load and its distribution on the mounds, useful for their geotechnical and structural design. The slush is modelled as a Bingham fluid, a non-Newtonian fluid exhibiting no movement under its yield stress threshold.

1. INTRODUCTION

During snowmelt periods and events of heavy rain a snowpack may become water-saturated and begin to move. This is known as a slushflow. Slushflows typically occur in Arctic and Alpine regions and have caused various degrees of economic and human harm and may become more frequent with climate change (Hestnes (1998), Relf et al. (2015)).

In January 1983 a catastrophic slushflow was released from the Stekkagil gully above the village of Patreksfjörður in Northwestern Iceland (Figure 1 and Figure 2). Three people perished and sixteen houses were destroyed or damaged (Tomasson and Hestnes (2000)).



Figure 1. Stekkagil gully above the village of Patreksfjörður, Iceland (photo: Hákonardóttir, 2006).

Stekkagil is a narrow and rocky gully that stretches from a bowl-shaped depression at the edge of a 400 m high plateau down to a debris cone at an elevation of 70 m a.s.l., roughly 200 m from the nearest houses (Figure 1). Slushflows are the primary natural hazard for the residents below the gully but the steep slope on the east side of the depression above it is a known avalanche release area where supporting structures have recently been placed. Small avalanches had been documented coming down the gully prior to the instalment of the supporting structures and all stopped before reaching the village (Tomasson and Hestnes (2000), Hilmarsson (2017)).

The volume of the 1983 slushflow is estimated to have been 30,000 m³ and it's the largest and most consequential slushflow to have come from Stekkagil (Tomasson and Hestnes (2000)). Other smaller slushflows have also been documented, as recently as 2023 (Helgadóttir et al. (2024)). Slushflows may start in the depression at the top of the plateau during heavy rain or thaw events or in the gully itself, e.g. if snow accumulation or avalanche debris blocks water discharge from the snowpack (SFL (2015)). Slushflows commonly entrain substantial amount of snow, soil and other loose material in their path and can grow significantly in size on their way down. The 1983 flow is believed to have started in the mouth of the gully (85 – 100 m a.s.l.) and entrained most of its mass on the debris cone below (Tomasson and Hestnes (2000), Gauer (2004)).

An appraisal study for defence measures from 1998 proposed a channel and deflecting dams below Stekkagil to direct slushflows into the ocean (Figure 3). The channel would require the removal of several houses and splitting the town into two (VST/NGI (1998)). The proposal was

rejected by the municipal council as it would cut off all road connection to the western part of the village in a major flow event - an unacceptable scenario, especially in circumstances surrounding a natural hazard of this kind which may be accompanied by bad or extreme weather (Hákonardóttir and Ágústsdóttir (2019), SFL (2015)).



Figure 2. Aerial photo of Stekkagil and the village below after the 1983 slushflow (photo: Ómar Ragnarsson. From Morgunblaðið, 25.01.1983).



Figure 3. Sketch of previously proposed defence measures (reproduced from VST/NGI (1998)).

Stefan Margreth of the SLF in Switzerland consulted authorities on the matter in 2015 and recommended investigating the feasibility of placing a catching dam below the gully to stop slushflows (SLF, 2015). Following this recommendation a series of small-scale laboratory experiments and numerical simulations were conducted to investigate this option (Hákonardóttir and Ágústsdóttir (2019), Hákonardóttir et al. (2024), and Pétursson et al. (2019)). This work has led to the current defence proposal which consist of two rows of braking mounds above a catching dam (Figure 4).

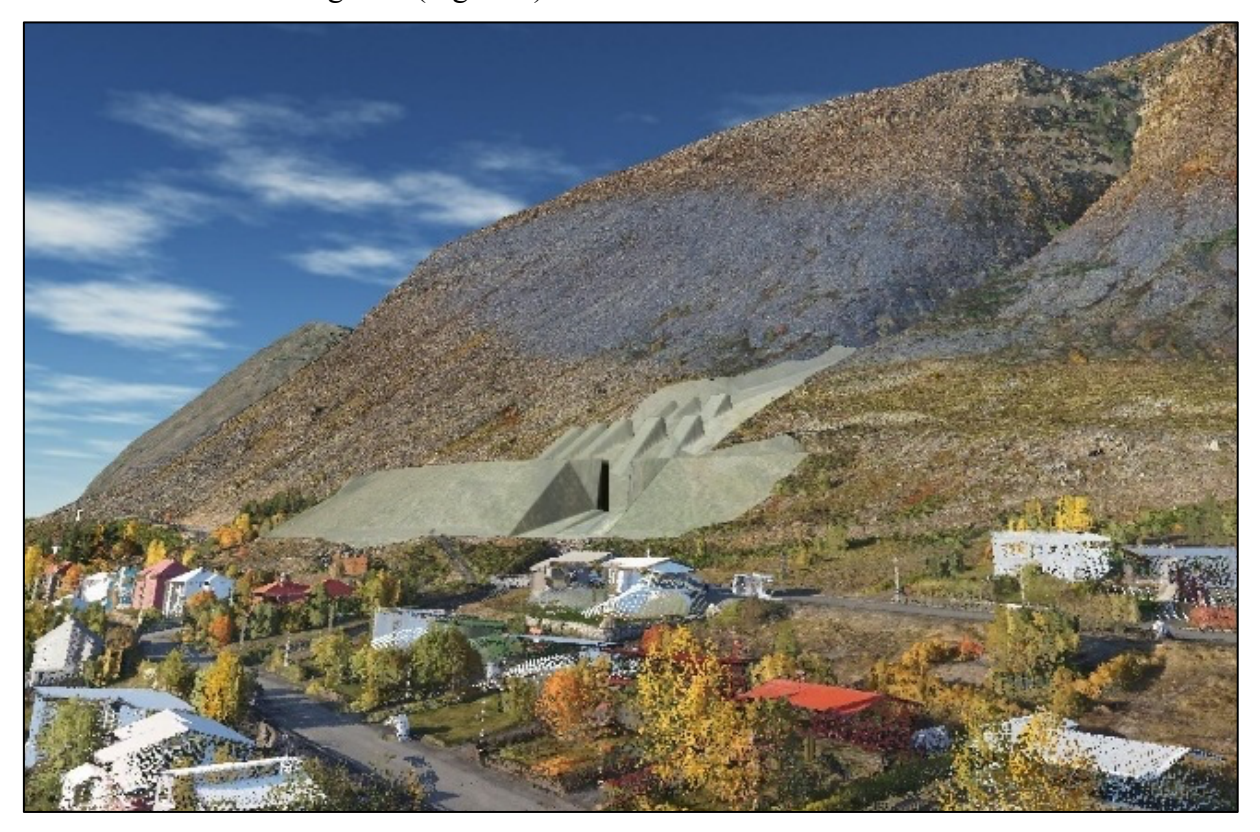


Figure 4. Proposed defence measures. View from the southeast.

Three-dimensional numerical simulations of slushflow were made to assess the effectiveness of the proposed protective measures. The assessment is achieved through three-dimensional numerical simulation of a 30,000 m³ slushflow starting in the gully. The flow was also simulated over the current terrain without protective structures and its distribution compared to the flow marks of the 1983 flow.

2. SLUSHFLOW CHARACTERISTICS AND PROPOSED DEFENCE MEASURES

Slushflows are generally slow moving compared to dry-snow avalanches and can be released from a relatively gentle slope. They most commonly start in drainage channels and streams where inflow of water into the snowpack is often greater than the outflow causing the snowpack to become saturated. Slushflows are, however, not limited to channels and streams as this condition can also occur in other kind of terrain, such as open slopes (Hestnes (1998)).

Despite their lower speed, their momentum can be of the same order as for faster moving dry snow avalanches due to the slush's high density, which can range from 600 to over 1000 kg/m³ depending on the composition of ice/snow, water and debris (Jaedicke et al. (2022), Hestnes

(1998)). Slushflows can be near laminar to fully turbulent and exhibit saltation layers and airborne particles (Hestnes, 1998). Gude and Scherer (1998) characterized slushflow as being either sub-critical minor slushflows that have Froude number less than 1, or supercritical slush torrents that have Froude number greater than 2.

Expected speed and thickness ranges of slushflows from Stekkagil gully are 10-20 m/s and 1-3 m, respectively, corresponding to a Froude number between 2 and 5. Hákonardóttir and Ágústsdóttir (2019) report on small-scale laboratory experiments intended to find an engineering design that effectively stops a slushflow of this magnitude upstream of an approximately 10 m high catching dam. Their work was based on the experience with designing mounds and dams for dry-snow avalanches, ocean breakwater, and obstacles in dam spillways and bottom outlets of hydropower plants. Water was used in the experiment as a substitute for slush. Slush composition can vary significantly in nature, and it is hard to re-produce in a small-scale experiment in a consistent manner. They identified three stages of water impact with an impermeable dam; first, a violent initial *splash* with a jet shooting twice as high as predicted by energy conservation, alike strong wave impacts with harbour walls. Second, *fountaining* follows the splash with height in accordance with energy conservation theory assuming no energy dissipation. Overtopping is most likely during the fountaining stage. Third, the formation of a *hydraulic jump* and its upstream propagation.

Further analysis and numerical simulations following the laboratory experiments were reported by Hákonardóttir et al. (2024). They concluded that the most effective design includes two rows of steep braking mounds upstream of a catching dam.

The design of the proposed defence measures to be located below Stekkagil is based on these foregoing experimental and numerical investigations. It consists of two rows of braking mounds above a catching dam (Figure 5). The braking mounds are earth-filled with a steep upstream side and a height of 5 and 6 metres for the upper and lower rows, respectively. The catching dam is likewise earth-filled and steep, with the height of its upstream side ranging from 10 to 12 metres. The dam is equipped with a 10 m wide steel grille for conveying water from upstream of the dam to the existing brook below. An overflow spillway is located on the west end of the dam.

The braking mounds serve to dissipate the flow's kinetic energy before reaching the catching dam, thereby reducing the risk of overflow and the necessary height of the dam. The flow over and past the mounds exhibits strong turbulence and three-dimensionality. Therefore, 3D simulations are needed to predict their performance as empirical or analytical models and depth averaged 2D simulation methods fail to capture the relevant flow dynamics.

3. NUMERICAL SIMULATION

3.1 Solver and numerical scheme

The simulations are made with interFoam, a three-dimensional OpenFOAM solver that simulates two incompressible, isothermal immiscible fluids using the Volume of Fluid method (VOF). Similar to the slushflow simulations by Hamre et al. (2024), the slush is modelled as a Bingham fluid; a non-Newtonian fluid exhibiting no movement under its yield stress threshold. This is achieved by using the Hershel-Bulkley viscosity model in OpenFOAM with the dimensionless shear-thinning constant n = 1:

$$\nu = \min\left(\nu_0, \frac{\tau_0}{\dot{\gamma}} + k\dot{\gamma}^{n-1}\right)$$

Where ν is the viscosity, $\dot{\gamma}$ is the shear rate, τ_0 is the yield stress, and k is the consistency index and ν_0 is the threshold viscosity, effective under very low shear rates (CFD Direct Ltd. (2025)).

Here, a yield stress of $\tau_0 = 1000$ Pa is applied, and the density of the slush is 1000 kg/m^3 .

To secure simulation stability, the convective fluxes were calculated using a first order upwind scheme. The k- ω SST turbulence model is used. We could not find any published studies on the effects of turbulence models in slushflow simulations. Therefore, the question regarding the applicability of the turbulence model, and which model in that case, remains open.

InterFoam returns a phase-fraction α which represents the fraction of the volume occupied by the phases in each cell. In our analysis we consider the boundary between slush and air to be at $\alpha = 0.5$ (i.e. the cell's volume is 50% occupied by slush). All visualisation of the slush surface is based on this criterion.



Figure 5. Overview of the proposed protective structures as they are in the simulation.

3.2 Simulation geometry, boundary conditions and computational grid

The simulated terrain with the proposed protective structures is shown in Figure 5. To reduce the simulation time, the release area is not included in the computational domain. A 2.6 m high

inlet boundary is applied near the gully's mouth and set to release 30,000 m³ of slush in 35 seconds into the domain. This corresponds to an inlet speed of 15 m/s and a Froude number of 3.0.

The model of the current terrain without the protective structures was acquired through an aerial LiDAR scan (Figure 6). The extent of the computational domain is the same in all simulations (Figure 6 and Figure 7).

The computational mesh with the protective structure consists of 14.2 million cells, primarily hexahedral (Figure 7 - Figure 9). The mesh with the current terrain is 13.7 million cells and of similar density. The mesh needs to be adequately fine near the terrain surface to capture the velocity boundary layer as it affects the flow distribution significantly. A proper mesh study was not performed; however, the resolution was kept as high as time and computational resources allowed for.

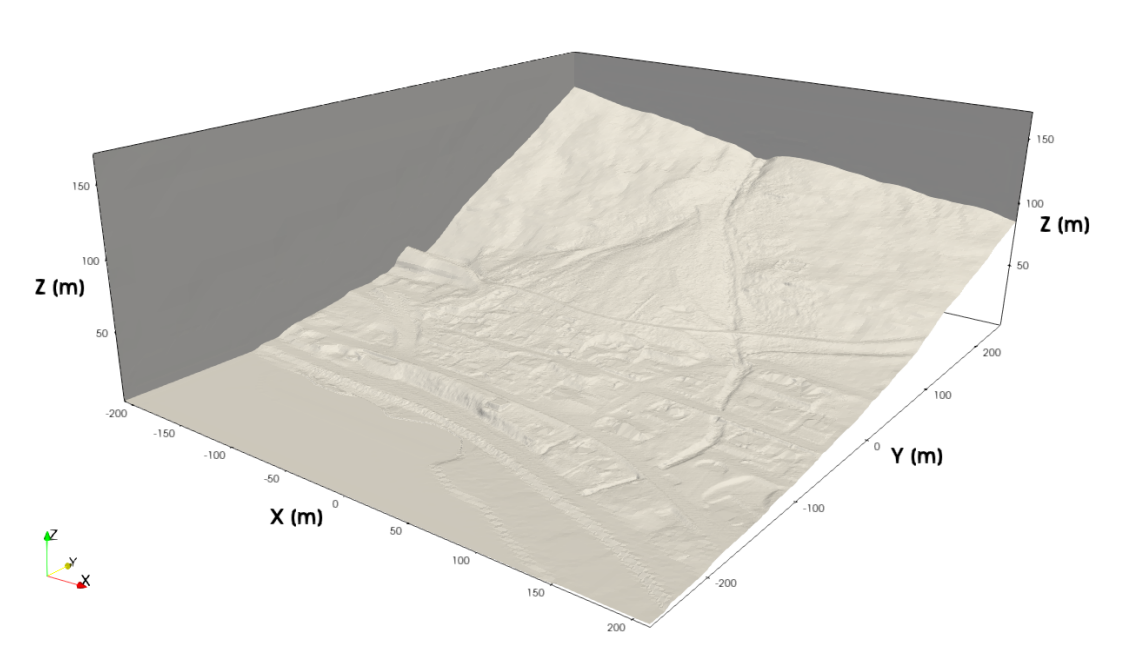


Figure 6. Computational domain. Current terrain without protective structures.

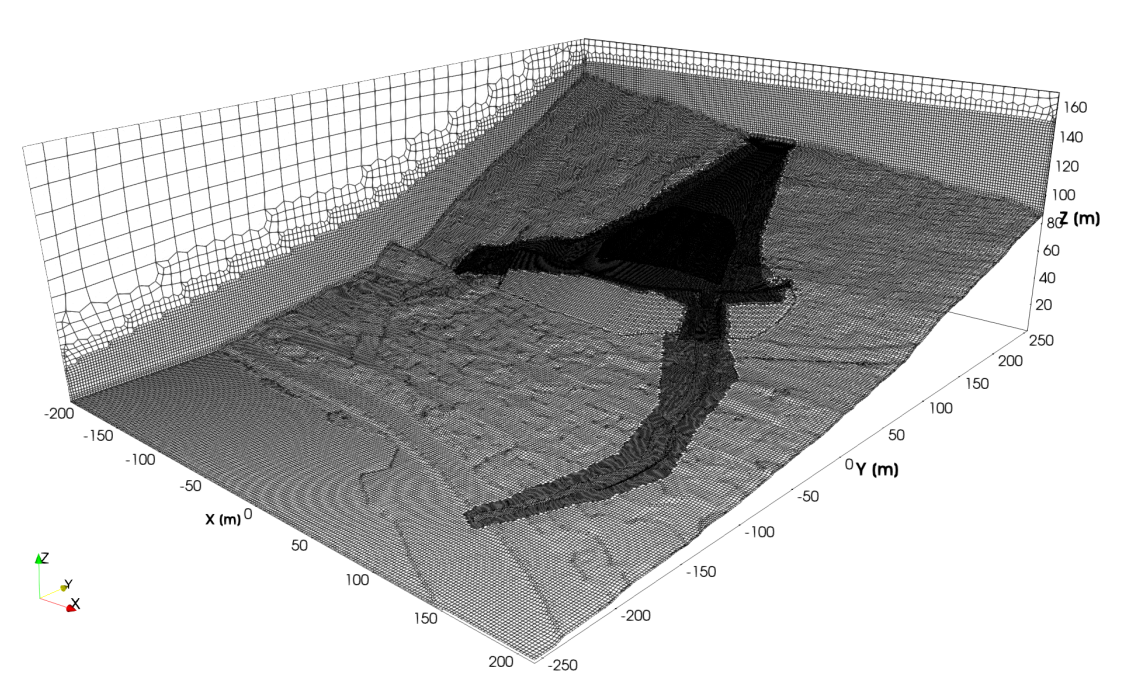


Figure 7. Computational mesh with proposed protective structures. Note the higher resolution in the channel leading to the dam.

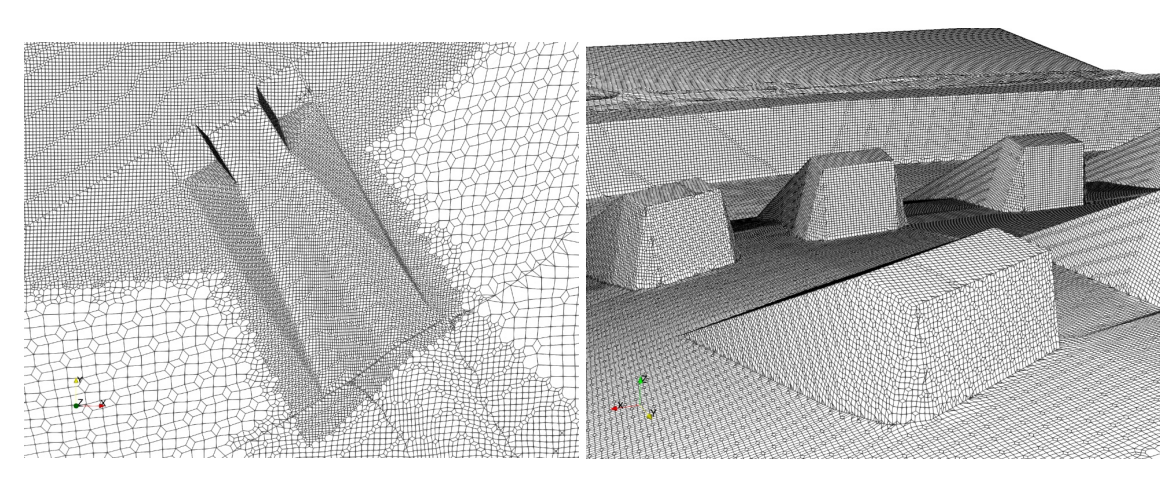


Figure 8. Closer view at the computational mesh. Left: top view of dam and steel grille gap. Right: Braking mounds.

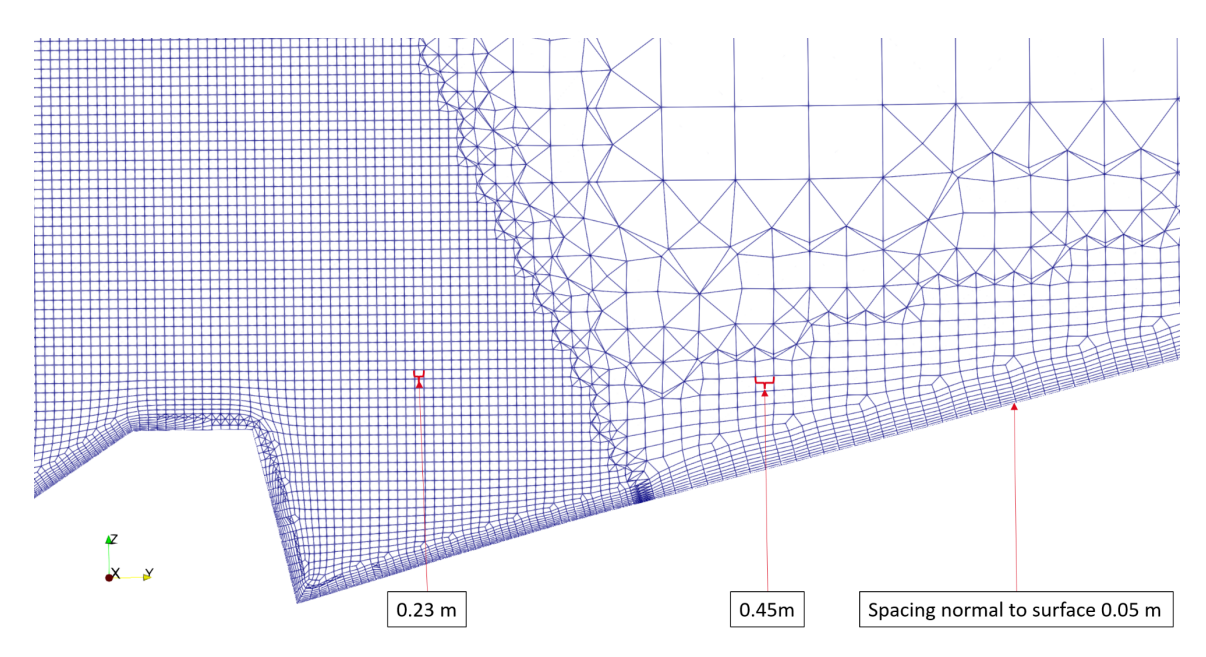


Figure 9. A YZ-plane through the computational mesh, cutting through a braking mound. Dimensions of cells in different locations in the flow path are shown.

4. RESULTS

In the simulation, 30,000 m³ of slush flowed into the domain in 35 seconds, corresponding to a 15 m/s inlet speed and Froude number of 3.0, which does not correspond to the 1983 flow. The 1983 slushflow started at an altitude similar to that of the inlet boundary and entrained most of its mass on the debris cone below. Entrainment is not simulated here. The simulated flow, while similar in volume, is therefore greater in terms of potential energy and momentum. However, the general direction and run-out distance are comparable between these two cases although the simulated flow has wider distribution on the debris cone and in the residential area directly below the gully (Figure 10 and Figure 11). This is likely due to its higher momentum, although the absence of an existing snowpack in the simulation and/or an underestimation of the fluid's viscosity may also influence the distribution.

The braking mounds and catching dam effectively stop the flow in the simulation without any overflow (Figure 10 - Figure 12). The steel grille is not included in the simulations, therefore the outflow through the grille gap is overpredicted. A simulation with the gap completely closed shows negligible difference in the flow dynamics around the braking mounds or impact with the dam away from the gap and there is no overflow in either case.

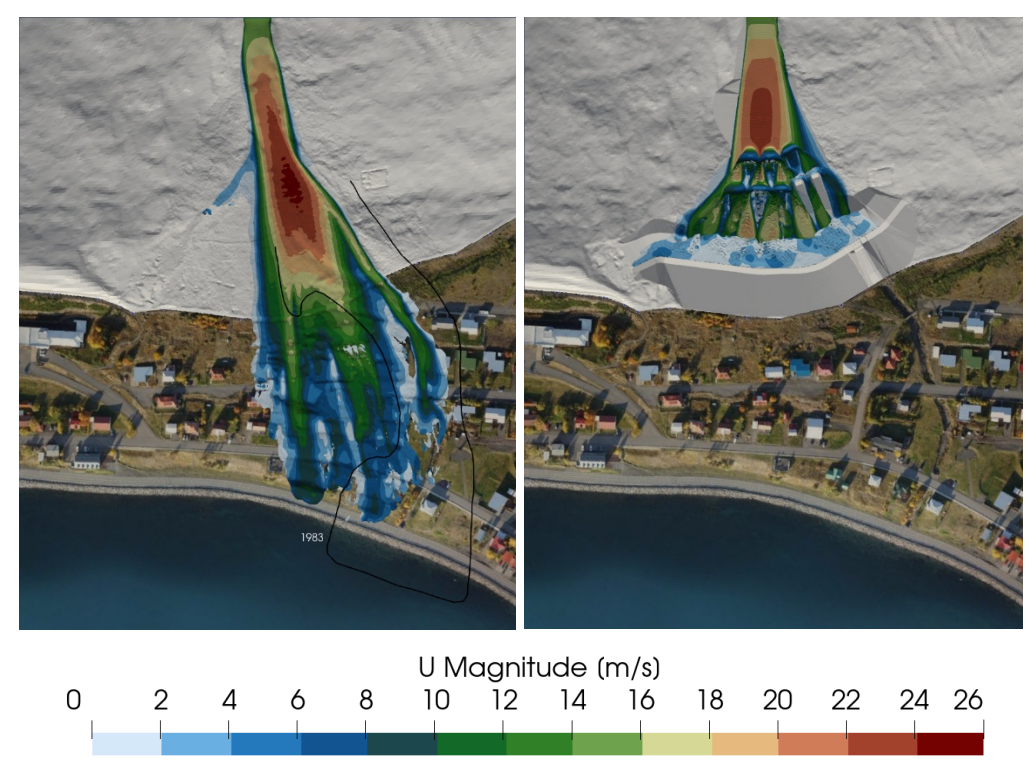


Figure 10. Velocity magnitude at slush surface. Time 34 s. Left: current terrain (the black line marks the 1983 flow distribution). Right: terrain with protective structures.

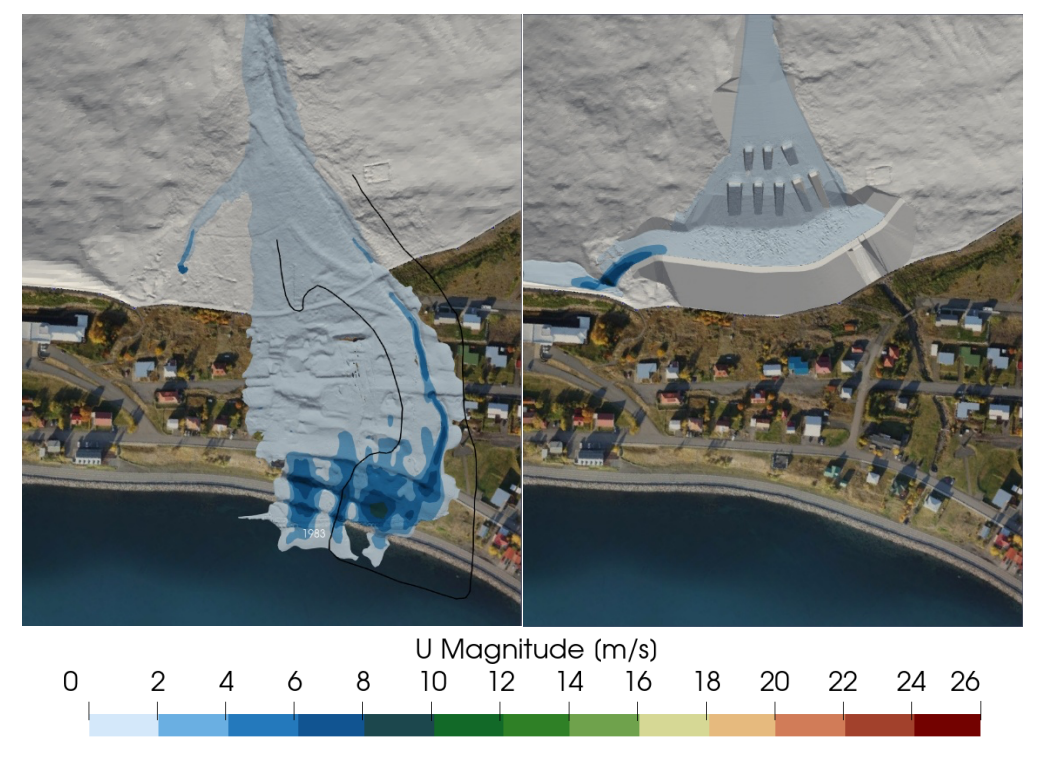


Figure 11. Velocity magnitude at slush surface. Time 60 s. Left: current terrain (the black line marks the 1983 flow distribution). Right: terrain with protective structures.

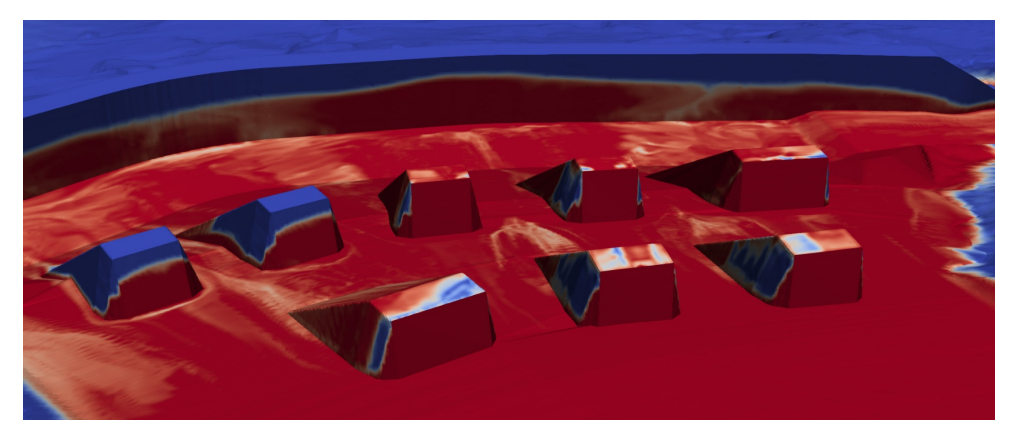


Figure 12. Maximum phase-fraction, α , on the surface of the mounds and dam. Red colour indicates that surface has been wetted.

Roughly one mound height, or 5 m, upstream of the upper mounds, the flow depth is 0.8 m (vertically), and the depth-averaged velocity is 21 m/s at the centre of the channel (Figure 13). This corresponds to a Froude number of 7.6. The surface velocity is 23 m/s. It is possible that the depth and width are underpredicted and overpredicted, respectively, as a result of an underestimated fluid viscosity.

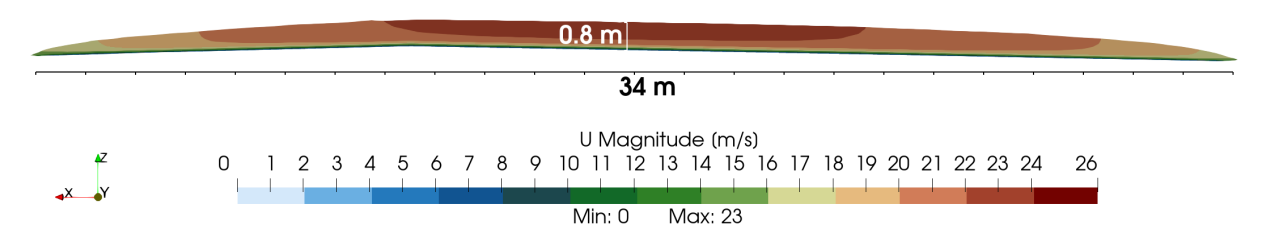


Figure 13. Vertical cross section of the flow 5 m upstream of the upper mounds. Time 6 s.

The slushflow forms quasi-stable jets, or ballistic flow trajectories, over the mounds of varying shape and height depending on the mound (Figure 14). In the upper row of braking mounds, the highest trajectory reaches 14 m vertically from the base of the mound. For the lower row this reduces to 12 m (Figure 15).

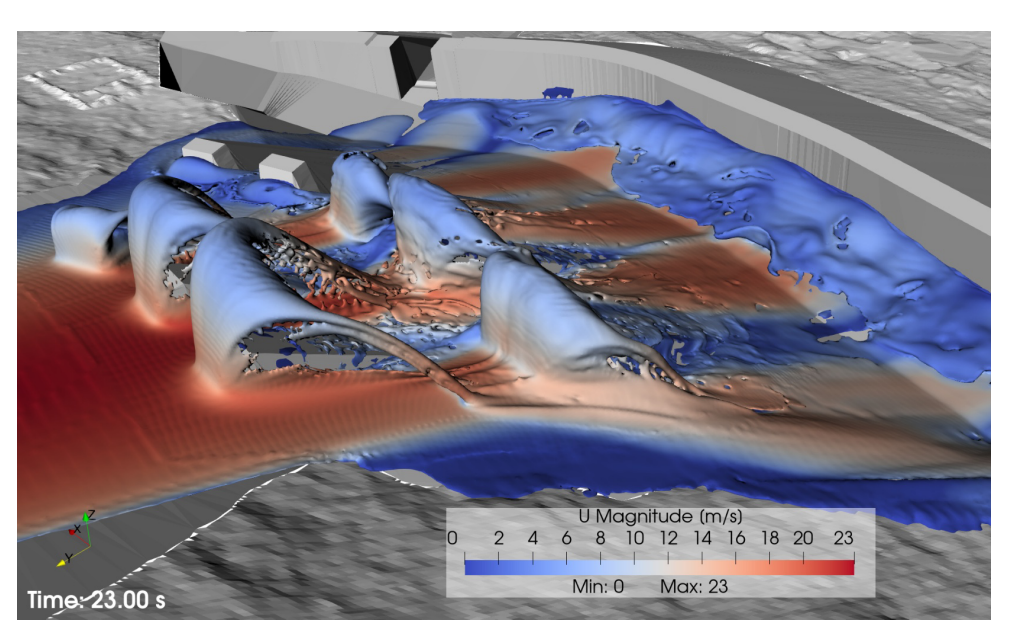


Figure 14. Slushflow at 23 s. Quasi-stable flow trajectories over mounds.

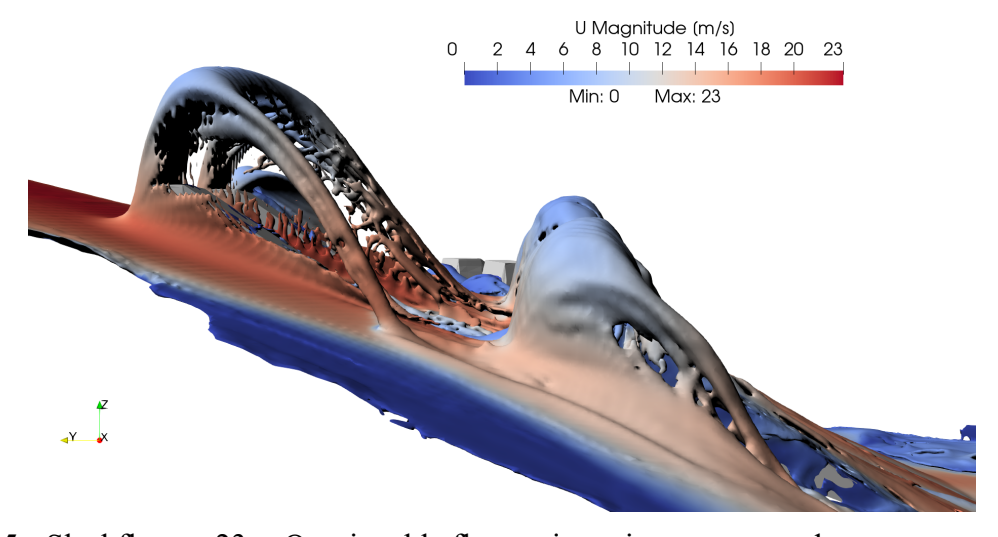


Figure 15. Slushflow at 23 s. Quasi-stable flow trajectories over mounds.

The simulation shows a run-up at the dam on impact that does not exceed the height during the fountaining stage (Figure 16). The maximum height occurs during that stage near the centre of the dam (Figure 17) and is sustained as the hydraulic jump forms and begins to propagate upstream (Figure 18).

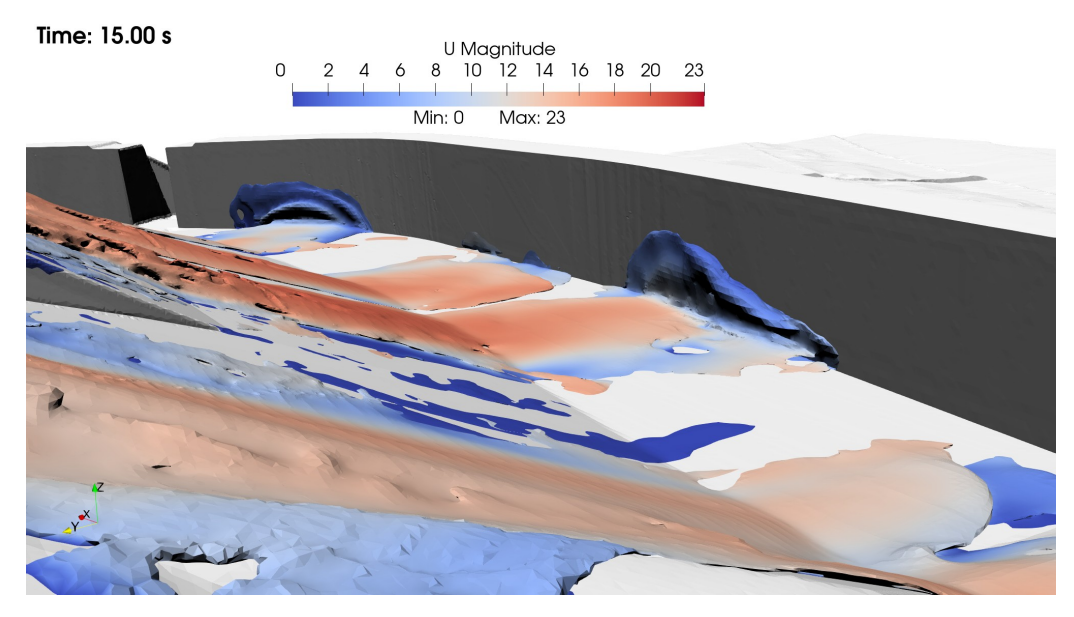


Figure 16. Slushflow at 15 s. Slush run-up at impact with the catching dam.

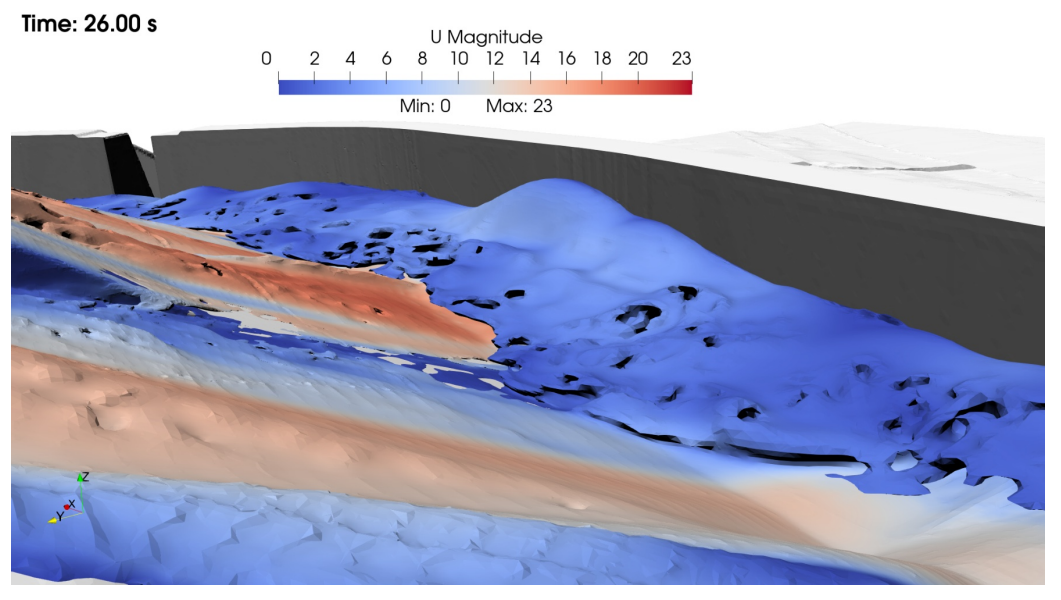


Figure 17. Slushflow at 26 s. Fountaining and hydraulic jump visible. Maximum height already achieved near the centre of the dam.

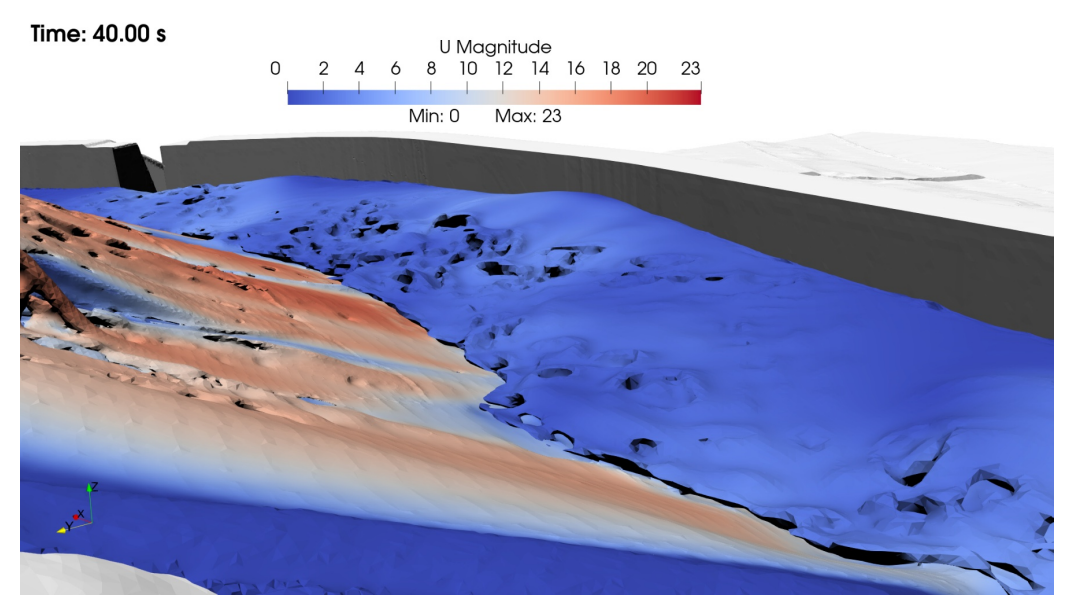


Figure 18. Slushflow at 40 s. Diminished fountaining. Hydraulic jump has propagated somewhat upstream.

The recorded maximum pressure on the braking mounds varies but is generally significantly greater than the pressure on the dam (Figure 19).

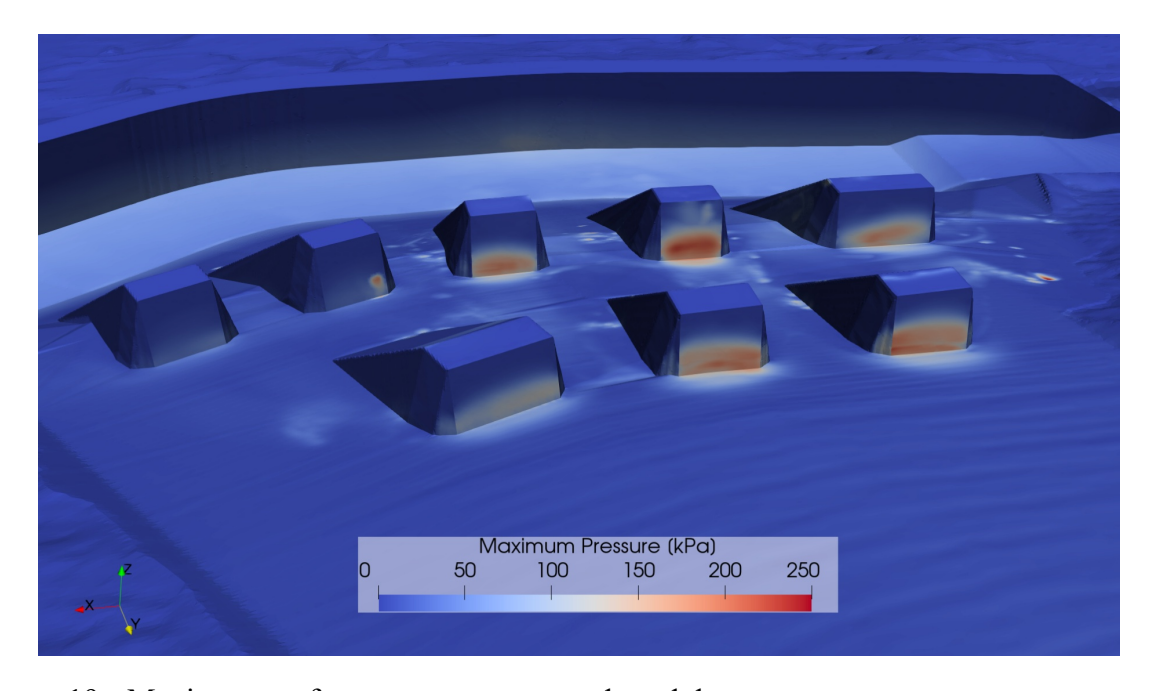


Figure 19. Maximum surface pressure on mounds and dam.

The largest force acts on mound 7 as it is directly in the flow path and receives slush deflected by the upstream mounds (Figure 20). Nevertheless, the flow trajectory over this mound does not reach the same height as the trajectories of the mounds above, as mentioned. Mound 8, west of mound 7, experiences a similar force magnitude. However, this mound is larger and when

normalized with the frontal area, the forces on the mound on either side of mound 7 are nearly identical during the semi-quasi state (i.e. after 20 s).

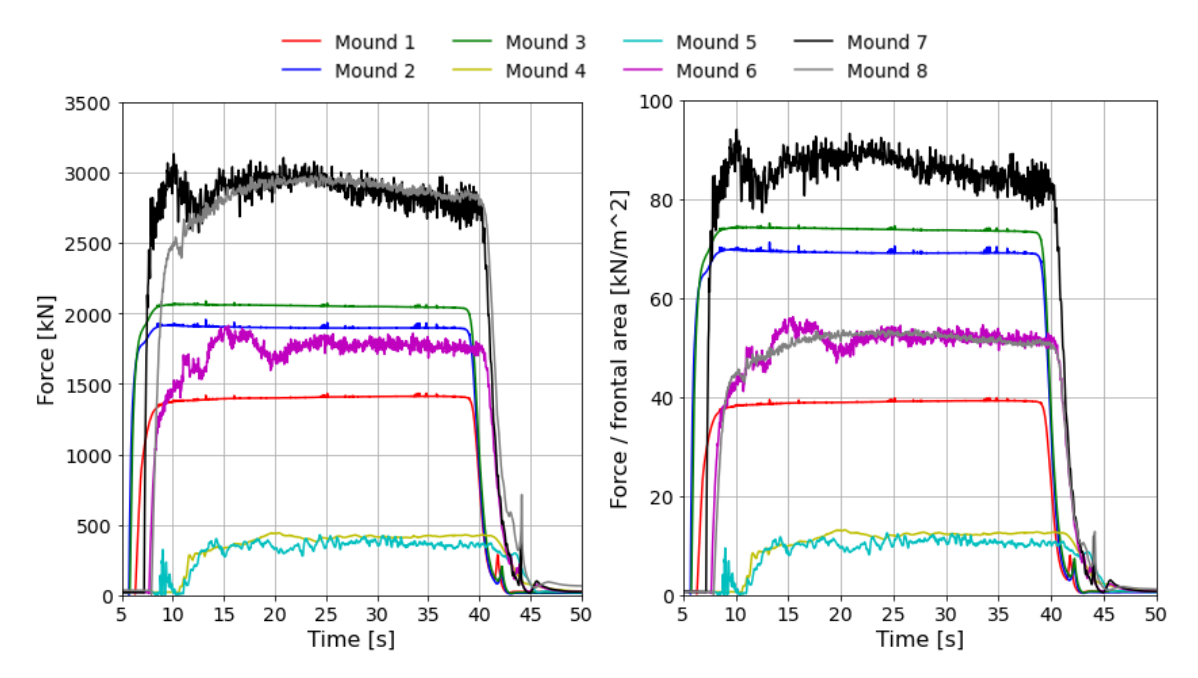


Figure 20. Left: Force on braking mounds. Right: Force on braking mounds normalized with their respective frontal area. See Figure 5 for mound numbers.

5. DISCUSSION AND CONCLUSION

The simulations predict satisfactory performance of the braking mounds and catching dam with no overflow. The flow dynamics are generally convincing and, interestingly, the flow structures around the mounds highly resemble what Hákonardóttir et al. (2003) observed in granular flow over a braking mound in laboratory experiment using glass particles (Figure 21).

As interFoam is a two-phase solver, the simulations also included an air phase surrounding the slush. The air is believed to have negligible effect on the bulk of the slushflow, while the airborne jets in the mound overflow might be somewhat affected. We, however, do not believe that this effect is influential on the performance of the mounds.

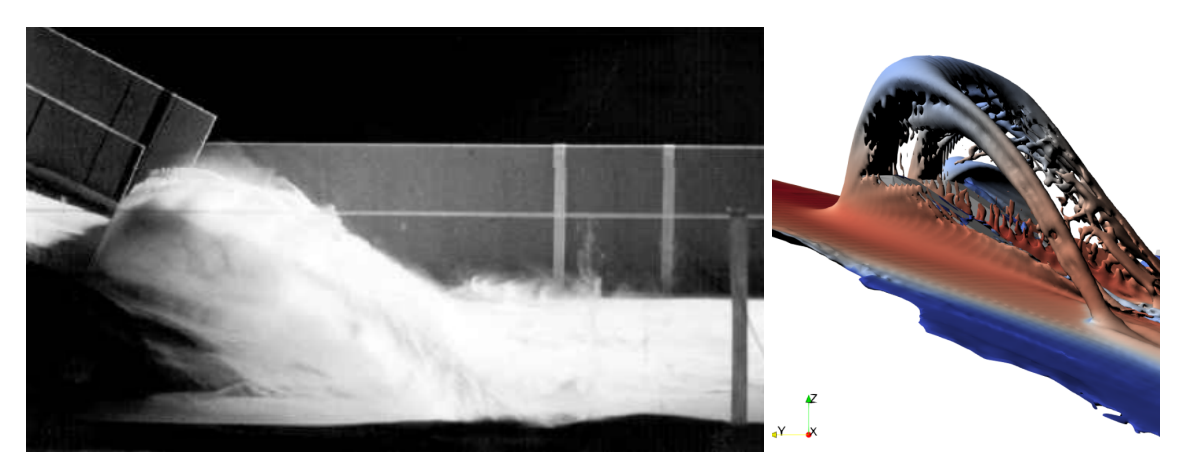


Figure 21. Left: Granular flow experiment. A quasi-steady jetting over a braking mound (reproduced from Hákonardóttir et al. (2003)). Right: a subsection of Figure 15.

The splash/run-up at first impact with the dam is not observed to reach as high as the splash reported in the laboratory experiments by Hákonardóttir and Ágústsdóttir (2019). The same is true for the impact with the braking mounds; no higher splash is observed, and the flow reaches its maximum height during the quasi-steady jet state. This could be due to insufficient mesh resolution or insufficient sampling frequency of the results as the splash is very short lived. The numerical diffusion of the 1st order scheme of the convective fluxes might also influence the splash. It could also be due to an incapability of the two-phase solver to capture the flow dynamics that produce a splash, although this must be considered unlikely given that previous simulations by Pétursson et al. (2019) showed a high initial splash on braking mounds under similar flow condition. They, however, simulated a Newtonian fluid, not a Bingham fluid. The Bingham fluid may become highly viscous near the stagnation point at the base of the braking mound, potentially affecting the initial impact splash in the simulations. This aspect was outside the scope of this study and would need further work to conclude.

The highest recorded surface pressure on the mounds is roughly 250 kPa in the simulation. Pétursson et al. (2019) recorded initial pressure peak of 620 kPa on a braking mound under similar flow conditions (Froude number). However, this peak was associated with the initial splash phase and was highly localized near the base of the mounds and only lasted a few milliseconds. It is possible that peaks of higher pressure than 250 kPa occurred in the current simulation but were too short for the sampling rate to capture.

Simulating slushflows remains highly challenging. Their flow dynamics are extremely complex and there is a high uncertainty and variability in their composition and properties, release location, and extent of entrainment. However, simulations of this kind are valuable in the engineering design of protective structures. In this work for example, the simulations led to adjustment of the width, spacing and location of the braking mounds as initial simulations showed room for improvement.

6. REFERENCES

CFD Direct Ltd. (2025, 07 31). *OpenFOAM v9 User Guide* . Retrieved from https://doc.cfd.direct/openfoam/user-guide-v9/transport-rheology

- Gauer, P. (2004). Numerical modeling of a slushflow event. *Proc. of the International Snow Science Workshop*, (pp. 39-43). Jacskon Hole, Wyoming.
- Gude, M., & Scherer, D. (1998). Snowmelt and slushflows: hydrological and hazard implications. *Ann. Glaciol*, 381-384.
- Hákonardóttir, K. M., Hogg, A. J., Jóhannesson, T., & Tómasson, G. G. (2003). A laboratory study of the retardin effects of braking mounds on snow avalanches. *Journal of Glaciology*, 191-200.
- Hákonardóttir, K. M., & Ágústsdóttir, K. H. (2019). The design of slushflow barriers: Laboratory experiments. *International Symposium on Mitigative Measures against Snow Avalanches and Other Rapid Gravity Mass Flows*. Siglufjordur.
- Hákonardóttir, K. M., Pétursson, H. Ö., Guðmundsson, R. L., Thoroddsen, Á., & Jóhannesson, T. (2024). Stopping slushflows: Small-scale laboratory experiments and full-scale numerical simulations. *International Snow Sceience Workshop*. Tromsø.
- Hamre, D., Blatny, L., Gaume, J., Gauer, P., & Mears, A. (2024). Observations and modeling of slushflows Atigun Pass, Alaska. *Proc. of the International Snow Science Workshop (ISSW)*. Tromsö.
- Helgadóttir, H. R., Jónasdóttir, S. B., & Hilmarsson, Ó. (2024). *Snjóflóð á Íslandi veturinn* 2022-2023. Reykjavík.: The Icelandic Meteorological Office (VÍ) report no. 2024-010.
- Helgadóttir, H. R., Jónasdóttir, S. B., & Hilmarsson, Ó. (2024). *Snjófóð á Íslandi veturinn 2022-2023*. Reykjavík : Veðurstofa Íslands.
- Hestnes, E. (1985). A contribution to the prediction of slush avalanches. Ann. of Glaciol., 1-4.
- Hestnes, E. (1998). Slushflow hazard where, why and when? 25 years of experience with slushflow consulting and research. *Ann. of Glaciol.*, 370 376.
- Hilmarsson, Ó. (2017). *Snjóflóð á Íslandi veturinn 2015-2016* . Reykjavík: The Icelandic Meteorological Office (VÍ) report no. 2017-010.
- Jaedicke, C., Kalsnes, B., & Anders, S. (2022). Sørpeskred. Egenskaper, historikk og sikringsløsninger (KLIMA2050: Rapport nr. 38-2022). SINTEF.
- Pétursson, H. Ö., Hákonardóttir, K. M., & Thoroddsen, Á. (2019). Use of OpenFOAM and RAMMS Avalanche to simulate the interaction of avalanches and slush flows with dams. *Proc. of the International Symposium on Mitigative Measures against Snow Avalanches and Other Rapid Gravity Mass Flows*. Siglufjörður.
- Relf, G., Kendra, J. M., Schwartz, R. M., Leathers, D. J., & Levia, D. F. (2015). Slushflows: science and planning considerations for an expanding hazard. *Nat Hazards*, 333-354.
- SLF. (2015). Analysis of the hazard situation and the proposed mitigation measures in Patreksfjörður and Bíldudalur, Iceland. Davos: WSL Institute for Snow- and Avalanche Research SLF.
- Tomasson, G. G., & Hestnes, E. (2000). Slushflow Hazard and Mitigation in Vesturbyggd, Northwest Iceland. *Nydrology Research*, 399-410.
- VST/NGI. (1998). Vesturbyggd. Slush flow defences. Appraisal for Geirseyrargil. VST/NGI.

Artificial intelligence supported extra long-range Doppler radar: avalanche activity measurement and RACS blasting verification in Evolène, Switzerland – Extended abstracts

Maxence Carrel^{1*}, Ólafur Y. Stitelmann¹, Martin Hahner¹, François Fellay², Pascal Mayoraz³

¹ Geoprevent, Zurich, Switzerland
² Canton of Valais (DNAGE), Valais, Switzerland
³ Town of Evolène, Valais, Switzerland
⁴ Nivalp SA, Valais, Switzerland
*Corresponding author, e-mail: maxence.carrel@geoprevent.com

ABSTRACT

The municipality of Evolène in the Swiss alps is exposed to high avalanche hazards and was hit tremendously during the 1999 winter. The municipality consists of several villages located below a mountain slope of 4.5 km length with an elevation difference of ca. 2000 m, with many small avalanche paths threatening the inhabitants of the valley. A massive avalanche protection and mitigation project has been set up over the last two decades to ensure the safety of the valley. Different snow supporting structures were rapidly installed in the 2000s and in a new project phase remote avalanche control systems (RACS) and radars are installed to further control avalanche hazard. 5 RACS and two radars were installed in 2023, with about twenty more RACS to be installed over the next years. The two radars were combined horizontally to detect small avalanches (size 1-2) over the entire slope, in all weather conditions, at more than 5.5 km of distance. Geoprevent implemented a convolutional network artificial intelligence model in addition to existing detection algorithms to improve the sensitivity of the system and increase its accuracy. The avalanche experts of the valley actively use the system for avalanche control operations and it provided key data during the critical week of mid-April 2025. While there is still some potential for further improving the accuracy of the system, the data generated will be helpful for validating the location chosen for the RACS to be installed.

1. INTRODUCTION

1.1 What is radar?

Radar stands for "radio detection and ranging", a system used to detect and locate objects. The radar transmitter generates radio waves, that are emitted in a specific direction. The radio waves propagate through the air and as they travel, encounter objects. Upon hitting an object, a part of the transmitted power is reflected towards the radar system. Receiving antennas of the radar collects the reflected energy and processes the signal. As the radio waves travel at the speed of light (ca. 200,000 km/s), objects can be detected in real-time. The frequency shift between the emitted and received radio waves can be exploited using the Doppler effect to measure the velocity of moving objects. Their position can be determined by measuring the travel time of the radio waves assuming a constant travel velocity.

Radar technology is widely applied in the military, aviation, marine and car industry. As it measures continuously in a robust manner, in real-time and in all weather conditions, Doppler radars have become a helpful tool for real-time avalanche detection.

More than 20 long-range Doppler radar systems for avalanche detection were installed in Switzerland in recent years. These systems are used by avalanche forecasters to assess the current avalanche situation. At certain locations, radars additionally close roads and railways automatically or monitor slopes where RACS are installed to verify blasting results, thus allowing efficient RACS operation independent of weather conditions and at any time of the day.

1.2 Radar physics

Radio waves are dampened by the atmosphere while traveling (Nathanson et al., 1999). The relationship between the power received by the radar (P_r), the distance between the detected object and the radar (R), the transmitted power (P_t), the antenna transmitter gain (G_t), the antenna received gain (G_r), the wavelength transmitted (λ), object size (σ) and diverse system losses (L_s) is expressed by the following equation (1):

$$P_r = \frac{P_t * G_t * G_r * \lambda^2 * \sigma}{(4\pi)^3 * R^4 * L_S} \tag{1}$$

When we unify the constant parameters that depend on the hardware (antenna gain, wavelength, system losses) and the object size into the constant value C, we receive the simplified equation (2):

$$P_r = \frac{P_t * C}{R^4} \tag{2}$$

The received power from a radar decreases in a relationship to the distance with a power of 4. The relation is symbolized in **Error! Reference source not found.** It assumes power to be 100% at 1000 m distance It dropts to 0.16% at 5000 m.

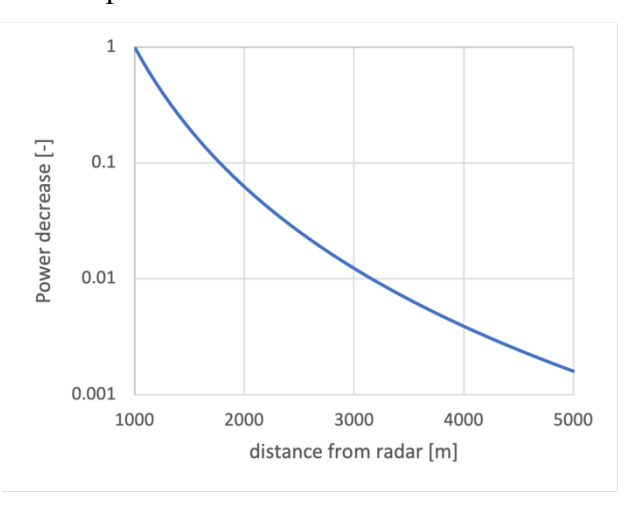


Figure 1 Relationship between received power and distance of the reflected object to the radar.

1.3 Finding the best radar location for a site

When considering avalanche detection, radars are optimally placed at the bottom of a slope or somewhere low at the counter slope, as the frequency shift detection is best, when an avalanche

approaches the radar in line of sight. However, the exact location a radar will be installed is always a compromise of different boundary conditions, such as (not exclusive):

- Radar physics,
- Topography (e.g. blind spots, incised channels),
- Access (ground access, helicopter only),
 Existing infrastructure (power, communication technology),
- Permission/landowner (e.g. national park, forest service, private person, sacred site, etc.),
- Environmental conditions of the site (geology, vegetation, etc.),
- Hazards for the system (vandalism, rockfall, avalanche danger, animals, etc.),
- Project scope (e.g. at what elevation does an avalanche need to be detected in order to close the road in time),
- Budget (difference in construction and operation costs),
- Purpose (e.g. rockfall detection, camera monitoring, etc.)

As a radar has horizontal and vertical opening angles, it can be desirable to mount it as far away as possible to cover the maximal terrain possible. At Evolène in southern Switzerland, Geoprevent has for the first-time operated avalanche detection radars at distances above 5 kms, hence working with a very high power reduction. At this distance, only 0.0016% of the transmitted power is received back to the antennas. This is 59% less power compared to the received signal at a distance of 4000 m.

2. MATERIAL & METHODS

Evonène has been tremendously hit by avalanches during the 1999 winter. Consequently, the entire ridge above the town has been subject to avalanche danger reducing measures. Among snow supporting structures, RACS and radars are part of the project that is realized in different phases over several decades. Here, radars serve to optimize the operation of RACS. As the slope above town has a relatively flat terrain feature, the radar had to be placed at the other side of the valley. Besides a road, power could be drawn and access by truck allowing a fast installation of the radar unit (Figure 2).



Figure 2 Installation of Doppler radar beside a mountain road in Evolène.

A critical factor is the distance between the radar and the release area, which for parts of the slope exceeds 5000 m. To increase antenna gain, special radar antennas were used, to funnel the power transmitted to the target area. Emitted radio waves use the X-Band, at a frequency of 10 GHz.

In order to detect avalanches for slopes located at more than 5 km from the radar, a convolutional neural network (CNN) was trained on results of the radar and acts as a binary data classifier. It evaluates an event after the other standard algorithms concluded that an event is over and confirms that it was indeed an avalanche.

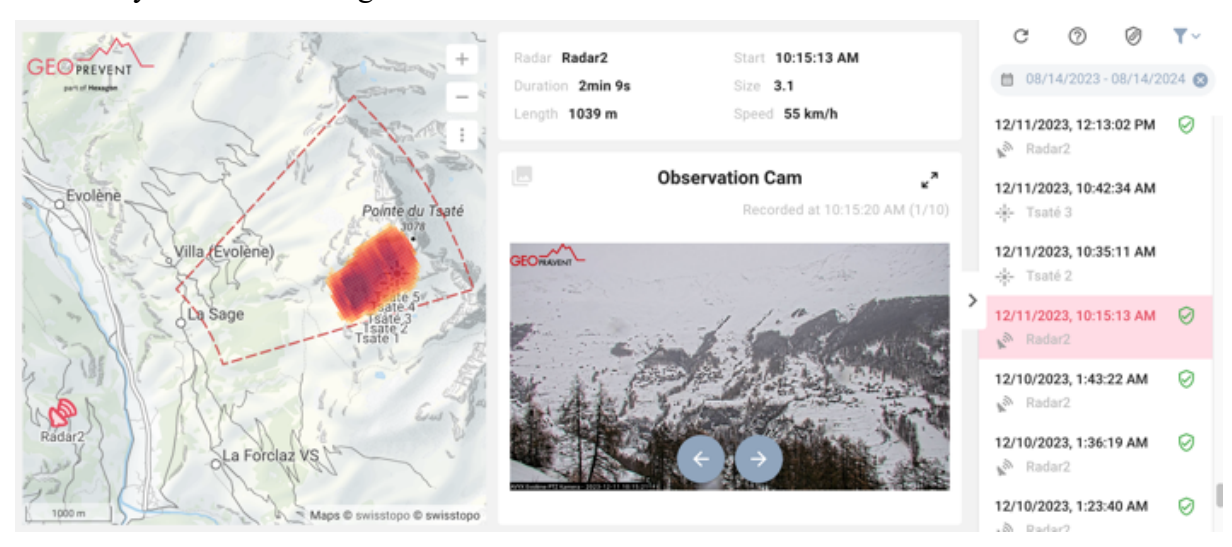
3. RESULTS & DISCUSSION

In winter 2023/2024 the radars recorded an activity of 81 avalanches in Evolène (94 in the 2024/2025 season). The detections contain small to large avalanches at distances ranging over 5000 m at all times of the day and during snowstorms as well as during sunny weather (see Figure 3).

Field reports from Evolène mention small avalanches just outside/at the border of the detection perimeter on slopes oriented in an angle of ca. 45° from the line of sight that were not detected by the radar (ca. size 1 or smaller). There is no feedback that an avalanche of size 2 or larger released without detection.

These observations can be described by the spatial distribution of the radar power. The transmitted power decreases in distances from the source and from the center line. A simple analogy can be made with a flashlight pointing to a wall at night. The center of the lightened wall is strongly illuminated. A spot further away from the center vanishes increasingly. However, A large object at the extremity of the light, where it is "half dark", is still visible, especially when at movement.

The CNN model allowed to substantially reduce the false positive detection rate and to thus effectively increase the range of the radar.



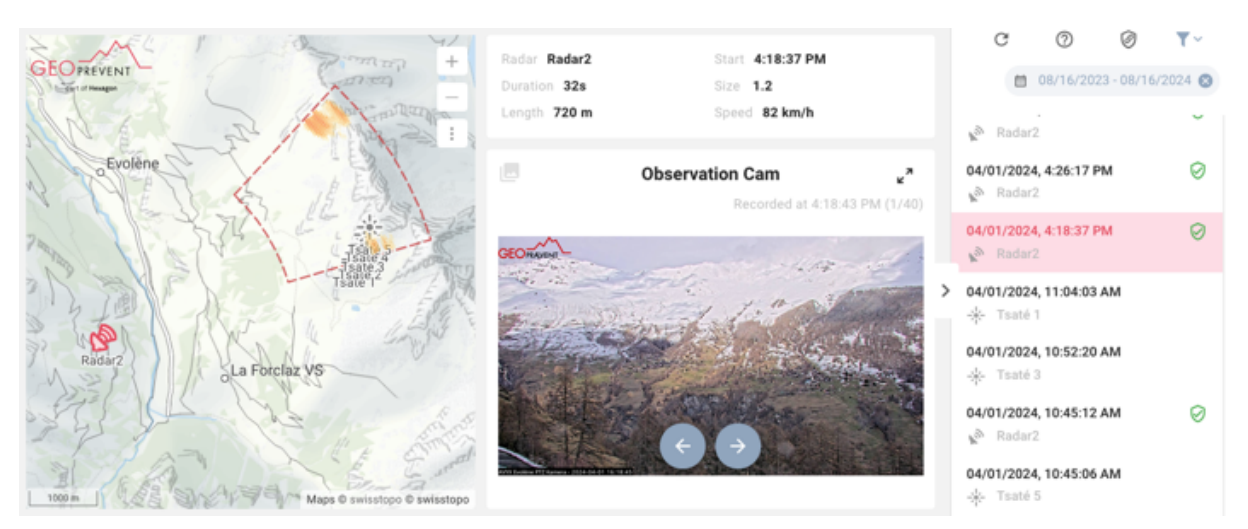


Figure 3 Detected avalanches in Evolène. Large avalanche that starts at the top of the release area, 4497m away from the radar (upper image). A small avalanche that is 4917 m away from the radar, triggered by RACS (lower image).

4. CONCLUSIONS

The avalanche radar in Evolène demonstrated that even small avalanches can be well detected at distances of 5000 m. This also applies to avalanches smaller size 1 and are of great benefit to the local avalanche forecasters in operating their RACS and assuring safety.

It is crucial that the location of a radar installation as well as the radar orientation are carefully assessed and planned to optimally detect avalanches of interest in the monitored terrain. The choice of radar location is especially important when detecting avalanches over important distances.

The implementation of a convolutional neural network allowed to increase the range of the system effectively, thus combining the best of two worlds, configurable rule-based (white-box) detection algorithms with the power of data-driven (black-box) artificial intelligence to discard false alarms. Up to now the timescale on which artificial intelligence based rejection occurs is of ca. 30 seconds, which remains quite long for real-time applications (on-site alarming or road-closure) but is sufficient for activity monitoring.

REFERENCES

Nathanson, F. E., Reilly, J. P., Cohen. M. N., 1999. Radar Design Principles: Signal Processing and the Environment (2nd ed.). SciTech Publishing.

Meier, L., Jacquemart, M., Blattmann, B., Arnold, B., 2016. Real-time avalanche detection with long-range, wide-angle radars for road safety in Zermatt, Switzerland. In: Proceedings ISSW, Breckenridge, Colorado, 304-308.

Persson, A., Venås, M., Humstad, T., Meier, L., 2018. Real-time radar avalanche detection of a large detection zone for road safety in Norway. In: Proceedings ISSW, Innsbruck, Austria, 597-600.

Stähly, S., Yount, J., Gorsage, B., Greene, E., Wahlen, S., 2023. Optimizing road management with Doppler radar for automatic avalanche detection at I-70. In: Proceedings ISSW, Bend, Oregon, 1565-1568.

Detailed, high temporal resolution snow distribution monitoring for avalanche hazard management: A case study from a controlled avalanche release

Pia Ruttner^{1,2,3*}, Julia Glaus^{1,2,4}, Annelies Voordendag³, Andreas Wieser³ and Yves Bühler^{1,2}

 WSL Institute for Snow and Avalanche Research SLF, Davos Dorf, SWITZERLAND
 Climate Change, Extremes, and Natural Hazards in Alpine Regions Research Center CERC, Davos Dorf, SWITZERLAND

³ Institute of Geodesy and Photogrammetry ETH Zurich, Zurich, SWITZERLAND
⁴ Institute for Geotechnical Engineering ETH Zurich, Zurich, SWITZERLAND
*Corresponding author, e-mail: pia.ruttner (at) slf.ch

ABSTRACT

Detailed snow depth measurements immediately before and after an avalanche event are rare but can provide valuable insights for avalanche forecasting and control as well as for the back calculation of the events with numerical simulations. In this study, we present a unique dataset from a slope near Davos in the Swiss Alps where an avalanche was artificially triggered as part of avalanche control work for road safety. The release area was scanned hourly throughout the winter with a low-cost terrestrial laser scanner (TLS), providing a high temporal and spatial resolution record of snowpack changes before the event. In addition, we measured the snow depth of the entire slope with a long-range TLS before the snowfall, and immediately before and after the avalanche release, allowing for precise mapping of the release area, track and deposition zone. After the event, we dug a snow pit close to the release zone including observations of snow grain types, snowpack temperature and snow density measurements.

The before-and-after scans enable accurate volume estimates of the released snow and mass distribution after the avalanche event. Measuring release and erosion conditions of avalanches with high spatial and temporal resolution at locations with differing terrain characteristics will substantially enhance the understanding of the formation, the prediction and the modelling of potential destructive avalanche events.

1. INTRODUCTION

Avalanche forecasting and hazard mitigation heavily rely on an accurate understanding of the snowpack evolution, spatial snow depth distribution, and the conditions leading up to avalanche release. Among the various snowpack parameters, snow depth distribution is a critical input for both operational forecasting and numerical avalanche modelling, as it influences loading patterns, slab development, and snowpack stability (Reuter et al., 2016; Schweizer et al., 2003).

Over the past two decades, remote sensing technologies, particularly terrestrial laser scanning (TLS) and photogrammetry, have revolutionized snow depth mapping by providing high-resolution, spatially continuous datasets over large patches of complex terrain (Bühler et al., 2015; Prokop, 2008). These tools allow for quantifying snow depths at the slope scale, offering detailed insights into snow depth distribution and terrain-driven variability. Recent

P. Ruttner and others O8.2 - Page 208

developments include high temporal resolution monitoring using low-cost lidar sensors, allowing for high spatial, as well as high temporal resolution (Ruttner et al., 2025).

In particular, the ability to map pre- and post-event snow depth distribution allows for an accurate estimation of release volumes, erosion patterns, and deposition characteristics, which are essential for validating and calibrating avalanche dynamics models such as RAMMS (Christen et al., 2010), SAMOS (Sampl & Zwinger, 2004) or AvaFrame (Oesterle et al., 2025). Such detailed datasets are not only valuable for back-calculation of individual avalanche events but also hold potential for improving data-driven avalanche forecasting systems, which increasingly incorporate machine learning and simulation approaches (Mayer et al., 2023).

In this study, we present a unique dataset collected on a slope near Davos, Switzerland, where an avalanche was artificially triggered during regular avalanche control operations. Using a low-cost TLS system operating throughout the winter, combined with long-range TLS scans taken immediately before and after the release, we document the snow depth evolution and distribution at high spatial and temporal resolution. Additional in-situ snow pit data were collected to validate snowpack layering and properties near the release zone. This dataset offers a rare opportunity to analyze avalanche initiation and deposition, contributing valuable input for both operational avalanche forecasting and the validation of numerical avalanche models.

2. DATA AND PROCESSING

2.1 Low-cost lidar

At the Braemabuel test site in Davos, south-eastern Switzerland we installed two stations in November 2023, each equipped with a low-cost lidar (Livox Avia), camera and some meteorological instruments (wind speed and direction, relative humidity, air temperature and snow surface temperature). The lidars observe the same region of interest (Figure 1, light purple line) from different viewing angles and together cover an area of approximately 14'500m² (Ruttner et al., 2025). The acquisition interval is 1 hour, resulting in around 3000-4000 epochs per season. After registration to the Swiss national coordinate system (LV95/LN02), the resulting point clouds are converted into gridded digital surface models (DSMs) with a spatial resolution of 0.5 m. Snow depth, or the amount of new snow, is calculated as the height difference between DSMs.

2.2 Long-range lidar

To acquire data over the entire slope of interest, we performed terrestrial laser scanning measurements using a Riegl VZ-6000, positioned on the opposite side of the valley (Figure 1, dark purple line; Figure 2). We acquired one scan on 07.11.2024, as a snow-free reference and during winter we acquired three additional scans: one on 27.01.2025 (before a major snowfall) and two on 29.01.2025 (after the snowfall and prior to the avalanche release and one immediately after the avalanche). We processed the data using the same workflow described above for the low-cost lidar.

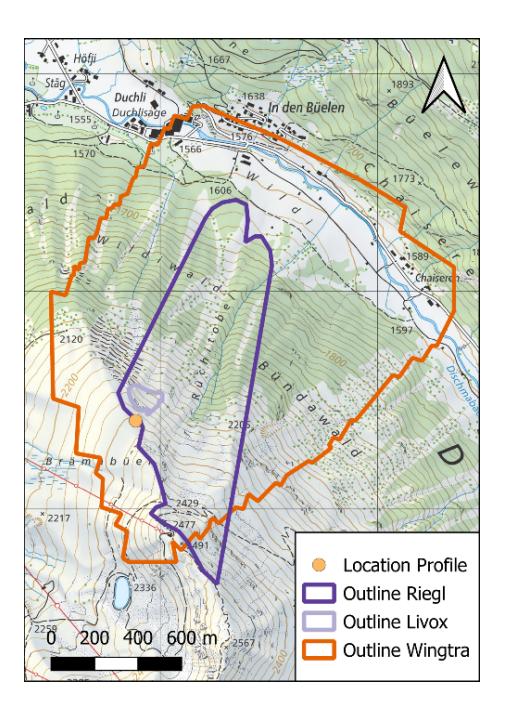


Figure 1 Overview of locations and extents of the acquired datasets (map source: Federal Office of Topography).

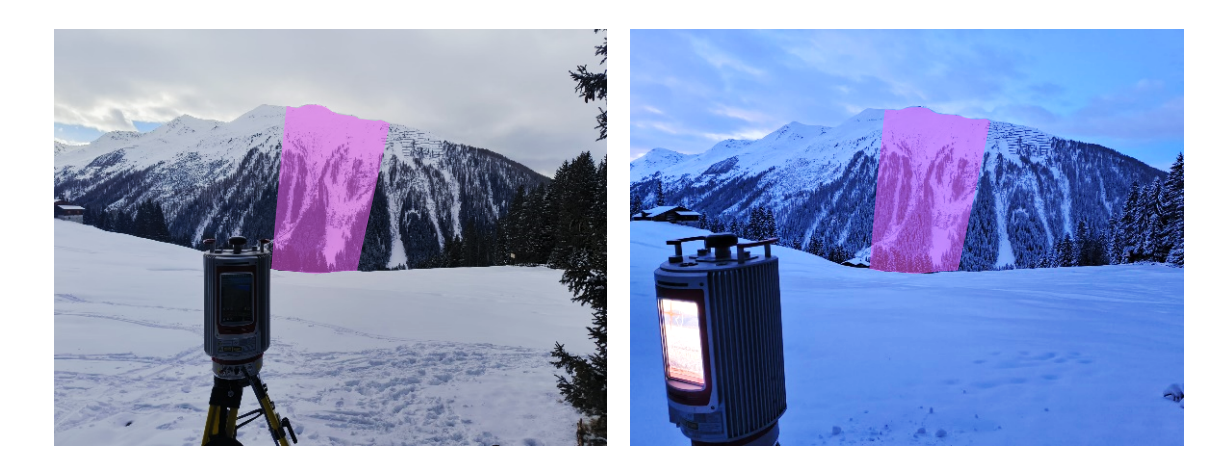


Figure 2 Acquisition of the Braemabuel slope on 27.01.2025 (left) and on 29.01.2025 (right) with a Riegl VZ-6000. The pink polygons indicate the scanned area.

2.3 Reference datasets

On the day of the avalanche event (29.01.2025), we conducted an aerial photogrammetric survey using a Wingtra One Gen II drone, with a Sony DSC-RX1RII 42 megapixel camera (Figure 1 orange line). We processed the data using Agisoft Metashape 2.1 (Agisoft, 2020), resulting in an orthophoto with 3 cm resolution and a DSM of 10 cm resolution.

To supplement the dataset, we dug a snow profile next to the slope of interest, in flat terrain just above the ridge, also at the day of the avalanche event on 29.01.2025 (Figure 1, yellow dot). The detailed stratigraphy is shown in the Appendix (Figure 4).

P. Ruttner and others O8.2 - Page 210

3. RESULTS AND DISCUSSION

The main outcome of the presented study is a set of snow depth maps of 0.5 m spatial resolution covering the entire slope of interest at three different points in time: before the snowfall, after the snowfall and before the avalanche and immediately after the avalanche. These maps allow for accurate (low centimeter level) estimation of release volume, erosion and deposition. Data from the Livox Avia scanner provide a time series of hourly snow depth maps, though over a smaller area.

The difference between the scans on 29.01.2025 (before and after the avalanche) clearly shows the outline of the avalanche release zone and path, as well as the release depth and deposition (Figure 3). By comparing the release depth with the measured amount of new snow, we can assess whether the weak layer was located at the boundary between old and new snow. The mean release depth was 0.60 m, while the average amount of new snow in the release area was 0.30 m, indicating that the weak layer was deeper than the old-new snow interface. Snow pit observations likewise suggest the presence of a weak layer at a height of 0.43 m, i.e. 0.63 m below the surface.

Comparing the two snow depth maps also provides a means to validate the results from the low-cost laser scanner against those from a more established high-end device. Although the low-cost lidar does not capture the entire release area, it provides a reasonable estimate of the average release depth.

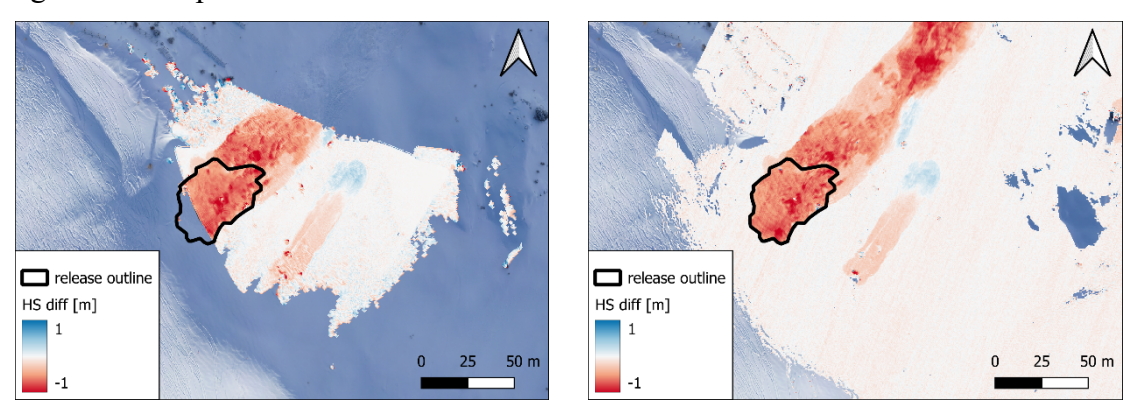


Figure 3 Differences of snow depth (HS diff) before and after the avalanche event on 29.01.2025. Left: HS diff, derived from Livox Avia measurements, right: HS diff, derived from Riegl VZ-6000 measurements. The background image is derived from UAV data from 29.01.2025.

4. CONCLUSIONS

This study presents a set of high-resolution maps of snow depth changes before and after an artificially triggered avalanche, including long-range and low-cost TLS measurements, a drone flight and snow pit observations. The combination of full-slope snow depth maps and a time series of hourly scans provides detailed insights into snowpack evolution, slab formation, and avalanche release dynamics under well-documented conditions.

The ability to accurately estimate release volume, erosion, and deposition, paired with supporting snow profile data, offers valuable input for validating avalanche simulation models and improving hazard assessment. Such datasets can support the development of more accessible and data-driven avalanche forecasting tools.

ACKNOWLEDGEMENT

The authors thank Vali Meier for the communication of the avalanche control work, as well as Christian Göhrig and Philipp Frieß for helping with the fieldwork. The authors acknowledge the use of ChatGPT for language refinement and assistance in drafting sections of this manuscript.

REFERENCES

- Agisoft, L. (2020). Agisoft Metashape User Manual—Professional Edition, Version 1.6. https://www.agisoft.com/pdf/metashape-pro_1_6_en.pdf
- Bühler, Y., Marty, M., Egli, L., Veitinger, J., Jonas, T., Thee, P., & Ginzler, C. (2015). Snow depth mapping in high-alpine catchments using digital photogrammetry. *The Cryosphere*, 9(1), 229–243. https://doi.org/10.5194/tc-9-229-2015
- Christen, M., Kowalski, J., & Bartelt, P. (2010). RAMMS: Numerical simulation of dense snow avalanches in three-dimensional terrain. *Cold Regions Science and Technology*, 63(1), 1–14. https://doi.org/10.1016/j.coldregions.2010.04.005
- Mayer, S., Techel, F., Schweizer, J., & van Herwijnen, A. (2023). Prediction of natural drysnow avalanche activity using physics-based snowpack simulations. *Natural Hazards and Earth System Sciences*, 23(11), 3445–3465. https://doi.org/10.5194/nhess-23-3445-2023
- Oesterle, F., Wirbel, A., Fischer, J.-T., Huber, A., & Spannring, P. (2025). avaframe/AvaFrame: 1.13_rc9 [Computer software]. Zenodo. https://doi.org/10.5281/zenodo.15781251
- Prokop, A. (2008). Assessing the applicability of terrestrial laser scanning for spatial snow depth measurements. *Cold Regions Science and Technology*, 54(3), 155–163. https://doi.org/10.1016/j.coldregions.2008.07.002
- Reuter, B., Richter, B., & Schweizer, J. (2016). Snow instability patterns at the scale of a small basin. *Journal of Geophysical Research: Earth Surface*, 121(2), 257–282. https://doi.org/10.1002/2015JF003700
- Ruttner, P., Voordendag, A., Hartmann, T., Glaus, J., Wieser, A., & Bühler, Y. (2025). Monitoring snow depth variations in an avalanche release area using low-cost lidar and optical sensors. *Natural Hazards and Earth System Sciences*, 25(4), 1315–1330. https://doi.org/10.5194/nhess-25-1315-2025
- Sampl, P., & Zwinger, T. (2004). Avalanche simulation with SAMOS. *Annals of Glaciology*, 38, 393–398. https://doi.org/10.3189/172756404781814780
- Schweizer, J., Bruce Jamieson, J., & Schneebeli, M. (2003). Snow avalanche formation. *Reviews of Geophysics*, 41(4). https://doi.org/10.1029/2002RG000123

P. Ruttner and others O8.2 - Page 212

5. APPENDIX

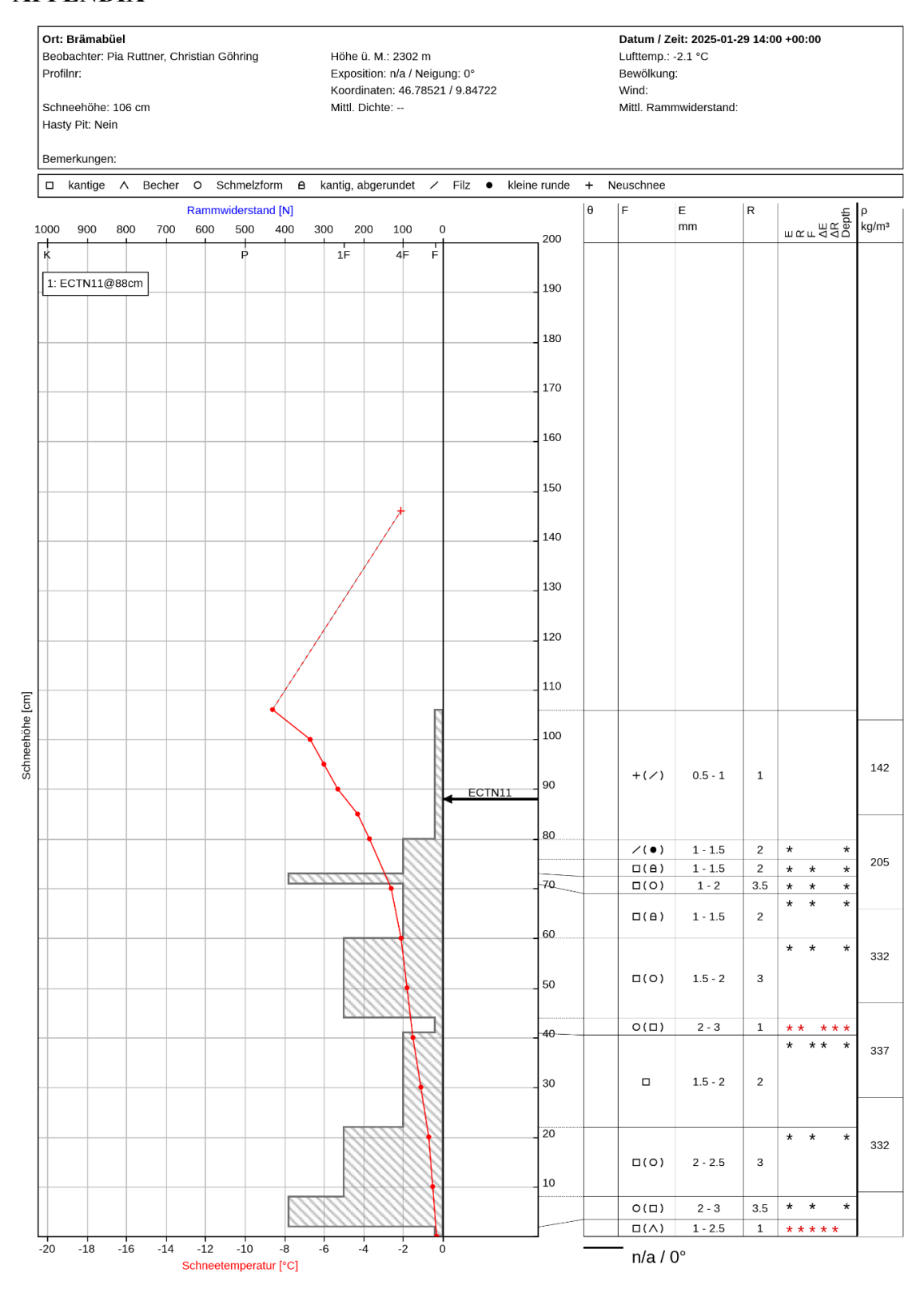


Figure 4 Snow profile, taken on 29.01.2025 14:00, in flat terrain next to the avalanche release.

Low Cost lidar monitoring for planning and operation of mitigation measures

Thomas Goelles, 1* Stefan Wallner 2 and Markus Eckerstorfer 3

University of Graz, Heinrichstraße 36, 8010 Graz, AUSTRIA
 FH Joanneum – University of Applied Science, Alte Poststraße 149, 8020 Graz, AUSTRIA
 Norwegian Public Roads Administration, Nygårdsgaten 112, NO-5008 Bergen, NORWAY

*Corresponding author, e-mail: thomas.goelles (at) uni-graz.at

ABSTRACT

Low-cost lidar sensors (0.5k–20k EUR), initially developed for robotics and automotive applications, are increasingly used for continuous snow monitoring. Their robustness, affordability, and suitability for near-infrared wavelengths, where snow and ice are highly reflective, make them well suited for permanent alpine installations. When mounted on fixed infrastructure, the Avia sensor by Livox, combined with a custom datalogger, enables continuous or scheduled 3D surface measurements up to 450 meters with a 70-degree field of view. These data are valuable for hazard assessment and mitigation planning.

We present a system for deploying low-cost lidar units for avalanche risk management, featuring multi-sensor integration, configurable scan intervals, and automated data processing. Snow thickness data and visualizations are accessible via a REST API, supporting calculations of snow depth changes between arbitrary time points. For further analysis, our open-source Python package, pointcloudset, provides statistical evaluation, anomaly detection, and additional insight from time-series point cloud data.

Long-term datasets produced by these systems support mitigation planning for snow fences, dams, and controlled release systems. By mapping snow accumulation, detecting changes in release zones, and quantifying deposition volumes, fixed lidar installations provide a basis for evidence-based decisions on protective infrastructure.

We present data from four lidar installations: since December 2024 in Lech am Arlberg, Austria, beneath avalanche blasting towers, and since March 2025 in Longyearbyen, Svalbard, on a lift mast near a snow fence.

1. INTRODUCTION

Information on snow depth is currently sparse and discontinuous, often limited to isolated point measurements that lack crucial data on wind redistribution and precipitation-driven variability. The spatial distribution of snow is typically assessed using lidar sensors and photogrammetric cameras, which can be deployed on mobile platforms or mounted in fixed positions. Among mobile platforms, Unmanned Aircraft Systems (UAS) are the most common. While UAS can

cover large areas, they currently need a human operator and are subject to weather limitations and regulatory constraints. Recently, aerial lifts have also been evaluated as a novel platform for lidar deployment (Dikic et al., 2024). In contrast, permanently installed sensors offer continuous monitoring without disturbing the snowpack or endangering personnel. Lidar provides the additional advantage of operating at night and in adverse weather conditions such as heavy snowfall, although at a reduced range. Its performance is also independent of surface texture, making it especially valuable in complex alpine environments.

Lidar has been used in snow-related research and monitoring for more than 17 years (Prokop, 2008). A wide variety of lidar systems is now available, each suited to different use cases. High-performance instruments such as the RIEGL VZ-6000 are capable of capturing snow depth across entire slopes or mountain sides, with a maximum range of up to six kilometers at a wavelength of 1064 nanometers. However, capturing a single high-resolution scan with such a system can take anywhere from several minutes to over an hour. These systems are expensive, with costs of around €150,000. As an alternative, the automotive and robotics industries have developed lidar sensors that are reliable, robust, and relatively inexpensive. These sensors are particularly well suited for continuous slope monitoring applications (Goelles et al., 2022; Ruttner et al., 2025).

Accurate information on the spatial distribution of snow is essential for both the planning and operation of avalanche mitigation infrastructure (Deems et al., 2015). Avalanche triggering is often more effective when shallow trigger points are located near deeper slabs, which can facilitate fracture initiation and propagation (Guy and Birkeland, 2013). During the planning phase, data collected from UAS flights can provide snapshots of the overall snow distribution over large areas, which is useful for identifying zones where mitigation structures are most effective without being snowed in. In contrast, permanently installed lidar systems, especially when combined with weather stations, can provide detailed insight into how snow accumulates and redistributes over time. Such data can be collected over multiple winters to inform the placement and design of mitigation structures.

Once mitigation structures are in place, lidar can be used to monitor their effectiveness. It can help determine whether roads need to be closed or reopened, support site-specific avalanche forecasting, and assess whether artificial avalanche triggering has been successful. Lidar systems also support the documentation of control actions, validation of snowpack and avalanche models, planning of explosive placement, and monitoring of cornice formation (Hancock et al., 2020).

In this study, we present preliminary data from four permanently installed lidar systems. Two of these are located in Lech am Arlberg in the Austrian Alps, and the other two are in Longyearbyen on Svalbard, in the High Arctic.

2. TECHNOLOGY

Our snow distribution monitoring system consists of the sensor (Livox Avia) and controller together with a power supply, housing and mounting pole which is installed on a slope, a server and a frontend which can be accessed by the end user (see Figure 1).

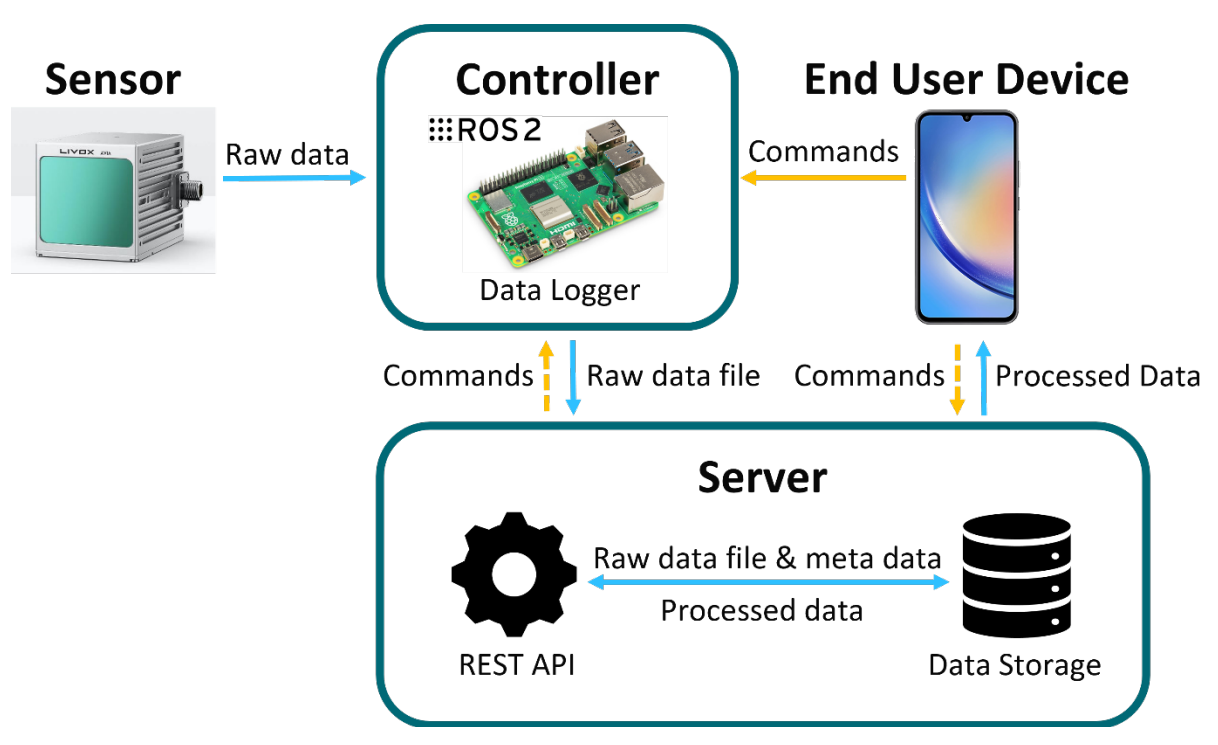


Figure 1 Components of the lidar sensing solution and the data flow between them (blue arrows) as well as the actual direct remote-control path with commands (yellow arrow) and the improved future one via the server (dashed yellow arrow, Wallner et al., 2025)

Using the API, difference plots for any sensor can be generated between two timestamps. This is done by sending a POST request to https://api.avalanchemonitoring.com/data/diff-plots/by-search following a successful user login. The request requires several parameters, including the sensor ID (sensor_location_id), a reference timestamp (datetime_ref), a comparison timestamp (datetime_to_compare), and the desired export format (e.g., "png"). Additionally, optional parameters can be specified to customize the output, such as the coordinate reference system (crs_to), the plot buffer size, and visualization limits for distance differences (vmin and vmax). The API returns a job ID in response, which can then be used to retrieve the generated plots once processing is complete.

3. CURRENT INSTALLATIONS

Two installed lidar systems are shown in Figure 2. Overall, more than 250 GB of raw data, i.e. point cloud time series and Inertial Measurement Unit (IMU) data has been collected time-synchronously on our server.

AT - Lech am Arlberg

NO - Longyearbyen



Figure 2 Setup in Lech am Arlberg (left, installed on 19.12.2024) with lidar sensor mounted on a pole and the setup in Longyearbyen (right, installed 09.03.2025) mounted on a ski lift mast with the measurement area highlighted in red.

According to the datasheet, the Livox Avia has a maximum range of 450 meters when measuring a target with 80 percent reflectivity. We evaluated the actual maximum range every 12 hours from the time of installation until the end of March, as shown in Figure 3. In practice, this theoretical maximum was not reached, most likely because the surfaces in the field of view are not oriented at a perfect 90-degree angle relative to the sensor and due to the complex topography. Among the four lidar systems, the average maximum range in the x-direction varied between approximately 160 and 320 meters. The observable area per lidar results from the max range and the horizontal field of view angle of 70.4 degrees and therefore ranges from 15727 to 62910 square meters. Note that this uses the full field of view angle while assuming flat topography. The observable area can be increased by combining multiple lidars, which is supported by the processing of the API server.

Figure 4 shows an example of a snow thickness difference map from Longyearbyen. In this case, a snow fence is visible within the sensor's field of view. The map displays M3C2 distances, which correspond to snow thickness in the flat terrain, but not in the area around the snow fence. The M3C2 algorithm quantifies differences between two point clouds by calculating distances along surface normals derived from the local geometry of the reference cloud. In addition, the plotting algorithm interpolates the data, which introduces artifacts in areas with abrupt changes in surface geometry, such as around the snow fence. For most applications, regions containing such structures should be excluded from visualizations and further evaluation. We kept the snow fence in the plot to illustrate these effects. The white area in front of the snow fence indicates locations where no M3C2 distance could be calculated because one of the two point clouds lacks data in this region due to shadowing. This data gap is a result of shadowing caused by the combination of topography and snow cover.

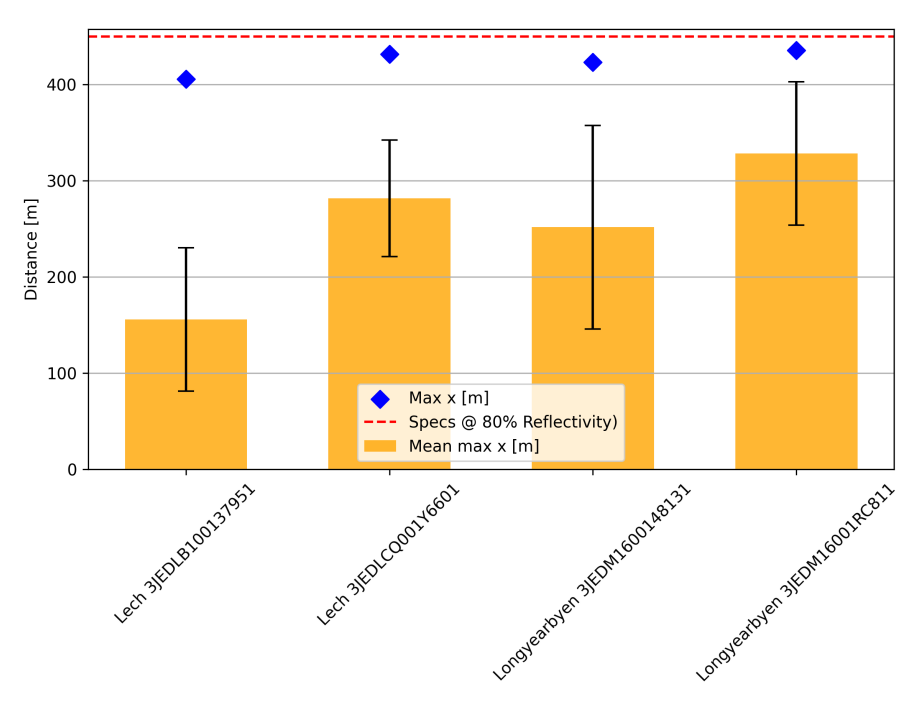


Figure 3 Maximum measurement distance from the data sheet for each sensor and the maximum value, the mean and the interquartile range measured (Wallner et al., 2025).

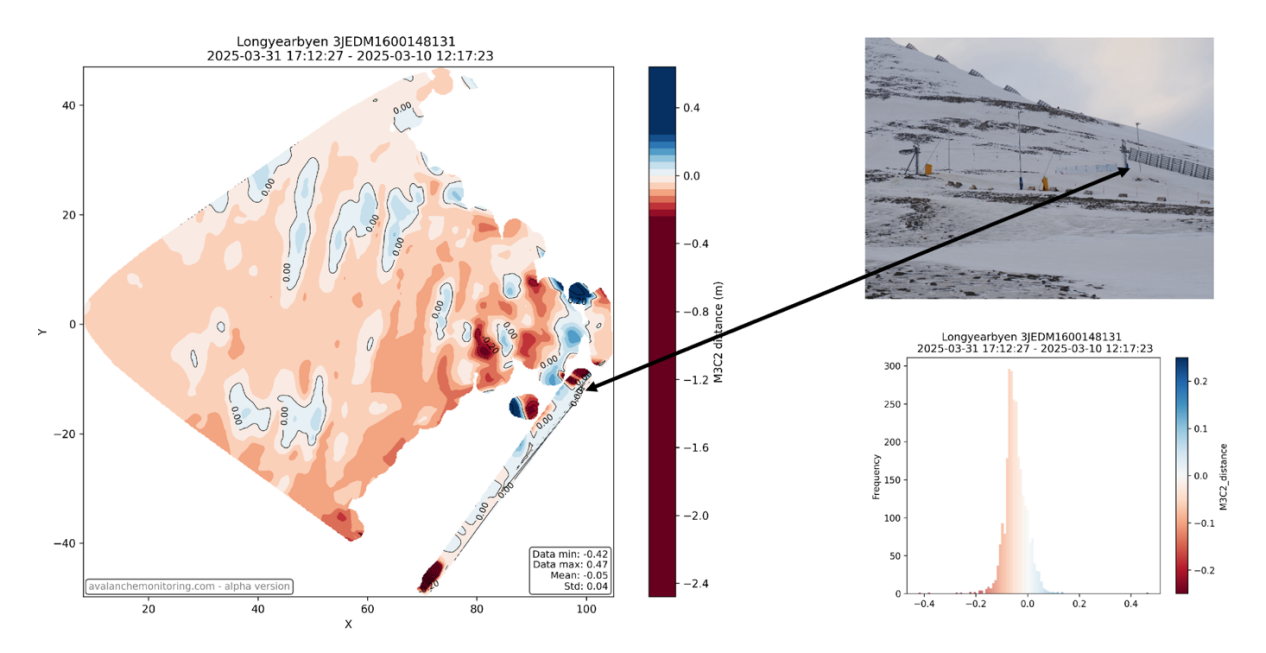


Figure 4 Change in snow depths from one sensor in Longyearbyen shown in a difference plot (left), photo of the area where the lidar is installed on top of the lift mast and a snow fence within its field of view. The arrow marks the snow fence in the photo which is also visible in the difference plot. A histogram of the distribution of the snow depth is at the bottom right.

4. CONCLUSIONS

Permanently installed lidar systems can provide critical insights for both the planning and operation of avalanche mitigation measures. To ensure optimal coverage and minimize shadowing effects caused by low incidence angles, the position and height of the lidar must be carefully planned.

ACKNOWLEDGEMENT

This work is supported by the FFG-funded project GEOTEQ. The installation in Longyearbyen was carried out with support from an Arctic Field Grant (RiS ID 12564).

REFERENCES

- Deems, J.S., Gadomski, P.J., Vellone, D., Evanczyk, R., LeWinter, A.L., Birkeland, K.W., Finnegan, D.C., 2015. Mapping starting zone snow depth with a ground-based lidar to assist avalanche control and forecasting. Cold Regions Science and Technology 120, 197–204. https://doi.org/10.1016/j.coldregions.2015.09.002
- Dikic, B., Goelles, T., Gaisberbger, C., Schlager, B., Muckenhuber, S., Pedro Batista, P., Keuschnig, M., Schratter, M., 2024. Lidar-based snow monitoring: cable car deployment in the Austrian Alps. https://doi.org/10.31223/X55Q6G (submitted)
- Goelles, T., Hammer, T., Muckenhuber, S., Schlager, B., Abermann, J., Bauer, C., Expósito Jiménez, V.J., Schöner, W., Schratter, M., Schrei, B., Senger, K., 2022. MOLISENS: MObile LIdar SENsor System to exploit the potential of small industrial lidar devices for geoscientific applications. Geoscientific Instrumentation, Methods and Data Systems 11, 247–261. https://doi.org/10.5194/gi-11-247-2022
- Guy, Z.M., Birkeland, K.W., 2013. Relating complex terrain to potential avalanche trigger locations. Cold Regions Science and Technology 86, 1–13. https://doi.org/10.1016/j.coldregions.2012.10.008
- Hancock, H., Eckerstorfer, M., Prokop, A., Hendrikx, J., 2020. Quantifying seasonal cornice dynamics using a terrestrial laser scanner in Svalbard, Norway. Nat. Hazards Earth Syst. Sci. 20, 603–623. https://doi.org/10.5194/nhess-20-603-2020
- Prokop, A., 2008. Assessing the applicability of terrestrial laser scanning for spatial snow depth measurements. Cold Regions Science and Technology 54, 155–163. https://doi.org/10.1016/j.coldregions.2008.07.002
- Ruttner, P., Voordendag, A., Hartmann, T., Glaus, J., Wieser, A., Bühler, Y., 2025. Monitoring snow depth variations in an avalanche release area using low-cost lidar and optical sensors. Natural Hazards and Earth System Sciences 25, 1315–1330. https://doi.org/10.5194/nhess-25-1315-2025
- Wallner, S., Gölles, T., Schlager, B., Prokop, A., Gaisberger, C., Schrattner, M., Muckenhuber, S., 2025. An affordable permanent monitoring solution of potential avalanche sites. Lawinensymposium 2025 (in press)

Impact of Snow Depth Initialization on Avalanche Modeling: Comparing Station Data with High-Resolution Measurements

Julia Glaus ^{1,2,3*}, Pia Ruttner^{1,2,4}, Johan Gaume^{1,2,3} and Yves Bühler^{1,2}

¹WSL Institute for Snow and Avalanche Research SLF, Davos Dorf, SWITZERLAND
²Climate Change, Extremes, and Natural Hazards in Alpine Regions Research Centre CERC, Davos Dorf, SWITZERLAND

³Institute for Geotechnical Engineering, ETH Zurich, Zurich, SWITZERLAND 4 Institute of Geodesy and Photogrammetry ETH Zurich, Zurich, SWITZERLAND *Corresponding author, e-mail: Julia.glaus (at) slf.is

ABSTRACT

Avalanches can increase significantly in volume due to erosion of snow cover, leading to longer runout distances, higher velocities, and increased impact pressures. Numerical avalanche models including erosion, require initialization of the erodible snow layer. This is often based on snow depth estimates from nearby weather stations. These estimates are commonly adjusted for terrain factors such as elevation and slope. During snowfall events with wind, snow redistribution can create highly variable snow depth patterns, making station-based assumptions potentially inaccurate in complex terrain. To evaluate the impact of snow depth initialization on simulation outcomes, we compare model results based on station data with those using detailed field measurements. Our case study involves an artificially triggered avalanche in the Brämabüel region near Davos, Switzerland. Snow depth was measured at high spatial resolution before the snowfall and both, before and after the avalanche event, allowing reconstruction of the snow distribution along the entire track prior to release. Using this dataset, we conduct avalanche simulations initialized with (1) the measured snow distribution and (2) approximations derived from two weather stations. This study highlights the importance of accurate snow cover initialization in improving the reliability of avalanche simulations, particularly in complex alpine terrain.

INTRODUCTION

Numerical simulation tools for avalanche dynamics are widely applied to analyse avalanche paths to support hazard mapping and risk assessment (Bühler et al. 2022). These models are essential for predicting potential run-out distances, impact pressures, and affected areas. Studies have shown that avalanches can run significantly farther than predicted by friction-only approaches (Issler, 2020). These simplified models account for resistance from basal friction but neglect additional processes such as snow entrainment, which increases avalanche mass. Snow entrainment, which depends on the snow amount, density, and slope angle, increases the avalanche's mass and momentum, thereby influencing both its dynamics and destructive potential. For some numerical simulation models, the initialization requires an estimate of the amount of erodible snow available along the avalanche path. This parameter strongly influences the simulated mass growth through entrainment (Glaus et al. 2025). However, suitable datasets to assess the distribution and characteristics of the erodible snow mass are barely existing. In practice, such estimates are often derived from measurements at nearby weather stations, assuming only the new snow can be eroded. The snow depth distribution within the terrain can be adjusted based on elevation gradient and local terrain

steepness. While these approaches can provide useful first-order estimates, they are subject to large uncertainties due to spatial variability in snowfall and wind redistribution as remote sensing measurements demonstrate (Bührle et al. 2023). In this study, we present a dataset of snow depth measurements collected within days before a snowfall, after snowfall, and immediately after an artificially triggered avalanche. We outline initial strategies for using these data to calibrate and validate existing erosion models, providing a first step towards improved representation of erosion in numerical avalanche simulations.

1. METHODS

1.1 Data acquisition and event description

In January 2025, an avalanche was artificially released as part of avalanche control operations above the Dischma road. A scan using the VZ 6000 from the opposite slope was conducted prior to the snowfall (27 January 2025), followed by another scan on 29 January 2025 at 6:53 o'clock, shortly before the release, and a final scan after the avalanche event at 7:40 o'clock.

Following the release, a photogrammetric drone survey with a Wingtra One Gen II drone was carried out using structure-from-motion photogrammetry to generate a reference dataset of the affected area. In addition, a snow pit was dug near the release zone to obtain additional information on the snowpack. The snow pit revealed a weak layer located 60 cm below the surface and around 30 cm of new snow. The average snow temperature in the weak layer was -3.5° C (excluding the surface), with an average snow density of 250 kg/m^3 .

To initialise the erodible snow cover, snow depth and temperature are typically estimated from weather stations. For this event, we focused on the last snowfall prior to the release, which began on 27 January 2025 around 12:00. Comparing snow depth at the IMIS stations Weissfluhjoch WFJ (2536 m a.s.l.) and SLF in the valley (1563 m a.s.l.) before the snowfall (WFJ: 86.6 cm; SLF: 49.9 cm) and just before release at 07:00 (WFJ: 116 cm; SLF: 59 cm) results in a snow cover gradient of 0.021 m per 100 m elevation. As the snowpack near the release zone was already relatively warm, a temperature gradient of 0°C per 100 m was assumed.

1.2 Evaluation

For data evaluation, an AI-based algorithm was used to identify the avalanche outline, with some manual adjustments (Hafner-Aeschbacher et al. 2024). To enable a comparison between measured and simulated snow cover, a central flow line was established, referred to as the main path. For the evaluation a 5 m resolution grid was used, matching the spatial resolution of the simulation. To mitigate the impact of outliers from single-pixel measurements, rectangular sampling areas with a width of 20 m were positioned perpendicular to the main path, over which the mean snow depth values were computed.

The average snow depth along the main avalanche path was calculated by subtracting the DEMs from the scans from the snow-free DEM acquired in October 2024 acquired with the Wingtra One Gen II drone.

1.3 Simulation of Erodible Snow

The erodible snow depth in RAMMS::Extended was initialised following the approach described in Glaus et al. (2025), where the fracture height is estimated based on nearby snow measurement stations. From the recent snowfall, an erodible snow cover gradient is derived, as outlined in the event description. For each raster cell, the snow depth perpendicular to the terrain is set according to this elevation gradient. Additionally, the erodible snow depth is adjusted based on the local terrain steepness.

2. Results and discussion

2.1 Measured snow cover

The snow depth measurements from the laser scan taken from the counter slope are shown in Fig. 1. The values represent vertical snow depth (not slope-normal). In the release area, a reduction of approximately 60 cm in snow depth is visible after the avalanche released (46 cm normal to slope for an average steepness of 40°). This matches the weak layer depth identified in the nearby snow pit.

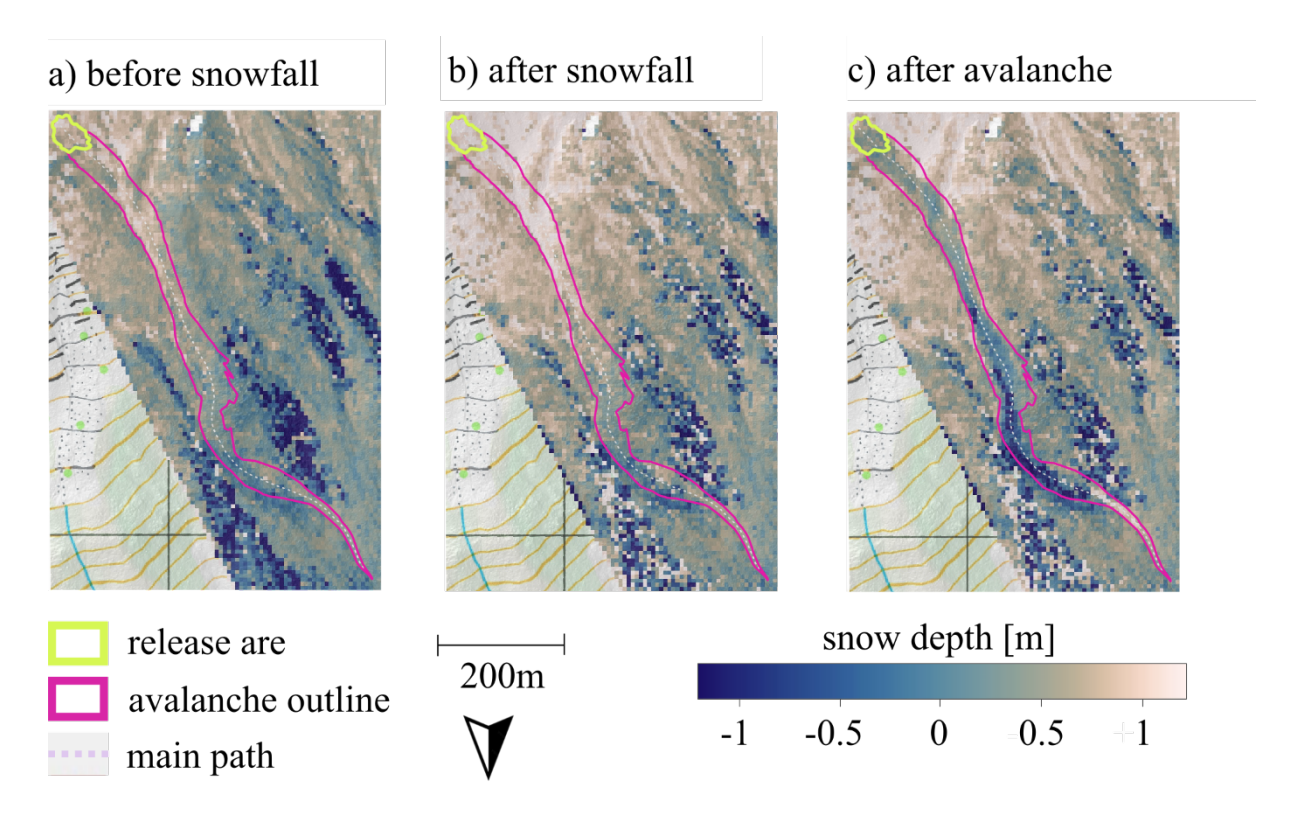


Figure 1: Visualization of snow depth derived from scans taken from the counter slope. (a) Snow cover before the snowfall began, (b) shortly before the avalanche release, and (c) immediately after the avalanche event. Negative values represent NaN entries, which occur in regions covered by forest or dense bush vegetation.

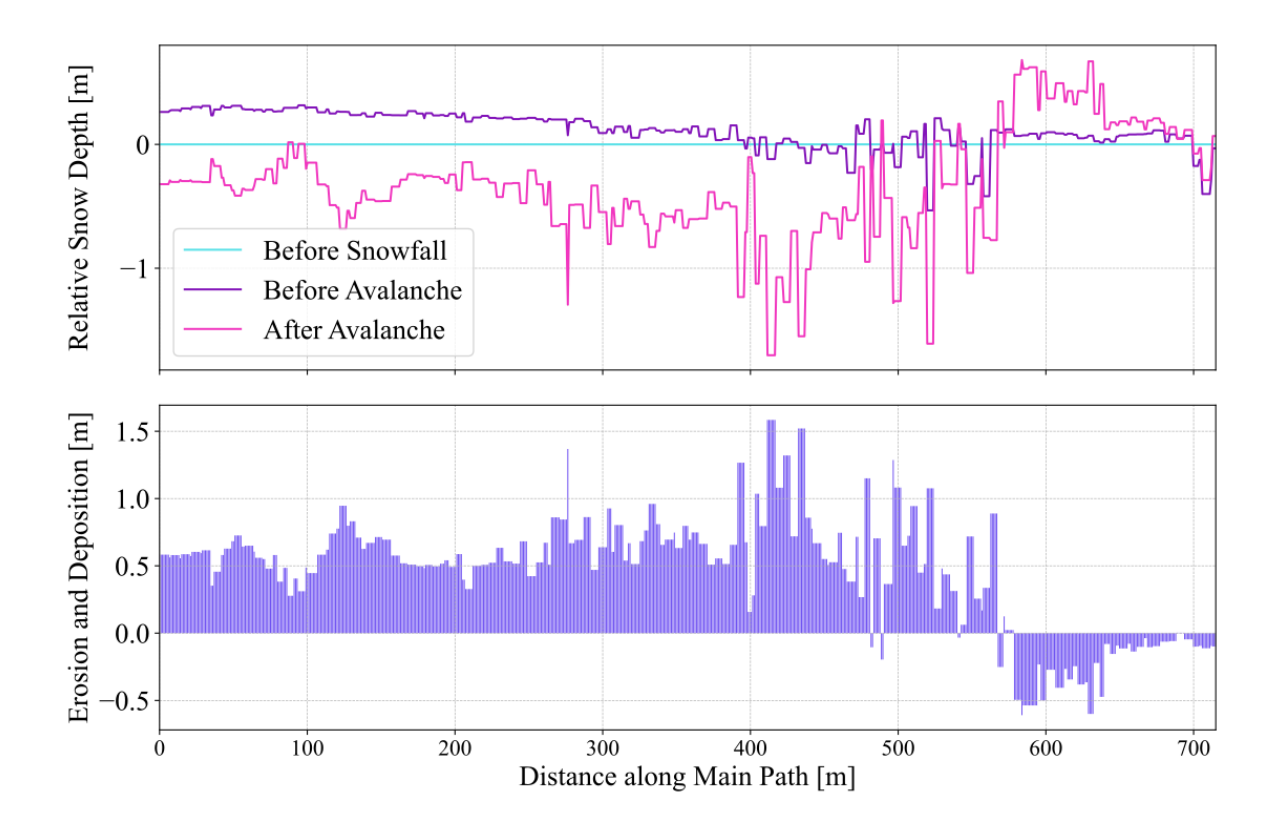


Figure 2: Snow depth after snowfall and after avalanche, shown relative to the snow depth before the snowfall—indicating new snow accumulation and snow erosion/deposition, respectively. (b) Difference in snow cover height before and after the avalanche, illustrating the net sum of erosion and deposition.

Fig. 2 shows the amount of new snow and the snow remaining after the avalanche relative to the snow depth before the snow fall. Hence, we can conclude, that the avalanche released and eroded deeper than the new snow layer (on average 30cm new snow in the release zone measured).

In Fig. 2 the panel (b) depicts the difference in snow depth before and after the avalanche event. This gives a rough picture where erosion and deposition happened. But we cannot distinguish where both processes occurred simultaneously. By analyzing the net change, we can approximate the maximum erosion depth, observed to reach approximately 0.5 m along the initial segment of the avalanche path (between 50 m and 400 m), accepting the fact that this also includes deposition that occurred along the avalanche path. At the end of the main path (580 - 715 m), the deposition is visible.

To analyze the erosion pattern, we calculated the surface roughness along the avalanche path using CloudCompare (CloudCompare, 2022). This method estimates roughness by measuring how much each point deviates from a best-fitting plane based on its nearby points. In case of a rough surface, we can conclude that the snow cover got eroded and in case of a very smooth the avalanche was just sliding on the snow.

2.2 Simulated snow cover

Applying the gradient approach based on weather station data to initialize the snow cover in the RAMMS::Extended results in an avalanche with a release volume of 820 m³ and a potential erosion volume of 2732 m³. The distribution is shown in Fig.3 b). A direct comparison to the measured erosion and deposition data set is not possible, as RAMMS simulates only the snow cover that could potentially be eroded, excluding the underlying snowpack.

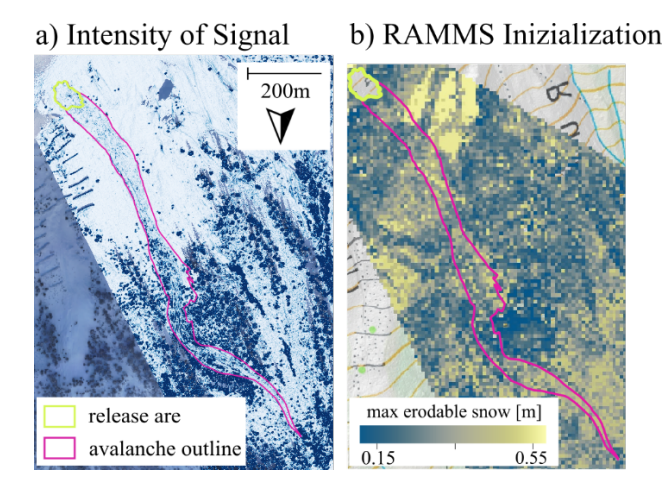


Figure 3: Qualitative comparison between the measured snow distribution and the RAMMS initialization based on the gradient approach. Panel (a) shows surface roughness, where darker blue indicates higher surface roughness and white represents a more homogeneous surface. Panel (b) depicts the RAMMS initialization of the erodible snow cover; lighter areas indicate zones where more snow is available for erosion.

3. CONCLUSION

For numerical avalanche simulations, datasets capturing snow conditions before and after avalanche events are essential to better understand mass balance and erosion processes. In this extended abstract, we present an initial analysis of a snow depth dataset acquired around an avalanche event. We outline a first approach for estimating the potentially erodible snow volume, providing a basis for calibrating numerical simulation tools. Our method applies a simple comparison of snow depth along the avalanche's main path. Additionally, we qualitatively demonstrate how surface roughness can provide insights into erosion and deposition patterns. While our current measurement setup enables detailed observations, it has so far only captured a relatively small avalanche event. Future work will focus on using the measured snow cover directly for initializing simulation models.

4. ACKNOLEDGEMNT

We sincerely thank everyone who supported our fieldwork days. In particular, we appreciate Vali Meier for managing the avalanche control efforts, and Philipp Frieß and Christian Göhrig for their help carrying the heavy laser scanner through fresh snow up the mountain and helping with the snowpit. We also acknowledge the assistance of ChatGPT (OpenAI) for support in drafting the manuscript.

REFERENCES

- Bühler, Y., Bebi, P., Christen, M., Margreth, S., Stoffel, L., Stoffel, A., Marty, C., Schmucki, G., Caviezel, A., Kühne, R., Wohlwend, S., & Bartelt, P., 2022. Automated avalanche hazard indication mapping on a statewide scale. *Natural Hazards and Earth System Sciences*, 22, 1825–1843. https://doi.org/10.5194/nhess-22-1825-2022
- Bührle, L., Marty, M., Eberhard, L., Stoffel, A., Hafner-Aeschbacher, E., & Bühler, Y., 2023. Spatially continuous snow depth mapping by aeroplane photogrammetry for annual peak of winter from 2017 to 2021 in open areas. *The Cryosphere*, 17, 3383–3408. https://doi.org/10.5194/tc-17-3383-2023
- CloudCompare, 2022. CloudCompare 3D point cloud and mesh processing software. Available at: https://www.cloudcompare.org/ (Accessed: 2025-08-11).
- Glaus, J., Wikstrom Jones, K., Bartelt, P., Christen, M., Stoffel, L., Gaume, J., & Bühler, Y., 2025. Simulation of cold-powder snow avalanches considering daily snowpack and weather situations. *Natural Hazards and Earth System Sciences*, **25**(7), 2399–2419. https://doi.org/10.5194/nhess-25-2399-2025
- Hafner-Aeschbacher, E., Kontogianni, T., Caye Daudt, R., Oberson, L., Wegner, J. D., Bühler, Y., 2024. Interactive snow avalanche segmentation from webcam imagery: results, potential, and limitations. *The Cryosphere*, 18, 3807–3823. https://doi.org/10.5194/tc-18-3807-2024
- Issler, D. 2020. Comments on "On a continuum model for avalanche flow and its simplified variants" by S. S. Grigorian and A. V. Ostroumov. *Geosciences*, 10, 96 https://doi.org/10.3390/geosciences10030096.

Comparing simulated pressure profiles with measurements from a power line assembly at the Ryggfonn test site

Peter Gauer^{1*}, Piotr Kupiszewski¹, and Callum Tregaskis¹

^{1 2} Norwegian Geotechnical Institute, P.O. 3930 Ullevål Stadion, NO-0806 Oslo, NORWAY *Corresponding author, e-mail: peter.gauer(at)ngi.no

ABSTRACT

Dry mixed avalanches with a substantial powder component pose a significant hazard in alpine regions. These avalanches typically consist of one or two denser core layers—the dense layer and the fluidized layer—accompanied by a more dilute powder/suspension layer characterized by variable density and flow height. While the denser cores travel rapidly and cause severe destruction along the avalanche path, the powder cloud can extend well beyond and above the main impact zone. This cloud exerts considerable forces on structures in its path and can affect areas not directly hit by the dense flow.

The dynamic force from a 1-meter-high dense flow with a density of 100 kg m⁻³ is equivalent to that from a 10-meter-high powder flow with a density of 10 kg m⁻³. Depending on how pressure is distributed within the suspension layer, the resulting structural loads—especially bending moments—can be dominated by the powder component. For structures such as free-hanging power lines, it is often the powder cloud's force that governs risk assessment. Therefore, accurately understanding the pressure distribution within the suspension layer is critical for engineering design.

In recent years, avalanche simulation models that incorporate both the dense core and the suspension layer have been developed to support engineering decisions. However, a key challenge remains: the scarcity of quantitative field data for model validation.

This paper presents a comparison between historical measurements taken in the 1980s from a power line assembly at the Ryggfonn avalanche test site and simulation results from three avalanche models: SAMOS-AT, RAMMS::Extended, and MoT-PSA. RAMMS::Extended and MoT-PSA use depth-integrated approaches to represent the suspension layer, while SAMOS-AT fully resolves the powder component in three dimensions. The comparison offers insights into each model's ability to reproduce observed pressure profiles and highlights their respective strengths and limitations.

1. INTRODUCTION

Dry-mixed avalanches are understood to consist of three distinct flow regimes (Gauer et al., 2008): a dense core, a more fluidized intermediate layer, and a powder cloud or suspension layer. Figure 1.1 presents FMCW radar measurements alongside a schematic illustrating the three flow regimes.

Although the powder part typically has a density less than one-tenth that of the fluidized or dense core, it can still cause significant damage. For instance, Figure 1.2 illustrates a case where

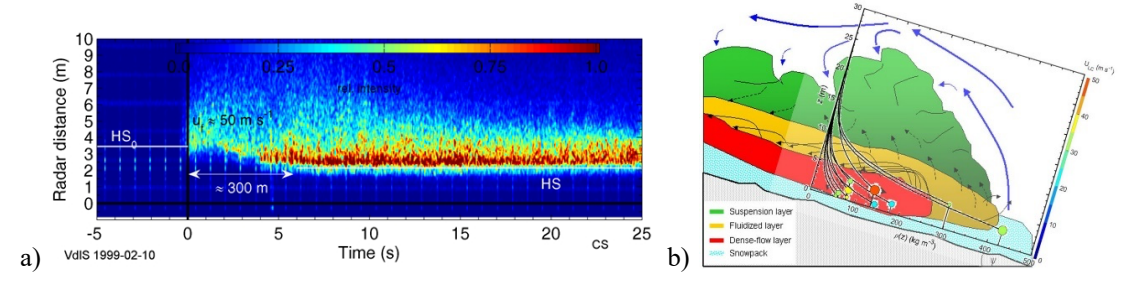


Figure 1.1 a) Moving target identification plot from FMCW-radar measurements; The plot shows relative intensity, where higher intensity indicates greater flow density. b) Schematic of a dry-mixed avalanche showing the dense core, the fluidized (saltation) layer, and the powder cloud (suspension layer, PSA). The three flow regimes become more or less pronounced depending on the velocity and properties of the snow

the powder cloud was powerful enough to partially dislodge the wooden frame of a chalet from its foundation.

The destructive potential of PSAs has long been recognized, as documented by early works such as Coaz (1889), Flaig (1935), and Rohrer and Greber (1956). Despite this well-established hazard, direct measurements of PSA properties—such as pressure profiles or density distributions within the powder cloud—remain scarce. Most estimates rely on indirect observations, with damaged flag trees commonly used as indicators of flow intensity and direction. Some information has been obtained from dedicated avalanche test sites, such as that reported by Turnbull and McElwaine (2007) from Vallée del Sionne, Switzerland or by Gauer and Kristensen (2016) from Ryggfonn, Norway.



Figure 1.2 a) Example from La Fouly, Switzerland (1999), where the powder cloud exerted enough force to partially dislodge a wooden chalet from its foundation. b) "Flag trees" observed in the aftermath provide indirect evidence of the powder cloud's intensity and direction, offering insight into the avalanche's dynamics.

On the other hand, over the past two decades, numerical avalanche models have been developed that include not only the dense flow component but also the powder-snow cloud. These models aim to support avalanche practitioners in hazard assessments related to dry mixed avalanches. Most practitioners currently rely on the Austrian model SAMOS-AT (Sampl and Granig, 2009) and partially, the pre-release version of RAMMS::Extended (Glaus and others, 2023). More recently, the MoT-PSA model was introduced by Vicari and Issler (2023). While SAMOS-AT

couples a depth-integrated dense flow with a fully 3-dimensional resolved powder part, both RAMMS::Extended and MoT-PSA employ depth-integrated formulations for the powder-snow cloud as well. Solving the depth-integrated balance equations for the field variables in both the dense and powder layers requires assumptions about how these variables vary with flow depth and boundary conditions at the interfaces. Typically, such assumptions rely on self-similarity principles to define shape functions (Tochon-Danguy and Hopfinger, 1975; Schweiwiller, 1986). In practical applications, empirical relations—such as the one proposed in Statens Vegvesen's Handbook V138 (2014)—are also used. However, due to the lack of sufficient validation data, it remains challenging to reliably assess the performance of both numerical models and empirical approaches.

This paper presents a comparison between historical measurements taken in the 1980s from a power line assembly at the Ryggfonn avalanche test site and simulation results from three avalanche models: SAMOS-AT, RAMMS::Extended, and MoT-PSA as well the empirical equation proposed in Statens Vegvesen's Handbook V138 (2014).

2. OBSERVATIONS

Aside from a few indirectly derived datasets—such as those presented by Takeuchi et al. (2011)—there is limited published data on direct measurements of forces within the PSA layer. McElwaine and Turnbull (2005) and Turnbull and McElwaine (2007) reported flow heights ranging between 18 m and 36 m and frontal velocities between 37 m s⁻¹ and 54 m s⁻¹ for seven PSA events near the measurement mast in Vallée de la Sionne.

In the early years of the Ryggfonn site, a transmission line assembly was installed in the lower part of the track. It consisted of three cables positioned approximately 8 m, 12 m, and 16 m above ground (see Figure 2.1). Some summary information on the measurements can be found in (Norem, 1995; Gauer and Kristensen, 2018; Gauer, 2023).





Figure 2.1 a) Power line assembly at the Ryggfonn test-site during the years 1983 to 1990. The cables were aluminum-conductor steel-reinforced (ACSR) with a diameter D = 34 mm, a weight of 3.0 kg m⁻¹ and elastic modulus EAt = 750 GPa. b) The avalanche from 1989-04-03 reaching the power line assembly. In this case, the frontal velocity at the assembly was about 22 m s⁻¹.

A limited set of data was collected between 1983 and 1989, offering some insight into the likely pressure distribution with height during avalanche events. The measurements generally showed sinusoidal tension forces, with peak tension forces occurring early in the avalanche passage.

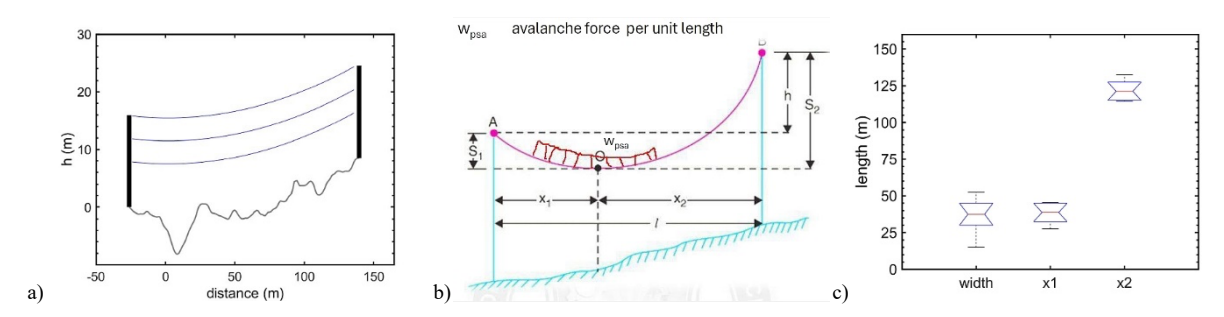


Figure 2.2 a) Schematic of the powerline assembly as seen looking downstream. b) Definition diagram for suspended cable used for the sag tension analysis. w_{psa} represents the force from the powder part on to the cable. c) Estimates of the avalanche widths and corresponding lengths x_1 and x_2 .

Converting the measured tension forces into avalanche impact pressures on the cables is not straightforward, as it depends on both the location of impact and the effective width of the area affected along the cable. The latter remains particularly uncertain. Nevertheless, rough estimates of impact pressure can be obtained through iterative sag-tension calculations (see, e.g., Task Force B2.12.3, 2016). In the following the pressure derived from the peak tension is used as a proxy for the PSA pressure.

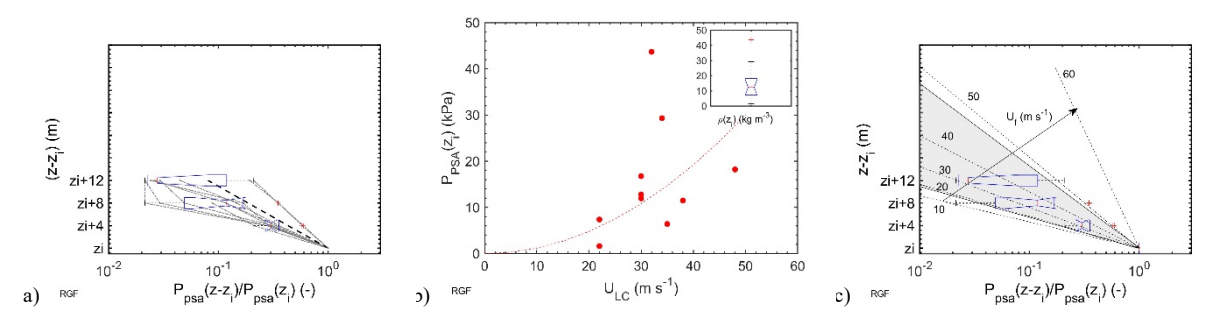


Figure 2.3 a) Estimates of the normalized pressure profile $P_{PSA}(z-z_i)/P_{PSA}(z_i)$ based on measurements from the RGF-site, where z_i denotes the assumed height of the interface between dense and powder layer. The gray lines depict the individual measurements, while the black dashed line indicates a mean trend line. Boxplots illustrate the spread of the data at the three cable heights. Note the log-scale of the x-axis. b) Estimated pressure $P_{PSA}(z_i)$ just above dense–powder interface plotted against the velocity U_{LC} . The red dashed line represents a trend line according to $P \sim 6 \ U_{LC}^2$. The inset shows the corresponding density estimates at the interface. c) The dashed lines show fits of $P_{PSA}(z-z_i)/P_{PSA}(z_i)$ according to eq. (1) using the frontal velocity as parameter varying from 10 to 60 m s⁻¹. The gray area depicts an extrapolated range spanned by the observational data.

Figure 2.3 shows the data from the 11 avalanches from which measurements were obtained. The normalization and extrapolation of the data downwards suggest that the typical dense–powder interface was about 4 m above the ground. This estimate is consistent with observed snow heights and estimated dense-layer flow heights. The back-calculated density at the interface $\sim 12 \text{ kg m}^{-3}$, aligns with commonly accepted values for PSAs. Figure 2.3 c shows fits of the normalized pressure profile, where the pressure at the interface z_i is given by:

$$P_{PSA}(z_i) = C_D \rho(z_i) \frac{U_f^2}{2}$$
 (1)

3. COMPARISON BETWEEN MODELS AND OBSERVATIONS

First, we compare the observations to the empirical formula proposed in Statens Vegvesen's Handbook V138 (2014):

$$P_{iPSA}(z=0) = C_D \rho_{iSVV} \frac{U^2}{2}$$
 (2)

and

$$\frac{P_{PSA}(z)}{P_{PSA}(z=0)} = \left(\frac{h_{PSA} - z}{h_{PSA}}\right)^3 \tag{3}$$

where the density at the interface is estimated to range between 4 and 10 kg m⁻³, with 8 kg m⁻³ as a best first estimate. The profile function additionally requires an estimate for the flow depth of the PSA, for which 30 m is adopted as a first-guess value. With this fixed flow height, the shape of the profile is assumed to be independent of velocity.

Figure 3.1 depicts a comparison of the empirical relation with the measurements from Ryggfonn. In the lower 25 m of the powder part the empirical function the empirical model tends to overestimate relative to the measured profiles, thus providing conservative estimates. However, the suggested density at the interface, z_i , appears lower than what was observed in the field, leading to an underestimation of the expected pressures.

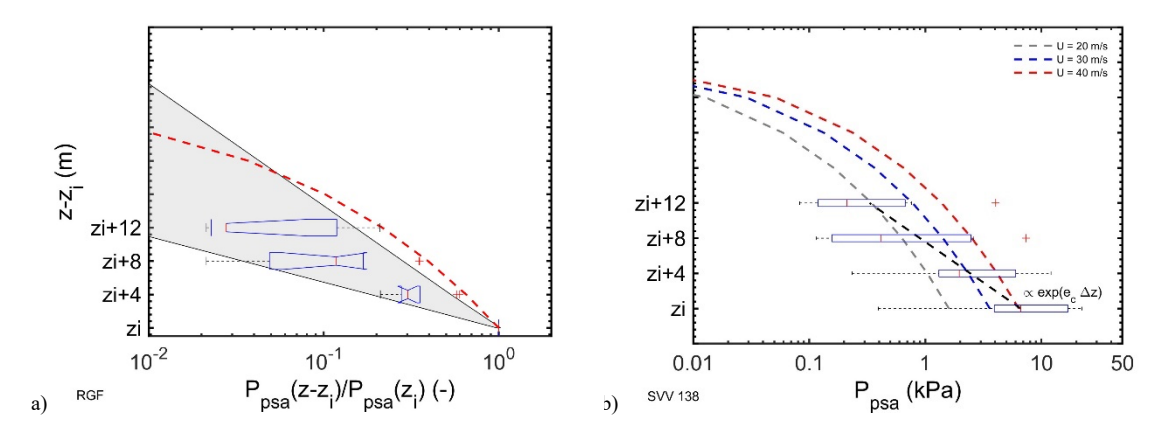


Figure 3.1 a) Comparison of the observational data with the proposed empirical profile function (red dashed line) given in eq. (3). b) Example of the proposed pressure distribution for the given velocities and $\rho_I = 8 \text{ kg m}^{-3}$, compared with observational data.

In the second part of this section we compare the observations with a series of simulations with three models that are in use by practitioners for hazard assessments: 1) MoT-PSA (Vicari and Issler, 2023); 2) RAMMS::EXTENDED (Glaus et al 2023; 2025); 3) SAMOS-AT (Sampl and Granig 2009) with an adapted bottom-friction inspired by Gauer (2020) and Gauer et al. (2023). Both MoT-PSA and RAMMS::EXTNDED must be regarded as pre-release versions.

The scope of this paper is not to perform a back-calculation of a specific event, nor to verify or validate the models. Rather, it aims to test the type of results a practitioner might obtain as a best first estimate, and how those results compare to actual measurements. To this end, the models were run using commonly proposed parameter values for relevant avalanches, i.e. avalanches of relative size $\geq R3$. While no specific observed event was selected for back-calculation, the avalanche event of 2021-04-11 was kept in mind as a representative reference.

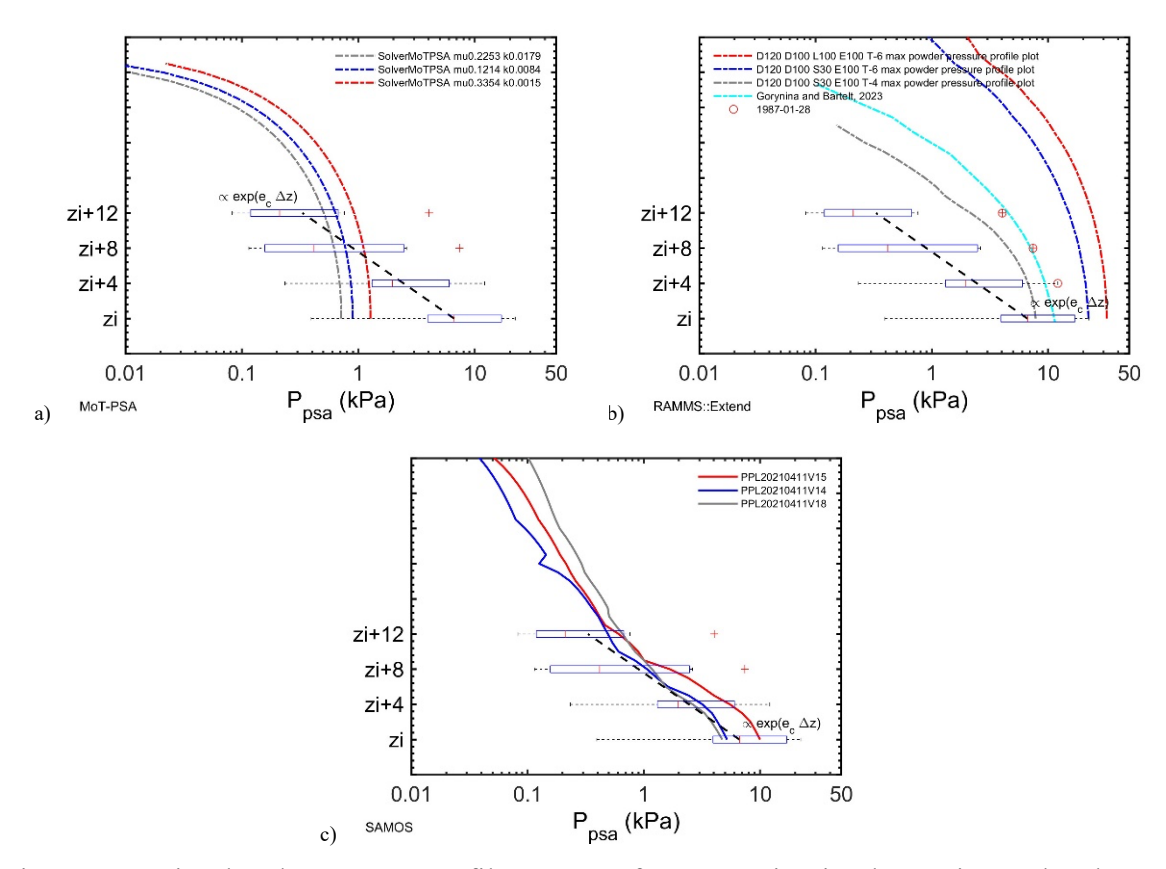


Figure 3.2 Simulated pressure profiles at a reference point in the main avalanche track, corresponding to the original location of the power assembly. Shown are peak pressures over time. For comparison boxplots of the observational data are included. a) MoT-PSA b) RAMMS::Extended c) SAMOS-AT

Figure 3.2 presents the tests of the three models, each with simulations with slightly changing parameters. The version tested for MoT-PSA corresponds to the one presented in Vicari and Issler (2023). It is evident that the pressures in the lower section of the powder part are consistently underestimated, while pressures above approximately 12 m above the interface tend to be overestimated. A significant portion of the underestimation at the interface can be attributed to the predicted densities being relatively low—typically less than 2 kg m⁻³—and only weakly dependent on avalanche velocity. At the same time, the predicted flow height of the powder part remains around 30 meters. This underestimation of interface pressures is also evident in Vicari and Issler (2023, Fig. 7 d).

The first back-calculations using RAMMS:EXTEND for the power line assembly at the Ryggfonn test site were conducted by Gorynina and Bartelt (2023). They focused on the event 1987-02-28, which, by coincidence, was the fastest event recorded at the power line and produced the highest PSA pressures in the measurements (marked in the figure). These pressure values were reproduced in the simulations. Additionally, three simulations from a sensitivity analysis (NGI, 2025) are presented. In terms of pressure, all these simulations tend to fall on the higher end—or even exceed—the observed values. Some of the simulations also indicate elevated pressures at significant heights. Moreover, certain simulations suggest flow densities for the powder-snow component that are higher than commonly assumed. The simulations further reveal that the model is sensitive to variations in certain input parameters.

The simulations using SAMOS were conducted with a Coulomb friction coefficient of $\mu = 0.28$, which allowed the avalanche to reach the dam in the valley bottom approximately 49 seconds after initiation—consistent with observations from the event on 2021-04-11. For testing purposes, only the parameters "ParticlesSuspensionCoeff" and "ParticlesDiameter", which influence the suspension behavior in SAMOS, were slightly varied. Under these conditions, the simulated pressures generally fell within the range expected from measurements. However, slightly higher pressures may be present at elevations above 12 m from the dense flow-powder interface.

4. CONCLUDING REMARKS

This paper presents a comparative analysis of unique historical pressure measurements from a power line structure at the Ryggfonn avalanche test site and simulation outputs from three powder snow avalanche models: SAMOS, RAMMS::Extended, and MoT-PSA—the latter two being prerelease versions. The comparison offers valuable insights into each model's ability to replicate observed pressure profiles within the suspension layer and highlights their respective strengths and limitations. However, due to the limited availability of suitable data, comprehensive model validation remains incomplete. A visual impression of the powder cloud alone can be misleading, as even a snow concentration as low as 0.001 can reduce visibility to range of approximately 1 m (cf. Mellor and Mellor, 1988).

These models can serve as valuable tools for practitioners, providing essential input for hazard assessments and the design of mitigation measures. To be truly effective in practical applications, they must deliver fast and reliable first-guess results, even when input data are limited. At the same time, the growing complexity of avalanche dynamics models demands a deeper level of understanding from users, as well as increased awareness of their sensitivity to key input parameters.

ACKNOWLEDGEMENT

Parts of this work was financially supported by the Norwegian Ministry of Oil and Energy through the project grant "R&D Snow avalanches 2023–2025" to NGI, administrated by the Norwegian Water Resources and Energy Directorate (NVE). We thank Marc Christen (RAMMS AG) and Perry Bartelt for the access to RAMMS::Extended (pre-release).

REFERENCES

- Coaz, J. W. (1889) Der Lawinenschaden im schweizerischen Hochgebirge im Winter und Frühjahr 1887–88, Stämpfli, p. 67
- McElwaine, J. N., Turnbull, B. (2005) Air pressure data from the Vallée de la Sionne avalanches of 2004, Journal of Geophysical Research: Earth Surface, Vol. 110, No. F3 p. No. F03010, doi:10.1029/2004JF000237.
- Gauer, P., Issler, D., Lied, K., Kristensen, K., Sandersen, F. (2008) On snow avalanche flow regimes: Inferences from observations and measurements. Proceedings of the

- International Snow Science Workshop 2008, September 21- 27, Whistler, British Columbia, Canada, p. 717-723
- Gauer, P., Kristensen, K. (2016) Four decades of observations from NGI's full-scale avalanche test site Ryggfonn---Summary of experimental results, Cold Regions Science and Technology, Vol. 125, p. 162-176, doi: 10.1016/j.coldregions.2016.02.009.
- Gauer, Peter (2020) Considerations on scaling behavior in avalanche flow: Implementation in a simple mass block model, Cold Regions Science and Technology, Vol. 180, p. 103165.
- Gauer, P. (2023) Cross-Comparison of Selected Avalanche Observations. International Snow Science Workshop Proceedings, Bend, Oregon, , 8-13 October 2023, p. 436-443
- Gauer, P., Body, N.S., Aalerud, A.H. (2023) What Avalanche observations tell us about the performance of numerical models, International Snow Science Workshop Proceedings, Bend, Oregon, 8-13 October 2023, p. 120-127,
- Glaus, J., Jones, K., Wikstrom, Bühler, Y., Christen, M., Ruttner-Jansen, P., Gaume, J., Bartelt, P. (2023) RAMMS::EXTENDED Sensitivity analysis of numerical fluidized powder avalanche simulation in three-dimensional terrain. International Snow Science Workshop Proceedings 2023, Bend, Oregon, p. 795-802
- Glaus, J.; Wikstrom Jones, K.; Bartelt, P.; Christen, M.; Stoffel, L.; Gaume, J.; Bühler, Y. (2025) Simulation of cold-powder snow avalanches considering daily snowpack and weather situations Natural Hazards and Earth System Sciences, Vol. 25, No. 7, p. 2399-2419
- Gorynina, O., Bartelt, P. (2023) Powder snow avalanche impact on hanging cables International Journal of Impact Engineering, Vol. 173 p. 104422, doi:10.1016/j.ijimpeng.2022.104422.
- Gerber, E., Rohrer, E. (1956) Wesen und Wirkung der Staublawinen. Die Alpen SAC p. 52-57.
- Mellor, M.; Mellor, A. (1988) Some characteristics of falling snow. Cold Regions Science and Technology, Vol. 15, No. 2 p. 201-206
- NGI 20230100-07-TN (2025) AARN-Applied Avalanche Research in Norway: RAMMS::Extended sensitivity analysis. Norwegian Geotechnical Institute.
- Norem, H. (1995) The Ryggfonn Project: Summary Report 1981—1995, No. A952-1, Dr. ing. Harald Norem A/S Consultant in Snow Engineering, Molde, Norway.
- Sampl, P., Granig, M. (2009). Avalanche simulation with SAMOS-AT. Proceedings of the International Snow Science Workshop Proceedings Davos 2009, p. 519–523
- Scheiwiller, T. (1986) Dynamics of powder-snow avalanches PhD thesis ETH Zurich.
- Statens vegvesen (2014) Veger og Snøskred, No. V138 Statens Vegvesen, Statens Vegvesen.
- Task Force B2.12.3 (2016). Sag-tension calculation methods for overhead lines. Technical report.
- Takeuchi, Y., Torita, H., Nishimura, K., Hirashima, H. (2011) Study of a large-scale dry slab avalanche and the extent of damage to a cedar forest in the Makunosawa valley, Myoko, Japan, Annals of Glaciology, Vol. 52, No. 58 p. 119-128
- Tochon-Danguy, J.-C. / Hopfinger, E. J. (1975) Simulation of the dynamics of powder avalanches, In Rodda, J. C. (Ed.), The International Symposium on Snow Mechanics,

- Grindelwald, Switzerland, April 1-5, 1974, Vol. 114 IAHS Publ. Int. Assoc. Hydrol. Sci.: Wallingford, Oxon OX10 8BB, UK p. 369-380
- Turnbull, B., McElwaine, J. N. (2007) A comparison of powder-snow avalanches at Vallée de la Sionne, Switzerland, with plume theories Journal of Glaciology, Vol. 53, No. 180, p. 30-40, doi:10.3189/172756507781833938.
- Vicari, H., Issler, D. (2023) MoT-PSA: a two-layer depth-averaged model for simulation of powder 1 snow avalanches on three-dimensional terrain, Annuals of Glaciology e16, (1-6) doi:10.1017/aog.2024.10.

Next-Generation Modular Avalanche Radar with Multi-Hazard Capabilities

Susanne Wahlen, 1* Lorenz Meier, 1 and Severin Staehly 1

¹ Gravimon Ltd. Zurich Switzerland

ABSTRACT

Doppler radars have proven highly effective for real-time avalanche detection in road safety alarms system, avalanche control verification, and forecasting. However, current radar systems often rely on radar hardware not originally intended for avalanche-detection, leading to limitations in spatial coverage, robustness, power requirements, reliance on experts, processing power, off-season applicability and ultimately costs.

To address these challenges, we developed a compact, fully modular and purpose-built Doppler radar system for avalanche detection, with the goal of simplifying radar-based monitoring and expanding its applicability.

The system features a 90° horizontal × 40° vertical field of view and up to 10 km range, optimized for monitoring of multiple avalanche paths with a single unit. It operates in the 9-11 GHz band and offers flexibility for frequency licensing in different regions. The radar unit has improved antenna geometry and optimized real-time algorithms to reduce false alarms, while faster processing allows for shorter reaction times. Power consumption is significantly reduced compared to conventional systems, enabling solar-only operation in most environments.

The compact, shoebox-sized modules allow for plug-and-play setup, rapid deployment and seasonal relocations without expert support, e.g. spring road clearance or summer rockfall detection. Trailer-mounted, the system offers flexible use and is well-suited for road agencies engaged in multi-hazard monitoring. A weather station is also integrated to support AI-based forecasting by identifying avalanche-related patterns in growing event datasets.

In this contribution, we present initial field results from pre-series (C-sample) deployments conducted during summer 2025 on ice avalanches in Switzerland.

Development of snow sensors in Ísafjörður

Harpa Grímsdóttir^{1*} and Örn Ingólfsson²

¹ Icelandic meteorological Office, IS-105 Reykjavík, Iceland
 ² POLS Engineering ehf, Urðarvegur 72, IS-400 Ísafjörður, Iceland
 *Corresponding author, e-mail: harpa (at) vedur.is

ABSTRACT

The SM4 snowsensor has been produced and developed by a small innovation company POLS Engineering in Ísafjörður since the year 2004. The aim was to create an instrument that would perform well during periods of heavy snowdrift and icing and would be relatively easy to install in steep mountain slopes.

The SM4 snow sensor consists of a cable with thermistors mounted at 20 cm interval. The basic output is a temperature profile and an algorithm calculates the snowdepth. The data from SM4 are displayed in various ways on www.snowsense.is. The website was redesigned in 2024 and the hardware of the SM4 is now being upgraded as well as the transmission unit, working towards an instrument that is simpler in production and more robust.

The SM4 snow sensors are currently installed at 32 locations in Icelandic mountains for the purpose of monitoring avalanche danger. It has evolved to be one of the most important instruments for the avalanche forecasting team at the IMO, which uses data on snow depth, air temperature and, no less importantly, the temperature gradient within the snowpack.

1. PRODUCTION OF SM4 AND RECENT UPDATES

Automatic snow-depth measurements are important for avalanche monitoring since the rate of loading is one of the most important variables for predicting triggering of avalanches. Following avalanche catastrophes in Súðavík and at Flateyri in 1995, avalanche monitoring in Iceland was strengthened. Snow stakes were installed in avalanche starting areas making it possible to read the snowdepth with binoculars. At a few selected locations, acoustic snow-depth sensors were installed in steep mountains on 5–6 m high aluminium masts.

The acoustic sensors worked well most of the time, but during periods of heavy snowdrift or icing, the measurements would often be disrupted. The aim with SM4 was to create an instrument that would perform well during these periods and would be relatively easy to install in steep mountain slopes. The SM4 snow sensor consists of a cable with thermistors mounted at 20 cm interval, a data logger and a data transmitter. The cable is mounted on a pole and an algorithm calculates the snow depth based on fluctuations of the temperature, which is greater in the air than within the snow. The data is transmitted via the GSM system.

Since 2004, the SM4 snow sensor has been installed at 32 locations in the Icelandic mountains. Most of the sensors are operated by the Icelandic Meteorological Office (IMO) while the Road Administration (IRCA) owns some of them.

In 2024 and 2025, a new version of SM4 has been developed. The new type has a simpler, yet more comprehensive control unit, which makes the construction of the instrument easier and

results in a more robust sensor. It also facilitates the addition of different types of sensors to the instrument. All new SM4s have a laser sensor as an additional way of measuring snow depth, and it is possible to add anemometer as well. It is possible to programme and control the instrument remotely in a better way than before. The older version was running on the 2G system, which will be shut down in Iceland at the end of the year 2025. Therefore, new data transmission units have been developed running on 4G, using the NB (NarrowBand) and LTE (Long Term Evolution) systems.

A new version of the snowsense is website was launched in 2024 and continues to be developed in cooperation with the avalanche monitoring group at the IMO. The data are displayed in various ways, giving information on snow depth in real-time, the temperature profile in the snow, rough depth of possible weak layers and air temperature. The web site also contains photos of the installation of each instrument and a log of maintenance and malfunctions.

2. UTILISATION

The SM4 sensor and snowsense is have been developed in cooperation with the avalanche monitoring group at IMO from the beginning, to ensure the usability of the data.

The data from SM4 are used in various ways:

- The direct output from SM4 is a temperature profile which implicitly shows *the temperature gradient* in the snow cover. Steep gradient is favourable for the formation of weak layers.
- Information on *snow depth* is derived from the data. Scrolling the temperature profile in time gives information about the snow depth because the temperature fluctuates more in the air than within the snow cover. An algorithm calculates the snow depth, which is displayed in a graph.
- Wet snow is constant at zero degrees Celsius and, therefore, the data give indications on how far into the snow cover *the effect of thaws* reach, which is useful when predicting wet snow avalanches or slushflows.
- Snow that has been through melt–freeze cycles is also at zero degrees Celsius. In Iceland, thaws and rain-on-snow events are common throughout winter. This means that the snowpack becomes wet throughout and then refreezes. A typical snowpack condition in Iceland consists of a melt–freeze crust at the bottom which may be up to a few meters thick in some places, with layered snow cover on top. The thick crust is stable, but the layered snow needs attention. The temperature profiles from SM4 show clearly the amount of layered snow and the thickness of the crust at the site where they are installed.
- An algorithm calculates a *faceting index* based on the temperature gradient. The algorithm is based on the snow model Crocus. Lines of different colours appear on snow-depth graphs where the temperature difference between two sensors matches the criteria for faceting, showing the calculated faceting index and the approximate depth of the possible weak layer.
- The air temperature is also useful output. It provides information about the temperature at different hights in the mountains, since SM4 are installed close to various potential starting areas.

3. CONCLUSIONS

The SM4 sensor was developed by a small innovation company in Ísafjörður to fulfil the need for a robust and simple instrument that could provide valuable information on the snowpack for avalanche forecasting. It was developed in cooperation with the avalanche monitoring team at the IMO and has become an important instrument for avalanche forecasting in Iceland. Recently, a new version of SM4 was built and is now being tested in the mountains. A few papers on SM4 are listed in the references section below, providing more detailed description and graphs.

REFERENCES

- Grímsdóttir, H., Ingólfsson, Ö., 2010. Sjálfvirkar snjódýptarmælingar á upptakasvæðum snjóflóða. Reynslan af SM4 snjómæli. Icelandic Meteorological Office. VÍ 2010-008.
- Grímsdóttir, H., Ingólfsson, Ö., 2016. Utilisation of the SM4 automatic snowpack sensor in avalanche forecasting. Proceedings Breckenridge 2016 International Snow Science Workshop, 642–644.
- Ingólfsson, Ö., Grímsdóttir, H., 2008. The SM4 snowpack temperature and snow depth sensor. Proceedings Whistler 2008 International Snow Science Workshop, 808–811.
- Ingólfsson, Ö., Grímsdóttir, H., 2012. Monitoring snowpack temperature gradient using automatic snow depth sensor. Proceedings Anchorage 2012 International Snow Science Workshop, 956–960.

Experiences in designing mitigation measures against slushflows

Elise Morken^{1*}, Sunniva Skuset¹ and Peter Gauer¹

¹ Norwegian Geotechnical Institute, Postboks 3930 Ullevål Stadion, NO-0806 Oslo, NORWAY *Corresponding author, e-mail: elise.morken@ngi.no

ABSTRACT

The Norwegian Geotechnical Institute, NGI, has collaborated as a subcontractor to Aas-Jakobsen, a construction consultancy in Norway, on a project for Bane NOR, the Norwegian railway authority responsible for the infrastructure. This project focused on designing mitigation measures to protect the northernmost section of the Norwegian railway, Nordlandsbanen, from gravity-driven mass flows, including debris- and slushflows.

As of today, the project has included the design of eight debris flow nets, each equipped with a secondary finer mesh behind the primary retention net, to mitigate both debris- and slushflows along the railway. The recommendation was based on the developing approach that a secondary mesh with smaller mesh sizes will better retain slushflows, which mainly consist of water-saturated snow, compared to using a single net with larger mesh sizes.

Debris flow nets were recommended due to their cost-effectiveness, minimal space requirements, and ease of transport by helicopter to remote locations. However, there is limited data and experience on the effectiveness of using debris flow nets against slushflows. Our concern is that for slushflows with high water-to-snow ratio, a debris flow net with a secondary mesh might not be able to retain the slushflow sufficiently enough. While debris flow nets have proven to retain debris and reduce the velocity, a snow- water mixture may continue downslope, as observed in an event in Straumen (Nordland County/ Northern Norway). To date, five of the nets have been constructed, but have not yet been tested. The presentation will include a summary of our experiences regarding designing mitigation measures against slushflows for the Norwegian railway authorities.

1. INTRODUCTION

"Nordlandsbanen" is the longest railway line in Norway, measuring 729 km. The line runs between Steinkjer and Bodø (Figure 1). The railway line is an important part of the Norwegian infrastructure, serving as the primary land-based transport route for freight between northern and southern Norway. Traffic delays are therefore highly critical and must be avoided, even at significant cost.



Figure 1 The railway line "Nordlandsbanen", shown as a black line, located between Steinkjer and Bodø, Norway.

The railway line is located in complex terrain exposed to rockfalls, snow avalanches, landslides, debris flows and slushflows. The climate in the region adds to the complexity, particularly regarding slushflows, which are strongly dependent on specific weather conditions.

The project presented is a continuation of a hazard mapping conducted by NGI and commissioned by Bane NOR, the Norwegian railway authority responsible for the infrastructure, in 2022. The hazard mapping included a risk assessment of rockfalls, snow avalanches, landslides, debris- and slushflows, as well as icefalls, originating from natural terrain along the railway. The mapping serves as a foundation for quantifying landslide risk along the railway and evaluating safety measures to mitigate hazards along exposed sections of the railway. A cost-benefit analysis of the proposed measures was carried out to enable Bane NOR to prioritize those offering the greatest risk reduction relative to their cost. Measures were proposed where the annual probability of landslides was considered to exceed 1/200. Based on the cost-benefit analysis, NGI has provided preliminary designs of mitigation measures from the priority list given by the analysis. Several of the recommended mitigation measures against debris- and slushflows ended up high up on the priority list. Thus, some of the measures recommended against these natural hazards have already been finalized.

In the following sections, a literature review, along with NGI's experience in the process—from recommending solutions to calculating loads—is presented.

2. METHODOLOGY

NGI's role as the subcontractor to Aas-Jakobsen, was to perform site inspections, model flow dynamics, recommend optimal mitigation measures and calculate the expected load on the structures. Aas-Jakobsen was responsible for drawing and describing the structures for the tender competition organized by Bane NOR for the construction of the mitigation measures. General rules regarding requirements and principles for safety and durability of structures were followed. In cases where existing standards did not cover the dimensioning of special structures, relevant guidelines from Alpine countries were adopted (Berger et al., 2021).

2.1 Mitigation aim

To calculate the appropriate type and required strength of the mitigation measures, a mitigation aim was selected by Bane NOR. The mitigation aim was to protect the railway line against debris- and slushflows with a nominal annual probability of 1/100.

2.2 Modelling

Several aspects of slushflow dynamics are poorly understood, including velocity, flow depth and pressure (Barbolini et al., 2024). Currently, there are no dynamic models specifically tailored for slushflows (Hamre et al., 2024; Jaedicke et al., 2022; Skred AS, 2021). And only a few attempts have been made to back calculate slushflows (Ragulina, 2015; Gauer 2004, Skred AS, 2021, Barbolini et al., 2024). Dynamical models tested for modelling slushflows include among others RAMMS::AVALANCHE, RAMMS::DEBRISFLOW, SAMOS, REEF3D and OpenFOAM. Although the models are not developed for modelling slush flows, the models can simulate various snow-related flows by adjusting friction parameters (Barbolini et al., 2024; Hákonardóttir, 2024; Hansen et al., 2024; Herberg, 2021; Jones, 2019; Pétursson, 2019; Skred AS, 2021).

When dimensioning the mitigation measures in this project, SAMOS was used for modelling flow dynamics such as velocity and height (Hamre et al., 2024; Barbolini et al., 2024). The mitigation aim provided guidance on the design impact magnitude that the structures need to withstand. Among other, SAMOS was used due to its ability to simulate flow interactions with mitigation measures.

2.3 Mitigation measures

There is limited empirical understanding of the dynamic interaction between moving slushflow masses and large-scale structural elements within the flow path. However, a few small-scale experiments have been conducted to investigate slushflow structure interactions (Herberg, 2021; Hákonardóttir, 2024; Jones, 2019; Pétursson, 2019) and recent efforts have explored the application of flexible net barriers as a mitigation strategy (Herberg, 2021; Skred AS et al., 2021). Such nets have for example been installed along ravines susceptible to slushflows. For instance, along the railway west of Voss, and along a road in Straumen, Nordland. Additionally, in Vannledningsdalen, Svalbard, 14 nets have been put up to mitigate large slushflows in the valley (Skred AS et al., 2021).

To mitigate debris and slushflows in several ravines along the railway, NGI recommended flexible net barriers equipped with secondary mesh featuring smaller openings than the primary retention net. Although using nets to mitigate slushflows has certain limitations, the use of permeable barriers is intended to capture larger debris and reduce flow velocities, thereby limiting potential damage to the railway line. Excessive water escaping through the barrier is assumed to have reduced velocities compared to upstream the net, thus the erosive potential is reduced. This approach was recommended due to its cost-efficiency, minimal spatial requirements, and logistical advantages, particularly its suitability for aerial transport via helicopter to remote or otherwise inaccessible locations.

2.4 Design criteria

The practical guide for debris flow and hillslope debris flow protection nets by Berger et al. (2021) served as a basis for the design of the mitigation measures. The height of the nets was calculated based on the expected snow height in the area and the calculated flow height of slushflows with a nominal annual probability of 1/100. However, in some cases the mitigation

aim was reduced to a nominal annual probability of 1/50 by request from Bane NOR due to cost constraints. Static and dynamic loads on the nets were calculated based on the modelling results in SAMOS. In most cases, the planned foundation sites were located on bedrock with only a thin soil cover, allowing the foundations to be anchored directly into the bedrock.

3. RESULTS

In total, NGI have dimensioned eight mitigation measures against debris- and slushflows within the project (NGI, 2023; NGI, 2024). As of May 2025, Bane NOR has finalized five of the debris flow nets along "Nordlandsbanen". As far as we know, none of these systems have yet been subjected to full-scale debris- or slushflows. Bane NOR, together with the net-manufacturer, made modifications to NGI's proposals. The flexible barriers that ended up being installed were the TECCO-SL-100 delivered by Geobrugg (Figure 2). Instead of a two-net system, a singular net with mesh sizes of 6,3 cm, typically used to mitigate shallow landslides, was installed.



Figure 2 One of the flexible barriers installed along the railway line (Photo: Bane NOR).

4. KEY POINTS TO BE SOLVED AND OUTLOOK

As stated by Gauer (2004) and still holds true, no direct measurements of velocity or pressure are currently available for slushflows, and flow dynamics remain poorly understood (Jaedicke et al., 2022). Due to scale effects, small-scale modelling has limited applicability (Herberg, 2021), underscoring the need for full scale experiments (Jaedicke et al., 2022). Further investigation into slushflow mitigation interaction is warranted (Herberg, 2021). Testing of protection measures in frequently affected areas is suggested. Additionally, small-scale tests using water saturated snowpacks may support evaluation of drainage and vegetation-based mitigation (Jaedicke et al., 2022).

ACKNOWLEDGEMENT

The authors want to thank all involved in this project; Bane NOR, Aas-Jakobsen Trondheim and our colleagues contributing to the project at NGI.

REFERENCES

Barbolini, M. et al. (2024) The Lillet Lake Avalanche – A potential slushflow case for Italian alps. Proceedings, International Snow Science Workshop, Tromsø, Norway, 2024.

Berger, C., Denk, M., Graf, C., Stieglitz, L., Wendeler, C., (2021) Practical guide for debris flow and hillslope debris flow protection nets. WSL Berichte 113. 79 p.

Gauer, P. (2004) Numerical modelling of a slushflow event. Proceedings of the International Snow Science Workshop 2004, Jackson Hole, Wyoming, United States p. 39-43.

Hákonardóttir, K. M. (2024) Stopping slushflows-small scale laboratory experiments and fullscale numerical simulations-2024. Proceedings, International Snow Science Workshop, Tromsø, Norway, 2024.

Hansen, V. E. et al. (2024) Limitations of RAMMS::DEBRISFLOW as a slushflow simulation tool. Proceedings, International Snow Science Workshop, Tromsø, Norway, 2024.

Hamre, D. et al. (2024) Observations and modelling of slushflows – Atigun Pass, Alaska. Proceedings, International Snow Science Workshop, Tromsø, Norway, 2024.

Herberg, T. S. (2021) Fleksible nettkonstruksjoner som sikringstiltak mot sørpeskred i Vannledningsdalen. Masteroppgave i Bygg- og miljøteknikk. NTNU. Veileder Arne Alberg. Juli 2021.

Jaedicke, C. et al. (2022) Sørpeskred – Egenskaper, historikk og sikringsløsninger. Klima2050 Rapport Nr. 38 -2022.

Jones, R. A. (2019) The Design of Slushflow Barriers: CFD Simulations. Magister Scientiarum degree in Mechanical Engineering. University of Iceland.

NGI (2024) Dimensjonering sikringstiltak: Bjerka – Fauske,561.524-561.534. Prosjektering av sikringstiltak på Nordlandsbanen. Dok.nr. 20240298-08-TN.

NGI (2023) Dimensjonering av prioritet 1: Lønsdal – Fauske, km 624.160-324.470. Prosjektering av sikringstiltak på Nordlandsbanen. Dok.nr. 20230456-02-TN.

NGI (2021) FoU 80606 – Identifisering av løsneområder for sørpeskred. Klassifikasjon og beskrivelse av de mest typiske løsneområdene for sørpeskred. NVE. Ekstern rapport Nr. 8/2021.

Pétursson, H. Ö. (2019) Use of OpenFOAM and RAMMSAVAl to simulate the interaction of avalanches and slushflows with dams. International Symposium on Mitigative Measures against Snow Avalanches and Other Rapid Gravity Mass Flows Siglufjörður, Iceland, April 3–5, 2019.

Ragulina, G., Lied, E., Smebye, H., Gauer, P. (2015) NGI 20140053 Annual report Results 2015 from SP 4 FoU Snøskred: Work Package 3 — Slushflows 2016 Norwegian Geotechnical Institute.

Skred AS (2021) FoU – Bruk av RAMMS::DEBRISFLOW på kjente sørpeskredhendelser. NVE. Ekstern rapport Nr. 9/2021.

Skred AS, HNIT (2021) Forprosjektering av nettløsning mot sørpeskred i Vannledningsdalen. Dokumentnummer 18241-25-1.

Skred AS, HNIT (2018) Forprosjektering av sikringstiltak – Fase B2. Dokumentnummer 18241-03-4.

Slushflows – A review of a poorly explored phenomenon and its protection measures

Nadine Feiger^{1*} and Corinna Wendeler¹

¹ Mountain Hazard Engineering GmbH, Nussweg 12, CH-4800 Zofingen, SWITZERLAND *Corresponding author, e-mail: nadine.feiger (at) mountainhazard.ch

ABSTRACT

Slushflows are a gravitative flowing mass movements that are most commonly found in Artic regions, and which pose a significant hazard to human life and infrastructure. Despite the clear general classification, a unique definition of the process is lacking among the scientific community. The prospect of enduring climate change and the subsequent increased likelihood of slushflows posing a serious hazard also to people and infrastructure in regions of lower latitude requires clarity on this process and calls for effective mitigation measures. In this study, we aim to shed some light on the main properties that characterise slushflows and the processes involved by reviewing the available literature. Next, we analyse the various protection and mitigation measures that can be used to counteract and mitigate this phenomenon. These range from traditional dams to more advanced solutions such as flexible nets and early warning systems. We elucidate how cutting-edge numerical simulations, precise hazard mapping, and effective protective measures help to advance the understanding of slushflows, contributing to the protection of communities and infrastructure, as well as mitigating the risks associated with these flowing mass movements.

1. INTRODUCTION

The terminology slushflow indicates a multi-phase flow consisting of a mixture of liquid and solid composed of the same material that is partially solidified (Reynier et al., 2010). When it comes to natural hazards, slushflows are gravitative mass movements composed of water saturated snow flowing downhill. These events are mostly found in arctic and subarctic regions, but are increasingly present also at lower latitudes as consequence of climate change (Jaedicke et al., 2007; Furdada et al., 1999; Hestnes and Jaedicke, 2018; Barbolini et al., 2024). Slushflows can come in different size and, besides snow and ice, carry along a variety of other components, ranging from rocks and soil to wood and, more generally, vegetation (D'Amboise et al., 2024, Fig. 1), making them a highly complex phenomenon to understand and model (e.g., Gauer, 2004).

Compared to well-known gravitational mass movements, such as debris flow or avalanches, slushflows can generate also on very shallow and gentle slopes, which can be way below 30° (e.g., Bozhinskiy et al., 1998, Gude and Scherer, 1998; Hansen et al., 2024; Jaedicke et al., 2024; Sund et al., 2024). While there is an obvious similarity with avalanches, slushflows share also several characteristics with debris flows, one of which is outlined in Jaedicke et al. (2007): slushflows move in surges, sharing thus an important movement characteristic with the debris flows. Additionally, slushflows result in higher impact forces than dry avalanches of similar

N. Feiger, C. Wendeler O10.2 - Page 244

size and velocity, outlining the importance of slushflow-specific design criteria when planning protective measures (Jaedicke et al., 2007).

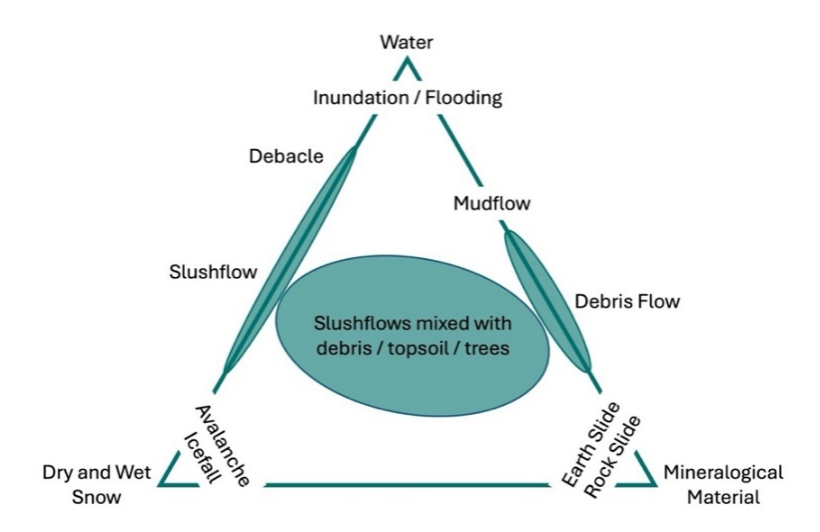


Figure 1 Classification of rapid gravitational mass movements, depicting the complex nature of slushflow events according to Hestnes and Jaedicke, 2018.

Despite many efforts to clearly identify the driving processes and the typical release areas of slushflows (e.g., Gauer, 2004; D'Amboise et al., 2024; Jaedicke et al. 2024), many uncertainties concerning these phenomena remain. Generally, slushflows occur during the snowmelt period or during heavy rains in wintertime, where the water inflow in the snowpack is higher than its outflow, leading to an increase of water saturation and lower grains attraction in the snow, creating, thus, perfect conditions for an abrupt release of a mass of slush (Gude and Scherrer, 1998). Similarly to the influence of snow-water content, coarse-grained snowpack also provides favourable conditions for the development of slushflows (Hestnes and Bakkehøi, 2004). Apart the hydraulic and snowpack characteristics, to meet ideal conditions for a slushflow to be released, terrain topography plays a crucial role. Terrain features leading to pooling of water in the snow cover can be ideal release areas for slushflows (Jaedicke et al., 2024). In their study, Jaedicke et al. (2024) concluded that although the majority of slushflow events happen in streams and depressions, open slopes and bogs cannot be neglected as starting zones. Despite identifying an overall trend, slushflows release areas characterisation remains difficult and a direct combination with weather, hydrological, and snow data is necessary to reduce possible starting locations to a reasonable number (Jaedicke et al., 2024). Uncertainties in the driving physics and in typical release areas lead to a reduced efficiency and accuracy of hazard mitigation measures.

To mitigate natural hazards, numerical models are widely used in spatial planning and the application of protection measures. Despite specific tools for debris flow, avalanches, and other flowing mass movements, no specific numerical tool for slushflow events has been entirely developed yet (Hansen et al., 2024). The high complexity of the slushflow process, coupled with the uncertainties and high sensitivity of the input parameters, makes accurately modelling of impact pressures and runout zones of flowing slush extremely difficult (Gauer P., 2004; Hansen et al., 2024). This calls for more and better data to calibrate numerical models and to develop new cutting-edge numerical tools that can accurately model such gravitational events. Thereby, spatial planning and application of protective measures improve significantly.

As of today, several measures are already applied to mitigate the slushflow hazard, such comprehend early warning systems (e.g., Sund et al., 2024), and technical protective measures (e.g., Hestnes and Sandersen, 1998). Despite their widespread use, these measures are mostly taken directly from those used to counteract other types of gravitational mass movement. While most systems are suitable for slushflows, several protective measures require adaptations and specific designs for this purpose. In this short study, we aim to show some key aspects that need to be considered in the design of protective measures against slushflows. We focus on different mitigation measures along the flow path of slushflows and point out where suitable measures can be installed and show the constraints of the measures.

2. APPROACH

2.1 General applied mitigation concept

The general concept applied to technical mitigation measures of flowing mass movements, and thus also slushflows, are subdivided into three main technical principles: conveyance, retention, and deflection. The first, avoids any direct action against the hazard. Instead, conveyance involves keeping the path clear, ensuring that infrastructure is not in the path of the hazard (e.g., building of galleries), and directing the flow in the desired direction and along the desired path. This can be achieved by proper area and land use planning aspects. This principle is especially suitable when the other two are disproportionate or impossible. The retention principle aims to reduce the menace directly at the source zone, along the flowing path or at the runout zone by a number of structural measures, such as retention basins, barriers, or landscape measures. These structural measures focus on reducing energy and/or volume of the moving mass before reaching the protected objects. Deflection tries to deliberately deflect the incoming flowing material by deflecting dams, embankments, or walls, away from the sensitive zones and endangered areas. This principle is often used when retention measures are not practicable or when the application of the conveyance principle would lead to severe damages and losses.

In practice, an effective mitigation measure is often the result of a combination of different principles. The best choice of these technical principles depends on the risk to be mitigated, technical feasibility and cost benefit of protection measures.

2.2 Location of mitigation measures

The technical measures for gravitational mass movements are spatially distributed along the flowing path in three main sections: release area, transition zone, and deposition zone. Depending on the hazard type and the local site conditions, it is more suitable to mitigate the hazard in the release area, transition zone, deposition zone, or eventually in several zones combined.

Mitigation measures in the release area are purely active measures, such as flexible or rigid support structures for the snowpack, or rigid walls, and serve to prevent the release of the hazard itself addressing directly the source of it. On the other hand, passive measures are widely used in the transition and deposition zone, where galleries, reinforced earth dams, walls, catchment basins, and flexible netting is used for guiding the flowing mass on a certain path, slowing it down, or stop it and catch the released mass.

N. Feiger, C. Wendeler O10.2 - Page 246

2.3 Slushflow mitigation measures classification

Construction and technical mitigation measures are classified based on Hestnes and Sandersen, (1998) according to the zone in which they operate and the variable/process they control (Fig. 2), or to the technical principles of mitigation measures: conveyance, retention, and deflection (Fig. 2). Most of the mitigation measures listed in Fig. 2 are well-known measures, which are used for avalanche and debris flow hazard mitigation measures. With the appropriate adaptation and consideration for the different physics and parameters, those well-known measures can be easily transposed to use them against slushflows. Early warning systems can be used, also in combination with protective mitigation measures outlined in Fig. 2, but they are not further addressed in this study.

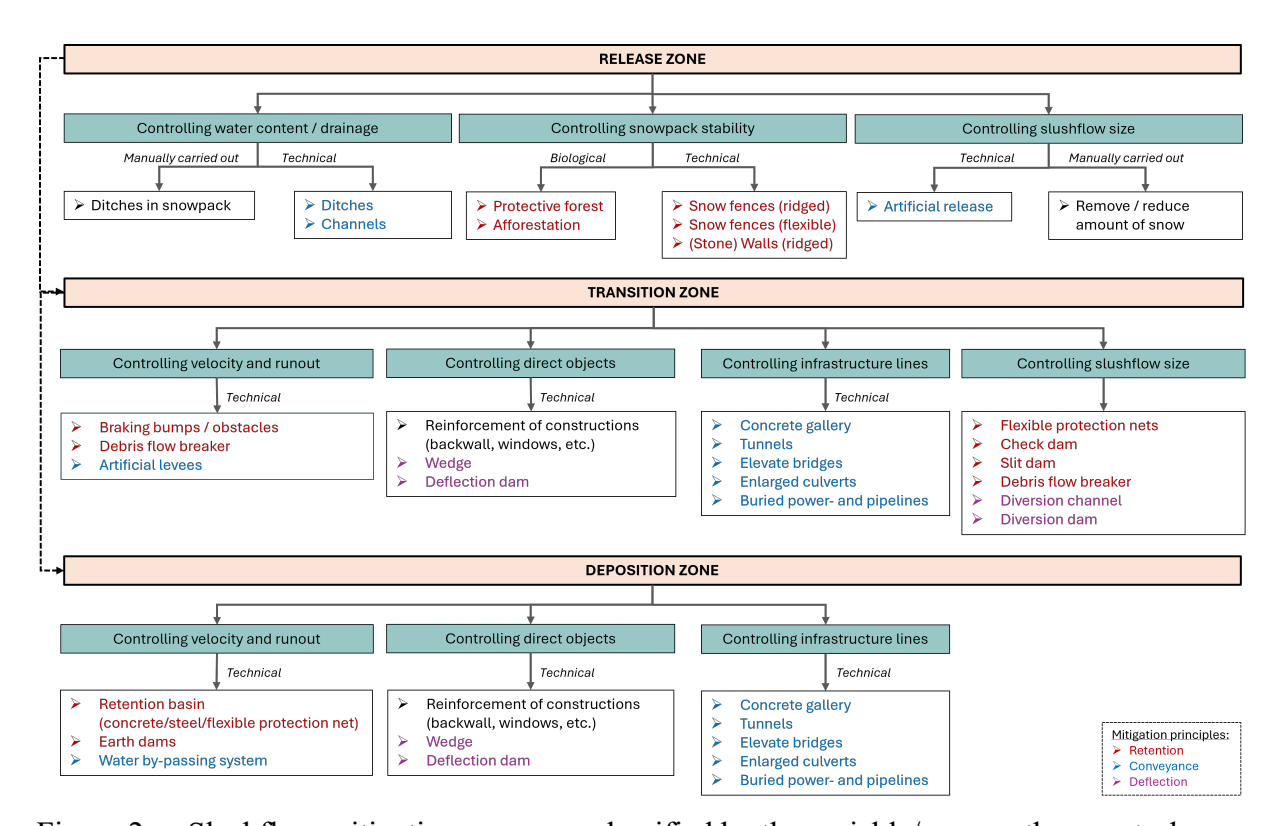


Figure 2 Slushflow mitigation measures classified by the variable/process they control.

2.3.1 Release zone

In the release zone, mitigation measures based on the retention principle, as well as some conveyance measures, are appropriate. Three control variables are identified to manage the risk of a slushflow release and its potential release volume. These are controlling the water content and drainage, controlling the stability of the snowpack, and controlling the size of the slushflow. The latter includes artificial release, which has not yet been fully effective for slushflows, and reducing the amount of snow, which must be carried out by someone on site. Trenching the snowpack must also be carried out by someone on site as for example it was done in Vannledningsdalen Valley (Longyearbyen, Norway). Protective forest and afforestation are non-technical measures. However, this requires that the climate zone remains suitable for forests. It can be said that protective forests and afforestation, ditches, channels and supporting structures (rigid and flexible) are considered as effective mitigation measures to use in the

release zone, provided that the climate, topography, construction access, and maintenance conditions are suitable.

2.3.2 Transition zone

All technical mitigation principles, such as conveyance, retention and deflection, are applied in the transition zone, where four control variables are outlined. These are controlling the size, velocity and runout of the slushflow, protecting direct objects (e.g. buildings) and infrastructure lines (e.g. roads, railways, power lines and pipelines). To mitigate using the deflection principle, wedges, deflection dams, diversion channels and dams are used. Retention mitigation is only used to control the size, velocity and runout of a slushflow. To achieve this, flexible protection nets, check dams, slit dams and drainage with a steel grid known as a 'debris flow breaker' are effective. Conveyance is used to control infrastructure lines with concrete galleries, tunnels, elevated bridges, enlarged culverts and buried power and pipelines. In addition, artificial levees can help control runout. Direct objects are controlled by reinforcing constructions (e.g. backwalls and windows) and by deflection measures such as wedges or deflection dams.

2.3.3 Deposition zone

Most of the mitigation measures classified for the transition zone can also be applied to the deposition zone. In addition, retention basins and earth dams are installed to control the velocity and runout. Due to the high liquid water content of slushflows, a water bypass system or drainage outlet is required when designing these structures.

2.4 Dimensioning slushflow mitigation measures

In order to identify an appropriate load case and model to determine the pressure acting on a mitigation structure, it is necessary to understand the slushflow process and its physical parameters. The main load cases for slushflow mitigation measures consist of static snow loads and high dynamic impacts. Design parameters addressing static snow loads, such as those for supporting structures, are well established and are defined in situ using guidelines (e.g. Margreth, 2007). However, design parameters for the dynamic impact P_{dyn} (Eq. 1) acting on mitigation measures (dams, wedges, protection nets, etc.) depend on the drag coefficient c_d , flow density ρ , and velocity v and are not as well established as those for the static snow loads.

$$P_{dyn} = c_d \cdot \rho \cdot v^2 \qquad (1)$$

The main driving design parameter is the velocity. Slushflows can occur at velocities of up to 30 m/s (Gauer, 2024), which exceeds the 15 m/s velocity range of debris flows (Berger et al., 2021). Another critical design parameter is the drag coefficient c_d. Most of the debris flow impact approaches for flexible mitigation measures with nets propose a drag coefficient value between 0.7 - 2.0 depending on the mesh size, flow density of the debris flow (granular, viscous or muddy) and the flexibility of the obstacle (Berger et al., 2021). For avalanches a new approach came up in Kyburz et al., 2022 through large scale tests at Valle de la Sion. The drag coefficient for avalanches depends on the Froude number. This new approach for avalanches should be proven for slushflows as well by testing instrumented obstacles.

N. Feiger, C. Wendeler O10.2 - Page 248

3. DISCUSSION

The classification of slushflow mitigation measures presented in Fig. 2 should provide a simple overview of technical measures for mitigating slushflow risk combined with the mitigation principles. Mentioned control variables can help to address the hazard and plan mitigation measures along the flow path. Nevertheless, limitations in the design of protective measures and use of them have to be considered.

Unfortunately, identification of release areas is associated with high uncertainties. This results in limitations in applying appropriate mitigation measures (Jaedicke et al., 2024). In most areas it is almost impossible to implement effective mitigation measures in terms of cost, technical feasibility, and coverage, as the area to be covered would be enormous. Therefore, channelised and already known release areas, such as debris flow channels, avalanche paths/channels, and lakes or pooling locations, where slushflows were already observed are appropriate for measures. On the other hand, mitigation measures in release areas would lead to simpler designs and dimensioning, as only static load, some gliding effects or drainage must be considered, instead of a combination of static and dynamic loads in the transition or the deposition zone. Furthermore, design parameters can be "easily" retrieved and several guidelines on such support structures already exist (e.g., Margreth 2007). Nevertheless, differences in the snowpack between different snow regions (e.g., alps vs. artic sphere) must be considered carefully, when approaching the design of supporting structures in release areas.

In most cases, effective protective measures in terms of cost, technical feasibility, and coverage will be implemented in the transition and/or deposition zones. Despite an easier zone identification, design and dimensioning of structures tailored for slushflows are complex. The distribution of velocity, drag coefficient and thus impact pressure, run-up height, and water content is broad and rarely known with precision. This makes it difficult to approximate the design input parameters resulting in challenging mitigation measures design, and great uncertainties in the effectiveness of the measures. Often, existing measures, such as dams and flexible nettings are implemented to counteract the effect of slushflows and protect people and infrastructure. However, these already well-established solutions for other gravitational mass movements, need careful attention and important adaptations. Compared to debris flows higher velocities, run-up heights, and impact pressures must be considered in the design of deflecting and catching dams. Similarly, drainage of the large amount of water present in slushflows must be taken into account as well. Slushflows exhibit surge-like behaviour similar to that of debris flows (Jaedicke et al., 2007). This behaviour must be considered carefully in the design and dimensioning of structures based on avalanche protection since subsequent surges can be as powerful and destructive as the first one.

In future, the most decisive factor in classifying slushflows may be the water content or debris/snow content of the mixture. The debris-to-snow content ratio may influence internal friction values, like in debris flows, where particles are impacted together. Therefore, more process studies carrying out lab testing, large-scale testing and field observations are necessary in order to calibrate simulation models carefully.

Recently, flexible net barriers have been applied as slushflow mitigation measures in Longyearbyen, Norway (Jonnson et al., 2024). Based on classic debris flow barriers, these solutions were adapted to withstand static snow loads, a different filling process, and a different flow behaviour than encountered in classic mixtures of debris and water. Very high velocities were given by the RAMMS simulation for the barrier design. These high velocities result in

high impact pressures (Eq. 1). In this project the drag coefficient for muddy debris flows was used. These aspects of design values should be investigated further with field tests as well as through measures of impact pressure and density to improve the understanding of the slushflow process and to calibrate numerical models. Modelling of the flow process and the flow-barrier interaction will help to improve the design of flexible nets for slushflow mitigation.

4. CONCLUSION AND OUTLOOK

Although slushflows share several characteristics with both avalanches and debris flows, they should be considered as a distinct hazard. Specific mitigation measures and mitigation guidelines/handbooks should be developed for this hazard. Besides, clear guidelines for protective measures against slushflows, as presented by Nordang and Jonsson, 2024, more lab and field tests are required to improve accuracy and effectiveness of such measures and to define the relevant design parameters. In addition, a more comprehensive understanding of these destructive yet poorly understood events is required, along with a unique and definitive classification. Therefore, further work is necessary to develop specific design parameters, resulting in guidelines and standards for decision-making workflows for mitigation measures. This will improve and unify the approach to mitigating slushflow-related hazards, and to improve protection and risk reduction for people and infrastructure, not only in Nordic countries, but in all affected regions.

5. ACKNOWLEDGEMENT

We would like to thank Claudio Petrini for proofreading of the manuscript and for insightful discussions that supported the development of this work.

6. REFERENCES

- Barbolini M., Gauer P., Stefanini F., 2024, *The Lillet Lake Avalanche: A Potential Slushflow Case for Italians Alps*, ISSW2024, conference proceedings, Norway.
- Berger C., Denk M., Graf C., Stieglitz L., Wendeler C., 2021, *Practical guide for debris flow and hillslope debris flow protection nets*, WSL Berichte, Vol. 113, Birmensdorf: Swiss Federal Institute for Forest, Snow and Landscape Research WSL, 79 p.
- Bozhinskiy A. N., Nazarov A. N., 1998, *Dynamics of two layer slushflows*, Norwegian Geotechnical Institute publication, 203, 74-78.
- D'Amboise C., Hansen V., Hendriks J., and Vick L., 2024, *Motivation for Slushflow Classification*, ISSW2024, conference proceedings, Norway.
- Furdada G., Martinez P., Oller P., Vilaplana J. M., 1999, *Slushflows at El Port del Comte, Northeast Spain*, Journal of Glaciology, Vol. 45, No. 151.
- Gauer P., 2004, *Numerical Modeling of a Slushflow Event*, ISSW2004, conference proceedings, WY, U.S.A.

N. Feiger, C. Wendeler O10.2 - Page 250

- Gude M., Scherrer D., 1998, Snowmelt and Slushflow: Hydrological and Hazard Implications, Annals of Glaciology, 26, 381-384.
- Hansen V., D' Amboise C., and Vick L., 2024, *Limitations of RAMMS:Debrisflow as Slushflow Simulation Tool*, ISSW2024, conference proceedings, Norway.
- Hestnes E., Bakkehøi S., 2004, *Slushflow Hazard Prediction and Warning*, Annals of Glaciology, 38, 45-51.
- Hestnes E. and Jaedicke C., 2018, *Global Warming Reduces the Consequences of Snow-Related Hazards*, ISSW2018, conference proceedings, Austria.
- Hestnes E. and Sandersen F., 1998, *Slushflow hazard control. A review of mitigative measures.*, NGI Publication, 203, 140-147, https://hdl.handle.net/11250/3082642.
- Jaedicke C., Kern M. A., Gauer P., Baillifard M.-A., Platzer K., 2007, *Chute Experiments on Slushflow Dynamics*, Cold Regions Science and Technology, 51, 156-167, doi:10.1016/j.coldregions.2007.03.011.
- Jaedicke C., Sund M., Grímsdóttir H., Helgason J. K., Bartsch U. B. A., Sandersen F., and Morken E., 2024, *Classification of Slushflow Release Areas in Norway and Iceland*, ISSW2024, conference proceedings, Norway.
- Jonsson A., Feiger N., Solli I. L., Pedersen M. B., Klotz M., Ringheim A., Kanstad S. B., Jansen J.-A., Sletten O., 2024, The Design and Construction of Slush-Flow Nets in Vannledningdsdalen Longyearbyen Svalvard, ISSW2024, conference proceedings, Norway.
- Kyburz M. L., Sovilla B., Gaume J., Ancey C., 2022. *Physics-based estimates of drag coefficients for the impact pressure calculation of dense snow avalanches*. Engineering Structures, 254, 113478, https://doi.org/10.1016/j.engstruct.2021.113478
- Margreth S., 2007: Lawinenverbau im Anbruchgebiet. Technische Richtlinie als Vollzugshilfe. Umwelt-Vollzug Nr. 0704. Bundesamt für Umwelt, Bern, WSL Eidgenössisches Institut für Schnee- und Lawinenforschung SLF, Davos, 137 S.
- Nordang S. F., Jonsson A., 2024, *Mitigation Measures Handbook a Practical Handbook about Reducing Snow Avalanche Hazard for Buildings with Avalanche Defence Structures*, ISSW2024, conference proceedings, Norway.
- Reynier Ph., Bugel M., and Lecoîntre J., 2010, Modelling of Slush Flows, conference paper.
- Sund M., Grønsten H. A., and Seljesaeter S. Å., 2024, *A Regional Early Warning for Slushflow Hazard*, Nat. Hazards Earth Syst. Sci., 24, 1185–1201, https://doi.org/10.5194/nhess-24-1185-2024.

Advancing Snowdrift Forecasting with Physically-Based Snow Models and High Resolution Weather Data

Sveinn Gauti Einarsson^{1*}

¹Veðurvaktin, Iceland

ABSTRACT

Snowdrift events present a persistent and significant challenge to transportation safety and winter road maintenance in Iceland. Current forecasting methods, largely based on simplified empirical models, often lack the physical fidelity to accurately predict the complex, non-linear dynamics of wind-driven snow. This report details a project that evaluates the efficacy of a modern, physically-based modeling framework, CRYOWRF, in comparison to a traditional empirical approach. The advanced model integrates high-resolution meteorological data and simulates detailed snowpack properties, including aging, wind transport, and vertical redistribution.

2. THE PHYSICALLY-BASED MODELING APPROACH WITH CRYOWRF

2.1. CRYOWRF: A Coupled Atmospheric and Cryospheric System

The project's advanced approach is centered on CRYOWRF, a new modeling framework that represents a significant advancement over existing land surface schemes. CRYOWRF achieves this by coupling the widely used atmospheric model WRF with the detailed snow cover model SNOWPACK. This is an online coupling, which means the two models are fully integrated and exchange data in real-time throughout the simulation.

The modeling philosophy of CRYOWRF is fundamentally different from that of empirical models. Instead of relying on statistical correlations, CRYOWRF is a physically-based system that uses fundamental physical laws to simulate the dynamics of a large number of snow layers, governed by grain-scale prognostic variables. This sophisticated approach makes it possible to perform multiscale simulations, capturing phenomena from large-scale synoptic conditions to small-scale turbulent processes. The online coupling is a critical innovation that directly addresses the limitations of legacy models. Previous climate and weather models often had a simplistic representation of snow, failing to capture the strong, two-way interaction between the snow surface and the atmosphere. CRYOWRF's tight coupling allows it to simulate complex feedback loops, such as the enhanced sublimation of snow due to wind, which in turn cools and moistens the near-surface air, a crucial detail that simpler models cannot resolve.

2.2. Advanced Model Physics: Key to Improved Forecasting

2.2.1. Snow Aging and Metamorphism

The ability to accurately model the evolution of snow is central to effective snowdrift forecasting. The SNOWPACK component of CRYOWRF excels in this area by simulating the

S.G.Einarsson O10.3 - Page 252

detailed stratigraphy and metamorphism of the snowpack over time, a clear contrast to simplified models that rely only on bulk properties like snow age. Accurate simulation of snow aging is critical because it directly affects the "transportability" of the snow, with aged snow being less susceptible to wind-driven drifting.

This process is a key differentiator between the two modeling approaches. For example, a fresh snowfall might be followed by a period of calm, with strong winds developing a day or two later. During this period, the snow undergoes metamorphism, which increases its shear strength and reduces its driftability index. In contrast, CRYOWRF's physically-based approach can account for the evolution of snow grain characteristics, density, and shear strength, providing a more accurate forecast of the drift potential for aged snow.

2.2.2. Wind Transport and Redistribution

It is necessary to improve the modeling of wind thresholds for transport. The CRYOWRF framework directly addresses this with the introduction of a new, detailed blowing snow scheme. This scheme models the three primary processes of snow transport: creep, saltation, and suspension. Saltation, the bouncing of snow particles along the surface, is a key focus as it is widely considered to contribute the most to the total volume of transported snow. To accurately capture this process, CRYOWRF employs a "fine mesh" of multiple vertical levels situated between the surface and the lowest atmospheric grid level, which is necessary to resolve the strong vertical gradients of particle concentration near the ground.

The ability of a model to account for the interplay between wind speed, temperature, and snowpack properties is paramount for accurate predictions. The CRYOWRF model's advanced physics allows it to simulate complex phenomena like airborne snow walls and the redistribution of snow from windward to leeward slopes.

2.2.3. Vertical Snowpack Dynamics

Beyond surface-level phenomena, the vertical dynamics of the snowpack play a direct role in road safety. The SNOWPACK model allows for the simulation of a large number of vertical layers, from 1 to 50, with their properties such as temperature, density, and liquid water content tracked dynamically. The online coupling with the atmospheric model facilitates both fast mass exchange (e.g., precipitation, blowing snow) and slower thermal processes (e.g., heat conduction and phase changes) between the atmosphere and the snowpack.

3. DATA INPUTS AND FORCING FOR HIGH-RESOLUTION MODELING

3.1. The Need for High-Resolution Forcing Data

The use of a physically-based model like CRYOWRF comes with a significant dependency on the quality and comprehensiveness of its input data. Unlike simpler models that can operate on minimal inputs, physically-based models require a more complete set of meteorological forcing data, including wind, humidity, shortwave radiation, and longwave radiation. These variables are often not available at standard automatic weather stations, especially in remote regions. The analysis shows that a lack of crucial data, particularly longwave radiation, can lead to substantial errors in model outputs, including discrepancies in snow disappearance timing by

weeks. This highlights a fundamental challenge: the superior predictive power of physically-based models is only realized when they are fed with a rich, high-resolution dataset.

3.2. Leveraging Reanalysis Datasets: CARRA

To overcome the data sparsity challenge in Iceland, the project leverages a high-resolution reanalysis dataset as a primary input source for the models. The Copernicus Arctic Regional Reanalysis (CARRA) is an optimal choice. Reanalyses combine historical observations with advanced models to create a best estimate of historical weather at locations where direct measurements are sparse. CARRA offers a high-resolution, 2.5 km grid spacing for the European Arctic, which is a significant improvement over the coarser resolution of global reanalyses like ERA5, which have a grid spacing of around 31 km. This high spatial resolution allows CARRA to more accurately represent near surface temperature and wind speed, particularly in regions with complex topography and coastlines, which are precisely the conditions that define Iceland's landscape. The CARRA dataset is available from 1990 to near present, making it a perfect fit for the historical case studies in the project.

4. AVALANCHE FORECASTING WITH CRYOWRF

In addition to its applications for snowdrift and road forecasting, the CRYOWRF model can be used to assess avalanche conditions. The SNOWPACK model, which is a component of CRYOWRF, was originally developed for avalanche warning purposes and simulates the detailed layering and microstructure of the snowpack. This model has been used in an operational capacity in the Alps, where it runs on a network of around 160 automatic weather and snow-measuring stations throughout Switzerland. It provides supplementary information on snowpack conditions, including new snow amounts, settling rates, and the metamorphic evolution of snow grains.

Avalanche forecasting is often a human judgment process, but snowpack simulations can provide an independent perspective and add value by offering quantitative links between weather, snowpack, and hazard characteristics. The model can be used to track snow layers across time and space, allowing for the calculation of spatial distributions of key avalanche problem characteristics, such as storm and persistent slabs. This capability can assist forecasters with difficult decisions, like the removal of persistent slab avalanche problems. While SNOWPACK is fundamentally a one-dimensional model for a soil/snow/vegetation column, its coupling with the atmospheric model in CRYOWRF allows for the use of terrain models to estimate snow transport on steep slopes, which is crucial for avalanche assessment.

5. CONCLUSIONS AND RECOMMENDATIONS

5.1. Key Findings

The CRYOWRF modeling framework, with its advanced physical representation of snowpack dynamics, including the nuanced effects of snow aging, wind transport, and vertical redistribution, is a significant advancement for snow forecasting. This detailed, physics-driven approach allows the model to capture the complex, non-linear processes that are oversimplified in legacy models, resulting in more accurate and reliable predictions.

S. G. Einarsson O10.3 - Page 254

5.2. Recommendations for Future Implementation

Based on the capabilities demonstrated by the CRYOWRF model, the following recommendations are proposed:

- **Phased Implementation:** It is recommended to proceed with a phased adoption of the CRYOWRF modeling framework for operational snow forecasting.
- Actionable User Interfaces: The outputs of the CryoWRF model are complex, physics-based simulations. A key next step is to develop user interfaces that translate the detailed, physics-based outputs (e.g., maps of snow accumulation and erosion, predicted road-surface conditions) into clear, actionable intelligence for road crews and other stakeholders.

LIST OF REFERENCES

- Bartelt, P., & Lehning, M. (1999). SNOWPACK model calculations for avalanche warning based upon a network of weather and snow stations. *Cold Regions Science and Technology*, 30(1-3), 145–157.
- Sharma, V., Sharma, K., Vionnet, A., & Masson, V. (2023). Introducing CRYOWRF v1.0: Multiscale atmospheric flow simulations with advanced snow cover modelling. *Geoscientific Model Development*, 16(2), 719-749.

Can wind simulation help optimize the function of snow avalanche mitigation measures?

Árni Jónsson^{1*} and Peter Gauer²

ORION Consulting slf, Foldarsmára 6, IS-201 Kópavogur, ICELAND
 Norwegian Geotechnical Institute, Postboks 3930 Ullevål Stadion, NO-0806 Oslo, NORWAY
 *Corresponding author, e-mail: arni (at) orion.is

ABSTRACT

For decades, the authors have observed how wind shapes drifting snow around structural measures intended to prevent or stop avalanches. Often, these structures were not designed considering wind or snowdrift. This oversight may have led to challenges as snowdrifts can accumulate in ways that compromise the effectiveness of these structures. Incorporating a better understanding of wind dynamics and snow behaviour into the design process could improve the reliability and safety of avalanche mitigation measures. In regions where trees do not obstruct wind flow, the wind is a critical factor for the effective functioning of mitigation measures.

In 1996, a group of experts discussed the layout of a catching dam in Neskaupstaður, Iceland. Concerns were raised regarding the draft of the dam layout, specifically about potential excessive snow accumulation above the dam due to snowdrift. The layout was later modified to reduce snow accumulation. Generally, wind and snow drift have not been prioritised during the design phase in Iceland or Norway but recently wind simulation has been incorporated into the design of two large ongoing projects in Honningsvåg and Mosjøen, both in Norway. Before these projects, two wind simulations were conducted for a large project in Longyearbyen, Svalbard. The examples presented here discuss the experience with wind and snowdrift in northern Norway, along with wind simulation (CFD) at the same locations. While the cost of wind simulation can be significant, the potential benefits may justify the expense.

1. INTRODUCTION

For several decades, the authors have been engaged in the design of infrastructure projects, including roads/highways, transmission lines as well as the development of mitigation strategies for rapid gravitational mass flows, with a particular focus on snow avalanches. In many of these projects, wind was either given very little attention as a design factor or even ignored in some cases. Still, there was clear understanding that drifting snow events could result, e.g., in road closures.

The term drifting snow is here used for drifting- and blowing snow and they refer to the suspension- and saltation processes; for further reading see (Tabler, 1994).

In recent years wind problems have gained more attention in planning mitigation measures against snow avalanches. Supporting structures are often partially or fully covered with snow during typical winters, raising concerns about their performance in unusually snowy winters. Frequently, the underlying cause is unanticipated drifting snow that has not been adequately considered.

G. Jónsson, P. Gauer O10.4 - Page 256

Snow drift fences can help reduce snow build-up in avalanche starting zones but installing them can be challenging in complex alpine terrain (Prokop and Procter, 2016). Gathering detailed snow condition data in winter is essential and can for instance be achieved through photos, aerial imagery, or lidar scanning. Detailed climate data matters, but it is rarely available for the specific site of interest. With current tools, it is possible to obtain information about wind conditions at locations of interest by transposing wind roses. The questions have been raised about how to interpretate the wind data from wind simulations and if it is worth the spendings. The following text highlights recent work by the authors and their colleagues.

The table below shows some of the projects where wind simulations have been used since 2002:

Table 1 The table below shows a list of some wind simulation projects in Iceland (IS) and Norway (NO) since 2002 till now.

Location	Type of project	What?
Bláfjöll, IS	Ski area	Wind map showing maximum and minimum wind across the area.
Klettsháls, IS	Road	Analysis of wind patterns and snow accumulation along the roadway: How do steep slopes and roadside excavations affect snow buildup?
Fljótsdalslínur, IS	Transmission lines	How are the wind fields in valleys crossed by the transmission lines in east Iceland? Where can we expect snow accumulation?
Mt. Hafnarhyrna, IS	Mitigation measures	What factors contribute to the formation of the snowpack at the summit of Hafnarhyrna in Siglufjörður, and can wind simulation provide an explanation for this phenomenon?
Mt. Bjólfur, IS	Mitigation measures	How is snow likely to accumulate in the mountain side above Seyðisfjörður?
New road Melrakkaslétta, IS	Road	Where is snow accumulation likely to occur along the new road alignment in northeast Iceland?
Mounds in Ísafjörður, IS	Mitigation measures	How does snow accumulate near mounds, and which wind direction is most influential?
Båtsfjord, NO	Village	What are the wind field characteristics in Båtsfjord and its surrounding regions?
Longyearbyen, NO	Mitigation measures	1) Wind fields on Mt. Sukkertoppen. 2) What are the wind conditions along the proposed deflecting dam at Haugen residential area?
Honningsvåg, NO	Mitigation measures	What are the wind field characteristics at Storefjellet prior to and following the installation of supporting structures and snow drift fences?
Mosjøen, NO	Mitigation measures	How do Øyfjellet's wind fields differ before and after adding supporting structures and snow drift fences?

2. WIND SIMULATION

Wind simulation uses numerical analysis and algorithms to simulate and analyse fluid flows such as wind movements and particle transport. This field, known as Computational Fluid Dynamics (CFD), has undergone significant development over several decades.

Below are two recent examples of wind simulation used in the design of mitigation measures in Norway in which two different models were used for the simulations.

2.1 Examples of wind simulation use

2.1.1 Longyearbyen, Svalbard

Following two avalanche incidents that resulted in the loss of two lives, Norwegian authorities made the decision to implement mitigation measures for the community of Longyearbyen. Mt. Sukkertoppen, Lia, and Vannledning valley are the main locations that present risks to both the town centre and the residential areas. For the former two snow avalanches are the main threat and for Vannledning valley slush-flow is the main threat. The landscape is open and lacks trees or shrubs, resulting in minimal reduction of snow drift. Wind significantly influences snow accumulation patterns on Mt. Sukkertoppen and within the Vannledning valley.

The mitigation project was divided into multiple phases. During the initial phase, Lia, wind simulations were conducted for the two primary boundary wind directions of 130° and 310°, resulting in the development of a simple wind velocity map (Windsim AS, 2017). Comparing the wind velocity maps to photos showing snow distribution, we found relatively good correlation between high wind speed and little snow and low wind speed and snow accumulation.

During slush-flow mitigation project at Haugen near the Vannledning valley outlet, a plan was made to build deflecting dams along the stream. A wind simulation was conducted for three wind directions—40°, 220°, and 340°—using boundary wind speeds of 10 m/s, 20 m/s, and 25 m/s (WindSim AS, 2018). This wind simulation is also briefly described in (Jonsson et al., 2019, p. 153). The client later selected an alternative mitigation approach for Vannledning valley, so the simulation results are not being further evaluated.

2.1.2 Mosjøen northern Norway

At Øyfjellet, situated above the town of Mosjøen in northern Norway, snow avalanche consultants are working on a preliminary plan for mitigation measures. This plan includes the installation of supporting structures on the mountainside as well as snow drift fences and wind baffles at the mountain top. Due to significant snow accumulation in many of the avalanche release zones on the mountainside, one strategy is to implement measures that reduce the buildup of snow in these areas.

G. Jónsson, P. Gauer O10.4 - Page 258

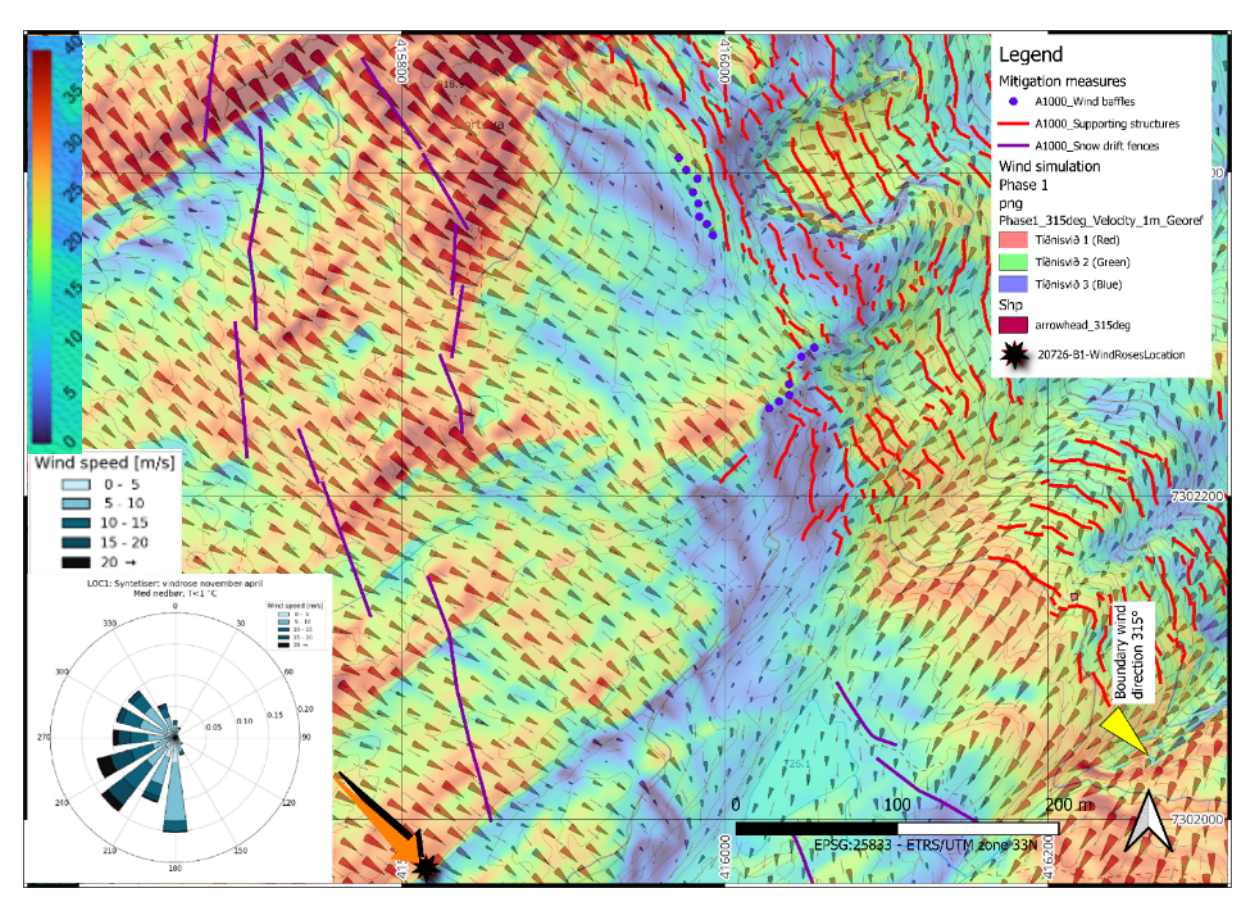


Fig. 1 The figure shows phase 1 of wind simulation for boundary wind from northwest (315°, yellow arrowhead in figure). The wind simulation is both shown as coloured background map and as arrow heads showing wind direction and intensity. Wind speed (m/s) for background map is shown at upper left corner. Mitigation measures from the preliminary design phase are shown as coloured lines and dots; note that final location might be different. Black star shows location of calculated/transposed wind for the period November to April with precipitation and temperature below +1°C.

The Norwegian Water and Energi directorate (NVE) engaged experts in wind simulation and weather analysis to:

- (1) analyse weather conditions before and during three major avalanche events from Øyfjellet.
- (2) Conduct a climate analysis for Øyfjellet and examine wind conditions at three locations.
- (3) Study wind fields on Øyfjellet by analysing eight wind directions at constant wind speeds and at 1 m elevation above the terrain; for phase 1 without mitigation measures, and for phase 2 with mitigation measures (work in progress). Also, study wind profiles for four locations.

Wind simulation was conducted on snow-free terrain using a 2 m grid for the lowest three vertical layers of the model. The consultant used a cylinder model (5 km radius, 3 km height) centred on the mountain top; for a full description of the methods see (Norconsult Norge AS, 2025). Boundary wind speed was set at 20 m/s at 10 m elevation, with surface roughness values

of 0.000075 m for snowy ground, 0.0007575 m for lake/sea, and 0.3 m for urban areas. The structures will be assigned the following porosity values: 1) rigid steel bridges, 50%; 2) snow and rock-fall nets, 85%; and 3) snow drift fences, 50%. The height of all structures is specified as 4 meters even though the height varies from 3.5 to 7.0 m; we are only looking at wind fields approximately 1 m above ground.

NVE recognises that winter snow fills low-lying terrain and changes its shape and wind fields, and that wind fields at Øyfjellet are complex because of the terrain roughness. The impact of wind on snow accumulation on mountain slopes, as well as the influence of structures on snow drift (work in progress, here we refer to other projects), is challenging to quantify; however, analysis of wind patterns offers valuable insights into potential outcomes.

Three snow scans of Øyfjellet are available: a terrestrial scan from the town centre that covers only the mountain side, and two UAV photogrammetry scans that include the entire area of interest. Data from these scans is relevant for interpreting the wind simulation results.

The wind rose presented in Fig. 1 illustrates the challenges involved in optimally positioning snow drift fences to minimise snow transport into the release zones in the mountain slope.

The preliminary design is still in progress, and the placement of snow drift fences may be subject to modification.

3. DISCUSSION

Since the beginning of wind simulations over complex terrain to support the planning for mitigation measures against rapid mass movements, both the methods and tools have undergone significant improvements. Similarly, the requirements and expectations for these simulations have evolved accordingly. CFD simulations of drifting snow have also evolved significantly.

The examples above show that all projects prioritize wind (CFD) simulations over simulating drifting snow, since wind patterns in complex terrain are crucial to understanding snow drift. Accurate drifting snow simulation requires knowledge of both wind behaviours and snow properties, as well as how wind alters snow accumulation across varied surfaces. Snow property variations can have a significant impact on form and size of the snow drifts and is still a large challenge to incorporate.

When preparing for wind simulations, several factors or boundary conditions must be considered:

- (1) What are the wind simulations for?
 - (i) Wind field studies, such as 45° sectors, 8 wind directions, 0°-360°.
 - (ii) Wind field studies for known avalanche incidents
 - (iii) Transpose of wind roses to locations of interest
- (2) Plan for large enough plan area outside the area of interest to consider the disturbance from complex terrain, see Fig. 2
- (3) Plan for high enough model (top of volume) for stable boundary conditions
- (4) Boundary conditions for incoming velocity profile (and turbulence intensity), for example at certain reference height.
- (5) Mesh size will vary within the model volume. Dense mesh is close to the observation site and thinner to the boundaries. In the horizontal plan the grid size has often been

G. Jónsson, P. Gauer O10.4 - Page 260

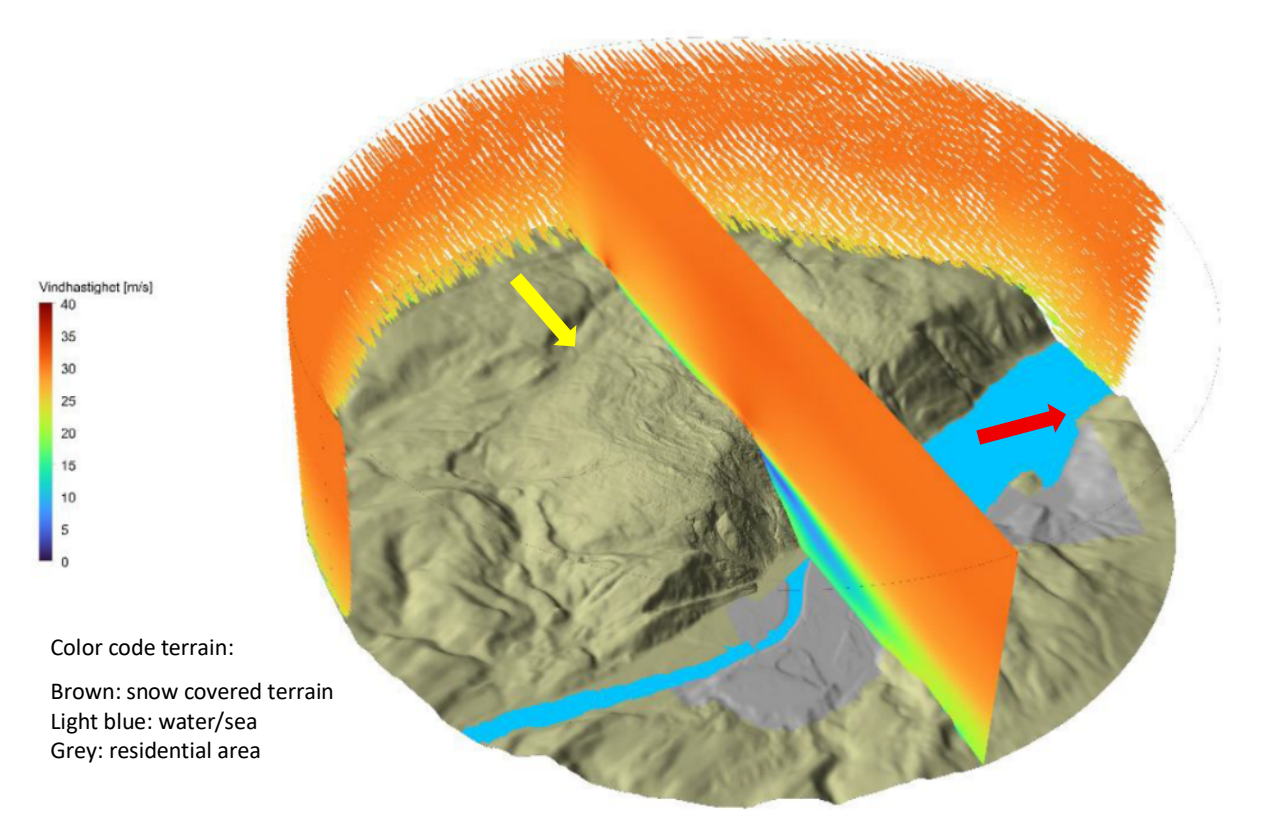


Fig. 2 Model domain for the Mosjøen project. It illustrates the boundary conditions and a profile with wind velocity. Red arrow shows north direction. The wind direction is from west, yellow arrow. Source: Norconsult Norge AS.

2 m and 1 m for the lowest three layers in the vertical plane. The higher resolution the longer is it to run and process the model and the more it costs.

- (6) The variations in air density are often neglected as the height of the observation site is small compared to the atmosphere
- (7) Coriolis forces can normally be neglected
- (8) Atmospheric conditions are considered neutral
- (9) Air humidity, condensing and heat transport is neglected
- (10) A fixed height above terrain should be used for presenting results; in our projects, 1 or 2 metres have been selected. Note, the terrain is without snow.

When evaluating structural mitigation measures in a windy environment, it is important to define the porosity of the structures and height for simulation. Similarly, consideration should be given to the amount of snow surrounding the structures. During early winter, when there is minimal snow on ground, the entire structures remain exposed to wind. In contrast, by late winter, typically only sections of the structures are left uncovered. We can argue that early winter with little snow on ground is the preferable situation to understand the effects of wind even though we acknowledge that snowy terrain is also of importance.

So far, our analysis has focused on a constant height of 1 or 2 meters above ground, which suits the structures involved. Multiple wind profiles are also used to assess wind conditions.

The porosity values are typically determined based on the geometric characteristics of the structures rather than experimental measurements. The following values have been used in recent analyses:

(1) Steel bridges: 50%

(2) Snow nets/rock-fall nets: 85 - 90%

(3) Snow drift fences: 50%

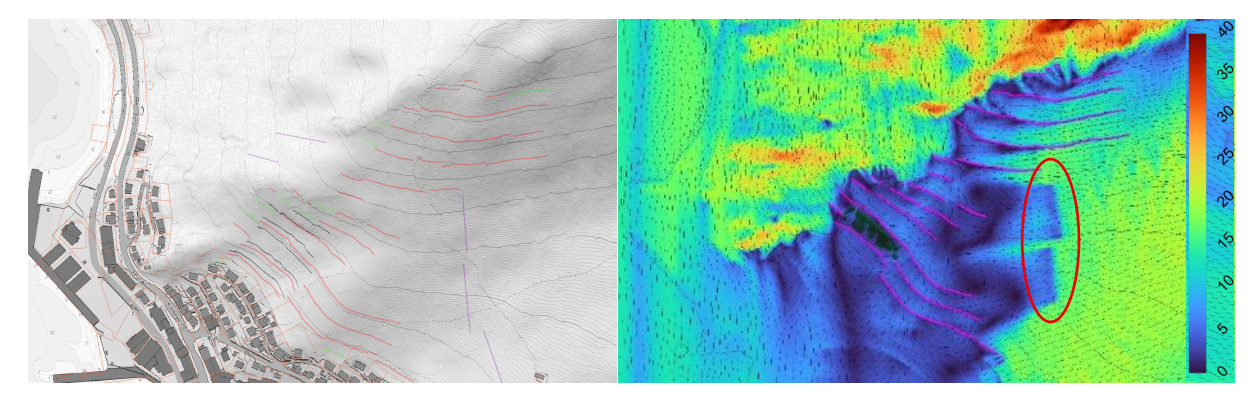


Fig. 3 These figures are from the design phase for mitigation measures in central Honningsvåg, northern Norway. In the left figure, red and green lines indicate supporting structures, while purple lines denote snow drift fences. The figure on the right presents early-stage location of mitigation measures (purple lines) and the background map displays wind simulation at 2 m distance from ground. The boundary wind originates from the north (top of the figure). Red ellipse indicates two snow drift fences with 50% porosity. A wind velocity scale (m/s) is provided on the right side.

Returning to our main question: Can wind simulation help optimize the function of snow avalanche mitigation measures?

Wind simulations are useful for understanding wind fields especially in complex terrain as can be seen in Fig. 1, and they are intended as a supplement to on-site observations and practical judgment rather than a replacement. Fig. 3 shows an example of design work where wind simulation was used in early stage to help understand the wind fields in planned area with supporting structures and snow drift fences. A wind simulation for the site depicted in Fig. 3, conducted without mitigation measures, was cross-compared to a photograph taken following northerly storm. Some adjustments of the snow drift fences were made during the final design but supporting structures have other boundary conditions than wind and reorganizing them partly follows other rules.

In our case wind maps were used to assist with estimation of snow cover thickness especially extra snow cover thickness caused by drifting snow.

4. CONCLUSION

Wind simulations for mitigations measures have been carried out for years in various locations in Iceland and Norway. Although improved models aid planning and mitigation, verification of these simulations remains limited. This is primarily due to limited funding, as after the design and construction phases are finished, clients—often municipalities—may lack the financial

G. Jónsson, P. Gauer O10.4 - Page 262

resources to continue the work. Additionally, clients typically cannot assign the follow-up work to a specific consultant and must instead conduct a tendering process which can be costly and in worst case be awarded according to lowest price instead of best snow drift knowledge.

In a recent project, the wind simulation results were cross-checked using photographs taken after stormy weather and in an ongoing project we see strong correlation between wind simulation and aerial photos of the snow cover.

Wind simulation and snow drift simulation are expected to receive wider recognition in the near future. However, it is also necessary to communicate to clients the importance of subsequent follow-up work to verify the wind- or snow drift results.

5. ACKNOWLEDGEMENT

Some of the authors original text in this article is rewritten with the help of Copilot.

6. REFERENCES

- Jonsson, A., Kronholm, K., Li, D., Gravdahl, A.R., 2019. Wind simulation for Longyearbyen mitigation measures, in: Jóhannesson, T., Gauer, P., Margreth, S., Martha Hákonardóttir, K., Pálsson, H., Sigtryggsdóttir, F.G. (Eds.), International Symposium on Mitigation Measures against Snow Avalanches and Other Rapid Gravity Mass Flows Siglufjörður 3–5 April 2019. Association of Chartered Engineers in Iceland (VFÍ), Reykjavik, pp. 1–6.
- Norconsult Norge AS, 2025. Vindforhold Øyfjellet Mosjøen. CFD-analyse, klimastudier og skredhendelser. Oslo.
- Prokop, A., Procter, E.S., 2016. A new methodology for planning snow drift fences in alpine terrain. Cold Reg Sci Technol. https://doi.org/10.1016/j.coldregions.2016.09.010
- Tabler, R.D., 1994. Design Guidelines for the Control of Blowing and Drifting Snow.
- WindSim AS, 2018. Wind conditions for security measures in Longyearbyen (No. 181203_HNIT_Longyearbyen_100). Tønsberg.
- Windsim AS, 2017. Wind Fields at Longyearbyen and Lia on Svalbard (No. 170601 NGI 100). Tønsberg.

Avalanche control systems and traditional mitigation structures (Environment and Society)

Ines Waltl^{1*} and Jón Páll Eyjólfsson²

¹ Inauen-Schätti AG, Im Tschachen 1, 8762 Schwanden, Switzerland ² 1001 Tindur ehf, Eyrarlandsvegur 8, 600 Akureyri, Iceland, *Corresponding author, e-mail: <u>iwaltl@seilbahnen.ch</u>

ABSTRACT

Remote avalanche blasting systems and traditional mitigation structures play vital roles in reducing avalanche risks in mountainous areas. While their environmental impacts differ, both offer effective solutions for managing avalanche hazards.

Traditional mitigation structures, while more resource-intensive, are proven to provide reliable and long-term protection against avalanches. They can be effective in managing avalanche risks in areas with consistent and predictable conditions. However, they do require land alteration, which can impact local flora and fauna during installation and maintenance.

Remote avalanche blasting systems offer advantages such as minimizing the need for permanent infrastructure, reducing soil erosion, and preserving wildlife. These systems can be more adaptable, with technology-driven solutions that respond to real-time conditions, reducing the need for continuous human intervention. Flexibility makes them an appealing choice for areas where traditional mitigation structures might be less practical or environmental preservation is a priority.

In conclusion, both remote systems and traditional mitigation structures contribute to avalanche risk management, each with its strengths. Remote systems present a more adaptable and eco-friendly approach, while traditional structures provide long-established, effective protection. Combining both methods where appropriate can provide a comprehensive and sustainable solution for avalanche risk reduction, balancing safety with environmental conservation.

Keywords: Avalanche mitigation, environmental impact, carbon footprint, societal acceptance, rapid mass movements, structural control, explosive control.

INTRODUCTION

Settlements in alpine regions face persistent risks from snow avalanches and related rapid mass movements. Mitigation strategies have evolved from traditional structural approaches to modern active control systems. While technical effectiveness has been widely studied (Margreth et al., 2000), comparative evaluations of environmental and societal impacts remain scarce. But first, let's take a brief look at the past and the origins and necessity of avalanche protection.

Avalanche protection in the Alps has a long history dating back to the 19th century. In Austria, the Forestry Service for Torrent and Avalanche Control was founded in 1884 and is responsible for ongoing avalanche protection. However, the development of modern support

structures as we know them today was significantly influenced by the avalanche disaster in Galtür in 1999 and the catastrophic winter of 1950/51, which led to a rethink in avalanche protection.

Between 1950 and 1997, almost all avalanche control measures involved the construction of permanent avalanche protection structures. The first manually operated blasting cableways came into operation in the mid-1960s. A good 30 years later, the first avalanche blasting systems, such as those sold today by Inauen-Schätti, were developed.

The system was revolutionary at the time, as a primary charge was used to throw the main charge into the desired slope, where it was detonated. The explosive charge was only armed when it left the magazine.

After many years of successful use of avalanche blasting systems, the system was further developed with the avalanche mast. The sequence and process of ejecting the charges was retained, but the system was optimized so that the magazine was now placed on a 7-metre-high mast, enabling more effective above-snow blasting. Overhead blasting releases up to 25% more energy than in-snow blasting.

Not only in Central Europe, but also in Iceland, the history of avalanche protection has gradually gained awareness through a series of devastating disasters, ultimately leading to a modern, multi-layered safety approach.

EARLY RESPONSES AND THE TURNING POINT

The threat of avalanches has long been a part of life in Iceland, with historical accounts of devastating events. However, the initial response to these disasters was limited. The 1974 avalanche in Neskaupstaður, which killed 12 people, was a pivotal moment for research and planning. It led to the creation of Iceland's first avalanche hazard maps but did not result in the immediate construction of protective dams. The political and public will for such large-scale, costly projects was not yet present.

The year 1995 marked the true turning point. Catastrophic avalanches in Súðavík and Flateyri, which killed 34 people in total, shocked the nation and led to a fundamental shift in policy. A nationwide program was launched to assess avalanche risk and build permanent, passive defense structures.

A NATIONWIDE PROGRAM OF PROTECTIVE STRUCTURES

Beginning in the late 1990s, extensive construction projects were initiated in high-risk areas.

- Flateyri: Between 1996 and 1999, deflecting and catching dams were built to protect the town.
- Neskaupstaður: Following the 1974 disaster and the new national directive, dams and braking mounds were constructed in the late 1990s and early 2000s.
- Other High-Risk Areas: Similar projects were undertaken in Siglufjörður, Ísafjörður, Seyðisfjörður, and Bíldudalur, with construction continuing into the 2000s and beyond.

These projects primarily focused on "passive" measures defecting and catching dams—designed to divert or stop avalanches before they could reach settlements.

EVOLUTION TO ACTIVE CONTROL MEASURES

While the construction of passive dams continued, the approach to avalanche safety also evolved to include "active" control and mitigation strategies. These measures are particularly important in recreational areas like ski resorts.

- Forecasting and Evacuation: The Icelandic Meteorological Office (IMO) is central to this effort, providing critical avalanche forecasts and warnings that can lead to the evacuation of at-risk areas.
- Snow Management: Ski resorts began using snow groomers not just to maintain slopes, but also to compact the snowpack and eliminate weak layers, thereby reducing the risk of avalanches on marked runs.

THE INSTALLATION OF MODERN AVALANCHE CONTROL SYSTEMS

The final piece of this modern safety strategy is the use of advanced, remote-controlled systems. The most significant example is the installation of the Inauen-Schätti Avalanche Master LM5400 system in Hlíðarfjall around 2020. This system of remotely detonated explosives, strategically placed in avalanche starting zones, allows ski patrols to proactively trigger controlled avalanches from a safe distance, making the ski resort a safer environment for everyone. This marked a major step in Iceland's shift toward a comprehensive, technologically advanced approach to avalanche control, moving beyond just passive defenses to include cutting-edge active measures.

ADVANTAGES AND DISADVANTAGES OF AVALANCHE BLASTING SYSTEMS AND PERMANENT AVALANCHE PROTECTION STRUCTURES

The combination of avalanche blasting systems and other avalanche protection measures is more widespread than it might appear at first glance. As history shows, people have always used the resources available to them to protect themselves against avalanches. But why not combine tried-and-tested avalanche barriers and steel structures with automatic avalanche blasting systems?

Traditional mitigation structures, while more resource-intensive, are proven to provide reliable and long-term protection against avalanches. They can be effective in managing avalanche risks in areas with consistent and predictable conditions. However, they do require land alteration, which can impact local flora and fauna during installation and maintenance.

Remote avalanche control systems offer advantages such as minimizing the need for permanent infrastructure, reducing soil erosion, and preserving wildlife. These systems can be more adaptable, with technology-driven solutions that respond to real-time conditions, reducing the need for continuous human intervention. Flexibility makes them an appealing choice for areas where traditional mitigation structures might be less practical or environmental preservation is a priority. Avalanche blasting systems can be used to guide snow down into the valley in portions, thus preventing damaging avalanches. If triggered at the right time, there is no need to wait until heavy snowfall and an unstable snow cover cause snow masses to descend uncontrollably into the valley or onto roads, causing considerable damage. No environmentally

harmful agents or materials are used to protect the environment. Both the explosives Rimon T1 and Ladin have a water quality class of 1 and are classified as non-harmful to the environment.

The charges are also made of environmentally friendly materials such as wood and cardboard and rot overtime.

In the Swiss ski resorts of Leukerbad and Andermatt, as well as in the Austrian ski resorts of Silvretta Montafon, Sölden, Serfaus and others, combinations of permanent installations and avalanche blasting systems are already in use. Avalanche blasting systems can be protected by steel structures, particularly in areas that are susceptible to rockfall and snow pressure from above.

METHODS

We reviewed existing literature and technical documentation on avalanche control measures in Andermatt and Leukerbad (Switzerland). No original field data was collected. The study relied on published information about the history of avalanche protection structures, avalanche mitigation and control. We reviewed existing data about carbon emissions, operational requirements, environmental disturbance, and social integration.

RESULTS AND DISCUSSION

3.1 Carbon and Operational Impacts

Permanent dams show high initial embodied emissions but low maintenance emissions (construction phase and installation). Active control systems such as explosive mast systems from Inauen-Schätti (e.g., in Andermatt and Leukerbad) emit CO₂ annually and require logistical support such as helicopter transport and charge handling. LM32 and LM5400 systems can store and remotely detonate up to 32 explosive charges via GSM/4G-controlled platforms (ATMS), improving safety and operational responsiveness. These systems eliminate the need for major terrain alteration and carbon emissions during construction of permanent dams and its modern designs use biodegradable materials to minimize environmental waste.

3.2 Environmental and Landscape Effects

Dams significantly alter terrain permanently and viewsheds. Active systems have minimal footprint but temporary disruption to wildlife and noise pollution.

3.3 Societal Acceptance and Perceived Safety

Communities are historically more exposed to permanent structures than active systems. In Andermatt for example, complex terrain requires both types of measures, with the public becoming more aware of the benefits of active systems.

CONCLUSIONS

No single solution fits all. Permanent structures excel in long-term, high-risk zones with stable topography. Active systems are more flexible. Sustainable planning must

environmental, economic, and social dimensions. Combining both approaches where suitable can provide comprehensive and resilient avalanche risk reduction strategies. Both blasting systems and traditional mitigation structures contribute to avalanche risk management, each with its strengths. Blasting systems present a more adaptable and eco-friendly approach, while traditional structures provide long-established, effective protection. Combining both methods where appropriate can provide a comprehensive and sustainable solution for avalanche risk reduction, balancing safety with environmental conservation and with reducing cost.

ACKNOWLEDGEMENTS

This work was inspired by the avalanche defense structures in Iceland, which protect the towns themselves but sometimes leave critical infrastructure like the road access or tunnels exposed to avalanche hazards. Observations of these limitations motivated a broader inquiry into avalanche mitigation strategies focused on combining them with avalanche defense structures. The author also thanks regional authorities in Iceland for their input and acknowledges insights gained through discussions with avalanche professionals.

REFERENCES

Margreth, S., Harvey, S., Wilhelm, C., 2000. Effectiveness of long term avalanche defense measures in winter 1999 in Switzerland.

Avalanche Monitoring in Flateyri using Doppler Radar

Ragnhild Lie and Lars Krangnes, Cautus Geo AS

Cautus Geo AS, Lysaker, Norway

EXTENDED ABSTRACT

Flateyri, located in the Westfjords of Iceland, is a village prone to avalanches. To protect Flateyri from such hazards, deflecting dams have been constructed.

In order to gain more insight into the avalanche activity in the five avalanche paths originating from the mountains behind Flateyri, Cautus Geo installed the Cautus Avalanche Radar in 2021. The radar is positioned near the harbour and has a clear view of all five paths. The Cautus Avalanche Radar is a Doppler radar with scanning capabilities, large field of view and high resolution. Cautus Geo has employed Doppler radar technology since 2014 for monitoring and detection of avalanches. A camera that documents the detections is also integrated into the radar system.

The radar in Flateyri has recorded several avalanches each winter. Avalanches have been detected in all five avalanche paths. Information about all events are available in Cautus Web. Cautus Web is a cloud-based data management system for processing and presenting data. For each avalanche event, basic information such as time, duration, intensity, velocity and location are displayed in Cautus Web. Additionally, a heatmap and video of the event are also available, along with the option to replay the raw data. Most of the events in Flateyri have occurred at night or during stormy weather, which has limited the usefulness of video documentation due to poor visibility. The heatmap is showing the outline of the avalanche on a map. The data from the radar measurements are used to create the heatmaps. If visibility is too low to verify the event on video, the heatmap is as a highly valuable product.

Due to the radar's location near the harbour, reflections from vessels initially interfered with the radar signals. Different approaches were developed and tested to filter out these strong reflections. Cautus Radar now uses a robust method to avoid being affected by vessels in the harbour. It also utilizes functionality to remove the influence of weather phenomena occurring between the radar and the mountainside.

Cautus Radar has also functionality for dividing the mountainside into zones, enabling it to identify in which zones avalanche activity is occurring. When the radar is used to close the road upon detecting avalanche activity, these zones can be used to determine whether the road should be closed and, if applicable, whether it should be automatically reopened.

The presentation will give information about the monitoring and early warning of avalanches in Flateyri from 2021 to 2025.

R. Lie and L. Krangnes P1.2 - Page 269

Samuelsberg catching dam partial failure and rebuild - Case studies

Árni Jónsson^{1,2*} and Anders Bjordal²

ORION Consulting slf, Foldarsmára 6, IS-201 Kópavogur, ICELAND
 Norwegian Water Resources and Energy Directorate (NVE), Middelthuns gate 29, Oslo, NORWAY
 *Corresponding author, e-mail: arni (at) orion.is

ABSTRACT

Samuelsberg a small fishing and agricultural village in northern Norway faced a challenge with snow avalanches threatening its outskirts. A 325-meter catching dam was constructed in 2019, designed to use tunnel rock from a nearby highway project. The dam's height ranged from 5 to 12 meters, with drainage trenches planned for stability. The facing material was gabions filled with stone material, taken from the tunnel project. However, in August 2020, heavy rain led to the collapse of two sections of tens of meters. An investigation found that the geogrid reinforcement was improperly installed and had only one third of the required capacity. The drainage could also have been more extensive.

The damaged sections of the 12-meter-high dam and transition to 5 meters high dam were removed and the material stored nearby for later use. A new plan was created for rebuilding using different facing material and reinforcement methods. Additionally, the storage capacity above the dam was increased, and larger ditches and culverts were planned. Reconstruction began early summer 2022 with the foundation work and connections to existing gabions. The construction work of the dam was completed in late 2024 but work with ditches and culvert will wait until summer 2025.

A significant learning outcome is enhanced coordination and improved information flow among various stakeholders during the construction process.

1. INTRODUCTION

The residential area in Samuelsberg (seen to the left in Fig. 1) is threatened by snow avalanches from two main avalanche paths in Mt. Juvravárri. Since 1882 six avalanches or debris flows have passed the residential area and reached the sea. Two residential houses and one hut are inside the hazard zone 1/100 and seven more are inside hazard 1/333 (Norges vassdrags- og energidirektorat NVE, 2013, 2015). The initial plan for protecting the residential area was made in 2013 when one deflecting dam and one catching dam with mounds were proposed (Norges vassdrags- og energidirektorat NVE, 2013). The deflecting dam was built shortly after, but the catching dam waited as the authorities planned to use rock mass from a new tunnel under construction nearby.

The project was a joint work between Kåfjord municipality, the Norwegian road authorities and NVE.



Fig. 1 This figure shows the catching dam at Samuelsberg Troms county northern Norway and the two locations of failure of the 12 m high facing side. Photo Anders Bjordal/NVE.

2. THE PLANNING AND DESIGN OF THE CATCHING DAM

According to the initial plan (Norges vassdrags- og energidirektorat NVE, 2015), a 12-meter high and approximately 325-meter-long catching dam with steep impact face was required to protect the area. Since a new tunnel would serve the municipality, the existing road was considered unnecessary, leading the road authority to abandon the roadside in favor of the construction of the catching dam. During the design phase the height of the catching dam was reduced to 5 m for approximately 80 m at the southern end.

The main part of the highest part of the dam was planned located at the existing road as it was thought to be well compacted and stable but the supporting fill at lee side stretched over a farmland downslope. Geotechnical investigations were carried out prior to the work, and it showed some silt close to the toe of the planned fill but otherwise the ground conditions were block-rich moraine and partly coastal debris. Test drilling showed depth to rock between 10 – 20 m (Norges Geotekniske Institutt NGI, 2014).

NVE conducted the preliminary and detailed designs of the dam, with assistance from NGI for the geotechnical aspects (Norges Geotekniske Institutt NGI, 2017). The initial design of the dam indicated very limited space for avalanche debris accumulation above the dam. Additionally, the landowners-imposed restrictions that would effectively reduce the dam's

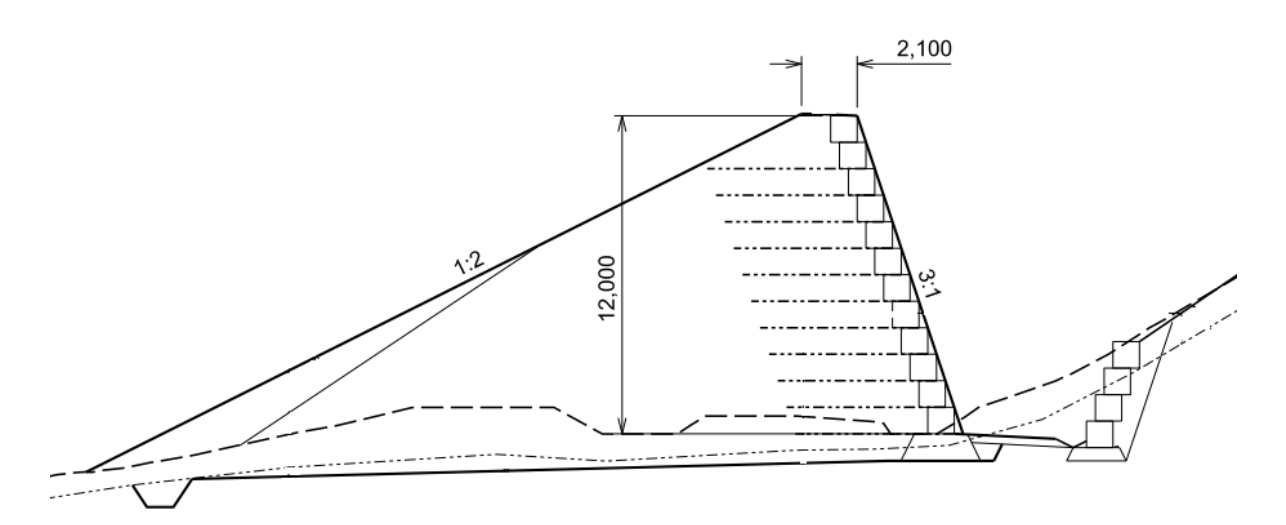


Fig. 2 The figure shows a typical cross section of the catching dam. Boxes in the front show gabions and dotted lines show planned geogrid. As can be seen the area above the dam (to right) is very limited and allows only relatively small machines.

capacity. The plan was to build the impact face of gabions filled with rock and reinforce the steep face with geogrid. The supporting fill downslope was planned material from the tunnel.

The dashed lines in Fig. 2Error! Reference source not found. indicate the existing surface and the old road beneath the geogrid. The stability of this road section was deemed adequate, given its prolonged use over several decades. It was crucial to drain the site to the left of the road before starting any filling operations.

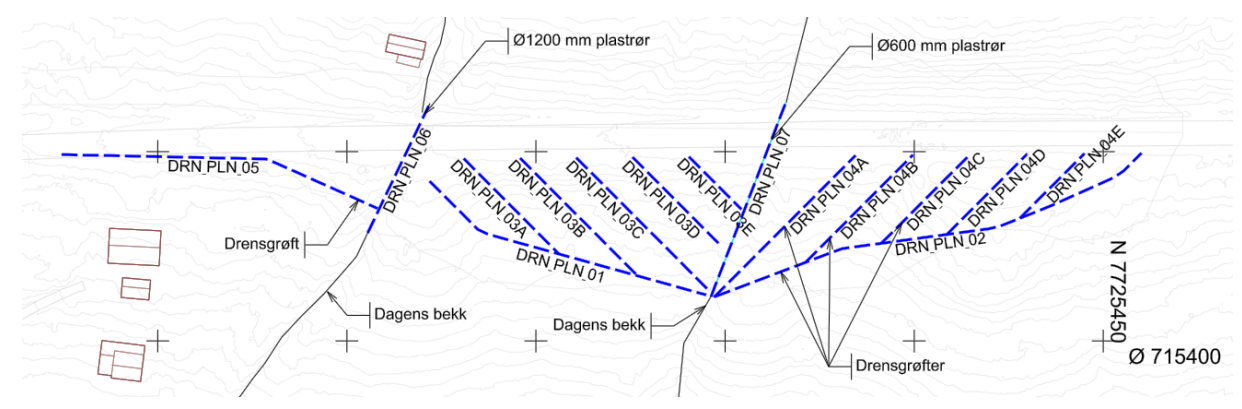


Fig. 3 Blue dashed lines in the figure show the drain system mainly under the supporting fill but also for part of the area around the geogrid. The existing road is visible above the blue dashed lines as a grey area. The distance between the crosses is 50 m. Drawing from the report.

Two main streams flow down the hillside through culverts in the dam. If the culverts become blocked, water can escape south (to left in Fig. 3) via the excavation above the dam. Drainage ditches were also established above the dam to help divert ground water from the dam.

A permeable geotextile was laid out on the foundation prior to the layout of gabions and filling to ensure drainage and soil stabilization.

3. THE CONSTRUCTION 2017 – 2019

The dam's construction began in 2017 by NVEs mechanical department and subcontractors. Despite its small size, completing it in two years is reasonable for Samulesberg, where work is limited from late May to October due to harsh winter conditions.

4. THE COLLAPSE

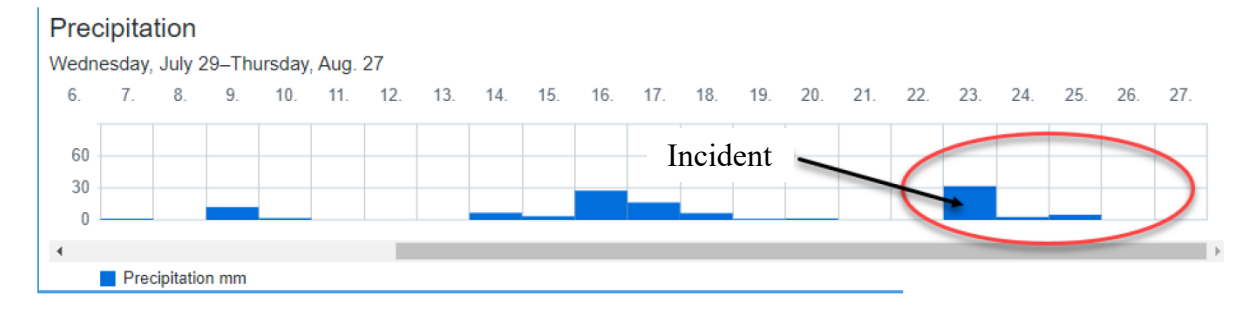


Fig. 4 Dayli precipitation in July 2020 at Løkvollen station some 1.3 km away from the catching dam. From MetNo and (Multiconsult AS, 2020).

Just one year after the construction of the dam part of it collapsed during heavy rain. Shortly after the initial collapse the second collapse occurred, see Fig. 1. These collapses occurred at the 12 m high section of the dam, the 5 m part seemed unaffected. NVE hired Multiconsult AS to investigate the dam collapse and recommend actions. They identified several causes:

- People passing just before the collapse notice bagging at the bottom gabions
- Heavy precipitation and assumed insufficient drainage seem destabilizing
- Information on local bad ground conditions during construction
- Geogrid laid out in wrong direction; it had only one third of necessary capacity.

Multiconsult AS did not explicitly conclude the reasons, but heavy precipitation and incorrect geogrid direction are likely the main causes.

During the initial phase of reconstruction, it was observed that the geotextile was fully impermeable and did not allow water to pass through. This observation was not included in the Multiconsult AS report.

5. THE REBUILT

The catching dam in Samuelsberg was constructed to protect the residential area below it. With the dam no longer functioning, a plan was made to rebuild it the dam and to monitor avalanche risk during construction time. Avalanche warning systems were reinstated, and a plan was established to dismantle the 12-meter-high dam and reconstruct it. Although the existing gabions of the 5 m high dam were not visually appealing, it was decided to retain them while constructing a new 12-meter dam using steel baskets, a system that has proved to be robust and reliable in many Icelandic dams. The remaining 12 m dam was excavated in 2021, and materials were stored nearby for later reuse. During the planning of the reconstruction new ground investigations were carried out. Most of the test pits were shallow as very compact and stable

moraine was found in many of the pits. That indicated that the excavation above the dam was quite stable and could not vibrate as was stated shortly after the collapse.

Steel baskets and strips from the company Geoquest were used for the facing and reinforcement of the steep face. The rebuild, starting in 2023 and finishing late 2024, involved challenging but successful connections between the old 1.0 m high gabions and new 0.5 m high steel baskets, Fig. 5.

The construction process was labour-intensive, requiring manual placement of stones (100–200 mm in size) at the front of the steel baskets. This also resulted in downtime for the machines operating on site. However, the result looks good and demonstrates craftsmanship.

Due to the 12 m height, the work was conducted from a lift in accordance with Norwegian regulations. No accidents were reported during the construction.



Fig. 5 The figure shows the 12 m high dam under construction. To the right is the 5 m high gabion wall. Photo taken in August 2023.

6. KEY TAKEAWAYS

This work provides several important conclusions, which are summarized. Most of them are general but some apply to this project:

• In general, there are only a limited number of contractors in Norway with expertise in constructing dams or barriers using steep facing materials. While the mechanical division of NVE has considerable experience in building erosion protections systems

- and levee systems for rivers, their expertise is not specifically suited for constructions aimed at mitigating rapid mass movements in steep terrains.
- Construction documents and drawings must be clear to ensure contractors understand what to build and how to build. Good documentation should include drawings and checklists.
- Contractors should be mandated to either employ a technical assistant or provide education to their staff on the complexity and functionality of various materials used in earthen dams.
- Supervisors should have education in geotechnical engineering to understand the functions of various materials.
- During a startup meeting, the principal designer or engineer and the client should clearly explain to the contractor how the construction works and the functions of various materials in the construction.
- Ditches above the upstream excavation limit are essential for diverting ground and surface water.
- Monitoring the salinity and chemical composition of the filling material is important for maintaining the longevity of steel baskets.
- Graded gravel (20 120 mm), making up about 15% of the fill, was added to decrease the amount of fine material.



Fig. 6 The figure from July 2025 shows completed catching dam above the residential area in Samuelsberg. Photo: NVE/Anders Bjordal.

7. LIST OF REFERENCES

- Multiconsult AS. (2020). Skredvoll Samuelsberg. Befaringsnotat og årsaksvurdering.
- Norges Geotekniske Institutt NGI. (2014). Grunnundersøkelser i Samuelsberg I Kåfjord kommune Geoteknisk datarapport (K. Kåsin, Ed.; 20140665-01-R).
- Norges Geotekniske Institutt NGI. (2017). Skredsikring ved Samuelsberg, Kåfjord kommune. Detaljprosjektering av sikringstiltak (A. Jonsson & Z. Liu, Eds.; NGI rapport 20170137-01-R).
- Norges vassdrags- og energidirektorat NVE. (2013). *Dimensjonering av sikringstiltak for Samuelsberg* (O.-A. Mikkelsen, Ed.; Vol. 15). Norges Vassdrags- og Energi Direktorat (NVE).
- Norges vassdrags- og energidirektorat NVE. (2015). *Tiltaksplan. Skredsikring ved Samuelsberg* (H. Strand, A. Bjordal, & O.-A. Mikkelsen, Eds.; 201404173).

Adapting and using active rigid modules in a passive way against avalanches

Rémy Martin, 1* Nadia Hassine 1 and Philippe Berthet Rambaud 2*

¹ ONF-RTM 9 quai Créqui 38000 GRENOBLE FRANCE ² Engineerisk 690 route de la Motte Servolex 73160 St SULPICE FRANCE *Corresponding author, e-mail: remy.martin(a)onf.fr and pbr(a)engk.fr

ABSTRACT

Snow supporting structures used to stabilize avalanche starting zones benefit interesting operational feedback regarding structural resistance and durability, manufacturers availability and installation experiences. Using these characteristics in a different passive way can bring new solutions for specific situations. Two cases are presented: the first one concerns the access road to Gourette ski resort in the French Pyrenees, which was completely closed during winter 2015. To secure this road, the "Mountain terrains restoration" (RTM) service, part of the national forestry office, has proposed a combination of artificial release systems and rack-type modules located downhill for an additional braking effect. This choice is adapted to the context of the Pyrenees where snow conditions change very quickly, moving from cold snow conditions (favorable to effective triggering) to wet snow conditions (with frequent natural avalanches). The paper presents the solutions proposed to achieve the corresponding design from a very classic model of active rack. The second case also adapts the design of existing active models but in a different context: the asset is the bottom station of the new gondola of famous "Mer de Glace" glacier at Chamonix-Mont-Blanc which is located near the exit of a narrow gully. Due to its steepness surrounded by rocky slabs, recurrent small flows accumulate downhill, creating a potentially prejudicial new terrain shape in case of larger event. Only four modules were installed, mono-anchored and reinforced types, mostly to change the geometry of the deposit by increasing lateral natural accumulation able to influence a subsequent event.

1. INTRODUCTION

Structural avalanche defenses in the starting zone (Margreth 2007) are not designed to withstand snow avalanches. Their use requires the stabilisation of the upstream zones and if, for reasons of heavy snow cover, it is desired to trigger an avalanche within the structures, major damage can occur. Unexpected snow avalanches are even listed as the main reason for damages (Harada et al. 2018)

However, it is sometimes necessary to protect nearby issues without necessarily equip an entire slope or install kind of obstacles for specific purposes. In such cases, it is possible to design adequate structures, but the idea here is to adapt existing structures to limit development (and therefore costs).

Two different applications are presented hereafter which show different possibilities and different approaches, all based on the adaptation of existing supporting structures models.

2. ROAD PROTECTION: A SNOW BRIDGE WHICH CAN RESIST TO TRIGGERED AVALANCHES

2.1 Context

During the winter 2015, the road #918 linking the village of "Les Eaux-Bonnes" to the ski resort of "Gourette" (Pyrénées Atlantiques) was closed due to avalanches, and the resort had to be evacuated. As a result, the local road administration decided to make the route safer.



Figure 1 February 2nd 2015, left : snow avalanche of "la cascade de Goua" (©D. Oulié), right: snow avalanche "des Blanques" (©D. Oulié).

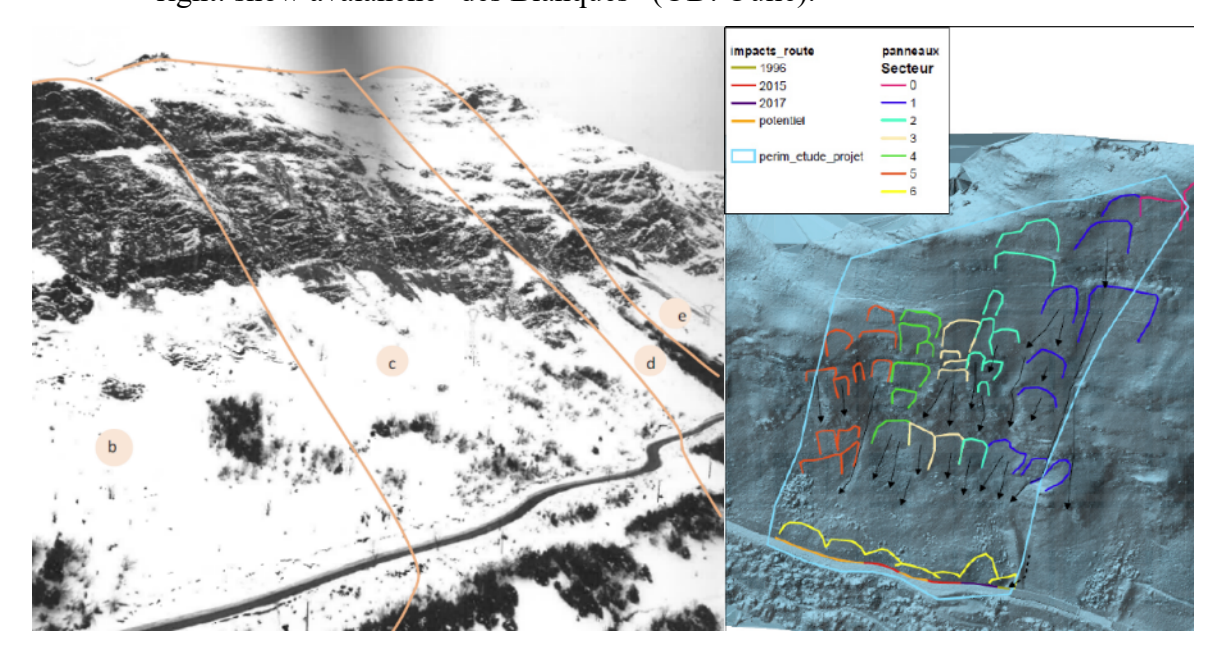


Figure 2 overview of the site (February 1978) and the different starting zones (ONF-RTM 2022)

A study carried out by ONF-RTM and Meffre (2018) enabled the road manager to adopt a protection strategy for its route using various solutions, concluding in a combination of Remote Avalanche Control Systems (RACS) and rake-type supporting structures. This design was then refined and sized in a project study (ONF-RTM, 2022): the rakes are designed to laminate/brake the snow flows within a combined strategy where avalanches from the upper panels are released (left avalanche in figure 1), while flows from the slopes downhill (just above the road – right in figure 1).

This choice stems from the context of the Pyrenees, where snow conditions change very rapidly, from cold snow (favourable for effective triggering) to wet snow. Almost during the same avalanche period, passive structures at the bottom of the slope can be subjected either to snow flows resulting from artificial shootings, but also from the spontaneous release of wet snow.

Thanks to their intrinsic resistance, passive structures are initially made from a 'classic' metal snow rake with a buried bar whose sizing had to be adapted to withstand the actions of the flow.

2.2 Snow load for the design

The design of the structure required the definition of the project situations and the action values to be taken into consideration for the structural calculations (metal assembly and foundation of the structure). These action values include the creep of the snowpack, for which a standard exists in France (NFP95-303, 2020) and the possible dynamic impact of snow flows/avalanches. The design situations will also depend on whether the structure has been previously filled with snow or not.

The calculation of the dynamic impact pressure is subject to a large number of parameters, including significant random uncertainties (which cannot be reduced). A precautionary approach has been chosen. The dynamic characteristics of the flow were assessed by modelling them using the RAMMS software. Among other hypotheses, the design is based on the propagation of a 100-years return period volume, as if artificial releases were ineffective. Finally, the most pessimistic case is assumed to be a speed of 15m/s and the corresponding pressure against this ''obstacle'' is calculated following usual equations (Barbolini et al. 2009).

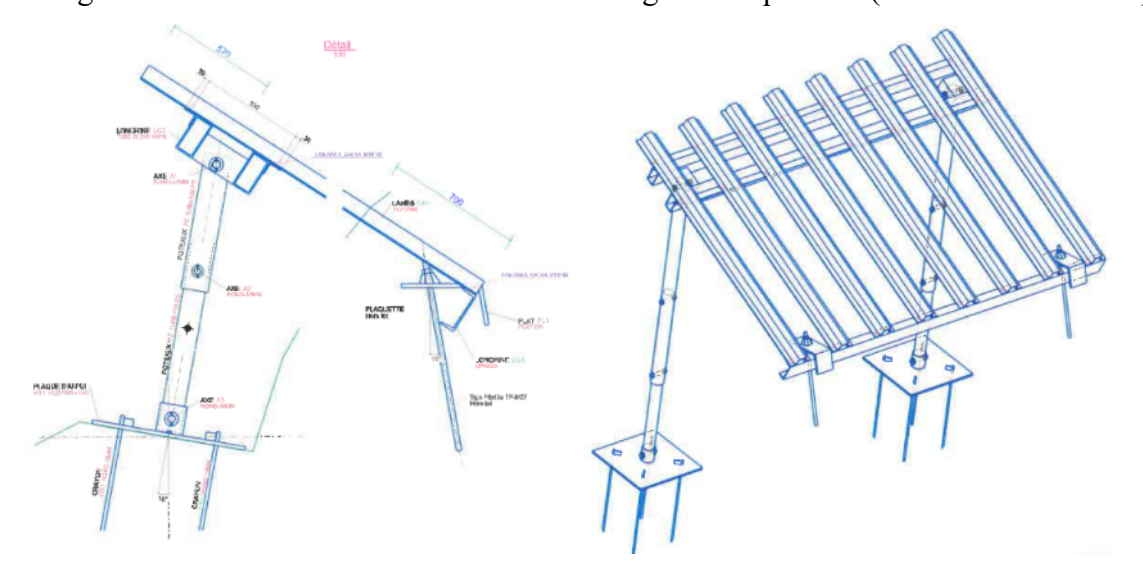


Figure 3 design of the snow rake

2.3 Adaptations of an existing snow supporting product

It was decided to adapt an existing steel buried-upstream-bar rake structure (Figure 3). The design was guided by two main constraints: The feasibility of heli-lifting and the reasonable feasibility of foundations. The thickness of the steel was increased (values of 6 mm instead of 4 mm were required), and the inclination was increased (20°) to better distribute resultant forces. To reduce them on the foundations, the width of the module was also limited to 4m and the surface area of the downstream plates has been increased.

2.4 Consequences in terms of construction

The foundation arrangements involved major earthworks (see Figure 4). Their feasibility will depend on the amount of machinery that can be brought to the site. Heli-lifting meant that the structure had to be lightened, and the crossbeams were assembled on site (see Figure 5).

The cost of the structures (supply and installation) was around 4,000 euros/ml, which is 2 to 3 times more expensive than 'conventional' structures.



Figure 4 View of the earthworks for the installation of the structures



Figure 5 Snow bridge for Heli lifting (the crossbeams were removed to reduce weight) and view of the finalised structure.

3. MONO-ANCHORED SNOW BRIDGES AS DEVIATING OBSTACLES

With the retreat of the glacier, a new gondola has been recently installed to access the Mer de Glace and its famous ice cave in Chamonix-Mt-Blanc. One of the specificities of the site is the coexistence of avalanches and rockfalls, each requiring structures that may have to "withstand" the other phenomenon.

Firstly, rockfall risk management required the installation of two superimposed dynamic falling rock protection kits, E1 and E2 (Figure 6) which are partly threatened by potential avalanches. However, this type of dynamic structure is not designed to withstand repeated pseudo-static pressures and/or the continuous loading of a large filling of snow. From this point of view, their installation on a relatively high point was an initial advantage that had to be further improved by channelling the main avalanche flow line and "breaking" its incident dynamics.

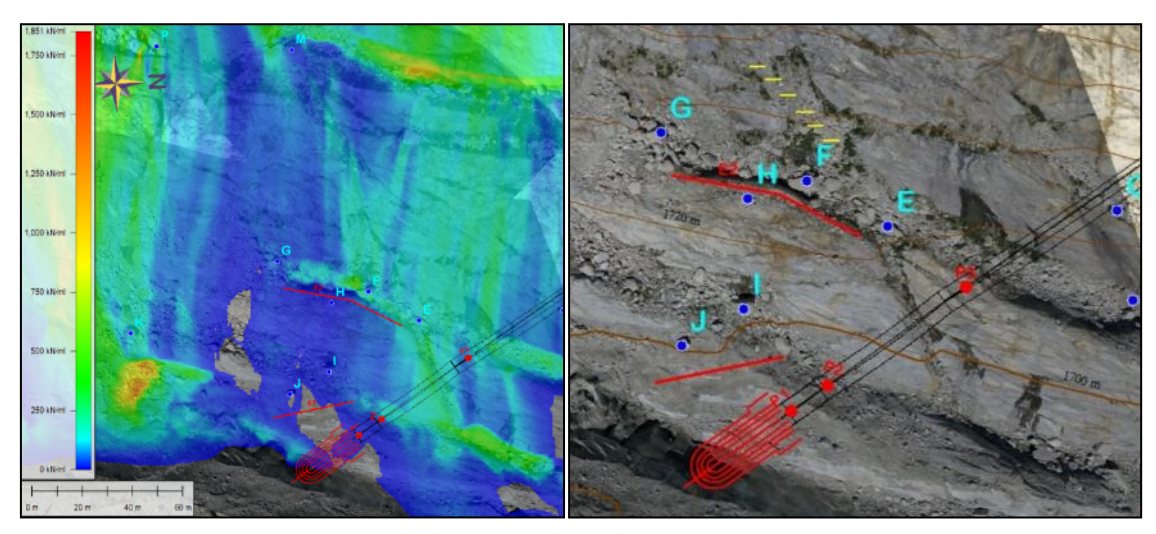


Figure 6 Left, snow avalanche potential intensity above the gondola station (ropeway in black). Right, view of the two main rockfall kits (red lines) and location of the staggered arrangement of the active-passe modules (in yellow)

To achieve this, rather than considering a complex, exploratory prototype structure, which would be all the more ambitious the higher it was on the slope, the reasonable choice was to use known structures in mountainous context, able to resist a certain pressure, from whatever it finally comes. From this point of view, the design of a normalised snow bridge is interesting as it effectively includes such a defined loading, all the more important the model is tall and considered as isolated. The ER50 size in accordance with the latest version of standard NF P 95-303 (2020) and under an individual modular approach, gave a first basis to obtain these new active-passive structures then to position them in such a way as to induce a lateral deflection of the flow.

To maximise the resistance, the frame based on ER50 steel profiles was furthermore reduce to a 3m x 3m panel with a strong connection to a rigid drawbar, itself assisted by cables braced to the corner of the structure (Figure 7). Apart from the main anchorage, no other fastening devices were permitted: each module must be able to slide and find its natural position in the event of an avalanche. Finally, a curved tube was added at the bottom to play the role of "ski" and facilitate lateral movements in the scree.

The desired deflecting effect, in order to extend the existing natural corridor, could be achieved by placing a series of modules globally close together in a frontal position and staggered transversely on the slope (Figure 7). By allowing small lateral movements thanks to a certain length of cables from the anchors made at the foot of the upper cliff where the ground resistance is maximum (unlike the lower scree), this ensures the best 'natural' positioning. It gives also a certain flexibility to provide better resistance to impacts from blocks, additionally to an acceptable "damageable" or even replaceable characteristics of crossbeams.

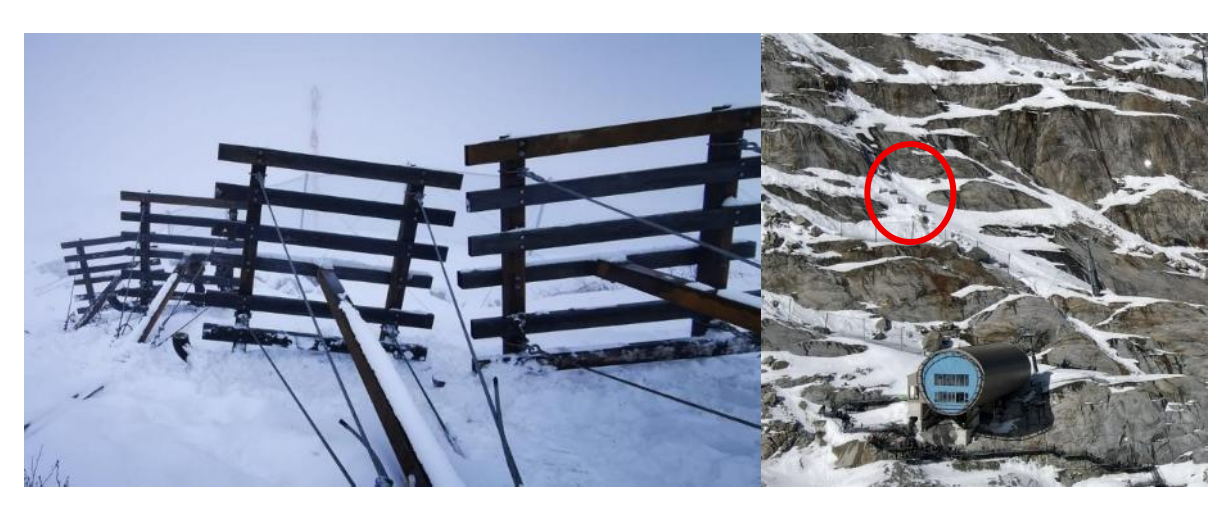


Figure 7 Left, view of the four modules located above the gondola bottom station (right)

4. CONCLUSIONS

The existing design of normalised active supporting structure models is interesting as it already takes into account pressure loadings which, with minimum adaptations, can withstand (small) snow-avalanches to influence them: two applications are presented but with only a reduced existence period: they need to be followed during the coming winters to verify that the underlying concepts and hypotheses were correct.

REFERENCES

Barbolini M., U. Domaas, Thierry Faug, P. Gauer, K.M. Hakonardottir, et al..2009. The design of avalanche protection dams Recent practical and theoretical developments. EUROPEAN COMMISSION, 212 p., 2009, Climate Change and Environmental Risks,

Harada Y., Matsushita H., Kanazawa A., 2018. An attempt to create a soundness evaluation fro snow bridges In: Proceedings of the International Snow Science Workshop, Innsbruck, Austria 2018

Margreth, S., 2007: Construction d'ouvrages paravalanches dans la zone de décrochement. Aide à l'exécution: directive technique. L'environnement pratique no 0704. Office fédéral de l'environnement Berne, WSL Institut Fédéral pour l'Étude de la Neige et des Avalanches ENA, Davos. 136 S.

NFP 95-303, 2020. Norme française Equipements de protection paravalanches, claie, râteliers ONF-RTM and JF. Meffre, 2018. Protection de la RD 18 contre les avalanches du village des Eaux-Bonnes à Gourette, tecnical report

ONF-RTM & JF. Meffre, 2022. Site de Siala-projet de protection paravalanche, tecnical report.

Detection of liquid water accumulations during snow block sliding experiments.

James Glover, 1* Fabian Wolfsperger, 2 Silvio Ziegler³

1 University of Applied Sciences Grisons Chur Switzerland 2 WSL, Institute for Snow & Avalanche Research, SLF Davos Dorf Switzerland 3 FPGA Company GmbH Tann Switzerland

ABSTRACT

Liquid water accumulation at the snow-ground interface is a key factor influencing glide snow avalanche activity. In this study, we use a calibrated capacitive sensor to detect the liquid water content (LWC) in snow during a series of controlled snow block sliding experiments. These experiments aim to assess how water accumulation affects the angle of dynamic friction at the snow-ground interface.

The LWC sensor module enables continuous, real-time measurements and was actively used throughout the experiments. Snow blocks were exposed to a radiant heat lamp to induce melting until sliding occurred. We analyze the relationship between LWC accumulation and the onset of sliding, characterized by the dynamic friction angle.

Preliminary results are presented for melting snow blocks sliding over two different substrates: smooth plastic glass and a low-friction geotextile surface.

J. Glover and others P1.5 - Page 283

Roof avalanche mitigation through photovoltaic panel heating to induce controlled snow removal

James Glover, 1* Michael Sattler, 2 Dylan Longridged, 1 Philip Crivelli, 1 Jann Ambühl, 3

¹ University of Applied Sciences Grisons Chur Switzerland ² Liestal Switcherland ³ BZG Ambühl/Ehrensperger Davor Frauenkirch Switzerland

ABSTRACT

Snow accumulations on photovoltaic (PV) systems installed on sloped roofs present structural and safety challenges in alpine regions. This study investigates the environmental and snowpack conditions associated with slab-like roof avalanches on a PV installation equipped with a reversely biased heating system. In this configuration, the temperature at the snow–panel interface can be increased to induce controlled release of accumulated snow.

A rooftop sensor module recorded panel surface temperature, snowpack temperature, snow depth, snow mass and density, and liquid water content within the snow. These measurements were complemented by local weather data, including air temperature, humidity, wind speed and direction, solar radiation, and precipitation. Thermal imaging was periodically conducted to assess the spatial distribution of surface heating across the installation.

The dataset enables identification of key physical parameters influencing roof snow avalanches on PV surfaces and supports the development of automated snow load mitigation systems for solar installations. Through this approach, the goal is to improve operational safety and energy production by regularly and safely clearing snow before it can accumulate dangerously

J. Glover and others P1.6 - Page 284

Engineering Approaches to Avalanche Mitigation in Japan: Current Status, Challenges, and Future Perspectives

Yusuke Harada 1*

¹ Civil Engineering Research Institute for Cold Region, 1-3-1-34 Hiragishi Toyohira Sapporo Hokkaido, JAPAN *Corresponding author, e-mail: harada-y (at) ceri.go.jp

ABSTRACT

In Japan, in addition to the increasing frequency and severity of natural disasters, the aging of the infrastructure and the decline in the working-age population have been progressing year-by-year, making efforts to maintain sustainable avalanche mitigation measures increasingly important. In October 2024, the Avalanche Mitigation Subcommittee of the Japan Society of Snow Engineering organized the first working group to examine the current status, challenges, and future perspectives of engineering approaches to avalanche mitigation in Japan. Based on understanding avalanche-prone sites through direct observation, the action plan of the subcommittee is to gather the approaches of domestic and foreign organizations engaged in avalanche mitigation through the working group in order to share insights and recommendations through a comprehensive report on the future of avalanche mitigation efforts. This paper presents the key findings and discussions generated through the activities of the first working group, along with an overview of the historical development of avalanche mitigation measures in Japan.

1. INTRODUCTION

In Japan, in addition to the increasing frequency and severity of natural disasters, the aging of the infrastructure and the decline in the working-age population have been progressing year-by-year, making efforts to maintain sustainable avalanche mitigation measures increasingly important.

Japan is one of the most snow-prone countries in the world, with approximately 70% of its land consisting of mountainous and hilly terrain. Although countermeasures against avalanches affecting roads, railways, forested areas, and settlements have progressed, unexpected avalanche events still cause damage to infrastructure and result in road closures. This indicates that protective measures remain insufficient in certain areas. To reduce avalanche-related damage, it is essential to enhance both avalanche research and practical implementation of the findings.

In October 2024, the Avalanche Mitigation Subcommittee of the Japan Society of Snow Engineering organized the first working group to examine the current status, challenges, and future perspectives of engineering approaches to avalanche mitigation in Japan (Harada, 2025). Based on understanding of avalanche-prone sites obtained through direct observation, the action plan of the subcommittee is for the working group to gather the approaches of domestic and foreign organizations engaged in avalanche mitigation in order to share insights and recommendations through a comprehensive report on the future of avalanche mitigation efforts. This paper presents the key findings and discussions generated through the activities of the first

working group, along with an overview of the historical development of avalanche mitigation measures in Japan.

2. AVALANCHE DAMAGE, COUNTERMEASURES, AND RESPONSES MAINLY SINCE THE 20TH CENTURY

In Japan, changes in the social environment during the 20th century significantly influenced the occurrence of avalanche disasters. Between 1867 and 2010, a total of 7,940 avalanche incidents were recorded, resulting in 6,167 fatalities (Izumi, 2014). According to the Snow Research Center of Japan (2000), the number of avalanche events and the corresponding number of deaths and missing persons between 1900 and 1999 peaked particularly between 1955 and 1985. Fatalities and missing persons were notably high between 1918 and 1963, with especially severe disasters occurring around 1910 to 1930, and during that period individual avalanche events caused over 80 deaths or designations as missing persons. These large-scale disasters were primarily associated with damage to settlements, railway lines that extended into snowy regions, and with field operations related to industrial expansion, such as mining and power infrastructure development. Although the total number of avalanche events during this period was relatively low, some individual avalanches resulted in particularly severe consequences. Legislation was enacted in 1956 to ensure road transportation in snowy and cold regions. Subsequently, the heavy snowfall event of January 1963 served as a turning point that prompted the development of avalanche countermeasures. Numerous avalanches occurred during the heavy snow years of 1981, 1984, 1986, and 2006. In January 1986, an avalanche disaster destroyed or severely damaged ten houses and resulted in 13 fatalities. In recent years, both the number of avalanche occurrences and the number of deaths or missing persons have shown a declining trend. However, a relatively high proportion of avalanche-related casualties now occur during winter mountain recreational activities such as mountaineering and skiing. This trend has continued more or less consistently to the present day (Izumi, 1998; Akiyama, 2012).

In Japan, for avalanches affecting roads, railways, power infrastructure, forested areas, and settlements, a combination of structural measures such as structural interventions based on historical records and hazard assessments, and non-structural measures such as regulatory controls have been implemented. As a result, large-scale avalanche disasters have rarely occurred since 1986. However, damage caused by avalanches has still been reported in the following cases:

- Large-scale storm slab avalanches caused by intense snowfall: Damage to bridges, dam construction or inspection workers, and settlements.
- Avalanches caused by heavy snowfall associated with low-pressure systems: Repeated avalanches that slipped through trees and existing snow bridges descended on roads and settlements.
- Earthquake-induced avalanches: Large and multiple slab avalanches occurred near the epicenters, characterized by irregular fracture patterns in snowpack on slopes, and accompanied by landslides.
- Large full-depth avalanches: Debris accumulated downstream of a snow shed; part of it reversed course and flowed back through the opening site, reaching the roadway.
- Wet slab avalanches due to rain-on-snow: Damage to infrastructure facilities.

• Slush avalanches: Damage to sediment control dams, roads, and bridges in the Mt. Fuji area.

3. AVALANCHE MITIGATION IN JAPAN: CURRENT STATUS AND CHALLENGES

3.1 Structural Measures for Design and Construction

3.1.1 Current Status

- Avalanche mitigation design practices in Japan generally follow the Snow Protection Handbook 2025 Revised Edition (Snow Research Center of Japan, 2025). In addition, the guidelines for avalanche mitigation and protection (draft version) and a photographic catalog of avalanche mitigation and protection structures (NPO Snowslide Disaster Prevention Technology Forum, 2017), and avalanche countermeasure considering regional characteristics of Hokkaido (draft version) (CERI, 2010) have also been published.
- The design snow pressure used for snow bridges in Japan follows the "Defense Structures in Avalanche Starting Zones" in the Swiss guideline. In southern Honshu, where wet snow predominates, the glide factor is set at 1.5 times the base value. While in northern Hokkaido, where dry snow is dominant, the same values as those used in Switzerland are applied (Takahashi et al., 2018).
- When the design snow depth is small, the distance between structures in the line of slope tends to decrease, resulting in overdesign. Field testing and discussions with domestic and international experts have led to the proposal of a broader range of acceptable distance between structures in the line of slope as a reference condition for design (Matsushita et al., 2012).
- Snow bridges with mesh panel have been shown to effectively prevent avalanches from flowing through gaps in the fence face and reaching roads. Their effectiveness has been quantitatively verified. It serves as reference material for design guidelines (Matsushita et al., 2010).
- Due to considerations such as cost-effectiveness and landscapes, suspended snow nets are increasingly being installed in avalanche starting zones, while vertical net-type fences are applied in deposition zones.

3.1.2 Challenges

- When probabilistic evaluations of avalanche scale and loading are unclear, designs tend to adopt conservative assumptions to ensure safety.
- There is ongoing discussion regarding the appropriate application ranges for avalanche mitigation structures. It is also necessary to consider the possibility of introducing new technologies to expand design options.
- Since the selection criteria and design approaches for avalanche mitigation measures
 vary by region and by the type of asset to be protected, there is a need to systematize
 these practices. While designs generally follow the guidelines presented in the
 handbook, flexibility to accommodate site-specific conditions is also considered
 important.

3.2 Avalanche Management in Planning, Maintenance, and Monitoring

3.2.1 Current Status

- In Niigata Prefecture, one of the snowiest regions in Japan, road administrators prepare an avalanche patrol logbook before each winter season. During snow seasons, they conduct on-site inspections and, when necessary, remove overhanging snow accumulating above snow bridges to mitigate risk. The cost of such snow removal measures amounts to approximately 400 million yen per year under average snowfall conditions on managed roads by the prefecture. Avalanche-related damage has been decreasing year by year, primarily due to the widespread installation of avalanche protection structures and preemptive overhanging snow removal from above snow bridges. In addition, conditions for the collapse of overhanging snow, including height and projection length, have also been characterized (Harada, 2025).
- Also, the Inspection Guidelines for Rock and Snow Prevention Facilities in Niigata Prefecture (Draft, 2013 revised edition) have been published. In addition, an attempt to create a soundness evaluation for snow bridges has been proposed (Harada et al., 2018).
- Failures such as collapsed, loosened wires, and dislodged anchors have been confirmed in snow bridges of the suspended type.
- In some cases, trail cameras equipped with communication functions have been installed on avalanche slopes along roads to allow remote monitoring. However, a fully operational real-time avalanche monitoring system has not yet been established.
- Conditions for avalanche occurrence in forested slopes have been considered, and a simplified method for estimating their frequency has been proposed (Matsushita et al., 2018).
- In recent years, increased avalanche risk has been observed in areas where tree fall or deforestation has reduced the glide-suppression effect of snowpacks on slopes.

3.2.2 Challenges

- Key challenges include aging infrastructure, rising maintenance costs, and a shortage of contractors available to conduct avalanche hazard inspections and remove overhanging snow from the abovementioned snow bridges in the future, preserving technical knowledge, and securing budgets. To address these issues, the use of machine learning, ICT, and UAVs is expected to play an increasingly important role.
- A standardized methodology for soundness evaluation of avalanche protection structures needs to be established. Based on this methodology, condition assessments of avalanche mitigation facilities should be conducted nationwide using consistent procedures and criteria.
- A balanced approach to avalanche management should be pursued through the integration of probabilistic assessments of avalanche occurrence and runout, along with practical discussions among administrative stakeholders.

4. AVALANCHE MITIGATION IN JAPAN: FUTURE PERSPECTIVES

In Japan, future avalanche mitigation must take into account several evolving challenges: the intensification of hazardous events such as short-duration heavy snowfall and increased winter rainfall, the impacts of global warming, the occurrence of earthquakes, and the decline in both

the working-age population and available budgets. In this context, to protect lives and maintain societal resilience, it is essential to develop new technologies and frameworks that address changes in snowfall patterns and snow characteristics. The following considerations are proposed:

- Continued efforts toward the long-term durability of existing structures through asset management.
- Installing and updating avalanche countermeasures that take into account previously unexperienced events, environmental impact, and landscape considerations, in addition to establishing prioritization methods for handling slopes (e.g., inspection, repair, or maintenance).
- Developing systems and technologies that enable broader area monitoring with fewer personnel, while also enhancing rapid response capabilities for lifesaving, damage assessment, and emergency measures. This includes the application of UAVs (for surveying, emergency response, and avalanche control), machine learning, ICT, and remote sensing technologies for purposes such as avalanche record accumulation, damage detection, monitoring, and support systems.
- Enhancing real-time and forecast-based information to support decisions on pre-emptive road closures, evacuation orders, and behavioral changes prior to avalanche events.
- Setting up teams to enable timely artificial avalanche release (e.g., via explosives) in high-risk roadside slopes.
- Building cross-sectoral collaboration frameworks that promote knowledge transfer, technical continuity, and enlightenment to reduce avalanche-related damage.

ACKNOWLEDGEMENT

The author appreciates those who presented and participated in the first working group in October 2024 for their cooperation.

REFERENCES

- Akiyama, K., 2012. Geometry and magnitude of snow avalanches. Dissertation of Niigata University, pp.1-5. [in Japanese with English abstract]
- Civil Engineering Research Institute for Cold Region (CERI), 2010. Avalanche Countermeasure Considering Regional Characteristics of Hokkaido (draft version), 47pp [in Japanese]
- Izumi, K., 2014. Database on snow avalanche disasters in Japan. Research Institute for Natural Hazards and Disaster Recovery, Niigata University. https://www.nhdr.niigata-u.ac.jp/records/nadare db/ [2025/07/28]
- Harada, Y., Matsushita, H., Kanazawa, A., 2018. An attempt to create a soundness evaluation for snow bridges. Proceedings of the International Snow Science Workshop, Innsbruck, Austria, October 7–12, 2018, pp. 278–282.
- Harada, Y., 2025. Reports on the 2024 workshop for the avalanche prevention committee present issues and draft proposal for avalanche mitigations of engineering. Japan Society of Snow Engineering, 41(1), 39-46. [in Japanese]

Y. Harada P2.1 - Page 289

- Matsushita, H., Matsuzawa, M., Nakamura, H., 2012. Possibility of increasing the slope distance between avalanche prevention bridges. Proceedings of the International Snow Science Workshop, Anchorage, Alaska, September 17–21, 2012, pp. 696–702.
- Matsushita, H., Matsuzawa, M., Sakase, O., Nakamura, H., 2010. Effect of mesh panel fences against the phenomenon of snow slides through support structures designed to prevent avalanches. Monthly Report of Civil Engineering Research Institute for Cold Region, 685, pp. 22-30. [in Japanese]
- Niigata prefecture, 2013. Inspection Guidelines for Rock and Snow Prevention Facilities in Niigata prefecture (Draft, 2013 revised edition). 40pp. [in Japanese]
- NPO Snowslide Disaster Prevention Technology Forum, 2017. Guidelines for Avalanche Mitigation and Protection (draft version). 254pp. [in Japanese]
- NPO Snowslide Disaster Prevention Technology Forum, 2017. Photographic catalog of avalanche mitigation and protection structures. 128pp. [in Japanese]
- Snow Research Center, 2000. Case studies of avalanche disaster (1618-1999). pp. 1-14. [in Japanese]
- Snow Research Center of Japan, 2025. Snow Protection Handbook 2025 Revised Edition. pp. 139-300. [in Japanese]
- Takahashi, W., Harada, Y., Matsuzawa, M., 2018. Changes in snow pressure on snow bridges in the Hokkaido region of Japan. Proceedings of the International Snow Science Workshop, Innsbruck, Austria, October 7–12, 2018, pp. 176–180.

Y. Harada P2.1 - Page 290

Snow net instrumentation at Snoqualmie Pass, Washington, USA

Chris Wilbur^{1*} and John Stimberis²

Wilbur Engineering, Inc., 150 E. 9th St. #201, Durango, Colorado, 81301 USA
 Washington State Department of Transportation, Seattle, Washington, USA
 *Corresponding author, e-mail: geowilbur@gmail.com

ABSTRACT

Interstate 90 is a critical transportation corridor with over 30,000 vehicle trips per day that connects the port city of Seattle, Washington with the interior U.S. The highway crosses the Cascade Mountains at Snoqualmie Pass at elevation 921 meters. More than 1200 meters of Dk 3.0 to 4.0-meter snow nets were installed at the Slide Curve avalanche path about 9 kilometers southeast of the pass to improve safety and reduce avalanche closures.

The project is in a maritime snow climate with heavy winter snows and mild temperatures. Annual snowfall is highly variable. Continuous long-term records at Snoqualmie Pass record an average annual snowfall of 11 meters. The maximum recorded snow height is 5.03 meters in 1956. Deep snow, common rain-on-snow events, high snow densities, and high glide areas required special designs for the project.

The Washington State Department of Transportation (WSDOT) installed instrumentation to monitor loads, deformations and deflections in the snow net components and an on-site weather station to measure snow heights, water content and other parameters. The purpose of the measurements is to improve our understanding of snow net performance in this deep maritime snowpack and to guide maintenance, repairs and future designs.

The measurement system has been operational for eight winters from 2018 to 2025. All years, except 2021, were near or below average and median snow heights. Maximum snow heights in 2021 were about 60-percent of design heights. Measured loads and deflections in 2021 were similar to below-average years. The largest snow net loads occurred in 2022, a below-average snow year. The authors believe that a likely explanation for the relatively large loads was due to a unique combination and sequence of rain, sleet, and snow accumulations.

1. INTRODUCTION

Interstate 90 is a critical transportation corridor that connects the port city of Seattle with the interior U.S. (Figure 1). The highway crosses the Cascade Mountains at Snoqualmie Pass at elevation 921 meters. Several avalanche paths can reach the highway near Snoqualmie Pass. Snoqualmie Pass has a rich history of avalanche management, structural and operational mitigation, and research (LaChapelle et.al., 1976, Schaerer, 2000). Closures often result in long detours and significant disruptions to commerce and the travelling public. Much of the highway follows the shore of Lake Kechelus, so consequences of avalanches can be severe to exposed traffic.

Between 2009 and 2018, I-90 was improved and widened from 4-lanes to 6-lanes. The Slide Curve avalanche path on the east side of the pass presented a challenging avalanche mitigation problem due to ground instabilities, steepness, high snow depths and densities, high glide areas, rockfall and lack of runout zone above the highway.



Figure 1 – Site location

Slide Curve was re-graded and rock-scaled, and over 1200 meters of Dk=3.0 to 4.0-meter snow nets were installed between elevations 812 m and 920 m. Dk=4.0m snow nets were installed on smooth rock surfaces at the upper elevations with artificial surface roughening. Dk=3.5m and Dk=3.0m snow nets were installed at lower elevations. Snow nets in two rows were instrumented to quantify snow pressures, deflections and structure performance. This paper describes the instrumentation and measurements to date.

2. CLIMATE

The project is in a maritime snow climate with heavy winter snows, mild temperatures, common rain-on-snow events and highly variable snow depths. Figure 2 shows the site and nearest weather stations. Long-term weather records (95 years) at Snoqualmie Pass (el. 921m) have an average annual snowfall of 11 meters and a maximum snow depth of 5.03 meters in 1956. Figure 3 shows the historic maximum snow heights at Snoqualmie Pass. Table 1 presents snow height data from the long-term weather station at Snoqualmie Pass. Snow depths at Slide Curve are about 30-percent lower than Snoqualmie Pass. Weather stations at Stampede and Ollalie indicate average snow densities of 400 to 450 kg/m³ in deep snow years. Similar high snow densities have been described in Norway and Iceland (Jóhannesson and Margreth, 1999).

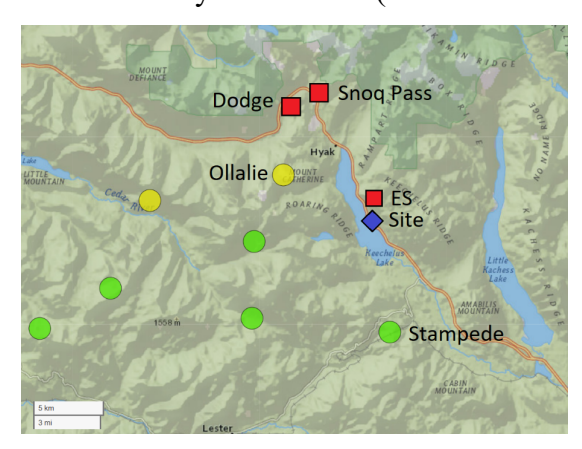


Figure 2 – Site with nearest weather stations

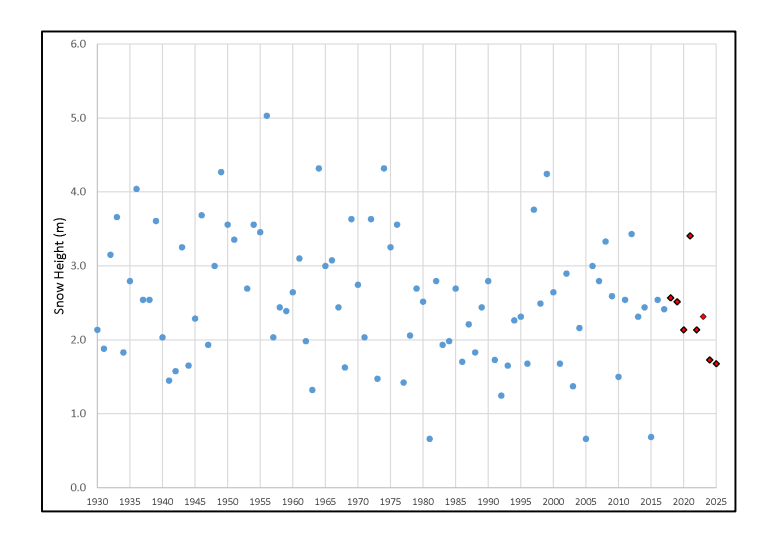


Figure 3 – Historic snow depths at Snoqualmie Pass The red symbols are the 8-years with snow net instrument data.

Table 1 – Snoqualmie Pass snow depth statistics

	max.	median	avg	std dev					
95 yrs*	5.03	2.50	2.54	0.86					
30 yrs	4.24	2.46	2.39	0.87					
8 yrs**	3.40	2.22	2.31	0.86					
* period of record									
**snow net measurement period									

3. TERRAIN & VEGETATION

The site is below timberline, but has sparce vegetation due to historic landslides, rock scaling, construction activities and avalanche mitigation with explosives since the mid-1970s. Figure 4 shows the site prior to snow net construction. Complex non-planar terrain and non-uniform roughness at upper Slide Curve may cause variable creep flows and snow net pressures.

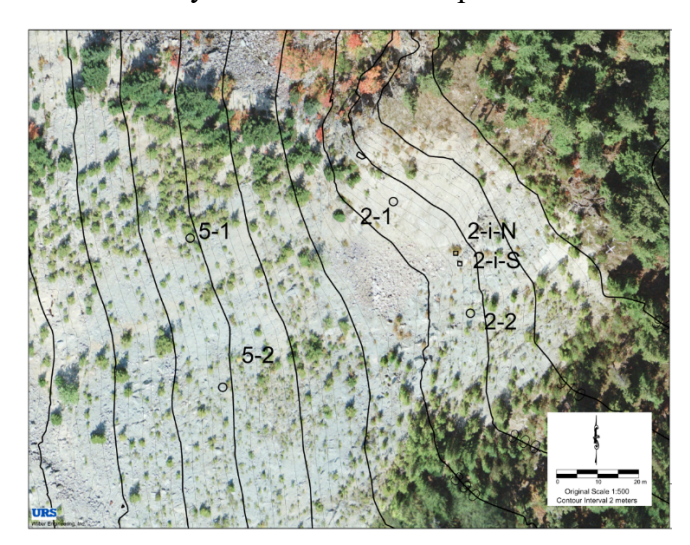


Figure 4 – Pre-construction site topography & vegetation

4. INSTRUMENTATION

WSDOT installed instrumentation to monitor loads, deformations and deflections in the snow net components. In addition, an automated weather station was installed at the upper elevations of the site to measure snow heights, water content and other weather data. Figure 5 shows the instrumented locations on a topographic map and Figure 6 shows the placement of the sensors on the structure. A moisture sensor was installed on the ground near site 2-1.

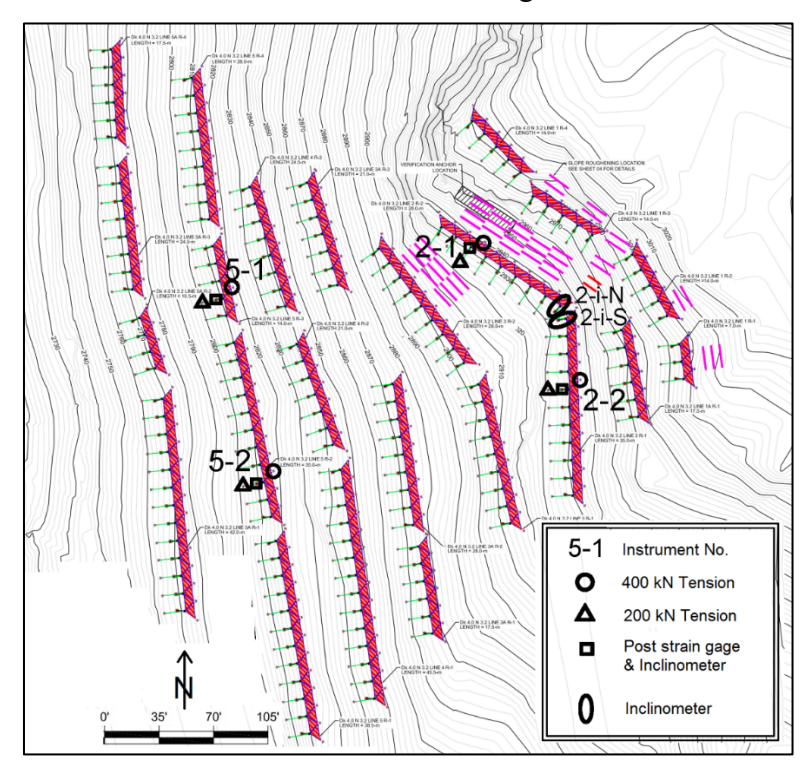


Figure 5 – Instrument locations and snow net layout on topographic map

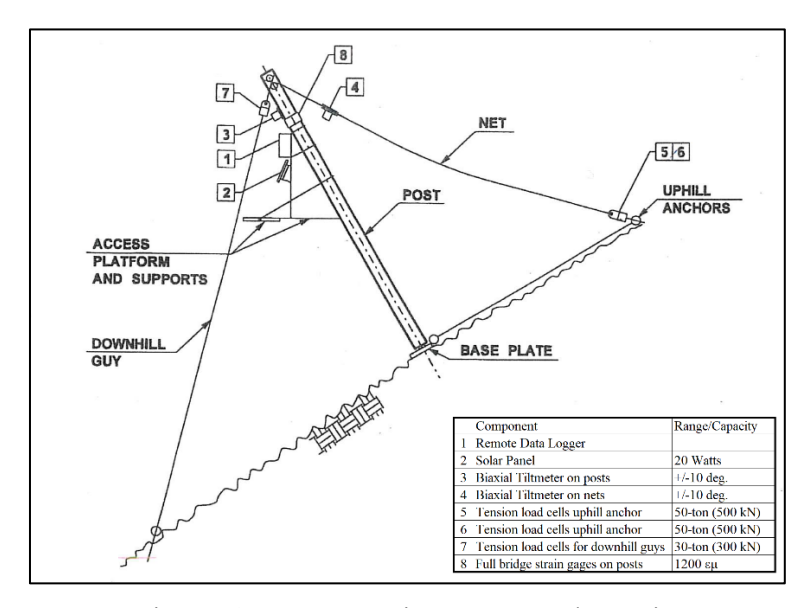


Figure 6 – Snow net instrument schematic

5. RESULTS

Due to the lack of deep snow years during the monitoring period, the forces on the system are small compared to the design loads. Figure 7 shows representative load measurements. Table 2 lists the largest loads and deflections for each instrumented location with the corresponding dates. Interestingly, while the maximum snow height and snow-water equivalent year was 2021, the maximum forces were recorded in mid-January 2022 during an average snow depth year. Unfortunately, the moisture sensor stopped working in 2021 prior to the largest loads and deflections.

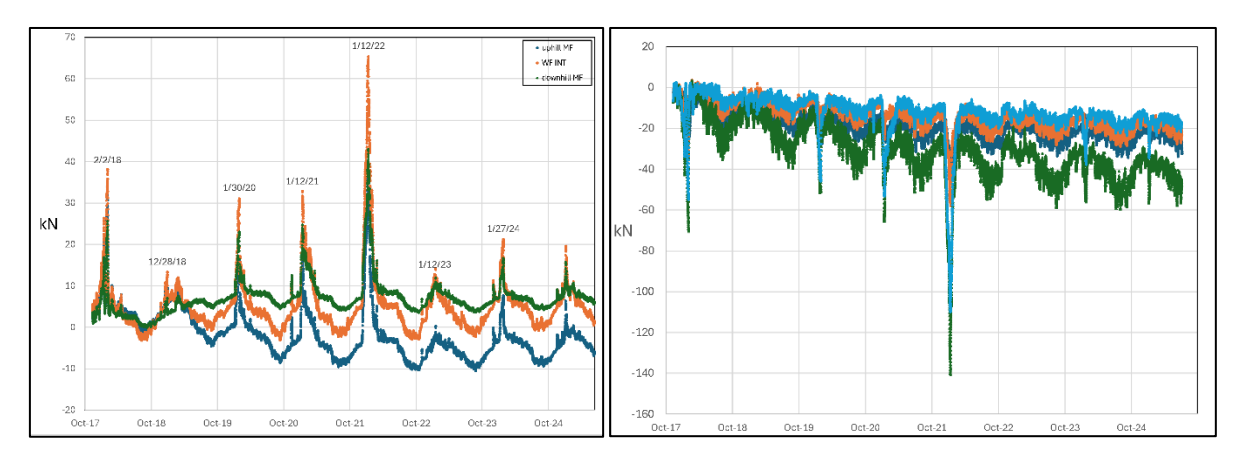


Figure 7 – Tension forces in the upper elevation high glide area 2-1 (left) and post compression force at 2-1 from strain gage measurements (right). Four plots correspond to strain gages installed 90-degrees apart.

	post tilt		net tilt		post compression		net tension	
2-1	1/15/22	1 deg	1/14/22	11 deg	1/11/22	115 kN	1/12/22	65 kN
2-2	12/20/20	2 deg	1/18/22	5 deg	1/12/22	113 kN	1/18/22	55 kN
5-1	1/17/22	2 deg	1/14/22	8 deg	1/12/22	151 kN	1/17/22	46 kN
5-2	3/18/23	2 deg	1/15/22	11 deg	1/11/22	116 kN	1/11/22	49 kN
2i-N	10/23/22	17 deg						
2i-S	9/6/22	34 deg						

Table 2 – Maximum loads and deflections with occurrence dates

6. DISCUSSION

Snow loads on the Slide Curve snow nets are expected to vary primarily depending on accumulated snowfall (HS), average snow density and precipitation type. Water flowing at the base of the snowpack is also an important factor affecting snow loads. The maximum loads and deflections over the 7-year measurement period occurred in mid-January 2022. Prior to maximum loads, the snow height at Snoqualmie Pass increased from 132 cm to 225 cm over a 5-day period ending January 6. Between January 6 and January 22, temperatures warmed to above freezing and 20 cm of rain fell, while snow height decreased by 70 cm. The measurements indicate that rain-on-snow resulted in the maximum snow loads and deflections for the snow nets.

Significant swivel post deflections were measured at the location where planar slopes of differing roughness converge near tiltmeters 2i-N and 2i-S. These deflections indicate the need for field assessment of post inclinations and possible adjustments.

The design snow heights for the snow nets relied on historic climate data without adjustments for climate change. While high variability in snowfall and snow heights characterize this maritime climate, long-term trends indicate lower probabilities of extreme snow heights in the future.

7. CONCLUSIONS & OUTLOOK

The lack of deep snow during the 7-year measurement period limits our ability to evaluate the performance of the snow nets under conditions that approach the 100-year design loads. Variability of measurements to date and the lack of strong correlations with snow heights appear to support the design assumptions of higher snow densities and elevated glide potential in this maritime climate. Future measurements will provide an opportunity for capturing above average snow heights and improving our characterization of snow net performance in this climate.

8. REFERENCES

- Rainer, E., Rammer, L., and Wiatr, T. (2008). Snow loads on defensive snow net systems. In International Symposium on Mitigative Measures against Snow Avalanches Egilsstadhir, Iceland.
- Margreth, S.: Defense structures in avalanche starting zones; Technical guide as an aid to enforcement, Environment in Practice no. 0704, Federal Office for the Environment, Bern; WSL Swiss Federal Institute for Snow and Avalanche Re-search SLF, Davos, 134 pp, 2007.
- Jóhannesson, Tómas and Margreth, Stefan, Adaptation of the Swiss Guidelines for supporting structures for Icelandic conditions, VÍ-G99013-ÚR07 Reykjavík, July 1999
- Stimberis, John & Rubin, Charles M., Glide avalanche response to an extreme rain-on-snow event, Snoqualmie Pass, Washington, USA, Journal of Glaciology, Vol. 57, No. 203, 2011
- LaChapelle, E.R., Bell, D.B., Johnson, J.B., Lindsay, R.W., Sackett, E.M., and Taylor, P.L., Alternate Methods of Avalanche Control, Final Report to WSDOT, July 1978.
- Schaerer, Peter, Snow Avalanche Control Snoqualmie Pass East Shed Area, prepared for WSDOT, unpublished report, 15 May 2000.

9. ACKNOWLEDGEMENTS

The authors acknowledge the important roles, contributions and support of the WSDOT Geotechnical Group, the installation contractor, Hi-Tech Rockfall Construction, Inc., the contractor's snow net consultant, Dr. Roberto Castaldini, the project geotechnical engineer Kane Geotech, Inc. and the project instrumentation specialist Erik Mikkelsen.

New experiments and measurements to improve operational practices for preventive avalanche triggering

Philippe Berthet-Rambaud^{1,*}, Jean-François Bellin², Eric Viallet³, Amandine Molinier¹, Sonam Bourlon de Rouvre¹, Fanny Bourjaillat¹ and Stéphane Bornet⁴

¹ ENGINEERISK, 690, route de la Motte Servolex, 73160 Saint-Sulpice FRANCE
 ² Compagnie du Mt Blanc, 35 Place de la Mer de Glace 74400 Chamonix-Mt-Blanc FRANCE
 ³ ADSP, French association of ski patrols director, 73450 Valloire FRANCE
 ⁴ ANENA, National Association for the Study of Snow and Avalanches 38000 Grenoble FRANCE
 *Corresponding author, e-mail: pbr (at) engk.fr

ABSTRACT

After decades of implementing PIDAs (''Plan d'Intervention de Déclenchement d'Avalanches'', French avalanche control plan), the French Association of Ski Patrols Directors (ADSP) still faces questions regarding certain operational practices: with a bomb tram, can a high overflight height be compensated by a larger quantity of explosives? Can the individual mass of each charge be optimized? For this reason, new experimental campaigns were organized first to measure the air shock waves generated by conventional explosives in different situations (positions, combinations, mass) and as a function of distance: do not considering the interaction with the snowpack might appear as a strong limitation but allows objective comparisons. However, this interaction was still considered with simple explosion tests in a very homogeneous spring snowpack: here too, different positions and configurations are tested with trends sometimes opposite to the effects in the air. At the same time, the database of these shock waves is being supplemented by measuring the pulses generated by gas exploders, considering both historical and innovative systems. The aim is to include these various results in the ANENA (National Association for the Study of Snow and Avalanches) program as national training center for new ski patrollers.

1. INTRODUCTION

If several thousands of artificial releases of avalanche are performed every winter in the French Alps ski resorts, habits can indirectly lead to a loss of knowledge to finally forget why things are done in such a way and progressively see wrong ideas emerging. That's why the French Association of Ski Patrols Directors (ADSP) have re-initiated new experiments since a few years to feed a database and use corresponding results in the initial and refresh trainings of ski patrollers in cooperation with ANENA (National Association for the Study of Snow and Avalanches) which faces the same questions as national training center: efficiency of products and methods including emerging systems, safety of operators.... Making it directly without using only the existing literature or commercial communications of provider is important to get a direct and independent interaction with what is done. In practice, most experiments were performed by La Flégère ski resort staff at Chamonix, using a bomb tram to hang solid charges and measurements (Walter 2004) being done by Engineerisk. If the main phasis focused on solid explosives, an additional one is being processed on gas exploder, ''invented'' and largely used in France with continuous and recent developments.

2. SOLID EXPLOSIVES

Although explosives have been used for much longer (the recipe for black powder was mentioned as early as the 10th century, nitroglycerine was discovered in the mid-19th century, and Alfred Nobel patented dynamite in 1867), it was only in the 1950s and the work of Ed LaChapelle (1956) that their civilian application on snow in 1939 (explosives) and 1949 (military cannons) was mentioned.

However, it was mainly during the 1970s that this field saw multiple developments: in France, the "Dynaneige" program supported various research projects mainly carried out by the Laboratory of Special Applications of Physics (ASP) at the Grenoble Nuclear Research Centre (CENG). This "program" was also directly connected with ANENA, CTGREF (now INRAe), the Snow Research Centre of Météo France and pioneers of the "eldorado" development of ski resorts (Bon Mardion and Cattelin 1972). With the "Bangavalanches" experiments, they went so far as to test the effect of sonic bangs on avalanche triggering, but without any real success (Alléra et al. 1973).

At the international level, equivalent research and experiments were conducted and H. Gubler (1977) is still considered a reference, especially regarding the maximum effect of a solid explosive charge a few meters above the snowpack.

From this background and recent contributions (Meier 2024), the main ideas were to focus first on the 'in the air' situation (corresponding to a bomb tram use) and to test additional configurations directly connected with practical operations and emulsion charge (named Emulstar): position of the charge (vertically, horizontally) to distinct axial and lateral effects, position of the detonator (upper or lower extremity, middle of the charge), combination of different charges attached together. Then, equivalent declinations were carried out with explosion experiments in a homogeneous spring snow cover.

The reliability of the measurements process was also confirmed by comparing results from equivalent experiments.

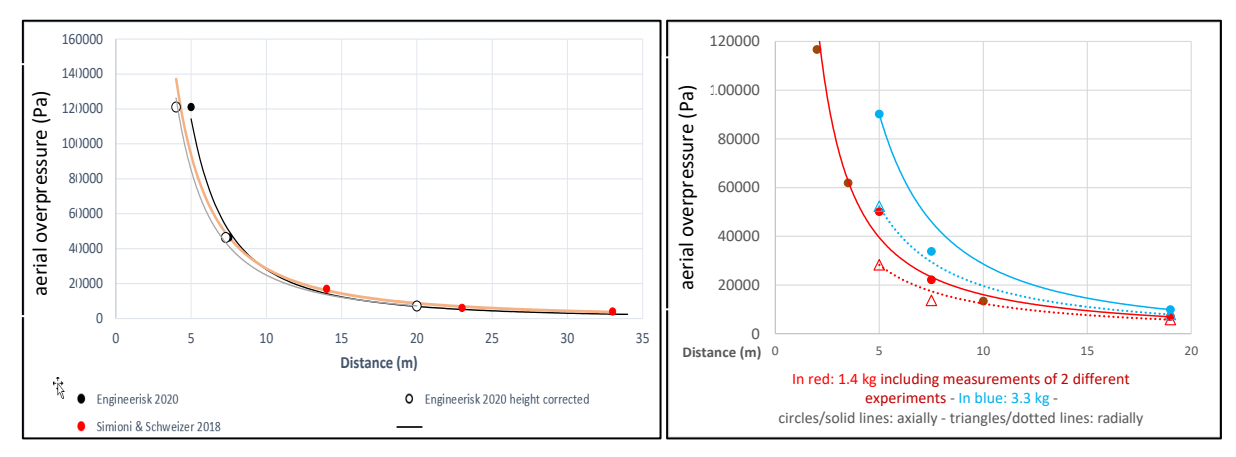


Figure 1 Left, comparison of a 4.8kg charge explosion with Simioni and Schweizer (2018) results including correction related to the initial deflection of the hanging (bomb tram) cable. Right, main results regarding charge mass, distance and direction (axially and radially).

At the same time, interpretations are sometimes complex, especially as they can show contradictory and even counterintuitive trends between the situation in the air and in the snow (with a huge attenuation in this last case and so a limited size of the initial influence zone). It is therefore important to apply these results as best as possible depending on the desired effect.

Indeed, and beyond physical aspects, there are also operational aspects and contexts in which the various techniques are applied. Thus, the main practical lessons that could be learned are:

- Overall, the effect of a greater mass is limited in any case, especially if the aim is to achieve an effect over a longer distance or over a larger area. In the air as in snow, the difference will be relatively small and, more than just power (unless enormous quantities are considered), the careful placement of the charge remains the main keypoint.
- With regard to mass, the difference between the 1.4 kg and 1.9 kg charges is minimal and does not justify the extra weight of the latter. Their axial effect is even virtually identical.
- With regard to placement, where possible, this includes the general orientation of the charge and the position of the detonator:
 - In the air (Bomb tram or charges fixed on a stick), the effect is greater in the axis of the charge on the opposite side of the detonator. Depending on the case, it may therefore be useful to use this "property" to maximise the effect on the slope in question.
 - In the snow (handcharges, helicopter bombing), results (Figure 2) and the literature show the advantage of a sufficient burial, particularly at the extremity where the detonator is placed. In fact, more than the burial itself (which directly allows to reach greater depth in the snowpack), the confining effect of the explosion plays surely the greatest role in maximising the effect... but which depends on the snow property and density. Further experiments should be done with (more) fresh snow.

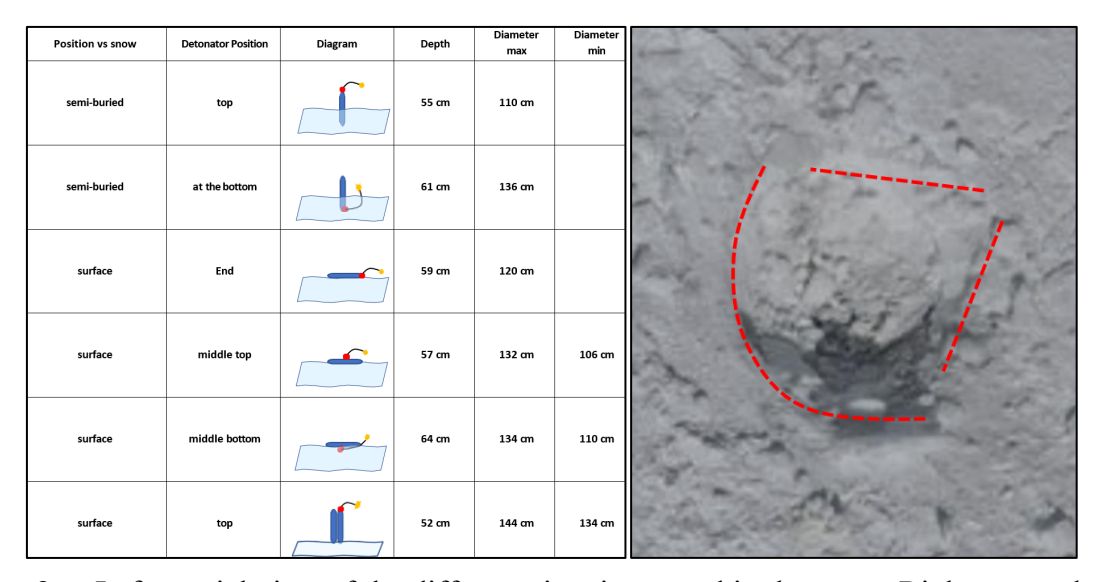


Figure 2 Left, partial view of the different situation tested in the snow. Right, example of a pear-shaped crater corresponding to the 3rd test in the table.

3. GAS EXPLODERS

In parallel to the versatile use of solid explosives for avalanche control, Remote Avalanche Control Systems (RACS) based on gas explosions have become a pillar of ski areas, roads and infrastructures safety management against avalanches. Their main advantages are all-weather all-time availability, power and safety for operators.

The first historical step was the Gazex system (Lieberman et al. 2002) initially patented by J. Schippers at the end of the 1980s through his company Technology Alpine de Sécurité TAS. Since that, several thousand were installed worldwide combining either standards, inertia or flex foundations. With the end of the validity of certain patents, Gazex-type exploders are now also produced freely by other companies like SAM-montagne in France, SATS in Austria. The gas mixture remains made of propane and oxygen, still using the well-known elbow-terminated tube installed near the top of the avalanche starting zone with the open extremity directed to the slope.

Avalhex (Duclos and Senabre 2002) was the first to compete in this market at the beginning of 2000s in France including a helicopter-borne prototype. It was itself competed with by the Avalanche Blast system developed initially in the Dolomites around 2003. Both were based on a latex balloon to contain the gas mixture before ignition and using hydrogen in combination with air (for Avalhex) or Oxygen (for Avalanche Blast). Facing different limitations, Avalhex systems (a few dozen was installed) progressively disappeared. From 2007, TAS, then part of MND group, started to develop a new family of systems still based on a steel explosion chamber (instead of a balloon) but adapted to a hydrogen+oxygen gas mixture: the shape of the Gazex (slightly inclined upwards) evolved towards a cone, directed rather vertically downwards and adapted to this lighter-than-air mixture. This cone was initially equipped for daily helicopter bombing mission with the DaisyBell system and was converted as the autonomous fixed but removable RACS O'Bellx (Berthet-Rambaud et al. 2010), recently combined with a ''+ option' consisting in a cylindric section on its foot to extend its cone.

Recently, new technical and patented developments are emerging: the BW "Boom Woosh" exploder from Alpine Infrastructure company is the first RACS device designed and made in North America. The first units have been installed in Alta (UT), Jackson Hole (WY) and Wolf Creek (CO). They use an almost straight pipe closed at the top and inclined downwards as explosion chamber fixed on a tower. According to the system description, the key words are reliability thanks to standard components, possibility of longer-distance gas supply to optimize installation configurations without helicopter refills need and single point foundations.

In France, Avenir Protections is developing the APeX system with 2 successful prototypes last winter at Les Arcs and Méribel ski resorts and a dozen foreseen for the next season. The company came back to the propane-oxygen mixture and aims at improving two main topics: an efficient use of the gas volume to obtain more powerful shockwaves with less gas thanks to an innovative steel explosion chamber which promotes multiple-reflections and therefore successive and superposed shockwaves. In terms of functionalities, the APeX system is composed of this explosion chamber on which a removable (by helicopter, mainly for summer maintenance and storage) technical module is simply placed: This module provides the power supply, remote control, and ensures the mixing, injection and ignition of the gas mixture thanks to its interface with the explosion chamber. The assembly is simply vertically stacked under the action of gravity without vertical fixing, making it possible to significantly limit tearing forces and therefore reduce the footprint of the foundation.

In this context, it is also interesting to complete the previous database to better know the main characteristics of each system in terms of shockwave: amplitude, duration, single or multiple peaks, direction in comparison to the usual steepness of a starting zone, lateral diffusion.... New measurements are progressively performed in addition to the existing literature. For now, they are first focused on the initial power of the explosion in the air at a few meters corresponding more or less to its maximal impact with the snowpack in usual situation. It is more objective for comparisons as long-distance measurements on the ground are also directly influenced by the terrain relief and cover.

Main findings (Figure 3) confirm a shorter peak shown by a rapidly decreasing impulse curve (area underneath the pressure - time curve) with hydrogen+oxygen mixture than with propane+oxygen. In the same way, a simple explosion chamber with direct straight exit is producing single peaks whereas more complex (Gazex pipe but especially that of the ApeX which was specifically designed for this purpose) are able to superimpose them with successive waves from internal reflections. The combination of these two physical parameters (type of mixture, shape of the explosion chamber) directly explain the lower power of configuration like DaisyBell / O'Bellx also demonstrated by Seitz (2021). On the contrary, the fact that the initial internal stage of the explosion is facing high compressive phases highly improves the overall efficiency: for instance and if Gazex remains a reference in this field, APeX system obtains an equivalent explosion but with 2 to 3 time less gas volume: less gas is lost by ejection and pushed outside from the growing explosion.

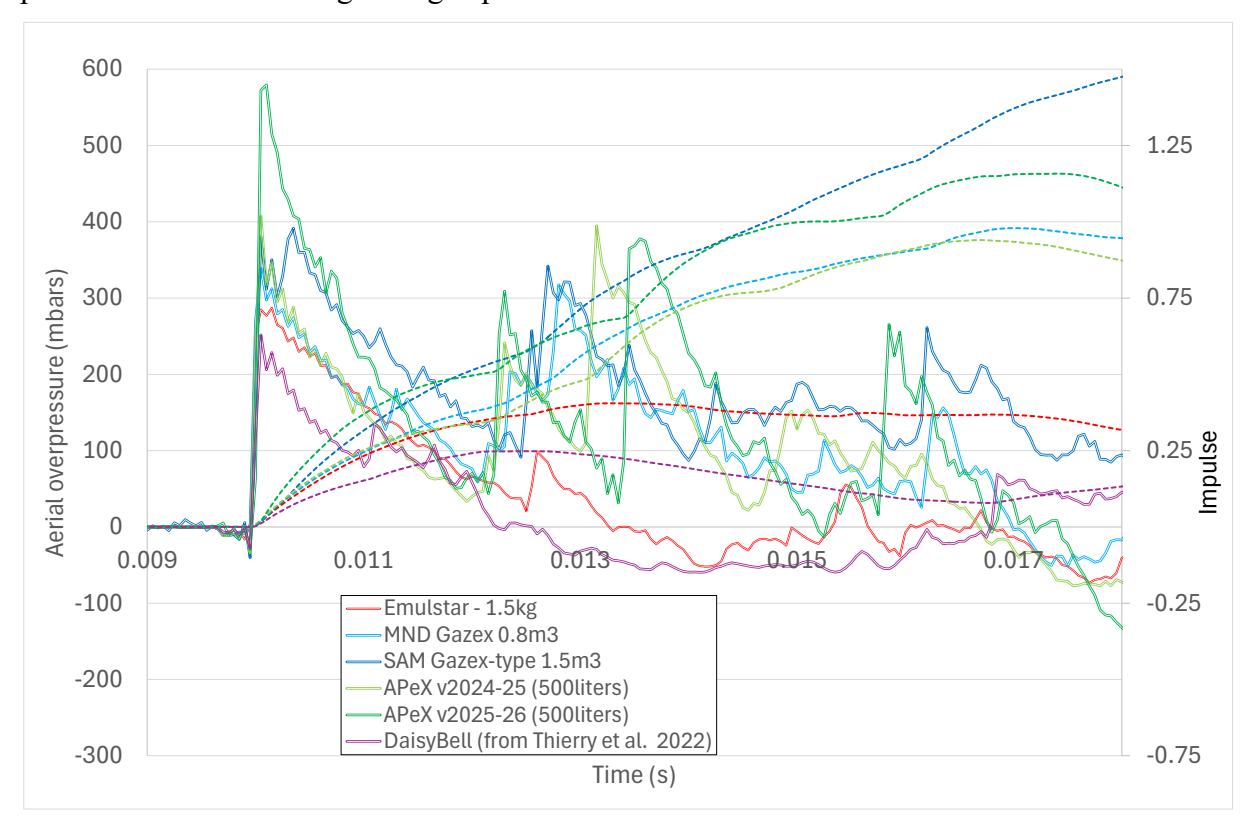


Figure 3 Graphs of different positive parts of shockwaves for different RACS (+1.4 kg Emulstar charge) at 4m distance: aerial pressure (solid lines) and corresponding impulse curves (dashed lines)

4. CONCLUSIONS

Studying RACS and solid explosives shockwaves and their interaction with the snow is important for both professionals and manufacturers/providers: it should improve the way artificial releases are performed for the reliability of avalanche control plan, including the right choice of RACS with the right power in comparison to the corresponding avalanche starting zone. The database initiated by ADSP is an on-going process which will continue also to include more experiments with snow and other types of explosives (for instance deflagrating instead of detonating).

ACKNOWLEDGEMENT

All these experiments could not have been possible without the support of the Compagnie du Mt Blanc and especially A. Trinquier. We thank also Prof. A. Limam and his team for their help with measurements also through the loan of various materials.

REFERENCES

- Alléra J-L, P. Amardeil, R. Béranger et al., 1973. Effet du Bang sonique sur le déclenchement d'avalanches, détermination de la trajectoire du Mirage III B au-dessus du Vallon de la Lavey, Compte-randu des essais du printemps 1973, Rapport d'avancement n°2, Note CENG/ASP n°73-10.
- LaChapelle, E.R. 1956, some effects of high explosives on snow: a report on preliminary investigations, US dept of Agriculture, Forest service, Internal Report.
- Bon Mardion G., Cattelin J., Manuel sur l'emploi des explosifs pour le déclenchement artificiel d'avalanches, ANENA 1972
- Gubler H, Artificial release of avalanches by explosives, Journal of Glaciology, Vol. 19, n° 81,
- Simioni S., Schweizer J, 2018. Comparing two methods of artificial avalanche triggering: gas vs solid explosives, In: Proceedings of the International Snow Science Workshop, Innsbruck, Austria 2018.
- Seitz B.K., 2021. Measuring explosive airblast of remote avalanche control systems, thesis, Montana state University
- V. Thierry, B. Tang, P. Joffrin, et al.2022. Characterization of blast waves using solid and gaseous explosives: application to dynamic buckling of cylindrical shells. Shock Waves, 2022, 32 (8), pp.703-713.
- Berthet-Rambaud P., Farizy B, Juge A. et al., 2010. A New Environment-Friendly Device for Avalanche Preventive Release, In: Proceedings of the International Snow Science Workshop, Squaw Valley, CA 2010
- Walter P.L. (2004). Introduction to Air Blast Measurements Part 1. Technical Note. PCB Piezoelectronics
- Meier B 2024. On triggering avalanches, what happens between explosion and release, In: Proceedings of the International Snow Science Workshop, Tromsø, Norway 2024
- Duclos A., Senabre P. 2002. AVALHEX: New Gas-Mix-Explosive System for Avalance Triggering Statement After Two Seasons of Use in Savoie, France, International Snow Science Workshop proceedings, Penticton BC
- Lieberman E., Schippers J., Lieberman S. C., 2002, The GAZEX avalanche release system, International Snow Science Workshop proceedings, Penticton BC

Monitoring site Ranalt – Flexible barrier designed for catching avalanches exposed to an unexpected debris flow event

Gernot Stelzer, ^{1*} Engelbert Gleirscher, ² Daniel Illmer, ³ Georg Nagl, ⁴ Marcel Fulde¹

¹ Trumer Schutzbauten GmbH Oberndorf Austria (Presenting
² BFW Innsbruck Austria
³ Ingenieurbüro Illmer Daniel GmbH Fulpmes Austria
³ BOKU Wien Austria

ABSTRACT

In 2018, a free-standing structure, known as a Snow Catcher, was installed in a gully at the monitoring site in Ranalt, Austria. It is instrumented with several load pins to measure forces at the hinges of the steel support structure (so-called "Lambda Frame") and load cells for measuring tension forces in the bearing and middle ropes. The site relies on the natural avalanche events that occurred multiple times in recent years in the time span between November to April.

Over the years, many small avalanches have impacted on the structure and resulted in the collection of data that has enhanced our understanding of how these structures function under dynamic and static snow loads. During this time, it was also noted that several small debris flow events occurred within the avalanche track, some of which have reached the barrier.

Heavy rainfall in the night between 21.06.2024 to 22.06.2024 triggered a significant debris flow event that impacted the structure and completely filled the 5 m high barrier. Deposited material caused the flow to divert around the barrier and eroded the lateral anchoring and interrupted data lines of the monitoring setup, while the area directly behind the structure stayed unaffected.

Presented herein is a summary of the events, the effects on the structure during the impact of June 2024. Furthermore, an outlook on the future of the monitoring site Ranalt will be given.

G. Stelzer and others P2.4 - Page 303

Snow fences on Eyrarfjall above Flateyri – A pilot study

Gísli Steinn Pétursson^{1*}, Þorbjörg Anna Sigurbjörnsdóttir¹, Kristín Martha Hákonardóttir², Tómas Jóhannesson³, Örn Ingólfsson³, Skúli Þórðarson, Áki Thoroddsen ¹

¹ Verkís, Ofanleiti 2, IS-103 Reykjavík, ICELAND

²Ministry of the Environment, Energy and Climate, Borgartún 26, IS-105 Reykjavík, ICELAND

³ Icelandic Meteorological Office, Bústaðavegur 7–9, IS-105 Reykjavík, ICELAND

*Corresponding author, e-mail: gsp (at) verkis.is

ABSTRACT

As a part of efforts to improve avalanche defenses for the village of Flateyri in northwest of Iceland following avalanches in January 2020, a pilot project was initiated to evaluate the effectiveness of snow fences. The fences are situated in a large snow catchment area on top of Eyrarfjall mountain above the village and are intended to reduce snow transport into avalanche starting zones.

In the summer of 2022, two 150-meter-long, and 5-meter-high steel fences were installed in the catchment area on the mountain perpendicular to the prevailing winter winds. Snow accumulation has been monitored over three winters. Results show substantial snow capture, although drift volumes are somewhat lower than predicted by Tabler's empirical formula.

The study focuses on fence performance under high-wind conditions, including the influence of ground clearance, an important factor given the deep snowpack on Eyrarfjall.

Snow accumulation and drift patterns were analyzed using drone-based photogrammetry and weather station data. The observed drift volumes reached about 220 t/m, slightly lower than predicted by Tabler's empirical formulas but consistent with the design expectations of 200–250 t/m. Reduced performance for one winter was attributed to atypical wind conditions and burial of fences. The results of the pilot study demonstrate the effectiveness of snow fences for avalanche mitigation in Iceland, with design adaptations such as increased ground clearance recommended before full-scale implementation.

1. INTRODUCTION

Flateyri, a village in the Westfjords of Iceland, lies at the base of the steep Eyrarfjall mountain. Two prominent gullies, Innra-Bæjargil and Skollahvilft, which are located directly above the settlement, are the primary avalanche starting zones threatening the village. The settlement at Flateyri was hit by many avalanches prior to the construction of two deflecting dams in 1997 following the catastrophic 1995 avalanche that claimed 20 lives and damaged numerous buildings.

Despite the construction of protective dams, the January 2020 avalanches demonstrated continued vulnerability. Although no fatalities occurred, the avalanches reached the residential area, buried one individual, and damaged homes and vehicles, revealing the limitations of the existing passive defenses.

These events reignited discussions on how to further reduce the avalanche risk. In response, the avalanche flow channel along the deflecting dam below Innra-Bæjargil has been deepened and widened, and work is ongoing to construct steep braking mounds above the dams to decelerate

G.S. Pétursson and others P2.5 - Page 304

avalanches descending from both starting zones. Among the additional mitigation strategies under consideration is the installation of snow fences on the plateau of Eyrarfjall. These structures are designed to control wind-blown snow transport and modify deposition patterns, with the aim of reducing snow accumulation in the avalanche starting zones, especially at the start of the winter.

Snow fences have been used in Iceland for road safety purposes, primarily by the Icelandic Road and Coastal Administration (2000). However, their use in avalanche mitigation remains largely unexplored in Iceland and international experience of those structures in high-wind conditions, as on Eyrarfjall, is limited. The theoretical basis for snow fence design in lower wind speeds has been established, particularly the empirical work of Tabler (1991, 1994 and 2003), who provided insight into snow drift formation based on fence geometry and porosity.

This pilot project was therefore initiated at Eyrarfjall to evaluate the performance of snow fences under high-wind conditions. The primary goals are to assess their effectiveness in trapping wind-transported snow and to determine whether design modifications are necessary to enhance their functionality for Icelandic terrain and climate conditions and observe weather icing occurs during winter, limiting the effectiveness of the structures.

2. SITE CHARACTERISTICS AND PROJECT DESIGN

Eyrarfjall rises steeply from sea level to about 660 m a.s.l., with a south-southwest facing slope above Flateyri. The summit is relatively flat, as is common for mountains in the northern Westfjords, with an approximate 1700 m fetch from Vatnsdalur to the edge above Flateyri. The dominant wind directions are from the northeast to east-northeast, which also corresponds with the most common wind direction during storm and snowdrift conditions. Cumulative winter precipitation at the summit is about 900 mm, 90% of which is snow, with peak accumulation in December and January (Petersen, 2021).

These conditions make Eyrarfjall well-suited for snow fence installation due to its flat terrain, exposure to prevailing winds, and heavy winter snowfall.

The full implementation concept (Hákonardóttir et. al., 2023) assumes about 2 km of 5 m high fences arranged in two rows, oriented perpendicular to the dominant wind direction (Figure 1). Due to limited experience with these fences in high-wind conditions, a pilot installation was constructed in summer 2022. A weather station was installed to record wind direction and wind speed, and a time-lapse camera for continuous visualization of snow accumulation and icing conditions. Two rows of galvanized steel fences were installed, each 150 m long and 5 m high, with 0.5 m ground clearance and 50% porosity, aligned with best practices (Tabler 1991, 1994, 2003).

The first fence row is situated approx. 320 m from the edge of Innra-Bæjargil, and the second about five times the fence height (H), 120–125 m, upwind. This setup assumed a leeward drift of about 25H and windward drift of about 15H, slightly reduced from Tabler's values to account for denser Icelandic drift snow (400 kg/m³) and higher wind speeds. Expected drift mass was estimated as 21.5 H² m³/m in accordance with Tabler's empirical formula, equivalent to approx. 200–250 t/m (Þórðarson, 2021).

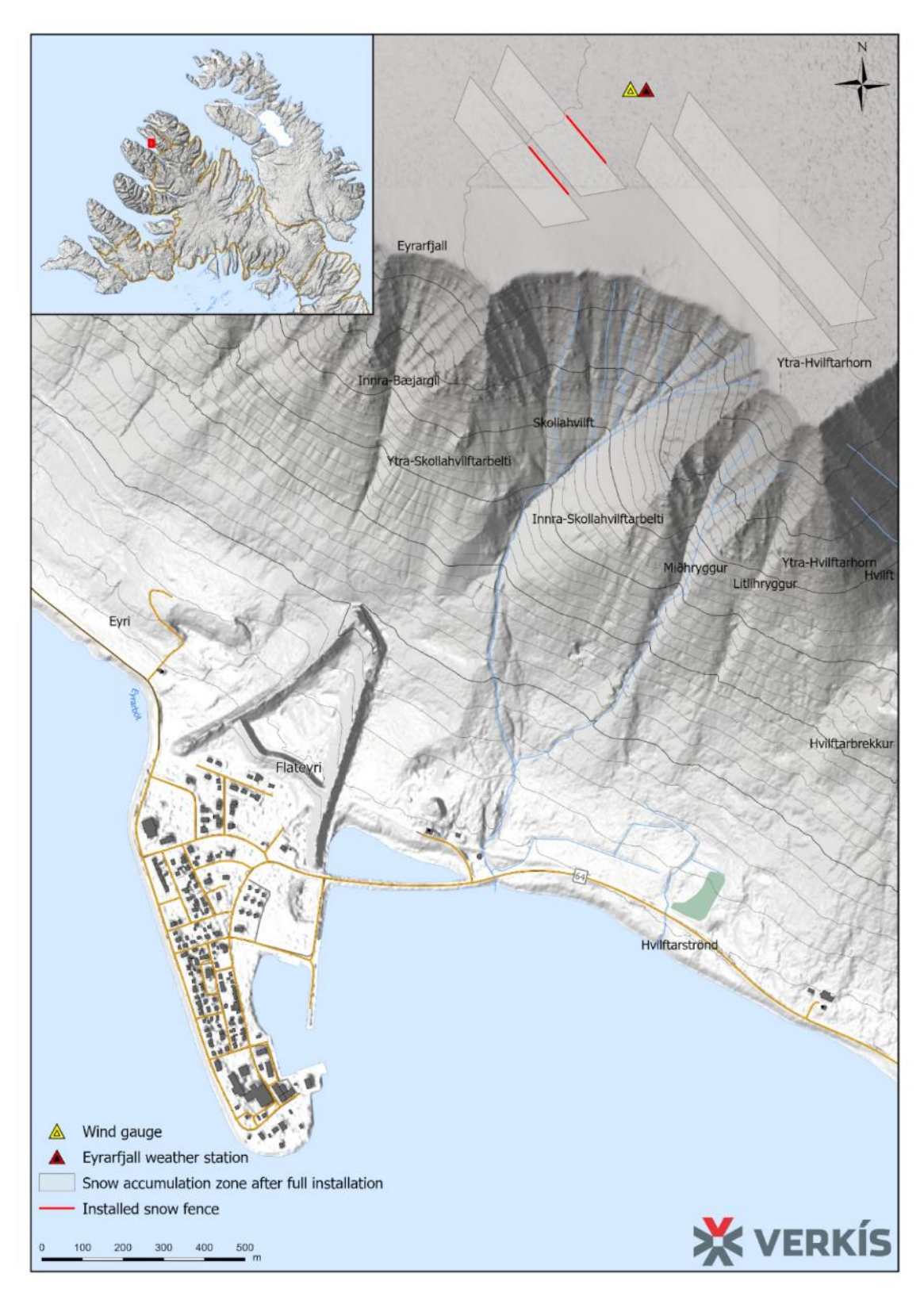


Figure 1 An airial view of Eyrarfjall, above Flateyri. Shown on the Figure: The location of the installed snow fences, key instruments, proposed snow accumulation zones after full installation and the gullies above Flateyri village.

G.S. Pétursson and others P2.5 - Page 306

3. MONITORING METHODS AND DATA ANALYSIS

An on-going monitoring program was implemented in November 2021 to quantify the effectiveness of the snow fences in capturing wind-transported snow. The monitoring strategy relied on three complementary components: high-resolution drones-based photogrammetry (Figure 2) conducted by the Icelandic Meteorological Office (IMO), comparative digital elevation model (DEM) analysis, and the integration of meteorological data from the Eyrarfjall weather station operated by the IMO. To date, three full winters have been captured (2022–2023, 2023–2024 and 2024–2025), each winter season defined as October 1st to June 1st.

3.1 Snow Accumulation Mapping

Each winter, IMO performed multiple drone flights. Each flight was processed using DATACT platform to generate point clouds of the snow surface elevation on Eyrarfjall. In total 23 flights were performed with 19 of them being usable for analysis of snow patterns around the fences (3 in 2022–2023, 9 in 2023–2024 and 7 during 2024–2025).

A snow-free reference DEM (from 2009) was used for estimating snow depth and accumulation volumes from the winter DEMs. In addition to volumetric analysis, drift shapes and profiles were analyzed. Cross-section perpendicular to the fences was extracted from the DEMs to assess drift height and length (Figure 3).

3.2 Meteorological Data and Snow Transport Thresholds

Meteorological data was obtained from the Eyrarfjall weather station, located approximately 200–320 m upwind of the fences, in the assumed prevailing wind direction.

To identify periods conducive to snow transport, thresholds for wind speed and temperature were applied in accordance with guidelines from the Icelandic Road and Coastal Administration (IRCA, 2000). Specifically, snow transport was considered likely when sustained wind speeds exceeded 7 m/s and air temperature was below 0°C. These criteria were applied to generate winter wind roses and assess wind directions during potential snow transport periods.



Figure 2 Photo of the fences taken from a drone on the 28.12.2023 by the IMO.

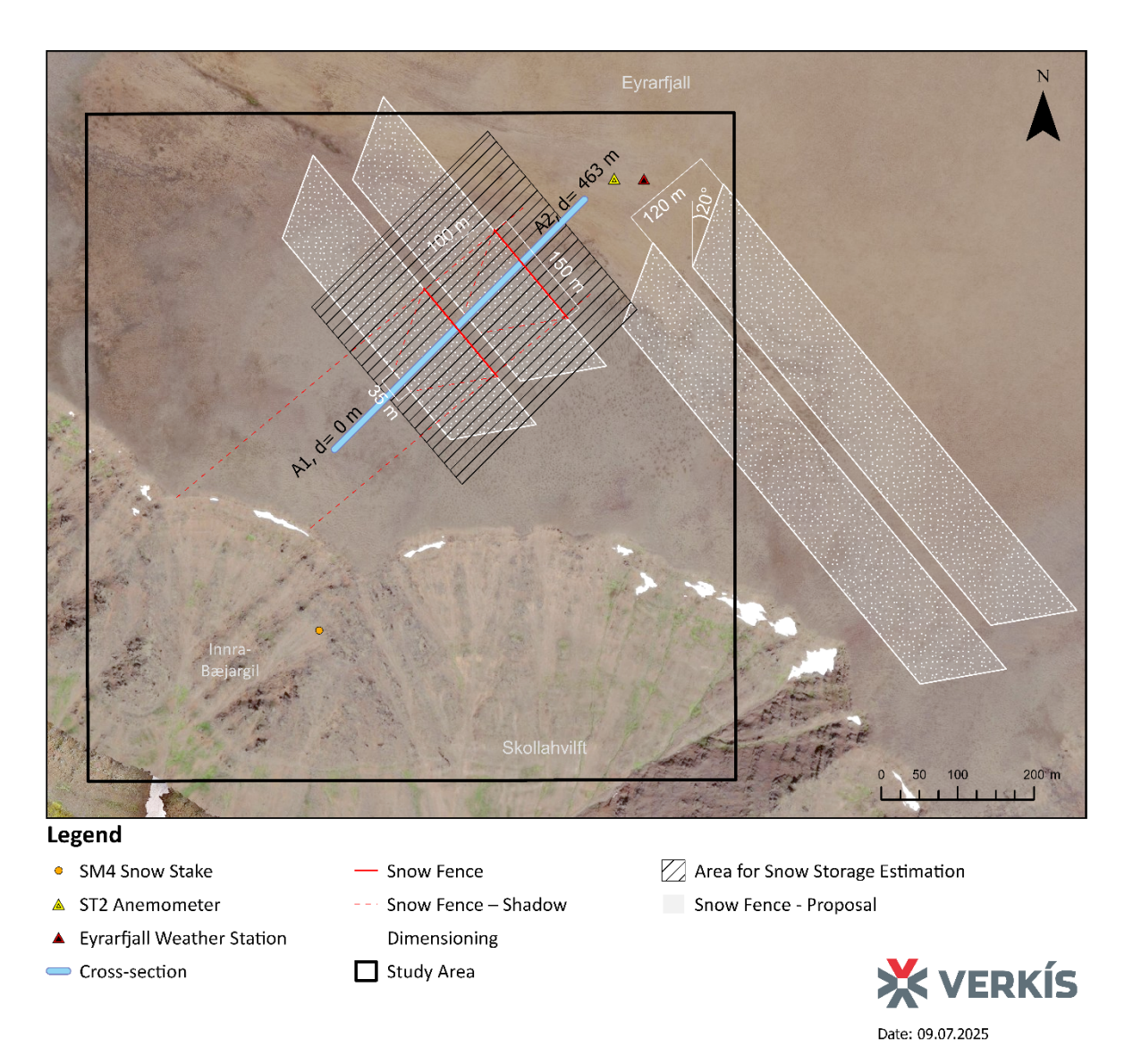


Figure 3 Airial photograph of the Eyrarfjall plateau. Location of the pilot study area is shown, along with the cross-section for snow surface profiles through the middle of the snow fences.

4. RESULTS AND INTERPRETATION

Wind data from the Eyrarfjall weather station confirmed that dominant snow transport events occurred during northeast to east-northeast winds (Figure 4). Winter winds predominantly originate from the northeast, south and southwest. During the 2022–2023 and 2023–2024 winters, the snow transport wind directions were almost exclusively northeast to east-northeast. However, for the winter 2024–2025 winds from the south and southwest contribute significantly to the snow drift period, while the north-northeast direction remained the dominant direction for snow drift. Less snowfall was observed during the 2024–2025 winter than for previous winters. The fetch of snow for the southwest direction is significantly smaller which impacts the total volume of snow expected to be captured by the fences for those wind directions.

G.S. Pétursson and others P2.5 - Page 308

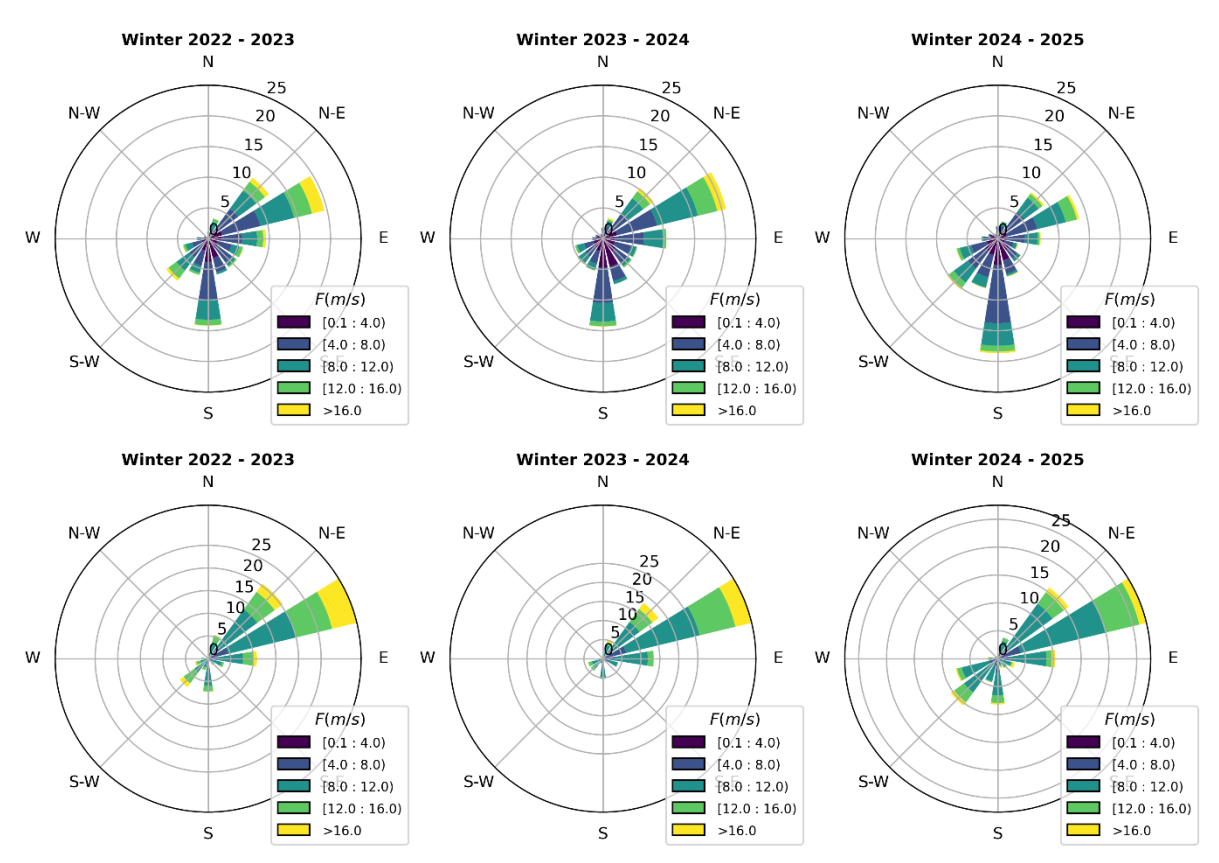


Figure 4 Winter wind roses from the Eyrarfjall weather station for winter period (above) and filtered by snow transport thresholds (below).

Snow surface elevations and images show the highest snow accumulation near the fences and close to the edge of the mountain, specifically below the edge (Figure 5) where the measurements indicate that the snow depth can reach up to 8 m. Snow depths at the mountain edge are subjected to higher uncertainties due to abrupt terrain change and the accuracy of the reference DEM (2009). Possible sources of error include DEM mismatch, measurement inaccuracies, or physical changes from rockfall, water scouring and avalanches.

No significant changes were observed in snow accumulation at the top of Innra-Bæjargil gully nor at the edge for the zones directly downwind from the fences and to the side of the fences. However, measurements show less snow downstream of the snow accumulation zones of the fences on the plateau compared to adjacent areas to the sides.

The snow accumulation patterns near the fences (Figure 6) were relatively uniform for the first two winters (2022–2023 and 2023–2024), with typical rounding that extends inward from the ends of each row, though less pronounced than described by Tabler. In 2024–2025, drift patterns deviated noticeably, with reduced length and westward slant to the drift, likely due to the more frequent southerly winds.

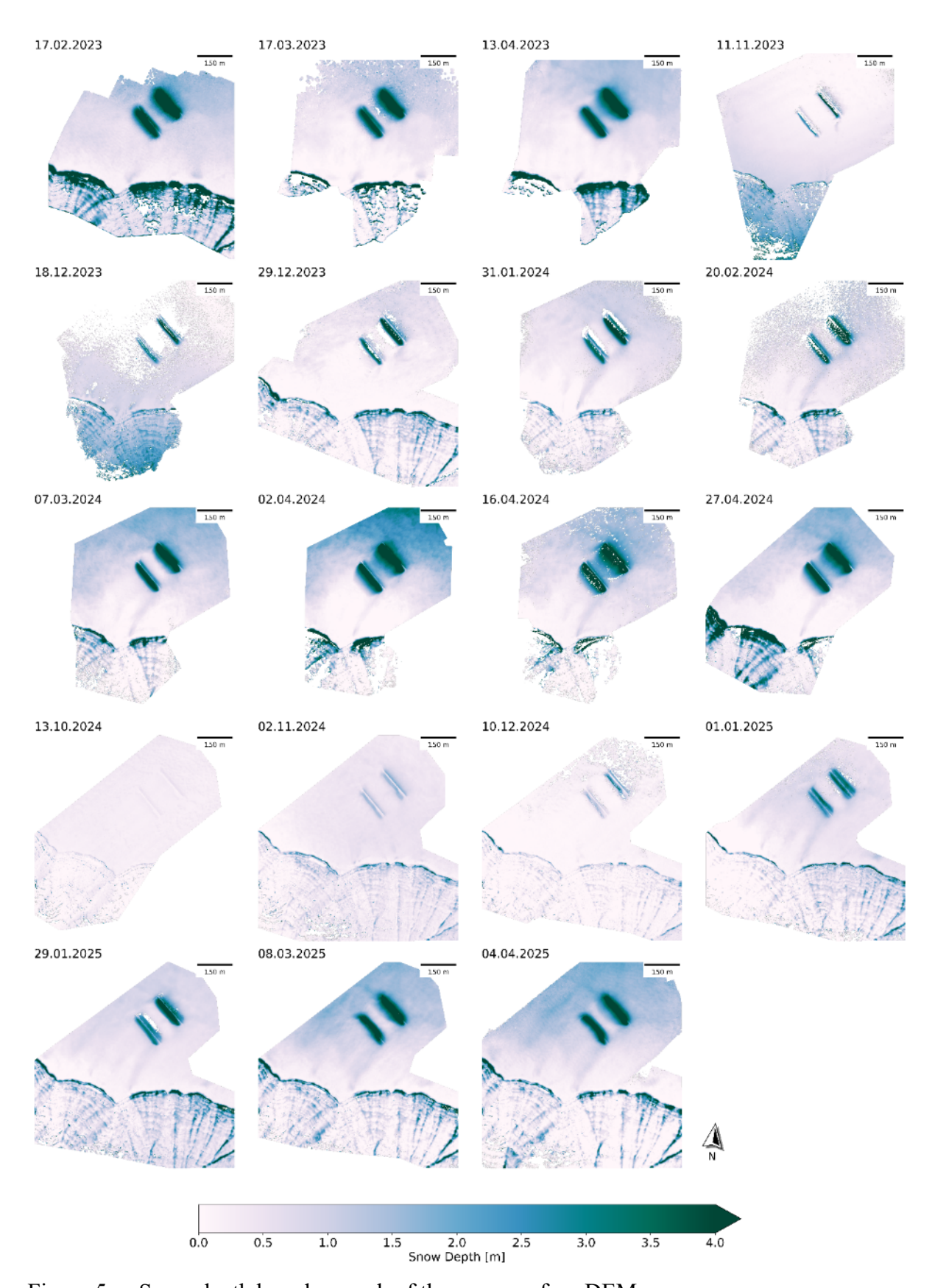


Figure 5 Snow depth based on each of the snow surface DEMs.

G.S. Pétursson and others P2.5 - Page 310



Figure 6 Late winter accumulation around the snow fences for each winter.

Snow surface profiles through the middle of the fences (Figure 7) show how the snow accumulation increases progressively through the winter, stabilizing in March or April, at which point the fences became largely buried, reducing or eliminating their effectiveness. For the first two winters, the drift patterns are similar to patterns as observed by Tabler (1991, 1994 and 2003) for fences with 50% porosity, although less drift length and height/depth. The drift patterns for winter 2024-2025 is unlike the others and is more consistent with the solid fence behaviour (Figure 8).

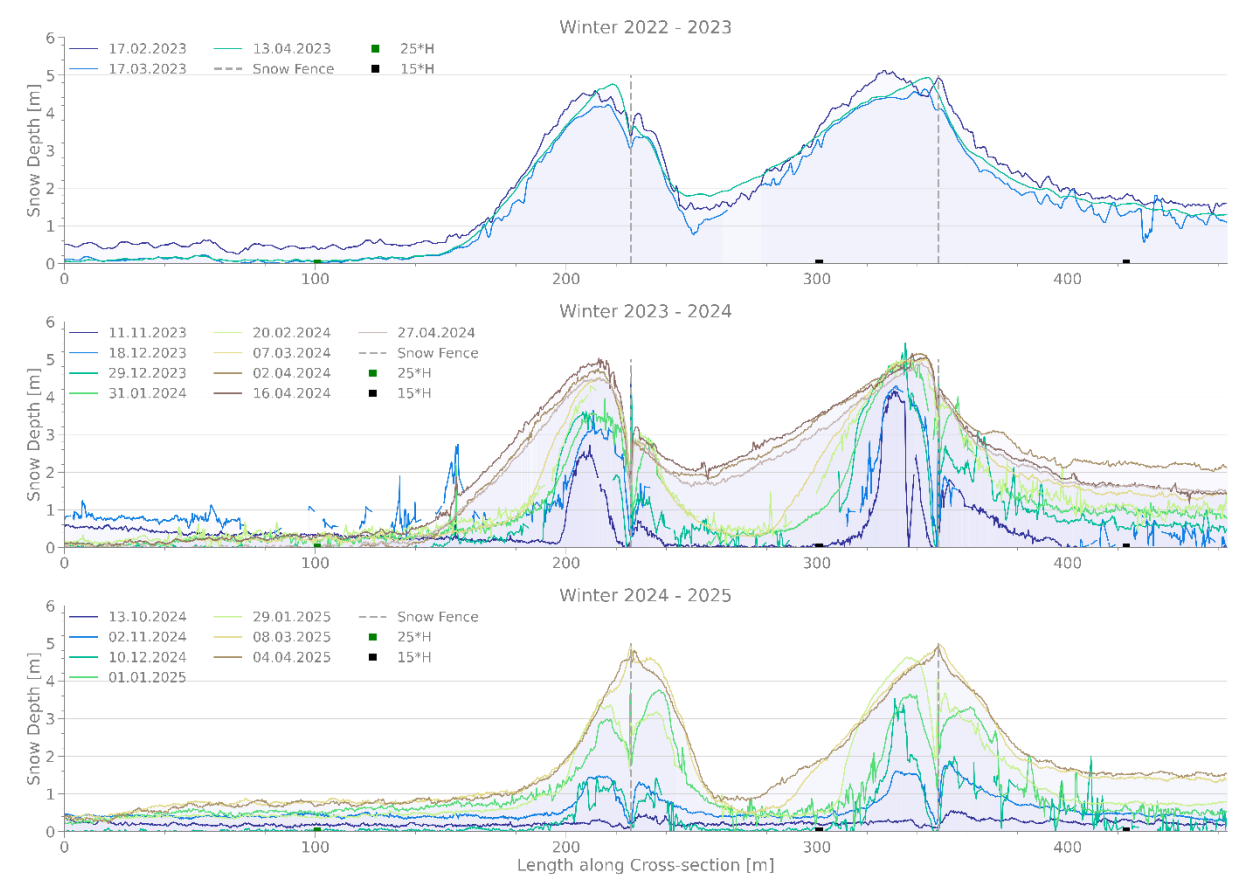


Figure 7 Snow surface profiles through the middle of the fences. The wind direction is from right to left. The locations of the design leeward drift (25H) and windward drift (15H) are shown as boxes on the ground for comparison.

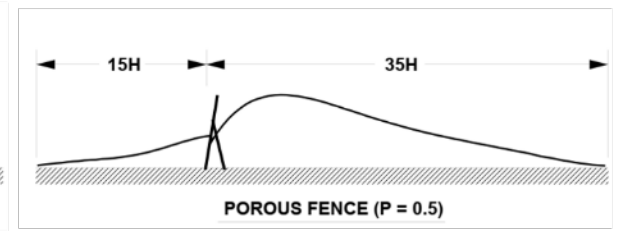


Figure 8 Comparison of drifts formed by solid and 50% porous fences (Tabler 1994). Wind direction s from left to right.

The leeward drift length for the first two winters is observed as about 17H (85 m), which is shorter than suggested by Tabler. For the third winter the drift length was about 12H (60 m), consistent with solid fence behavior. The windward drift is observed as about 15H for all three winters. The highest point of the drift is about the same height as the fences, but fences in lower wind conditions show up to 1.2H height of the drift (Tabler, 1991, 1994, 2003). Higher wind speeds may cause reduced height of the drift above the fence height, limiting the total storage capacity of the fences.

Observed drift volumes are about 214–223 t/m in all three winters. This aligns well with the design expectations (200–250 t/m). Despite high wind speeds and dense snow conditions, the observed drift volumes and shapes largely align with predicted behaviour, indicating that the fence design remains effective under Icelandic conditions. The consistency of measured drift volumes across the first two winters demonstrates that the fences operate within their intended capacity. However, performance can degrade due to burial as is observed in the third winter.

Observations during irregular direct inspection of the fences during winter as well as oblique drone photographs did not indicate serious problems due to icing, that is, icing did probably not reduce the porosity such that the snow-catching effectiveness of the fences was adversely affected. The time-lapse camera did, however, not work well due to riming and/or icing and was taken down in the summer 2025. The camera did, for this reason, not provide useful information regarding this problem.

5. CONCLUSIONS

The pilot study demonstrates that snow fences on the plateau of Eyrarfjall mountain can perform effectively under the site's high-wind conditions, particularly during typical snow transport events from the northeast. Measured snow drifts align with design expectations. However, performance can be limited during some winters due to more southerly winds. Continued monitoring is needed to better understand this variability.

The ground clearance of the fences is currently set as 0.1H (0.5 m) which might be insufficient, given the observed snowfall on the mountain plateau. It is recommended to increase the clearance to 0.2H (1 m) to improve drift storage and delay burial later in the season.

While the fences effectively capture snow in their immediate vicinity, their influence on snow accumulation in the nearby avalanche starting zones remains uncertain. It is plausible that they reduce snow in the starting zone in early winter, but their impact likely diminishes as they become buried later in the season. This may reduce the frequency of avalanche releases but is unlikely to significantly mitigate avalanche hazard during large storm-driven snow avalanche cycles, particularly in middle to late winters.

G.S. Pétursson and others P2.5 - Page 312

Before proceeding with further implementation, a structural inspection of the existing fences is advised, as anchoring tall structures in such exposed, wind-prone terrain presents challenges. Finally, continued multi-year monitoring is recommended, extending to the starting zones of

both gullies to further understand the impact of these structures.

REFERENCES

- Hákonardóttir, K. M., Gíslason, S., Thoroddsen, Á., Guðmundsson, R. L., Pétursson, H. Ö. (2023). Snjóflóðavarnir á Flateyri. Endurskoðun frumathugunar. Verkís, report nr. 291189.
- Icelandic Road and Coastal administration. (2000). Snjósöfnunagrindur Handbók. Orion ráðgjöf.
- Petersen, G. N. (2021). Vetrarúrkoma á Eyrarfjalli samkvæmt ICRA endurgreiningunni. Icelandic Meteorological Office, report nr. GNP/2021-01.
- Tabler, R. D. (1991). Snow Fence Guide. Strategic Highway Research Program. National Research Council. Washington, DC. Report nr. SHRP-W/FR-91-106.
- Tabler, R. D. (1994). Design Guidelines for the Control of Blowing and Drifting Snow. Strategic Highway Research Program. National Research Council. Washington, DC. Report nr. SHRP-H-381.
- Tabler, R. D. (2003). Controling Blowing and Driffting Snow with Snow Fences and Road Design. National Cooperative Highway Reasearch Program. Transportation Research Board of the National Academies. Report nr. 20-7(147).
- Þórðarson, S. (2021). Eyrarfjall ofan Flateyrar. Athugun á forsendum fyrir snjósöfnunargirðingum til þess að draga úr snjóflóðahættu. Vegsýn ehf. Memo dated 14.02.2021.

Development of a calculation method for flexible rockfall barriers under static and dynamic snow loads

Dennis Gasteiger^{1*}, Peter Utz¹, Gabriel Marc², Alexander Michalski³ and Maximilian Kramer¹

Geobrugg AG, Aachstrasse 11, 8590 Romanshorn, SWITZERLAND
 BKW Energie AG, Viktoriaplatz 2, 3013 Bern, SWITZERLAND
 HTWG Konstanz, Alfred-Wachtel-Straße 8, 78462 Konstanz, GERMANY
 *Corresponding author, e-mail: dennis.gasteiger@geobrugg.com

ABSTRACT

Flexible rockfall barriers are primarily designed to absorb high-energy point impacts caused by falling rocks. However, when installed in high-altitude environments, they are exposed to substantial snow loads. These loads act as areal rather than point forces, representing a fundamentally different loading scenario for which the systems are not originally designed. If snow loads are not adequately considered during design and planning, they may lead to damage of individual components or, in the worst case, complete failure of the barrier. This highlights the need for flexible barrier systems with multi-hazard resistance, capable of withstanding both rockfall impacts and snow loads.

The objective of this study is to develop a calculation method for all flexible rockfall barrier types produced by *Geobrugg AG* that are exposed to static and dynamic snow loading. To achieve this, key aspects such as the mechanical properties of ring nets, fundamentals of rope statics, and principles of snow and avalanche mechanics were analyzed to model areal loading scenarios on flexible structures. Missing material properties were determined through targeted tensile testing in the laboratory.

The proposed method was calibrated and validated using field data collected from previous research projects, including measurements of barrier deformation and loading of individual components during interactions with static and dynamic snow events. The final calculation approach combines Excel-based workflows with structural analysis in *RSTAB*. The method is fully parametric, allowing for efficient adaptation to a wide range of environmental and loading conditions in practical applications.

1. INTRODUCTION

The present study is the result of my master's thesis conducted in the field of civil engineering at HTWG Konstanz – University of Applied Sciences, in collaboration with Geobrugg AG.

Rockfall and snow avalanches are gravitational natural hazards that predominantly occur in alpine regions. One possible technical mitigation measure against rockfall is the use of flexible rockfall barriers, which are designed to catch falling rocks. These systems are subjected to highenergy, dynamic point loads. In contrast, avalanche protection structures are intended to prevent the release of avalanches in advance and are therefore exposed to large-area, static snow loads.

When flexible rockfall barriers are installed in alpine environments, they are also exposed to snow pressure and snow slides for which they were not primarily designed. If this type of

D. Gasteiger and others P2.6 - Page 314

loading is not taken into account during the design phase, it may lead to damage of individual components or, in the worst case, complete failure of the barrier.

Since the structural behavior of flexible rockfall barriers is highly deformation-dependent, it is particularly challenging to incorporate snow loading scenarios into standard design calculations. To address this issue, two research projects were conducted in 2003-2006 and 2023-24, during which several barriers were exposed to snow loads (Margreth and Roth 2007; Marc et al., 2024). The findings from these studies contributed to the development and verification of the calculation method described in this work.

2. AIM OF THE STUDY

To date, only rudimentary methods have been used to model the structural behavior of flexible barriers under snow loads.

The aim of this study was to develop a calculation method for flexible rockfall barriers produced by *Geobrugg AG* under snow and avalanche loads. The method is intended to realistically capture the complex structural behavior resulting from the interaction of steel nets, support ropes, steel posts, brake elements, and anchor ropes.

The approach was designed to be fully parametric, allowing for the consideration of varying terrain conditions, snow loads, barrier heights, and post spacing. It enables the determination of internal forces within the individual components, forming the basis for structural design and verification.

3. SNOW AND AVALANCHE LOAD

For the calculation procedure, load models for static snow pressure and avalanche impact had to be defined first.

For static snow pressure on sloped terrain, the method described in the Swiss guideline "Lawinenverbau im Anbruchgebiet" was adopted (Margreth, 2007). This approach is based on Haefeli's snow pressure theory, in which slope-parallel and slope-perpendicular pressures act uniformly over the snow depth on the obstacle (Haefeli, 1939).

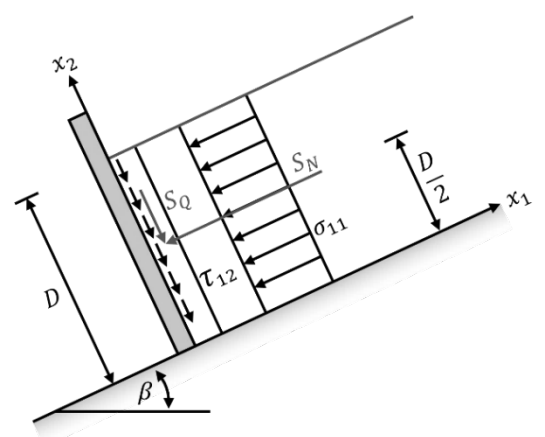


Figure 1 creep pressure according to Haefeli

For avalanche impact loading, the method by Voellmy and Salm was selected (Voellmy, 1955; Salm et al., 1990). In this approach, the avalanche pressure is assumed to be constant within the flow height and decreases linearly within the run-up height.

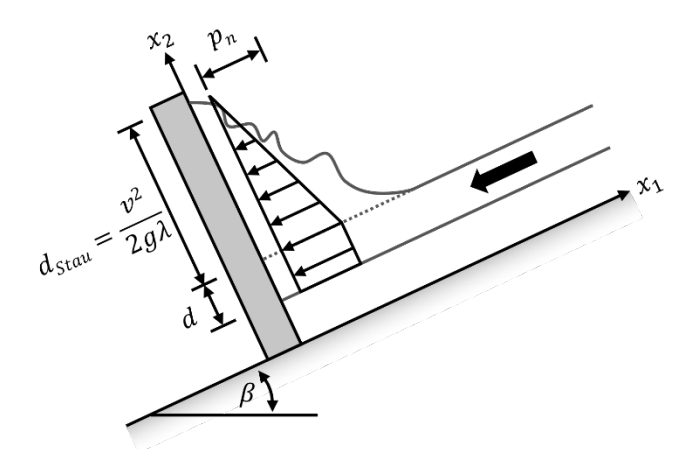


Figure 2 avalanche pressure distribution on an obstacle

The calculation assumes that the avalanche impacts a rigid obstacle. However, when the flow hits a net structure, such as those used in flexible rockfall barriers, the actual pressure can be significantly reduced due to the net's permeability. To date, no reliable reduction factor is available. The described approach can therefore be regarded as a conservative upper bound for avalanche loading.

4. DEVELOPMENT OF THE CALCULATION METHOD

The calculation method is divided into two main parts. First, the snow load calculation, net analysis, and support rope analysis are carried out parametrically in Excel. Through an import function, the system geometry and the support rope forces, which were calculated in Excel, can be automatically transferred to the structural analysis software *RSTAB*.

In RSTAB, the remaining structural components, namely the posts and anchoring ropes, are analyzed. In this method, the internal forces are passed sequentially from one structural component to the next, ensuring clear traceability and transparency of the results.

To improve the understanding of the following section, a system drawing of a typical rockfall barrier by *Geobrugg AG* is provided below:

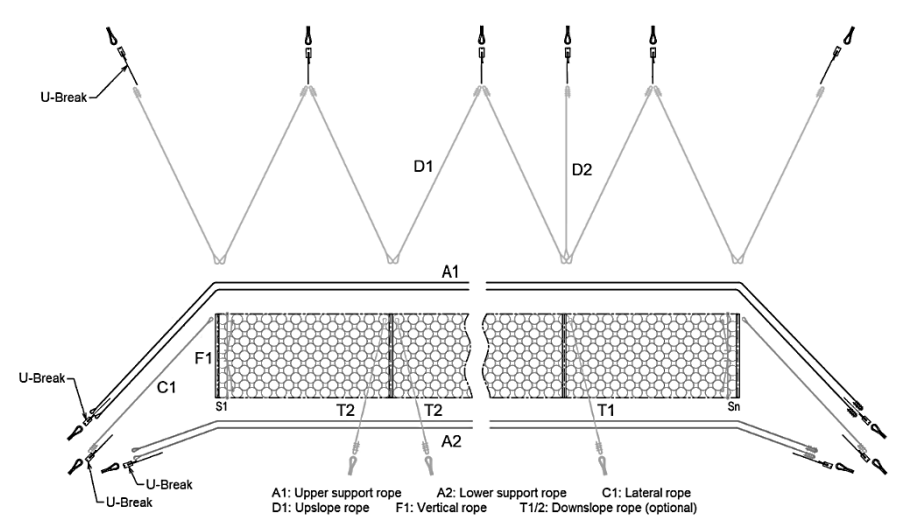


Figure 3 system drawing of a rockfall barrier from Geobrugg AG

D. Gasteiger and others P2.6 - Page 316

4.1 Snow and avalanche load calculation

The snow and avalanche loads can either be specified in advance based on existing design criteria or external input, or they can be calculated using the methods described above, considering site-specific factors such as slope angle, snow depth, and avalanche characteristics.

4.2 Net calculation

To improve transparency and simplify the calculation model, the individual components of the barrier are analyzed step by step, with the resulting forces passed on to the subsequent elements. The process begins with the net, which is subjected to snow loading and is suspended between an upper and a lower support rope.

The aim is to determine the resulting net shape as well as the forces transmitted from the net to the support ropes. It is conservatively assumed that the entire snow pressure is transferred to the net, as snow cones are expected to form behind each mesh opening, enabling full load transfer despite the net's open structure. A planar load-bearing behavior is assumed, allowing the net to be idealized as vertical strips behaving like single ropes suspended between supports.

Based on this assumption, the net can be analyzed using basic rope theory. This requires information about the load distribution, the initial net height, the material elongation behavior, and the position of the supports. The calculations are carried out parametrically in Excel. An iterative solution of the rope equations allows the determination of the net shape, the resulting forces, and their direction.

In the final step, the support reactions are calculated, which then serve as input for the calculation of the support ropes.

4.3 Support rope calculation

The upper and lower support ropes run continuously from the beginning to the end of the barrier and are only deflected at the top and bottom of the posts. Since the same snow load is assumed in every span, a rope segment between two posts can be analyzed separately and modeled as a sagging single rope.

The post tops and bases act as support points. The load is taken from the previous net calculation and applied as a constant distributed load along the rope. The calculation is done in Excel using the same iterative rope theory approach as for the net.

4.4 Transfer of geometry and loads to RSTAB

RSTAB offers the possibility to import and export input data such as nodes, members, materials, and loads via Excel tables. To ensure that RSTAB correctly interprets the data, a predefined table structure must be followed. Each table contains structured information that defines the geometry and loading of the structural model.

The required table templates are integrated into the Excel tool. Parameters such as the selected system, slope inclination, the orientation of the support ropes, and the resulting forces acting on the posts influence the entries in these tables. To maintain a fully parameterized workflow, all table entries are generated dynamically using Excel formulas.

By importing the generated tables into a blank *RSTAB* model, the system is automatically created with the correct geometry, materials, number of spans, and load conditions. The sagging

support ropes are modeled as non-structural members for visualization purposes, while the lateral and upslope anchor ropes are modeled as straight tension members. All posts and ropes are modeled with pinned supports. Rigid links are used at the top of the posts to account for eccentricities in the rope connections.

The following figure shows an example of a generated system in RSTAB:

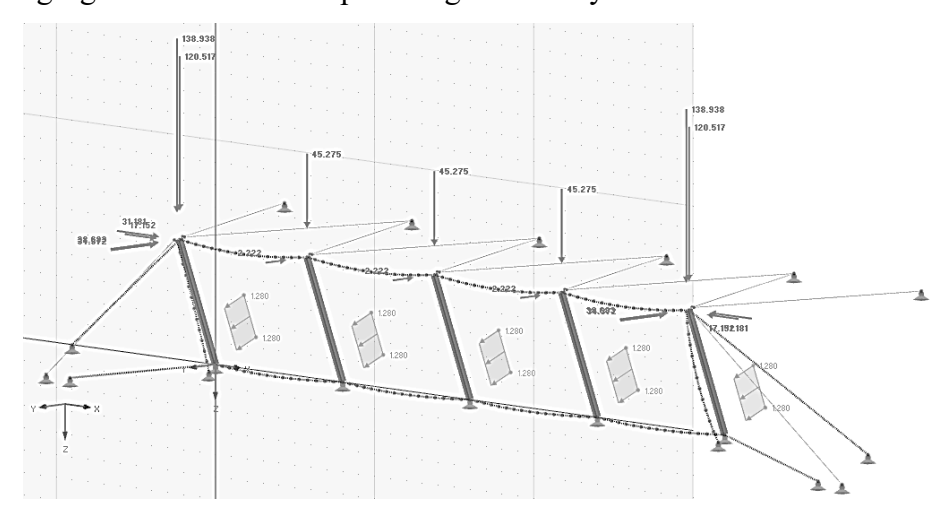


Figure 4 generated system in *RSTAB*

4.5 Calculation of posts and anchor ropes

The internal forces for the posts and anchor ropes are then determined in *RSTAB*. Since the structure is a rope-supported system, the analysis is performed according to the theory of third-order. The posts are primarily subjected to compression but also experience bending moments due to eccentricities at the post head and the explicit snow load perpendicular to the post. The lateral and uphill anchor ropes are subjected to pure tensile forces. The forces in the net and in the upper and lower main ropes have already been calculated in the Excel tool, as previously described.

5. RESULTS AND DISCUSSION

The objective of this study was to develop a calculation procedure for *Geobrugg* rockfall barriers exposed to static snow and avalanche loads. The calculations are performed in Excel and *RSTAB* and are fully parameterized. After entering the system parameters and site-specific factors, the expected snow load can either be calculated using the described approaches or specified directly. Due to the fully parametric setup, the internal forces of the individual components can be determined with minimal effort, and the subsequent structural design of the system components can also be performed.

To validate the developed calculation procedure, measured rope forces from the previous field tests were compared with calculated values. The results showed very good agreement, with the exception of the forces in the lower support rope. In this case, the calculated forces were significantly higher than the measured ones. A plausible explanation for this discrepancy could be friction between the lower support rope and the ground, which was not considered in the calculation procedure. However, this deviation results in conservative estimates, which is favorable from a safety perspective.

D. Gasteiger and others P2.6 - Page 318

6. CONCLUSIONS

The developed calculation procedure provides an efficient tool for assessing the structural response of flexible rockfall barriers under static snow and avalanche loads. The strong agreement with field measurements confirms the validity of the approach, while its parametric structure ensures adaptability to various system configurations and site conditions.

ACKNOWLEDGEMENT

I would like to express my sincere thanks to my supervisors at *Geobrugg AG*, Peter Utz and Gabriel Marc, for their valuable guidance, support, and practical insights throughout the course of this thesis. I am also grateful to Prof. Dr.-Ing. Alexander Michalski from the *HTWG Konstanz* – *University of Applied Sciences* for his academic supervision and constructive feedback. Lastly, I would like to thank Maximilian Kramer for his assistance with the introductory abstract of this extended abstract.

REFERENCES

- Haefeli, R., 1939. Schneemechanik mit Hinweisen auf die Erdbaumechanik. Beiträge zur Geologie der Schweiz, Geotechnische Serie, Hydrologie, Lieferung 3, ETH Zürich, Zürich.
- Marc, G., Halsen, S., Peterson, J., Lanter, A., Lanter, H., 2024. ALPS2.0: Interaction of flexible rockfall barriers with static and dynamic snow pressure. ISSW, Tromsø, Norway.
- Margreth, S., 2007. Lawinenverbau im Anbruchgebiet. Technische Richtlinie als Vollzugshilfe. Umwelt-Vollzug Nr. 0704, Bern, Davos, Bundesamt für Umwelt BAFU, WSL Eidgenössisches Institut für Schnee- und Lawinenforschung SLF.
- Margreth, S., Roth, A., 2007. Interaction of flexible rockfall barriers with avalanches and snow pressure. Cold Regions Science and Technology.
- Salm, B., Burkard, A., Gubler, H. U., 1990. Berechnung von Fliesslawinen. Eine Anleitung fuer Praktiker mit Bleispielen. Davos, Eidgenössisches Institut für Schnee- und Lawinenforschung, Mitteilungen Nr. 47.
- Voellmy, A., 1955. Über die Zerstörkraft von Lawinen. In: Schweizerische Bauzeitung, 73 (12, 15, 17, 19, 37), Zürich, Verlag W. Jegher & A. Ostertag, 1955, pp. 159–162, 212–217, 246–249, 280–285.



The Association of Chartered Engineers in Iceland Engjateig 9, IS-105 Reykjavík, tel. +354 535 9300